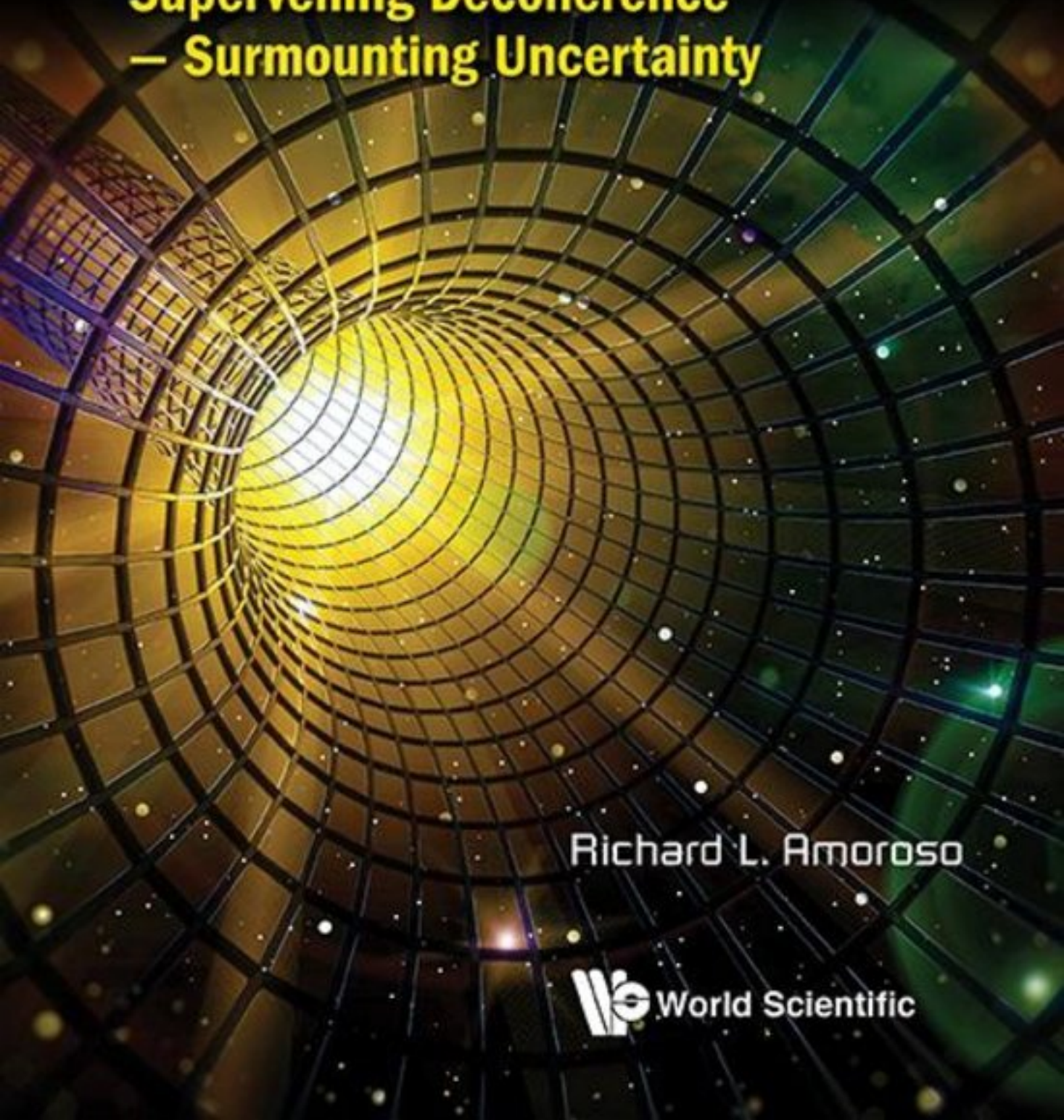


UNIVERSAL QUANTUM COMPUTING

**Supervening Decoherence
— Surmounting Uncertainty**



Richard L. Amoroso



World Scientific

UNIVERSAL QUANTUM COMPUTING

**Supervening Decoherence
— Surmounting Uncertainty**

This page intentionally left blank

UNIVERSAL QUANTUM COMPUTING

**Supervening Decoherence
– Surmounting Uncertainty**

Richard L. Amoroso
Noetic Advanced Studies Institute, USA



World Scientific

NEW JERSEY • LONDON • SINGAPORE • BEIJING • SHANGHAI • HONG KONG • TAIPEI • CHENNAI • TOKYO

Published by

World Scientific Publishing Co. Pte. Ltd.

5 Toh Tuck Link, Singapore 596224

USA office: 27 Warren Street, Suite 401-402, Hackensack, NJ 07601

UK office: 57 Shelton Street, Covent Garden, London WC2H 9HE

Library of Congress Cataloging-in-Publication Data

Names: Amoroso, Richard L., author.

Title: Universal quantum computing : supervening decoherence — surmounting uncertainty /
Richard L. Amoroso, Noetic Advanced Studies Institute, USA.

Description: Hackensack, NJ : World Scientific, [2016] |

Includes bibliographical references and index.

Identifiers: LCCN 2016022859| ISBN 9789813145993 (hardcover)

Subjects: LCSH: Quantum computing. | Quantum theory.

Classification: LCC QA76.889 .A46 2016 | DDC 006.3/843--dc23

LC record available at <https://lccn.loc.gov/2016022859>

British Library Cataloguing-in-Publication Data

A catalogue record for this book is available from the British Library.

Copyright © 2017 by World Scientific Publishing Co. Pte. Ltd.

All rights reserved. This book, or parts thereof, may not be reproduced in any form or by any means, electronic or mechanical, including photocopying, recording or any information storage and retrieval system now known or to be invented, without written permission from the publisher.

For photocopying of material in this volume, please pay a copying fee through the Copyright Clearance Center, Inc., 222 Rosewood Drive, Danvers, MA 01923, USA. In this case permission to photocopy is not required from the publisher.

Preface

This breakthrough volume touts having conceptually dissolved the remaining barriers for immediate implementation of Bulk Universal Quantum Computing (UQC), and as such most likely describes the most advanced basis for developing Quantum Information Processing (QIP). Numerous books, many 100s of patents, 1,000s of papers and a Googolplex of considerations fill the pantheon of QC R&D. Of late QC mathemagicians claim QCs already exist; but by what chimeric definition. Does flipping a few qubits in a logic gate qualify as quantum computing?

In physics, theory bears little weight until it is supported by rigorous experimental confirmation, less if new, radical or an untested paradigm shift. This volume develops quantum computing based on ‘3rd regime’ physics of Unified Field Mechanics (UFM). What distinguishes this work from myriad other avenues to UQC under study? Virtually all R&D paths struggle with refining technology and decoherence. If the highly favored room-sized cryogenically cooled QCs ever become successful, they would be reminiscent of the 1946 city block-sized Eniac computer that contained 17,468 vacuum tubes. Does the proposed by-pass of that step retard acceptance of the UFM model; maybe, maybe not as UFM modeling also puts an end to the need for large supercolliders like the CERN LHC.

The QC prototype proposed herein is room temperature, tabletop, surmounts uncertainty and supervenes decoherence during the general process of operation. It is dramatically different in that it is also not limited to the ‘locality and unitarity’ confines of the basis of quantum mechanics itself. Since it is based on principles of UFM, the Uncertainty Principle and Decoherence no longer apply. Thus generally speaking, the UFM UQC model could putatively be implemented on any of the other viable quantum platforms. Albeit, here’s the rub: a conundrum still exists; the complex algebra for correlating relativistic (r-qubits) with a new class of algorithms designed for a transform beyond the Galilean-Lorentz-Poincaré cast in HD UFM brane topology remains. A program is in place to finish the final mathematical derivation by spring 2017 and perform the

1st experiment by 2019 if our proposal is accepted and allocated a spot in the que applied to.

The last age of discovery occurred about 100 years ago. Incorporating the remaining requirements for UQC will usher in the next one. Scott Aaronson of MIT said, ‘*quantum computing requires a new discovery in physics, and if that discovery has been made is not been revealed to the physics community.*’ Since the CIA has purchased a D-wave ‘toy’ QC, it seems reasonably clear no clandestine discovery is in the hands of the US government. Gazing over the landscape of the QC research community, everyone seems to be about on the same page in battling decoherence as the final problem. With relative certainty then, the claim, ‘*Hypothesis non-Fingo*’ as Newton is want to say, that the discovery is revealed in this volume is reservedly ballyhooed. The transition to UFM is not one discovery, but a ‘bucket of discovery’, perhaps that could be said of a similar bucket ladling out quantum mechanics a hundred years ago by the seventeen eventual Nobel laureates who attended the world of physics changing *Conseil Solvay* conferences in Brussels.

The framework for the imminent age of discovery we term unified field mechanics (UFM); a third regime of reality in the progression Classical Mechanics → Quantum Mechanics → UFM. Just as infinities (ultraviolet catastrophe) in the Raleigh-Jeans Law describing blackbody radiation led to Planck’s 1900 formulation of the process of energy absorption and emission, becoming known as the quantum hypothesis - *any energy-radiating atomic system can theoretically be divided into a number of discrete ‘energy elements’, ϵ* with each element proportional to the frequency, v individually radiating energy, by: $\epsilon = hv$.

There is an obvious parallel today in the renormalization of the troublesome infinities in quantum field theory. It is quite curious that in this case a reversal occurs and quantization is undone again by entry into the 3rd regime. Since quantum mechanics can no longer be considered the ‘basement of reality’ an initial discovery popping out of the UFM bucket is that QM uncertainty is a ‘complex manifold of finite radius’. The new set of UFM transformations beyond the Galilean-Lorentz-Poincaré naturally cancel the infinities from fundamental principles, not in an *ad hoc* manner.

Physicists still ‘believing’ in a quantum universe where the Planck scale is the ‘basement of reality’, adamantly proclaim the impossibility of violating the quantum uncertainty principle. Here is the manner in which science fiction writer Isaac Asimov put it, “*You can’t lick the uncertainty principle, man, any more than you can live on the sun, there are physical*

limits to what can be done.” [1]. Physical limits apply of course to the tools available to us. Currently, the smaller the scale we hope to observe the larger and larger the supercollider needs to be to create a definitive particle spray cross-section. As you will hopefully be able to comprehend from my primitive ruminations, UFM provides a new type of low energy cross-section. The 4-space observation of microscopic matter demands a supercollider. From the point of view of a cosmology with a Planck-scale basement that is all there is; particles are singularities in spacetime. But the fundamental nature of matter is profoundly different once one is able to ‘see’ beyond the rigid barrier kept in place by the uncertainty manifold. In HD space, each particle is comprised additionally of a mirror-symmetric brane topology of conformal scale-invariant components. A Dirac-like spherical rotation occurs, cyclically separating each mirror symmetric half and reconnecting it again. If the ‘measurement’ is taken when the symmetry is reconnecting, the cross-section is revealed; the 3-sphere able to ‘see’ the insides of the circles in Abbot’s book Flatland.

If this volume could evolve to a 3rd edition; I think I might finally be satisfied with it. Those who write ‘books’ suffer with the experience that a volume in many ways is never completely finished; and one polishes and rubs until a convenient or often inconvenient stopping place intervenes. I would not bother my dear readership with this misanthropic complaint if it were just a matter of time constraints, which of itself can be a serious derailment; but in performing the usual study and research to embellish, supplement and check for accuracy, something totally unexpected occurred. This has by no means been a more typical monograph preparation solidifying research done over a past five to ten or even twenty years; but *avant-garde* and thus perhaps sadly may be seen as a bit too radical for some mentalities. I remember a 1st reading Newton’s *Principia*, it took effort for me to find the basis for his historical introduction of Calculus. More pertinently however, what I mean is that the work has been a broad avenue of profound discovery, not a few, but many; that like the shift to quantum mechanics will take the next 100 years to develop.

For example, and this is not the kind of discovery I mean – something already out there that I didn’t notice before: In preparing this manuscript I was delighted, surprised and nonplussed to find in what at first appeared to be an obscure nook and cranny in 2015, a discussion of relativistic quantum information processing and relativistic qubits. The originator of the concept, Vlasov, a Russian postdoc at the time, briefly introduced relativistic qubits at PhysComp96 [2]. On emailing him, I said, ‘it looks like it took about 20 years, but finally the community is starting to catch

up with your idea'. He promptly emailed me back with a link to a 2006 paper hinting at the concept [3]. As often is the case with a seminal thought, the presenter is timid, not sure himself and has less clarity than will appear soon afterwards, which almost immediately did, and now a new field of relativistic information processing (RIP) is in full swing. I'll only mention one more item at the moment – I never would have guessed in pondering solutions to the inherent problem of anyonic ‘topologically protected’ TQC, that I would discover the need for what I decided to term an ‘Ontological-Phase Topological Field Theory (OPTFT).

When the great innovation appears, it will almost certainly be in a muddled, incomplete and confusing form. To the discoverer himself it will be only half-understood; to everybody else it will be a mystery. For any speculation which does not at first glance look crazy, there is no hope. - Freeman Dyson [4].

If the author has an obvious shortcoming, while he is a practicing mathematical-theoretical physicist, he is equally or more so a philosopher of physics revealed in the more axiomatic approach peppered with *dessin enfant* (pun intended) utilized in this presentation.

OPTFT, essential UFM bulk UQC will end up taking us far into the future; with it, one leaves polynomial and quadratic algorithmic speedup in the dust as it will soon enough be possible to develop ‘instantaneous algorithms’ by utilizing the full EPR aspects of nonlocal holography and some sort of dual-amplituhedron as being developed by Nima Arkani-Hamed. Now let’s get back to more immediate promulgations.

The salient premise of this volume is that UQC cannot be achieved without utilizing UFM. This is not a simple premise, but represents a major paradigm shift of the caliber of switching from classical mechanics to quantum mechanics. But to confound us, it is in addition more like a Galilean class paradigm shift complicated by additional epistemological issues involved; which even this ‘fall guy’ is too timid to address here without guile. The rest of the physics community is still lollygagging around finishing the standard model in 4D. I think dimensionality of the TOE is not addressed as a requirement in that escapade. Additional dimensionality (XD) is however, now testable by proposed experiments at CERN (or the low energy tabletop protocol outlined herein). It may be that the putative utility of UFM required for UQC here garners little attention until a version of M-theory becomes pragmatically realized.

Also note that, for a variety of reasons discussed, our version of M-theory differs dramatically on several key premises, because we feel Gravity is not quantized and that the regime of interaction is rather with

the regime of UFM. This is also not a trivial dilemma, we have defined a duality between Newton's and Einstein's gravity; and it seems likely in that guise that in the semi-quantum limit some sort of quantized-like residue operates elevating the concept of wave-particle duality to a principle of cosmology applied to brane topology. This stems from our discovery that 'uncertainty' is a complex manifold of finite radius. Certainly, at the time of writing, the majority of QC developers still work within the confines of Bloch sphere Hilbert space concepts. Before even approaching the cornucopia of landmines proposed here; one must pass through the briar patch of leaving unitarity and locality behind, and also view differently the very recent forays into relativistic modes of QIP before coming to the threshold of what we think should be called a Ontological-Phase Topological Field Theory (OPTFT).

In Chap. 3 the author felt it necessary to take liberty and include material relating to the physical basis for the 'Mind of the Observer' as part of delineating the need for a new cosmological paradigm to fully develop UQC. For real progress to occur, even as the likes of von Neumann claimed, observer physics needs to be fully addressed sometime - Feynman said in his Nobel lecture:

If [all physicists] follow the same current fashion in expressing and thinking about ... field theory ... hypotheses being generated ... is limited ... possibly the chance is high that the truth lies in the fashionable direction. But, on the off chance that it is in another direction - a direction obvious from an unfashionable view of field theory - who will find it? Only someone who sacrifices himself ... from a peculiar and unusual point of view, one may have to invent for himself - *Richard Feynman*, Nobel Prize lecture.

There is still a lot of chatter about classical mechanics and classical field theory. The situation has been steadily evolving from quantum mechanics to quantum field theory. The concept of Quantum Computing (QC) began in 1981 when Nobelist Richard Feynman queried if '*quantum physics could be simulated on a computer*'. The discussion led to the insight that simulating quantum physics would require a new kind of computer called a '*quantum computer*'; thought to be the very first mention of the term. Later Feynman suggested: '*There is nothing in the laws of physics prohibiting quantum computers*' [5]. Feynman also proposed that quantum computation could be facilitated by incorporating the utility of a concept he termed a '*synchronization backbone*'. Until now this construct has remained mysterious and considered intractable by the QC development community. This impasse essentially occurred because

the rational for attempting to implement a synchronization backbone approach is classed in terms of what is known as a ‘bi-local’ phenomenon [3,4] that didn’t really add a proper ‘backbone’ to the quantum system in that style of attempt. In the extended model delineated here, based on elements of UFM [5-7], a viable synchronization backbone is discovered to be an inherent part of the topology of the higher dimensional (HD) M-Theoretic Calabi-Yau mirror symmetric backcloth; which turns out to be essentially like getting half the quantum computer for ‘free’! In terms of UFM the perceived local state is only a shadow of the HD nonlocal quantum reality; thus our perception of Feynman’s synchronization backbone is not feasible bi-locally but requires a duality of locality and HD nonlocal aspects of UFM. This key aspect of bulk UQC modeling could not have been discovered without the paradigm shift to UFM [8-10] revealing the true synchronization backbone as part of the mirror symmetry backcloth.

The purpose of the first two chapters is generally to review the current state of affairs in QC development and give a semblance of self-containment for the volume. Chapter 1 - *From Concept to Conundrum* briefly delineates the origins of Quantum Computing in terms of Feynman’s ruminations on the subject; followed by a short description of the dozen or more research approaches currently considered most promising. Chapter 2 - *Cornucopia of Quantum Logic Gates* surveys and compares salient aspects of many of the main types of quantum logic gates studied.

Chapter 3 *Multiverse Cosmology – A New Basis of Reality* provides the initial foray into the basis for UFM providing a glimpse of the radical extension from the historical and current concept of observed reality as a Euclidean 3-space and outlines the new multiverse cosmology needed to go beyond the 4D Minkowski-Riemann spacetime of the standard model into the HD 3rd regime of Calabi-Yau mirror symmetric M-Theory.

Chapter 4 - *A Revolution in the Conception of Matter* sets the stage for Chap. 5 extending understanding of the ages old conundrum of the nature of the fermionic singularity or point particle; and defining why the current Bloch sphere rendition of a qubit must now be considered grossly inadequate and a relativistic r-qubit with more degrees of freedom is required. Chapters 4 and 5 tell us about conformal scale-invariant mirror symmetric ‘copies’ of a quantum state found in the topology of the HD brane world. In Chap 5 - *From Qubits to Relativistic Qubits (R-Qubits)* the basis for the standard definition of a qubit is redefined and extended to relativistic form for RIP where the additional degrees of freedom create

compatibility with a 12D OPTFT which as shown later in Chaps. 6,7 and 8 provides the foundation for surmounting uncertainty and completely eliminating the problem of decoherence in the operation of a quantum computer. Chapter 9 - *Topological Quantum Field Theory* gives a technical review of TQFT and its utility in our model of bulk quantum computing. Chapters 7 and 8 - *Surmounting Uncertainty Supervening Decoherence*, and - '*Measurement*' With *Certainty*, respectively begin to explain more fully the core thrust of the volume. This is where the principles for actualizing a universal bulk quantum computer are explained for final prototyping in Chap. 15 and operation in Chap. 14.

Chapter 6 - *Utility of Unified Field Mechanics* describing a 3rd regime of reality beyond Classical and Quantum Mechanics provides clarity in understanding the bridge between TQFT, the essential large scale additional dimensionality (LSXD) of our new understanding of reality and utility of relativistic qubits (r-qubits). When the reader gets to Chapter 13 - *New Classes of Quantum Algorithms*, it should become obvious that an r-qubit with additional degrees of freedom cast in an LSXD cosmology associated with UFM requires a radical extension of existing quantum logic gates.

In Chapters 14 - *Class II Mesoionic Xanthines as Potential Ten Qubit Substrate Registers*, and 15 - *Universal QC Prototype Modeling* the class II mesoionic xanthine molecule chosen for prototyping and its bonding substrate is described. The mesoionic xanthine forms a stable crystal at room temperature with a 100-year shelf life and has 10 evenly spaced quantum states suitable for uniform scalability.

There is currently a program in the process of performing an experimental protocol aimed at falsifying the paradigm of unified field mechanics required to operate the quantum computer design offered herein. Success of the experiment will essentially confirm near term implementation of universal scalable bulk quantum computing as the methodology required parallels computer operations, albeit applied to the quantum system in a different manner.

The fins structure constant will be shown to be relevant to refinements in initial empirical tests and corrections to rf-resonance applied to operation.

The easiest to implement and most obvious primary applications of quantum computing are cryptography, database search, pharmaceutical and software development. For example, Microsoft will no longer need to introduce new versions of operating systems riddled with errors.

It will take time to understand how to develop the more complex algorithms to best manipulate the deep structure of reality required to implement 2nd generation quantum computers. Examples, some seemingly fantastic from the myopic perspective of the moment, are utilizing ‘Coherent Control’ of quantum systems to produce orders of magnitude refinements in transistor lithography or solving the remaining problems in nuclear fusion confinement finally producing nearly limitless clean energy. ‘Perfect’ weather prediction leads to satellite based weather control. Ballistic quantum information processing of the cellular automata structure tessellating deep reality will also lead to de Broglie matter-wave defense shields making nuclear ordnance obsolete.

Other aspects of quantum computing will introduce new classes of medical technologies, communication devices and wondrous engineering feats like practical FTL warp drive space ship design!

Final note: The author is proud of this volume as it represents his most significant work to date; however too many of the chapters are disappointing as they do not nearly fulfill their purpose. I say this because the concern is that because of these shortcomings of the author readers will overlook what albeit as yet primitive, and somewhat inscrutable are its ‘profound discoveries’.

Certainly, the most salient feature not to be overlooked is the model (plus experimental design) for routine surmounting of the uncertainty principle [9]. I say routine in contrast to the IFM or ‘interaction free measurement’ model. Cramer suggests IFM works because of the Everett model. We disagree with his interpretation; rather it is because the additional degrees of freedom required arise from HD Calabi-Yau mirror symmetry, allowing a ‘single pass’ rather than the numerous passes or interferometers required by IFM. Do not miss this obvious key insight.

There are numerous insights relevant to Unified Field Mechanics (UFM), our adapted version of M-Theory that includes a completion of quantum mechanics based on extensions of the Cramer Transactional and de Broglie-Bohm-Vigier Causal interpretations. Currently we consider the fermionic singularity or point particle the fundamental object of physics. As difficult as it may be to imagine at first, in UFM there exists a conformal scale-invariance ‘up’ through brane topology such that actual real component copies of the 3-space ‘particle in a box’ exist within this HD regime. In addition to violation of uncertainty this UFM aspect is key to supervening decoherence. The relativistic (r-qubit) has been considered for 20 years, now finally, the important new field of Relativistic Information Processing (RIP) has begun. This is all now experimentally

falsifiable, which ‘when’ successful presents the 1st viable test of M-Theoretic additional dimensionality, putting an end to the need for supercolliders (Gödelized cross section) and of course founding the 3rd regime field of UFM.

The author himself gives severe criticism that the important chapter on OPTFT is far too conceptual and axiomatic, as is the mention of instantaneous algorithms. The imminent age of discovery will most certainly be described topologically; wherein the utility of the development of the Octonion Fano Snowflake is not carried through to completion. There is some urgency felt as UQC leads to new classes of medical technologies, weather control, beam weapons, flying car infrastructure, and defense shields. Finally, the heresies of the observer will be solved.

References

- [1] Asimov, I. (1989) The dead past, in Hartwell, D.G. (ed.) *The World Treasury of Science Fiction*, Little Brown.
- [2] Vlasov, A.Y. (1999) Quantum theory of computation and relativistic physics, PhysComp96 Workshop, Boston MA, 22-24 Nov 1996, arXiv: quant-ph/ 9701027v4.
- [3] Terno, D.R. (2006) Introduction to relativistic quantum information, arXiv:quant-ph/0508049v2; Peres, A. & Terno, D.R. (2003) Quantum information and relativity theory, arXiv:quant-ph/0212023v2.
- [4] Dyson, F. (1958) Innovation in physics, *Scientific American*, 199, Collected in, *From Eros to Gaia*, 1993.
- [5] Feynman, R.P. (1986) Quantum mechanical computers, *Found. of Phys.* 16: 507-531.
- [6] Floerchingerar, S. (2010) Quantum field theory as a bilocal statistical field theory, arXiv:1004.2250v1 [hep-th].
- [7] Acatrinei, C. (2002) Bilocal dynamics in quantum field theory, arXiv:hep-th/0210040v1.
- [8] Amoroso, R.L., Kauffman, L.H. & Rowlands, P. (2016) *Unified Field Mechanics: Natural Science Beyond the Veil of Spacetime*, Singapore: World Scientific.
- [9] Amoroso, R.L. (2010) Simple resonance hierarchy for surmounting quantum uncertainty, *AIP Conf. Proc.* 1316, 185 or <http://vixra.org/pdf/1305.0098v1.pdf>.
- [10] Amoroso, R. L. (2013) Evidencing ‘tight bound states’ in the hydrogen atom: Empirical manipulation of large-scale XD in violation of QED, in *The Physics of Reality: Space, Time, Matter, Cosmos*, Singapore: World Scientific.

*Richard L. Amoroso,
Los Angeles, CA USA
7 May 2016*

This page intentionally left blank

Dedication

For Epaphroditus,

Mikołaj Kopernik and

Galileo Galilei,

who grieved, *nigh unto death*, and/or were
nearly executed for their scientific innovations

...

This page intentionally left blank

Contents

Preface	v
Dedication	xv
Chap 1 From Concept to Conundrum	1
1.1 Preamble – Bits, Qubits and Complex Space	1
1.2 Panoply of QC Architectures and Substrates – Limited Overview	4
1.2.1 <i>Quantum Turing Machine</i>	4
1.2.2 <i>Quantum Circuit Computing Model</i>	5
1.2.3 <i>Measurement Based Quantum Computing</i>	5
1.2.4 <i>Adiabatic Quantum Computer</i>	6
1.2.5 <i>The Kane Nuclear Spin QC</i>	9
1.2.6 <i>QRAM Models of Quantum Computation</i>	10
1.2.7 <i>Electrons-On-Helium Quantum Computers</i>	11
1.2.8 <i>Fullerene-Based ESR Quantum Computer</i>	13
1.2.9 <i>Superconductor-Based Quantum Computers</i>	14
1.2.9.1 <i>SQUID-BASED SUPERCONDUCTOR QC</i>	14
1.2.9.2 <i>TRAPPED ION-BASED SUPERCONDUCTOR QC</i>	15
1.2.10 <i>Diamond Based Quantum Computers</i>	18
1.2.11 <i>Quantum Dot Quantum Computer</i>	19
1.2.12 <i>Transistor-Based Quantum Computer</i>	21
1.2.13 <i>Molecular Magnet Quantum Computer</i>	22
1.2.14 <i>Bose–Einstein Condensate-Based Quantum Computer</i>	23
1.2.15 <i>Rare-Earth-Metal-Ion-Doped Inorganic Crystal QC</i>	25
1.2.16 <i>Linear Optical Quantum Computer (LOQC)</i>	26
1.2.17 <i>Optical Lattice Based Quantum Computing (OLQC)</i>	28
1.2.18 <i>Cavity Quantum Electrodynamics Quantum Computing</i>	29
1.2.19 <i>Nuclear Magnetic Resonance (NMR) Quantum Computing</i>	30
1.2.19.1 <i>LIQUID-STATE NMRQC</i>	31
1.2.19.2 <i>SOLID-STATE NMRQC</i>	33
1.2.20 <i>Topological Quantum Computing (TQC)</i>	33

1.2.21 <i>Unified Field Mechanical Quantum Computing</i>	35
1.3 Concept	35
1.4. Conundrum - <i>Hypotheses non Fingo</i>	37
1.4.1 <i>The Church-Turing Hypothesis</i>	38
1.4.2 <i>The Church-Turing-Deutsch Thesis</i>	39
1.4.3 <i>Perspicacious Perspicacity – Who Has it?</i>	
<i>Where can I get Some?</i>	40
References	41
Chap 2 Cornucopia of Quantum Logic Gates	46
2.1 Fundamental Properties of Gate Operations	46
2.2 Unitary Operators as Quantum Gates	48
2.3 Some Fundamental Quantum Gates	50
2.4 Properties of the Hadamard Gate	56
2.5 Rotation Gate Quantum Multiplexer	57
References	60
Chap 3 Multiverse Cosmology: A New Basis of Reality	62
3.1 Overview	62
3.2 Introduction to Cosmological Issues	63
3.3 Clarification of Pertinent Cosmological Nomenclature	66
3.4 Parallel Interpretations of Cosmological Data	70
3.5 Euclidean/Minkowski Geometry as Basis for Observed Reality	70
3.6 Philosophy of Space in Multiverse Cosmology- Origin of Structure	72
3.7 Space: Relational Versus Absolute	74
3.8 Physical Cosmology of Fundamental Least Cosmological Unit	79
3.9 Holographic Anthropic Multiverse Cosmology	81
3.10 Overview of the Formalism for Anthropic Cosmology	83
3.11 Transformation of Space into Time	87
3.12 Energy Dependent Spacetime Metric	88
3.13 The Wheeler Geon Concept Extended to Noetic Superspace	88
3.14 The Hyper-Geon Domain of Multiverse Noetic Field Theory	89
3.15 Interregnum	90
3.16 Ambulatory Hoopla	92
3.17 Ultimate Evolution of M-Theory	97
3.18 String/Brane Dynamics	99
3.19 New Horizons Beyond the Standard Model	101

3.20 Ultimate Geometry of Reality, Dimensionality, Arrow of Time	103
3.21 New Cosmological Framework	104
3.22 Current Philosophy of Temporal Science	105
3.23 Complementarity of Physical Time and Observer Time	107
3.24 The Vacuum Origin of Thermodynamics and Entropy	115
3.25 Spin-Exchange Compactification and the Noetic Transformation	117
3.26 Dirac Spherical Rotation Inherent to LCU Transformation	120
References	124
Chap 4 A Revolution in the Conception of Matter	131
4.1 Point-Particle Infinite Mass-Energy	131
4.2 Space-Antispace as a UFM Intermediary	132
4.3 The Nilpotent Quaternionic Representation of Fermions	134
4.4 The Nature of Quantum Reality	143
4.5 Revolution in Concept of Matter	148
References	157
Chap 5 From Qubits to Relativistic (R-Qubits)	160
5.1 Introduction	161
5.2 Case for Relativistic Information Processing	164
5.3 Microphysical Computation Limits: The Relativistic R-Qubit	165
5.3.1 <i>Aspects of the Lorentz Transformation</i>	165
5.3.2 <i>Massive Particles</i>	168
5.3.3 <i>Aspects of the Poincaré Transformation</i>	169
5.4 Additional Aspects of R-Qubits and Relativistic Computing	170
5.5 Current Thinking on Relativistic Information Processing	172
5.6 Relativistic Quantum Information Theory and Computation	175
5.7 Physical Reality of Quantum States	178
5.8 Unified Field Mechanical Ontological-Phase TFT	180
References	180
Chap 6 Utility of Unified Field Mechanics	183
6.1 Unified Field Mechanics: What is it, What are the Implications?	183
6.2 Précis	185
6.3 The LCU Concept Key to Developing Unified Field Mechanics	188
6.4 Pragmatic Testing of the UFM Paradigm	192

6.5 Exploring Novel Cyclic Extensions of Hamilton's Dual-Quaternion Algebra	195
6.6 Brief Quaternion Review	195
6.7 Background and Utility of New Quaternion Extensions	197
6.8 A New Concept in Quaternion Algebra - The 1 st Triplet	198
6.9 Vectors, Scalars, Quaternions and Commutativity	200
6.10 Toward Completing the Hypercube: The 2 nd Triplet	202
6.10.1 <i>Higher Doublings - Planar to Riemann Sphere</i>	203
6.10.2 <i>Nilpotent Idempotent Vacuum Doublings</i>	204
6.10.3 <i>As Generalized Equation</i>	204
6.10.4 <i>As Tensor Transformation</i>	204
6.11 Quaternion Mirrorhouses	204
6.11.1 <i>Observation as Mirroring</i>	206
6.11.2 <i>Mirror Symmetry Experiment</i>	208
6.12 Calabi-Yau Manifolds - Brief Review	208
6.13 Search for Commutative – Anticommutative Cyclical Algebra	209
6.14 Indicia for Unified Field Mechanics by	
Tight-Bound States (TBS)	218
6.15 Building the UFM TBS Experimental Protocol	223
6.16 Some Concluding Remarks – Realm of Observation	231
References	233
 Chap 7 Surmounting Uncertainty Supervening Decoherence	236
7.1 Phenomenology Versus Ontology	237
7.2 The Turing Paradox and Quantum Zeno Effect	245
7.3 From the Perspective of Multiverse Cosmology	246
7.4 Micromagnetics and LSXD Topological Charge	
Brane Conformation	251
7.5 Catastrophe Theory and the M-Theoretic Formalism	259
7.6 Protocol for Empirically Testing Unified Theoretic Cosmology	265
7.7 Introduction to a P ≡ 1 Experimental Design	268
7.8 Conclusions	280
References	281
 Chap 8 Measurement with Certainty	288
8.1 Introduction – Summary of Purpose	289
8.2 The Principle of Superposition	292
8.3 Oscillatory Rabi NMR Resonance Cycles	294
8.4 The Problem of Decoherence	295

8.5 Insight into the Measurement Problem	297
8.6 New Physics from Anthropic Cosmology	300
8.6.1 <i>Spacetime Exciplex - U_F Noeon Mediator</i>	303
8.6.2 <i>Quantum Phenomenology Versus Noetic UFM Field Ontology</i>	305
8.7 The Basement of Reality - Through the Glass Ceiling	309
8.8 Empirical Tests of UFM Cosmology Summarized	311
8.8.1 <i>Summary of Experimental Protocols</i>	312
8.8.2 <i>Review of Key Experimental Details</i>	314
8.9 Unified Field Mechanical (UFM) Précis - Required Parameters	318
8.10 Formalizing the Noeon, New Physical Unit Quantifying UFM Energy	320
8.11 Quarkonium Flag Manifold Topology	323
8.12 Singularities, Unitary Operators and Domains of Action	326
8.12.1 <i>Semi-Classical Limit</i>	326
8.12.2 <i>Semi-Quantum Limit</i>	327
8.13 Measurement	327
8.14 The No-Cloning Theorem (NCT)	330
8.14.1 <i>Proof of the Quantum No-Cloning Theorem (NCT)</i>	331
8.14.2 <i>Quantum No-Deleting Theorem</i>	333
8.15 The Tight-Bound State Protocol	333
8.16 Indicia of the UFM Tight Bound State CQED Model	336
8.17 Building the UFM TBS Experimental Protocol	338
8.18 Issues of Experimental Design	351
References	356
 Chap 9 Topological Quantum Field Theory	364
9.1 Topological Quantum Field Theory (TQFT)	364
9.2 Schwarz-Type Topological Field Theories	366
9.3 Witten-Type Topological Field Theories	366
9.4 Dodecahedral AdS^5/CFT Duality	367
9.5 Chern-Simons Theory with Knots and Links	367
9.6 The Alexander Polynomial Skein Relation	371
9.7 The Jones Polynomial and Trefoil Knot Crossings	372
9.8 Cobordism in TQFT - Atiyah's Definitions	375
9.9 <i>Ab Infinito Ad Infinitum</i>	379
References	380
 Chap 10 Topological Quantum Computing	382
10.1 The Topological Quantum Computer (TQC)	382

10.2 Topological Quantum Computing	383
10.2.1 <i>Quasiparticles in $v = 5/2$ FQH States</i>	385
10.2.2 <i>Theoretical Models for the $v = 5/2$ State</i>	386
10.2.3 <i>Spin Polarization of the $v = 5/2$ State</i>	386
10.3 Quantum Hall Quasiparticle Anyon Braiding	387
10.3.1 <i>Topological Insulators</i>	388
10.3.2 <i>Quasiparticle Interferometry and Topological Protection</i>	390
10.4 The Jones Polynomial	392
10.5 Anon ye Fabled Anyon	393
References	394
 Chap 11 A New Group of Transformations	399
11.1 Introduction	400
11.2 Metric Space and the Line Element	401
11.3 Why a New Transformation Group?	403
11.4 Micromagnetics and LSXD Topological Charge Driving Brane Conformation	403
11.5 Lorentz Condition in Complex 8-Space and Tachyonic Signaling	404
11.6 Velocity of Propagation in Complex 8-Space	411
11.7 Metaphor Series to Clarify the Transformation of HD Topology	413
11.8 Spin Exchange Compactification Dynamics and Permutation of Dimensions in the UFM Transformation	418
11.9 Preparing the UFM Spacetime Transformation	421
11.10 Developing the Line Element for UFM Superspace	422
11.11 Dirac Spherical Rotation Inherent to Transformation of the Fundamental Least-Unit	429
11.12 Final Thought on the UFM Spacetime Transformation	431
References	433
 Chap 12 Ontological-Phase Topological Field Theory	437
12.1 Abductive <i>a Priori a Posteriori</i> Tautology	438
12.2 The Phasor (Phase Vector) Complex Probability Amplitude	439
12.2.1 <i>Complex Phase Factor</i>	441
12.2.2 <i>Geometric Phase - Berry Phase</i>	443
12.2.3 <i>The Toric Code</i>	445
12.3 Transitioning from TQFT to OPTFT	447
12.3.1 <i>The A and B-Models of Topological Field Theory</i>	448

12.3.2 Dualities Between Topological String Theories (TSTs)	448
12.3.3 The Holomorphic Anomaly	449
12.4 Topological Vacuum Bubbles by Anyon Braiding	449
12.5 Topological Switching – Key to Ontological-Phase	451
12.6 Dual Amplituhedron Geometry and ‘Epiontic’ Realism	467
References	471
Chap 13 New Classes of Quantum Algorithms	475
13.1 Introduction - From al-Khwarizmi to Unified Field-Gorhythms	475
13.2 The Church-Turing Hypothesis	477
13.3 Algorithms Based on the Quantum Fourier Transform	477
13.4 Exponential Speedup by Quantum Information Processing	479
13.5 Classical Holographic Reduction Algorithms	482
13.6 Ontological-Phase UFM Holographic Algorithms	484
13.7 The Superimplicate Order and Instantaneous UQC Algorithms	488
13.8 Some Ontological-Phase Geometric Topology	491
13.9 Summation	496
References	497
Chap 14 Class II Mesoionic Xanthines as Potential Ten Qubit Substrate Registers	501
14.1 Introduction	501
14.2 Resonance stabilization in Class II Mesoionic Xanthines	503
14.3 Projectors and Projection Operators	506
14.4 Tensor Products and Associated Operators	509
14.5 Commutation Relations for the Pauli Matrices	511
14.6 Quantum Superposition and Quantum Probabilities of 10-Qubit Mesoionic Registers	515
14.7 Projectors and Projection Operators	518
14.8 Density Measurement Operator and Quantum State Ensembles	519
14.9 State-Function Time Evolution of a Closed Quantum System	521
14.10 Quantum Simulations of Hamiltonians	522
14.11 Initialization of Mesoionic Xanthine Registers	524
14.12 Xanthine Molecule Electrostatic Potentials	533
14.13 Conclusion	533
References	535
Chap 15 Universal Quantum Computing Prototype Modeling	537
15.1 Introduction – Basics of Quantum Computing (QC)	538

15.2 Overview of New Fundamental Parameters	540
15.3 The Causal Separation of Phenomenology from Ontology	541
15.4 Review of Angular Momentum and Pauli-Dirac Spin Matrices	543
15.5 Noumenal Reality Versus Phenomenology of Quantum Theory	546
15.6 Justification for the Incursive UFM Model	547
15.7 Essential Properties of Complex 12-Space	550
15.8 Geometric Introduction to the UFM QC Ontology	564
15.9 Essential Parameters of the Incursive Oscillator	568
15.10 Ontological I/O by Superseding Quantum Uncertainty	570
15.11 A Twistor Approach to the UQC I/O Ontology	574
15.12 Class II Mesoionic Xanthines as Potential 10-Qubit Quantum Computer Substrate Registers	578
15.13 Initialization of Mesoionic Xanthine Registers	580
15.14 Conclusions	589
References	590
Index	594

Chapter 1

From Concept to Conundrum

“... Trying to find a computer simulation of physics, seems ... an excellent program to follow ... I’m not happy with all the analyses that go with just the classical theory, because nature isn’t classical, ... and if you want to make a simulation of nature, you’d better make it quantum mechanical ...”, R. Feynman [1].

The concept of quantum computing (QC) is generally credited to ratiocination by Nobelist Richard Feynman during the 1980’s, who saw ‘nothing in the laws of physics that precluded their development’. During the ensuing decades accelerating progress has been made in the ongoing development of quantum logic gates, a variety albeit dearth of algorithms and most assuring a plethora of potentially viable substrates for QC implementation. Proponents generally consider the remaining hurdle preventing bulk universal QC centers on problems associated with decoherence. In this chapter for the purpose of bringing the reader up to speed and a semblance of self-containment, a precis of the dominant platforms under development is given; each platform is unique in substrate technology, implementation format and scaling challenges. This also prepares the reader for later chapters where we move from qubits to a new class of relativistic qubits (r-qubits) whereby additional degrees of freedom are deemed essential for crossing the ‘semi-quantum limit’ into the realm of Unified Field Mechanics (UFM) allowing routine violation of the Quantum Uncertainty Principle and thereby supervening decoherence.

1.1 Preamble – Bits, Qubits and Complex Space

A classical Turing bit (short for binary digit) is the smallest unit of digital data and is limited to the two discrete binary states, 0 and 1; but a quantum bit (qubit) can additionally enter an entangled superposition of states, in which the qubit is effectively in both states simultaneously. While a classical register made up of n binary bits can contain only one of 2^n possible numbers, the corresponding quantum register can contain all 2^n

numbers simultaneously. Thus in theory, a QC could operate on seemingly infinite values simultaneously in parallel, so that a 30-qubit QC would be comparable to a digital computer capable of performing 10^{13} (trillion) floating-point operations per second (TFLOPS) which is comparable to currently fastest supercomputers.

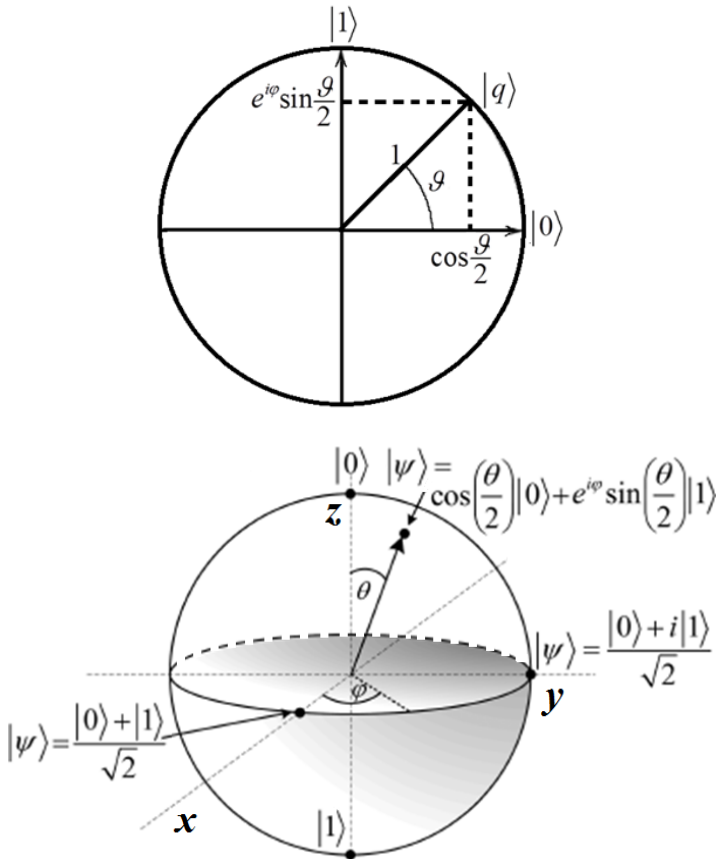


Fig. 1.1. Geometrical qubit representations. a) The qubit resides on the complex circle in the Hilbert space of all possible orientations of $|qi\rangle$. The complex unit circle is called the Hilbert space representation. In the logical basis, the two degrees of freedom of the qubit are expressed as two angles geometrically interpreted as Euler angles. b) The Bloch sphere in spin space showing the geometric representation of a qubit where $|\psi\rangle = \alpha|1\rangle + \beta|0\rangle$ for orthogonal eigenstates $|1\rangle$ and $|0\rangle$ of a single qubit on opposite poles, with superpositions located on the sphere's surface. Adapted from [2].

The qubit, a geometrical representation of the pure state space of a 2-level quantum mechanical system, is described in Dirac's 'bra-ket notation' by the state $\alpha|0\rangle + \beta|1\rangle$ where α and β are complex numbers satisfying the absolute value parameter $|\alpha|^2 + |\beta|^2 = 1$; such that measurement would result in state $|0\rangle$ with probability $|\alpha|^2$ and $|1\rangle$ with probability $|\beta|^2$. Formally, a qubit is represented in the 2D complex vector space, \mathbb{C}^2 where the $\alpha|0\rangle + \beta|1\rangle$ can be represented in the standard orthonormal basis as $|0\rangle = \begin{bmatrix} 1 \\ 0 \end{bmatrix}$ for the ground state or $|1\rangle = \begin{bmatrix} 0 \\ 1 \end{bmatrix}$ for the excited state, or on the Bloch sphere as in Fig. 1.1b.

A qubit is shown in Fig. 1.1 in both its SU(2) Hilbert space representation (top), and the same qubit on the Bloch sphere in its O(3) representation (bottom). The SU(2) and O(3) representations are homomorphic, i.e. mapping preserves form between the two structures.

Vincenzo itemized what he felt were the major requirements for implementing practical bulk QC [3]:

- Physically scalable, allowing the number of qubits to be sufficiently increased for bulk implementation.
- Qubits must be able to be initialized to arbitrary values.
- Quantum gates that operate faster than the decoherence time.
- A universal gate set for running quantum algorithms.
- Qubits that can be easily read correctly.

None of Vincenzo's requirements are yet fulfilled; some are further along than others; system decoherence is among the most challenging aspects remaining. Recently, the fundamental basis of quantum information systems is undergoing an evolution in terms of the nature of reality with radical changes in the nature of the measurement problem. The recent introduction of parameters for relativistic information processing (RIP), including relativistic r-qubits, has brought into question the historical sacrosanct basis of 'locality and unitarity' in terms of Bell's inequalities, overcoming the no-cloning theorem [4,5]. The epistemic view of the Copenhagen Interpretation is challenged by ontic considerations of objective realism and additionally as merged by W. Zurek's epi-ontic blend of quantum redundancy in quantum Darwinism [6].

1.2 Panoply of QC Architectures and Substrates – Limited Overview

The following list represents many prominent QC architectures and substrates currently under development. It seems useful to briefly review the challenges and merits of each system as distinguished by the computing model and physical substrates used to implement qubits.

- Quantum Turing Machine
- Quantum Circuit Quantum Computing Model
- Measurement Based Quantum Computing
- Adiabatic Quantum Computing
- Kane Nuclear Spin Quantum Computing
- QRAM Models of Quantum Computation
- Electrons-On-Helium Quantum Computers
- Fullerene-Based ESR Quantum Computer
- Superconductor-Based Quantum Computers
- Diamond-Based Quantum Computer
- Quantum Dot Quantum Computing
- Transistor-Based Quantum Computer
- Molecular Magnet Quantum Computer
- Bose-Einstein Condensate-Based Quantum Computer
- Rare-Earth-Metal-Ion-Doped Inorganic Crystal Quantum Computers
- Linear Optical Quantum Computer
- Optical Lattice Based Quantum Computing
- Cavity Quantum Electrodynamics (CQED) Quantum Computing
- Nuclear Magnetic Resonance (NMR) Quantum Computing
- Topological Quantum Computing
- Unified Field Mechanical Quantum Computing

1.2.1 *Quantum Turing Machine*

The quantum Turing machine (QTM) generalizes the classical Turing machine (CTM); the internal states of a CTM are replaced by pure or mixed states in a Hilbert space; The QTM is an idealistic platform not currently being developed. A QTM is a simple universal quantum computer used for modeling all the powerful parameters of quantum computing.

The QTM was proposed by Deutsch where he suggested that quantum gates could function similarly to traditional binary digital logic gates [7]. QTMs are not usually used for analyzing quantum computation; the quantum circuit model (QCM) is a more commonly used for such purposes.

1.2.2 Quantum Circuit Computing Model

The quantum circuit model (QCM) computes sequences of quantum gates which are reversible transformations on a quantum mechanical analog of a classical n -bit register. The QCM has only two observables, preparation of the initial state and observation of the final state in the same basis for the same variable at the end of the computation [8].

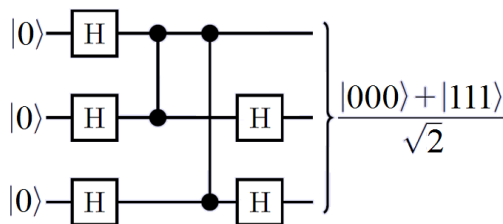


Fig. 1.2. Quantum circuit for 3 qubits using Hadamard gates.

1.2.3 Measurement Based Quantum Computing

The measurement based quantum computer (MBQC) model is also called the one-way model because the entangled resource state (usually a ‘cluster state’) is destroyed by the series of single qubit measurements on it. For a MBQC computation one starts with a given fixed entangled state of numerous qubits and performs a computation by applying a sequence of measurements to specific qubits in designated bases. The choice of basis for future measurements often depends on prior measurement outcomes. The final computation result is determined from the classical outcome data of all the measurements. In contrast to the more common gate array model in which computational steps are unitary operations, a large entangled state prior to some final measurements for the output is developed.

There are two principal schemes of MBQC:

- 1) Teleportation quantum computation (TQC) and the
- 2) Cluster state model or one-way quantum computer (1WQC)

Any one-way computation can be made into a quantum circuit by using quantum gates to prepare the resource state. For cluster and graph resource states, this requires only one 2-qubit gate per bond, which is very efficient [9-13].

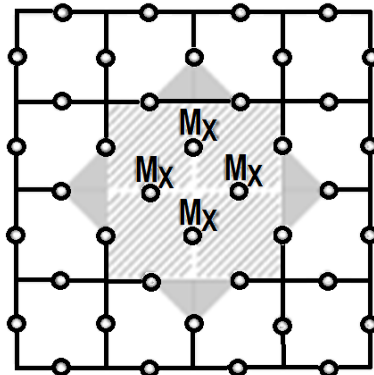


Fig. 1.3. Topological Cluster-State Quantum Computing (CSQC) on a 2D Cluster state surface code with 1° of freedom introduced via the measurement M_x of 4 qubits in the X basis and removal of 5 stabilizers. Note that new 3-term X stabilizers are not necessarily created with positive sign as in the shaded triangles. Redrawn from [14].

The face or region of such faces (shaded squares) is called a smooth defect. The degree of freedom can be phase flipped by any ring of Z-operators encircling the defect and bit flipped by any chain of X operators connecting the defect to a smooth boundary. The qubit inside the defect plays no further role in the computation unless the defect moves.

For the cluster-state model of quantum computation, in which coherent quantum information processing is accomplished via a sequence of single-qubit measurements applied to a fixed quantum state known as a cluster state; it has been proven that the cluster state cannot occur as the exact ground state of any naturally occurring physical system, proving that measurements on any quantum state which is linearly prepared in one dimension can be efficiently simulated on a classical computer, and thus are not candidates for use as a substrate for quantum computation [10,11].

1.2.4 Adiabatic Quantum Computer

Adiabatic quantum computation (AQC) is an alternative to the more common gate model which is based on the Turing approach to

computing. It has been mathematically shown that the adiabatic model and the gate model are equivalent. The gate model approach creates quantum equivalents of digital logic gates and puts these gates together to build a quantum computer; it is a one-way quantum computer using quantum gates. It operates by setting up an initial entangled resource state pertaining to the problem, applies logic gates, then takes a measurement destroying the initial resource state. There is a high amount of error in this method requiring many trials or error correction sequences.

An AQC is based on Quantum annealing (finding the global minimum of a function over a given set of solutions by using quantum fluctuations), a process where computation is decomposed into a slow continuous transformation of an initial Hamiltonian into a final Hamiltonian, where the ground states of the system contain the solution [15].

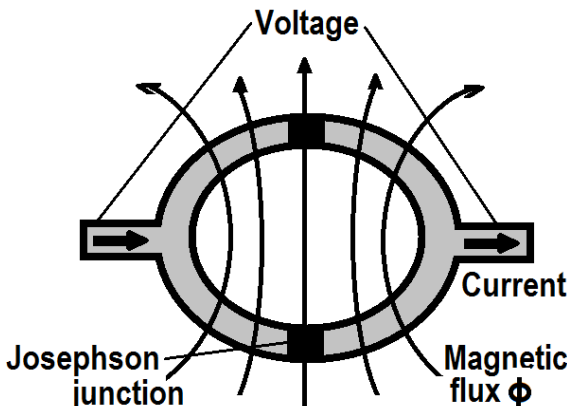


Fig. 1.4. An rf-SQUID with a Josephson junction from a D-Wave device. An array of coupled superconducting flux qubits acts as an artificial Ising spin system with programmable spin-spin couplings and transverse magnetic fields. Josephson junctions are integral elements in SQUID QC as flux qubits and other substrates where phase and charge act as conjugate variables.

A system of connected qubits in SQUID form is prepared with a magnetic field going a certain way. Then the initial state is slowly turned off while slowly turning on the final state. Basically processing a mixed state of initial and final energy, and by the end there will be essentially no initial parts left in the state leaving only the final state. Alternatively, one can start with both states on, with the initial state much stronger than the final part of the state, and then slowly turn off the very large, initial state as shown in

$$H = \sum_i h_i Z_i + \sum_{i < j} J^{ij} Z_i Z_j + \sum_{i < j} K^{ij} X_i X_j, \quad (1.1)$$

where H is the Hamiltonian, (matrix for total energy of the system). The three terms could be grouped into two terms because Z and X refer to the spin matrices; therefore, the initial state is governed by the last term, and the final state is governed by the first two terms. The spin matrices show the change from the X -basis state to the Z -basis state. When preparing the initial system of qubits, they are all put into the X -spin state and then ‘annealed’ to the Z -spin state. Imagine that h and J are tiny compared to K initially. When annealing, K is slowly turned off so that in the finished state, you’re only left with the content of first two terms. This is how the annealing process works; when annealing, you need to be in the ground state. This is why you must move slowly, because if you move too quickly energy is imparted into the system, causing excitations and jumps to higher energy levels causing errors [15].

Researchers have performed the largest protein-folding problem solved to date using a quantum computer. The researchers solved instances of a lattice protein folding model, known as the Miyazawa-Jernigan model, on a D-Wave I quantum computer [16]. The D-Wave Systems QC has a quantum annealing processor, currently increased to 1,000 qubits.

The AQC unit cell array of coupled superconducting flux qubits is designed to solve instances of the classical optimization problem - given a set of local longitudinal fields, $\{h_i\}$ and an interaction matrix, $\{j_{ij}\}$ find the assignment, $s^* = s_1^* s_2^* \dots s_N^*$ that minimizes the objective function $E(s)$, where,

$$E(s) = \sum_{1 \leq i \leq N} h_i s_i + \sum_{1 \leq i < j \leq N} j_{ij} s_i s_j, \quad (1.2)$$

with $|h_i| \leq 1, |j_{ij}| \leq 1$, and $s_i \in \{+1, -1\}$. Finding the optimal s^* is equivalent to finding the ground state of the corresponding classical Ising Hamiltonian,

$$H_p = \sum_{1 \leq i \leq N} h_i \sigma_i^z + \sum_{1 \leq i < j \leq N} j_{ij} \sigma_i^z \sigma_j^z \quad (1.3)$$

where σ_i^z are Pauli matrices acting on the i th spin [16].

Experimentally, the time-dependent quantum Hamiltonian implemented in the superconducting qubit array is given by

$$H(\tau) = A(\tau)H_b + B(\tau)H_b, \quad \tau = t / t_{\text{run}}, \quad (1.4)$$

with, $H_b = -\sum_i \sigma_i^x$ responsible for quantum tunneling among the localized classical states, which correspond to the eigenstates of Hp (computational basis). The time-dependent functions, $A(\tau)$ and $B(\tau)$ are such that $A(0) \gg B(0)$ and $A(1) \ll B(1)$; t_{run} denotes time elapsed between preparation of the initial state and the measurement [16].

1.2.5 The Kane Nuclear Spin QC

The Kane QC is based on an array of phosphorus donor atoms embedded in a silicon lattice is considered a hybrid between quantum dot and NMR QC platforms. The Kane QC utilizes the nuclear spins of the donors and the spins of the donor electrons in the computation. Phosphorus donors are placed in an array with a 20 nm spacing. An insulating oxide layer is grown on top of the silicon. As shown in Fig. 1.5 Metal A-gates are deposited on the oxide above each donor, and J-gates between adjacent donors [17].

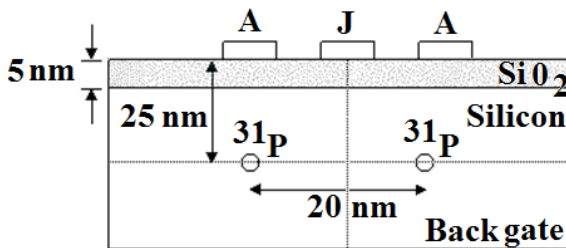


Fig. 1.5. Kane Nuclear Spin QC substrate with $^{31}\text{P}^+$ impurities embedded in ^{28}Si .

The phosphorus, ^{31}P donors and silicon, ^{28}Si substrate are isotopically pure, with nuclear spins of $\frac{1}{2}$ and spin 0 respectively. The nuclear spin of the P donors used to encode qubits has two important advantages;

- 1) The state has an extremely long decoherence time, on the order of 1018 seconds at mK temperatures.
- 2) Qubits can be manipulated by applying an oscillating NMR field.

Theoretically, altering the voltage on the A gates, makes it possible to alter the Larmor frequency (precession of angular momentum about the axis of an applied external magnetic field) of individual donors allowing them to be addressed individually, by bringing specific donors into resonance with the applied oscillating magnetic field [17,18].

Nuclear spins alone will not interact significantly with other nuclear spins 20 nm away. Nuclear spin is useful to perform single-qubit operations, but to make a quantum computer, 2-qubit operations are also required. This is the role of electron spin in this design. Under A-gate control, the spin is transferred from the nucleus to the donor electron. Then, a potential is applied to the J-gate, drawing adjacent donor electrons into a common region, greatly enhancing the interaction between the neighboring spins. By controlling the J-gate voltage, 2-qubit operations are possible [18].

Kane's proposal for readout is to apply an electric field to encourage spin-dependent tunneling of an electron to transform two neutral donors to a D+-D- state, where two electrons orbit the same donor. The charge excess is then detected using a single-electron transistor. This method has two major difficulties. Firstly, the D- state has strong coupling with the environment and hence a short decoherence time. Secondly, it's not clear that the D- state has a sufficiently long lifetime to allow for readout because the electron tunnels into the conduction band. Unlike many quantum computation schemes, the Kane quantum computer is in principle scalable to an arbitrary number of qubits. This is possible because qubits may be individually manipulated by hyperfine electrical means above each impurity [17,18].

1.2.6 QRAM Models of Quantum Computation

Quantum Random Access Machine (QRAM) Models of Quantum Computation have a quantum processor controlled by classical instructions. The processor follows the QRAM model, a quantum memory and a quantum ALU (qALU) Arithmetic and Logical Unit using a reversible control unit [19] containing a group of quantum gates, which are controlled by classical signals. The processor's instructions are written using a quantum assembly (QASM) language. As test cases, several well-known quantum circuits are described using the QASM language and executed by the model. The QRAM model hopes to be integrated with classical components forming a hybrid quantum computer [20].

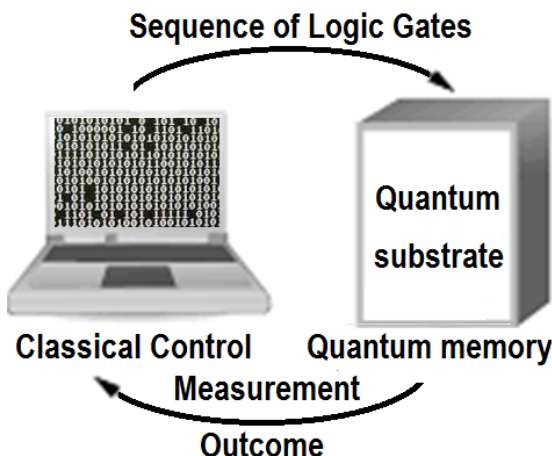


Fig. 1.6. Hybrid QRAM Quantum Computer with classical input.

1.2.7 Electrons-On-Helium Quantum Computers

Electrons-On-Helium Quantum Computers (EOH) are attractive because the scalable electron traps have very long relaxation times, and the highest mobility known in a condensed-matter system [21]. The system of electrons on the surface of superfluid ^4H is made by submerging a system of individually addressed micro-electrodes beneath the helium surface. The large $\sim 1 \mu\text{m}$ interelectron simplifies fabrication of an electrode array. The electrode potential, the high barrier that prevents electrons from penetrating into the helium, and the helium image potential together create a single-electron quantum dot above each electrode. The parameters of the dot can be controlled by the electrode potential [22,23].

The Hamiltonian describing $|2\rangle \rightarrow |1\rangle$ transitions induced by excitations in helium has the form

$$H_i^{(d)} = \sum_n |2\rangle_n \langle 1| \sum_q \hat{V}_q e^{iqr_n} \quad (1.5)$$

where, $|1\rangle_n$ and $|2\rangle_n$ are the states of the n th electron normal to the surface, and \hat{V}_q is the operator depending on the coordinates of helium vibrations, such as phonons or ripplons. The wavelengths of the vibrations involved

in electron scattering are much smaller than the interelectron distance so that each electron has its own thermal bath of helium excitations [22].

As shown in Fig. 1.7, the EOH QC is operated by a constant voltage, V applied to the rings creating a static electric field with voltage valleys that trap electron bubbles along the z-axis. The oscillating voltage, \tilde{V} is applied to opposing rods trapping electrons in the x-y plane.

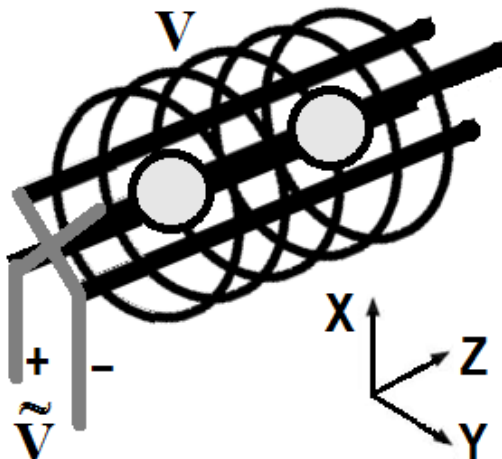


Fig. 1.7. Architecture for electrons on liquid helium QC. The qubit is the electron spin. At each end of the qubit array is a single-electron transistor (SET) detector.

The spin of electrons floating on the surface of liquid ^4H makes excellent qubits because these electrons can be electrostatically held and manipulated like electrons in semiconductor heterostructures, and being in a vacuum the spins on ^4H are less likely to decohere. The spin-orbit interaction is reduced so that moving the qubits with voltages applied to gates has little effect on coherence times which can be expected to exceed 100 s which is enough time for more than 105 operations at 10 mK [23].

The $|0\rangle$ and $|1\rangle$ qubits are assigned the ground and 1st excited Rydberg states of the electrons above the liquid ^4H . An electron can be excited from $|0\rangle$ to $|1\rangle$ with a microwave pulse at frequency, f_R with individual qubits tuned by voltages on the underlying electrodes using the linear Stark effect. Quantum gates are operated by tuning neighboring qubits through mutual resonance generating entangled quantum states in XOR, $\sqrt{\text{swap}}$ or other quantum gates [22,23].

1.2.8 Fullerene-Based ESR Quantum Computer

Endohedral buckyball or Fullerene-based ESR quantum computer qubits are based on the electronic spin of atoms or molecules encased in fullerenes. Atoms can be embedded in a permanent nanoscale molecular scaffolding to form an array. Electron paramagnetic resonance (EPR) or electron spin resonance (ESR) spectroscopy is a technique for manipulating materials with unpaired electrons. The basic concepts of EPR/ESR spectroscopy is similar to nuclear magnetic resonance (NMR), but electron spins are excited instead of the spins of atomic nuclei as in NMR spectroscopy.

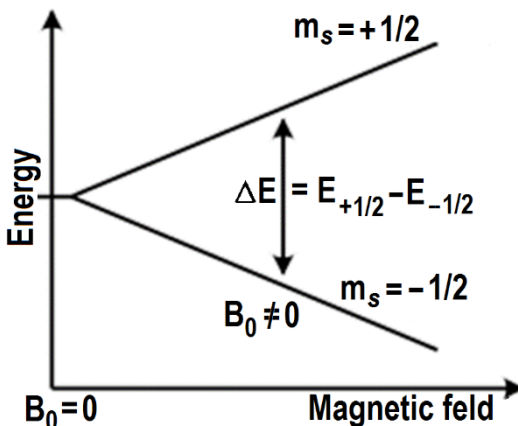


Fig. 1.8. Splitting of the electrons magnetic moment in the presence of an external magnetic field with strength, B_0 .

All electrons have a magnetic moment and spin quantum number, $s=1/2$, with magnetic components $m_s=+(1/2)$ and $m_s=-(1/2)$. In the presence of an external magnetic field with strength, B_0 the electron's magnetic moment aligns itself either parallel, $m_s=-(1/2)$ or antiparallel $m_s=+(1/2)$ to the field with each alignment having a specific energy due to the Zeeman effect, $E=m_s g_e \mu_B B_0$, where g_e is the electron g-factor, $g_e=2.0023$ for the free electron and μ_B is the Bohr magneton [24]. Therefore, the separation between the lower and the upper state is $\Delta E=g_e \mu_B B_0$ for free unpaired electrons implying that the splitting of

the energy levels is directly proportional to the magnetic field strength, as shown in Fig. 1.8.

An unpaired electron can move between the two energy levels by either absorbing or emitting a photon of energy, $\hbar\nu$ such that the resonance condition, $\hbar\nu = \Delta E$ is obeyed. This leads to the fundamental equation of EPR spectroscopy: $\hbar\nu = g_e\mu_B B_0$.

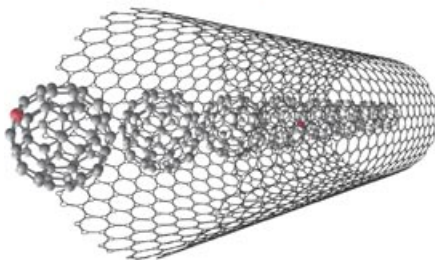


Fig. 1.9. ‘Peapod’ – Carbon nanotube filled with nitrogen doped buckyball fullerenes.

A nitrogen atom is bonded to the center of the fullerene cage with its electron wavefunction extending the cage boundary with a 2% overlap. ‘Peapod’ nanotubes contain fullerenes packed in a pseudo-helical phase. These nanotube ‘Peapods’ could help in the implementation of quantum computing. A pea pod is made up of a tiny carbon nanotube filled with buckyball fullerenes [25].

1.2.9 Superconductor-Based Quantum Computers

There are two main types of Superconductor-Based Quantum Computers under study:

- SQUID-based Superconductor quantum computers with the qubit implemented by the state of small superconducting circuits such as Josephson junctions.
- Superconductor-based quantum computers with qubits implemented by the internal state of near Absolute Zero, mK trapped ions.

1.2.9.1 SQUID-BASED SUPERCONDUCTOR QC

The SQUID quantum annealing QC is summarized briefly in Sect. 1.2.4, Adiabatic Quantum Computers, as the two models are very similar.

Quantum annealing (QA) is a classical randomized algorithm. Meaning, there is no part of QA that necessarily depends on quantum hardware. In classical annealing (CA), temperature is the source of random perturbations that allow the algorithm to explore a problem's solution space. In QA, the temperature is replaced by a term analogous to the quantum tunneling field strength, where quantum tunneling would be carried out directly in hardware.

D-Wave processors are designed to harness a fundamental principle operating in both quantum and classical regimes - the propensity for all physical systems to minimize their free energy. Free energy minimization in a classical system is referred to as annealing. Free energy minimization in a quantum system is referred to as quantum annealing. D-Wave has demonstrated that quantum annealing can hasten the energy minimization process. D-Wave processors compute by piggybacking on quantum annealing which can be operated as a UQC. In this regime of operation, the computational model is referred to as adiabatic quantum computation (AQC), which can be thought of as the long-time limit of quantum annealing [26].

1.2.9.2 TRAPPED ION-BASED SUPERCONDUCTOR QC

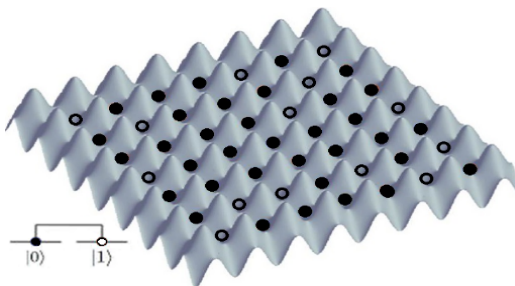


Fig. 1.10. Cold atoms confined in an optical lattice formed by multidimensional optical standing-wave potentials, with solid balls depicted as $|0\rangle$ and clear spheres as $|1\rangle$.

The most successful demonstrations of quantum computing have involved atoms trapped in magnetic fields. One method for building a trapped-ion computer connects ions through common motions of a string of ions electrically levitated between two arrays of electrodes. Because the positively charged particles repel one another, any oscillatory motions imparted to one ion by a laser will oscillate the whole string of ions. Lasers

can also flip an ions' magnetic orientations encoding the data carried by the string [27].

Scaling these systems is difficult because longer strings containing more than ~ 20 ions seem impossible to control because the collective modes of common motion would interfere with one another. Now grid-like-traps (Fig. 1.10) allow ions to be moved from a string in the system's memory to another data processing string. Quantum entanglement of the ions allows data to be transferred from one trap zone to another [26-29].

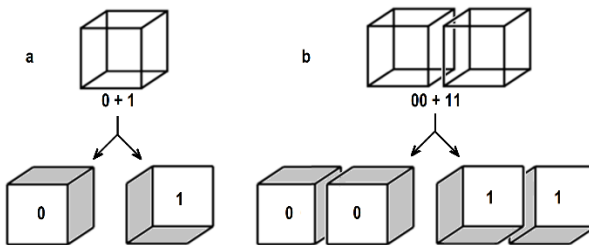


Fig. 1.11. The “ambiguous cube” (a) is like an ion in a superposition state—a measurement of the ion will lock it into one of two definite states (0 or 1). When two ions are in an entangled superposition (b), a measurement will force both ions into the same state (either 0 or 1) even though there is no physical connection between them. Redrawn from [30].

It should be easy to scale trapped ions to large numbers of qubits by merely connecting several types of quantum logic gates made from trapped ions; and if the qubits are encoded with multiple ions, the system should be fault tolerant. In this manner, Wineland suggests “*a useful trapped-ion quantum computer would most likely entail the storage and manipulation of at least thousands of ions, trapped in complex arrays of electrodes on microscopic chips*”. Wineland’s team created a 4-qubit quantum computer by entangling four ionized beryllium atoms in an em-trap. After linearly confining the ions, they were laser cooled to a few mK and their spin states synchronized. Finally, a laser was used to entangle the particles, creating a superposition of both spin-up and spin-down states simultaneously for all four ions. Wineland goes on to say:

‘Firstly, a UQC requires reliable memory where decoherence will not occur before the data is processed and measured. Trapped ions have been shown to have coherence times over 10 minutes long’.

‘Secondly, the ability to manipulate individual qubits is essential. Oscillating magnetic fields applied for a specified duration, can be used to flip a trapped ion qubits magnetic orientation. Currently, the small

distances between trapped ions (millionths of a meter), make it difficult to localize the oscillating magnetic fields to an individual ion' [30].

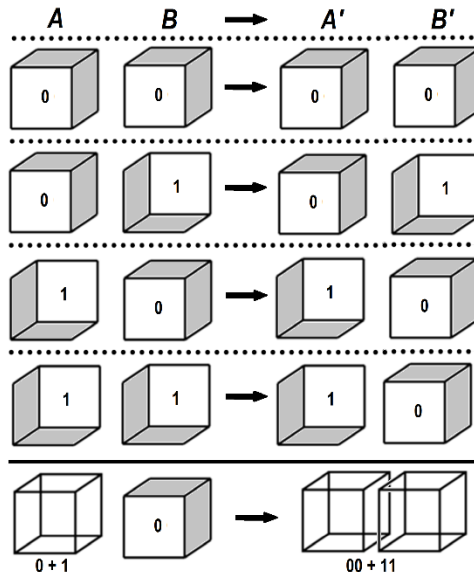


Fig. 1.12. Trapped ion truth table from ambiguous cubes. A trapped-ion computer would rely on logic gates such as the CNOT, which consists of two ions, A and B . The truth table shows that if A (control bit) has a value of 0, the gate leaves B unchanged. But if A is 1, the gate flips B , changing its value from 0 to 1, and vice versa. And if A is in a superposition state of 0 and 1, the gate puts the two ions in an entangled superposition state identical to the one in Fig. 1.11. Redrawn from [30].

Trapped atom qubits can also be measured with nearly 100% efficiency through the use of state dependent fluorescence detection. Trapped atomic ions are particularly attractive quantum computer architectures, because the individual charged atoms can be confined in free space to nanometer precision, and nearby ions interact strongly through their mutual Coulomb repulsion. A collection of atomic ions can be confined with appropriate em-fields from nearby electrodes, forming a 3D harmonic confinement potential, as depicted in Fig. 1.10. When the ions are laser cooled to a center of the trap, the balance between the confinement and the Coulomb repulsion forms a stationary atomic crystal. The most typical geometry is a 1D linear atomic crystal, where one dimension is made significantly weaker than the other two. In such a linear trap, the collective motion of the ion chain can be described accurately by quantized normal modes of

harmonic oscillation, and these modes can couple the individual ions to form entangled states and a variety of quantum gates [29-31].

1.2.10. Diamond Based Quantum Computers

Diamond-based quantum computers are being realized by qubits with an electronic or the nuclear spin of nitrogen-vacancy centers in synthetic diamond crystals. Among solid-state systems, the nitrogen-vacancy (NV) in diamond is found to have an excellent optically addressable memory with satisfactory electron spin coherence times. Recent efforts have demonstrated quantum entanglement and teleportation between two NV-memories, but as true for scaling virtually any proposed QC substrate to larger networks, NV diamond qubits will require more efficient spin-photon interfaces such as optical resonators. Situating nitrogen atoms next to gaps in a diamond's crystal lattice produces 'nitrogen vacancies', which enable optical control of the magnetic orientation (spin) of individual electrons and atomic nuclei.

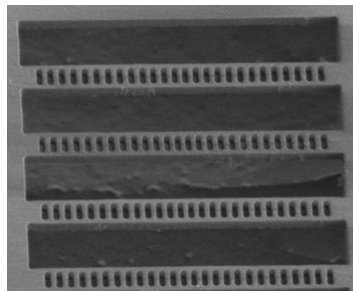


Fig. 1.13. Nitrogen-vacancy (NV) diamond qubit substrate. The NV consists of a substitutional nitrogen atom adjacent to a vacancy in the diamond lattice. The diamond photonic cavities are integrated on a Si substrate with metallic strip lines for coherent spin control. They are optically addressed using a confocal setup with 532 nm CW excitation and photoluminescence collected > 630 nm ladder-like structure etched into diamond. The gaps between the ladder's 'rungs' act like a mirror, temporarily trapping light particles emitted at the ladder's center. Adapted from [32].

Among all crystals, diamond is particularly good for capturing an atom, because the diamond nuclei are essentially free of magnetic dipoles, which can cause noise on the electron spin. Diamond NV spin superpositions have been found to last almost a second. But in order to communicate with each other, NV qubits need to be able to transfer information via photons, requiring the vacancy to be positioned inside an optical resonator. As

shown in Fig. 1.13 a Diamond NV device consists of a ladder-like diamond structure with a NV at its center suspended horizontally above a silicon substrate.

Shining light perpendicularly onto the ladder kicks an NV electron into a higher energy state. When it drops back to ground, it releases the excess energy as a photon. The gaps in the diamond structure - spaces between rungs in the ladder, act as a photonic crystal, confining the photon so that it bounces back and forth across the vacancy thousands of times. When the photon finally emerges, it has a high likelihood of traveling along the axis of the ladder, so that it can be guided into an optical fiber [32].

1.2.11. *Quantum Dot Quantum Computer*

A quantum dot (QD) is a type of nanoscale atomic/molecular structure or nanocrystal made of silicon and semiconductor materials of which there are at least 200 kinds. Generally, a QD is any nanocrystalline material which tightly confines its excitons in all three spatial directions. A QD can be designed as a single qubit. There are numerous methods for utilizing quantum dots in quantum information processing; and QD technology is among the more promising candidates being studied for use in solid-state quantum computation.

In semiconductors, thermal energy is sufficient to cause a small number of electrons to escape from the valence bonds between the atoms (valence band); allowing them to orbit in the higher energy conduction band instead where they are relatively free. Gaps in the valence band are called holes. The hole within an exciton is called the Bohr radius of the exciton; and Excitons are coupled electron-hole pairs via a Coulomb force.

A significant factor for using QDs for quantum information processing is that QDs can have a radius close to or smaller than the Bohr radius value, which in a typical semiconductor is a few nanometers. This is the scenario where a particle reveals its specific quantum mechanical properties:

“In bulk semiconductors, the exciton can move freely in all directions. When the length of a semiconductor is reduced to the same order as the exciton radius, i.e., to a few nanometers, quantum confinement effect occurs and the exciton properties are modified. Depending on the dimension of the confinement, three kinds of confined structures are defined: quantum well (sometimes termed QW), quantum wire (QWR) and quantum dot (QD). In a QW, the material size is reduced only in one direction and the exciton can move freely in other two directions. In a QWR, the material size is reduced in two directions and the exciton can move freely in one direction only. In a QD, the material size is reduced in all directions and the exciton cannot move freely in any direction” [33].

By applying small voltages to the leads, the flow of electrons through the quantum dot can be controlled and thereby precise measurements of the spin and other properties therein can be made. With several entangled quantum dots, or qubits, plus a way of performing operations, quantum calculations and the quantum computers that would perform them might be possible.

The two main types of QD quantum computing being studied are:

- Spin-based Quantum dot computer, such as the Loss-Di Vincenzo quantum computer where the qubit occurs as the spin states of trapped electrons [34-36].
- Spatial-based Quantum dot computer, where the qubit occurs from the position of electrons in double quantum dot. QC researchers have been focusing on QDs formed in GaAs heterostructures, nanowire-based QDs, and self-assembled QDs [37].

In Fig. 1.14 a gallium arsenide semiconductor is coated with plastic and the nanoscale lines are cut into the plastic with a beam of electrons. Then the lines were filled with metal and the plastic dissolved, leaving lines ~ 50 nanometers wide (5-10 atoms). The quantum dots (center of the image) are pools of $\sim 20\text{-}40$ electrons. Each dot is ~ 180 nanometers in diameter. The modulated Swap operation is achieved by applying a pulsed gate voltage between the dots, making the exchange constant in the Hamiltonian time-dependent:

$$H_s(t) = J(t) \vec{S}_L \cdot \vec{S}_R. \quad (1.6)$$

which is valid only if the level spacing in the quantum-dot is much greater than kT , the pulse time scale, τ_s is greater than $\hbar / \Delta E$, so there is no time for transitions to higher orbital levels to happen and also the decoherence time Γ^{-1} is longer than τ_s [37].

According to Jeong and his team, the QD are defined by ten independently tunable QD gates on a GaAs/AlGaAs heterostructure containing a 2D electron gas (2 °K) located 80 nm below the surface. The low temperature sheet electron density and mobility are $n = 3.8 \times 10^{11} \text{ cm}^{-2}$ with $\mu = 9 \times 10^5 \text{ cm}^2/\text{Vs}$, respectively. The lithographic dot size is 180 nm in diameter and each dot contains about 40 electrons. To reduce unnecessary degrees of freedom in controlling the double dot, gates sitting on the opposite side are connected together, giving a total of five pairs of

controllable gates. Gate pair V1 and V5 are used to set tunneling barriers, while the V3 sets the inter-dot tunnel coupling. V2 and V4 control the number of electrons and energy levels in each dot separately [37].

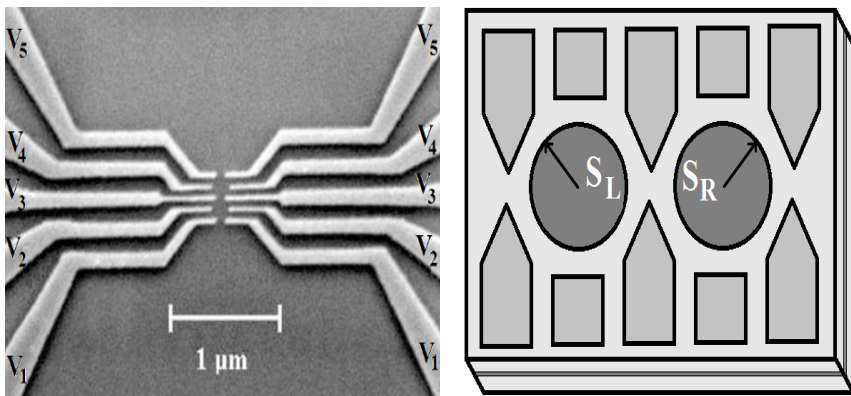


Fig. 1.14. a) Depicting a double quantum dot. Each S_L or S_R electron spin defines one 2-level system (qubit) in the ‘Loss-Di Vincenzo Model’. The narrow gate between the two dots modulates the spin coupling, allowing swap operations. b) Physical realization of the quantum dots utilizing electron beam lithography. Figs. Redrawn from [37].

1.2.12. Transistor-Based Quantum Computer

A Transistor-based quantum computer is a string quantum computer with an entrainment of positive holes using an electrostatic trap. A microwave field is used to gain control over an electron bound to a single phosphorous atom implanted next to a specially-designed silicon transistor, a device made in a manner similar to making common silicon computer chips.

According to team member Morello: “*This is the quantum equivalent of typing a number on your keyboard. This has never been done before in silicon, a material that offers the advantage of being well understood scientifically and more easily adopted by industry. Our technology is fundamentally the same as is already being used in countless everyday electronic devices, and that's a trillion-dollar industry.*”

Veldhorst’s team presents a 2-qubit logic gate, which uses a single spin in isotopically enriched silicon and is realized by performing single- and 2-qubit operations in a QD system using the exchange interaction, as envisaged in the Loss-Di Vincenzo proposal discussed briefly in 1.2.11, the Quantum Dot Quantum Computer [34,35]. He realizes CNOT gates by

controlled-phase operations combined with single-qubit operations. Direct gate-voltage control provides single-qubit addressability, together with a switchable exchange interaction that is used in the 2-qubit controlled-phase gate. By independently reading out both qubits, the transistor-based QC can measure anti-correlations in the 2-spin probabilities of the CNOT gate [38].

1.2.13. Molecular Magnet Quantum Computer

A Molecular Magnet Quantum Computer (MMQC) is an additional form of the Loss-Di Vincenzo proposal [34-35]. The potential of molecular magnets as the building blocks of a UQC is the attractive simplification in the control procedure for the quantum gates provided by many-spin systems coming from the high symmetry shown to lead to a relatively simple way to address spin degrees of freedom in molecular magnets. The advantage of an anisotropic effective spin interaction in QC memory applications is demonstrated by using Grover's quantum search algorithm in a generic easy-axis molecular magnet. Electric control of spin-spin coupling has been shown to enable 2-qubit quantum gates in polyoxometalates [39,40].

It is of interest to briefly summarize the Leuenberger & Loss [40] proposal for what they call 'a feasible implementation of Grover's factoring algorithm' utilizing ^{8}Fe and ^{12}Mn as molecular magnets. The initial state, $|\psi_0\rangle = |s\rangle$ is prepared by applying a strong field in the z direction. Then field brought near zero (to bias δH_z) so that all $|m\rangle$ -states become localized.

Once a state is marked and amplified (decoded) readout is performed by standard pulsed ESR spectroscopy. Then the magnet is irradiated with a single pulse of duration, T with frequencies, $\omega_{m-1,m}$, with $m = s - 2, \dots, m_0$, inducing transitions of 1st order amplitudes, $S_{m-1,m}^{(1)}$. To illustrate, Leuenberger & Loss assume state, $|7\rangle$ is populated, from which stimulated emission can be observed in the transition from $|7\rangle$ to $|8\rangle$ at frequency, $\omega = \omega_{6,7}$ uniquely identifying the marked level. They go on to say generally that, if states, $|m_1\rangle, |m_2\rangle, \dots, |m_k\rangle$, where $1 \leq k \leq n$, are marked, the following absorption/emission intensity is measured:

$$I_{s-2}^{m_0} = \sum_{i=1}^k \left(\left| S_{m_i-1, m_i}^{(1)} \right|^2 + \left| S_{m_i+1, m_i}^{(1)} \right|^2 \right). \quad (1.7)$$

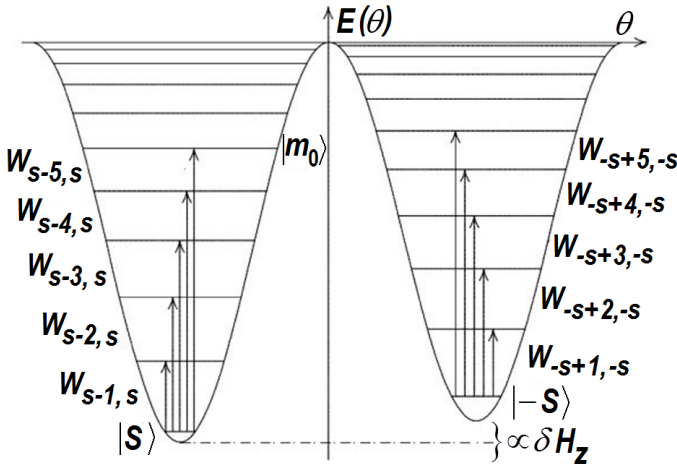


Fig. 1.15. High symmetry properties of single-molecule magnets for QC. Shows the double well potential of the spin due to magnetic anisotropies in ^{12}Mn with the initial state, $|\psi_0\rangle = |s\rangle$. Arrows depict transitions between spin eigenstates driven by the external magnetic field H . Figure adapted from [40].

The spectrum identifies all marked states clearly. In this manner implementing the entire Grover algorithm (input, decoding, read-out) is achieved by three pulses of duration, T with $\tau_d > T > \omega_0^{-1} > \omega_m^{-1}, \omega_{m,m\pm 1}^{-1}$, giving a clock speed of ~ 10 GHz for Mn_{12} such that the complete process takes only 10^{-10} s [40].

1.2.14. Bose–Einstein Condensate-Based Quantum Computer

In 1924 Einstein pointed out that unlimited bosons could condense into a single ground state [41,42]. Recently QC based on Bose–Einstein condensation (BEC), the state of matter composed of a dilute gas of bosons cooled close to absolute zero, has been proposed.

Recent progress in solid-state quantum computing using superconducting qubits on Cooper pairs of charged electrons met limitations due to decoherence effects caused by the strong Coulomb interaction of the superconducting qubit with the environment. To solve the problem,

Andrianov and Moiseev have proposed a solution by trying another BEC setup utilizing uncharged long-lived magnons, where the magnon BEC qubit can be realized due to a magnon blockade isolating pairs of the magnon condensate energy levels in mesoscopic and nanoscopic ferromagnetic dielectric samples [43].

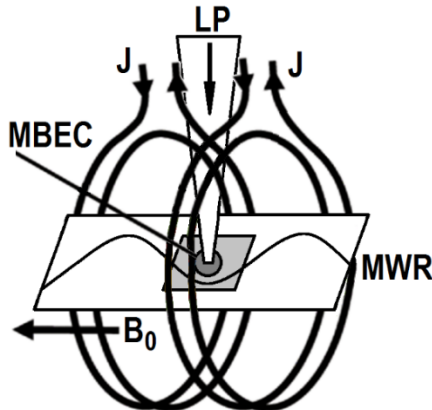


Fig. 1.16. Layout of the single qubit gate, Magnon Bose-Einstein Condensate (MBEC), laser pumping (LP), microwave resonator (MWR), current in the magnetic coil, J and the magnetic field, B_0 . The MBEC is excited by laser pulse. Qubit rotation is achieved by the interaction with a standing microwave field in a high-quality resonator. Redrawn from [43].

Andrianov and Moiseev want to demonstrate single-qubit gates by operating quantum transitions between these states in the external microwave field. They are also studying implementation of the 2-qubit gate by using the interaction between the MBEC qubits due to exchange of virtual photons in a microwave cavity. They hope to achieve conditions for long-lived MBEC qubits, a scalable architecture, and utility of the promising advantages of the multi-qubit QC the MBEC qubit offers [43].

Hecht presents a different scheme for BEC quantum computation utilizing atomic many-body states. The system she has in mind consists of a 2-species interacting BEC, which, under the right conditions, behaves like a robust 2-level system protected by an energy gap from higher excited levels. The two states can be used to encode a qubit. Hecht claims to show how to create a universal set of quantum gates by inducing energy shifts on the atomic levels, by changing the Raman coupling between atomic states and allowing tunneling between pairs of the BEC condensates. The scheme is limited by particle losses as a key source of decoherence, but Hecht suggests that for small numbers of particles and

weak Feshbach resonance, maximally entangled states between two qubits can be produced [43,44].

1.2.15. Rare-Earth-Metal-Ion-Doped Inorganic Crystal QC

Rare-earth-metal-ion-doped inorganic crystal based quantum computers are being developed to use the internal electronic state of dopants put in optical fibers. The aim of initial experiments towards constructing simple quantum gates in such solid state materials using these specially tailored crystals, is to select a subset of randomly distributed ions in the ion-doped material, ones which have the interaction necessary to control each other and can therefore be used for quantum logic operations. Experimental results demonstrate that part of an inhomogeneously broadened absorption line can be selected as a qubit and that a subset of ions in the material can control the resonance frequency of other ions. This is the key to opening the way for the construction of quantum gates in rare-earth-ion doped crystals.

Rare-earth-ion doped crystals have several attractive features for implementing quantum gates. Because of the existence of a partially filled inner shell (4f) that is shielded from the environment by outer electrons, they have optical transitions with very narrow line-widths. For Eu doped into Y_2SiO_5 for example, some transitions have homogeneous line-widths of less than 1 kHz. The narrow line-width makes it possible to coherently manipulate the ions with long sequences of laser pulses. Most rare-earths have a hyperfine splitting of the ground state, due to nuclear quadrupole interactions. Any nucleus with more than one unpaired nuclear particle (protons or neutrons) will have a charge distribution which results in an electric quadrupole moment. NMR of the anisotropy of the magnetic hyperfine and nuclear quadrupole interactions in rare-earth orthochromites in the vicinity of the order-order type magnetic phase transition, with GdCrO_3 , as the rare-earth example, show that the nuclear quadrupole interactions, along with the magnetic anisotropies of the hyperfine interactions, contribute to the splitting of the NMR lines of ^{53}Cr in the transition region [45].

The relaxation between different hyperfine levels is very slow and lifetimes are as long as hours or days. Measurements of the dephasing time between the hyperfine levels are lacking for many materials, but it is at least of the order of milliseconds for some combinations of dopants and hosts. When doped into inorganic host crystals, the differently located ions experience shifts of their optical absorption frequencies because of imperfections in the crystal host lattice. Because of the differences

between different positions in the lattice, the shifts will be different for different ions, creating an inhomogeneous broadening of the optical transition. The broadening can be several GHz, making it possible to address more than 10^6 different spectrally distinct channels. [46]

Another rare-earth-ion doped crystal QC research team headed by Walther is studying a high fidelity readout scheme for a ‘single instance’ approach to quantum computing in rare-earth-ion-doped crystals. The scheme is based on using a different species of qubit and readout ions; Walther shows that by allowing the closest qubit ion to act as a readout buffer, readout error can be reduced by more than an order of magnitude. The scheme is shown to be robust against certain experimental variations, such as varying detection efficiencies. Walther’s team has found a way to use the scheme to predict the expected quantum fidelity of a CNOT gate in a variety of solid state systems that he predicts are scalable.

By monitoring the cavity-enhanced fluorescence from one rare-earth ion using another long-lived rare-earth ion species as a buffer stage that can be repeatedly cycled, several buffer stages can be concatenated to yield a very long effective detection times reaching $\varepsilon = 10^{-3}$ for a wide variety of collection efficiencies and background levels. The team then used this result, together with known error sources, to obtain expected fidelities for a CNOT gate of 99 % and for larger GHz states remaining above 92 % for up to 10 qubits. One of the present limitations of his assumptions is that the expected increase in performance for qubit rotations when switching from Pr to Eu has not been fully experimentally verified as of yet [47,48].

1.2.16. Linear Optical Quantum Computer (LOQC)

Linear optical quantum computer (LOQC) development attempts to realize qubits by processing different modes of light as quantum states (photonic qubits) through linear elements like mirrors, beam splitters and phase shifters, which is a form of the quantum circuit model as in 1.2.2 [8]. Optical quantum technologies are highly sought for quantum information processing (QIP) because they link QC with quantum communications in the same framework.

Up to $N \times N$ unitary matrix $U(N)$ operations can be realized using just mirrors, beam splitters and phase shifters which preserve the quantum state of light; but the intrinsic challenge as well-known, is that photons only interact minimally. Initially this problem was partly solved by adding nonlinearity via the Kerr effect to LOQC; this allowed operations such as

the single-photon CNOT gate. This was followed by discovery of the KLM protocol by Knill, Laflamme and Milburn that uses linear optical elements to promote nonlinear operations [49].

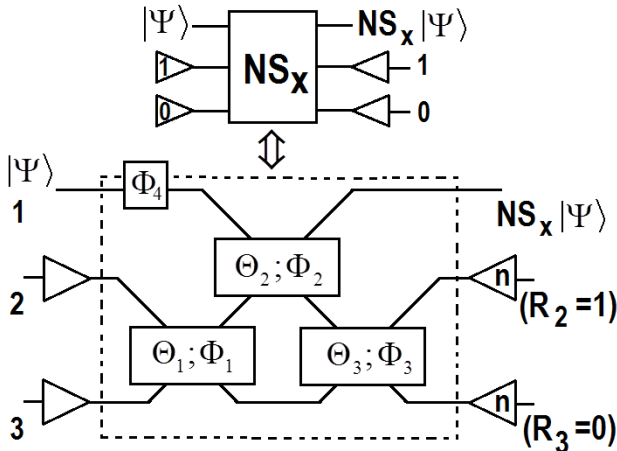


Fig. 1.17. Linear optics implementation of Nondeterministic Sign-Flip gate (NS-gate). The elements framed in the box (dashed border) is the linear optics implementation with three beam splitters and one phase shifter. Modes 2 and 3 are ancilla modes. Adapted from [49].

Photon states for a 2-qubit representation could be written as $|01\rangle_{\alpha\beta} \equiv |0\rangle_\alpha |1\rangle_\beta$ for two orthogonal photon polarization modes prepared by optical parametric down-conversion which emits EPR correlated photons. Linear optics in LOQC is supported by a complete set of $SU(2)$ operators. If a unitary matrix is correlated with an optical beam splitter, $B_{\theta,\phi}$, the 2×2 matrix is

$$U(B_{\theta,\phi}) = \begin{bmatrix} \cos \theta & -e^{-i\phi} \sin \theta \\ e^{-i\phi} \sin \theta & \cos \theta \end{bmatrix}; \quad (1.8)$$

the reflection and transmission amplitudes determine θ and ϕ [49-51].

A nonlinear sign-flip gate implements the transform:

$$\text{NS}: \alpha_0 |0\rangle + \alpha_1 |1\rangle + \alpha_2 |2\rangle \rightarrow \alpha_0 |0\rangle + \alpha_1 |1\rangle - \alpha_2 |2\rangle, \quad (1.9)$$

which is the basis, along with ancilla, for implementing the CNOT-gate [52]. The nonlinear sign gate can be implemented non-deterministically by three beam splitters, two photo-detectors, and one ancilla photon. The implementation of conditional sign flip gate is then made by the combination of the nonlinear sign gate and the physics of Hong-Ou-Mandel (HOM) interferometer. For an arbitrary two qubits [53]

$$\begin{aligned} |\mathcal{Q}_1\rangle &= \alpha_0 |0\rangle_L + \alpha_1 |1\rangle_L = \alpha_0 |0\rangle_1 |1\rangle_2 + \alpha_1 |1\rangle_1 |0\rangle_2, \\ |\mathcal{Q}_2\rangle &= \alpha'_0 |0\rangle_L + \alpha'_1 |1\rangle_L = \alpha'_0 |0\rangle_3 |0\rangle_4 + \alpha'_1 |1\rangle_3 |0\rangle_4. \end{aligned} \quad (1.10)$$

The NS-gate in Fig. 1.17 gives a nonlinear phase shift on one mode conditioned on two ancilla modes. The output is accepted only if there is one photon in mode 2 and zero photons in mode 3 detected, where the ancilla modes 2 and 3 are prepared as the $|10\rangle_{2,3}$ state [49, 53-55].

1.2.17. Optical Lattice Based Quantum Computing (OLQC)

In an Optical Lattice Based Quantum Computer (OLQC) qubits are implemented by internal states of neutral atoms such as, ${}^6\text{Li}$ and ${}^{133}\text{Cs}$ trapped in an optical lattice as shown in Fig. 1.18.

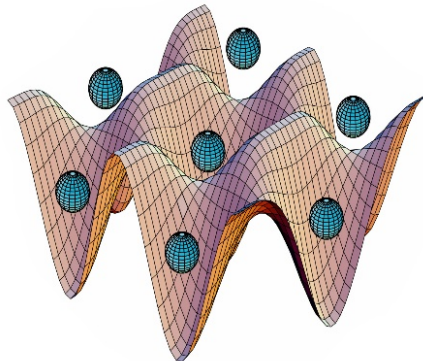


Fig. 1.18. Optical lattice of qubits trapped potential minima by the Stark shift.

Optical lattices are often formed by counterpropagating laser beams, interfering to form spatially periodic polarization patterns. The resulting periodic potential traps neutral atoms by the Stark shift (shifting and splitting of spectral lines of atoms and molecules due to presence of an

external electric field). The neutral atoms are cooled and congregate in locations of potential minima where the trapped atoms resemble a crystal lattice [56-58].

One novel scheme uses Li-Cs molecular states to entangle ultracold ^6Li and ^{133}Cs atoms held in independent optical lattices. The ^6Li atoms act as the qubits, and the ^{133}Cs atoms serve as messenger qubits aiding in q-gate operations to mediate entanglement between distant qubit atoms. The separated species can be overlapped by translating the lattices. When the ^{133}Cs messenger and ^6Li qubit atoms are overlapped, targeted single spin operations and entangling operations would be performed by coupling the atomic states to a molecular state with rf-pulses. By controlling frequency and duration of the rf-pulses, entanglement can either be created or swapped between a qubit messenger pair [59].

1.2.18. Cavity Quantum Electrodynamics Quantum Computing

In Cavity Quantum Electrodynamics Quantum Computing (CQEDQC) a qubit is based on the internal state of trapped atoms coupled to high-finesse cavities. Following Burell, an essential component of CQEDQC is the Fabry-Perot partially silvered mirror cavity, which partially reflects and transmits incident light E_a and E_b , which has the effect of producing output fields $E_{a'}$ and $E_{b'}$, which are related by the unitary transformation:

$$\begin{bmatrix} E_{a'} \\ E_{b'} \end{bmatrix} = \begin{bmatrix} \sqrt{R} & \sqrt{1-R} \\ \sqrt{1-R} & -\sqrt{R} \end{bmatrix} \begin{bmatrix} E_a \\ E_b \end{bmatrix} \quad (1.11)$$

where R is the reflectivity of the mirror. A Fabry-Perot (FP) cavity is made from two plane parallel mirrors of reactivities R_1 and R_2 , incident upon which is light from outside the cavity E_{int} . Inside the cavity, light bounces back and forth between the two mirrors acquiring a phase shift $e^{i\phi}$ on each trip. The internal cavity field is

$$E_{\text{cav}} = \sum_k E_k = \frac{\sqrt{1-R} E_{\text{in}}}{1 + e^{i\phi} \sqrt{R_1 R_2}} \quad (1.12)$$

One of the most important things about the Fabry Perot cavity for purposes of CQEDQC is the power in the internal cavity field mode as a function of the power and frequency of the input field,

$$\frac{P_{\text{cav}}}{P_{\text{in}}} = \left| \frac{E_{\text{cav}}}{E_{\text{in}}} \right|^2 = \frac{1 - R_1}{\left| 1 + e^{i\phi} \sqrt{R_1 R_2} \right|^2} \quad (1.13)$$

Frequency selectivity arises because of constructive and destructive interference between the cavity mode and the reflected light front. Another indispensable feature is that on resonance, the cavity field achieves a maximum which is approximately $(1 - R)^{-1}$ times the incident field [60].

An optical CQEDQC could be almost entirely comprised of optical interferometers. The quantum information would be encoded in both the photon number states and the photon phase. The Interferometers would perform the switching function between the two representations. Stability is a major issue, because the relatively short scale of the de Broglie wavelengths of the qubits would make stable interferometers a challenge to construct [60].

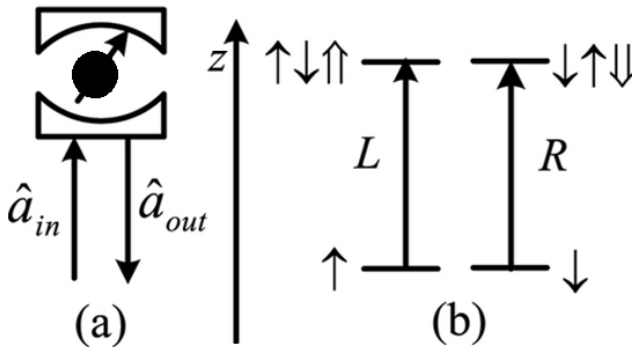


Fig. 1.19. Schematic CQED dipole spin-dependent transitions with circularly polarized photons for utility in CQEDQC modeling. a) A charged quantum dot inside a 1-side micropillar-microcavity interacting with circularly polarized photons, where \hat{a}_{in} and \hat{a}_{out} are the input and output field operators of the waveguide, respectively. (b) Optical selection rules by the Pauli exclusion principle. L and R denote left and right circular polarization respectively, \uparrow and \downarrow represent spins of excess electrons and $\uparrow\downarrow\uparrow\uparrow$ and $\downarrow\downarrow\downarrow\downarrow$ negatively charged excitons. Figure redrawn from [61].

1.2.19. Nuclear Magnetic Resonance (NMR) Quantum Computing

Nuclear Magnetic Resonance Quantum Computing (NMRQC) is among the 1st and most mature technologies for implementing quantum

computation. It utilizes the motion of spins of nuclei in a variety of molecules such as the hydrogen and the carbon nuclei of chloroform, manipulated by rf-pulses. The spin-lattice (T_1) and spin-spin (T_2) relaxation processes in NMR are key factors in the ability to implement NMRQC quantum algorithms. NMRQC has taken two forms:

- Liquid-state NMRQC on molecules in solution with the qubit provided by nuclear spins within the dissolved molecule [62].
- Solid-state NMR Kane quantum computers with qubits realized by the nuclear spin state of phosphorus donors in silicon [17].

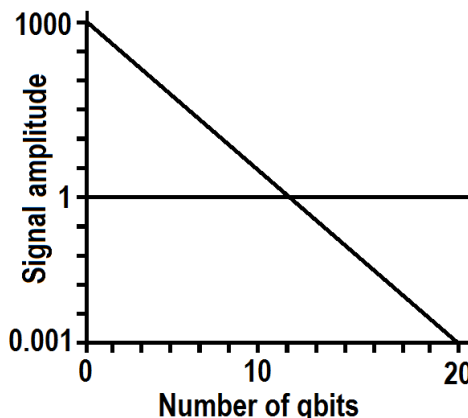


Fig. 1.20. Signal amplitude loss in NMRCC due to preparation of pure states as a function of the size of the quantum register, causing NMR QC to be difficult beyond a few qubits.

1.2.19.1 LIQUID-STATE NMRQC

NMR differs from other implementations of QC in that it uses an ensemble of systems, in this case molecules. The ensemble is initialized to be the thermal equilibrium state as given by the density matrix:

$$\rho = \frac{e^{-\beta H}}{\text{Tr}(e^{-\beta H})}, \quad (1.14)$$

where H is the Hamiltonian matrix for a single molecule with $\beta = 1/kT$, k Boltzman's constant and T the temperature. Ensemble operations are performed through rf-pulses applied orthogonally to a strong, static field, created by a large NMR magnet [62].

It is very difficult to prepare NMRQC systems in pure spin states because of the tiny energy gap between nuclear spin states. This seriously challenges the scalability of NMRQC because the procedure for preparing the required pseudo-pure states averages all the populations but one. As long as the spin system can be described by the high temperature approximation, the population of an individual spin state is inversely proportional to the number of states. But this scenario decreases as 2^{-N} with an increase in the number of spins, N . The detectable signal size therefore limits the possible number of spins to be used in NMR quantum information processors. The reduction of sensitivity associated with the preparation of pseudo-pure states can be avoided by using algorithms that do not require pure states to work with [63].

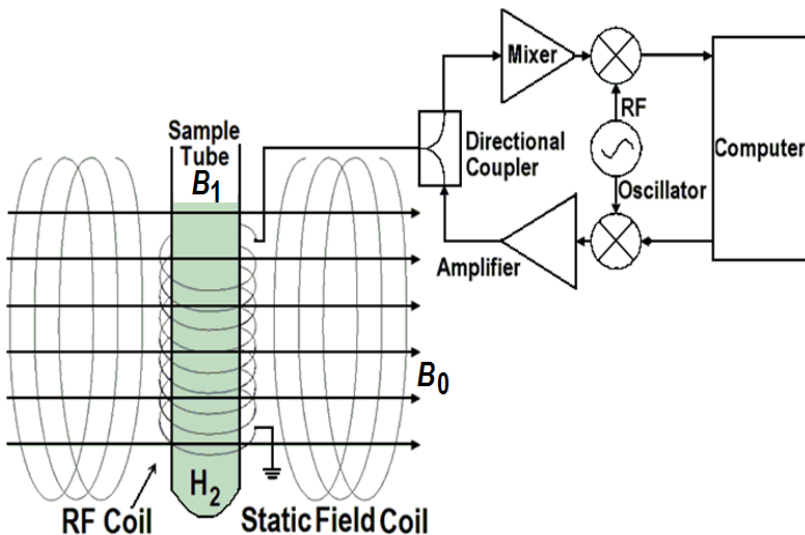


Fig. 1.21. Experimental set up for Liquid-state NMRQC on molecules in solution with the qubit provided by nuclear spins within the dissolved molecule. For a time, NMRQC was very appealing leading model for QC research, but as shown in Fig. 1.20 severe tactical problems have removed it from the limelight until these problems are solved.

It has also been shown that liquid state ensemble NMRQC do not possess quantum entanglement as required for quantum information processing; thus it appears that NMRQC are only classical simulations of a QC. Quantum ensembles represent possible states of a mechanical system of particles that are maintained thermodynamically with a reservoir. The system is open in the sense that it can exchange energy and particles with a reservoir, so that various possible states of the system can

differ in both their total energy and total number of particles. The system's volume, shape, and other external coordinates are kept the same in all possible states of the system [64].

1.2.19.2 SOLID-STATE NMRQC

For solid-state NMRQC see Sect. 1.2.5, the brief review of Kane Nuclear Spin QC where:

- 1) The state has an extremely long decoherence time, on the order of 10^{18} seconds at mK temperatures.
- 2) Qubits can be manipulated by applying an oscillating NMR field [17].

1.2.20. *Topological Quantum Computing (TQC)*

Topological Quantum Computing (TQC) is based on the braiding of anyons in a 2D lattice at cryogenic temperatures near absolute zero. TQC is among the most promising considerations for Bulk UQC; and the scenario that Microsoft has placed it's bet on [65]. Anyons are 2D quasiparticles that are neither Bosons or Fermions operating with the Fractional quantum Hall effect. Common substrates are doped GaAs, Pb or Si, InSb and InAs semiconducting nanowires some of which support Majorana Zero Modes (MZM). Non-Abelian anyons are the key requirement for the anyonic model of TQC, but their existence has not yet been experimentally confirmed. But recent experimental work following theoretical predictions, has shown signatures consistent with the existence of Majorana modes localized at the ends of semiconductor nanowires in the presence of a superconducting proximity effect [66].

The topological braiding of these anyonic non-Abelian fractional quantum Hall effect quasiparticle Majorana fermions provides a high degree of error protection from decoherence by interaction with the environment (the braid state has remained experimentally inaccessible). The actual TQC is done by the edge states of a fractional quantum Hall effect. When anyons are braided the quantum information which is stored in the state of the system is impervious to small errors in the trajectories. Braiding acts as a matrix on a degenerate space of states. The relevant quasiparticle in the Moore-Read state is a 'Majorana fermion' which is its own antiparticle, 'half' of a normal fermion. The effect of the exchange on the ground state need not square to 1. 'Anyon' statistics: the effect of an exchange is neither +1 (bosons) or -1 (fermions), but a phase [67].

Freedman, Kitaev, Larsen, & Wang (FKLW) found that a conventional QC device, with an error-free operation of its logic circuits, gives a solution with an absolute level of accuracy, whereas a FKLW device with flawless operation will give the solution with only finite accuracy; but any level of precision for a readout can be obtained by adding more anyon braid twists (logic circuits) to the TQC, in a simple linear relationship. In other words, a reasonable increase in elements (braid twists) can achieve a high degree of accuracy in the answer [68]. Note that this solution can be considered the same as applying the Quantum Zeno Effect (QZE) to Interaction Free Measurement (IFM) as discussed in detail in Chap. 7.

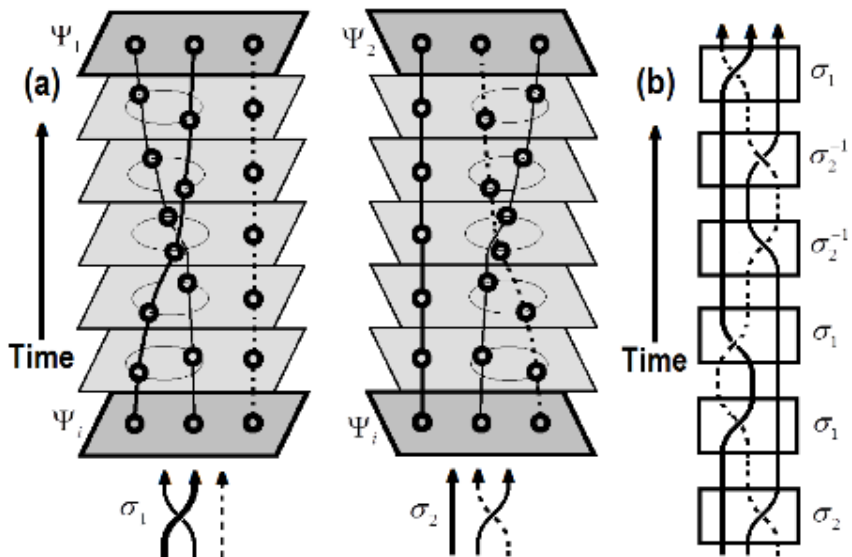


Fig. 1.22. Topological quantum computing schema of quasiparticle exchange. (a) Basic operations, σ_1 and σ_2 on a system of three quasiparticles. Top: Temporal evolution of the system from the initial state Ψ_i to the final state $\Psi_{1(2)} = \sigma_{1(2)}\Psi_i$. Bottom: diagrammatic representations of the quasiparticle exchange operations. (b) Example of logic gate operations for the basic operations σ_1 and σ_2 shown in (a) and their inverses σ_1^{-1} and σ_2^{-1} . Redrawn from [67].

Even though quantum braids are inherently more stable than trapped quantum particles, there is still a need to control for error inducing thermal fluctuations, which produce random stray pairs of anyons which interfere with adjoining braids. Controlling these errors is simply a matter of

separating the anyons to a distance where the rate of interfering strays drops to near zero [67].

TQC provides a possible new architecture for QC with a low error rate by exploiting anyon braiding in the topology of quasiparticles. Anyons have different statistics than Bosons (Bose-Einstein spin 1 statistics) and Fermions (Fermi-Dirac spin 1/2 statistics). Semiconductor devices are expected to host these exotic quasiparticle states, predicting that TQC will have properties sufficient for error-free quantum computation. A more detailed analysis of TQC is given in Chaps. 9 and 10. TQC is considered a ‘toy model’ for the introduction of the Unified Field Mechanical (UFM) Ontological-Phase Topological Field Theoretic QC presented as the main purpose of this volume. See Chap. 12.

1.2.21. Unified Field Mechanical Quantum Computing

Unified Field Mechanical Quantum Computing (UFMQC) is probably the newest QC model; although under theoretical development for over a decade, understanding its formulation only began to gel while writing this volume. Its Group Theory is not fully known yet; and its basis has been given the provisional name: Ontological-Phase Topological Field Theory or in terms of quantum information processing: Ontological-Phase Topological Quantum Computing (OPTQC), which we will do our best to make a case for in Chaps. 12, 13 and 15.

What this currently highly speculative model has to offer is pointed out acutely in the subtitle of this volume ‘Surmounting Uncertainty – Supervening Decoherence’. Those UFM scenarios, if correct totally remove conditions plaguing virtually all the other QC models outlined in this chapter. Its most redeeming factor is that it is experimentally testable; and preparations are underway to do such [69,70].

1.3 Concept

Computation whether classical or quantum is Boolean, utilizing a symbolic system of algebraic notation for binary variables that are used to represent logical propositions or logical operators having two possible values denoted as ‘true’ and ‘false’, 1 and 0 or $|\uparrow\rangle$ or $|\downarrow\rangle$ [71]. Information is physical and cannot exist without a physical representation. The question is how to move from current more symbolic representations to methods of representing algorithms in a manner connoting physical reality

to the extent now required by UFM? The supposition is that a purely mathematical space such as the multidimensional Hilbert space currently in use can no longer be considered adequate for implementing universal quantum information processing (QIP). It is a fairly recent idea to worry about the fact that information is physical in this respect [72-74], and that while mere binary representations have been adequate for Turing machines for the last 70 years, and even all the QIP done to date at the semi-classical limit; the scenario is not sufficient for QC at a UQC level, especially as we pass beyond the historical basis of Unitarity and Locality to the requirements for relativistic QIP effects and further to incorporate the necessary phenomena imposed by UFM and the associated OPTFT.

Moore's Law has approached unity as we speak; and as everyone knows computing at the quantum level is plagued by a lack of control of quantum degrees of freedom by interaction with the environment and vacuum fluctuations. The wavefunction, $|\psi\rangle = \alpha|0\rangle + \beta|1\rangle$ complicates the concept of reality for Euclidean observers. In order to determine the state of a physical object we have to interact with it; don't we?

Two quantum systems as represented by the wavefunction above are entangled by a standard unitary operation, $U_{\text{ent}}|\psi\rangle|0\rangle = \alpha|0\rangle|0\rangle + \beta|1\rangle|1\rangle$. $|\psi\rangle$ can be unknown and $|0\rangle$ a known state, that can be extended to an N -qubit product state which can be operated on simultaneously by U :

$$\begin{aligned} U_{\text{ent}} \underbrace{|0\rangle|0\rangle|0\rangle|0\rangle|0\rangle\dots|0\rangle|0\rangle}_{N \text{ times}} &\sim |00000\dots00\rangle + |00000\dots01\rangle + |00000\dots10\rangle + \\ &+ \dots + |1111\dots00\rangle + |1111\dots01\rangle + |1111\dots10\rangle + |1111\dots11\rangle \left(2^N \text{ terms}\right). \end{aligned} \quad (1.15)$$

We have been at this point for a long time for all QC systems under study; all plagued by decoherence with severity increasing with the number of qubits. Error correcting techniques have been proposed for arbitrary size qubit registers [75-77].

Any quantum system such as electron spin whose state space can be described by a 2D complex vector space can be used to implement a qubit. By current thinking, 'The QC must operate in a Hilbert space whose dimensions may be grown exponentially as an infinite-dimensional analog of Euclidean space such that an abstract vector space possessing the structure of an inner product allows length and angle to be measured'. This

scenario has been good in principle until now, and probably retains utility in some QC mathematical and algorithm preparation processes; but since the Bloch 2-sphere representation is not physical, it can no longer be considered a sufficient description for practical implementations of UQC.

1.4. Conundrum - *Hypotheses non Fingo*

Newton claimed he did not make use of fictions, "*Whereas the main business of natural Philosophy is to argue from Phaenomena without feigning Hypotheses*" [78]. I have no idea what the most myopic hypothesis in the history of science is; I do know that theory drives experiment and experiment drives theory and that finally the much criticized string/M-Theory has finally become testable after several decades of criticism. I say this because a very radical model of UQC is presented in this volume. It has been tinkered with for 20 years and finally is sufficiently testable to promote. One corner of the QC community has finally caught up with the premise of relativistic qubits in the last couple years. The TQC anyon quasiparticle Hall effect model seems to be a 2D toy model of our model. As far as the penultimate requirement of UFM; we seem first to use the term.

Few physicists consider Large-Scale Additional Dimensionality (LSXD), but sufficiently so, that experiments at CERN are being developed to search for them. Our UFM protocol to find them is table top and low energy, which if successful will put an end to the need for supercolliders. We are formulating an Ontological-Phase Topological Field Theory (OPTFT) to address the putative parameters. Our view of a UFM fortunately makes easy correspondence to HD extensions of the Wheeler-Feynman-Absorber Cramer-Transactional De Broglie-Bohm-Vigier causal interpretations of quantum theory as well as dual 3-tori Calabi-Yau brane mirror symmetry (thus OPTFT). Even though I'm riding a wild stallion, it is a very radical paradigm shift that blows even the author's mind. The most difficult part for colleagues to embrace/comprehend is the 'continuous-state' evolution of the HD brane topology; along with the fact that 'the Earth is not the center of the Universe', flagrantly meaning that we, as physical observers, must give up observation from the perspective of Euclidean 3-space as the primary vantage. It's always like this in a paradigm shift; get over it, leap-frog over and beyond me and enter the 'brave new world'. The late Karl H. Pribram, noted Stanford neuroscientist (holographic brain model), once asked me

on a beach approaching sunset, in Long Beach, CA USA “*Aren’t we all in this together?*”, while we were pondering the reflection of the sun on the water, arguing about how many images there were...

1.4.1 The Church-Turing Hypothesis

The Church-Turing Hypothesis states, every function naturally regarded as computable can be computed by the universal Turing machine, interpreted quasi-mathematically as the conjecture that all possible formalizations of the mathematical notion of algorithm or computation are equivalent to each other. But Deutsch says, “*we shall see that it can also be regarded as asserting a new physical principle, which I shall call the Church-Turing principle to distinguish it from other implications and connotations of the conjecture. My statement of the Church-Turing principle is manifestly physical ... computable as the functions which may in principle be computed by a real physical system*” [79].

Deutsch then states, “*I can now state the physical version of the Church-Turing principle: ‘Every finitely realizable physical system can be perfectly simulated by a universal model computing machine operating by finite means’. This formulation is both better defined and more physical than Turing’s own way of expressing it, because it refers exclusively to objective concepts such as ‘measurement’, ‘preparation’ and ‘physical system’, which are already present in measurement theory.*” [79]. And further:

Every existing general model of computation is effectively classical. That is, a full specification of its state at any instant is equivalent to the specification of a set of numbers, all of which are in principle measurable. Yet according to quantum theory there exist no physical systems with this property. The fact that classical physics and the classical universal Turing machine do not obey the Church-Turing principle in the strong physical form is one motivation for seeking a truly quantum model. The more urgent motivation is, of course, that classical physics is false. Benioff (1982) has constructed a model for computation within quantum kinematics and dynamics, but it is still effectively classical in the above sense. It is constructed so that at the end of each elementary computational step, no characteristically quantum property of the model - interference, non-separability, or indeterminism - can be detected. Its computations can be perfectly simulated by a Turing machine [79].

The Church-Turing thesis generally defines an ‘algorithm’ as a description of a calculation that needs to be realized physically; thus, the device executing the calculation has to be considered a physical system also. In this regard a calculation is defined as the execution of a physical

process, where the result is provided by the observation of the process. Underlying the Church-Turing hypothesis there is an implicit physical assertion, which as Deutsch states:

“is presented explicitly as a physical principle: ‘every finitely realizable physical system can be perfectly simulated by a universal model computing machine operating by finite means’. Classical physics and the universal Turing machine, because the former is continuous and the latter discrete, do not obey the principle, at least in the strong form above. A class of model computing machines that is the quantum generalization of the class of Turing machines is described, and it is shown that quantum theory and the ‘universal quantum computer’ are compatible with the principle. Computing machines resembling the universal quantum computer could, in principle, be built and would have many remarkable properties not reproducible by any Turing machine. [79].

This includes ‘quantum parallelism’, whereby certain probabilistic tasks can be performed faster by a UQC than by any classical restriction of it. “*The intuitive explanation of these properties places an intolerable strain on all interpretations of quantum theory other than Everett’s*” [79].

1.4.2. The Church-Turing-Deutsch Thesis

The idea of the Turing machine dates back to the year 1936. At this time, the physical world seemed to be dominated by mechanical forces; correspondingly, the definition of a Turing machine is based on the ideas of classical mechanics. And though the physical realization of a Turing machine, the digital computer, actually uses quantum mechanics, its construction principles aims at the suppression of any effect associated with the quantum world. With ever-tighter package density, however, this is not achievable anymore in a perfect way. The effects of quantum theory may begin to have an influence on the outcome of the calculation.

Consequently, it seems to be questionable whether the Turing machine provides a ‘natural’ model of computation. Searching for alternatives and taking the quantum nature of the world into consideration, Feynman had the idea of quantum computation in 1982. As a model executing such a quantum computation, he proposed the quantum Turing machine as quantum theoretical analogon to the Turing machine. Similar ideas were developed independently by Manin [80]. Accordingly, David Deutsch famously generalized the Church-Turing thesis to the Church-Turing-Deutsch thesis in 1985, which states that every computation, which can be realized physically, can be executed using a quantum Turing machine [81, 82].

1.4.3. Perspicacious Perspicacity – Who Has it? Where can I get Some?

I remember when I was about 12 years old and my father would take the old fashioned steam locomotives from West Medford, MA to Boston to work. That railroad company had kept a few steam locomotives about a decade longer than any others in the country. The last age of discovery occurred at the beginning of the 20th century; this next one will pale all others in the history of human consciousness. A big part of me wishes I wasn't with the utmost alacrity, becoming a codger and could transfer my mind to an android for a couple hundred years; Yea, I mean 'where's my flying car', less than a decade ago it took four guys to barely be able to move a 50-inch TV out the door, now they can be carried with one arm, and paper thin, roll up into a tube, wallpaper TVs are coming out the door. The toys UCQ will provide are not unimaginable; I want some. Let's get with the program...

WHAT'S BEYOND A VEIL OF UNCERTAINTY?

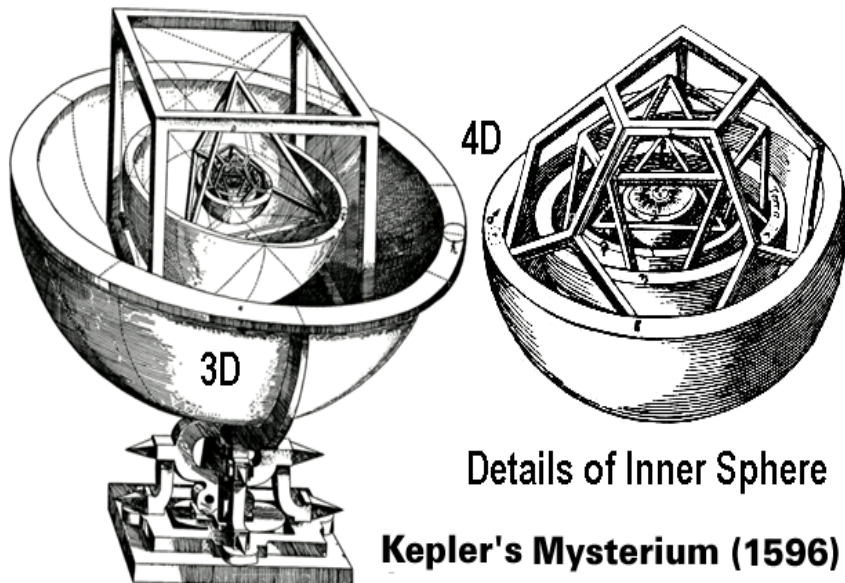


Fig. 1.23. Kepler's *Mysterium Cosmographicum* Platonic solid solar system model [83].

We offer Kepler's *Mysterium Cosmographicum* Platonic solid as a metaphor suggesting the additional hidden semi-quantum dimensionality

for UFM required to represent QC operations in a physically real manner. It is important to realize, that just as the Earth was found not to be the center of the universe, as difficult as it may seem at the moment; Euclidean 3-space can no longer be considered the sole basis of observation.

For that important reason we repeat Feynman's message quoted at the beginning of this chapter:

“... Trying to find a computer simulation of physics, seems ... an excellent program to follow ... I'm not happy with all the analyses that go with just the classical theory, because nature isn't classical, ... and if you want to make a simulation of nature, you'd better make it quantum mechanical ...”, R. Feynman [1].

Thirty-four years have passed. I take liberty to impress upon you the necessity for updating it:

I'm not happy with all the analyses that go with just classical and quantum theory, because nature isn't classical or quantum, ... if you want to make a simulation of nature, you'd better make it unified field mechanical, R.L. Amoroso.

References

- [1] Feynman, R.P. (1982) Simulating physics with computers, *Intl J Theoretical Physics* 21, pp. 467-488.
- [2] Vandersypen, L.M.K. & Chuang, I.L. (2004) NMR techniques for quantum control and computation, *Rev Mod Phys*, 76, 1037-1069.
- [3] Di Vincenzo, D.P. (2000) The physical implementation of quantum computation, arXiv:quant-ph/0002077.
- [4] Bell, J.S. (1966) On the problem of hidden variables in quantum mechanics, *Reviews of Modern Physics*, 38(3), 447.
- [5] Lindblad, G. (1999) A general no-cloning theorem, *Letters in Mathematical Physics*, 47(2), 189-196.
- [6] Zurek, W.H. (2009) Quantum Darwinism, arXiv:0903.5082v1 [quant-ph].
- [7] Deutsch, D. (1985) Quantum theory, the Church-Turing principle and the universal quantum computer, *Proceedings Royal Society, A* 400 (1818): 97-117.
- [8] Benioff, P. (1980) The computer as a physical system: A microscopic quantum mechanical Hamiltonian model of computers as represented by Turing machines, *Journal of Statistical Physics*, 22(5):563-591.
- [9] Jozsa, R. (2005) An introduction to measurement based quantum computation, arXiv:quant-ph/0508124v2.
- [10] Raussendorf, R., Browne, D.E. & Briegel, H. J. (2003) Measurement based quantum computation on cluster states, *Phys Rev A* 68 (2):022312; arXiv:quantph/0301052.
- [11] Raussendorf, R., Harrington, J. & Goyal, K. (2007) Topological fault tolerance, *New Journal of Physics* 9: 199; arXiv:quant-ph/0703143.
- [12] Walther, P., Resch, K.J. Rudolph, T., Schenck, E. Weinfurter, H. Vedral, V. M. Aspelmeyer, M. & Zeilinger, A. (2005) *Nature* 434 (7030): 169-76; arXiv:quant-ph/0503126.

- [13] Fowler, A.G., Stephens, A.M. & Groszkowski, P. (2009) High-threshold universal quantum computation on the surface code, *Phys Rev A*, 80: 052312.
- [14] Nielsen, M.A. (2005) Cluster-state quantum computation, arXiv:quant-ph/0504097v2.
- [15] Johnson, M.W. et al. (2011) Quantum annealing with manufactured spins, *Nature*, 473, 194-198.
- [16] Perdomo-Ortiz, A., Dickson, N., Drew-Brook, M., Rose, G. & Aspuru-Guzik, A. (2012) Finding low-energy conformations of lattice protein models by quantum annealing, *Scientific Reports* 2, 571.
- [17] Kane, B.E. (1998) A silicon-based nuclear spin quantum computer, *Nature*, 393, p. 133.
- [18] O'Gorman, J., Nickerson, N.H., Ross, P., Morton, J.L. & Benjamin, S.C. (2015) A silicon-based surface code quantum computer, arXiv:1406.5149v3 [quant-ph].
- [19] Dixit, A. & Kapse, V (2012) Arithmetic & logic unit (ALU) design using reversible control unit, *Intl J Eng and Innovative Tech (IJEIT)* Vol 1, No. 6.
- [20] Elhoushi, M., El-Kharashi, M.W. & Elrefaei, H. (2011) Modeling a quantum processor using the QRAM model, in *Communications, Computers and Signal Processing (PacRim), 2011 IEEE Pacific Rim Conf.*, pp. 409-415.
- [21] Shirahama, K., Ito, H.S., Suto, S.I. & Kono, K. (1995) *J. Low Temp. Phys.* 101, 439.
- [22] Platzman, P.M. & Dykman, M.I. (1999) Quantum computing with electrons floating on liquid helium, *Science*, Vol. 284, No. 5422, pp. 1967-1969.
- [23] Platzman, P.M., Dykman, M.I. & Seddighrad, P. (2003) Dynamics in quantum dots on helium surface, arXiv:cond-mat/0308572v1.
- [24] Odom, B., Hanneke, D., D'Urso, B. & Gabrielse, G. (2006) New measurement of the electron magnetic moment using a one-electron quantum cyclotron, *Physical Review Letters* 97 (3): 030801.
- [25] Harneit, W. (2002) Fullerene-based electron-spin quantum computer, *Phys. Rev. A* 65, 032322.
- [26] Rose, G. & Macready, W.G. (2007) An Introduction to quantum annealing, DWAVE/ Technical Document 0712.
- [27] Clarke, J. & Wilhelm, F. (2008) Superconducting quantum bits, *Nature* 453 (7198): 1031-1042.
- [28] Kaminsky, W.M. (2004) Scalable superconducting architecture for adiabatic quantum computation, arXiv:quant-ph/0403090.
- [29] Bouchiat, V., Vion, D., Joyez, P., Esteve, D. & Devoret, M.H. (1988) Quantum coherence with a single Cooper pair, *Physica Scripta*, T76: 165.
- [30] Monroe, C.R. & Wineland, D.J. (2008) Quantum computing with ions, *Scientific American*, pp. 64-71.
- [31] Monroe, C.R. (2002) Quantum information processing with atoms and photons, *Nature*, Vol. 416, No. 6877, pp. 238-246.
- [32] Li, L. et al. (2015) Coherent spin control of a nanocavity-enhanced qubit in diamond, *Nature Communications*, 6, 6173.
- [33] Xu, S.J. Physics of nanomaterials, www.physics.hku.hk/~phys2235/lectures/lecture9.pdf.
- [34] Loss, D. & DiVincenzo, D.P. (1998) Quantum computation with quantum dots, *Phys. Rev. A* 57, p120; arXiv.org.
- [35] DiVincenzo, D.P. (1997) in *Mesoscopic Electron Transport*, Vol. 345, NATO Advanced Study Institute, Series E: Applied Sciences, L. Sohn, L. Kouwenhoven, & G. Schoen (eds.) Dordrecht: Kluwer; arXiv.org.

- [36] Kloeffel, C. & Loss, D. (2012) Prospects for spin-based quantum computing, arXiv:1204.5917v1 [cond-mat.mes-hall].
- [37] Jeong, H., Chang, A. M., Melloch, M. R. (2001) The Kondo effect in an artificial quantum dot molecule, *Science* 293, 2221-2223.
- [38] Veldhorst, M. et al. (2015) A two-qubit logic gate in silicon, *Nature*, 526, 410-414.
- [39] Stepanenko, D., Trif, M. & Loss, D. (2008) Quantum computing with molecular magnets, *Inorganica Chimica Acta*, Vol. 361, Is. 14-15, pp. 3740-3745.
- [40] Leuenberger, M.N. & Loss, D. (2001) Quantum computing in molecular magnets, arXiv.org/ftp/cond-mat/papers/0011/0011415.pdf.
- [41] Andrianov, S.N. & Moiseev, S.A. (2014) Magnon qubit and quantum computing on magnon Bose-Einstein condensates, *Phys. Rev. A* 90, 042303.
- [41] Bose, S.N. (1924) *Plancks gesetz und lichtquantenhypothese*, *Zeitschrift für Physik* 26: 178–181.
- [42] Einstein, A. (1925) *Quantentheorie des einatomigen idealen Gases*, *Sitzungsberichte der Preussischen Akademie der Wissenschaften*, 1: 3.
- [43] Hecht, T. (2004) Quantum computation with Bose-Einstein condensates, www2.mpq.mpg.de/Theorygroup/CIRAC/wiki/images/7/79/Hecht_Diplomarbeit.pdf.
- [44] Timmermans, E., Tommasini, P., Hussein, M. & Kerman, A. (1999) Feshbach resonances in atomic Bose-Einstein condensates, *Physics Reports-Review Section of Physics Letters*, 315(1-3):199–230.
- [45] Karnachev, A.S., Klechin, Y.I., Kovtun, N.M., Moskvin, A.S., Solov'ev, E.E. & Tkachenko, A.A. (1983) Spin-flip and nuclear quadrupole interactions in the rare-earth orthochromites $GdCrO_3$, *Sov. Phys. JETP* 58 (2), *Zh. Eksp. Teor. Fiz.* 85, 670-677.
- [46] Nilsson, M., Levin, L., Ohlsson, N., Christiansson, T. & Kröll, S. (2001) Initial experiments concerning quantum information processing in rare-earth-ion doped crystals, arxiv.org/ftp/quant-ph/papers/0201/0201141.pdf.
- [47] Chang, H., Xie, J., Zhao, B., Liu, B., Xu, S., Ren, N., Xie, X., Huang, L. & Huang, W. (2015) Rare earth ion-doped up conversion and surface modification, *Nanocrystals: Synthesis, Nanomaterials*, 5, 1-25.
- [48] Walther, A., Rippe, L., Yan, Y., Karlsson, J., Serrano, D., Nilsson, A.N., Bengtsson, S. & Kroll, S. (2015) High fidelity readout scheme for rare-earth solid state quantum computing, arXiv:1503[quant-ph].
- [49] Knill, E., Laflamme, R., Milburn, G.J. (2001) A scheme for efficient quantum computation with linear optics, *Nature* (Nature Publishing Group) 409 (6816): 46-52.
- [50] Kok, P., Munro, W.J., Nemoto, K., Ralph, T.C., Dowling, J.P. & Milburn, G.J. (2007) Linear optical quantum computing with photonic qubits, *Rev. Mod. Phys.*, 79: 135-174; arXiv:quant-ph/0512071.
- [51] Adami, C. & Cerf, N.J. (1999) Quantum computation with linear optics, in *Quantum Computing and Quantum Communications*, Lecture Notes in Computer Science, Springer, 1509: 391-401.
- [52] Malinovskaya, S.A. & Novikova, I. (2015) From Atomic to Mesoscale: The Role of Quantum Coherence in Systems of Various Complexities, Singapore: World Scientific.
- [53] Ralph, T.C., White, A.G., Munro, W.J. & Milburn, G.J. (2001) Simple scheme for efficient linear optics quantum gates, *Phys. Rev. A* 65, 012314.
- [54] Hong, C.K., Ou, Z.Y. & Mandel, L. (1987) Measurement of subpicosecond time intervals between two photons by interference, *Phys. Rev. Lett.* 59, 2044.
- [55] Knill, E. (2002) Quantum gates using linear optics and postselection. *Physical Review A* 66 (5): 052306; arXiv:quant-ph/0110144.

- [56] Hutchinson, G.D. & Milburn, G. J. (2004) Nonlinear quantum optical computing via measurement, *Journal of Modern Optics* 51 (8): 1211-1222; arXiv:quant-ph/0409198.
- [57] Lloyd, S. (1992) Any nonlinear gate, with linear gates, suffices for computation, *Physics Letters A* 167 (3): 255-260.
- [58] Bloch, I. (2005) Ultracold quantum gases in optical lattices, *Nature Physics* 1 (1): 23-30.
- [59] Soderberg, K-A B., Gemelke, N. & Chin, C. (2008) Ultracold molecules: Vehicles to scalable quantum information processing, arXiv:0812.1606v1 [quant-ph].
- [60] Burrell, B. (2012) An introduction to quantum computing. arXiv:1210.6512v1 [quant-ph].
- [61] Luo, M-X, Deng, Y., Li, H-R & Ma, S-Y (2015) Photonic ququart logic assisted by the cavity-QED system, *Scientific Reports* 5, No.: 13255.
- [62] Vandersypen, L.M.K., Yannoni, C.S. & Chuang, I.L. (2002) Liquid state NMR quantum computing, in D.M. Grant & R.K. Harris (eds.) *Encyclopedia of Nuclear Magnetic Resonance*, Vol. 9, pp 687-697, Chichester: John Wiley & Sons.
- [63] Peng, X., Zhu, X., Fang, X., Feng, M., Gao, K., Yang, X. & Liu, M. (2000) Preparation of pseudo-pure states by line-selective pulses in Nuclear Magnetic Resonance, arXiv:quant-ph/0012038v2.
- [64] Menicucci, N.C. & Caves, C.M. (2002) Local realistic model for the dynamics of bulk-ensemble NMR information processing, *Phys Rev Lett* 88 (16); arXiv:quant-ph/0111152.
- [65] Freedman, M.H., Kitaev, A., Larsen, M.J. & Wang, Z. (2002) Topological quantum computation, *Bulletin (new series) Am Mathematical Society* vol. 40, no. 1, pp. 31-38.
- [66] Sarma, S.D., Freedman, M. & Nayak, C. (2015) Majorana zero modes and topological quantum computation, *NPJ Quantum Information* 1, 15001.
- [67] Muraki, K. (2012) Unraveling an exotic electronic state for error-free quantum computation, *NTT Technical Review*, Vol. 10 No. 10.
- [68] Sarma, S.D., Freedman, M. & Nayak, C. (2005) Topologically protected qubits from a possible non-abelian fractional quantum Hall state, *Physical Review Letters* 94 (16): 166802; arXiv:cond-mat/0412343.
- [69] Amoroso, R.L. (2013) Evidencing ‘tight bound states’ in the hydrogen atom: Empirical manipulation of large-scale XD in violation of QED, in R.L. Amoroso (ed.) *The Physics of Reality: Space, Time, Matter, Cosmos*, Singapore: World Scientific.
- [70] Amoroso, R.L. (2010) Simple resonance hierarchy for surmounting quantum uncertainty, *AIP Conf. Proc.* 1316, 185 or <http://vixra.org/pdf/1305.0098v1.pdf>.
- [71] Nielsen, M.A. (2002) Rules for a complex quantum world, *Scientific American*, Vol. 287, No. 5, pp. 66-75.
- [72] Shannon, C.E. (1958) Channels with side information at the transmitter, *IBM journal of Research and Development*, 2(4), 289-293.
- [73] Landauer, R. (1991) Information is physical, *Phys. Today* 44 (5) 22.
- [74] Landauer, R. (1996) The physical nature of information, *Phys Let. A* 217, 188-193.
- [75] Lidar, D. & Todd Brun T. (eds.) (2013) *Quantum Error Correction*, Cambridge: Cambridge University Press.
- [76] Shor, P.W. (1996) Fault-tolerant quantum computation, *37th Symposium on Foundations of Computing*, IEEE Computer Society Press, pp. 56-65.
- [77] Preskill, J. (1998) Fault-tolerant quantum computation, in *Introduction to Quantum Computation*, H-K Lo, S. Popescu, T. P. Spiller (eds.) Singapore: World Scientific.

- [78] Newton, I. (1689) Scholium to the Definitions in *Philosophiae Naturalis Principia Mathematica*, Bk. 1; Andrew Motte (trans.) (1729), rev. F. Cajori (1934) Berkeley: University of California Press, pp. 6-12.
- [79] Deutsch, D. (1985) Quantum theory, the Church-Turing principle and the universal quantum computer, Proceedings of the Royal Society of London, A 400, pp. 97-117.
- [80] Manin, Y.I. (1980) *Vychislomoe i nevychislomoe* [Computable and Noncomputable] (in Russian) Sov.Radio. pp. 13-15.
- [81] Quantum Turing machine, Encyclopedia of Mathematics, www.encyclopediaofmath.org/index.php/Quantum_Turing_machine.
- [82] Aaronson, S. (2008) The limits of quantum computers, Scientific American, Vol. 298, No. 3, pp. 62-69.
- [83] Kepler, J. (1596) *Mysterium Cosmographicum*, Platonic solid model of the Solar system.

Chapter 2

Cornucopia of Quantum Logic Gates

A logic gate is the elementary building block of a computing circuit or algorithm practically applying the concept of binary Boolean bits to circuits using combinational logic. Logic gates are of recent origin. From the time that Leibniz refined binary numbers and showed that mathematics and logic could be combined in 1705, it took well over a hundred years before Babbage devised geared mechanical logic gates in 1837 for use in his proposed Analytical Engine. Another sixty years passed before the first electronic relays appeared in the late 1890s. Then it wasn't until the 1940s that the first working computer was built. Now, with the arrival of quantum logic gates the evolution continues; and universal quantum computers (UQC) wait in the wings while finishing the absorption of required remaining discovery in physics.

2.1 Fundamental Properties of Gate Operations

Linear algebra concerns vector spaces and linear mappings between such spaces. The 3D Euclidean space \mathbb{R}^3 is a vector space, where lines and planes passing through the origin are vector subspaces in \mathbb{R}^3 . The most important space in basic linear algebra is \mathbb{R}^n , a Euclidean space in n dimensions where a typical element is an n -element vector of real numbers. The space of infinite-dimensional vectors defines the Hilbert space, $\ell^2(\mathbb{N})$. Such a Hilbert space, H is a vector space endowed with an inner or dot product, $\|x\|$ and associated norm and metric, $\|x - y\|$ such that every Cauchy sequence (converges to a limit) in \mathbb{R}^n making \mathbb{R}^n a Hilbert space. Complex Hilbert spaces are used to represent the pure states of a quantum mechanical system utilizing unit vectors, called state vectors.

What is the difference between classical and quantum information? As shown in the matrices below, the classical bit is described by two nonnegative real numbers for probabilities $P(0) = 1/3$ and $P(1) = 2/3$. In contrast the quantum bit has two complex amplitudes giving the same probabilities by taking the square of the absolute value.

$$\text{Classical bit: } \begin{bmatrix} 1/3 \\ 2/3 \end{bmatrix} \quad \text{Qubit: } \begin{bmatrix} -1/\sqrt{3} \\ 1+i/\sqrt{3} \end{bmatrix} \quad (2.1)$$

A quantum system described like this with nonzero amplitudes is said to be in a superposition of the 0 and 1 configurations.

The basis of all computing is the logic gate [1]. A quantum logic gate is most often represented by a matrix. For example, a gate acting on n qubits takes the form of a $2^n \times 2^n$ unitary matrix. The number of qubits input and the number of qubits output from any gate must be equal. The operation of the gate is determined by multiplying the gate's unitary matrix by the vector representation of the quantum state. For example, the vector representation of a solitary qubit and of two qubits is represented respectively as:

$$v_0|0\rangle + v_1|1\rangle \rightarrow \begin{bmatrix} v_0 \\ v_1 \end{bmatrix}, \quad v_{00}|00\rangle + v_{01}|01\rangle + v_{10}|10\rangle + v_{11}|11\rangle \rightarrow \begin{bmatrix} v_{00} \\ v_{01} \\ v_{10} \\ v_{11} \end{bmatrix}. \quad (2.2)$$

For the 2-qubit state $|ab\rangle$, a represents the value of the 1st qubit and b represents the 2nd qubit.

A single qubit wave function takes the form $|\Psi\rangle = \psi_0|0\rangle + \psi_1|1\rangle$ such that $|\psi_0|^2 + |\psi_1|^2 = 1$; with this as the case observation gives a result of either a 0 or a 1 with a probability for 0 as $|\psi_0|^2$ and the probability for observing a 1 is $|\psi_1|^2$.

2.2 Unitary Operators as Quantum Gates

The state of a quantum computer is described by a state vector, Ψ which is a complex linear superposition of all binary states of the qubits

$$x_n \in \{0,1\} :$$

$$\Psi(t) = \sum_{x_n \in \{0,1\}^n} \alpha_x |x_1, \dots, x_n\rangle, \quad \sum_x |\alpha_x|^2 = 1. \quad (2.3)$$

The state's evolution in time, t is described by a unitary operator, U on the same vector space, meaning any linear transformation is bijective and length-preserving. This unitary evolution on a normalized state vector is known to be the correct physical description of an isolated system evolving in time according to the laws of quantum mechanics [2-5]. Quantum physics is reversible because the reverse-time evolution specified by the unitary operator, $U^{-1} = U^\dagger$ always exists; as a consequence, reversible computation could be executed within a quantum-mechanical system.

Quantum physics postulates that quantum evolution is unitary (reversible); i.e., if we have an arbitrary quantum system, U taking an input state, $|\phi\rangle$ that outputs a different state, $U|\phi\rangle$, then we describe U as a unitary linear transformation, defined as follows. If U is any linear transformation, the adjoint (functions related by transposition) of U , denoted U^\dagger , is defined in the relation $(U\vec{v}, \vec{w}) = (\vec{v}, U^\dagger \vec{w})$. In a basis,

U^\dagger is the conjugate transposition of U ; for example,

$$U = \begin{pmatrix} a & b \\ c & d \end{pmatrix} \Rightarrow U^\dagger = \begin{pmatrix} \bar{a} & \bar{c} \\ \bar{b} & \bar{d} \end{pmatrix}. \quad (2.4)$$

By definition U is unitary if $U^\dagger = U^{-1}$. Thus, rotations and reflections are unitary. Also, the composition of two unitary transformations is also unitary, and for a unitary transformation U , the rows and columns also form an orthonormal basis [6].

Evolution of the state, $|\psi\rangle$ of a quantum system in time, t is a unitary transform, $|\psi\rangle \rightarrow \hat{U}|\psi\rangle$. Temporal evolution of a quantum system is linear because it does not depend on the state, $|\psi\rangle$. For example, any linear combination in t of state, $|\psi\rangle$ and $|\phi\rangle$ has the same operator

$$(\alpha|\psi\rangle + \beta|\phi\rangle) \rightarrow \hat{U}(\alpha|\psi\rangle + \beta|\phi\rangle) = \alpha\hat{U}|\psi\rangle + \beta\hat{U}|\phi\rangle. \quad (2.5)$$

Unitary operators conform to the Schrödinger equation

$$\frac{d|\psi\rangle}{dt} = -i\frac{\hat{H}(t)|\psi\rangle}{\hbar} \quad (2.6)$$

with $\hat{H}(t) = \hat{H}^\dagger(t)$ the system's Hamiltonian.

The general Hamiltonian for a spin-1/2 system is $\hat{H} = b\hat{X} + c\hat{Y} + d\hat{Z} = E_0\vec{n} \cdot \hat{\sigma}$ with $E_0 = \sqrt{b^2 + c^2 + d^2}$, $\vec{n} = (n_x, n_y, n_z) = (b/E_0, c/E_0, d/E_0)$, $n_x^2 + n_y^2 + n_z^2 = 1$ and $\hat{\sigma} = (\hat{X}, \hat{Y}, \hat{Z})$. Thus the unitary is

$$\exp\left(-\frac{i\hat{H}t}{\hbar}\right) = \cos\left(\frac{E_0 t}{\hbar}\right)\hat{I} - i\sin\left(\frac{E_0 t}{\hbar}\right)\vec{n} \cdot \hat{\sigma}. \quad (2.7)$$

This is a rotation about the \vec{n} axis in the Bloch sphere representation with a rotation rate of E_0/\hbar . For spin-1/2 this is the most general unitary transform [6].

Assuming we can turn the Hamiltonian off and on, the state can be rotated by a specific angle; again for spin-1/2 a unitary transform takes the form, $\hat{U}(\theta) = \cos(\theta/2)\hat{I} - i\sin(\theta/2)\vec{n} \cdot \hat{\sigma}$. It is important to realize that any product of unitary operators is also unitary [7]

$$\hat{U}^\dagger\hat{U} = \hat{V}^\dagger\hat{V} = \hat{I} \Rightarrow (\hat{U}\hat{V})^\dagger(\hat{U}\hat{V}) = \hat{V}^\dagger\hat{U}^\dagger\hat{U}\hat{V} = \hat{I} \quad (2.8)$$

The Copenhagen Interpretation's restriction of time evolution to unitary operators suggests that certain kinds of evolution are deemed impossible. Two such operations are the quantum no-cloning and non-erasure theorems [8-15]. In ensuing chapters, we intend to show that this is a condition of the 4D standard model Copenhagen Interpretation up to the 'semi-quantum limit' and is no longer the case for UFM topology.

2.3 Some Fundamental Quantum Gates

Unitary transformations, or quantum gates can be built from sets of unitaries, \hat{U} . The simplest spin-1/2 quantum system, the qubit, has two quantum states with the basis $|0\rangle \equiv |\uparrow Z\rangle$, $|1\rangle \equiv |\downarrow Z\rangle$. Some examples of simple single and 2-qubit unitary transforms, or ‘quantum gates’ follow:

- **The Hadamard Gate:**

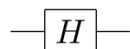
The Hadamard transform, known as the Hadamard gate in quantum computing is an example of a generalized class of Fourier transforms. It is able to perform orthogonal, symmetric, involute and linear operations. The Hadamard gate acts on a single qubit. It maps the basis state $|0\rangle$ to $|0\rangle + |1\rangle / \sqrt{2}$ and $|1\rangle$ to $|0\rangle - |1\rangle / \sqrt{2}$ representing a rotation of π about the axis $(\hat{x} + \hat{z}) / \sqrt{2}$. This is equivalent to the combination of the two rotations, $\pi/2$ about the y-axis followed by π about the x-axis. The Hadamard gate is represented by the Hadamard matrix which is a square matrix with mutually orthogonal rows with entries of ± 1 .

$$H = \frac{1}{\sqrt{2}} \begin{bmatrix} 1 & 1 \\ 1 & -1 \end{bmatrix}. \quad (2.9)$$

Since $HH^* = I$ and I is an identity matrix, H is a unitary matrix. The Hadamard gate operates as a reflection around $\pi/8$, or as a $\pi/4$ rotation followed by a reflection. Notice that $H^\dagger = H$ and $H^2 = I$ because H is real and symmetric.

$$H = \frac{1}{\sqrt{2}} \begin{pmatrix} 1 & 1 \\ 1 & -1 \end{pmatrix} = -\boxed{H} = \begin{bmatrix} \frac{1}{\sqrt{2}} & \frac{1}{\sqrt{2}} \\ \frac{1}{\sqrt{2}} & -\frac{1}{\sqrt{2}} \end{bmatrix} \quad (2.10)$$

The circuit representation of Hadamard gate is



- **The Phase Shift Gate:**

Phase Shift gates are a family of single qubit gates that leave basis state $|0\rangle$ unchanged and map $|1\rangle$ to $e^{i\theta}|1\rangle$. The Phase Shift Gate 2×2 matrix and symbol are:

$$R_\theta = \begin{bmatrix} 1 & 0 \\ 0 & e^{i\theta} \end{bmatrix} \quad \text{with symbol} \quad -\boxed{R_\theta}-$$

The phase shift gate is a generalization of an infinity of gates. The Pauli-Z gate, Phase shift gate, and $\pi/8$ gates are all special cases of the phase shift gate for specific values of θ (the phase shift).

- **The Swap Gate:**

The Swap Gate swaps two qubits in terms of the basis $|00\rangle, |01\rangle, |10\rangle, |11\rangle$ and is represented by the matrix:

$$\text{SWAP} = \begin{bmatrix} 1 & 0 & 0 & 0 \\ 0 & 0 & 1 & 0 \\ 0 & 1 & 0 & 0 \\ 0 & 0 & 0 & 1 \end{bmatrix} \quad \begin{array}{c} \diagup \diagdown \\ \diagdown \diagup \end{array}$$

- **The Pauli X (NOT) Gate:**

The Pauli-X gate acts on a single qubit. It is the quantum equivalent of a classical NOT gate (with respect to the standard basis $|1\rangle, |0\rangle$, which privileges the Z-direction). It equates to a rotation of the Bloch Sphere around the X-axis by π radians; and maps $|0\rangle$ to $|1\rangle$ and $|1\rangle$ to $|0\rangle$. Due to this operation, it is sometimes called the bit-flip gate. It is represented by the Pauli matrix:

$$\begin{bmatrix} 0 & 1 \\ 1 & 0 \end{bmatrix} = -\boxed{X}-$$

- **The Pauli Y Gate:**

The Pauli-Y gate acts on a single qubit. It equates to a rotation around the Y-axis of the Bloch Sphere by π radians. It maps $|0\rangle$ to $i|1\rangle$ and $|1\rangle$ to $-i|0\rangle$. It is represented by the Pauli Y matrix:

$$\begin{bmatrix} 0 & -i \\ i & 0 \end{bmatrix} = -[\boxed{Y}] -$$

- **The Pauli Z Gate:**

The Pauli-Z gate acts on a single qubit. It produces a rotation around the Z-axis of the Bloch Sphere by π radians. Thus, it is a special case of a phase shift gate with $\theta = \pi$. It leaves the basis state, $|0\rangle$ unchanged and maps $|1\rangle$ to $-|1\rangle$. Due to this nature, it is sometimes called the phase-flip gate. It is represented by the Pauli Z matrix:

$$\begin{bmatrix} 1 & 0 \\ 0 & -1 \end{bmatrix} = -[\boxed{Z}] -$$

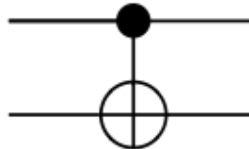
- **The CNOT (Controlled NOT) Gate:**

Controlled gates act on 2 or more qubits, with one or more qubits acting as a control for a specific operation. For example, a CNOT Gate acts on 2 qubits, and performs the NOT operation on the second qubit. The first bit of a CNOT gate is the ‘control bit’; the second is the ‘target bit’. The control bit never changes, while the target bit flips if and only if the control bit is 1. Here is the matrix representation of CNOT, and its operation upon a general 2-qubit state column vector:

$$\text{CNOT} = \begin{bmatrix} 1 & 0 & 0 & 0 \\ 0 & 1 & 0 & 0 \\ 0 & 0 & 0 & 1 \\ 0 & 0 & 1 & 0 \end{bmatrix}$$

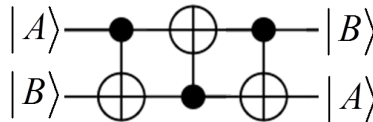
$$\text{CNOT } \Psi = \begin{bmatrix} 1 & 0 & 0 & 0 \\ 0 & 1 & 0 & 0 \\ 0 & 0 & 0 & 1 \\ 0 & 0 & 1 & 0 \end{bmatrix} \begin{bmatrix} \alpha \\ \beta \\ \gamma \\ \delta \end{bmatrix} = \begin{bmatrix} \alpha \\ \beta \\ \delta \\ \gamma \end{bmatrix}$$

The CNOT gate is usually depicted as follows, with the control bit on top



and the target bit on the bottom.

When unitary gates are combined they form a quantum circuit; the example below uses three CNOT gates to swap the 1st and 2nd qubits.



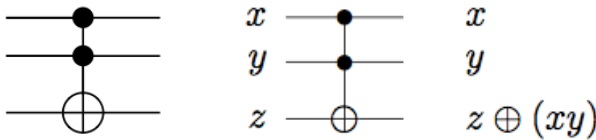
$$\begin{aligned} \hat{U}_{\text{CNOT}}|00\rangle &= |00\rangle, & \hat{U}_{\text{CNOT}}|01\rangle &= |01\rangle, \\ \hat{U}_{\text{CNOT}}|10\rangle &= |11\rangle, & \hat{U}_{\text{CNOT}}|11\rangle &= |10\rangle. \end{aligned} \quad (2.11)$$

This has two inputs and two outputs. The first input is passed through unchanged to the corresponding output. When this first input is 0, the second input is also passed through unchanged to its corresponding output. But when the first input is 1, the second input gets inverted as through an X gate.

- **The Toffoli Gate:**

Introduction of an additional control line to the CNOT gate results in the CCNOT gate (controlled-controlled NOT) which is also called the Toffoli gate. The Toffoli Gate is a 3-bit controlled gate also called the CCNOT gate which is universal for classical computing. The quantum Toffoli gate is the same gate defined instead for 3 qubits; but this gate is not universal for quantum Computing.

The Toffoli gate is depicted as follows:



If the first two bits are in the state $|1\rangle$, a Pauli-X is applied on the 3rd bit, otherwise it does nothing. Its permutation matrix is:

$$\text{CCNOT} = \begin{pmatrix} 1 & 0 & 0 & 0 & 0 & 0 & 0 & 0 \\ 0 & 1 & 0 & 0 & 0 & 0 & 0 & 0 \\ 0 & 0 & 1 & 0 & 0 & 0 & 0 & 0 \\ 0 & 0 & 0 & 1 & 0 & 0 & 0 & 0 \\ 0 & 0 & 0 & 0 & 1 & 0 & 0 & 0 \\ 0 & 0 & 0 & 0 & 0 & 0 & 1 & 0 \\ 0 & 0 & 0 & 0 & 0 & 0 & 0 & 1 \\ 0 & 0 & 0 & 0 & 0 & 0 & 1 & 0 \end{pmatrix}$$

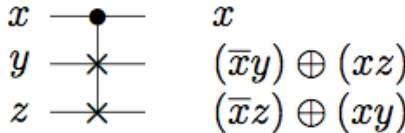
Essentially, the Toffoli gate reverses the bottom qubit if the top two qubits are 1, otherwise it leaves the qubit the same. This lets us simulate the classical AND gate if we initialize the bottom qubit in state $|0\rangle$, then we know it is in state $|1\rangle$ if and only if both top qubits are in state $|1\rangle$, thus the bottom qubit is essentially the output of an AND operation.

Any reversible gate can be implemented on a quantum computer, thus the Toffoli gate is a quantum operator. However, the Toffoli gate cannot be used by itself for UQC, it has to be implemented along with some inherently quantum gate(s) in order to be universal for quantum computation. Any single-qubit gate with real coefficients that can create a nontrivial quantum state suffices [6]. Recently a quantum mechanical Toffoli gate has been realized [16,17].

- **The Fredkin Gate:**

The Fredkin Gate, also called the CSWAP gate, is logic gate combining the logic of the SWAP and CNOT gates, is a universal reversible 3-bit gate that by performing a controlled-swap operation, swaps the last two bits if

the first bit is 1. The Fredkin gate is universal for classical computation. As with the Toffoli gate it has the useful property that the number of 0s and 1s are conserved throughout operation, which in the billiard ball model means that the same number of balls are output as input.



$$\begin{bmatrix} 1 & 0 & 0 & 0 & 0 & 0 & 0 & 0 \\ 0 & 1 & 0 & 0 & 0 & 0 & 0 & 0 \\ 0 & 0 & 1 & 0 & 0 & 0 & 0 & 0 \\ 0 & 0 & 0 & 1 & 0 & 0 & 0 & 0 \\ 0 & 0 & 0 & 0 & 1 & 0 & 0 & 0 \\ 0 & 0 & 0 & 0 & 0 & 0 & 1 & 0 \\ 0 & 0 & 0 & 0 & 0 & 1 & 0 & 0 \\ 0 & 0 & 0 & 0 & 0 & 0 & 0 & 1 \end{bmatrix}$$

- **The Controlled U Gate:**

The Controlled- U Gate is a gate that operates on two qubits in such a way that the 1st qubit serves as a control. It maps the basis states as:

$$\begin{aligned} |00\rangle &\mapsto |00\rangle \\ |01\rangle &\mapsto |01\rangle \\ |10\rangle &\mapsto |1\rangle U|0\rangle = |1\rangle (x_{00}|0\rangle + x_{10}|1\rangle) \\ |11\rangle &\mapsto |1\rangle U|1\rangle = |1\rangle (x_{01}|0\rangle + x_{11}|1\rangle) \end{aligned}$$

$$C(U) = \begin{bmatrix} 1 & 0 & 0 & 0 \\ 0 & 1 & 0 & 0 \\ 0 & 0 & x_{00} & x_{01} \\ 0 & 0 & x_{10} & x_{11} \end{bmatrix}, \quad \text{Diagram: Control line (dot), Target line (square labeled } U\text{), Control line (dot), Target line (square labeled } U\text{)}.$$

- **The Rotation Gate:**

This gate rotates the plane by θ :

$$U_R = \begin{bmatrix} \cos \theta & -\sin \theta \\ \sin \theta & \cos \theta \end{bmatrix} \quad (2.12)$$

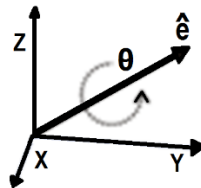


Fig. 2.1 The rotation gate showing axis of rotation.

2.4 Properties of the Hadamard Gate

The Hadamard Gate is an important special transform that maps qubit basis states $|0\rangle$ and $|1\rangle$ to two superposition states with a 50/50 weight of the computational basis states $|0\rangle$ and $|1\rangle$:

$$H|0\rangle = \frac{1}{\sqrt{2}}|0\rangle + \frac{1}{\sqrt{2}}|1\rangle; \quad H|1\rangle = \frac{1}{\sqrt{2}}|0\rangle - \frac{1}{\sqrt{2}}|1\rangle \quad (2.13)$$

This is the reason the Hadamard Gate is often used in the first steps of quantum algorithms to test all possible parallel input values.

$$-\overline{[H]} = \begin{bmatrix} \frac{1}{\sqrt{2}} & \frac{1}{\sqrt{2}} \\ \frac{1}{\sqrt{2}} & -\frac{1}{\sqrt{2}} \end{bmatrix}; \quad H|0\rangle = \frac{|0\rangle + |1\rangle}{\sqrt{2}}; \quad H|1\rangle = \frac{|0\rangle - |1\rangle}{\sqrt{2}}$$

The Hadamard operator is also hermitian and unitary, being its own inverse, $U(H, t|\psi(0)\rangle)$, where $U(H, t)$ is a unitary operator called the propagator. The propagator gives the probability amplitude for a particle to travel from one point to another in a given time, t , or to travel with a certain energy and momentum.

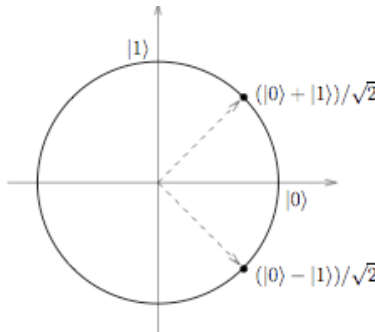


Fig. 2.2. Hadamard gate shown as R_y, R_z state rotations on the Bloch plane.

$$R_y(\pi/2)R_z(\pi) = -iH, \quad R_y(\pi/2) = \frac{1}{\sqrt{2}} \begin{bmatrix} 1 & -1 \\ 1 & 1 \end{bmatrix}, \quad R_z(\pi) = \begin{bmatrix} -i & 0 \\ 0 & i \end{bmatrix} = -iZ \quad (2.14)$$

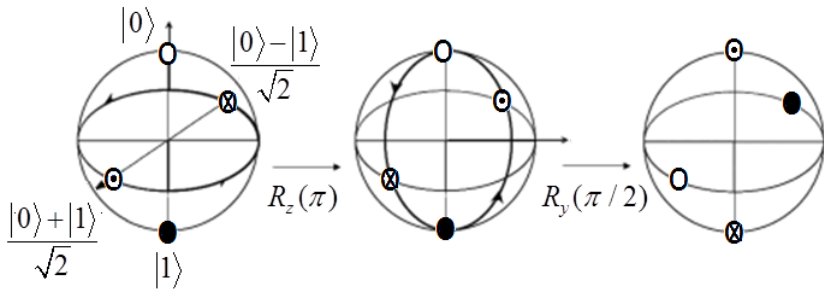


Fig. 2.3. Hadamard Bloch sphere rotation.

2.5 Rotation Gate Quantum Multiplexer

Finally, we give a brief review of recent work by Abdollahi and colleagues on their proposed multiple-control Toffoli gates for a quantum multiplexer [18]. The approach explores the synthesis of reversible functions by gates other than generalized Toffoli and Fredkin gates. They show that applying the proposed approach improves circuit size for multiple-control Toffoli gates from exponential in [19] to polynomial and circuit size for quantum multiplexers [19,20].

The θ -rotation gate ($0 \leq \theta \leq 2\pi$) around the x,y,z axes acting on a single qubit is defined as

$$R_x(\theta) = \begin{bmatrix} \cos \frac{\theta}{2} & -i \sin \frac{\theta}{2} \\ -i \sin \frac{\theta}{2} & \cos \frac{\theta}{2} \end{bmatrix}, \quad R_y(\theta) = \begin{bmatrix} \cos \frac{\theta}{2} & -\sin \frac{\theta}{2} \\ \sin \frac{\theta}{2} & \cos \frac{\theta}{2} \end{bmatrix},$$

$$R_z(\theta) = \begin{bmatrix} e^{\frac{-i\theta}{2}} & 0 \\ 0 & e^{\frac{i\theta}{2}} \end{bmatrix}.$$
(2.14)

In review, the single qubit NOT gate, $X = \begin{bmatrix} 0 & 1 \\ 1 & 0 \end{bmatrix}$, the (controlled NOT), CNOT =

$$\begin{bmatrix} 1 & 0 & 0 & 0 \\ 0 & 1 & 0 & 0 \\ 0 & 0 & 0 & 1 \\ 0 & 0 & 1 & 0 \end{bmatrix}, \text{ acting on two qubits (control and target) and the Hadamard gate, } H = \frac{1}{\sqrt{2}} \begin{bmatrix} 1 & 1 \\ 1 & -1 \end{bmatrix} \text{ are represented. A unitary matrix, } U \text{ implemented by several gates acting on several qubits can be calculated by the tensor products of their matrices; and two or more q-gates can be cascaded to form a quantum circuit. For a set of } k \text{ gates, } g_1, g_2, \dots, g_k \text{ cascaded in a q-circuit, } C \text{ sequentially, the matrix of } C \text{ can be calculated as } M_k M_{k-1} \dots M_1 \text{ where } M_i \text{ is the matrix of the } i^{\text{th}} \text{ gate } (1 \leq i \leq k). \text{ For a quantum circuit with unitary matrix, } U \text{ and input vector, } \psi_1 \text{ the output vector is, } \psi_2 = U\psi_1 [18].$$

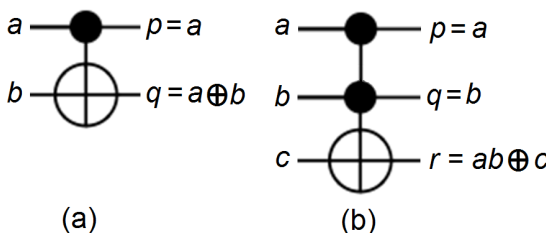


Fig. 2.4. a) CNOT gate, b) Toffoli gate.

Given any unitary, U over m qubits $|x_1 x_2 \dots x_m\rangle$, a Controlled- U gate with k control qubits $|y_1 y_2 \dots y_k\rangle$ can be defined as an $(m + k)$ -qubit gate

that applies U on $|x_1 x_2 \dots x_m\rangle$ if $|y_1 y_2 \dots y_k\rangle = |11 \dots 1\rangle$. For example, CNOT is the controlled-NOT with a single control, the Toffoli gate is a NOT gate with two controls, and $CR_x(\theta)$ is an $R_x(\theta)$ gate with a single control. Likewise, a multi-control Toffoli gate C^k NOT is a NOT gate with k controls as shown below [17,18].

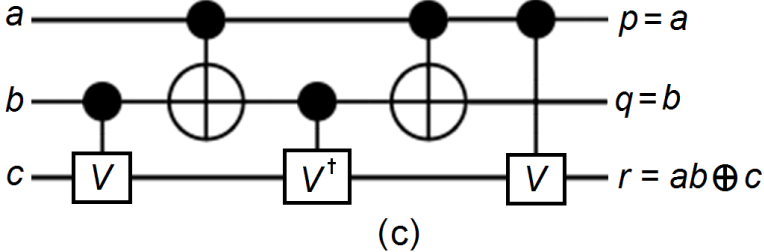


Fig. 2.5. c) Decomposition of a Toffoli gate into 2-qubit gates where $V = (1 - i)(I + iX)/2$. Redrawn from [16].

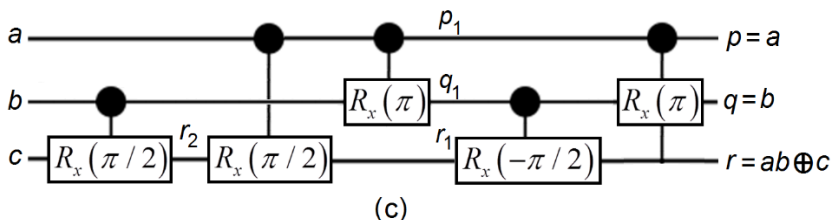
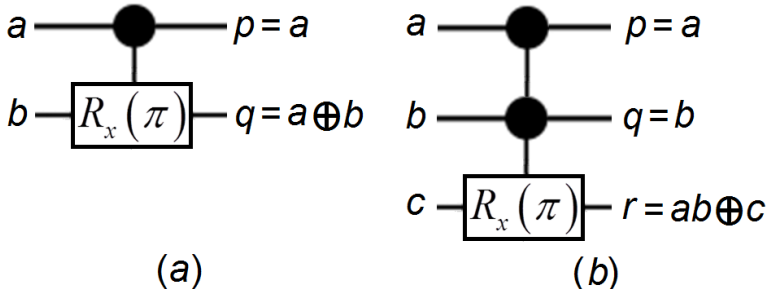


Fig. 2.6. New definitions for CNOT (a) and Toffoli (b) gates using controlled rotation gates. Decomposition of a Toffoli gate into five 2-qubit controlled-rotation gates (c). Redrawn from [16].

Under these parameters Boolean functions can be automatically synthesized by using rotations and controlled- $R_x(\pi)$ rotation gates around the x axis [18], which changes the basis states to $\hat{0} = [1 \ 0]^T$ and $\hat{1} = R_x(\pi)\hat{0} = [0 \ -i]^T$. The superscript, T stands for the conjugate transpose matrix of a vector provided the bases are orthonormal. By this basis definition of $\hat{0}$ and $\hat{1}$, the basis states remain orthogonal and inversion (NOT gate) from one basis state to the other is easily obtained by a $R_x(\pi)$ rotation gate. This means that the CNOT gate can be described using the $CR_x(\pi)$ operator shown in the figure. Additionally, the Toffoli gate can be described by the $C^2R_x(\pi)$ operator also illustrated in the figure. Finally, recall that a 3-qubit Toffoli gate needs five 2-qubit gates if $|0\rangle$ and $|1\rangle$ are used as the basis states [19].

References

- [1] Peirce, C.S. & Eisele, C. (eds.) (1976) The New Elements of Mathematics, Atlantic Highlands: Humanities Press.
- [2] Dirac, P.A.M. (1958) The Principles of Quantum Mechanics, Oxford: Oxford Univ. Press.
- [3] Feynman, R.P. (1985) Quantum mechanical computers, Optics News, 11, p. 11; reprinted in Foundations of Physics 16(6) 507-531.
- [4] Nielsen, M. & Chuang, I. (2000) Quantum Computation and Quantum Information, Cambridge: Cambridge University Press.
- [5] Barenco, A. et al. (1995) Elementary gates for quantum computation, Phys. Rev. 52 (5): 3457-3467; arXiv:quant-ph/9503016v1.
- [6] <http://www-inst.eecs.berkeley.edu/~cs191/sp05/lectures/lecture4.pdf>
- [7] <http://www-bcf.usc.edu/~tbrun/Course/lecture05.pdf>.
- [8] Abramsky, S. (2008) No-Cloning in categorical quantum mechanics, in I. Mackie & S. Gay (eds) Semantic Techniques for Quantum Computation, Cambridge: Cambridge University Press.
- [9] Bužek V. & Hillery, M. (1996) Quantum copying: Beyond the no-cloning theorem, Phys. Rev. A 54, 1844.
- [10] Bužek, V. & Hillery, M. (2001) Quantum cloning, Physics World 14 (11), pp. 25-29.
- [11] Wootters, W. K. & Zurek, W. H. (1982). A single quantum cannot be cloned, Nature 299 (5886): 802-803.
- [12] Dieks, D. (1982) Communication by EPR devices, Phys. Let. A 92 (6): 271-272.
- [13] Herbert, N. (1982) FLASH-A superluminal communicator based upon a new kind of quantum measurement, Found. Physics 12 (12): 1171-1179.
- [14] Peres, A. (2003) How the no-cloning theorem got its name, *Fortschritte der Physik* 51 (45): 458-461; arXiv:quant-ph/0205076.

- [15] Vlasov, A.Y. (2002) Comment on ‘How the no-cloning theorem got its name’, arXiv:quant-ph/0205195.
- [16] Monz, T., Kim, K., Hänsel, W., Riebe, M., Villar, A. S., Schindler, P., Chwalla, M., Hennrich, M. & Blatt, R. (2009) Realization of the quantum Toffoli gate with trapped ions, Am Phys Soc, 102 (4): 040501; arXiv:0804.0082.
- [17] Toffoli, T. (1980) Reversible computing, in J. W. de Bakker & J. van Leeuwen (eds,) Automata, Languages and Programming, Seventh Colloquium, Noordwijkerhout, Netherlands: Springer Verlag, pp. 632-644.
- [18] Abdollahi, A., Saeedi, M. & Pedram, M. (2013) Reversible logic synthesis by quantum rotation gates, arXiv:1302.5382v2 [cs.ET].
- [19] Barenco, A., Bennett, C.H., Cleve, R., DiVincenzo, D.P., Margolus, N. & Shor P. (1995) Elementary gates for quantum computation, Physical Review A, 52:3457-3467.
- [20] Cuccaro, S.A., Draper, T.G., Kutin, S.A. & Moulton, D.P. (2004) A new quantum ripple-carry addition circuit, arXiv:0410184.

Chapter 3

Multiverse Cosmology: A New Basis for Reality

The cosmological term Multiverse refers to the set of finite and infinite types of possible interconnected universes. Since the study of physical systems is typically to isolate and restrict the principle under investigation to the smallest domain feasible, why should issues of cosmology enter into a discussion of Quantum Information Processing (QIP)? As we hope to adequately demonstrate in this volume, the situation has dramatically changed recently; QIP has not and cannot be achieved beyond a few qubits by continuing to utilize the nonphysical mathematical representation of qubits on a Bloch sphere in Hilbert space as its basis. One might do better to define a qubit as a ‘realiton’, a complete microcosm of reality itself; and emphatically, since reality can no longer be considered fundamentally quantum, that microcosm must encompass whatever a localized segment of the multiverse entails in order to holistically process information! Therefore, an operationally sufficient understanding of the penultimate basis of reality (cosmology) appears mandatory in order to incorporate the newly perceived requirements of relativistic information processing and topological QC from the point of view of Unified Field Mechanics (UFM).

It is sensible and prudent...to think about alternatives to the standard model, because the evidence is not all that abundant...and we do know that the standard cosmological model is pointing to another surprise...because (it) traces back to a singularity. – P.J.E. Peebles [1].

3.1 Overview

Multiple universes are posited to occur by infinitely extending spacetime, or by ‘eternal inflation’; the idea that the universe expanded rapidly after the Big Bang (like a balloon), suggests some pockets of space stop

inflating, while other regions continue to inflate, producing numerous isolated ‘bubble universes’. There are numerous ‘eternal’ Big Bang scenarios such as the ‘Big Crunch, or the ‘Big Bounce’ where expansion stops, reverses and then collapses back into itself with various posited results. There is the ever popular ‘Parallel Universe’ model with several scenarios like the prospects of alternate braneworlds suggested by string theorists, where multiple dimensions beyond the three we observe contain other 3D braneworlds similar to ours but hidden from us in the non-observed higher dimensional (HD) branes. Weinberg suggested that if the multiverse existed, *“the hope of finding a rational explanation for the precise values of quark masses and other constants of the standard model that we observe in our Big Bang is doomed, for their values would be an accident of the particular part of the multiverse in which we live.”* [2]. This is not the only interpretation; we have, among others, suggested that the fundamental constants of nature may be fine-tuned or vary subtly according to precise parameters occurring in other ‘pockets’ of the multiverse [3]. Our mantra is: *‘The multiverse has room for an infinite number of nested Hubble spheres (universe we observe) each with their own fine-tuned laws of physics’*. Under this panoply we postulate that, the Hubble sphere is finite and closed temporally, but open and infinite beyond the temporal limit of observation. This is the antinomy pointedly argued by Leibniz and Newton.

Although popular, Big Bang cosmology still contains critical untested assumptions and unresolved logical conflicts. Recent observational and theoretical insights suggest it has become feasible to consider developing a new standard model of cosmology. Parameters for developing such a Continuous-State Holographic Anthropic Multiverse cosmology are developed herein. The new Multiverse cosmology is based primarily on a fundamental least cosmological unit (LCU) tiling the spacetime backcloth of a 12D superspace making correspondence with SUSY parameters of M-Theory, introduces the origin of complexity in self-organization and refines the long sought role and nature of the observer in physical theory.

3.2 Introduction to Cosmological Issues

We have recently entered one of the periodic transitional phases in the evolution of fundamental theories of physics, giving sufficient pause to reinterpret the general body of empirical data. Recent refinements in observation of cosmic blackbody radiation [4] and various programs of theoretical modeling [5,6] suggest it might be reasonable to explore

replacing or modifying the naturalistic Big Bang cosmology. A Continuous-State Holographic Anthropic Multiverse based on alternative interpretations of the observational data is introduced in preliminary form. We begin by reexamining the main pillars of the Big Bang, briefly review alternate interpretations, and then introduce some of the alternative general parameters for a holographic anthropic multiverse cosmology [3,5].

Reviewing the historical development of physical theory illustrates the fact that two general models, one unitary and the other dualistic, have evolved simultaneously in the scientific literature:

- Unitary Model. Naturalistic, Darwinian, Newtonian; a classically oriented model aligned with current interpretations of the standard models - i.e. Big Bang Cosmology, Bohr's phenomenological interpretation (Copenhagen) of Quantum Theory, standard Maxwellian Electromagnetism (em) and Einstein's General theory of Relativity. Many unanswered questions like the breakdown of Maxwell's equations at singularities remain.
- Dualistic Model. Includes all conventional wisdom pertaining to the above model plus extended theory like the de Broglie, Bohm, Vigier, Cramer models of quantum theory implying a covariant polarizable Dirac vacuum with additional parameters and interactions like a massive photon, m_γ and where Maxwell's equations do not cutoff at the vacuum. Best evidences are the Casimir, Zeeman & Aharonov-Bohm effects. Offers plausible explanations for unanswered questions like the Proca equation for em theory. The model also allows room for teleological causalities.

Only in the context of the dualistic parallels of *extended theory* can a multiverse cosmology of the type we envision be viably presented. The concept of a covariant polarizable Dirac vacuum introduces an additional causal order not deemed acceptable in physical theory because it was considered unreasonable that spacetime could contain such an ordered periodicity or significant additional symmetry [3]. As discussed below, a dual causality and additional vacuum symmetry invites extension of the Wheeler/Feynman [7] radiation law beyond Cramer's [8] transactional interpretation of quantum theory to string/brane topological dynamics of spacetime topology itself where an 'eternal' *present state* [9] is comprised of a continuous *future-past advanced-retarded HD standing-wave* [10,11].

The multiverse is intended as the next evolutionary step in the progression of modern cosmological modeling stemming from Einstein's

1917 proposal of a Static Universe (ESU) [12] and the banner 1948 development of both the Steady-State Universe (SSU) of Bondi, Gold [13] & Hoyle [14] and the Big Bang by Alpher, Bethe & Gamow [15]. Although multiverse cosmology could be considered a form of ESU or SSU modeling, it is sufficiently different to require a proliferation of nomenclature. For example the multiverse has neither inflation or expansion; and the multiverse is not confined to the limits of the $3(4)D + N_c$ Einstein/Minkowski/Riemann/Hubble sphere, H_R incorporated in the currently touted standard Big Bang and SSU models.

The multiverse paradigm introduces a revolutionary structural change in the universe. The Hubble sphere, H_R represents only an observational limit, not the physical limit as in Big Bang cosmology. Fundamental multiverse space is a complementarity of a new absolute 12D space and our observed E_3/M_4 relational spacetime. Multiverse cosmology has non-local holographic-like properties entailing a Multiverse of a potentially infinite number of nested *relational* Hubble-type domains, each with different fine-tuned laws of physics and complete causal separation from our 3D Euclidean, 4D Minkowski, E_3/M_4 realm [16]. The additional compact subspace dimensions, N_c [17,18] hypothesized as compactified in the initial Big Bang event are not a subspace of our E_3/M_4 domain, rather in multiverse cosmology E_3/M_4 is the subspace of the 12D superspace.

‘Our’ whole *relational* Hubble sphere, H_R is a subspace of an absolute 12D hyperspace without dimensionality as now defined. Additional dimensions are not compact, but ‘open’ and of infinite size, LSXD [19,20], undergoing a process of ‘continuous compactification and spin exchange dimensional reduction’ for the benefit of the Euclidean 3-spaced Earth observer as the complex HD ‘standing wave’ of the present is continuously created and recreated by future-past advanced-retarded SUSY breaking dynamics. They are unobserved not because they are microscopic, but because of a ‘subtractive interferometry’ inherent in the topology of the hyperspherical ‘future-past’ present. The idea of dimensionality in multiverse cosmology is a tricky business on first bite. Under the umbrella of a 12D atemporal, timeless or eternal absolute space of LSXD (the footstool of the Multiverse relative to our H_R) a domain of spacetime drops out. The properties of this spacetime are solely for the benefit of the observer imbedded in it. Spacetime dimensionality is a scaled continuum; SUSY properties are for large XD $> 4D$ and symmetry breaking $< 4D$ compactifying to $\sim 0D$ where an Ising flip of the Riemann 3-sphere (LCU) [21] begins the cyclic process over again. As will be clarified, this is what

gives rise to the arrow of time and why the XD are not directly observed. It is the basis of observed reality as a virtual UFM multiverse subspace.

3.3 Clarification of Pertinent Cosmological Nomenclature

Since the terms Holographic, Anthropic and Multiverse have many disparate uses it seems reasonable to clarify these key terms before we begin to earnestly delineate the properties of multiverse cosmology. This discussion is not exhaustive or even very detailed; it is only to provide an introduction and to distinguish our view of requirements for bulk QIP from the others. Obviously our viewpoint is neither the popular or politically correct view. But this is the way it sometimes is in the history of science, leapfrogging from one antipode to the another.

Multiverse Cosmology

Generally, Multiverse, is the hypothetical set of multiple possible universes (including our Einstein-Hubble universe) that together comprise all of reality. The different universes within the multiverse are sometimes called parallel universes. The structure of the Multiverse, the nature of each constituent universe and the connection between them depends on the particular multiverse hypothesis being considered by the theory. But the term universe is supposed to represent the entirety of all existence; however, with usages like ‘Mr. Tompkins Universe’ or the universe of the ant, one has become accustomed to the idea of many universes at least in the common vernacular. Interestingly the term Multiverse was first coined in 1895 by American psychologist William James. In scientific circles many disparate definitions of Multiverse exist such as parallel universes, Bubble universes, alternate realities as in Everett’s Many Worlds interpretation of quantum theory containing every possibility, or the 11D extension of string theory known as M-theory where our universe and others are purported to be created by collisions between membranes in an 11D space. An attempt to clarify and classify the various forms of possible Multiverse cosmologies into four types has been presented [22], but the attempt has caused some controversy of its own. Unfortunately, we contribute to the diversity of multiverse forms. For our multiverse cosmology the multiverse is an ensemble of holographically embedded Hubble domains, H_R each causally separated in their own domain with their own fine-tuned laws of physics. Each H_R domain is a self-organized complex system and as such operates with the principles and dynamics attributed to such systems such as incursion and scale-invariance [10,11].

Anthropic Principle

The term ‘anthropic principle’ was first used at a 1973 symposium in honor of the 500th birthday of Copernicus by astrophysicist Brandon Carter. The anthropic principle refers to the assertion that scientists need to take into account the fact of the existence of life when developing their theories. This stems from the observation that the physical constants of nature all seem to be fine-tuned in a significantly balanced manner that promotes the existence of complex living systems [23]. If the four fundamental forces or fine-structure constant differed very much there would be no stars, chemical elements, or chemical elements beyond lithium and then of course life as we know it could not exist.

Carter defined the two forms of the Anthropic Principle currently in use, the ‘weak’ anthropic principle referring to the idea of privileged spacetime locations in the universe, and the ‘strong’ form of the anthropic principle which addressed the values of the fundamental constants of nature. Barrow and Tipler [24,25] in a detailed work formed different definitions of the weak and strong anthropic principles. They also argue extensively that it is highly probable that human life is the only intelligent life in the Milky Way galaxy. We strongly disagree. We believe that intelligent life is the rule, not the exception and that this is what the anthropic principle is all about. This is suggested twice in Carl Sagan’s Hollywood film *Contact*, if not: “*it would be an awful waste of space*”.

Weinberg suggests the Anthropic Principle could be utilized by cosmologists opposed to theism as a ‘turning point’ in science by applying it to the string landscape to “... *explain how the constants of nature that we observe can take values suitable for life without being fine-tuned by a benevolent creator*” [26]. Interesting that the same principle can be used for opposite purposes. Weinberg’s view is opposite to the anthropic views presented here. We propose that teleological or eutaxiological bases are tantamount to the essence of anthropic cosmology itself suggesting that the anthropic principle entails an additional action principle driving or guiding cosmological evolution in opposition to the postulate of random Darwinian or naturalistic evolution of Big Bang cosmologies. This new action is believed to be synonymous with the action of the unified field which historically has also been equated with chi, ki, *prana*, the *élan vital* or spirit of God [10,11]. Please allow this politically incorrect ‘heresy’ in passing: Copernicus waited until he was on his death bed; Galileo was nearly executed for his views, perceived to conflict with the theism held by those with untoward control of society at the time. A quick search easily shows that there are no verses promulgating

requirements for ‘perfect spheres’ or an Earth centered universe. Theology and science then are not mutually exclusive, but opposite ends of the long spectrum of human epistemology. Greek mathematician Hipparchus discovered heliocentricity 2,000 years before Copernicus, but tossed it because of the ‘perfect sphere’ issue. Apologies if we have offended anyone’s reason; hopefully sufficient academic freedom exists to venture an opinion without myopically tossing out the smiling baby herein along with the gray bathwater.

String theory predicts a universe with a virtually infinite number of possibilities (Googolplex, 10^{∞}) for a unique string background or vacuum. This set of vacua has been called the Multiverse, anthropic landscape or string landscape. Susskind suggests this possibility for a large number of vacua strengthens anthropic reasoning: “*only universes whose properties are such as to allow observers to exist are observed, while a possibly much larger set of universes lacking such properties go unnoticed*” [27].

Holographic Principle

The holographic principle was developed as a property of quantum gravity theories by 't Hooft [28] and Susskind [27,29] to explain the information paradox of black holes in terms of string theory. Susskind states the principle as a description of a volume of space encoded on a boundary of the region, usually a light-like boundary such as the Schwarzschild gravitational horizon for a black hole. For black holes the holographic principle states that the information of all objects falling in is entirely contained in surface fluctuations of the black hole’s event horizon.

In a more speculative manner, it has been suggested that the multiverse is a 2D information structure like a 2-brane hologram [28,30]. To create a theory of holographic cosmology is considered a challenge because of expansion of the cosmological horizon in the Big Bang model where a finite area expands over time. We don’t see that this would necessarily be a problem as the structure could still remain invariant under the transformation. However, there is no expansion or inflation in our model where we take the ‘world as a hologram’ idea fairly literally. We don’t consider the 2D information surface of ‘t Hooft and Susskind [28,30] sufficient for a cosmology; for information of a black hole event horizon perhaps [31]. But for our multiverse model we postulate that the hologram is a duality of a local spacetime (image) projected from an HD topological hypersurface with the fundamental Gabor ‘logons’ being the dynamic system of cosmological LCUs tesselating it. This can only be elucidated

by solving some of the fundamental issues of string theory such as: Does gravity require 6D, or Schöenflies Theorem [32] which states that there can be no torsion in the plane; and does this preclude the lower limit suggested by 't Hooft and Susskind for information on the surface of a holographic 2-brane. Of course their purpose was concerning black holes and not a complete multiverse cosmology. Tired-light, by minute photon mass, $m_\gamma = 10^{-62}$ g is an alternative interpretation for Doppler redshift.

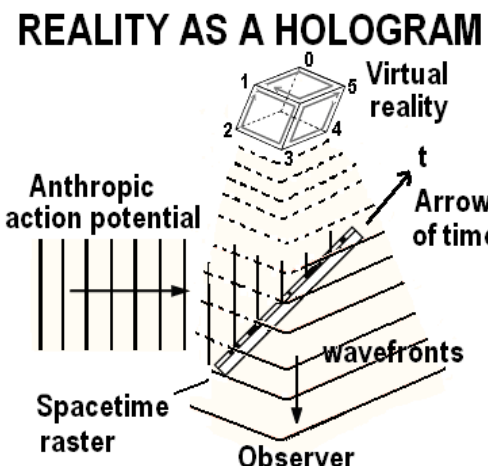


Fig. 3.1 Reality modeled as an HD holographic construct in continuous motion, with the 'laser' being the coherent anthropic UFM action principle, an inherent extended de Broglie Bohm-like super-quantum potential 'piloting' its continuous evolution.

A hologram is formed by simultaneously exposing a photographic plate to laser light from a reference beam and laser light reflected from the object employed. The two beams are out of phase which creates interference; it is the interference pattern that is recorded on the 2D photographic plate. A 3D image of the object is reconstructed by illuminating the hologram (plate) with coherent light. Eventually one might suppose an HD holographic multiverse cosmology could be fully developed to rigorously describe reality, matter and living systems [11] by the continuous-state action of the anthropic unified field.

In summary, multiverse cosmology is a hyper-dimensional hologram with room for an infinite number of nested Hubble spheres all in local causal separation and out of phase with each other (invisible). This allows each Hubble sphere to have its own fine-tuned laws of physics; and also can explain dark energy as weakly interacting multiverse energy.

3.4 Parallel Interpretations of Cosmological Data

TABLE 3.1

PARAMETER	BIG BANG	MULTIVERSE COSMOS
REDSHIFT	Doppler recession of an inflationary expanding universe. ($m_\gamma = 0$)	'Tired light' phenomena, non-zero mass photon ($m_\gamma \neq 0$) couples to vacuum dissipating energy.
CMBR	2.75° K blackbody remnant of initial hot cataclysmic explosion ~ 15 billion years ago.	Result of continuous-state blackbody emission by spacetime cavity-QED electrodynamics inherent in a continuous compactification D reduction process.
OLBER'S PARADOX	Expansion of the universe accounts for dissipation of luminosity.	Lifetime of stars insufficient to illuminate heavens; absorption by vacuum coupling and dispersion by interstellar media.
MATTER	Matter creation at initial Big Bang. Missing dark matter or dark energy required to explain galactic rotation etc.	Dark energy - balances the gravitational potential, Λ by multiverse matter. Results in flat spacetime. Spontaneous creation of matter; black hole evaporation removes evolved material.

3.5 Euclidean Minkowski Geometry as Basis for Observed Reality

- The Euclidean line is assumed to be the real line [16] because it is what is observed. Logical reasons from supersymmetry and super-gravity suggest there are a number of additional unobserved dimensions [17] leaving the issue of dimensionality as an open question. Euclidean space in classical Newtonian terms is a continuous 3D absolute space with time an independent parameter.
- Einstein's theories of relativity provided a discrete 3(4)D transmutable relational spacetime manifold. The debate between absolute space or substantivism and relational space still continues unabated. Utilizing the standard definition of a straight line as the intersection of two rigid planes, measurements could be taken to observe whether the angles of a triangle add up to 180°; but settling the question definitively would require

astronomical scale measurements where it appears physically impossible to apply the concept of a rigid body or to define a straight line in terms of a light ray by stellar parallax because of the effects of general relativity. Therefore, all physics knows with certainty at the present time is that observed space is approximately Euclidean as is Minkowski space [16,33].

- According to the proof of Schöenflies theorem [32] there can be no torsion or topological knots in a plane. Therefore, there can be no torsion in a 2D reality; thus the real line must be at least 3D Euclidean where the standard Pythagorean line element is:

$$ds^2 = dx_1^2 + dx_2^2 + dx_3^2 \quad (3.1)$$

- This assumption that the Euclidean line is the real line is intuitive. Currently there is no known method of empirical proof; and since the Euclidean line is what the human mind apprehends it has remained the formal basis for all scientific fact until now [16,24]. But this assumption remains profoundly problematical with issues stemming from both the foundations of mathematics and the nature of physical theory itself concerning the fundamental basis for sets, discreteness versus continuity, geometry and topology, and the relationship of real numbers to rational numbers for example [16]; leaving sufficient wiggle room to move beyond 3-space as the fundamental basis for observation or QIP.
- In general, the class of theories unifying gauge and gravitational fields by utilizing XD is called Kaluza-Klein theory. In these theories spontaneous symmetry breaking by coordinate transformation in 5D is a product of the standard 4D transformation and a local U(1) gauge group arising in basic form in a general relativistic framework of 5D described according to the Einstein-Hilbert action

$$A = \int d^5x \sqrt{g} R . \quad (3.2)$$

Where in Eq. (3.2) instead of postulating a 5D Minkowski space, \hat{M}^5 as the ground state, the ground state is taken to be the product $M^4 \times S^1$ where the circle S^1 is a U(1) group of rotations [17]. In conventional supersymmetry models the radius of circle S^1 is considered to be microscopically small on the order of the Planck scale, (10^{-33} cm , 10^{-43} s) very short and very fast, used to explain why these XD are not observed.

This will be discussed in more detail below where Planck's constant is reevaluated utilizing the Larmor radius of hydrogen as it relates to non-compactified Kaluza-Klein theory [34].

An $SU(3) \times SU(2) \times U(1)$ gauge symmetry group can be used to describe all known particle interactions. Following Witten [17], the minimum number of dimensions of a manifold with this symmetry is 7D. In this $SU(3) \times SU(2) \times U(1)$ symmetry group gauge fields arise in the gravitational field as components of more than 4D. This yields a dimensionality for our reality of at least four non-compact and seven compact spacetime dimensions, $M^4 \times S^7 = 11D$, which Witten [17] calls a *remarkable numerical coincidence* since this 11D maximum for supergravity is the minimum for $SU(3) \times SU(2) \times U(1)$ symmetry which also for symmetry reasons observed in nature is in practicality the largest group one could obtain from Kaluza-Klein theories in 7XD. As shown in Chaps. 6,15 our XD interpretation is different, $M^4 \times \mathbb{C}^{14} = 12D$ with the additional dimension a required control factor of the unified field.

This gauge group for gravitational field components is insufficient to describe nature; for a complete theory quarks and leptons plus a Higgs or alternative type mechanism triggering symmetry breaking must be added to the Kaluza-Klein framework. In attempting to complete the theory, the gauge coupling constants are determined by calculating the Einstein action over the compact dimensions. This scales at a high power of $1/(M_p R)$, where M_p is the Planck length and R the radius of the XDs showing that R must actually be in the $10^{-33} cm$ range for these standard model gauge theories. If one adds the Lagrangian of a cosmological constant, Λ , Witten finds one can form a reasonable theory [17]. Our UFM XD are part LSXD.

Although only introduced in a preliminary form here, a different view is required by UFM theory because the Einstein gauge is both classical and incomplete. Multiverse Cosmology like any new theory must however bear correspondence to the established Einstein gauge. The existing derivation of Planck's constant represents classical mathematical limits only, and are not actual physical limits in Multiverse Cosmology [34].

3.6 Philosophy of Space in Multiverse Cosmology-Origin of Structure

Although the concept of Absolute Space (AS) as defined by Newton is discarded in contemporary physics, a deeper more fundamental form of AS nevertheless seems to exist and is a required foundation for LSXD

UFM Multiverse Cosmology. The multiverse reintroduces a complementary AS that is non Newtonian because Newtonian AS, once considered the basis of ‘our space’, first of all is only a form of Euclidean space without sufficient degrees of freedom to incorporate Quantum or Relativity theory. Multiverse AS is different, but similar enough that Newton deserves credit for realizing the importance of AS. Secondly, the relational space of the Einstein universe contains insufficient symmetry parameters to describe the additional causal properties of a supralocal UFM Multiverse. The AS proposed by the multiverse (defined in postulate 3.1) represents the ground of all existence and possibly ‘resides’ beyond the observed Hubble universe or even the infinite number of other possible supralocal nested Hubble-type spheres (with varied laws of physics) [3,13]. The ultimate nature of multiverse AS remains ineffable at the moment, but empirical tests are being prepared [35,36]. In the meantime, we can deduce some AS properties to steer empirical investigations to higher order properties these deductions suggest.

Postulate 3.1: *Space is the most fundamental ‘form or substance’ of existence; and the origin of all structure. The metrical demarcation and translation of which constitutes the basis of all energy or phenomenology. Space takes two forms in multiverse cosmology, Absolute Space and the temporal relational subspaces that arise from it. A basis for energy (space geometry) is a fundamental form of information which signifies the cosmological foundation of causality. This postulate also connotes the most rudimentary basis of structural-phenomenology.*

The complementarity between the new concept of AS in Multiverse Cosmology and the contemporary relational space suggested by Einstein’s theories of relativity can be simplistically represented as a ‘virtual reality’ by interpreting UFM multiverse AS as a fundamental background space of the related space fields referred to by Einstein’s quote below regarding the nature of space and time.

Time is a complex process only just beginning to be addressed by physicists [37]. One can say that all forms of time [37-39] represent various types of motion and in that sense time can be discounted as a concept (i.e. - not absolutely fundamental). Then geometric translation or field propagation becomes more fundamental. Thus space (whatever it is) is the most fundamental concept of the universe. Space with boundary conditions or energy is fundamental to all forms of matter.

3.7 Space: Relational Versus Absolute

The conceptual disparity regarding the fundamental nature of space arises in terms of correspondence between the Newtonian worldview of a continuous Absolute Space in opposition to the current Einsteinian view of discreteness of the spacetime manifold. This debate about the nature of space has continued at least since Aristotle. Einstein in his last published statement regarding the nature of space and time said:

The victory over the concept of absolute space or over that of the inertial system became possible only because the concept of the material object was gradually replaced as the fundamental concept of physics by that of the field...The whole of physical reality could perhaps be represented as a field whose components depend on four space-time parameters. If the laws of this field are in general covariant, then the introduction of an independent (absolute) space is no longer necessary. That which constitutes the spatial character of reality is then simply the four-dimensionality of the field. There is then no 'empty space', that is, there is no space without a field [40].

Einstein's view is a form of the *relational theory* of space introduced initially by Leibniz and Huygens [41,42]. Relationalism is in opposition to *substantivism* which gives space the ontological status of an independent reality as a kind of *substance* [43]; the Newtonian concept of absolute space being the prime example.

Finding the founding fathers of quantum theory credible in their declaration that the standard model is incapable of describing biological systems; means awareness can only be defined adequately by extending all the standard models since they are so intertwined. This means that:

- The standard cosmological model - the Big Bang is insufficient.
- The standard mechanistic model of biological naturalism is inadequate.
- The standard Turing model of computation is inadequate.
- The standard model of gravitation is insufficient.
- The standard Copenhagen phenomenological model of quantum theory is inadequate.
- The standard model of electromagnetism is inadequate.
- The standard cognitive model of neuroscience is also insufficient.

This criticism does not mean these seven models are wrong; only that they go part way. The focus here is primarily on the cosmological model as it is the root of the problem. The required parameters of the post Big Bang universe will be stated axiomatically for simplicity. The domain of

the Big Bang is defined in terms of the Hubble radius, H_R for the large-scale structure of the universe and the Planck scale for the microscopic. The large-scale observational limit according to Big Bang philosophy is caused by the Doppler effect on light propagation due to the recessional velocity of expansion of the universe. This observational limit occurs where light becomes attenuated to zero by the redshift.

The Hubble radius, H_R remains an observational limit in Continuous-State Anthropic Multiverse cosmology also but is not caused by the Doppler effect. It is due to a minute non-zero rest mass for the photon [3,43]. As a photon propagates it couples to the polarized Dirac vacuum and loses energy also attenuating to zero observability; but if one were able to travel to the Hubble limit, observation would extend for another H_R ad infinitum. Thus a critical difference in interpretation of redshift – a physical limit for the Big Bang and an observational illusion in multiverse cosmology.

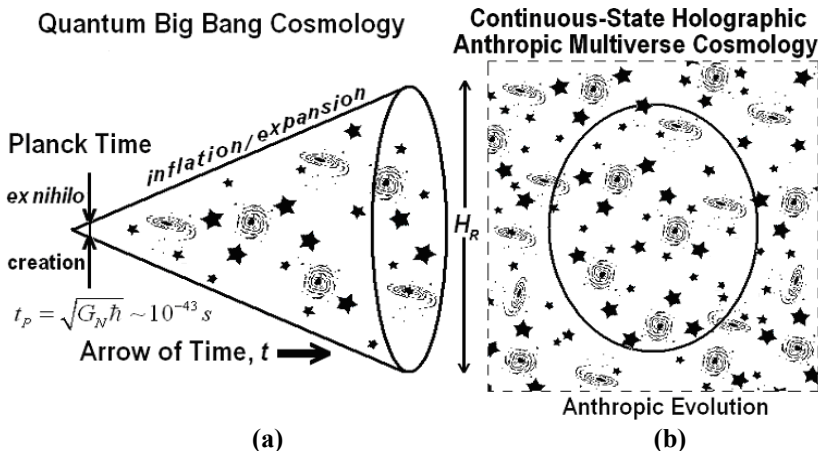


Fig. 3.2 a) Symbolic lightcone view for the origin of the universe from an initial temporal singularity showing spatial inflation/expansion as in a Big Bang cosmology. b) Atemporal multiverse cosmology with H_R observational limit. Planck time $t_p = \sqrt{G_N \hbar} \sim 10^{-43} s$.

Einstein by the introduction of special and general relativity replaced the absolute 3D Newtonian continuum with a discrete 3(4)D E^3/\hat{M}^4 , $+, +, +, -$ relational spacetime manifold. This space can still be interpreted as a potential Big Bang space terminating at the impenetrable Planck backcloth of stochastic foam. Noetic cosmology changes the interpretation of this limit. The Planck barrier is only a virtual mathematical barrier to

Fermions as the present recedes into the past as interpreted by Cramer's transactional model with a present instant as a standing-wave future-past.

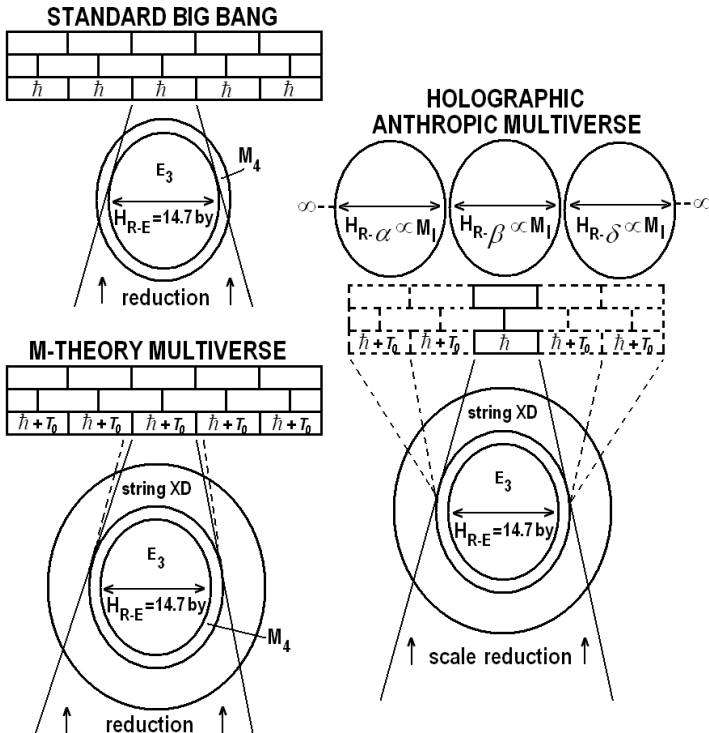


Fig. 3.3 Contrast of the three main cosmological models illustrating dimensionality relative to the Planck constant, \hbar and dimensionality. H_{R-E} is the Hubble radius for an Earth observer, E_3 & M_4 Euclidean and Minkowski space. In c) other fine-tuned H_R s exist beyond the virtual Planck barrier, not experimentally accessible by standard quantum theory.

The multiverse [3,43] has the potential for an infinite number of nested Hubble spheres in causal separation and thus with their own fine-tuned laws of physics [44]. In the Big Bang the XDs laid down at the beginning of time are curled up at the Planck scale as a compactified subspace. In the multiverse cosmology, the opposite is true. A new form of HD Absolute Space is comprised of a periodic 12D space. The standard observed relational Einstein reality, $3(4)\text{D } E^3/\hat{M}^4$, is a subspace projection of the 12D AS space. An extension of the Wheeler-Feynman absorber theory of radiation [7] is utilized to define an eternal *present* as a standing wave of

the *future-past* that is ‘covered’ at each level of scale by an HD Wheeler Geon-like [45] unified field ‘ball of light’. However, the UFM Geon is not electromagnetic as Wheelers is, but a noeon field filling the ubiquity of nonlocal space; it is the unified field acting as an energyless ontological ‘topological charge’. Noeon flux is equated to Mach’s principle and the reason gravity is not quantized. As will be derived below this action principle can be described by a simple fundamental Noetic equation $F_{(N)} = \mathbf{x} / \rho$ [43,46,47].

The world lines of relational space are virtual extensions created and recreated harmonically by the torsion of the continuous compactification process. Therefore, instead of a rigid impenetrable Planck barrier covered by a stochastic foam of particle creation and annihilation, multiverse cosmology has a periodic ordered spacetime with a complex hyperstructure that is closed and finite in time for fermions, but open and infinite atemporally for noeons. In the multiverse model, stochasticity, i.e. zero-point string or brane dynamics, arises in the wake of unitary graviton propagation guiding the dynamics of the continuous-state. Again note that XD are not observed because they are curled up microscopically at the Planck scale, but rather because of a subtractive interferometry process related to the nature of the arrow of time.

The noetic UFM graviton, is a quadrupole photon complex (Fig. 3.21) confined to the spacetime metric like quarkonium [6]; a probably seemingly absurd statement standing alone, but it is beyond the investment we are willing to make for this chapter (see Chap. 12). The Planck singularity (10^{-33} cm), 10^{-43} s is *virtual*, a geometric orientation that arises as the present recedes into the past during a Cramer transaction compactification process [43]. The Big Bang is said to originate from an initial singularity; this is an observational illusion in a multiverse where the arrow of time arises from continuous-state spin-exchange dimensional reduction compactification by an uncoupling recoupling process during deficit angle production during parallel transport of topological charge around the close-packed cosmological least-units tessellating spacetime. That mantra is a lot to swallow and is addressed more adequately in [3].

In Fig. 3.3 H_R is an observational limit, not because of temporal Doppler expansion of the universe as postulated in Big Bang cosmology but because of infinitesimal photon mass, m_γ [5,48]. Because Gauge

Theory is only an approximation, the Planck constant, \hbar is not a fundamental ultra-microscopic singularity and is reformulated in multiverse cosmology utilizing the original hadronic form of string theory

with variable string tension [49]. Its zero point oscillates from the usual \hbar to $\hbar + T_0$ which has an upper limit of the Larmor radius of the hydrogen atom. This is because the new singularity is the Witten string vertex [50].

Evolving concept of extra dimensions from Planck scale Riemann spheres to Calabi-Yau 3-forms.

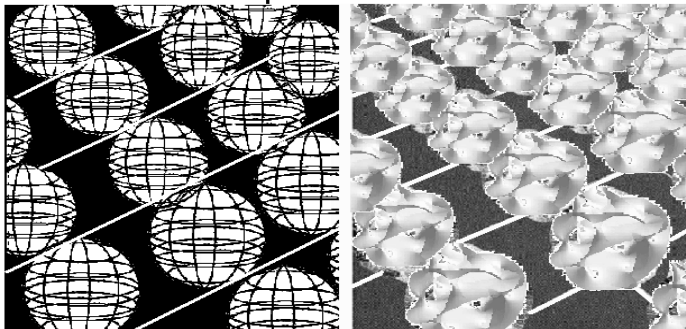


Fig. 3.4. a) Kaluza-Klein XDs as originally considered curled up microscopically at each spacetime point. b) More complex view 30 years later in terms of Calabi-Yau dual 3-torus topology. With the application of multiverse string tension, $\lambda + T_0$ compactified lower dimensional (LD) 3-forms provide a manifold of uncertainty of finite radius hiding infinite size LSXD beyond. λ is based on the original em Stoney precursor to \hbar .

Because our observed Euclidean temporal reality is a virtual subspace of an HD atemporal realm, the arrow of time, the propagation of which ‘creates’ our observed 3-space Euclidean reality, time is a complex system. The Hubble radius, H_R is still an observational cosmological limit, but instead of being indicative of a Doppler expansion of spacetime, arises as part of the complex self-organized structural-phenomenology of the continuous-state dynamics. The energy of the photon with infinitesimal mass, m_γ anisotropy [5,48] attenuates to zero such that an observer traveling to H_R would be able to see out to an additional H_R .

According to Cramer: The transactional interpretation of quantum mechanics is a nonlocal relativistically invariant alternative to the Copenhagen interpretation. It requires a ‘handshake’ between retarded, (ψ) and advanced waves, (ψ^*) for a quantum event which he calls a ‘transaction’ in which energy, momentum, angular momentum, and other conserved quantities are transferred as a standing wave [8]. As a 1D standing wave, this has been criticized as too primitive; but when extended

hyperspherically to 12D along with de Broglie-Bohm potentials associated with a force of coherence relegated to the unified field, it is sufficient.

Table 3.2 PROCESSES FORMING THE STANDING WAVE PRESENT

Dimensional reduction	Continuous Compactification
Spin exchange	Parallel Transport
Deficit Angle	Continuous-state 'Free Fall'
Holographic Principle	Future-Past Transaction
Super Quantum Potential	Anthropic Action Principle
Advanced / Retarded	Complex HD
Mirror symmetry/duality	Coordinate leapfrog

3.8 Physical Cosmology of Fundamental Least Cosmological Unit

Theories avoiding completely the notion of the continuum are, of course possible in principle. But the attempt is not so simple as you seem to believe. The interesting question is if on logical grounds (simplicity) a plausible choice of axioms is possible. Of course, the concept of time (continuum) could not enter such a theory. – Einstein, 1952.

Least Cosmological Unit and its Basic Complex

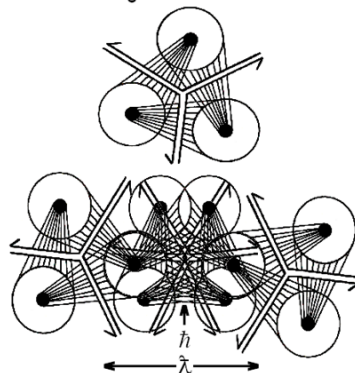


Fig. 3.5 a) Conceptualization of the triune nature of an isolated least-unit with a central Witten string vertex not existing free in nature. b) The central portion denoted by \hbar represents one virtual Euclidean point which oscillates harmonically to \sim the Larmor radius of a hydrogen atom here denoted as λ which represents the new Stoney representation of \hbar plus string tension, $T_s = (\lambda + T_0)$ modeled as an HD Cramer transaction.

In Fig. 3.8 an advanced-retarded future-past transaction is represented as an instant of the eternal present. The Planck constant, \hbar still exists in multiverse cosmology but represents a virtual lower limit of the SUSY

topology as constituents of the least-unit complex are compactified as they cyclically recede into the past in preparation for the next HD Cramer-type transaction cycle. The *Stoney* representation, λ signifies the ‘open’ future orientation of this portion of the continuous-state cycle and is also chosen because of the extended em properties of the Dirac polarized vacuum.

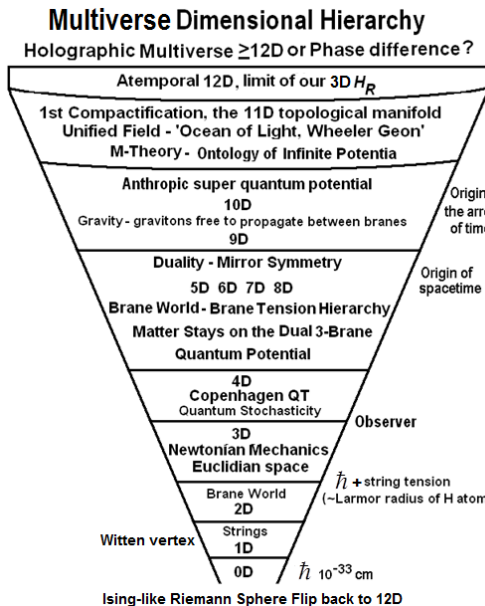


Fig. 3.6 The 12D multiverse cosmology hierarchy underlying the continuous-state compactification process that produces our observed virtual reality with subtractive interferometry of the LSXD hidden behind the quantum ‘veil of uncertainty’.

Conventional 11D M-Theory searches for one unique compactification within which to formalize a completed string theory model. This line of reasoning is a product of Big Bang cosmology and the Copenhagen interpretation of quantum theory suggesting nucleons were created around the time of the original singularity and a particular compactification was produced forming the basis of our reality. Multiverse cosmology does not have these constraints. Compactification is a self-organized continuous-state process through all possible dimensional compactification formats. This gives the cosmology unique characteristics; especially an anthropic UFM action principle driving its self-organization.

Time and space are modes by which we think and not conditions in which we live. - Albert Einstein, 1941.

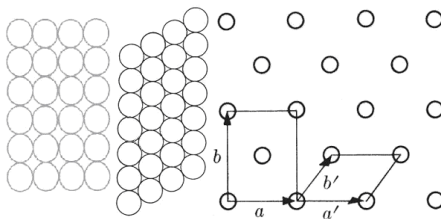


Fig. 3.7 Conceptualization of close-packed least cosmological units (LCU) and how Euclidean/Minkowski geometry might naturally emerge from its domain walls. Transformation from square to hexagonal close-packing can aid the compactification process in deficit angle parallel transport caused by gravitational curvature.

The new multiverse UFM cosmology is based on principles of the Wheeler-Feynman absorber theory of radiation extended to the topology of a periodic 12D spacetime. The fundamental *least-unit* is shown to be a scale invariant complex cosmological system. Time arises naturally as a ‘beat frequency’ in the translating boundary conditions of a spin exchange ‘continuous state’ dimensional reduction compactification process. A new set of UFM transformations beyond the Galilean and Lorentz-Poincaré are called for to cancel infinities in renormalization of quantum field theory and allow experimental entry into the 3rd regime by utilizing action principles allowed by the Dirac polarized vacuum. The inherent topology of the UFM transformation is derived by coupling superluminal Lorentz boosts with non-compactified Kaluza-Klein theory in the context of an Einstein energy dependent spacetime metric, \hat{M}_4 .

3.9 Holographic Anthropic Multiverse Cosmology

WHAT IS THE HOLOGRAPHIC ANTHROPIC MULTIVERSE?

- There is no big bang (temporal singularity), expansion or inflation.
- Redshift is non-Doppler due to periodic photon mass (tired light).
- CMBR is a cavity-QED blackbody (BB) radiation.
- Thus CMBR is emission & redshift absorption for BB equilibrium.
- The Multiverse is closed & finite in time/open and infinite eternally.
- This relates to the holographic principle – a multiverse with potential for an infinite number of nested Hubble spheres (H_R) each with their own fine-tuned laws of physics.
- Dark energy arises from the rest of the multiverse beyond our H_R .

- Cosmological constant based on this horizon-fluctuates near zero as ± 0 .
- The Multiverse is not static, steady-state or inflationary, but a cyclic continuous-state (CS).
- The CS provides a standing-wave present from future-past elements in a spin exchange dimensional reduction compactification process - i.e. The XD can range from infinitely large $> 4D$ and to asymptotic \hbar (never reached before next Riemann sphere rotation) C Planck scale $< 3D$.
- 3D reality is a ‘pocket space’ or temporal subspace of a new form of absolute 12D atemporal UFM space.
- An anthropic multiverse requires an additional teleological or anthropic UFM super-quantum potential action principle guiding evolution and governing hierarchical complex self-organization.

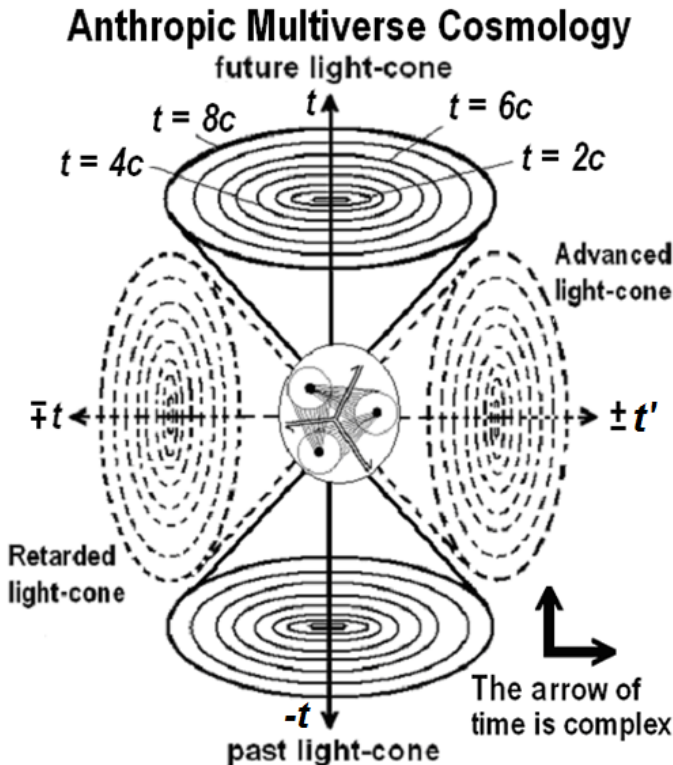


Fig. 3.8 Limited 3D conceptualization of temporal dimensions only in the XD topological backcloth of continuous-state Holographic Anthropic Cosmology showing a central LCU vertex. It is also representative of a Cramer transaction extended to three time dimensions.

§1: The Holographic Principle¹ is extended from 2D to HD.

§2: By the anthropic principle of the physical basis of intelligence and Einstein's mass-energy relation, $E = mc^2$, a tenet of multiverse cosmology is that the mass-energy of the Earth is equivalent to the mass-energy of all life over its ~ 5 billion year history [3].

- §2A: This mass-energy relation determines the observational limit in cosmology equated with the Hubble radius, H_R .
- §2B: Through parameters of string tension/coupling and the fine-structure constant $c \equiv c$ as empirically measured rather than of infinite velocity.

§2A and §2B are fine-tuned variables, different in each multiversal nested Hubble 3-sphere. An associated principle relates to conformal scale invariance. At the microscopic limit the Anthropic field equation balances the oscillation of the Planck constant, \hbar ; at the cosmological scale, the Anthropic field equation balances the fluctuation of the cosmological constant, Λ ; offering an explanation for dark energy/matter.

Apologies for including some aspects of the anthropic nature of awareness; but as they will become important in defining the physical nature of the observer in the future we leave some indicia that can easily be skipped by those wishing to exclude anthropic principles from the discussion on multiverse cosmology.

3.10 Overview of the Formalism for Anthropic Cosmology

Anthropic Cosmology is cast in a 12D harmonic superspace $S_N = S_0 + S_1 + S_2$ in the context of an extended Wheeler/Feynman

¹ The usual rendition of the Holographic Principle attributed to 't Hooft, Susskind and Wheeler [26,28,29] is a conjecture about quantum gravity theories, claiming that all of the information contained in a volume of space can be represented by information living in the boundary of that region. In other words, if you have an empty sphere, all of the events within can be explained by the arrangement of information on the surface of the sphere. The theory also suggests that the entire universe can be seen as a 2D information structure 'painted' on a boundary surface, and that the three observed dimensions are illusory. String theorists (11D M-theory) claim the holographic principle could form the theory of everything (TOE).

absorber theory [5] where standard Minkowski space M_4 is a ‘standing wave’ of the future-past [6]. This takes the general form

$$R_{symM_4}^{S_{N0}} = \frac{1}{2} \left[R_{ret\mathbb{C}_4}^{S_{N1}} + R_{adv\mathbb{C}_4}^{S_{N2}} \right] \quad (3.3)$$

or simplistically stated the 12D noetic superspace, S_N represents a complex Minkowski metric $M_4 + \mathbb{C}_8$ (or $\pm \mathbb{C}_4$ in terms of Calabi-Yau mirror symmetry). S_N thus combines the standard M_4 four *real* dimensions (D) plus 8 imaginary D representing a *retarded* and *advanced* complex hyperspace topology which adapts the complex ($M_4 + \mathbb{C}_8$) Minkowski metric from the standard stationary form to a periodic form. $S_0 = M_4$ represents the noetic 3(4)D ‘standing wave’ Minkowski ‘present’ spacetime; $S_1 = -\mathbb{C}_{4(ret)}$ represents the past component and $S_2 = +\mathbb{C}_{4(adv)}$ represents the future for complex correspondence to the standard 4 real dimensions utilizing 8 imaginary dimensions. The 8 imaginary dimensions, while not manifest generally (locally) on the Euclidean real line, are nevertheless ‘physical’ in the multiverse and can be represented by complex coordinates

$$X = \pm(x + i\xi), Y = \pm(y + i\eta), Z = \pm(z + i\zeta) \text{ and } t = \pm(t + i\tau) \quad (3.4)$$

designating correspondence to real and retarded/advanced continuous spacetime transformations. For symmetry reasons the standard Minkowski line element metric $ds^2 = g_{ij}dx^i dx^j$ is expanded into periodic *retarded* and *advanced* topological elements fundamental to relational space ‘extension’ giving Noetic Superspace S_N its continuous state dimensional reduction standing wave periodicity. This is illustrated conceptually in Fig. 3.9 below which reveals some of the main parameters of multiverse cosmology; in Fig. (3.9a) the baby and old man represent the *relational* periodic basis of spacetime by applying extended Wheeler-Feynman-Cramer absorber theory where the present is a standing wave of the future-past. The 11(12)D harmonic superspace translates in a continuous state dimensional reduction compactification process (Fig. 3.9b). A 12D

multiverse provides enough degrees of freedom so that two complex imaginary $\pm 3(4)\text{D}$ spacetime packages (Calabi-Yau) can topologically transform into a ‘standing wave’ present, i.e. the present has a future-past basis by extending the Wheeler-Feynman radiation law to include the continuous state transformation of the topology of spacetime dynamics itself. Fig. (3.9c) is a 3-torus illustrating a virtual standing wave ‘creation’ of a discrete virtual Fermionic Euclidian point; a different conceptual view of Figs. 3.9a and 3.9b. The three $3(4)\text{D}$ ($S_0 = M_4$, $S_1 = -\mathbb{C}_{4(\text{ret})}$ and $S_2 = +\mathbb{C}_{4(\text{adv})}$) spacetime packages surround a virtual Planck scale singularity, (in the form of a 3-torus $[\sqrt{(x^2 + y^2)} - R]^2 + z^2 = r^2$) the continuous propagation of which ‘create and recreate’ periodically the ‘standing wave’ Euclidean real line illustrating the virtual basis of relational Einsteinian reality as a subspace of absolute HD UFM multiverse space. This Noetic ‘least unit’ represents a Wheeler-Feynman future-past periodicity and a continuous cycling of *classical* \rightarrow *quantum stochasticity* \rightarrow *fundamental unitary*, $R_C \rightarrow R_Q \rightarrow R_U$ in the D reduction compactification $D_s \rightarrow D_t \rightarrow D_E$ transformation process [11].

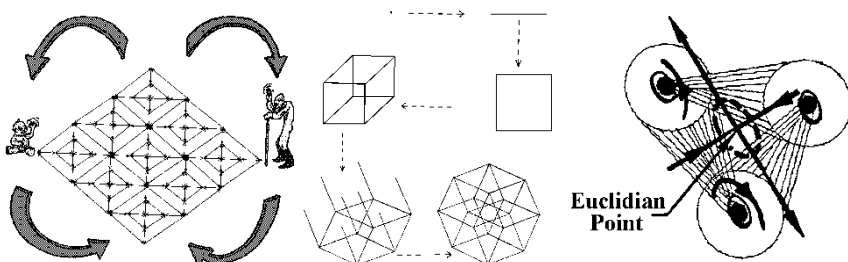


Fig. 3.9 Basic topological premises of Noetic Cosmology shown by three different conceptual views representing future-past dimensional reduction least cosmological unit.

The Kaluza-Klein model utilized is set in a noncompactified $D = 12$ harmonic Noetic Superspace S_N . For symmetry reasons shown in the text this superspace is comprised of an 11D hypersurface in a 12D universe, giving it theoretical correspondence to 10D superstring theory and 11D supergravity and providing a context to solve the disparity between them. The general appeal of the Kaluza-Klein model is that physics seems simplified in HD, especially integration of the electromagnetic (em) and gravitational field [6].

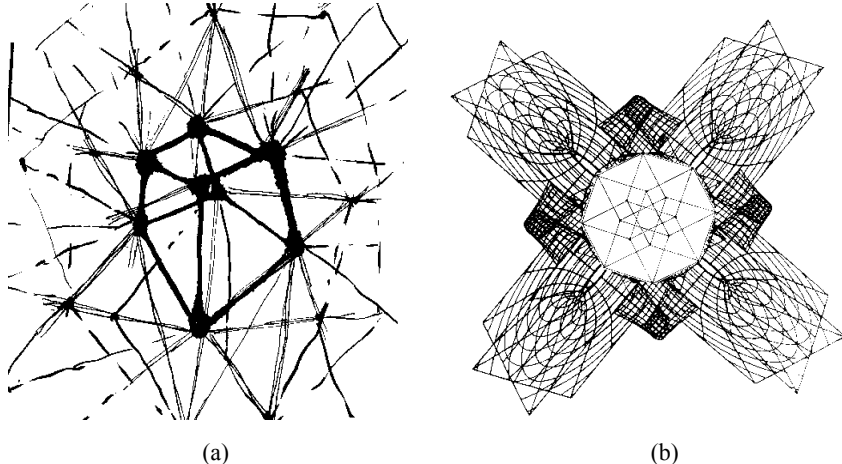


Fig. 3.10 Two additional conceptual views of Fig. 3.9. Fig. 3.10a conceptualizes the relational nature of Minkowski space emerging from the polarized vacuum 3.10b represents a snapshot in time. The central hypersphere represents the atemporal hidden HD covering the standing wave present. The larger peripheral tubes represent open orientation toward the future; and the narrower coupled tube forming a square represents a phase of recessional compactification toward the past, the final phase of which would end up like that of Fig. 3.9c – a virtual Planck scale singularity. This figure hints at why the Planck constant needs to be recalculated. Related to the past – the resultant of measurement, the Planck constant applies as usual. In the *eternal now*, the Planck constant takes the form of the Larmor radius of the hydrogen atom and is an unbounded component of the unitary field in the future orientation.

Periodic Noetic superspace S_N entails a continuous state of dimensional reduction that operates under transformations beyond the Poincaré / Lorentz where spatial dimensions D_S through superluminal boosts are transformed into temporal dimensions D_t and further in terms of a noncompactified Kaluza-Klein model [34] into energy dimensions D_E by $D_S \rightarrow D_t \rightarrow D_E$. This requires the properties of an energy dependent spacetime metric first developed by Einstein where standard Minkowski space, M_4 is a topologically invariant homeomorphic manifold of an Einstein energy dependent spacetime metric \hat{M}_4

$$f : M_4 \rightarrow \hat{M}_4. \quad (3.5)$$

According to the principle of relativity a spacetime region which is a ‘perfect vacuum’ (no matter and no fields) must be isotropic and covariant

in the Lorentz sense [30]. The deformed region \hat{M}_4 of S_N and the symmetry of S_N itself reduces to the Einstein relativistic metric and is assumed compatible with a covariant polarized Dirac vacuum.

3.11 Transformation of Space into Time

It is well known that Superluminal Lorentz Transformations (SLT) change real quantities into imaginary ones. Following Cole [51] and Rauscher [3,52] we illustrate the transformation of complex spatial dimensions into temporal dimensions by orthogonal superluminal boosts (SLB). For example, an SLB in the x direction with velocity $v_x \pm \infty$ the SLT is $x' = \pm t$, $y' = -iy$, $z' = -iz$, $t' = x$. In complex Minkowski space the coordinates are $z^u = x_{\text{Re}}^u + ix_{\text{Im}}^u$ where z is complex and x_{Re} and x_{Im} are real and the index u runs over 0,1,2,3. Using classical notation for simplicity

$$t = t_{\text{Re}} + it_{\text{Im}}, \quad x = x_{\text{Re}} + ix_{\text{Im}}, \quad y = y_{\text{Re}} + iy_{\text{Im}}, \quad z = z_{\text{Re}} + iz_{\text{Im}}. \quad (3.6)$$

To clarify the meaning of imaginary quantities in an SLT it is helpful to represent time as a 3D vector t_x , t_y , t_z ; therefore, time is defined as $t = t_x \hat{x} + t_y \hat{y} + t_z \hat{z}$ where

$$t_x = t_{x\text{Re}} + it_{x\text{Im}}, \quad t_y = t_{y\text{Re}} + it_{y\text{Im}}, \quad t_z = t_{z\text{Re}} + it_{z\text{Im}}. \quad (3.7)$$

Finally, for the SLB for velocity $v_x \pm \infty$ along x the transformations are

$$\begin{aligned} x'_{\text{Re}} + ix'_{\text{Im}} &= t_{x\text{Re}} + it_{x\text{Im}}, \quad y'_{\text{Re}} + iy'_{\text{Im}} = y_{\text{Im}} - iy_{\text{Re}}, \\ z'_{\text{Re}} + iz'_{\text{Im}} &= z_{\text{Im}} - iz_{\text{Re}}, \quad t'_{x\text{Re}} + it'_{x\text{Im}} = x_{\text{Re}} + ix_{\text{Im}}, \\ t'_{y\text{Re}} + it'_{y\text{Im}} &= t_{y\text{Im}} - it_{y\text{Re}}, \quad t'_{z\text{Re}} + it'_{z\text{Im}} = t_{z\text{Im}} - it_{z\text{Re}} \end{aligned} \quad (3.8)$$

where the SLT in the x direction of M_4 spacetime transforms real components into imaginary and imaginary complex quantities into real quantities as one major property of the periodic nature of Noetic multiverse spacetime [51-53].

3.12 Energy Dependent Spacetime Metric

Einstein originated the concept of an energy dependent spacetime for explaining temporal rate change in the presence of a gravitational field by generalizing the special relativistic line element

$$ds^2 = (1 + 2\phi/c^2)c^2 dt^2 - dx^2 - dy^2 - dz^2 \quad (3.9)$$

with the introduction of time curvature [1] where ϕ is the Newtonian gravitational potential. This utilizes the deformed Minkowski metric \hat{M}_4 (introduced above by Eq. 3.5) which is imbedded in the periodic HD Noetic space chosen axiomatically for multiverse cosmology to take the form of a noncompactified Kaluza-Klein theory [34].

Kaluza's initial demonstration of gravity in 5D, ${}^5G_{AB} = 0$ with AB running 0,1,2,3,4 contained 4D General Relativity with an EM field ${}^4G_{\alpha\beta} = {}^4T_{\alpha\beta}^{EM}$, with α, β running 0,1,2,3 [17,18]. The currently less common non-compactified Kaluza-Klein model is utilized by Noetic Cosmology where also dependence on the extra D is required; this yields the same result for Einstein's equations ${}^5R_{AB} = 0$ except that the EM energy momentum tensor ${}^4T_{\alpha\beta}^{EM}$ is replaced by a general one ${}^4T_{\alpha\beta}$ instead [17,18]. We demonstrate the feasibility of an energy domain pervading HD spacetime with properties similar to Wheeler's Geon proposal discussed in section 3.13 below. In a generalized deformed spacetime metric \hat{M}_4 , spacetime is fixed by the energy and has the metric

$$\eta(E) = \text{diag.}(a(E), -b(E), -c(E), -d(E)). \quad (3.10)$$

3.13 The Wheeler Geon Concept Extended to Noetic Superspace

Wheeler [45] postulated a photonic mass of sufficient size to self-cohere into a spherical ball of light. In Wheeler's notation the Geon is described by three equations. The first (3.11) is the wave equation, followed by two field equations the first (3.12) of which gives a mass distance relationship and the second (3.13) variation of the factor Q :

$$d^2 f / d\rho^{*2} + [1 - (l^* Q / \rho)^2 (1 - 2L / \rho)] f = 0 \quad (3.11)$$

with circular frequency $c\Omega$ related to the dimensionless radial coordinate $\rho = \Omega r$ such that $d\rho^*$ is the abbreviation for $d\rho^* = Q^{-1}(1 - 2L/\rho)^{-1} d\rho$

$$dL/d\rho^* = (1/2Q)[f^2 + (df/d\rho^*)^2 + (l^*Qf/\rho)^2(1 - 2L/\rho)] \quad (3.12)$$

$$dQ/d\rho^2 = (\rho - 2L)^{-1}[f^2 + (df/d\rho^*)^2] \quad (3.13)$$

L and f are mass and field factors respectively; Q is a scale correction factor. The factor l relates to a family of modes with distinct frequencies associated with the well-known completeness theorem of spherical harmonics. HD extended modes of l are key elements in propagation of the noetic field. Wheeler states that these equations permit change of distance scale without change of form [45] which is compatible with the Noetic action principle $F_N = \aleph / \rho$ derived below [46,47].

Postulate 3.2: *The Supralocal Hyper-Geon is the most fundamental energy or phenomenology of existence. This Energy arises from the ordering and translation of AS ‘space’ (i.e. information or change of entropy). This fundamental Geon-like energy, is synonymous with the ubiquitous unified field, the primary action driving all temporal existence; filling the immensity of space (nonlocally) and controlling the evolution of the large scale structure of the universe.*

3.14 The Hyper-Geon Domain of Multiverse Noetic Field Theory

As summarized in section 3.13 above Wheeler defined the Geon as a theoretical classical spacetime construct not yet observed in nature. A complex Hyperdimensional Geon (not em, but redefined as the noeon exchange unit of the unified field) is postulated to cover our observed 3(4)D relational spacetime and filters through each dimensional reduction like a waterfall as the de Broglie-Bohm pilot-wave quantum potential. This is described by a new set of Noetic transformations for multiverse cosmology [37]; acting on all levels of scale from the Einstein/Hubble radius to the Planck scale. Because of its contact with the Multiverse it relates also to balancing the cosmological constant, Λ , by the ‘dark energy’ responsible for the postulated missing dark matter that causes galaxy rotation to be like a solid disk rather than with a centripetal vortex

with increasing speed with distance from the center. multiverse cosmology postulates this missing energy to arise from the rest of the Multiverse. The Geon also forms the lower energy boundary of a projected 12D space making it synonymous with the unified field. This unitary Noetic field is the origin of the teleological anthropic action principle [54] guiding evolution. This coalesced region of nonlocal photon-gravitons – The hyper-geon superspace cover acts as:

- Gravitation (The graviton in multiverse cosmology is a confined quadrupole photon \hat{M}_4 complex; thus teleological action of the unified field orders the large scale structure of the universe – which is a non-Darwinian guided evolution). (not em but UFM noeon).
- Causal action of the quantum potential or pilot wave (An additional causal action principle pertinent to extended quantum theory and its completion).

3.15 Interregnum

Scientific theory, whether popular or unpopular at any point in history, must ultimately be based on description of natural law, not creative fantasies of a scientist's imagination. Only by adequate determination of natural law can a theory successfully model reality. “*There is good reason for the taboo against the postulate of new physics to solve new problems, for in the silly limit one invents new physics for every new phenomenon* [7]”. Not long ago cosmology was not considered to be a viable science; one saying went – ‘first there is speculation, followed by speculation squared, then comes cosmology’. Is Cosmology becoming a mature science; mature enough that there is no room for surprises? We don't think so; and we have hinted at some of the surprises here.

A new model of the universe called the Holographic Anthropic Multiverse provides a fundamental framework for introducing a scale-invariant complex cosmological system where life is the rule not the random exception because of the anthropic principle guiding its evolution. Many controversial principles stated emphatically; but Noetic cosmology is empirically testable so it will now be possible to settle many of these questions experimentally.

...maybe we should not try to quantize gravity. Is it possible that gravity is not quantized and all the rest of the world is? ... Now the postulate defining quantum mechanical

behavior is that there is an amplitude for different processes. It cannot be that a particle which is described by an amplitude, such as an electron, has an interaction which is not described by an amplitude but by a probability ... seems that it should be impossible to destroy the quantum nature of fields. In spite of these arguments, we should like to keep an open mind. It is still possible that quantum theory does not absolutely guarantee that gravity has to be quantized [55] - R.P. Feynman.

Even though a Nobel Prize has been given for the Big Bang, the issue of fundamental cosmology is not settled. The prize could have been phrased differently in terms of interpreting the nature of Cosmic Microwave Background (CMB) and redshift satellite data; as Hubble discovered redshift, not Doppler expansion of the universe. Neutrinos had no mass for decades; we suspect that some UFM scenario will also demonstrate photon mass. We believe the speed of light, c would be infinite otherwise. A Holographic Multiverse provides very simple concepts for dark energy/matter. Assuming the Hubble sphere is closed and finite in time, and open and infinite into infinite size additional dimensionality (LSXD) in ‘eternity’; there is room for an infinite number of nested Hubble spheres each with their own fine-tuned laws of physics in the multiverse beyond the 13.7 billion light year observational limit. In this scenario, dark energy/matter are simply due to the matter balancing the cosmological constant, Λ , with tiny fluctuations around zero. The recent purported discovery of gravitational waves, does not change anything as there is still an issue of what kind of waves were discovered.

String Theory, recast as M-Theory after the 1995 superstring revolution, has remained highly controversial because until now direct methods for empirical tests of its parameters have remained elusive. There are purported to be a googolplex, 10^{∞} candidates for the unique string background sought. One impetus for string theory in XD was the work of Kaluza and Klein showing that gravity and em could be integrated by introducing a 5th dimension. We believe as Feynman wonders, that a search for a quantum gravity is not the way to orient the quest for a Theory of Everything (TOE). M-Theory has made great strides in developing, tinkering with and finding rich associations between the infinite parameters of string theory. Because string theory is still aligned with a Big Bang cosmology, researchers seek one unique compactification from which the standard model of particle physics will drop out. Here because multiverse cosmology is a complex self-organized continuous-state system we profess that all dimensionalities of compactification occur by what we call the multiverse mantra: ‘a continuous-state spin-exchange parallel transport deficit angle dimensional reduction compactification

process' – a concatenation that is merely a fancy way of trying to elucidate SUSY breaking parameters.

3.16 Ambulatory Hoopla

Logically, since not long ago it appeared we lived in a Newtonian world, one might now assume we live in a Quantum world. By this logic should it not follow that after the unitary field is discovered one might surmise the universe is a form of unitarity as some monistic Eastern philosophies suggest. We believe this is not the case either, and suggest that the multiverse is a continuous-state Kantian antinomy [56] between the three. We realize this appears strange; but our evidence so far in examining the applications we have been able to develop based on such a view, i.e. surmounting uncertainty or universal quantum computing for example seem to indicate such a view should be embraced rather than ignored.

It appears logical in particle physics that supersymmetry (SUSY) is a symmetry that relates elementary particles of one spin to another particle that differs by a half unit of spin known as superpartners. In other words, in a supersymmetric theory, for every type of boson there exists a corresponding type of Fermion, and vice-versa. As of 2016 there is no direct evidence that supersymmetry is a symmetry of nature, a situation that physicists hope will change with newly designed experiments for the supercollider at CERN. We surmise the experimental protocol outlined in Chap. 8 provides a much simpler and direct low energy avenue for plumbing the HD domain making string theory readily testable. Other *avant garde* postulates of the continuous-state multiverse cosmology are:

- There is no quantum gravity (not the regime of unification)
- There are no superpartners (sparticles) in the usual sense, but charged brane mirror symmetry topology occurs
- Photon mass anisotropy, oscillating duality, $m_\gamma \neq 0 \leftrightarrow m_\gamma = 0$
- Anthropic evolution drives self-organization within the Einstein H_R

The first three constructs, while intellectually appealing for some decades are remnants of Gauge Theory, although enormously successful, is only an approximation soon to be shown unable to continue to sustain such predictions. It is obvious that the standard model of particle physics-cosmology is incomplete (recent discovery of neutrino mass for example) justifying the alternative considerations presented here [57-59].

By current considerations supersymmetries are generated by objects transforming under a spin-statistics theorem, where spin-1 Bosonic fields commute while spin- $\frac{1}{2}$ Fermionic fields anticommute according to the tenets of the Copenhagen interpretation of quantum theory. By current thinking in order to combine the two fields a super-Lie-algebra is needed that doubles the number of fundamental particles (superpartners often called sparticles). The Higgs mechanism has been a primary motivation for SUSY because it entails inherent Boson-Fermion renormalization /symmetry breaking that can be formalized in XD. We believe the renormalization paradox is indicative of the immanent need for new physics in the same manner that the Rayleigh-Jeans Law was indicative of the immanent appearance of quantum mechanics and that the infinities should not be considered a ‘plague’ but indicative of a lower order cut-off of the unitary field requiring a new set of transformations (See Chap. 11) beyond the current Lorentz/Poincaré to reveal their place in nature.

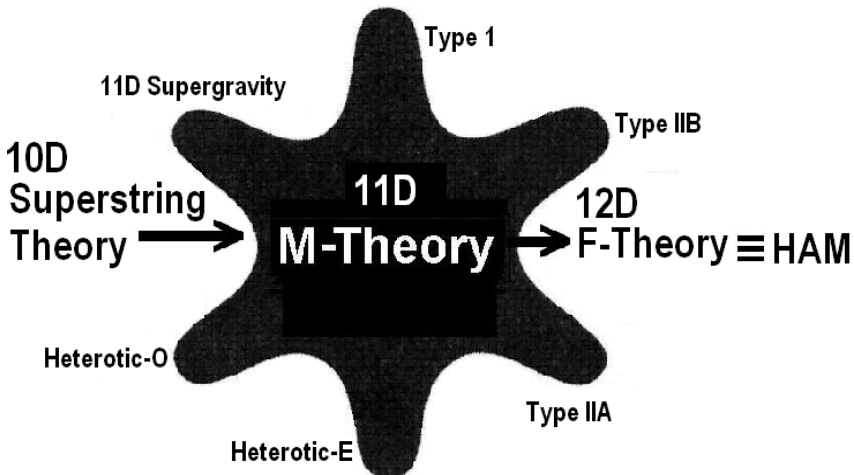


Fig. 3.11 Various types of string theory combined to form M-Theory and a 12D form of F-Theory utilized by multiverse cosmology to introduce the anthropic principle driving complex self-organization in the static Einstein 3-sphere, H_3 .

Recent M-Theory modeling has been able to resolve the hierarchy problem [20,60] yielding insight into the disparity between the weak and gravitational interaction scales. The maximum number of supersymmetries is 32 (curiously the same as the number of crystal forms) suggesting the maximum number of dimensions is 11 [61]; but we implement a 12th XD in order to introduce the anthropic action principle

driving the evolution of the complex self-organized continuous-state structural-phenomenology of the static-temporal Einstein-Hubble 3-sphere, H_R . Interestingly Smolin, architect of Loop Quantum Gravity (LQG) postulates that LQG does not require sparticles either and that LQG may turn out to be a component of M-Theory. Our problem with LQG is that it is limited to 4D; but it has the interesting feature of a background independent vacuum [62-67].

As stated the recently discovered Higgs mechanism requirement is an artifact of Gauge Theory being an approximation waiting for new physics. If no superpartners are found, what then? The worm-hole-like topological dynamics of HD branes. Starting from the perspective of the Dirac spinor spherical rotation of the electron requiring $360^\circ - 720^\circ$; where the additional 2π rotation is indicative of rotation through an HD space-antispace topology before returning to the 3D point of origin. This ‘Klein bottle’ raising-lowering effect is amenable to a Wheeler wormhole concept where ‘charge is topology’. According to Wheeler lines of force in a wormhole can thread through a handle and emerge through each mouth to give the appearance of charge in an otherwise charge free spacetime [7,68,69]. Wheeler originally failed; we believe because his approach was only 4D. An HD elaboration of this concept could extend the Higgs mechanism replacing sparticles with brane topologies (Fig. 3.12).

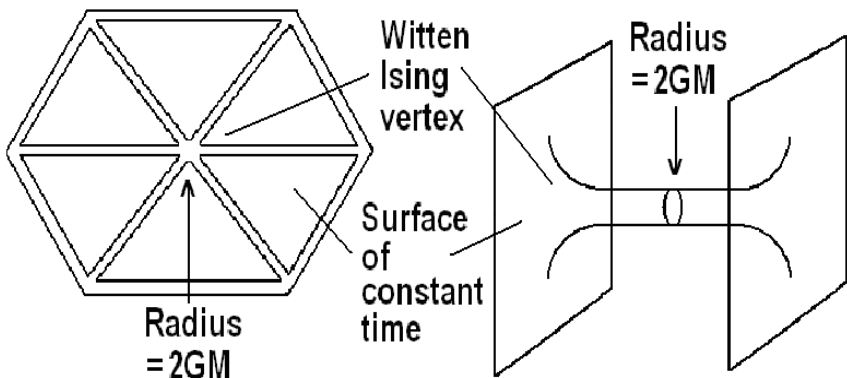


Fig. 3.12 Wormhole modeling for M-Theory. When the continuous-state topological dynamics are fully understood it is postulated a form of Ising model wormhole lattice-gas structure of brane tension-coupling might be able to replace sparticles by extending the Higgs mechanism. If topology is charge as Wheeler postulated the standing-wave hysteresis loop in the multiverse continuous-state least-unit transformation will enable such developments. Figure redrawn from [70].

Table 3.3 MULTIVERSE COSMOLOGY SUSY PARAMETERS

General Cosmological Parameters	Symmetry Breaking Parameters
<ul style="list-style-type: none"> • 12D Multiverse • Anthropic Guidance Principle • Holographic Principle • Non-Compactified K-K Model • Cosmological Least-Unit (LCU) • Large Scale XDs (LSXD) • Cosmos - A Self-Organized Complex System • Scale Invariance • Conformal Invariance • New HD Form of Absolute Space • Teleological Action – Evolution • Super Quantum Potential • Finite Photon Mass Anisotropy • Dark Energy from Λ Multiverse • 12 Dimensions • Unitary Wheeler Geon • Wheeler Wormholes • Continuous-State • Fine Tuning • Unitary Field (UFM)-Quadrupole Photon - Graviton • Noeon – Topological exchange parameter of the Unitary Field • Holographic Multiverse – Closed & finite in t, open and infinite in atemporal XD 	<ul style="list-style-type: none"> • Continuous-State • Continuous Compactification • Dimensional Reduction • Spin Exchange • Parallel Transport • Deficit Angle • Bianchi Identities • Regge Calculus – Oscillating Spacetime Curvature ± 0 • Spin-Spin Coupling of Spacetime Topology • T-Duality / Mirror Symmetry • Ising Model Rotation of Riemann Sphere, $0 \leftrightarrow \infty$ • Topological Switching • Coordinate Leapfrogging • Dirac Spherical Rotation • Dirac Style Annihilation/Recreation of mass / Topology • Dynamic/Static Casimir Coordinate Leapfrogging • Strings / Branes • Standing Wave Symmetry • Rotations – circular, spherical, cylindrical, chiral, hyperspherical • Unique Vacuum Symmetry
DUAL STATIC - DYNAMIC PARAMETERS	
Higgs Mechanism - Extension	:: No Superpartners – Alternative
Arrow of Time From Large XDs	:: Oscillating String Tension,
$\hbar + T_0$ Oscillating Cosmological Constant, $\Lambda \pm 0$:: Unitary Formalism,
$F_{(N)} = \mathbf{x} / \rho$	
\hbar Not Fundamental, New Stoney Basis	:: Complex Self-Organization
Structural-Phenomenology	:: Future-Past Transaction

Table 3.3 SUSY parameters required by multiverse cosmology for the continuous-state spin-exchange topological dynamics of dimensional reduction compactification process.

Although we propose radical changes for M-Theory we still consider it to be the best hope for a Theory of Everything (TOE); but it needs to take a lesson of some sort from LQG, revamp the concept of the Higgs mechanism and the origin of the fundamental parameters of particle physics forming sparticles such as the tension-coupling effects in the associated HD continuous-state topology. It is a ‘torque’ of some form in the energy dynamics of the spacetime least-unit [10,71] hysteresis loop in the SUSY breaking parameters of the ‘continuous-state spin-exchange parallel transport deficit angle dimensional reduction process’ that could be developed to fill this conceptual disparity if the Large Hadron Supercollider (LHC) fails to find neutralinos (lightest sparticles). M-Theory could still easily remain on track with SUSY requirements by incorporating the SUSY breaking parameters inherent in the alternatives presented by multiverse cosmology.

String theory is currently aligned with the Copenhagen interpretation of quantum theory and Big Bang cosmology which have led to the quest for a putative ‘quantum gravity’. In multiverse cosmology none of these ideas form the correct basis for string theory and need to be replaced by new considerations that include a new cosmological perspective and an HD completed form of the de Broglie-Bohm-Vigier causal stochastic interpretation of quantum theory [72,73] compatible with the Transactional Interpretation of quantum theory [8] because it entails a mirror symmetry compatible with the dual Calabi-Yau 3-form and the associated SUSY breaking parameters being developed in string theory.

A snippet should be given regarding the TOE search. Recently some well-known scientists like Hawking and Dyson have suggested that a TOE is impossible according to Gödel’s incompleteness theorem [11,74] which simplistically states that nothing can be described in terms of itself because by definition that would be too limited a view; any complete description must come from outside the boundaries of the principle to be fully understood. If accepted this would appear to be a challenging philosophical conundrum; but from the multiverse perspective, it turns out to have a simple answer allowing one not to know everything and still have a TOE. The TOE is essentially about unifying the four fundamental forces and having essentially complete theories of particle physics with a connection between quantum theory and gravitation in a proper cosmological context. An anthropic cosmology by supposition is a complex self-organized system with the properties associated with such systems such as incursion, hierarchy and an inherent external action principle driving its self-organization. By applying Kant’s antinomies [57]

the Hubble sphere is closed and finite temporally, but open, infinite and causally separated in eternity such that in a Multiverse there is room for an infinite number of nested Hubble spheres each with their own fine-tuned laws of physics [3]. So a TOE is sufficiently developed for parameters within our Einstein-Hubble sphere as we begin peeking into the holographic Multiverse beyond it, is compatible with Gödel's theorem.

3.17 Ultimate Evolution of M-Theory

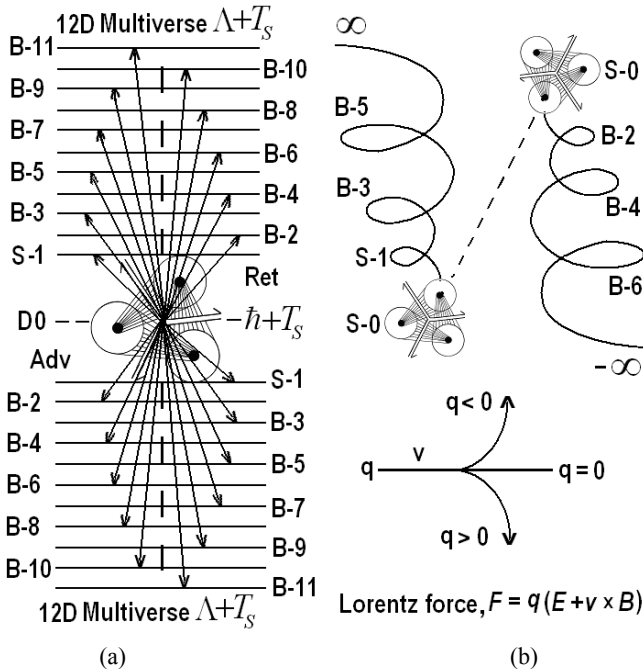


Fig. 3.13 Conceptualized string (S) and brane (B) couplings in Advanced-Retarded spacetime arising from a least-cosmological unit, D0, S-0. a) String-brane duality couplings from 0 to 12D for odd-even Fermi-Bose topologies. b) Ising model spin-glass rotations which may be driven by an internal Lorentz-like force of the anthropic principle or external resonances for vacuum engineering.

Every Calabi-Yau manifold with mirror symmetry or T-duality admits a hierarchical family of supersymmetric toroidal 3-cycles as shown conceptually in Fig. 3.13. Figure 3.13a shows possible duality couplings and 3.13b is meant to illustrate the compactification-boost hierarchy as modeled by a Genus-1 helicoid ‘parking garage structure’ (Fig. 4.11). It is currently unknown whether the attempt to formalize this continuous-state

structure should follow a Kaluza-Klein spin tower, logarithmic or golden ratio spiral, cyclotron resonance hierarchy, genus-1 helicoid ‘parking-garage’ or some other HD structure. We currently find the Genus-1 helicoid the most intellectually appealing because of its ability to incorporate Kähler manifolds compatible with M-Theory parameters listed in Table 3.3. Also of note is that the heterotic SO(32) Bosonic string introduces a tachyon which we do not consider anomalous but part of the internal field coupling of a Lorentz vacuum contraction. Type IIA & Type-IIB open/closed strings are cast in odd/even string/brane dimensionality which we postulate is an inherent part of the Ising model rotation of the Riemann sphere for ‘parking-garage’ helicoid raising-lowering indices of the continuous-state dimensional reduction compactification process. These complex constructs can only be adequately worked out with a move away from a Big Bang cosmology and limits imposed by 4D Copenhagen-Gauge approximations such as the uncertainty principle.

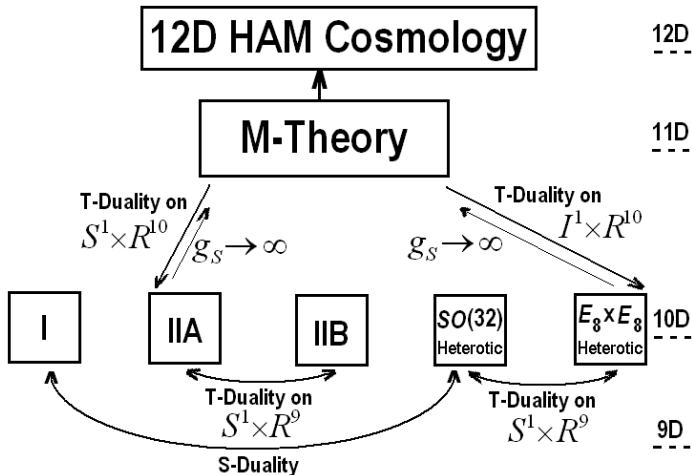


Fig. 3.14 Mirror/duality transformations relating the 5 superstring theories to each other and the anthropic principle of multiverse cosmology. Adapted from [75].

It is well known that it is possible to have supersymmetry in alternate dimensions. Because the properties of spinors change dramatically with dimensionality; each dimension has its own characteristics. In d dimensions, the size of spinors is roughly $2^{d/2}$ or $2^{(d-1)/2}$. Since the maximum number of supersymmetries is 32, the largest number of dimensions a supersymmetric theory can have is 11D. It is possible to have multiple supersymmetries and also have supersymmetric XDs.

If we accept the postulate of M-Theory that matter resides on the 3-brane along with the associated boundary conditions underlying the spinor elements of matter; along with duality/mirror symmetry this takes care of 6D. Multiverse cosmology is cast in 12D – 3 more for time and the final 3 for ‘piloting’ or the anthropic teleology for the continuous-state evolution of spacetime. Multiverse cosmology is built on the premises of extended em theory [76-80], a covariant polarized Dirac vacuum [73,81,82], with photon mass anisotropy [5,83] giving the photon an internal motion coupling it to the vacuum. Since minutely massive photons are not fermions their brane dynamics are different (simpler). Further we posit the photon as a periodic temporal ‘pinch’ of the continuous coherent unitary field – a geon or 12D ocean of light [45]. This could be one of the greatest contributions of this volume when properly understood.

3.18 String/Brane Dynamics

The purpose of this section is to illustrate the richness of string/brane transformations and to review the myriad fundamental component bases of the transformations not to necessarily demonstrate any particular action. In general, this includes:

- String/brane action in 0 to 9D
- Linear, circular, cylindrical, spherical, chiral and hyperspherical rotations, boosts, transformations and compactifications.
- SUSY breaking
- Calabi-Yau mirror symmetry, T-Duality
- Open – closed string-brane transformations
- String/brane tension-coupling dynamics
- Mass/energy/gravitation deficit angle parallel transport
- Annihilation/creation dynamics
- Teleological/anthropic UFM action driving /piloting complex systems.



Fig. 3.15 Five possible open-closed string interactions as forms of topological transforms.

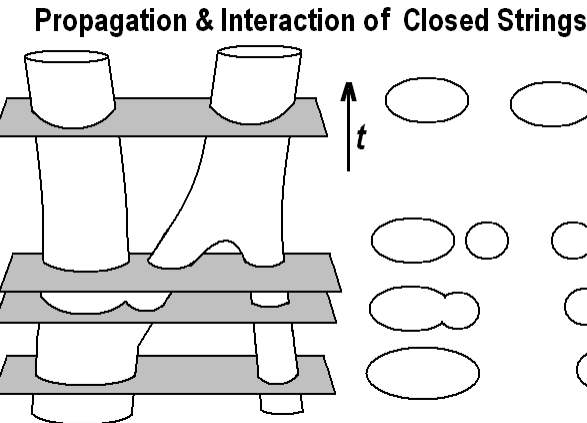


Fig. 3.16 2D & 1D ‘Pants diagram’ for the topology of string interactions.

The five superstring models of M-Theory are:

- Type-I strings having one supersymmetry in 10D. Type-I strings are unoriented and open or closed while all the other types are oriented closed strings.
- Type-IIA & IIB string theories contain two 10D supersymmetries which differ in that IIA theory is non-chiral or parity conserving and IIB theory is chiral or parity violating.
- Heterotic strings, so named because they are left-moving and right-moving, are a hybrid of a type-I and Bosonic strings. There are two kinds of heterotic strings, the $E_8 \times E_8$ and SO(32) string.

In type-II string theories closed strings are free to move through the 10D bulk of spacetime, but the ends of open strings attach to D-branes. In type-IIA their dimensionality is odd – 1,3,5,7 and even in type IIB – 0,2,4,6. See Fig. 3.13. Through different gauge symmetry conditions various types of strings or branes are related by S-duality which relates the strong coupling limit of one type to the weak coupling limit of another type. T-duality relates strings/branes compactified on a circle of radius R , to strings/branes compactified on a circle of radius $1/R$.

Following work by Sundrum [60] for 5D General Relativity where the Einstein action is $\exists \partial_\mu$ or $\partial_5 Gr_{MN}^0(x) \rightarrow 0$ for large XD fluctuations

$$ds^2 \exists Gr_{55}(dx^5)^2 = Gr_{55} R^2 d\theta^2 \Rightarrow Gr_{55}^{(0)}(x) \equiv \text{dynamical XD radius.}$$

Randall and Sundrum [19] have found an HD method to solve the

hierarchy problem by utilizing 3-branes with opposite tensions, $\pm\sigma$ residing at the orbifold fixed points which together with a finely tuned cosmological constant from sources for 5D gravity for a spacetime with a single S_1/Z_2 XD orbifold [84-86] These 3-branes with opposite tensions residing at the orbifold fixed points along with their model of a finely tuned cosmological constant serve as sources for 5D gravity.

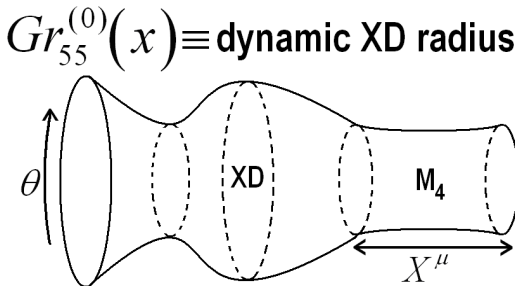


Fig. 3.17 Sundrum's view of the dynamic oscillations of bulk large size XD readily making correspondence to the continuous-state dimensional reduction parameters inherent in the multiverse cosmology paradigm. Redrawn from [63].

3.19 New Horizons Beyond the Standard Model

We did not choose to model our new cosmology after the steady-state or quasi-steady-state models of Bondi, Gold, Hoyle and Narlikar because they are set in expanding universe models. However, in our continuous-state model continuous matter creation must still be addressed, which we do briefly in [13,14]. It is interesting that the matter creation requirement can be satisfied with ‘one atom per cubic meter each 10 billion years, or about 1 atom per 10 cubic kilometers per year’ [87].

The Standard Model of particle physics provides a good correlation with experimental data, but there are phenomena not accurately described by the theory which physicists hope might be resolved by experiments performed with the LHC large hadron collider:

- The hierarchy problem
- The missing mass problem (dark matter and dark energy)
- The cosmological constant problem
- The strong CP problem
- Higgs Boson
- Non-zero neutrino mass

In the mid 1970's a postulate was bandied about the Stanford University physics department by a young graduate student (name forgotten) that went like this: '*if one assumes matter is a vector gluon, the leading light-cone singularity is modulated by a phase of the quark-gluon field*' which is not considered a sufficient descriptor. String theory postulates that matter is coupled vibration modes of string topology. The other element required is a mass producing Higgs spinor/twistor mechanism or an alternative like the one suggested here with wormhole dynamics as the basis. One might be willing to loosely accept that these elements provide an adequate conceptual framework for describing matter. The Stanford student's mantra adds an essential consideration especially if one embraces the de Broglie-Bohm model of relativistic quantum field theory where the wave-particle duality is not an either-or statistical complement, but a physically real piloted matter-wave simultaneity considered highly relevant to our continuous-state self-organized postulate. The electron is probably the simplest Fermion and the photon the simplest Boson. If string tension-coupling considerations are introduced into the Dirac spinor spherical rotation parameters one might begin to rigorously formalize the electron in terms of string theory. This is especially interesting in terms of the fact that high energy photons will undergo electron-positron pair production. The highly symmetric supersymmetry of the Cramer-multiverse vacuum might make it an easy task to design scattering experiments to reveal the electrons ultimate fundamental structure. We predict that these high energy collisions produce a momentary superluminal boost (Lorentz transformation) to the photon's ($m_\gamma \neq 0$) internal motion, which because of the 'perfect' symmetry conditions, allows an electron-positron pair (of equal total energy) creation. Already Chatterjee & Banerjee [88] have shown that angular momentum is conserved in the 5th dimension. We delve into this relative to the black-body cavity-QED exciplex model. Unraveling the fundamental structure of the photon may be simpler because the photon does not have the additional domain walls the electron has to keep it from unraveling when brought to rest. But as Einstein said '*every Tom, Dick and Harry believes they comprehend the photon nowadays; but they are sadly mistaken*'.

Icosahedral symmetry has been used to illustrate how higher-lower dimensionality (HD-LD) might enfold the vacuum state through an HD polyhedron that Coxeter [89] described as Polytope 2,21 consisting of 27 points evenly distributed over the surface of a 5D sphere embedded in a 6D space that may have relevance to the study of stringy vacuum geometric topology [90].

Currently few physicists have reason to suspect that gravity should not be quantized. Geometrodynamics is a classical theory. Physicists have been busy quantizing or trying to quantize all classical domains. Because of the move from Newtonian mechanics to quantum mechanics most physicists have decided that we live in a quantum universe. Physicists might suppose that this includes the idea that the unified field is not a similar cosmological condition but just the integration of all forces and fields from within this 4D quantum cosmology. Here we suggest that the multiverse in the reductionist sense is ultimately unitary, not in a monistic sense but rather one of a continuous-state complementarity between classical, quantum and unified. Much of our motivation arose by noetic insight from Plato ‘no matter how great one’s intelligence or how broad one’s knowledge base, noetic or transcendent insight is greater because it comes from beyond the individual’s abilities’ [91].

3.20 Ultimate Geometry of Reality, Dimensionality, Arrow of Time

...the right hand side includes all that cannot be described so far in the Unified Field Theory, of course, not for a fleeting moment, have I had any doubt that such a formulation is just a temporary answer, undertaken to give General Relativity some closed expression. This formulation has been in essence nothing more than the theory of the gravitational field which has been separated in a somewhat artificial manner from the unified field of a yet unknown nature. - Einstein [92].

In fact this new feature of natural philosophy means a radical revision of our attitude as regards physical reality. – Niels Bohr [93].

Utilizing the natural projection of fundamental parameters inherent in a Holographic Anthropic Multiverse cosmology we introduce a delineation of dimensionality, awareness and the arrow of time as they might arise relative to a temporal subspace of an absolute timeless HD space – a regime of the unitary field. Temporal asymmetry - the observed arrow of time has remained one of the most paradoxical problems in physics, recently considered more fundamental than quantum theory. The noetic approach delineated here assumes a ‘supra-local’ domain more fundamental than the sub-quantum hidden variable regime proposed by de Broglie and Bohm and introduces a whole new cosmology defining time and its origin. Current thinking suggests that there are five arrows of time, four physical and one psychological; in this chapter it is suggested that all arrows of time are a function of the phenomenology of the observer which calls for a reformulation of the basis of physical theory. Incorporating this

assumption into scientific epistemology requires a ‘continuous-state anthropic multiverse’ entailing an additional set of transformations beyond the Galilean, Lorentz-Poincaré groups of transformations and a description of the correspondences reducing to the current standard models of particle physics and quantum theory. Chapter 11.

3.21 New Cosmological Framework

This work attempts to demonstrate the utility of an emerging new cosmological framework by increasing our understanding of the arrow of time in a putative new context pertaining to the nature of reality itself and role of the observer which was irrelevant in Newtonian Mechanics; this mentality has continued to persist among physicists where time is looked at with a certain amount of abhorrence because it seems to demand addressing the nature of the observer in a fundamental way including addressing the nature of consciousness or awareness itself [11].

Although resistance to Big Bang cosmology has remained since its inception, only recently have such criticisms become more acceptable. We assume cosmology to be a multiverse, a form of covariant scale-invariant self-organized complex system within which the spacetime backcloth is a dynamical process of the inherent self-organization. We consider this fundamental backcloth to be a form of Dirac covariant polarized vacuum [94,95]. The dynamical surface of this vacuum is purported to be a zero-point field. In this context the arrow of time is defined as a locus of events conjoined with the continuous transformation of this spacetime. At the fundamental level an event is generally defined as an interaction of reversible trajectories in the dynamics of a physical system; because the dynamical equations of physics are time-reversible no preferred direction of time is considered relevant. A new event requires a preferred direction which produces a change in the initial conditions of the dynamical trajectories because such transformations of the dynamical trajectories of a system consist of shifts in the spatial and momentum coordinates within the limits of the uncertainty principle $\langle \delta x^2 \rangle^{1/2} \langle \delta p_x^2 \rangle^{1/2} = \hbar / 2$ [96].

At this fundamental level the vacuum structure is stochastic and quantum fluctuations of vacuum radiation [97] randomize the momentum distribution of particle coordinates and by the uncertainty principle there is a continuous fundamental ambiguity relating to any direction for an arrow of time. This is in contrast to the concept of Heisenberg ‘potentia’ where all properties of a system remain unresolved before occurrence of

an event. Thus an arrow of time can be defined as a cumulative resultant of oriented new events producing a hierarchical long-range order in the dynamics. From this starting point a new continuous-state HD offshoot is developed.

3.22 Current Philosophy of Temporal Science

In Newtonian clockwork mechanics awareness was irrelevant or nonexistent. The advent of quantum mechanics introduced a troublesome observer involved measurement. Although highly successful quantum mechanics is deemed incomplete - unable to describe biological systems suggesting that extended theory is required. The additional theory must describe the fundamental nature of time and fully include the observer.

Traditionally five arrows of time [98-101] have been described:

- ELECTROMAGNETIC: It is generally observed, which leads to the belief that all electromagnetic waves propagate into the future only. However, this is not necessarily true in interpretations of the transactional /absorber theory of radiation [7,8,11]; and represents a component of the illusion represented in Fig. 3.19 [3,43,102]. This is consistent with Maxwell's equations which are symmetrical in time.
- PERCEIVED EXPANSION OF THE UNIVERSE: Distinguishes between a past and future in the evolution of matter in the universe. In multiverse cosmology this arrow of time has no fundamental significance because it is an observational illusion proposed by an incorrect interpretation of astrophysical data [3,43,102].
- THERMODYNAMIC: The observation of temporal asymmetry in thermodynamic processes represents the most important arrow of time because it provides all of our phenomenological experience, and the existence of biological activity. Irreversible processes move toward a thermodynamic equilibrium of maximum entropy.
- KAON DECAY: Nuclear reactions may occur in either direction with one exception occurring between elementary particles that are not part of ordinary matter - Neutral Kaons. There are three kinds of K meson but only the neutral Kaon exhibits a temporal asymmetry. Because neutral Kaon decay asymmetry is a spacetime property not associated with ordinary matter its description can be formalized into evidence of the supralocality of the multiverse [3,43,102] by illustrating the variation of decay paths in terms of gravitational coupling to spatial and temporal nonlocal spacetime spin-exchange dynamics.

- THE OBSERVER: The subjective flow of time that reveals to our moment by moment experience that all actions flow from the present into what we define as the past. The contrast between the four arrows of time defined by physical laws and the subjective arrow of time has often led to the belief that time is an illusion.

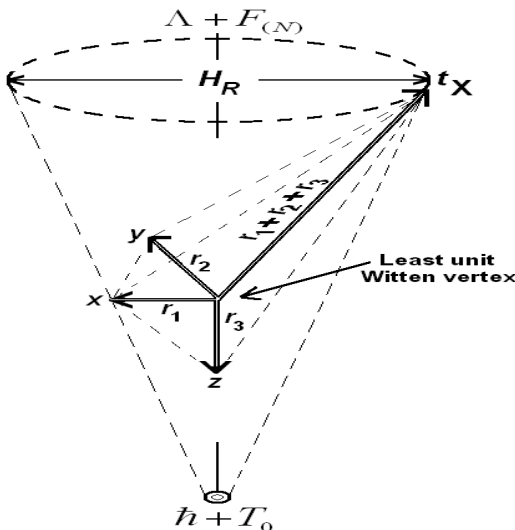


Fig. 3.18 Arrow of time as an oriented vector summation of continuous-state dimensional reduction deficit angle spin-exchange compactification of spacetime least-units (LCUs).

Currently physicists describe: 1) Physical time and 2) Psychological time separately, both of which are incompletely understood. A major premise of this work is that all five arrows of time are an illusion related to the phenomenology of the observer's awareness. But because mind in multiverse cosmology is completely physical; all the arrows of time are likewise actually 'physical' and can be investigated with new experimental methods leading to discovery of the teleology of the noetic field [35]. The unified nonlocal noetic field couples classical dynamics and general relativistic effects in a complementarity through the pathways of neural dynamics [3]. This is directly responsible for the perceived arrow of time because this matter-spacetime medium is what 'we' are made of and 'imbedded' in. The noetic timeless domain is the entry point of awareness coupling eternal time through special relativistic dynamic transformations independent of classical gravitation to temporality.

3.23 Complementarity of Physical Time and Observer Time

Einstein remarked that ‘*if one could ride on a photon, one could circumnavigate the universe without the passage of time*’. We postulate that the view from sitting in the saddle of that photon is of an ocean of light or universal Wheeler geon [45] that would be equated with an HD regime of the unified field. This view is shielded from the observer by the uncertainty principles action on the arrow of time which forms the temporal domain walls of our virtual reality. Virtual pretty much in the sense depicted in the Hollywood trilogy, *The Matrix*. This view is readily metaphorized by Plato’s ‘analogy of the cave’ from antiquity or by the more contemporary view of an observer seated in a movie theater. See Figs. 3.19 & 3.20. Discrete frames of film passing over the projector lens appear smooth on the screen because the motion of the film at a few cm/sec is too fast for the eye. In reality, of course, the effect is relativistic.

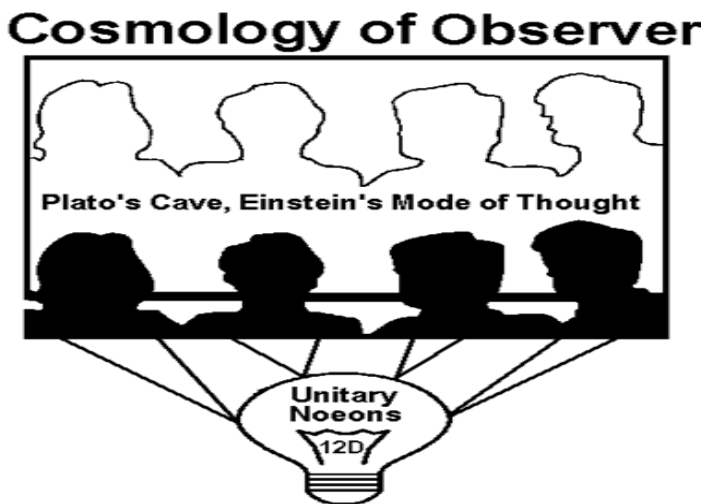


Fig. 3.19. Plato’s allegory of the cave. Plato said ‘reality is as if we are dwellers in a darkened cave chained up facing a wall viewing events as shadows by the light of a fire projected from behind and never knowing the true nature of existence. If we were released to turn toward the light, at first we would be blinded by its brightness still having our perception clouded. Elaborated in the movie theater model of perceived 4D virtual holographic reality in Fig. 3.20.

In a more modern interpretation of Fig. 3.19, we would not be blinded by ‘brightness’, but our vision system is not equipped to see 4D or $>$ 4D objects.

We may extend this to a holographic model in which the observer is imbedded in the cosmology itself and made out of the same materials as the surrounding matter. Because of the relativistic effects, the observer does not notice the virtual nature of the reality (See Fig. 3.20). The anthropic action of UFM noeons (exchange unit of the unitary field) is the ‘light’ of the projector bulb or laser for the spacetime hologram. This is an extension of the Holographic Principle [30,31] to its penultimate form. The nonlocal nature of quantum theory and the EPR principle give the best indicia of this kind of fundamental basis for reality.

As discussed elsewhere anthropic reasons for the 1st person – 3rd person barrier and why we are not easily able to perceive the 3rd regime UFM ‘ocean of light’ relates to the nature of the arrow of time [10,11]. In multiverse cosmology the additional dimensions are not invisible because they are curled up at the Planck scale, but because of a spin-exchange deficit-angle subtractive interferometry mechanism.

Now that some cosmological properties are reviewed it is easier to show the relationship of physical time to conscious time. All arrows of time reduce to the spacetime topology of the Dirac polarized vacuum [10,100]. From within the microscopic action of the complex hierarchical cosmology of the least-unit of awareness, macrophysical phenomena, which include thermodynamic processes, appear asymmetric because of a complementarity of Cramer-like standing-wave boundary conditions related to human awareness and other physical conditions. There is no preferred temporal direction in the microphysical laws of physics. When this atemporality is reduced to the temporal domain (when it becomes a subspace) many parameters are subtracted out through the symmetry breaking of the spin exchange compactification dimensional reduction process occurring relativistically. But this microscopic annihilation governed by teleological causality produces an orthogonal summation creating the macroscopia of perception. The velocity c of the reduction / compactification receding from the eternal present has a discrete microscopic beat frequency perceived macroscopically as continuous.

We introduce the suggestion by Franck [9] that an eternal now occupies the center of awareness and all points in spacetime. We assume that awareness, a fundamental physical UFM principle, like the concept of ‘charge’ [10,11,103], is associated with the ‘least unit’ in multiverse cosmology. The LCU is governed by a new Noetic Transform for the self-organized anthropic action guiding the evolution of information from the Planck scale continuously boosting it through M_4 into the 12D Hyper-Geon domain of the unified field as an Ising model rotation of the Riemann

sphere modeled after extended Wheeler-Feynman-Cramer future/past standing-wave parameters [7,8].

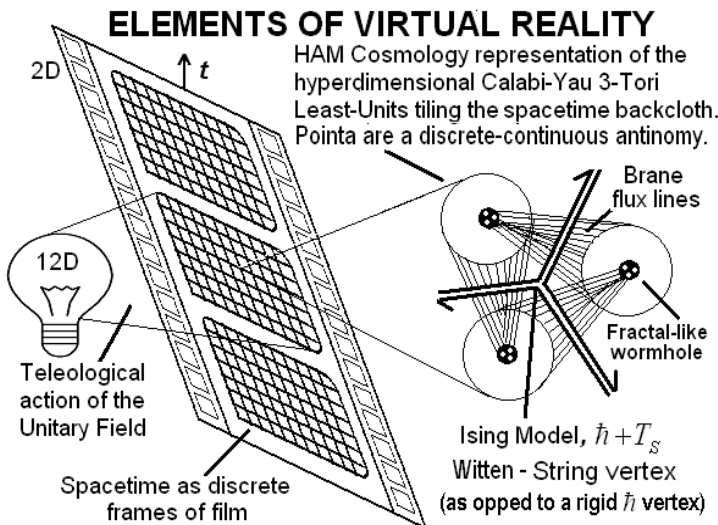


Fig. 3.20 Cosmology of holographic reality. Anthropic action of the unified field pilots the continuous-state evolution of spacetime and quantum dynamics through modulation of the supersymmetric topology of fundamental close-packed Calabi-Yau LCU as a finite regime tiling the spacetime backcloth.

If we utilize the metaphor of a movie theater (Figs. 3.19 and 3.20) to describe the structural-phenomenology of the mind-body and apply Huygens' principle of wave train addition in a manner similar to how sunlight shines through discrete raindrops summing into the smooth image of a rainbow, we can begin to understand the human psychosphere [10,11,102,104]. The psychosphere is the standing wave light-cone domain wall surface of human awareness impinged by qualia [10]. It is not confined to the brain; but occupies the total boundary conditions of the human mind-body that extends from the Euclidean brain occupying M_4 to the limits of the HD UFM Noetic Geon. There is a complementarity between these two domains of the human psychosphere. Fermi-Dirac statistic describe the temporal dynamics in the M_4 brain-body region and Einstein-Bose statistics describe the atemporal HD domain applicable to the holophote action of the Noetic hyper-geon. This is the view of Franck's 'eternal now' [9]. The two domains are mediated by the noeon of the unified field.

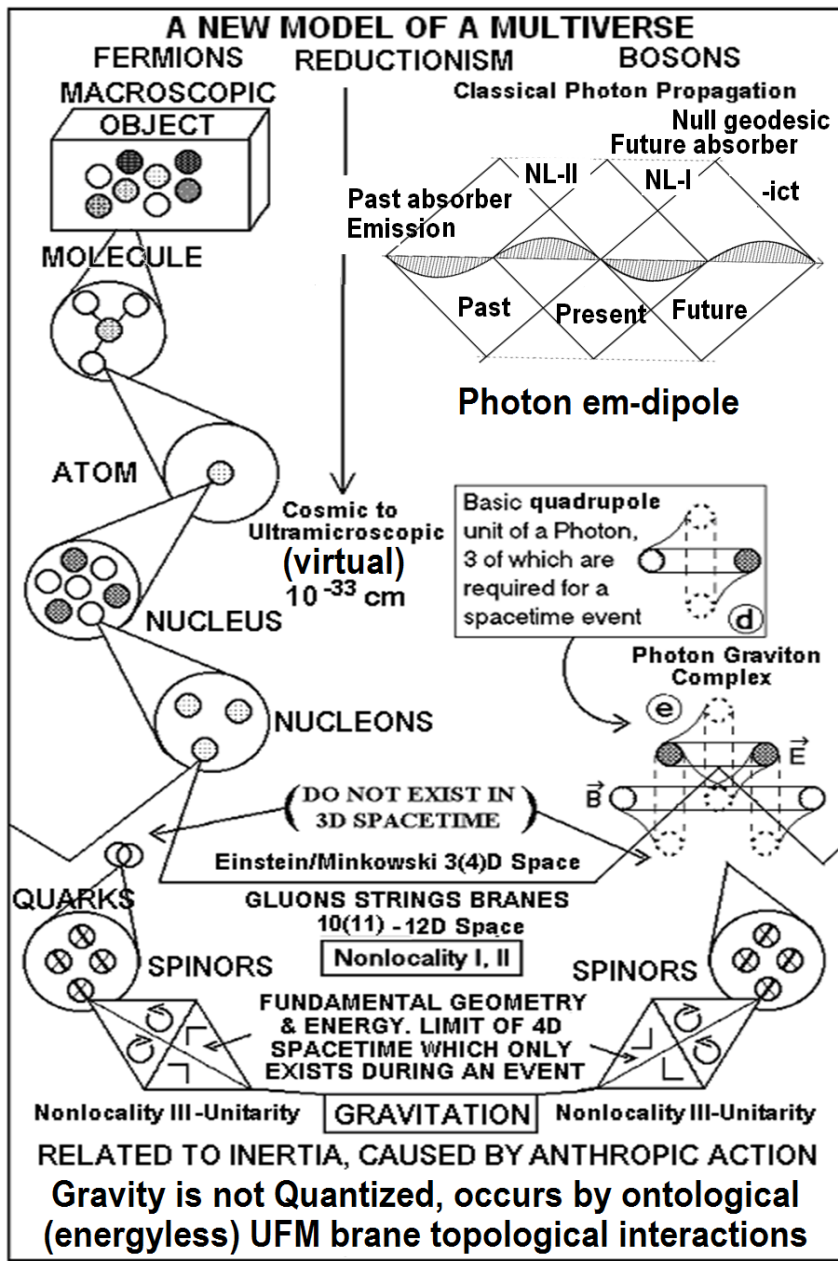


Fig. 3.21 Bose-Fermi reductionist model of matter from macroscopic wave-particles to the photon-graviton noeon-quadruplex of the 3rd regime unified field.

Clock time appears absolute in the Newtonian sense or mutable for relativistic observers. The perception of time is coupled to dynamical processes often associated with entropic flow; but entropic time does not correlate with clock time. And clock time only correlates with psychological time for certain states of consciousness. If a process is harmonic or occurs at a microscopic level where the laws of physics are temporally symmetric all conception of time can be lost; thus the nature of time has maintained itself as a dilemma. As Einstein said ‘The distinction between past, present, and future is an illusion’.

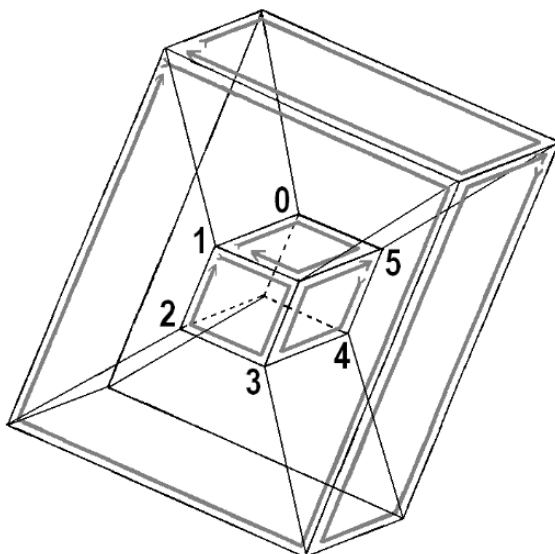


Fig. 3.22. Parallel transport by the Bianchi identities through a 3D Witten Ising model vertex. As the 4D hypercube transforms the small central cube becomes the larger outer cube. In the 12D standing-wave model of multiverse cosmology these small central x,y,z cubes continuously rotate in and out through three complex, $x = x_{\text{Re}} + ix_{\text{Im}}$, $y = y_{\text{Re}} + iy_{\text{Im}}$, $z = z_{\text{Re}} + iz_{\text{Im}}$ orientations simultaneously. This provides part of the basis of our Euclidean virtual reality.

Einstein’s notion of eternal time in a static universe is extended to develop a framework for correspondences that unify all aspects of time within the new multiverse cosmological model [35,102]. Within the multiverse framework human existence is composed of a two-fold complementarity; a Cartesian type body/mind dualism comprised of a Cartesian *res extensa*, and *res cogitans* [11]. The former component

associated with the body (obeying Fermi-Dirac statistics); the latter component (obeying Bose-Einstein statistics) is imbedded in an ‘eternal’ 12D HD space mediating a Cartesian ‘life principle’ [105] through teleological action synonymous with the unified noetic field [10,11].

Time, which is not considered fundamental, is inexorably connected with space in the evolution of the entity spacetime, and within which ‘We’ and the properties of all the matter we perceive is imbedded. It is the properties of this matter, that the awareness of the observer is imbedded in, with which we define the measuring rods of duration and extension that are the fundamental basis of all physical science [92]. To understand the nature or foundations of time we must be able to comprehend more fully the nature of space and the potentia from which it arises. As Einstein obviated the absolute space of Newtonian mechanics; we must now obviate the classical basis of measurement used up to this point in the history of empiricism, and in the process obviate and reformulate the whole fundamental basis of physics itself by inclusion of the true basis of the observer by adding the 3rd regime of UFM. It is mandatory that a new scientific methodology is devised to investigate the ‘absolute noumenon of existence’ that resides behind the ‘façade of phenomenological virtual reality’. If scientists are finally ready to open this Pandora’s box?

It has been suggested that fundamental awareness is comprised of three base states imbedded in spacetime that evanesce into our perceived reality in a manner metaphorically similar to a movie theater [10,11,46,47,100, 102,106-112]. This concept was described in antiquity by Plato’s ‘analogy of the cave’ as shown in Fig. 3.19. More recently, Einstein said: “*Time and space are modes by which we think and not conditions in which we exist.*” [113]. Awareness arises as a complementarity of three fundamental interacting base states

$$|\Psi_M\rangle = |B|\psi_b\rangle + |\psi_e\rangle + |\psi_a\rangle \quad (3.14)$$

where $|B|\psi_b\rangle$ represents the Fermi brain, $|\psi_e\rangle$ an individual’s components of eternal nonlocal elemental intelligence [114] and $|\psi_a\rangle$ the teleological anthropic action principle [10,11,46,47,100,102,106-112]. Within the current adamant vogue of cognitive theory this represents an extremely unpopular position which is also quite complicated. We have made our preliminary case elsewhere [10,11,46,47,100,102,106-112]. especially in the companion mind-body volume [11]. Suffice it to say here

that within the bounds of an individual psychosphere the above triune base states produce a superradiance that becomes awareness. This occurs through the holophote injection of the anthropic action principle into the unique hyperdimensional ‘standing wave’ domain of an individual coupled to their local eternal spacetime present.

The physics of time (thermodynamic processes, kaon decay etc) seems independent of psychological time. But in an *anthropic multiverse*, all arrows of time are interrelated and arise from one central process in the hierarchy of unitary translation of the close-packed noetic least cosmological unit tiling the spacetime backcloth. An understanding can be garnered by explaining the amplification of microscopic phenomena by processes inherent in fundamental awareness. Observation synonymous with measurement is the obverse of the process of awareness. William James stated that ‘there is no splitting of experience into consciousness and what the consciousness is of’. So between experience *A* and experience *B* there is no gap; no collapse of the wave function is observed in thought processes. If one attempts to bring a photon to rest, it destructs. This observed reduction of the wave function in the external world has confused conceptions of what occurs in the mind where there is no collapse and as in the photon analogy there cannot be. With large-scale XD the ‘continuous-state spin-exchange compactification dimensional reduction process’ occurring at the speed of light suggests why large XD are not readily observed. The deficit angle arising in the parallel transport of the continuous-state topology subtracts out one half of the HD standing wave parameters during the compactification process between the gaps in the film so to speak (Figs. 3.19 to 3.21) leaving us with a limited view which is the geometric origin of time.

According to the Copenhagen interpretation all quantum measurements are associated with reduction of the wave function, a thermodynamically irreversible process. Only the final observed component of the ensemble is considered to be *real* [39] by

$$\sum_i c_i \psi_i \rightarrow \psi_i . \quad (3.15)$$

This action directly creates boundary conditions separating the fundamental reversible aspects of microscopic natural law into the perceptual macroscopia and an additional HD physical realm not perceived by neurophysiology. Noetic cosmology proposes that this temporal asymmetry is completely observer related and the ensuing boundary conditions delete

essentially half of the systems information cosmology. Bohr stated from the beginning that the Copenhagen interpretation did not describe biological systems; therefore, a full physical description must utilize extended de Broglie/Bohm ontological forms of quantum theory without state reduction and therefore loss of systems information by Ψ collapse. The big question then is what is the utility of the unobserved parameters of this cosmology? Here is where the main utility of the Noetic least unit transform enters in.

The complementary superluminal boosting of the ‘standing wave’ eternal present undergoing the continuous cycling spatial, s temporal, t and energy, E dimensions through unified, U quantum, Q and classical, C states

$$D_s \rightarrow D_t \rightarrow D_E : R_U \rightarrow R_Q \rightarrow R_C \quad (3.16)$$

that produces and maintains the perceptual macroscopic amplification of microscopic phenomena. The Noetic boosts reduce the flux of all physical fields at the domain wall boundary conditions by absolute parallelism of the Bianchi identities, $\partial \circ \partial = 0$ where the boundary of a boundary equals zero [40] facilitating this whole cosmological process. We begin with the description of the electromagnetic field. Following Kafatos and his collaborators [44] suggesting the importance of $\dot{R} \equiv c$ for universal continuous-state boundary conditions which are also relevant to the velocity required for the observer’s mind to escape microphysics and become coupled to a virtual macroscopia for em by

$$\bar{c} = \frac{2\vec{E} \times \vec{B}}{\vec{E}^2 + \vec{B}^2} \quad (3.17)$$

where, according to Wheeler [115,116] velocity $\bar{c} = \vec{n} \tanh \alpha$ and the numerator is the Poynting flux and the denominator the energy density. This boost equation describes the reduction of the em-field to mutual parallelism which according to the Bianchi identity describes how the boundary of a boundary equals zero [40] (See Fig. 3.22). Allowing half the universe to cancel out of awareness into the resultant standing wave covering. The covering is piloted by the de Broglie-Bohm wave-particle energy. An application of Huygens’ principle of wave addition might produce the smooth feel of the evanescence of reality we observe while we are *surfing* as it were on the face of the discrete elements of atemporal microphysics!

3.24 The Vacuum Origin of Thermodynamics and Entropy

Temporal asymmetry is a fundamental problem because the microscopic laws of physics are time reversible. The macroscopic arrow of time arises from translation of the complex boundary conditions of the observer, which ultimately is a property of the unified field. Although this is a perceptual phenomenology it is still physical. The most fundamental basis, more fundamental than for quantum interactions of matter is the unified electromagnetic-gravitational arrow of time; from which the thermodynamic and all other arrows arise. The continuous-state dimensional reduction compactification process within the topological structure of the polarized Dirac vacuum has a *beat frequency* associated with the inherent *Jacob's ladder-holophote* of least unit translation.

Entropy increase in thermodynamic systems can be accounted for by vacuum radiation; and this interaction of vacuum radiation with matter is time-reversible. Therefore whether entropy increase in thermodynamic systems can be considered to produce an arrow of time depends on what controls the vacuum photons. Both cases are consistent with quantum mechanics. Position and momentum perturbation on particles by vacuum zero-point radiation is limited by uncertainty to

$$\langle \delta x^2 \rangle^{1/2} \langle \delta p_x^2 \rangle^{1/2} \quad (3.18)$$

where the first root mean square value is position and the second momentum respectively, Burns [96,97]. According to Zeh, [39]

$$\langle \delta x^2 \rangle^{1/2} = (\hbar t / m)^{1/2}, \quad (3.19)$$

(where m is particle mass), can be obtained both from classical SED and the stochastic interpretation of quantum mechanics. Substituting the result into the uncertainty principle yields a fractional change in momentum coordinates, $\langle \delta x_x^2 \rangle^{1/2} / p$, p is the total momentum, $2^{-3/2} (\hbar / Et)^{1/2}$, E is the kinetic energy. As vacuum radiation interacts with particles, momentum is exchanged. When an initial fractional change $\langle \delta x_x^2 \rangle^{1/2}$ in momentum is amplified by the lever arm of molecular interaction,

$$\langle \delta p_x^2 \rangle^{1/2} / p \geq 1 \quad (3.20)$$

becomes greater than one in only a few collision times [39,96,97]. Therefore the momentum distribution of a collection of interacting particles is randomized in that time, and the action of vacuum radiation on matter can account for entropy increase in thermodynamic systems; i.e. it can be related to the atemporal / temporal microscopic / macroscopic cosmology of fundamental awareness.

Dynamical interactions occurring at the molecular level are time-reversible, but thermodynamic processes associated with entropy increase, like diffusion and heat flow, only proceed unitarily in time. Entropy increase appears to be only a macroscopic phenomenon, appearing when a coarse-grained average is taken of microscopic processes. No averaging of time-reversible processes has been shown to account for temporally irreversible phenomena [39]. The reduced or temporal subspace nature of human perception filters out half of the microscopic action by the continuous dimensional reduction process. This action occurs at the speed of light explaining perspective – narrowing of the railroad tracks into the distance; which would not occur for a HD atemporal observer like ‘God’.

In the standard model (utilizing only the positive set of Maxwell’s equations) electromagnetic waves emanate from a source to infinity only, and do not converge from infinity to a source. Collapse of the wave function is a one-way process [117,118]. Burns [96,97] has shown that entropy increase in thermodynamic systems is produced by the interaction of vacuum radiation with matter. This interaction is time reversible. Whether an arrow of time is ultimately involved in entropy increase depends on how vacuum radiation is produced. In Noetic UFM cosmology which utilizes an extension of the Wheeler / Feynman absorber theory of radiation em-waves from infinity do converge with the standing wave source. There are extended quantum domains without collapse of the wave function where noncomputable ontological superpositions occur; and vacuum radiation is governed by teleological cosmological action principles inherent in the HD vacuum topology [119,120].

The exchange particle of the Noetic Unified Field, we term the noeon, follows preferred paths within the continuous spin-exchange dimensional reduction compactification process. It should be noted that ‘exchange particle of the unitary field’ is a bit of a misnomer as the exchange is energyless and ontological – a form of topological switching; we will deal with that conundrum later. It is reminiscent of a quantized traveling arc or *Jacob’s ladder* where the ‘charge’ enters with a harmonic *holophote action* at the bottom (Planck scale) and travels to the HD region where it is released or reabsorbed cyclically as the *eternal present* [9] remains a

continuous-state of the future-past HD topology. This again is the movie theater metaphor where discrete frames of film pass over the projector bulb (Planck scale holophote noeon emission into every point and atom in spacetime) propagating *up* the Jacob's ladder (psychosphere light cone surface) to the *screen* (smooth continuous raster of awareness) as qualia².

UFM Noeon flux, the super-quantum potential force of coherence organizing matter, also represents both the life principle, and light of awareness [10,11] propagating with an inherent beat frequency along preferred paths of a Jacob's ladder-like holophote by the UFM transform of multiverse cosmology. The smoothness of reality is the leading edge of the lightcone kept in phase by a Huygens' like principle of wave train addition of the oscillating Planck scale holographic least-units (LCU).

3.25 Spin-Exchange Compactification and the Noetic Transformation

Photon mass is not continuously maintained in multiverse cosmology but occurs only during a period of internal motion (angular momentum) when the centrum of the wave - the particulate moment, couples to the vacuum (a leap frog mechanism); so the photon in propagation cycles harmonically from mass to massless as a property of the future-past symmetry of its wave-particle duality. This is a new property of photon propagation introduced by the continuous-state parameters of multiverse cosmology.

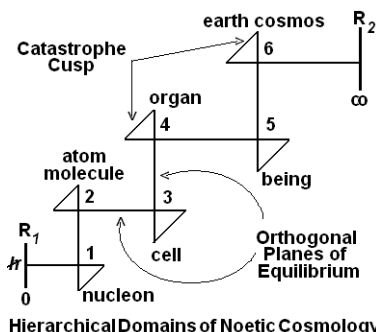


Fig. 3.23 Basic conceptualization of the covariant scale-invariant hierarchical standing-wave catastrophe structure and function of multiverse cosmology, microscopic to cosmic.

² Qualia- In philosophy of mind 'The quality of the feel' of a moment of awareness, the sensation of 'redness' for example. We take this much further here in that the duality of the reality of the observer is like a 'Qualia of the Multiverse'; part of the cosmologies inherent conformal scale-invariance [11].

Photon mass anisotropy is a major feature of the UFM multiverse model. It is indicative of the ubiquitous occurrence of the properties of spherical rotation discovered by Dirac initially attributed only to the spin of the electron where it takes 720° instead of 360° to return to the origin. The multiverse spacetime Cavity-QED paradigm is based on the fundamental premise that the energetic interplay of the fundamental forces of nature, mass, inertia, gravitation and spacetime is based on a unified symmetry of internal spin-spin coupling and spin exchange compactification with a ‘super quantum potential’ [121] ultimately being the anthropic unified action and control principle of the evolution of spacetime which within the Einstein Hubble 3-sphere is considered a complex self-organized system giving the known properties of such systems [10].

Spin exchange symmetry breaking through the interplay of a unique topological control package orders the compactification process providing a template from which superstring or twistor theory could be clarified if the tenets of Chap. 4 are applied (assuming they are correct of course).

One purpose of compactification dynamics is to allow the Einstein 3-sphere of temporal reality to stochastically ‘surf’ as it were on the atemporal LSXD superstructure creating our virtual reality and the perceived arrow of time allowing nonlocal interactions not possible in a Newtonian absolute space. Stated another way, the inherent purpose of the domain of quantum uncertainty is to stochastically separate the classical regime from the UFM regime by subtractive interferometry, revealing why the LSXD can be relativistically unobservable, a problem of the observer.

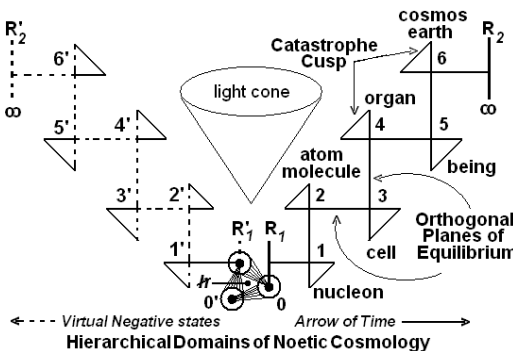


Fig. 3.24 Further conceptualization of the advanced-retarded future-past mirror symmetry/duality of the scale-invariance and function of the standing-wave properties of multiverse dimensionality from a 0D LCU to the 12D limit of the Hubble 3-sphere, setting the stage for application to a multiverse model arrow of time.

By parallel transport of the topological boundary conditions of the continuous-state dimensional reduction compactification process the deficit-angle produced in the hysteresis loop of the standing-wave eternal present allows half of the parameters to drop out during the ‘leap-frogging’ of coordinate fixing and re-fixing as the awareness of the observer relativistically couples, uncouples and re-couples, as a baton passing in a relay race, to observed reality. This seemingly complicated process creates the arrow of time and also reveals why the XD are not perceived even though they are large in scale during the retarded portion of the process. Only certain pathways for parallel transport by spin exchange dimensional reduction (D down scaling) and superluminal boosting (D up scaling) are allowed by the Wheeler-Feynman symmetry breaking relations in the continuous maintenance of the standing wave present.

Scale-Invariant Hierarchical Domains of Anthropic Cosmology

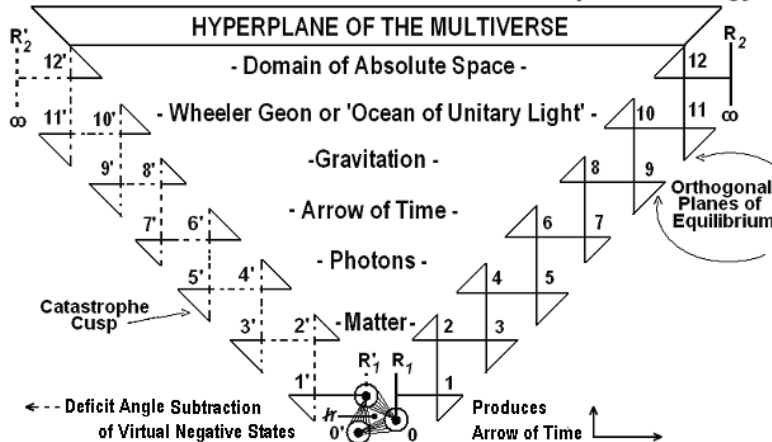


Fig. 3.25 By deficit angle parallel transport during the continuous-state spin-exchange dimensional reduction compactification process the arrow of time emerges naturally by subtraction of the advanced portion of the standing-wave topological elements of spacetime relative to the quantum state of the observer.

It is useful to further clarify the utility of parallel transport begun in association with Fig. 3.22 above in terms of the Regge equations [40] relation to the Bianchi identity of a boundary of a boundary being equal to zero ($\partial \circ \partial \equiv 0$) [40,122,123]. Figure 3.26 shows the three counter-propagating circular permutations of the face plane of a tetrahedron representing parallel transport which creates a deficit angle [124] allowing

uncoupling from Euclidean reality. Allowed pathways and orientations restricted by the symmetry breaking conditions allow boosting of the information or energy associated with one domain to transform by topologically switched parametric up-down conversion into another regime.

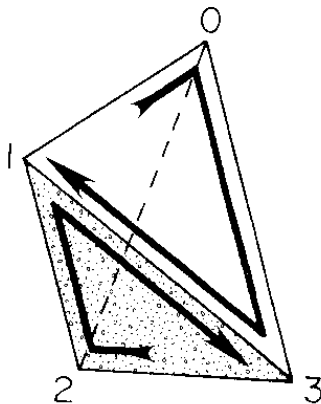


Fig. 3.26 Bianchi identities of absolute parallelism for a tetrahedron.

Ordering vertices as shown in Fig. 3.26 induces an orientation on the tetrahedron's two dimensional boundary, which consists of four oriented triangles by $\partial(0123) = (012) - (013) + (023) - (123)$. This in turn induces an orientation on the edges of the one dimensional boundaries $\partial(012) = (01) - (02) + (12)$. Summing the dimensional boundaries cancels them in pairs [$(01) - (01) = 0$]. This is the Bianchi identity $\partial \circ \partial = 0$ described by the Regge equations for parallel transport where the boundary of a boundary is zero. Or suggesting the tetrahedron is edgeless because the 1D boundary of the 2D boundary of the 2D region is zero [122-124].

3.26 Dirac Spherical Rotation Inherent to LCU Transformation

Typically, the Dirac dual (2π) spinor rotation applies to the observation that an electron undergoes 720° of rotation (not the usual 360°) before returning to the initial orientation. Traditional thinking has assumed this to be some property of matter. But the discovery of the complex structure of

spacetime has shown that this is not a property fundamental to the electron; but rather to the superspace the electron is imbedded in and part of Dirac spherical rotation as it is also called. The Dirac rotation is more fundamentally a primary property of space than it is matter. This is revealed in the complex hierarchical structure of the LCU discussed here.

The Dirac String Trick

Tie the four corners of a cube to another larger cube by loose strings as shown in the figure below (alternatively, tie the initial square to the four corners of a room). Now rotate the small cube by 360° about a vertical axis, that is, in a horizontal plane. The strings will become somewhat tangled, and it is not possible to untangle them without rotating the cube. If we rotate through another 360° , for a total of 720° ; it is now possible to untangle the string without further rotation of the cube by simply allowing enough space for the strings to be looped over the top of the cube. You may not believe it unless you check it out for yourself. It is advisable to use clips to attach the strings to the squares, so that it can be undone easily if it gets too tangled. A similar idea works for a rotation through 720° about any axis.

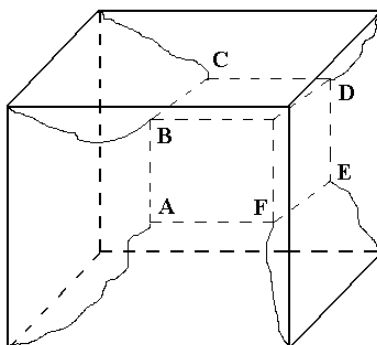


Fig. 3.27 Demonstration of the Dirac string trick to illustrate how spin $\frac{1}{2}$ particles like the electron must undergo 720° of rotation instead of the usual expected 360° to return to the starting point. Figure adapted from [40].

Another version of the Dirac string trick is called the Philippine wine dance. A glass of water held in the hand can be rotated continuously through 720° without spilling any water. These geometrical demonstrations are related to the physical fact that an electron has spin $\frac{1}{2}$. A particle with spin $1/2$ is something like a ball attached to its surroundings with

string. Its amplitude changes under a 360° (2π) rotation and is restored by rotation of 720° (4π). The formal description of such complex phenomena typically requires sophisticated mathematics (algebra, group theory, topology, quaternions...) since they are not part of everyday experience.

According to Kauffman [125] features of certain spin networks can be viewed as particles with similarities to Bosons and Fermions of the standard model of particle physics by looking at topological elements of the Artin braid group [126-128] that could be used as the basis for introducing quantum numbers. The focus of Kauffman et. al. is the manipulation of braid forms, not specific correlations to actual physics, but the work establishes a useful basis for physical implications in future works especially for twists for fermions that can be matched to quantum numbers such as weak isospin, hypercharge, baryon number or lepton number for example [125]. Kauffman says '*The spinor rotation does not contain a twist of a knot*' (A knot is the closure of specific braids). What occurs in the Dirac 'knot trick' is that a certain kind of belt twist can model the fact that the first homotopy group of the rotation group $\text{SO}(3)$ is $\text{Z}/2\text{Z}$. This can be easily visualized (Fig. 3.27) giving an understanding of how the phase change in a fermion wave-function can occur as the result of a rotation in 3-space which can be represented via $\text{SU}(2)$ on the quantum wave function with $\text{SU}(2)$ appearing relative to $\text{SO}(3)$ as its double 'covering space' [129].

The twist as demonstrated with a belt (Fig. 3.27) happens in 3-space. But this topology is not directly associated with a geometric linking of an electron with its surroundings. We only get there (using present theory) by noting that any quantum process must be modeled by a family of unitary transformations. And then a 360° rotation will be mapped up into $\text{SU}(2)$ and end up on the second sheet of the two sheeted covering space $\text{SU}(2)\text{-}\text{SO}(3)$. The topology of this covering space contains the essence of the Dirac belt trick (Fig. 3.27). But the belt trick itself is part of something occurring in 4D, namely the quaternions. See [130] for a discussion of this relationship. A topological theory of the electron where the Dirac 'belt trick' rotation property is connected directly with the physical properties of a particle is currently stymied by the standard Copenhagen quantum theory because there is no 'physical particle' only the result of measurements of an electron wave function which gives only statistical parameters of the wave function.

But as well-known this is not true in the de Broglie-Bohm-Vigier (DBV) causal stochastic interpretation of quantum theory where wave and

particle are physically real and may both exist simultaneously [131]. But DBV has not been completed. We believe when this explanatory gap has been filled it will show that there is no Quantum Gravity. The quantum regime ends with Copenhagen and the unification of quantum theory and gravity will be shown to occur at the level of 3rd regime UFM. Our view here is initially more conceptual, we think that a certain rotation point of the belt, where the twist occurs in 3D, becomes like a Klein bottle that can only be untwisted by rotation through 4D where it is not intertwined. We encourage the reader to perform the little trick with belts or strings from Fig. 3.27. When the electron is rotated 360° the 3D observer sees the twist that in that perspective cannot be untied except by another 360° rotation that occurs in 4D.

In string/brane theory there is a putative Kaluza-Klein spin tower compactification gradient of T-duality/Mirror symmetry for a pair of Calabi-Yau 3-forms or Kähler manifolds where the raising and lowering of the dimensionality with the string/brane tension-coupling parameters passes through Fermi-odd and Bose-even spin symmetries relating the branes to each other. Our postulate is that the rotation of the electron is indicative of a topological process that might be conformally scale-invariant through this whole convoluted hierarchy of dimensionality. We assume, the Dirac 360°-720° spherical spinor rotation of the electron contains a 'pinch or twist' in the midst of the transformation assumed to be indicative of a 4D topological background component of the rotation.

Is there a braid-form that might be scalable to even HD; a form that might require the mirror/dual symmetry conditions purported to occur in string-brane topologies to perform the periodic pinch and unpinch? The Dirac spherical rotation concept appears to be indicative of a covariant scale invariant cosmological principle applying to the entire dimensional nature of reality itself not just the electron. This cosmological twist then would occur as the Copenhagen regime separating Newton classical mechanics from unitarity. We have done our best to introduce an empirical protocol to falsify this prediction (low energy methods without accelerator that can also test string theory).

In several places Vigier refers to the 'negative result' of the 1887 Michelson-Morley ether-drift experiment [132-134]. However, contrary to what numerous textbooks and popular science books claim, this famous experiment did not give a null result. Vigier himself acknowledges this in an article not included in the collected works volume, or even mentioned in its bibliography. In it Vigier states [131]: *'the observed effect was not zero in Michelson's famous experiment, as later confirmed by a (presently*

almost forgotten) set of very detailed and very careful experiments by Morley and Miller' [135,136]. He presents a brief overview of the 'long set of remarkable experiments' conducted from 1881 to 1926, which 'are now completely ignored in the physics community'. These experiments detected a small but consistent and systematic ether drift of about 9 km/s [131,135,136].

Although relativity theory assumed a zero ether drift (and a constant velocity of light), Vigier [131] argues that a positive ether drift is compatible with special relativity if photons are assumed to have a very small mass [3,5]. He also argues that Sagnac's discovery in 1910 of fringe shifts in rotating interferometers (the Sagnac effect) can be reconciled with general relativity on the same assumption [131]. Whether the results of ether-drift experiments, including more recent ones [136], are best understood in terms of standard relativity theory is hotly contested [134,137-139]

According to Vigier, non-zero photon mass, m_γ (originally proposed by the likes of Einstein, Schrödinger, and de Broglie):

"If confirmed by experiment, it would necessitate a complete revision of present cosmological views. The associated tired-light models could possibly replace the so-called expanding Universe models. Non-velocity redshifts could explain the anomalous quasar-galaxy associations, etc., and the Universe would possibly be infinite in time" [131].

References

- [1] Peebles, P.J.E (1993) Principles of physical cosmology, Princeton: Princeton University Press.
- [2] Weinberg, S. (2007) Physics: What we do and don't know about physics, Nov. 20, The New York Review of Books.
- [3] Amoroso, R.L., & Rauscher, E.A. (2009) The Holographic Anthropic Multiverse Formalizing the Complex Geometry of Reality, London: World Scientific.
- [4] de Bernardis, P. et al. (2000) A flat universe from high-resolution maps of the cosmic microwave background radiation, *Nature*, 404, 955-959.
- [5] Amoroso, R.L., Kafatos, M. & Ecimovic, P. (1998) The origins of cosmological redshift in spin exchange between Planck scale vacuum compactification and nonzero rest mass photon anisotropy, in G. Hunter, S. Jeffers & J-P Vigier (eds.) *Causality & Locality in Modern Physics*, Dordrecht: Kluwer.
- [6] Vigier, J-P & Amoroso, R.L. (2002) Can one unify gravity and electromagnetic fields? in R.L. Amoroso, G. Hunter, S. Jeffers & M. Kafatos, (eds.) *Gravitation & Cosmology: From the Hubble Radius to the Planck Scale*, Dordrecht: Kluwer Academic.
- [7] Wheeler, J.A. & Feynman, R. (1945) *Rev. Mod. Physics*, 17, 157.
- [8] Cramer, J.G. (1986) *Reviews of Mod. Physics*, 58:3, 647-687.

- [9] Franck, G. (2000) Time and presence, in Science and The Primacy of Consciousness, R.L. Amoroso et al, (eds.) Orinda: Noetic Press.
- [10] Amoroso, R.L & Amoroso, P.J. (2004) The fundamental limit and origin of complexity in biological systems: A new model for the origin of life, in D. Dubois, (ed.) Computing Anticipatory Systems, Proceedings of CASYS04, 6th Int, Conf., Liege, Belgium, 11-16 Aug, 2003, AIP Proceedings Vol. 718, pp. 144-159.
- [11] Amoroso, R.L (ed.) (2009) The Complementarity of Mind and Body: Realizing the Dream of Descartes, Einstein and Eccles, New York: Nova Science Pubs.
- [12] Einstein, A. (1917) *Kosmologische Betrachtungen zur allgemeinen Relativitätstheorie, Königlich Preußische Akademie der Wissenschaften* (Berlin) *Sitzungsbericht*, pp. 142–152, Reprinted facsimile as Doc. 43 in Kox et al. (ed.) 1996, Translation: Cosmological Considerations on the General Theory of Relativity. In: H. A. Lorentz et. al. (eds.) The Principle of Relativity, New York: Dover, 1952, 177–188.
- [13] Bondi, H. & Gold, T. (1948) MNRAS, 108, 252.
- [14] Hoyle, F. (1948) A New Model for the Expanding Universe, MNRAS, 108, 372-82.
- [15] Alpher, R.A., Bethe, H. & Gamow, G. (1948) The origin of chemical elements, Physical Review, 73: 7; 803-804.
- [16] Sen, R.N. (1999) Why is the Euclidian line the real line? Found. Phys, 12:4;328-345.
- [17] Witten, E. (1981) Search for realistic Kaluza-Klein theory, Nuc Phys B186:412-428.
- [18] Overduin, J.M. & Wesson, P.S. (1997) Kaluza-Klein gravity, Physics Reports, 283, pp. 303-378.
- [19] Randall, L & Sundrum, R. (1999) An alternative to compactification, Physical Review Letters, 83, 4690-4693.
- [20] Randall, L. (2005) Warped Passages, New York: Harper-Collins.
- [21] Einstein, A. (1952) Letter to H. Stevens, from Stevens, H (1989) Size of a least unit, in M. Kafatos (ed.) Bell's Theorem, Quantum Theory and Conceptions of the Universe, Dordrecht: Kluwer Academic.
- [22] Ellis, G.F.R., Kirchner, U. & Stoeger, W.R. (2004) Multiverses and physical cosmology, Monthly Notices of the Royal Astronomical Society, 347: 921-936; or arXiv:astro-ph/0305292v3.
- [23] Dicke, R.H. (1957). Gravitation without a principle of equivalence, Reviews of Modern Physics 29: 363–376.
- [24] Barrow, J.D. & Tipler, F.J. (1988) The Anthropic Principle, Oxford Univ. Press.
- [25] Tipler, F. (1998) The Physics of Immortality: Modern Cosmology, God and the Resurrection of the Dead, New York: Doubleday.
- [26] Weinberg, S. (2007) Living in the Multiverse, in B. Carr (ed) Universe or multiverse? Cambridge: Cambridge University Press, arXiv:hep-th/0511037v1 (2005).
- [27] Susskind, L. (2008) The Black Hole War - My Battle with Stephen Hawking to Make the World Safe for Quantum Mechanics, Boston: Little, Brown & Co.
- [28] 't Hooft, G. (2000) The holographic principle, hep-th/0003004.
- [29] Susskind, L. (2003) Superstrings (Features: November 2003) Physics World 16 (11).
- [30] Susskind, L. (1994) The World as a Hologram, arXiv:hep-th/9409089 v2.
- [31] Bousso, R. (2002) The holographic principle, Rev Mod Phys 74: 825-874; arXiv:hep-th/0203101.
- [32] Brown, M. (1960) A proof of the generalized Schöenflies theorem, Bull. Amer. Math. Soc., vol. 66, pp. 74-76.

- [33] Smart, J.J.C. (1972) Space, V. 7, 506-511, Encyc. Philosophy, New York: Macmillan.
- [34] Darabi, F., Saikoand, W.N. & Wesson, P.S. (2000) Quantum cosmology of 5D non-compactified Kaluza-Klein theory, *Class. Quantum Grav.* 17; 4357-4364, or arXiv:gr-qc/0005036v1.
- [35] Chu, M-Y & Amoroso, R.L. (2008) Empirical mediation of the primary mechanism initiating protein conformation in prion propagation, in D. Dubois (ed.) *Proceedings of CASYS07, IJCAS*, vol. 22, pp. 292-313, Liege, Belgium.
- [36] Amoroso, R.L. & Rauscher, E.A. (2008) Emergence of generalized F-theory 2-branes from SUSY spacetime parameters of the discrete incursive oscillator in D. Dubois (ed.) *Proceedings of CASYS07, IJCAS*, Vol. 22, pp. 283-291, Liege, Belgium.
- [37] Amoroso, R.L. (2000) The parameters of temporal correspondence in a continuous state conscious universe, in L. Bucccheri & M. Saniga (eds.) *Studies on the Structure of Time: From Physics to Psycho(patho)logy*, London: Plenum.
- [38] Burns, J.E. (2002) Vacuum radiation, entropy and the arrow of time, in R.L. Amoroso, G. Hunter, S. Jeffers & M. Kafatos, (eds.) *Gravitation & Cosmology: From the Hubble Radius to the Planck Scale*, Dordrecht: Kluwer Academic.
- [39] Zeh, H.-D. (1989) *The Physical Basis of the Direction of Time*, NY: Springer-Verlag.
- [40] Misner, C.W., Thorne, K. & Wheeler, J.A. (1973) *Gravitation*, San Francisco: Freeman.
- [41] Sklar, L. (1995) *Philosophy and Spacetime Physics*, Berkeley: Univ. Cal. Press.
- [42] Reichenbach, H. (1957) *Philosophy of Space and Time*, NY: Dover.
- [43] Amoroso, R.L. (2002) The continuous state universe, in R.L. Amoroso, G. Hunter, S. Jeffers & M. Kafatos, (eds.) *Gravitation & Cosmology: From the Hubble Radius to the Planck Scale*, Dordrecht: Kluwer Academic.
- [44] Kafatos, M. Roy, S. & Amoroso, R. (2000) Scaling in cosmology & the arrow of time, in Bucccheri, di Gesu & M. Saniga, (eds.) *Studies on Time*, Dordrecht: Kluwer.
- [45] Wheeler, J.A. (1955) Geons, *Physical Review*, 97:2, 511-536.
- [46] Amoroso, R.L. (2002) *The Physical Basis of Consciousness: A Fundamental Formalism*, Part 1 Noesis, XXVI, Romanian Academy.
- [47] Amoroso, R.L (2000) Derivation of the fundamental equation of consciousness, Part I, Boundary conditions, *Noetic Journal*, 3:1, pp. 91-99.
- [48] Amoroso, R.L. & Vigier, J-P (2002) The origin of cosmological redshift and CMBR as absorption/emission equilibrium in cavity-QED blackbody dynamics of the Dirac vacuum, in R.L. Amoroso, G. Hunter, M. Kafatos, & J-P Vigier (eds.) *Gravitation & Cosmology: From the Hubble Radius to the Planck Scale*, Dordrecht: Kluwer.
- [49] Amoroso, R.L. & Rauscher, E.A. (2008) Derivation of the string tension formalism, and super quantum potential as inherent parameters of a holographic conscious multiverse cosmology, in R.L. Amoroso, I. Dienes & Cs. Varga (eds.) *Unified Theories*, Oakland: The Noetic Press.
- [50] Witten, E. (1996) Reflections on the fate of spacetime, *Physics Today*, pp. 24-30.
- [51] Cole, E.A.B. (1977) *Il Nuovo Cimento*, 40:2, 171-180.
- [52] Rauscher, E. (2002) Non-Abelian gauge groups for real and complex Maxwell's equations, in R.L. Amoroso, G. Hunter, S. Jeffers & M. Kafatos, (eds.), *Gravitation & Cosmology: From the Hubble Radius to the Planck Scale*, Dordrecht: Kluwer Academic.
- [53] Rauscher, E.A. & Targ, R. (2001) The speed of thought: investigation of a complex space-time metric to describe psychic phenomena, *J Sci Exp.*, 15:3; 331-354; or www.bibliotecapleyades.net/archivos_pdf/speedthought_rauscher_targ.pdf.
- [54] Eccles, J.C. (1986) Do mental events cause neural events analogously to the probability fields of quantum mechanics?, *Proc. Royal Soc. London B*227, pp. 411-428.

- [55] Feynman, R.P., Morinigo, F.B. & Wagner, W.G. (1971) Lectures on Gravitation, 1962-63. California Institute of Technology.
- [56] Kant, E. (1787) *Kritik der Reinen Vernunft*, Critique of Pure Reason, (1996) W. Pluhar (trans.) Indianapolis: Hackett.
- [57] Ahmad, Q.R., Allen, R.C., Andersen, T.C., Anglin, J.D., Barton, J.C., Beier, E.W. & Blevis, I. (2002) Direct evidence for neutrino flavor transformation from neutral-current interactions in the Sudbury Neutrino Observatory, Phys Review Letters, 89(1), 011301.
- [58] Gonzalez-Garcia, M.C. & Nir, Y. (2003) A review of evidence of neutrino masses and the implications, Revs. Mod Phys 75, p.345-402.
- [59] Pontecorvo, B. (1983) Pages in the Development of Neutrino Physics, *Usp.Fiz.Nauk*, 141, 675; English Ed. Sov. Phys. Usp. 26, 1087.
- [60] Sundrum, R. (2005) SSI lecture notes part 2, www.slac.stanford.edu/econfl/C0507252/lec_notes_list.htm.
- [61] Schwarz, J.H. (1996) Anomaly-free supersymmetric models in six dimensions Physics Letters B, 371: 3-4; 223-230.
- [62] Ling, Y. & Smolin, L. (1999) Supersymmetric spin networks and quantum supergravity, arxiv.org/abs/hep-th/9904016.
- [63] Konopka, T., Markopoulou, F. & Smolin, L. (2006) Quantum graphity, arxiv.org/abs/hep-th/0611197.
- [64] Smolin, L. (1992) The future of spin networks, in quantum gravity and cosmology, J. Perez-Mercader et al. (eds.) Singapore: World Scientific; or gr-qc/9702030.
- [65] Barrett, L. & Crane, L. (1998) Relativistic spin networks and quantum gravity, J. Math. Phys. 39, 3296-3302; or gr-qc/9709028.
- [66] Smolin, L. (2000) A candidate for a background independent formulation of M-Theory, Arxiv: hep-th/9903166.
- [67] Smolin, L. (2006) The case for background independence, in D. Rickles, et. al. (eds.) The Structural Foundations of Quantum Gravity.
- [68] Lemos, N.A. & Monerat, G.A. (2003) A quantum cosmological model with static and dynamic wormholes, General Relativity and Gravitation, Vol. 35, No. 3.
- [69] Hawking, S.W. (1988) Wormholes in spacetime, Phys. Rev. D 4: 37; 904-910.
- [70] Hawking, S.W. (1994) Wormholes in dimensions 1-4, in P. Nath & S. Reucroft (eds.) Proceedings of the 1st Intl. Symposium on Particles, Strings & Cosmology, New Jersey: World Scientific.
- [71] Amoroso, R.L. (2006) The Holographic Conscious Multiverse, in R.L. Amoroso, B. Lehnert & J-P Vigier (eds.) Beyond the Standard Model: The Search for Unity in Physics, Orinda: Noetic Press.
- [72] Bohm, D. & Vigier, J-P (1954) Model of the causal interpretation of quantum theory in terms of a fluid with irregular fluctuations, Phys Rev 96:1; 208-217.
- [73] Vigier, J-P (2000) Selected papers, in S. Jeffers, B. Lehnert, N. Abramson, & L. Chebotarev (eds.) Jean-Pierre Vigier and the Stochastic Interpretation of Quantum Mechanics, Montreal: Aperion.
- [74] Smulyan, R.M. (1992) Gödel's Incompleteness Theorem, Oxford Univ. Press.
- [75] Szabo, R.J. (2002) Busstepp lectures on string theory: An introduction to string theory and d-brane dynamics, arXiv: hep-th/0207142v1.
- [76] Lehnert, B. (2002) New developments in electromagnetic field theory, in R.L. Amoroso, G. Hunter, M. Kafatos & J-P Vigier (eds.) Gravitation & Cosmology: From the Hubble Radius to the Planck Scale, Dordrecht: Kluwer Academic.
- [77] Lehnert, B. (1998) Electromagnetic theory with space-charges in vacuo, in G. Hunter,

- S. Jeffers & J-P Vigier (eds.) *Causality and Locality in Modern Physics*, Dordrecht: Kluwer Academic.
- [78] Proca, A. (1936) *Compt. Rend.* 202, 1420.
- [79] Evans, M. & Vigier, J-P (1994) *The Enigmatic Photon* Vol. 1-5, Dordrecht: Kluwer.
- [80] Roy, S. & Lehnert, B. (1998) Extended Electromagnetic Theory; Space Charge in Vacuo and the Rest Mass of the Photon, Singapore: World Scientific.
- [81] Dirac, P.A.M. (1952) *Nature* (London) 169, 702.
- [82] Cufaro, N., Petroni, C. & Vigier, J-P (1983) Dirac's ether in relativistic quantum mechanics, *Found. Phys.*, 13; 253-286.
- [83] Vigier, J-P (1990) Evidence for nonzero mass photons associated with a vacuum-induced dissipative redshift mechanism, *IEEE Trans Plasma Sci*, 18:1;64-72.
- [84] Arkani-Hamed, N., Dimopoulos, S., Kaloper, N. & Sundrum, R. (2000) A small cosmological constant from a large extra dimension, arxiv:hep-th/0001197v2.
- [85] Rizzo, T.G. & Wells, J.D. (1999) Electroweak precision measurements and collider probes of the standard model with large extra dimensions, arXiv:hep-ph/9906234v1.
- [86] Randall, L. & Schwartz, M.D. (2002) Unification and the hierarchy from AdS5, *Phys. Rev. Let.* 88, 081801; Arxiv/hep-th/0108115.
- [87] Silk, J. (1989) *The Big Bang*, New York: W.H. Freeman & Co.
- [88] Chatterjee, S. & Banerjee, A. (2004) C-field cosmology in higher dimensions, *General Relativity & Gravitation*, 36:2; 303-313.
- [89] Coxeter, H.S.M. (1940) The polytope 2,21, whose twenty-seven vertices correspond to the lines on the general cubic surface, *American J. of Mathematics*, v62, pp. 457-486.
- [90] Saniga, M. (2000) Twenty-seven lines on a cubic surface and heterotic string spacetimes, arXiv:physics/0012033v1.
- [91] Mitchell, E. (1974) *Psychic Exploration; a Challenge for Science*, NY: Putnam.
- [92] Einstein, A. (1950) *The Meaning of Relativity*, Princeton: Princeton Univ. Press.
- [93] Bohr, N. (1935) Can quantum mechanical description of physical reality be considered complete? *Physical Rev.* 48; 696-702.
- [94] Dirac, P.A.M. (1952) *Nature* (London) 169, 702.
- [95] Cufaro, N., Petroni, C. & Vigier, J-P (1983) Dirac's Ether in Relativistic Quantum Mechanics, *Found. Phys.*, 13, 253-286.
- [96] Burns, J.E. (1998) Entropy and vacuum radiation, *Found. Phys. L.* 28:7; 1191-1207.
- [97] Burns, J.E. (2002) Vacuum radiation, entropy and the arrow of time, in R.L. Amoroso, G. Hunter, S. Jeffers & M. Kafatos, (eds.) *Gravitation & Cosmology: From the Hubble Radius to the Planck Scale*, Dordrecht: Kluwer Academic.
- [98] Morris, R. (1984) *Time's Arrows*, New York: Simon & Schuster.
- [99] Davies, P. (1974) *Physics of Time Asymmetry*, Berkeley: Univ. of California Press.
- [100] Amoroso, R.L. (2000) The parameters of temporal correspondence in a continuous-state conscious universe, in L. Buccheri & M. Saniga (eds.) *Studies on the Structure of Time: From Physics to Psycho(patho)logy*, London: Plenum.
- [101] Amoroso, R.L., Kauffman, L.H., & Rolands, P. (2013) *The Physics of Reality: Space. Time, Matter, Cosmos*, Hackensack: World Scientific.
- [102] Amoroso, R.L. (2005) Paradigm for the cosmology of a continuous-state holographic conscious multiverse, in R.L. Amoroso, B. Lehnert & J-P Vigier (eds.) *Beyond the Standard Model: Searching for Unity in Physics*, Oakland: The Noetic Press.
- [103] Chalmers, D. (1996) *The Conscious Mind*, Oxford: Oxford: University Press.
- [104] Amoroso, R.L. & Martin, B. (1995) Modeling the Heisenberg matrix: Quantum coherence and thought at the holospace manifold and deeper complementarity, in J. King & K. Pribram (eds.) *Scale in Conscious Experience*, Mahwah: Lawrence Earlbaum.

- [105] Bergson, H. (1911) Creative Evolution, A. Mitchell (trans.) New York: Henry Holt.
- [106] Amoroso, R.L. (1999) An Introduction to Noetic Field Theory: The Quantization of Mind, *Noetic Journal*, Vol 2, No. 1, pp. 28-37.
- [107] Amoroso, R.L. (1997) Consciousness, a radical definition, *Noetic Journal*, Vol.1 No.1, p.19-27.
- [108] Amoroso, R.L. (1997) A Brief Introduction to Noetic Field Theory: The Quantization of Mind, pp. 297-302, In *Brain & Consciousness*, L. Rakic, G. Kostopoulos, D. Rakovic & D. Koruga (eds.) ECPD: Belgrade.
- [109] Amoroso, R.L. (1997), Engineering a conscious quantum computer, In M. Gams, et al (eds.) *Mind Versus Computer*, IOS Press.
- [110] Amoroso, R.L. (1996) The production of Fröhlich and Bose-Einstein coherent states in in vitro paracrystalline oligomers using laser phase control interferometry, *Bioelectrochemistry & Bioenergetics*, 40: 39-42.
- [111] Amoroso, R.L. (1995) The extracellular containment of natural intelligence, *Informatica*, 19: 585-90.
- [112] Amoroso, R.L. (2000) Consciousness, a radical definition: Substance dualism solves the hard problem, In Amoroso, R.L., Antunes, R., Coelho, C., Farias, M., Leite, A., & Soares, P. (eds.) *Science and the Primacy of Consciousness*, Orinda: Noetic Press.
- [113] Einstein, A. (1954) Ideas and Opinions, New York: Crown.
- [114] Smith, J. (1989) *The Doctrine and Covenants*, Salt Lake City: The Church of Jesus Christ of Latter-day Saints.
- [115] Wheeler, J.A. (1977) Gravitational and Electromagnetic wave flux compared and contrasted, *Phys. Rev. D*, 16:12, 3384-3389.
- [116] Wheeler, J.A. (1962) *Geometrodynamics*, N.Y.: Academic Press.
- [117] Prigogine, I. (1997) From Poincaré's divergences to quantum mechanics with broken time symmetry, *Zeitschrift für Naturforschung* 52a, 37-47.
- [118] Petrosky, T. & Rosenberg, M. (1997) Microscopic non-equilibrium structure and dynamical model of entropy flow, *Foundations of Physics* 27: 2; 239-259.
- [119] Puthoff, H.E. (1989) Source of vacuum electromagnetic zero-point energy, *Phys. Rev. A* 40(9), 4857-4862.
- [120] Puthoff, H.E. (1991) Reply to Comment on 'Source of vacuum electromagnetic zero-point energy', *Phys. Rev. A* 44(5), 3385-3386.
- [121] Holland, P.R. (1995) *The Quantum Theory of Motion: An Account of the de Broglie-Bohm Causal Interpretation of Quantum Mechanics*, Cambridge: Cambridge Univ. Press.
- [122] Cartan, E. (1966) *The Theory of Spinors*, New York: Dover.
- [123] Cartan, E. (1979) Elie Cartan - Albert Einstein Letters on Absolute Parallelism 1929-1932, R. Debever (ed.) Princeton: Princeton Univ. Press.
- [124] Schutz, B.F. (1980) *Geometrical Methods of Mathematical Physics*, Cambridge: Cambridge Univ. Press.
- [125] Bilson-Thompson, S., Hackett, J. & Kauffman, L.H. (2009) Particle topology, braids and braided belts, arXiv:0903.1376v1.
- [126] Bilson-Thompson, S.O., A topological model of composite preons, arXiv:hep-th/0503213.
- [127] Bilson-Thompson, S.O., Markopoulou, F. & Smolin, L. (2007) Quantum gravity and the standard model, *Class. Quant. Gravity* 24; 3975-3993; arXiv:hep-th/0603022.
- [128] Magnus, W (1974) Braid groups: A survey, In *Lecture Notes in Mathematics*, vol. 372, pp. 463-487; or (1974) Proceedings of the 2nd Intl Conf. on the Theory of Groups, Canberra, Australia, 1973, New York: Springer.
- [129] Personal communication, Lou H. Kaufman (2009).

- [130] Kaufman, L.H. (2001) Knots and Physics, 3rd ed., Singapore, World Scientific.
- [131] Vigier, J-P (2000) Selected papers, in S. Jeffers, B. Lehnert, N. Abramson, & L. Chebotarev (eds.) Jean-Pierre Vigier and the Stochastic Interpretation of Quantum Mechanics, Montreal: Aperion.
- [132] Vigier, J. P. (1997) Relativistic interpretation (with non-zero photon mass) of the small ether drift velocity detected by Michelson, Morley and Miller, *Apeiron*, 4, 71-76.
- [133] Vigier, J. P. (1997) New non-zero photon mass interpretation of the Sagnac effect as direct experimental justification of the Langevin paradox, *Phys Letters A*, 234, 75-85.
- [134] Múnera, H. A. (1997) An absolute space interpretation (with non-zero photon mass) of the non-null results of Michelson-Morley and similar experiments: An extension of Vigier's proposal, Montreal: *Apeiron*, 4, 77-79.
- [135] Miller, D. C. (1933) The ether-drift experiment and the determination of the absolute motion of the earth, *Reviews of Modern Physics*, 5, 203-242.
- [136] Silvertooth, E.W. & Whitney, C.K. (1992) A new Michelson-Morley experiment, *Physics Essays*, 5, 82-89.
- [137] Spolter, P. (1993) Gravitational Force of the Sun, Granada Hills: Orb Publishing.
- [138] Galeczki, G. (1995) Uniform time, relative velocity, and special relativity, *Physics Essays* 8: 10.
- [139] Hazelett, R., & Turner, D. (1979) The Einstein myth and the Ives papers, In Counter Revolution in Physics, Devin-Adair Company.

Chapter 4

A Revolution in the Conception of Matter

Physics, simplistically, is the study of matter and energy; or as Einstein called it, ‘extension and duration’. A hundred and twenty years ago, our understanding of the physical world was described by the Newtonian Classical Mechanical belief in indivisible billiard ball-like atoms as the fundamental building blocks of matter. Discovery of the electron in 1897 by J.J. Thompson demonstrated that atoms are not indivisible, ushering in modern atomic theory. The advent of quantum mechanics showed that matter had wave properties. Now on the brink of discovering additional dimensions (XD) another advance beckons; extending our understanding of the structure of matter to include Calabi-Yau mirror symmetric topological brane phenomena hidden until now behind the veil of the uncertainty principle in a 3rd regime of Unified Field Mechanics (UFM). Classical observation seemingly straight forward, became compounded by uncertainty in quantum mechanics. Just as infinities in the Raleigh-Jeans Law were an indicia of quantum theory; likewise, the renormalization problem of infinite self-energy of a charged point particle in both classical and quantum theory are deemed inconsistencies, certainly suggesting incompleteness, that point the way to a new horizon of additional physics that can be accessed by utilizing a new class of HD commutation rules allowing the uncertainty principle to be ontologically overcome.

4.1 Point-Particle Infinite Mass-Energy

The term point particle is not rigorously defined causing inconsistencies in usage, but is generally used to denote a spherical 0D object with no spatial extension and as described by the inverse square law has all its matter concentrated at the 0D point. From classical electromagnetism (em) we know that the energy of a charge configuration increases as the distance between them decreases. For two general charges q_1 and q_2 separated by a

distance r , the electrostatic energy is:

$$E = \frac{1}{4\pi\epsilon_0} \frac{q_1 q_2}{r}. \quad (4.1)$$

Ignoring the 1st term, a constant, it is in the 2nd term where we see that the energy of the charges q_1 and q_2 , increases to infinity the closer we bring them together. Assuming that electrons are point particles carrying a charge density as a charged spherical shell; if we shrink its size to 0D, it is supposed to mean the electron has infinite electrostatic energy.

From the equation for a spherical shell of charge, e with radius, r we obtain a result similar to that for the two charges in (4.1):

$$E = \frac{1}{8\pi\epsilon_0} \frac{e^2}{r}, \quad (4.2)$$

where similarly if the spherical shell is brought to a point, the electron's self-energy goes to infinity. Since QED predicts that virtual electron-positron pairs can emerge from the vacuum for up to the Planck time, one can violate the conservation of energy with quantum mechanics at the Planck scale, $\delta t \delta E \leq \hbar$ allowing renormalization techniques to provide an *ad hoc* solution to this conundrum by letting quantum effects cancel out classically infinite contributions to electron mass at a scale similar to the scale of electron mass [1]. The 'Heisenberg Microscope' at CERN's LHC is said to 'see' to 10^{-16} . Quantum mechanics appears as the 'basement of reality' only because the Uncertainty Principle acts as a gating mechanism limiting observation. With the imminent advent of 3rd regime UFM we can take the next step in understanding the structural-phenomenology of matter beyond the traditional 3-space arena of current observation [2,3].

4.2 Space-Antispace as a UFM Intermediary

The Standard Model, a quantum field theory, is incomplete, while it seems theoretically self-consistent, with some phenomena unexplained (dark energy, non-zero neutrino mass); as well-known, it is not yet a complete theory. At the fundamental level Physics reduces to the structure and interaction of fermions. In 3-space Fermions appear to be 0D singularities rather than extended objects, a sufficient rendition until now.

However, Rowlands has found that the algebra associated with the Dirac equation suggests that the fermion requires a double, rather than a single, vector space for its full representation, confirmed by the dual 360° - 720° rotation needed by spin $\frac{1}{2}$ objects to return to the origin, and the associated effects of Berry phase shift and *zitterbewegung*, where it continually switches between real space and a second vacuum space, because the fermion is only in real space half the time. Further investigation of the ‘second space’ shows that it is an ‘antspace’ containing the same information as real Euclidean space, but in a less accessible form. The two nilpotent spaces effectively cancel to produce a norm 0 object which has the precise mathematical structure required to be a fermionic singularity as experimentally observed [4-8].

Physics assumes that we can define dynamic physical objects (‘particles’ or fermions) as existing ‘in space’. It is not at all obvious what this actually means, for, though the concept of space is inconceivable without matter, 3D space has no mechanism within itself for constructing the physical singularities that make up material particles. So, how are such singularities constructed within ordinary space? [9].

When the two spaces are combined in a norm 0 object (singularity or nilpotent), the symmetry of one of the two spaces is broken. Essentially, the space with the unbroken symmetry (lower case symbols in next sections) is the space of observation. The one with the broken symmetry (upper case symbols in next sections) is an unobservable dual space, that determines what happens in the observed space. The key fact is that the act of creating a singularity using these two spaces determines that they are precisely dual and that each contains the same information as the other, though in a different form as regards observation [9].

To express this in algebraic form, we require a double Clifford algebra of 3D space, which can also be expressed as a double multivariate vector algebra, a vector quaternion algebra, a complexified double quaternion algebra, or by using a tensor product of two sets of Pauli matrices. This is recognizable as the 64-part algebra of the Dirac equation for the fermion. It is also the algebra created by the four symmetrical parameters mass, time, charge and space, which have been identified as the only truly fundamental parameters required by physics [4,8]. A key fact is that the minimum number of generators for this structure, (5 generators) requires the symmetry of one of the two spaces to be broken, and this becomes the origin of the broken symmetry ($SU(3) \times SU(2) \times U(1)$), forming the Standard Model of particle physics [9].

4.3 The Nilpotent Quaternionic Representation of Fermions

A particularly powerful method of quantum mechanics and quantum field theory, which also brings into focus the question of dimensionality, can be found by exploiting the fact that the gamma algebra is also a Clifford algebra and can be represented algebraically, without matrices, in a number of different ways: as a double vector algebra, a vector quaternion algebra, or a complexified double quaternion algebra. In Clifford algebra, vectors are constructed from complexified quaternions, and also automatically include both complex numbers and quaternions as subalgebras. All three representations are significant in different ways. The vector quaternion algebra (which also includes real complex numbers as subalgebras) arises from a direct combination of the algebras of the four fundamental parameters in physics: space gives us vectors, charge quaternions, time complex numbers, and mass real numbers. The double vector algebra expresses the fact that the whole of physics, and in particular the representation of a point-like fermion, can be seen as a combination, and even a cancellation at a point, of two vector ‘spaces’: real space and the ‘antspace’ constructed out of the combination of charge, time and mass. A complexified double quaternion algebra can be seen as the basis of the representation of a physical object using the parameters space, charge, time and mass as a broken octonion, an octonion in which the antiassociative parts are deemed unphysical [4,10-16].

The origin of this approach lies in two fundamental propositions. One is that reality represents a fundamentally zero totality. The other is that this can be achieved through a fundamental symmetry between the parameters mass, time, charge and space. [4-7,9-11,17-20].

mass	conserved	real	commutative
time	nonconserved	imaginary	commutative
charge	conserved	imaginary	anticommutative
space	nonconserved	real	anticommutative

The symmetry is obtained by placing ‘properties’ against ‘antiproperties’, which are their *exact opposites*. Group information about the universe is assumed to be absolutely exclusive. That is, *there is no information about the universe, other than what comes from the parameter group*. The properties and antiproperties are absolutely opposite in every respect, though the designation of which are properties (say, conserved, real and commutative) and which antiproperties (say, nonconserved, imaginary

and anticommutative) is completely arbitrary. An investigation of the foundations of physics tells us that the properties and antiproperties are very exact, but not easily encompassed in a single word description.

We can choose to represent the properties and antiproperties algebraically in a way that makes the zero totality even more explicit.

mass	x	y	z
time	$-x$	$-y$	z
charge	x	$-y$	$-z$
space	$-x$	y	$-z$

The combination of property and anti-property in each parameter is associated with a particular algebraic structure, which happens to be either the Clifford algebra of 3D space, also known as multivariate vectors, and isomorphic to Pauli matrices and complexified quaternions, or one of its 3 subalgebras: bivector (or pseudovector), trivector (or pseudoscalar) and scalar. The pseudovectors are also equivalent to the imaginary parts of a quaternion and the pseudoscalars to complexified scalars or the imaginary parts of complex algebra. The subalgebras can be seen either as decompositions of the full Clifford algebra of space, or as stages leading towards the complete algebra generated by a ‘universal rewrite system’ [10]. Space itself incorporates the 3 subalgebras as volume (trivector), area (bivector), and scalar magnitude.

The algebras of the other 3 parameters that exist independently of those of space; charge and time also incorporate scalar magnitude as subalgebras of their own pseudovectors and pseudoscalars. Commutative terms, however, can be combined by simple multiplication in a way that anticommutative ones cannot; in principle, there is a division in the parameter group between two 3D structures. We can combine the parameters in various ways, but the most suggestive is one which opposes space to an alternative space-type concept constructed from the units of the anticommutative charge with the commutative time and mass. We can describe this as an ‘antispace’, because, according to the principle of zero totality, the combination of space, charge, time and mass, or the combination of space with everything else yields a totality of zero [10].

Space	i	j	k
Charge	\bar{i}	\bar{j}	\bar{k}
Time	i		
Mass	1		

vector	complexified quaternion
bivector	pseudovector quaternion
trivector	pseudoscalar complexified scalar
scalar	

Since the two ‘spaces’ originate independently, though combining to a zero totality, it is convenient to represent the ‘ordinary space’ by the units \mathbf{i} , \mathbf{j} , \mathbf{k} and the ‘antispace’ by the units \mathbf{I} , \mathbf{J} , \mathbf{K} . Each of these spaces is described by a Clifford or geometrical 3D algebra, with + and – versions of 8 base units [4,5]. That is:

$$\begin{array}{ccc} \mathbf{i} & \mathbf{j} & \mathbf{k} \\ \mathbf{\bar{i}} & \mathbf{\bar{j}} & \mathbf{\bar{k}} \\ i & & \\ 1 & & \end{array}$$

Vector	complexified quaternion
Bivector	pseudovector quaternion
Trivector	pseudoscalar complexified scalar
scalar	

and:

$$\begin{array}{ccc} \mathbf{I} & \mathbf{J} & \mathbf{K} \\ \mathbf{\bar{I}} & \mathbf{\bar{J}} & \mathbf{\bar{K}} \\ i & & \\ 1 & & \end{array}$$

Vector	complexified quaternion
Bivector	pseudovector quaternion
Trivector	pseudoscalar complexified scalar
scalar	

The tensor product or commutative combination of the two spaces produces an algebra structured on 64 units:

$$\begin{array}{cccccc} 1 & & & & & \\ \mathbf{Ii} & \mathbf{Ij} & \mathbf{Ik} & \mathbf{k} & \mathbf{ij} & \\ \mathbf{Ji} & \mathbf{Jj} & \mathbf{Jk} & \mathbf{k} & \mathbf{ij} & \\ \mathbf{Ki} & \mathbf{Kj} & \mathbf{Kk} & \mathbf{k} & \mathbf{ij} & \end{array}$$

$$\begin{array}{ccccc} -1 & & & & \\ -\mathbf{Ii} & -\mathbf{Ij} & -\mathbf{Ik} & -\mathbf{k} & -ij \\ -\mathbf{Ji} & -\mathbf{Jj} & -\mathbf{Jk} & -\mathbf{k} & -ij \\ -\mathbf{Ki} & -\mathbf{Kj} & -\mathbf{Kk} & -\mathbf{k} & -ij \end{array}$$

$$\begin{array}{ccccc} i & & & & \\ i\mathbf{Ii} & i\mathbf{Ij} & i\mathbf{Ik} & i\mathbf{k} & j \\ i\mathbf{Ji} & i\mathbf{Jj} & i\mathbf{Jk} & i\mathbf{k} & j \\ i\mathbf{Ki} & i\mathbf{Kj} & i\mathbf{Kk} & i\mathbf{k} & j \end{array}$$

$$\begin{array}{ccccc} -i & & & & \\ -i\mathbf{Ii} & -i\mathbf{Ij} & -i\mathbf{Ik} & -i\mathbf{k} & -j \\ -i\mathbf{Ji} & -i\mathbf{Jj} & -i\mathbf{Jk} & -i\mathbf{k} & -j \\ -i\mathbf{Ki} & -i\mathbf{Kj} & -i\mathbf{Kk} & -i\mathbf{k} & -j \end{array}$$

Notably, the set of 64 is made up of the 4 complex units and 12 pentads of very similar structure. Because we can exchange vectors for complexified quaternions, and quaternions for complexified vectors, an alternative version would be a vector-quaternion algebra of the form:

$$\begin{array}{ccccc} 1 & & & & \\ \mathbf{\ddot{i}} & \mathbf{\ddot{ij}} & \mathbf{\ddot{ik}} & \mathbf{\ddot{ik}} & j \\ \mathbf{\ddot{j}} & \mathbf{\ddot{jj}} & \mathbf{\ddot{jk}} & \mathbf{\ddot{ii}} & k \\ \mathbf{\ddot{k}} & \mathbf{\ddot{kj}} & \mathbf{\ddot{kk}} & \mathbf{\ddot{ij}} & i \end{array}$$

$$\begin{array}{ccccc} -1 & & & & \\ -\mathbf{\ddot{i}} & -\mathbf{\ddot{ij}} & -\mathbf{\ddot{ik}} & -i\mathbf{k} & -j \\ -\mathbf{\ddot{j}} & -\mathbf{\ddot{jj}} & -\mathbf{\ddot{jk}} & -i\mathbf{i} & -k \\ -\mathbf{\ddot{k}} & -\mathbf{\ddot{kj}} & -\mathbf{\ddot{kk}} & -i\mathbf{j} & -i \end{array}$$

$$\begin{array}{ccccc} i & & & & \\ i\mathbf{\ddot{i}} & i\mathbf{\ddot{ij}} & i\mathbf{\ddot{ik}} & i\mathbf{k} & j \\ i\mathbf{\ddot{j}} & i\mathbf{\ddot{jj}} & i\mathbf{\ddot{jk}} & i\mathbf{i} & k \\ i\mathbf{\ddot{k}} & i\mathbf{\ddot{kj}} & i\mathbf{\ddot{kk}} & i\mathbf{j} & i \end{array}$$

$$\begin{array}{ccccc} -i & & & & \\ -i\mathbf{\ddot{i}} & -i\mathbf{\ddot{ij}} & -i\mathbf{\ddot{ik}} & -i\mathbf{k} & -j \\ -i\mathbf{\ddot{j}} & -i\mathbf{\ddot{jj}} & -i\mathbf{\ddot{jk}} & -i\mathbf{i} & -k \\ -i\mathbf{\ddot{k}} & -i\mathbf{\ddot{kj}} & -i\mathbf{\ddot{kk}} & -i\mathbf{j} & -i \end{array}$$

This is isomorphic to the algebra of the Dirac equation, or the γ matrices, doubling the algebra of the single vector space which is isomorphic to that of the Pauli or σ matrices. All possible versions of the γ matrices can, in fact, be derived from a commutative combination of two sets of σ matrices, which we could write as σ_1 , σ_2 , σ_3 and Σ_1 , Σ_2 , Σ_3 . The very significant aspect of the algebra from the point of view of physics, however, is that only 5 generators are needed to produce the entire set of units. While it is possible to produce the units from something like i , \mathbf{i} , \mathbf{j} , \mathbf{i} , \mathbf{j} , all the sets of 5 which include the units of the two 3-dimensional structures on an equivalent basis are structured exactly to the same plan as the pentads in these tables. A typical set might be of the form

$$\mathbf{K} \quad i\mathbf{Ii} \quad i\mathbf{Ij} \quad i\mathbf{Ik} \quad i\mathbf{J}$$

which becomes

$$ik \quad ii \quad ij \quad ik \quad j$$

in the vector-quaternion set [4,5,10].

The creation of the pentads has a very significant physical consequence. If we take the base units of time, space, mass and charge, the pentads emerge if we incorporate the three units of charge onto the respective ones of time, space and mass. So

Time	space	mass	charge
i	$\mathbf{i} \mathbf{j} \mathbf{k}$	1	$i j k$

becomes

i	$\mathbf{i} \mathbf{j} \mathbf{k}$	1
k	i	j

or

$$ik \quad ii \quad ij \quad ik \quad j$$

exactly as in the pentad, which map directly onto the respective γ^0 , γ^1 , γ^2 , γ^3 and γ^5 matrices, with which they are isomorphic. Physically, this incorporates both relativity and quantization and is equivalent to the *creation* of quantized energy, three components of quantized momentum,

and rest mass. We simply define respective scalar values E , p_x , p_y , p_z , and m , to be applied to the units of the pentad whose algebraic structures carry the defining characteristics of these quantities. Then, we restore the zero totality by defining a norm-zero package or nilpotent as containing the entire set of fundamental information constituting physics. That is, we define the ‘fundamental unit’ or zero-singularity of physics as $(\mathbf{KE} + i\mathbf{I}ip_x + i\mathbf{I}jp_y + i\mathbf{I}kp_z + i\mathbf{J}m)$ or $(ikE + \mathbf{i}ip_x + \mathbf{i}jp_y + \mathbf{i}kp_z + jm)$ or $(\mathbf{KE} + i\mathbf{I}ip_x + i\mathbf{I}jp_y + i\mathbf{I}kp_z + i\mathbf{J}m)$. The nilpotent condition means that

$$(\mathbf{KE} + i\mathbf{I}ip_x + i\mathbf{I}jp_y + i\mathbf{I}kp_z + i\mathbf{J}m)^2 = 0$$

And

$$(ikE + \mathbf{i}ip_x + \mathbf{i}jp_y + \mathbf{i}kp_z + jm)^2 = 0$$

in line with the Einstein energy-momentum-mass equation

$$E^2 - p^2 - m^2 = 0 . \quad (4.3)$$

In more general terms, we can collect all the momentum components and use all the sign variations in energy and momentum to write

$$(\pm ikE \pm ip + jm) (\pm ikE \pm ip + jm) = 0, \quad (4.4)$$

with the four terms in the first bracket arranged as a row vector and the four terms in the second bracket as a column vector. Then, bringing in the nonconservation properties of space and time in an explicit fashion, a canonical quantization applied to the first bracket gives us the Dirac equation for a free particle:

$$\left(\mp k \frac{\partial}{\partial t} \mp i\nabla + jm \right) (\mp ikE \pm ip + jm) e^{-i(Et - \mathbf{p.r})} = 0 . \quad (4.5)$$

Using the convention that E and \mathbf{p} represent operators as well as amplitudes, we can also express this as

$$(\pm ikE \pm ip + jm) (\pm ikE \pm ip + jm) e^{-i(Et - \mathbf{p.r})} . \quad (4.6)$$

The condition that must always be applied is that the amplitude is always nilpotent. The differential operator is a way of codifying the space and time variation of the fundamental physical singularity or fermionic nilpotent. The phase factor (in this case, $e^{-i(Et - \mathbf{p} \cdot \mathbf{r})}$) represents the decoding to produce the amplitude term ($\pm ikE \pm i\mathbf{p} + jm$). If the particle is not assumed to be free, we can replace E and \mathbf{p} with covariant derivatives (e.g. $\partial / \partial t + e\phi + \dots, -\nabla - e\mathbf{A} + \dots$), or incorporate any number of field terms after the differential operators. The general expression

$$(\pm ikE \pm i\mathbf{p} + jm)(\pm ikE \pm i\mathbf{p} + jm) \rightarrow 0 \quad (4.7)$$

will still apply. The phase factor will no longer be a simple exponential, but we can assume that the amplitude will continue to be nilpotent and produce a norm zero amplitude [4,5,10].

As a consequence, the entire relativistic quantum mechanics applicable to a fermion in any state, subject to any number of interactions, is derived simply by defining an operator of the form

$$(\pm ikE \pm i\mathbf{p} + jm). \quad (4.8)$$

The operator then uniquely determines the phase factor which makes the amplitude nilpotent. The coding requires a unique decoding. In fact, there is no need to define any equation at all. Everything can be expressed using the fact that

$$\begin{aligned} & (\text{operator acting on phase factor})^2 \\ &= \text{amplitude}^2 = 0. \end{aligned}$$

The nilpotent representation has immediate physical meaning as the realization of the Pauli exclusion principle. If two fermionic wavefunctions are identical, they will create a zero combination state. A huge number of important results become simple consequences of the algebra, and wholly new calculations become possible. We can, for example (using an appropriate sign convention), immediately specify the four amplitude states as derived from four creation operators:

- $(ikE + i\mathbf{p} + jm)$ fermion spin up
- $(ikE - i\mathbf{p} + jm)$ fermion spin down
- $(-ikE + i\mathbf{p} + jm)$ antifermion spin down
- $(-ikE - i\mathbf{p} + jm)$ antifermion spin up

The 1st term in the column represents the fermion's physical state; if both right and left-handed helicity states are present (for any massive particle), the 1st two terms in superposition determine the state. The other terms then represent the vacuum state for this particular fermion. If the state represented was an antifermion with spin down, then $(-ikE + ip + jm)$ would be the 1st term in the column and the other terms would be decided by making the same sign changes to E and \mathbf{p} [5,10].

The many results that have been determined for the nilpotent Dirac formalism can be sought in the appropriate technical publication. They include C , P and T transformations and the CPT theorem. The reduction of all information about any fermion state to the instantaneous direction of its spin vector; the specification of locality as occurring within the fermion bracket and nonlocality as outside it; full derivation of spin, helicity and *zitterbewegung*. The description of all known boson states (for the first time) in terms of fermion combinations, and the derivation of the $SU(2)$ structure of the weak interaction. The first explicit representation of baryon wavefunctions, with the consequent explanation of baryon mass and the $SU(3)$ structure of the strong interaction; the first explanation of vacuum as the dual structure to a fermion which maintains zero totality.

The use of the quaternion operators to partition the vacuum into strong, weak and electric components; the first explanation of the symmetry-breaking between the three gauge forces; the proof that the only interactions which can emerge from a point source and obey the nilpotent condition are the three known gauge interactions. A Dirac equation structured for charges; a discrete version of the Dirac equation using commutators for differentials allowing a simple classical transition. A specification of 4-spinors in terms of a norm 0 Berwald-Moor metric; a complete specification of particle states based on nilpotent wavefunctions.

A complete derivation of the interactions based on the nonlocal descriptions creation equivalent local ones, fermion and boson propagators with no infrared divergence; the automatic cancellation of the self-energy terms in renormalization; and intrinsic supersymmetry without extra particles. The calculations include the analytic derivation of the three gauge interactions referred to a point source, the strong and weak ones being calculated for the first time, and the Coulomb interaction by the most efficient known process (in just six lines); the derivation of QED from the nilpotent structure without second quantization; and electroweak interaction calculations derived directly from the bosonic states without using trace theorems [4,5].

The nilpotent representation was not set up on the basis of any particular dimensionality, but it incorporates a number of different dimensionalities in different ways. The expression ($i\mathbf{k}E + i\mathbf{p}_x + i\mathbf{j}\mathbf{p}_y + i\mathbf{k}\mathbf{p}_z + \mathbf{j}\mathbf{m}$) is clearly 5D in E , \mathbf{p} and m (or, equivalently, in t , \mathbf{r} and τ), but there are also 5D of charge in the structure. This is consonant with the 10D of string theory (11 if you include the commutative ‘space’ in which the nilpotents are embedded). Of course, until now [2,3], there is here no ‘string’ or ‘membrane’ structure because the object described is a point-singularity. It is interesting in this connection that several other ideas that are now fundamental components of string theory have been present in the fundamental symmetry of the parameter group from the beginning, including R, S and T dualities and gravity-gauge theory correspondence [4-11,17-20]. The Kaluza-Klein connection is also apparent from the inclusion of the fifth term in the nilpotent, which, dually, represents invariant mass and electric charge.

In addition, the gravitational aspects are close to the holographic principle, of which the nilpotent structure is a perfect expression, being equivalent to an ‘area’ enclosing the E and \mathbf{p} terms (equivalent t and \mathbf{r}), with the third term numerically redundant. Significantly, the idea of ‘4D’ for energy-momentum or time-space has to be modified into a new 3D structure, represented by \mathbf{k} , \mathbf{i} and \mathbf{j} , for energy-momentum-mass or time-space-proper time: ($i\mathbf{k}E + i\mathbf{p}_x + i\mathbf{j}\mathbf{p}_y + i\mathbf{k}\mathbf{p}_z$), unlike ($iE + \mathbf{i}\mathbf{p}_x + \mathbf{j}\mathbf{p}_y + \mathbf{k}\mathbf{p}_z$), is not a true 4-vector because \mathbf{k} and \mathbf{i} are different.

If we take the dimensionality from the constituent parameters, then we have 4 of these; if we take it from their algebras, then we have 8. The fundamental symmetry-breaking in physics appears to be a matter of breaking the relatively perfect symmetry of 8 into the imperfect symmetry of 5, and the same has been observed also in key aspects of chemistry, biology, and information theory, where the same patterns are observed repeatedly at each successive level. [4,10-12,21-24] In every case the combination of two ‘spaces’ or equivalent to produce a ‘discrete’ state, or self-organizing system. The 6-fold perfection of the double space with units I, j, k, I, J, K becomes the 5-fold imperfection of \mathbf{K} , $i\mathbf{Ii}$, $i\mathbf{Ij}$, $i\mathbf{Ik}$, i , though nature prefers the imperfection because it is a more efficient packaging. As we have seen, the 5-fold structure means that the symmetry of one vector space is preserved (here, the one with the lower case symbols, \mathbf{i} , \mathbf{j} , \mathbf{k}) while that of the other is broken (here, the upper case symbols, \mathbf{I} , \mathbf{J} , \mathbf{K}) in precisely the same way. Physically, the space with the unbroken symmetry (\mathbf{i} , \mathbf{j} , \mathbf{k}) is the parameter space as we know it, the space of observation. The ‘space’ with the broken symmetry (\mathbf{I} , \mathbf{J} , \mathbf{K}) is a dual

space, the one we call vacuum space, which is unobservable (until now), but which determines what happens in the observed space. The act of creating a zero-norm singularity by combining the two spaces determines that they are precisely dual and that each contains the same information as the other, though the methods of observation will differ.

We can interpret the creation of the norm zero ‘singularity’ state as indicating that the totality of the universe is zero, so that the creation of a fermion (with all its special energy conditions, potentials, etc.) as a singularity simultaneously creates a kind of ‘hole in nothing’, which we describe as vacuum, or the rest of the universe. Source and sink are created simultaneously, one point-like and localized, and the other diffused throughout the whole of space and delocalized. Effectively, this duality is the same as that between amplitude and phase. Though only the space related to the localized state can be observed directly, the asymmetry between the two spaces – unbroken and broken symmetries – can be seen as the origin of mass, both through *zitterbewegung* and through the vacuum asymmetry involved in the Higgs mechanism. If we need a physical analogy to understand how the combination of two spaces, one observed and one unobservable, produces the discrete singularities known as nilpotent fermions, we can see it as a kind of knot between two pieces of string, say colored red and blue, neither of which is aware of the other’s existence (which is effectively the meaning of commutativity).

If we picture the universe from the point of view of one of them, say, the blue, the blue string will be straight, and we need to devise some special contortion to create the state of the red string from the blue’s perspective. The spatial ‘double twist’ will be equivalent to a singularity, an additional structure within the space. Penrose has used twistor theory to examine something similar, but, though the twistor algebra has a family resemblance to the algebra of the dual space in that it is constructed of four real units and four imaginary. Visually, the effect can be represented in the Robinson congruence [25]. However, the distribution of these units is different and the twistor algebra, based on a reality of 4D space-time which is denied by the nilpotent construction, is unable to create fermion or other particle structures. The nilpotent theory suggests that the only way to do this is to base it upon the fundamental algebras of mass, time, charge and space [26-35].

4.4 The Nature of Quantum Reality

The probabilistic Copenhagen approach was strongly opposed by Einstein, Planck, and Schrödinger. De Broglie proposed that the motion of physical

particles is guided by ‘pilot waves’, extended by Bohm and Vigier to a more realistic model. The ontology of the de Broglie-Bohm-Vigier causal interpretation claims that *a particle is a complex structure associated with a pilot wave* guiding its motion by exerting a potential force [36]. Particles thus follow causal trajectories even though measuring the trajectory is still governed by the uncertainty principle.

Bohm believed this quantum potential operates from a deeper level of reality called the ‘implicate order’, associated with the electromagnetic zero-point field which according to Vigier is a covariant polarized Dirac-type ether consisting of superfluid states of particle-antiparticle pairs [36,37]. Bohm postulated that observed particles are *not fundamental, but ‘forms’ produced by a continuous convergence and divergence of waves in a ‘superimplicate order’* [38]. The structural-phenomenology of these so-called forms is precisely what UFM reveals for a completed picture of a particle; before knowing of these ideas of Bohm, we independently termed the ‘continuous convergence and divergence of waves’, a ‘continuous-state process’ and develop a LSXD picture of Vigier’s concept of matter where a *particle is a complex structure associated with a pilot wave guiding its motion* by exerting a potential force, which turns out to be the inherent action of the unified field [2,3,39,40].

According to the Copenhagen interpretation a single particle passes through both slits simultaneously, in an undefinable manner, interfering with itself by wave-particle duality. In the de Broglie-Bohm-Vigier approach, a particle passes only through one slit and the quantum wave passes through both, causing the interference pattern. In the de Broglie-Bohm-Vigier model, the quantum world exists even when it is not being observed or measured, a rejection of the positivist view that something that cannot be measured does not exist. Probabilities calculated from the wavefunction indicate the chances of a particle being at different positions regardless of whether a measurement is made, whereas in the conventional Copenhagen Interpretation probabilities indicate the chance of a particle coming into existence at different positions when a measurement is made [36]. To clarify, fundamentally, the Copenhagen Interpretation, as developed by Bohr, Heisenberg, Born, and Pauli, claims a quantum world is nonexistent, and that only an abstract description of probability waves that ‘collapse’ into classical particle-like objectivity when measurements are taken exists. We believe, like other theorists, that localization only occurs whenever a conscious mind is impinged. This complicated conundrum is beyond the scope of this volume, but we register it here

periodically in preparation for the inevitable debate regarding the role of the observer which cannot be ignored much longer [40-42]. But like 2nd quantization, let's call it 2nd localization, the mere existence of the observer is a '1st collapse' generating the virtual 3-space reality housing mind.

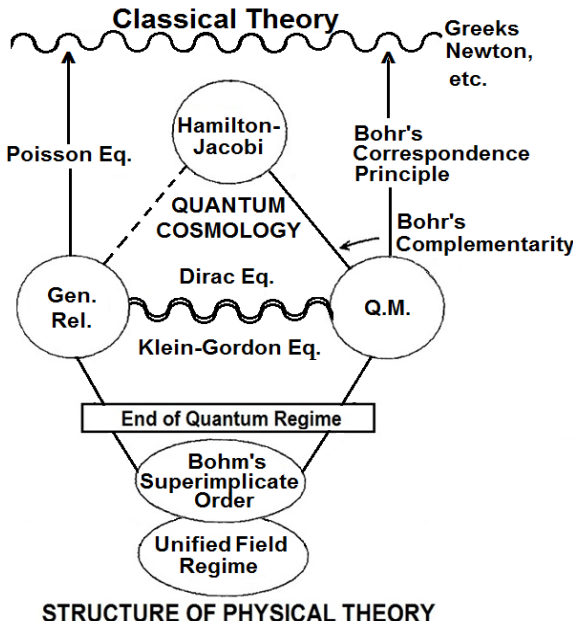


Fig. 4.1. A schematic representation of the history and structure of the fundamental equations of physics. Earlier time to present is represented from top to bottom. Gravity is not quantized if the quantum regime is a domain wall separating two infinite size dimensionalities (Euclidean and Implicate Order UFM space).

The probabilistic approach was strongly opposed by Einstein, Planck, and Schrödinger, to which de Broglie, Bohm and Vigier developed a viable alternative, albeit ignored by the main-stream physics community. Chebotarev had this to say:

The central idea of the Stochastic Interpretation of Quantum Mechanics consists in treating a microscopic object exhibiting a dual wave-particle nature as composed of a particle in the proper sense of the word (a small region in space with a high concentration of energy), and of an associated wave that guides the particle's motion. Both the particle and the wave are considered to be real, physically observable, and objectively existing entities [36].

Pratt's summary states that 'particles are pictured as oscillators (or solitons) beating in phase with their surrounding pilot waves, which in turn result from the superposition of superluminal phase waves carried by a subquantal etheric medium subject to constant stochastic fluctuations. The force, or quantum potential, determining particle motions therefore carries information from the entire environment, accounting for the 'wholeness' of quantum phenomena' [43].

And further that, the causal stochastic approach can account for all the quantum properties of matter disproving the claim that the quantum formalism requires abandonment not only the quest for an explanation of quantum phenomena but also the concepts of causality, continuity, and the objective reality of individual microobjects. In Vigier's view, the Copenhagen interpretation is based on 'arbitrary philosophical assumptions', and its insistence on the absolute and final character of indeterminacy is dogmatic [36,43].

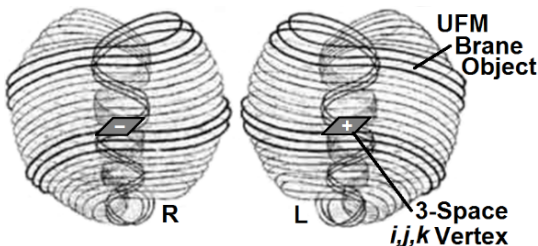


Fig. 4.2. Leadbeater & Besant 'ultimate physical atom' [44] which we tweaked with a traditional 3D fermionic singularity in the center to symbolize a global picture of matter. The two R-L forms are identical to each other, differing as an object and its mirror image. Mirror symmetric components are essential to the UFM particle dual regime model.

In the de Broglie-Bohm causal stochastic interpretation all quantum effects are explained by causal continuous motions in space and time with no place for the ill-defined concept of wave-packet collapse. There is only a 'pseudo-collapse', 'simply representing a change of our knowledge and not corresponding to any real physical changes in the state of the system. Vigier says that even if the quantum-potential approach 'is not taken as a fully satisfactory description of quantum mechanical reality, it at least shows in a clear way the features that such a description must entail' [36]. In the causal approach, therefore, 'the material world has an existence independent of the knowledge of observers' [36,45].

Interpreting the double-slit experiment is quite a concatenation of mysteries, if both slits are open an interference pattern occurs on the screen

even if electrons are sent to the slits one at a time. For Copenhagen, a single particle passes through both slits indefinitely interfering with itself; in the causal approach particles pass through only one slit and in the pilot wave approach particles pass through both. If a device is used to detect which slit a particle passes through, the interference pattern disappears. In the Copenhagen interpretation, the measurement collapses the wave function, whereas in the causal approach it affects a real pilot wave.

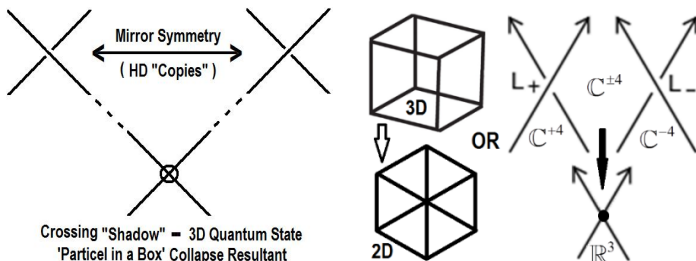


Fig. 4.3. Deconstructing the fermionic singularity. In 3-space a point (shown in a 2D x,y plane) is a fixed shadow having lost degrees of freedom inherent in HD space. To clarify: The mirror symmetric HD copies are real; while the Euclidean shadow is a virtual and transient production of a *continuous convergence and divergence* of the topological field (waves).

Now we get to important reasoning for extending the de Broglie-Bohm-Vigier approach. The Copenhagen interpretation claims that any path-determining measurement will destroy the interference pattern; however, the key idea to latch onto is that the causal interpretation predicts that interference will persist if future techniques allow a sufficiently subtle, non-demolition measurement to be performed. There is quite a body of literature referring to the evolution of the Elitzur-Vaidman Interaction Free-Measurement scenario [39,46-50]; which is abandoned as unnecessary in our experimental approach for surmounting uncertainty (Chaps. 7 & 8) [39,51], demonstrating the incompleteness of the Copenhagen description of reality, beckoning for new physics.

Vigier proposes that nonlocal interactions are not absolutely instantaneous but causal and superluminal; they are mediated by the quantum potential, and carried by superluminal phase waves in a covariant Dirac-type ether consisting of superfluid states of particle-antiparticle pairs [36,43]. We have noticed a duality between Newton's and Einstein's gravity (instantaneous versus luminal) [52], in addition to a complex 'manifold of uncertainty' bridging the gap between quantum mechanics

and UFM; it may turn out experimentally that this duality is a real condition.

Vigier writes:

In my opinion the most important development to be expected in the near future concerning the foundations of quantum physics is a revival, in modern covariant form, of the ether concept of the founding fathers of the theory of light ... it now appears that the vacuum is a real physical medium which presents some surprising properties [36].

Considerable effort was expended to review the causal-stochastic approach to hint at its foundation for UFM; and to show, at least from my point of view that the multiverse format for UFM is not *hypothesis non fingo* [55]. Whether one is inclined to accept anything to do with the parameters of the de Broglie-Bohm-Vigier interpretation at all; one must even if myopically, agree that the interpretation has sufficient richness to point in the direction we want to take it. Bias was so strong against heliocentricity that it literally took thousands of years before its pieces could be placed into the fabric of reality. While progress seems to be inevitable, it can be thwarted for lengthy periods. The de Broglie-Bohm-Vigier scenario has been waylaid for nearly 100 years; but finally the day of reckoning persistently looms.

4.5 Revolution in Concept of Matter

Since UFM does not exist yet empirically, currently only a dollop of theory, experiments designed, but not yet performed [53] loom in the entelechies (*εντελεξεία*) of potentia [54]; this key section can at the moment only be unavoidably conceptual and axiomatic. In doing customary book writing research, we discovered exquisite correspondence to insights of other theorists, making some of our radical proposals seem much tamer. Noted among these are Bohm's description of an *implicate and superimplicate order*, with observed particles *not fundamental, but forms' produced by a continuous convergence and divergence of waves*; and Vigier's concept of matter where a *particle is a complex structure associated with a pilot wave guiding its motion* by exerting a potential force, which we begin to formally describe in terms of an inherent action (guiding force of coherence) of the unified field [2,3]. If we momentarily sit alone in a chair provided by the *Zeitgeist*, soon teeming hordes will overrun us on another hundred years' adventure; indubitably the greatest heretofore in the history of science.

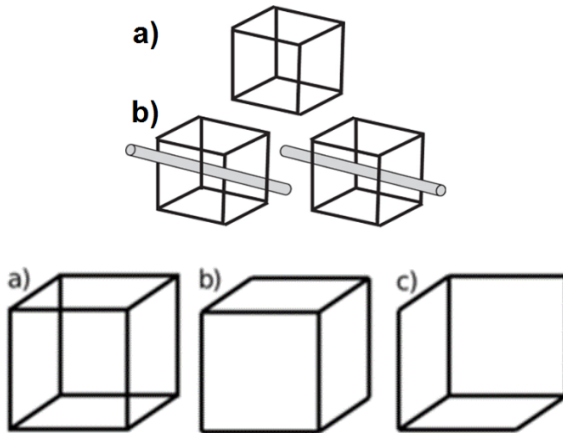


Fig. 4.4. The ambiguous Necker cube undergoes a process of ‘topological switching’ that acts as raising and lowering indices in the annihilation and recreation of knotted vertices.

What form does the revolution in the nature of matter take? About 100 years ago Leadbeater and Besant took an esoteric stab at what the extended model of an atom might look like as shown in Fig. 4.2, [44] which is good as any metaphor to start our discussion with.

We begin by repeating Rowlands view that in current thinking all of ‘*Physics reduces to the structure and interaction of fermions*’ [4-8]; what comes next as we enter the brane world regime of UFM? Figure 4.3 illustrates the 1st step into the ‘superimplicate order’ of topological forms. The Euclidean ‘shadow’ is a fixed knotted shadow of the Bohmian *continuous convergence and divergence* (which we term ‘Continuous-State’) of mirror symmetric topological field dynamics occurring in the 3rd regime of UFM [2,3]. The Euclidean 3-space shadow regime has been the space of observation for thousands of years. The utility of UFM insists that we give this tradition up (except for the Galilean/Lorentz transforms and some semi-quantum limit observations); and change the arena of observation to the HD brane-world vantage point. Any 3-space centered observation remains indelibly handicapped by the inherent attributes of the uncertainty principle, where the complete nature of a *particle as a complex structure associated with a pilot wave guiding its motion*, remains inaccessible.

Continuous-state aspects are further hinted at by the ambiguous or ‘Necker cube’. Crossover knots or braids become important in HD descriptions. In the next figure the complex structure of the superimplicate order begins to be revealed.

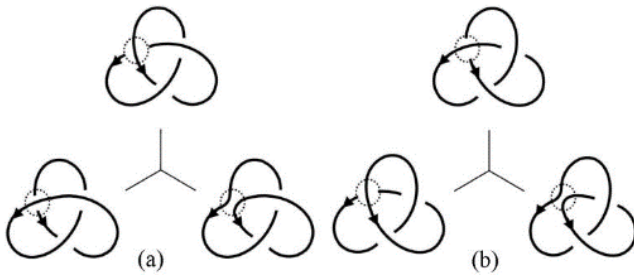


Fig. 4.5. Left-Right trefoil knots as 1st tier into into the symmetry operations of superimplicate order UFM topology.

For Fig. 4.5, assume the central vertex is the same as the Euclidean fermionic shadow vertex-singularity in Fig. 4.3a. The trefoil crossover – undercrossing can be manipulated in several ways or their combination, such as the 3 Reidemeister moves (Fig. 4.6) or by reflection, translation, raising and lowering, links, crossings and Markov moves [55], which with the addition of ontological-phase suffices for UFM matter cyclicity.

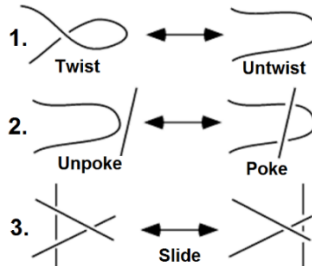


Fig. 4.6. The 3 Reidemeister moves.

Reidemeister was first to prove that distinct Knots exist that differ from the Unknot. He proved that all Knot deformations can be reduced to a sequence of three types of moves: 1) the Twist Move – Twist and untwist in either direction, 2) the Poke Move – Move a loop completely over another and 3) The slide Move – Move a line completely over or under a crossing [56].

Continuing our brief conceptual introduction to the superimplicate structure of matter, we next look at the fermionic vertex from the point of view of the Rowlands space-antispace model in quaternionic form. The pair of vertices, i,j,k and i',j',k' are transforming relativistically in the

spacetime backcloth. Because at this dimensional level the uncertainty principle is still in effect, stochasticity is still applicable and interaction of the vertices is chaotic. But as one notices, periodically they commute producing the Euclidean shadow; the cyclicity of which entails a hidden inherent ‘beat frequency’ of spacetime.

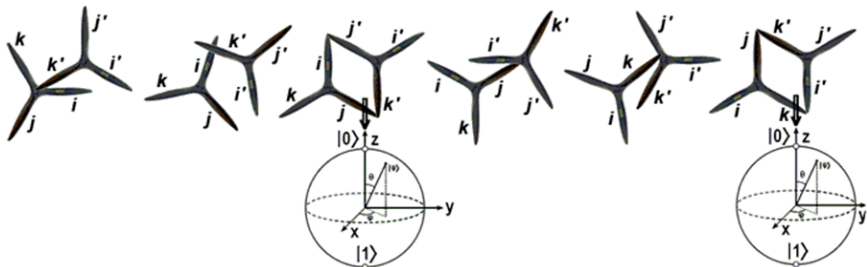


Fig. 4.7. Cyclic interaction (coupling) of space-antispace vertices becoming a realized Euclidean shadow point in 3-space (Fig. 4.3), suggesting a hidden periodic ‘beat frequency’ in the fabric of spacetime.

It is important to think of Figs. 4.7 & 4.8 as different views of the same continuous-state process; a dual mapping between the local Riemannian Bloch sphere as a shadow point in Euclidean 3-space and the quaternion ‘propellers’, top of Fig. 4.7 and as the contour spheres in Fig. 4.8, where the tiny central sphere would be a Bloch sphere in Fig. 4.7.

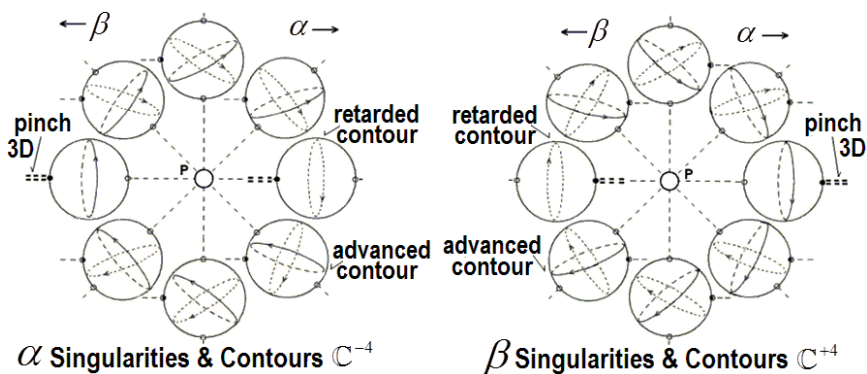


Fig. 4.8. Transformation of the forms making up the superimplicate order is both complex and complicated. The complex α and β mirror symmetric contours represent the 8 unit spheres of a $\pm\mathbb{C}$ -hypersphere. Similar to Fig. 4.7, when two pinches cyclically coincide a localized Euclidean shadow point occurs.

We realize expectation to accept such radical views for the nature and origin of matter in UFM space before experimental tests are performed is limited; but we do hope that sufficient ‘*dessin enfant*’ engender one to ‘Grok’ what we are driving at. In recalling an initial thumb through of Newton’s *Principia*; I remember myopically wondering where the origin of the calculus was...

To allow the cycle of ‘extension’ to operate properly (completely), such that the ‘mirror image of the mirror image in 12-space is causally free of the CQED quantum shadow in 3-space a 2nd duality is required. This is conceptualized in Fig. 4.9.

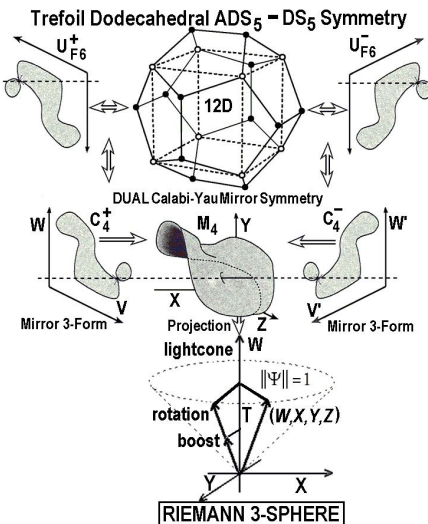


Fig. 4.9. The complete 12D UFM superimplicate order space, not enfolded. The Euclidean cube embedded in the 12D dodecahedron is causally free of the Euclidean shadow in 3-space and thus beyond the semi-quantum limit of the manifold of uncertainty.

As defined in more detail elsewhere, but put in here for the sake of continuity; Fig. 4.10 symbolizes the essential feature of extending Cramer’s transactional model of the present as a hyperspherical standing-wave of the future-past. It is to illustrate more of the same reasoning illustrated in Figs. 4.7 and 4.8, of the HD brane topological components comprising the new nonlocal parameters UFM adds to the basis of local matter. We finally feel secure in postulating that the finite radius semi-quantum manifold of uncertainty corresponds to the Calabi-Yau dual 3-torus. This is key to designing the experimental resonance hierarchy.

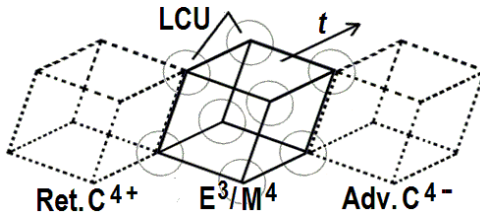


Fig. 4.10. Euclidean shadow illustrated by the central cube produced from two mirror symmetric complex cubes; not in Trefoil involute form so that cyclicity is not obvious.

With the addition of a super-quantum potential synonymous with the force of coherence of the unified field, a conceptual picture of the superimplicate order is complete. It is comprised of six spatial dimensions, a dual mirror symmetric Calabi-Yau 3-torus, able to translate by the utility of three temporal dimensions, as guided by three UFM control dimensions. The remaining and most important feature of course, is developing the complex quaternion Clifford algebra defining operation of the continuous transformation so the experimental design can be implemented [2,3].

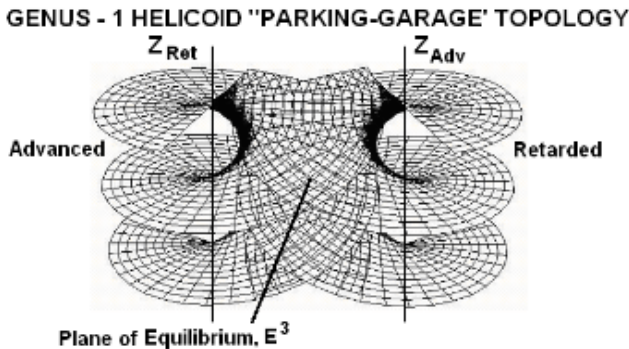


Figure 4.11 The Helicoid, a minimal embedded surface, is swept out by a line rotating about and moving down the z axis. Here a double Genus-1 Helicoid is joined into a “parking garage” ramp topological structure representing the future-past hierarchical topology of UFM space. An ordinary 2D plane can be twisted into a helicoid.

If Fig. 4.11 contained involute properties, it would probably look like the commonly drawn Calabi-Yau ‘floret’ brane topology. We separate it here as a Genus-1 helicoid to illustrate the T-duality nature of its hierarchical 3-fold properties.

The scalar equation in spherical coordinates of wave motion in spacetime which has spherical symmetry is [57].

$$\nabla^2 \Phi - \frac{1}{c^2} \partial^2 \frac{\Phi}{\partial t^2} = 0 \quad (4.9)$$

where Φ is the wave amplitude. The equation has two solutions

$$\begin{aligned}\Phi_{out} &= \frac{1}{r} \Phi_{max} \exp(i\omega t - ikr) \\ \Phi_{in} &= \frac{1}{r} \Phi_{max} \exp(i\omega t + ikr)\end{aligned}\quad (4.10)$$

which for the programming of spacetime can be applied to the propagation of Cramer's advanced retarded waves from an emission locus at $x, t = 0, 0$ by Eqs. 12.9 & 12.10 shown in Fig. 4.12.

$$F_{1-Ret} = F_0 e^{-ikx} e^{-2\pi ift}, \quad F_{2-Ret} = F_0 e^{ikx} e^{-2\pi ift} \quad (4.11a)$$

$$F_{3-Adv} = F_0 e^{-ikx} e^{2\pi ift}, \quad F_{4-Adv} = F_0 e^{ikx} e^{2\pi ift} \quad (4.11b)$$

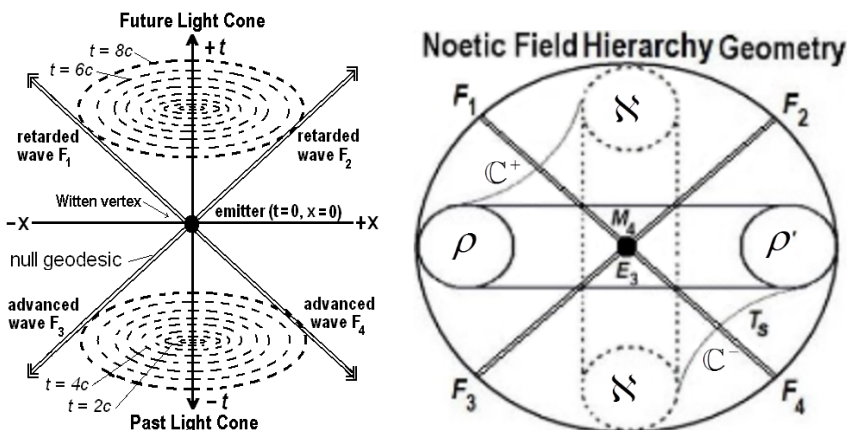


Fig. 4.12. a) Cramer advanced-retarded transaction emission locus illustrating Eqs. (4.11a) and (4.11b) at event point, $x, t = 0, 0$, which must be an unknotted Witten string vertex instead of a Euclidean/Minkowski fermionic 'knotted shadow' singularity for HD parameters to operate. The future-past lightcone is segmented into a superluminal hierarchy. b) Similar to 4.12a, taking the next step up the dimensional ladder to reveal one of two mirror symmetric brane topologies governed by the super quantum potential or force of coherence of the unified field equation, $F_{(N)} = \aleph / \rho$ guiding its evolution.

The UFM paradigm shift entails a plethora of new parameters. One can create an interesting mathematical equation for any idea; but finding one to represent physical reality is another thing. We dance around quite a bit with the perceived concepts of UFM, but since we do not fully understand yet how to ‘close pack’ the LCU configuration tessellating space we have held off. We have come to realize that the finite radius ‘manifold of uncertainty’ most likely corresponds to the Calabi-Yau dual 3-torus; but the general volumetric equation for hyperspheres suggests that these XD are not evenly spaced. The struggle of the moment is whether the LCU limit also applies to the Calabi-Yau manifold or if extends to 3rd regime LSXD. We are confident that there is an LCU exciplex that pumps UFM noeons into 4-space; but we do not know if that entails a rotating LCU scoop holophoting the UFM force of coherence. Since we know inertia is a cosmological flux, we probably have our answer, and will be spending the rest of 2016 developing a complex quaternion Clifford algebra to incorporate all these degrees of freedom and dimensional parameters to finish our empirical protocol, i.e. telling us how to program the resonance hierarchy. In the meantime, we hope the reader at least gets a glimmer of the ‘Golem’ being developed to account for a 12D model of matter.

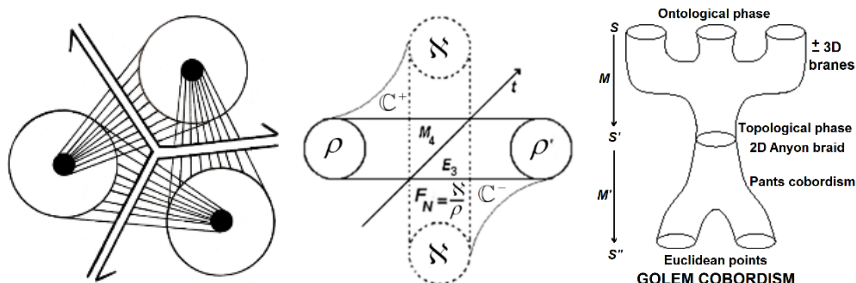


Fig. 4.13 Conceptualization of an isolated multiverse least cosmological unit (LCU) which like a quark would be confined. The continuous-state cyclic ‘static and dynamic’ Casimir boundary conditions around a central Witten Ising model string vertex. Compare Fig. 4.12b where the central square extended to a cube would contain 8 LCU. This form must at least be extended to the hypercube of 32 LCU vertices in some type of close-packed spheres coherently controlled by the Golem cobordism.

In Fig. 4.13a we say, ‘continuous-state cyclic ‘static and dynamic’ Casimir boundary conditions around a central Witten Ising model string vertex’, because the Euclidean shadow point (static) is continuously realized and recreated (dynamic) in the semi-quantum limit, a duality of the space and anti-space components [2,3].

Figure 4.13b is also a geometric representation of the Unified Field equation, $F_N = \aleph / \rho$ for an isolated LCU as in Fig. 4.13a. Solid lines represent extension, dotted lines represent field. Where $F_{(N)}$ is the coherent force of the unified field driving self-organization of the structural-phenomenology, \aleph equals the hysteresis loop energy of the hypervolumes ontological topological-phase charge, ρ is the scale-invariant radius of the action and the $\aleph - \rho$ connection curves refer to alternating variable string tension, T_0 part of the piloting of the static-dynamic Casimir conditions.

The ‘force of coherence’ is applied like a light house beacon with a beat frequency, which is a mechanism transforming the topology. This symbolically means that the ‘railroad tracks’ alternately recede into a point in the distance or remain parallel. If this were not so, the observer’s vision would not be confined to the accustomed Euclidean 3-space of observation, but the observer would ‘see’ the full 12D space, a perfect application for Plato’s analogy of the cave.

We have stated earlier that dimensionality beyond the manifold of uncertainty is of infinite size (LSXD). These XD are unseen not because they are curled up at the Planck scale as generally promoted, but because as in a movie theater film passing through the projector, they are invisible because of subtractive interferometry. Again all this concatenation of parameters is required to create the resultant Euclidean shadow out of the continuous evolution of the ‘forms’ of the superimplicate order.

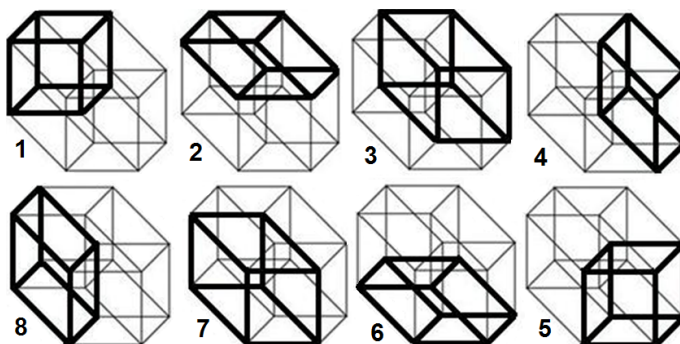


Fig. 4.14. Exploded view of a hypercube, an 8-unit cycle with each cube cyclically taking its turn as the Euclidean shadow. With mirror symmetry the 4D hypercube extends to 8D ($\pm C^4$) to handle all the required rotations. Alternatively, like the number of lines per second traced on the old style electron gun TV tubes.

In Fig. 4.14 for 8 cubes there are 32 LCU vertices, and with mirror symmetry 64 LCUs, same as the number of quaternion parameters. Because not all dimensions are spatial, involution in the topology, and the Euclidean ‘shadow’ many are redundant and thus we are not sure yet how to close-pack or tessellate them in spacetime. We think it will be based on a 6D dual Calabi-Yau 3-torus of spatial dimensions, 3 temporal dimensions that allow crossovers in the topology and 3 control dimensions for guidance by the unified field super quantum potential. Without the additional dimensionality of mirror symmetry, the cyclic operation will not work because the 4D quaternion algebra remains closed and the knot remains tied; it is only with 8D (2D probably lost for raising and lowering) that the algebra can be cyclically opened and closed under topological moves to allow surmounting uncertainty. We are in the process of developing the new set of transformations beyond the Galilean-Lorentz-Poincaré to handle this scenario which we believe is best handled by a complex quaternion Clifford algebra generally known to be able to mix a variety of dimensionality with other types of degrees of freedom [58,59].

References

- [1] Murayama, H. (2000) Supersymmetry phenomenology, arXiv:hep-ph/0002232v2.
- [2] Amoroso, R.L., Kauffman, L.H. & Rowlands, R. (eds.) (2013) *The Physics of Reality: Space, Time, Matter, Cosmos*, Singapore: World Scientific.
- [3] Amoroso, R.L., Kauffman, L.H. and Rowlands, R. (eds.) (2016) *Unified Field Mechanics: Natural Science Beyond the Veil of Spacetime*, Singapore: World Scientific.
- [4] Rowlands, P. (2007) *Zero to Infinity*, Singapore: World Scientific.
- [5] Rowlands, P. Physical interpretations of nilpotent quantum mechanics, arXiv: 1004.1523
- [6] Rowlands, P. (2010) What is vacuum? arXiv:0810.0224.
- [7] Rowlands, P. (2010) Dual vector spaces and physical singularities, AIP Conference Proceedings, 1316, 102-111.
- [8] Rowlands, P. Are there alternatives to our present theories of physical reality? arXiv:0912.3433.
- [9] Rowlands, P. (2013) Space and Antispace, in R. L. Amoroso et al. (eds.), *The Physics of Reality: Space, Time, Matter, Cosmos*, Singapore: World Scientific.
- [10] Rauscher, E.A., Rowlands, P. & Amoroso, R.L. (2016) Dirac equations in nilpotent quaternionic space-antispace and eight dimensional (8D) complex Minkowski space, in R.L. Amoroso, L.H. Kauffman & P. Rowlands (eds.) *Unified Field Mechanics: Natural Science Beyond the Veil of Spacetime*, Hackensack: World Scientific.
- [11] Rowlands, P. (2014) *The Foundations of Physical Law*, World Scientific, Singapore.
- [12] Rowlands, P. (2015) *How Schrödinger’s Cat Escaped the Box*, World Scientific.
- [13] Rowlands, P. (1994) An algebra combining vectors and quaternions: A comment on James D. Edmonds’ paper, *Speculat. Sci. Tech.*, 17, 279-282.

- [14] Rowlands, P. (1996) Some interpretations of the Dirac algebra, *Speculat. Sci. Tech.*, 19, 243-51.
- [15] Rowlands, P. (1998) The physical consequences of a new version of the Dirac equation, in G. Hunter, S. Jeffers, and J-P. Vigier (eds.), *Causality and Locality in Modern Physics and Astronomy: Open Questions and Possible Solutions* (Fundamental Theories of Physics, vol. 97, Kluwer Academic Publishers, Dordrecht, pp. 397-402).
- [16] Rowlands, P. & Cullerne, J.P. (2001) The connection between the Han-Nambu quark theory, the Dirac equation and fundamental symmetries, *Nuc Phys A* 684, 713-5.
- [17] Rowlands, P. (2010) The nilpotent Dirac equation and its applications in particle physics, arXiv:quant-ph/0301071.
- [18] Rowlands, P. (2004) Symmetry breaking and the nilpotent Dirac equation, *AIP Conference Proceedings*, 718, 102-115.
- [19] Rowlands, P. (2005) Removing redundancy in relativistic quantum mechanics, arXiv.org:physics/0507188.
- [20] Rowlands, P. (2006) Fermion interactions and mass generation in the nilpotent formalism, *AIP Conference Proceedings*, 839, 225-35.
- [21] Rowlands, P. (2014) A Dual space as the basis of quantum mechanics and other aspects of physics, in J.C. Amson & Louis H. Kauffman (eds.) *Scientific Essays in Honor of H Pierre Noyes on the Occasion of His 90th Birthday*, World Scientific, 318-338.
- [22] Rowlands, P. (2014) Nilpotent Quantum Theory: A Review, *Bulletin of the Transilvanian University of Brașov*, 7(56), No. 2, 99-120.
- [23] Rowlands, P. (1979) The laws of physics and fundamental particles, NVA.
- [24] Rowlands, P. (1982) The fundamental parameters of physics, ASIS/NAPS microfiche 04068.
- [25] Rowlands, P. (1983) Fundamental parameters of physics, *Spec Sci. Tech.*, 6, 69-80.
- [26] Rowlands, P. (1991) *The Fundamental Parameters of Physics: An Approach towards a Unified Theory*, PD Publications, Liverpool.
- [27] Rowlands, P. A foundational approach to physics, arXiv:physics/0106054.
- [28] Rowlands, P. (2008) Are there alternatives to our present theories of physical reality? (Invited presentation at the 20th Anniversary Seminar of the Finnish National Society for Natural Philosophy in debate with Anton Zeilinger, 18 September 2008), arXiv:0912.3433
- [29] Rowlands, P. (2010) Mathematics and Physics as Emergent Aspects of a Universal Rewrite System, *International Journal of Computing Anticipatory Systems*, 25, 115-131.
- [30] Rowlands, P. (2013) Symmetry in physics from the foundations, *Symm.*, 24, 41-56.
- [31] Hill, V.J. & Rowlands, P. (2008) Nature's code, *AIP Conf Proc*, 1051, 117-126.
- [32] Hill, V.J. & Rowlands, P. (2010) Nature's Fundamental Symmetry Breaking, *International Journal of Computing Anticipatory Systems*, 25, 144-159.
- [33] Hill, V.J. & Rowlands, P. (2010) The Numbers of Nature's Code, *International Journal of Computing Anticipatory Systems*, 25, 160-175.
- [34] Marcer, P. & Rowlands, P. (2010) The 'Logic' of self-organizing systems, *AAAI Technical Reports*.
- [35] Penrose, R. (2004) *The Road to Reality*, Jonathan Cape, p. 982, Fig. 33.15.
- [36] Jean-Pierre Vigier and the Stochastic Interpretation of Quantum Mechanics (2000) S. Jeffers, B. Lehnert, N. Abramson & L. Chebotarev, Montreal: Apeiron.
- [37] Dirac, P.A.M. (1951) Is there an aether?, *Nature* 168, 906-907.
- [38] Bohm, D. (1952) A suggested interpretation of the quantum theory in terms of "hidden" variables. I. *Physical Review*, 85(2), 166; A suggested interpretation of the quantum theory in terms of "Hidden" variables. II. *Physical Review*, 85(2), 180.
- [39] Amoroso, R. L., & Rauscher, E. A. (2009) *The Holographic Anthropic Multiverse Formalizing the Complex Geometry of Reality*, London: World Scientific.

- [40] Amoroso, R. L. (2010) Complementarity of Mind and Body: Realizing the Dream of Descartes, Einstein, and Eccles, New York: Nova Science Publishers.
- [41] Shimony, A. (1963) Role of the observer in quantum theory, American Journal of Physics, 31(10), 755-773.
- [42] Singh, I., & Whitaker, M.A.B. (1982) Role of the observer in quantum mechanics and the Zeno paradox, American Journal of Physics, 50(10), 882-887.
- [43] Pratt, D. (2002) Book review: Jean-Pierre Vigier and the Stochastic Interpretation of Quantum Mechanics, S. Jeffers, B. Lehnert, N. Abramson & L. Chebotarev (eds.) Montreal: Apeiron, 2000, J. Scientific Exploration, vol. 16, no. 2, pp. 283-7; <http://www.davidpratt.info/vigier.htm>.
- [44] Leadbeater, C.W. & Besant, A. (1919) Occult Chemistry, A.P. Sinnett (ed.) Revised Edition, Project Gutenberg.
- [45] Pratt, D. (1997) Consciousness, causality, and quantum physics, J Scientific Exploration, 11, 69-78.
- [46] Elitzur, A.C. & Vaidman, L. (1993) Quantum mechanical interaction-free measurements, Found. Phys. 23; 987-997.
- [47] Simon, S.H. & Platzman, P.M. (1999) Fundamental limit on “interaction free” measurements, arXiv:quant-ph/9905050v1.
- [48] Vaidman, L. (1996) Interaction-free measurements, arXiv:quant-ph/9610033v1.
- [49] Paraoanu, G.S. (2006) Interaction-free measurements with superconducting qubits, Physical Rev. Letters 97, (2006) 180406.
- [50] Vaidman, L. (2001) The meaning of the interaction-free measurements, arXiv:quant-ph/0103081v1.
- [51] Amoroso, R.L. (2010) Simple resonance hierarchy for surmounting quantum uncertainty, in R.L. Amoroso, P. Rowlands & S. Jeffers (eds.) AIP Conference Proceedings-American Institute of Physics, Vol. 1316, No. 1, p. 185.
- [52] Amoroso, R.L. (2013) Unified geometrodynamics: A complementarity of Newton’s and Einstein’s gravity, in The Physics of Reality: Space, Time, Matter, Cosmos, pp. 152-163, World Scientific.
- [53] Amoroso, R.L., & Vigier, J-P (2013) Evidencing ‘tight bound states’ in the hydrogen atom: Empirical manipulation of large-scale XD in violation of QED, in The Physics of Reality: Space, Time, Matter, Cosmos, pp. 254-272, World Scientific.
- [54] Duchesneau, F. (1998) Leibniz’s Theoretical Shift in the *Phoronomus* and *Dynamica de Potentia*, Perspectives on Science 6 (1&2): 77-109.
- [55] Markov, A. (1935) *Über die freie Äquivalenz der geschlossenen Zöpfe, Recueil Mathématique De La Société Mathématique De Moscou* (German and Russian) 1: 73-78.
- [56] Reidemeister, K. (1927) *Elementare Begründung der Knotentheorie, Abh. Math. Sem. Univ. Hamburg* 5 (1): 24-32.
- [57] Wolf, M. (2008) Schrödinger’s Universe, Colorado: Outskirts Press.
- [58] Rowlands, P. (2016) How many dimensions are there? in R.L. Amoroso (eds.) Unified Field Mechanics: Natural Science Beyond the Veil of Uncertainty, World Scientific.
- [59] Amoroso, R. L., Rowlands, P., & Kauffman, L. H. (2013) Exploring Novel Cyclic Extensions of Hamilton’s Dual-Quaternion Algebra, in R.L. Amoroso, L.H. Kauffman & P. Rowlands (eds.) The Physics of Reality: Space, Time, Matter, Cosmos, pp. 81-91 London: World Scientific.

Chapter 5

From Qubits to Relativistic (R-Qubits)

Quantum Computing (QC) has remained elusive beyond a few qubits. One of Feynman's initial premises was to recommend the use of a "synchronization backbone" for achieving the bulk implementation of Universal Quantum Computing (UQC); unfortunately, that has generally been abandoned as intractable; a conundrum we believe arises from limitations imposed by the standard Copenhagen Interpretation of Quantum Theory (QT) and current incomplete models of Cosmology. In this work it is proposed that not only can Feynman's synchronization backbone model be utilized, but in fact it is a required key element for implementing UQC if done with the addition of valid higher dimensional (HD) extensions of QT and cosmology. Requisite additional degrees of freedom are introduced by defining a relativistic basis for the qubit (r-qubit) in an HD conformal invariant context, and by defining a new anticipatory based cosmology (cosmology itself cast as a hierarchical form of complex self-organized system) making correspondence to dual 3-tori 6D Calabi-Yau mirror symmetries in M-Theory. An additional control parameter required by Unified Field Mechanics (UFM) is added bringing dimensionality to 12 (12D). The causal structure of these conditions reveal an inherent new UFM 'action principle' (not a 5th force, but an ontological 'force of coherence' of the UF) driving self-organization and providing a basis for applying Feynman's synchronization backbone principle. Attempts by the few researchers for a synchronization backbone, should at best be called 'bi-local'; when as we shall show the symmetry for synchrony is an inherent component of HD brane topology. Operationally a new set of transformations (beyond the standard Galilean/Lorentz-Poincaré) ontologically describe how to surmount the quantum condition, $\Delta x \Delta \rho \cong \hbar$ (supervening decoherence during both initialization and measurement) by an acausal energyless topological brane interaction.

5.1 Introduction

It is proposed that the difficulties encountered in attempting to implement bulk Universal Quantum Computing (UQC) [1-7] can only be solved by introducing a new relativistic approach to quantum information processing (QIP) that includes a new physically real coordinate transformation beyond the current Riemann Block 2-sphere rendition in Hilbert space and a relativistic definition of the qubit (r-qubit). As described in detail later on, this is part of an end to the historical pillars of ‘unitarity and locality’.

The Bloch 2-sphere representation of the qubit

$$|\Psi|^2 = \cos \frac{\theta}{2} |0\rangle + e^{i\phi} \sin \frac{\theta}{2} |1\rangle \quad (5.1)$$

maps to the polar coordinates along the z axis as a linear combination of $|0\rangle$ and $|1\rangle$ between $-\hat{z}$ and \hat{z} , and where $e^{i\phi}$ is a phase factor. In this regard we have $|\Psi(\theta=0, \phi=0)\rangle = |0\rangle$, and $|\Psi(\theta=\pi, \phi=0)\rangle = |1\rangle$ yielding $|\Psi(\theta, \phi)\rangle = \cos(\theta/2)|0\rangle + \sin(\theta/2)e^{i\phi}|1\rangle$ since $\cos(\theta/2)=0$ and $\sin(\theta/2)=1$. This scenario is very useful when applying π or $\pi/2$ pulses to basis states.

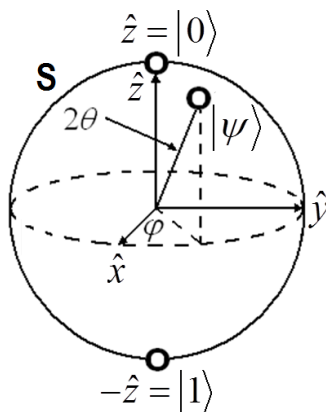


Fig. 5.1. Bloch sphere qubit representation. Note that the Bloch 2-sphere, $S^2 = \partial B^3$ representation of pure qubit states is the boundary of the Bloch 3-ball, B^3 for mixed qubit states. The Bloch sphere qubit is a mathematical model and as such not a physically real representation as now required to develop relativistic QIP.

Note that angle $\theta/2$ [8] doubles when going from the Dirac ket

$$|\psi\rangle = \begin{bmatrix} \cos \frac{\theta}{2} \\ e^{i\phi} \sin \frac{\theta}{2} \end{bmatrix}, \quad \|\psi\| = 1, \quad (5.2)$$

to the operator for the density matrix

$$\rho = |\psi\rangle\langle\psi| = \frac{1}{2}(1_{2\times 2} + \vec{r} \cdot \vec{\sigma}), \quad \text{tr}\rho = 1. \quad (5.3)$$

From (5.2)

$$\vec{r} = \begin{bmatrix} x \\ y \\ z \end{bmatrix} = \begin{bmatrix} r \cos \phi \sin \theta \\ r \sin \phi \sin \theta \\ r \cos \theta \end{bmatrix}, \quad r = 1, \quad (5.4)$$

the vector for the radius in spherical coordinates, and with σ_i as the Pauli matrices.

For a spin $1/2$ 2-state quantum system (qubit), the quantum state is $\psi = c_0|0\rangle + c_1|1\rangle$, c_0 and c_1 are complex numbers in Hilbert space and ψ is the norm:

$$\|\psi\|^2 \equiv \psi^*\psi = |c_0|^2 + |c_1|^2 = 1, \quad c_0, c_1 \in \mathbb{C}. \quad (5.5)$$

A qubit state is considered a superposition of the two usual logical bit states, False, True or 0,1 with complex coefficients described by a ray in complex Hilbert space or as a complex projective space, $\mathbb{C}P \sim \mathbb{C} \cup \{\infty\}$. Every ray (c_0, c_1) is represented by the complex number, $\xi = c_0 / c_1$ where the $|0\rangle$ corresponds to 0 and the $|1\rangle$ to ∞ on opposite poles of the Bloch sphere. The plane, ξ and the 2-sphere, S make correspondence because of stereographic projection, $\xi = (x - iy) / (1 - z)$ as in Fig. 5.2 [9].

Coordinates (x, y, z) are represented on the unit 2-sphere as:

$$\begin{aligned}
 x &= \frac{2 \operatorname{Re} \xi}{|\xi|^2 + 1} = \frac{c_0 \bar{c}_1 + c_1 \bar{c}_0}{c_0 \bar{c}_0 + c_1 \bar{c}_1} \\
 -y &= \frac{2 \operatorname{Im} \xi}{|\xi|^2 + 1} = \frac{-i(c_0 \bar{c}_1 - c_1 \bar{c}_0)}{c_0 \bar{c}_0 + c_1 \bar{c}_1} \\
 z &= \frac{|\xi|^2 - 1}{|\xi|^2 + 1} = \frac{c_0 \bar{c}_0 - c_1 \bar{c}_1}{c_0 \bar{c}_0 + c_1 \bar{c}_1}.
 \end{aligned} \tag{5.6}$$

Because of (5.5) this can be simplified to (X, Y, Z) instead:

$$\begin{aligned}
 X &= c_0 \bar{c}_1 + c_1 \bar{c}_0 \\
 Y &= i(c_0 \bar{c}_1 - c_1 \bar{c}_0) \\
 Z &= c_0 \bar{c}_0 - c_1 \bar{c}_1
 \end{aligned} \tag{5.7}$$

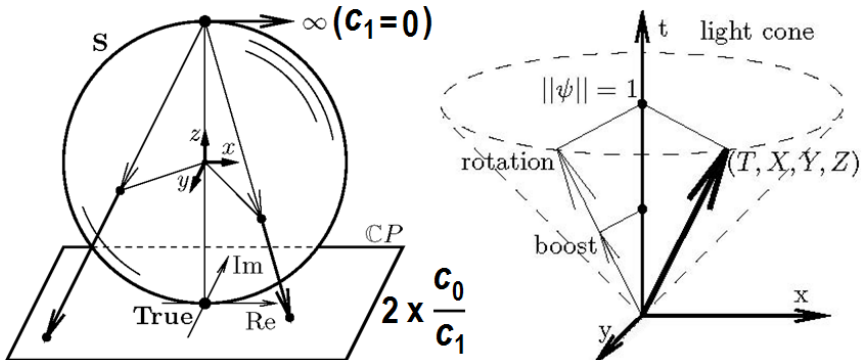


Fig. 5.2. a) Riemann sphere stereographic projection usual qubit representation. b) Relativistic lightcone null vector (T, X, Y, Z) qubit representation.

In terms of group theory, the 2D complex Hilbert space, $H = \mathbb{C}^2$ for the qubit is a 2-spinor representation of the $G = SU(2)$ Lie group, a double cover of the 3D rotation group $SO(3)$ [8]. State transformation from spatial rotation of the coordinate system can be described by a unitary matrix

$$\psi' = \begin{bmatrix} a & b \\ c & d \end{bmatrix} \psi, \quad \begin{aligned} \bar{a} &= d, \quad \bar{c} = -b \\ ad - bc &= |a|^2 + |b|^2 = 1. \end{aligned} \tag{5.8}$$

This is the $SU(2)$ group of unitary 2×2 matrices corresponding to the principle that transformation of the wave vector is described by a group coordinate transformation. The $SU(2)$ group represents the $SO(3)$ group of spatial rotations in a 2D complex vector space, where due to 2-1 $SU(2)$ and $SO(3)$ isomorphism any rotation corresponds to a unitary matrix up to sign allowing transition to other coordinate systems [9].

The $SO(3)$ $SU(2)$ relationship is shown by (5.6). Applying a unitary transformation (5.7) gives $U : (c_0, c_1) \rightarrow (c'_0, c'_1)$ such that

$$X^2 + Y^2 + Z^2 = \left(|c_0|^2 + |c_1|^2 \right)^2. \quad (5.9)$$

The angles between the vectors do not change; These unitary transformations of the qubit state correspond to rotations of the sphere as in Fig. 5.2a; and the two matrices U and $-U$ produce the same rotation because of (5.6) [9].

5.2 Case for Relativistic Information Processing

Here we describe steps for merging Relativistic Quantum Theory (RQFT) with the theory of computation. One must consider transformation of a qubit state due to rotation, boost and translation of the coordinate system. The $SL(2, \mathbb{C})$ Lorentz transformation is considered. New properties of this transformation suggest the usual Riemann Bloch 2-sphere model of the qubit must be changed. For RQFT it is necessary to consider a qubit in different coordinate systems. For the simplest case this may be 3D local rotations and $SU(2)$ spinors. In considering temporal coordinates, it is necessary to use Lorentz transformations and 4D spinors. The best general approach needs to include the full Poincaré group of transformations plus RQFT. As also shown, in order to meet the penultimate requirement of surmounting uncertainty and supervening decoherence, a new set of HD unified field mechanical (UFM) transformations is introduced. The UFM transform likewise obviates the no-cloning and quantum erasure theorems.

Quantum theory, relativity and Shannon's information theory are inseparably connected [10,11]. The speed of transmission of information signals has been bounded by the velocity of light (standard model only). Because information requires a material carrier obeying the laws of physics, Landauer proposed that information is physical [12].

5.3 Microphysical Computation Limits: The Relativistic R-Qubit

In the conventional consideration of quantum computing a quantum bit or qubit is any 2-state quantum system defined as a superposition of two logical states of a usual bit with complex coefficients that can be mapped to the Riemann Bloch sphere by stereographic projection. Geometrically, stereographic projection is a mapping projecting each point on a sphere onto a tangent plane along a straight line from the antipode of the point of tangency, with the exception that the center of projection, is not projected to any point in the Euclidean plane; but corresponds to a ‘point at infinity’ (Fig. 5.2a).

Formally a qubit is represented as: $\Psi = \xi|0\rangle + \eta|1\rangle$ with each ray $\xi, \eta \in C$ in complex Hilbert space and $\|\Psi\|^2 = \xi\bar{\xi} + \eta\bar{\eta} = 1$, where $|0\rangle$ corresponds to the south or 0 pole of the Riemann sphere and $|1\rangle$ corresponds to the opposite, north or ∞ pole of the Riemann complex sphere. The conventional (non-relativistic) qubit maps to the complex plane of the Riemann Bloch sphere in Hilbert space as:

$$\xi\bar{\eta} + \eta\bar{\xi} \rightarrow X, \quad \xi\bar{\eta} - \eta\bar{\xi} \rightarrow iY, \quad \xi\bar{\xi} - \eta\bar{\eta} \rightarrow Z. \quad (5.10)$$

5.3.1 Aspects of the Lorentz Transformation

The Lorentz group of all transformations for Minkowski spacetime is the Lie group upon which special relativity is based, preserving the quadratic form $(t, x, y, z) \rightarrow t^2 - x^2 - y^2 - z^2$ on \mathbb{R}^4 . The Lorentz group is also an $SO(3,1)$ group analogous to the $SO(4)$ 4D rotation group. There are 6 generators in the Lorentz group, three of them are related to boosts and the other three are related to 3D rotations. Specifically, the Lorentz group is defined by the set of all (4×4) real matrices leaving the line element, s invariant, $s^2 = c^2 t^2 - x' x' = (x^0)^2 - (x')^2$, where the minus sign distinguishes the $SO(3,1)$ group from the $SO(4)$ 4D rotation group [13].

For QC we employ unitary representations of a symmetry group, because they preserve the probabilities between eigenstates measured in different reference frames.

Following Yeh [13] for spinor representations of the Lorentz group we can define the generators **A** and **B** utilizing **J** and **K**:

$$\mathbf{A} = \frac{1}{2}(\mathbf{J} + i\mathbf{K}), \quad \mathbf{B} = (\mathbf{J} - i\mathbf{K}). \quad (5.11)$$

Since the conditions, $\mathbf{J} = i\mathbf{K}$ and $\mathbf{J} = -i\mathbf{K}$ correspond to spin zero in one of the states we can define two types of spinors:

$$\xi \equiv \left(\frac{1}{2}, 0 \right): \quad \mathbf{J}^{1/2} = \boldsymbol{\sigma}/2, \quad \mathbf{K}^{1/2} = -i\boldsymbol{\sigma}/2, \quad (5.12)$$

$$\eta \equiv \left(\frac{1}{2}, 0 \right): \quad \bar{\mathbf{J}}^{1/2} = \boldsymbol{\sigma}/2, \quad \bar{\mathbf{K}}^{1/2} = -i\boldsymbol{\sigma}/2. \quad (5.13)$$

If (θ, φ) represent parameters of both a rotation and a Lorentz boost, the spinors ξ and η transform as:

$$\xi \rightarrow \exp(-i\mathbf{J}^{1/2} \cdot \boldsymbol{\theta} - i\mathbf{K}^{1/2} \cdot \boldsymbol{\varphi}) \xi = \exp\left[-i\frac{\boldsymbol{\sigma}}{2} \cdot (\boldsymbol{\theta} + i\boldsymbol{\varphi})\right] \xi \equiv M\xi, \quad (5.14)$$

$$\eta \rightarrow \exp(-i\bar{\mathbf{J}}^{1/2} \cdot \boldsymbol{\theta} - i\bar{\mathbf{K}}^{1/2} \cdot \boldsymbol{\varphi}) \eta = \exp\left[-i\frac{\boldsymbol{\sigma}}{2} \cdot (\boldsymbol{\theta} - i\boldsymbol{\varphi})\right] \eta \equiv N\eta. \quad (5.15)$$

The **M** and **N** Lorentz group representations are not equivalent and cannot be transformed into one another by a similarity transform $\mathbf{N} = \mathbf{S}\mathbf{M}\mathbf{S}^{-1}$ where \mathbf{S} is a matrix. **M** and **N** are actually (2×2) complex matrices related by the Pauli matrix, $\boldsymbol{\sigma}_2$, $\mathbf{N} = \xi \mathbf{M}^* \xi^{-1}$ with

$$\xi = -i\boldsymbol{\sigma}_2 = \begin{pmatrix} 0 & -1 \\ 1 & 0 \end{pmatrix}. \quad (5.16)$$

These (2×2) complex matrices form the relativistic group, $SL(2, \mathbb{C})$ constituting irreducible spinor representations [13].

The Lorentz coordinate transform has various isomorphic similarities with groups $SO(3,1)$, $SL(2, \mathbb{C})$ and $SU(2)$; but we should not directly apply the relativistic group, $SL(2, \mathbb{C})$ to a qubit, because (5.17)

$$\|\psi\|^2 \equiv \psi^* \psi = |c_0|^2 + |c_1|^2 = 1, \quad c_0, c_1 \in \mathbb{C} \quad (5.17)$$

relativistically is not scalar invariant, but a temporal component of a 4-vector breaking the coordinate transformation relation with unitary matrices. In matrix notation, $\psi^*\psi$ or $(\langle\psi|\psi\rangle)$ is a scalar and $\psi\psi^*$ or $(|\psi\rangle\langle\psi|)$ is a 2×2 matrix [9].

If we write:

$$T = \|\psi\|^2 \equiv \psi^*\psi = c_0\bar{c}_0 + c_1\bar{c}_1. \quad (5.18)$$

We can use

$$\begin{aligned} X &= c_0\bar{c}_1 + c_1\bar{c}_0 \\ Y &= i(c_0\bar{c}_1 - c_1\bar{c}_0) \\ Z &= c_0\bar{c}_0 - c_1\bar{c}_1 \end{aligned} \quad (5.19)$$

and (5.17) to produce:

$$\begin{aligned} \mathbf{V} &\equiv \begin{pmatrix} T+Z & X-iY \\ X+iY & T-Z \end{pmatrix} = 2 \begin{pmatrix} c_0\bar{c}_0 & c_0\bar{c}_1 \\ c_1\bar{c}_0 & c_1\bar{c}_1 \end{pmatrix} \\ \frac{1}{2}\mathbf{V} &= \begin{pmatrix} c_0 \\ c_1 \end{pmatrix} (\bar{c}_0 \quad \bar{c}_1) = \psi\psi^* \\ \det \mathbf{V} &= T^2 - X^2 - Z^2 = 2c_0\bar{c}_0 2c_1\bar{c}_1 - 2c_1\bar{c}_0 2c_0\bar{c}_1 = 0. \end{aligned} \quad (5.20)$$

The linear transformation for a qubit with determinant unity corresponds to the Lorentz transformation of the relativistic null vector (T, X, Y, Z) :

$$\begin{aligned} \psi' &= \mathbf{A}\psi; \quad \det \mathbf{A} = 1 \\ \mathbf{V}' &= 2\mathbf{A}\psi(\mathbf{A}\psi)^* = 2\mathbf{A}\psi\psi^*\mathbf{A}^* = \mathbf{A}\mathbf{V}\mathbf{A}^* \\ \det \mathbf{V}' &= T'^2 - X'^2 - Y'^2 - Z'^2 = \det \mathbf{V} = T^2 - X^2 - Y^2 - Z^2. \end{aligned} \quad (5.21)$$

Only if matrix \mathbf{A} is unitary, $\mathbf{A}\mathbf{V}\mathbf{A}^* = \mathbf{A}\mathbf{V}\mathbf{A}^{-1}$ and *Trace* \mathbf{V} , the norm of (5.18) does not change; or (5.18) would be the T -component of a 4-vector. The relation (5.21) between $SL(2, \mathbb{C})$ and the Lorentz group (5.21) is not only valid for null vectors; but any vector is the sum of two null vectors and $\mathbf{A}(\mathbf{V}+\mathbf{U})\mathbf{A}^* = \mathbf{A}\mathbf{V}\mathbf{A}^* + \mathbf{A}\mathbf{U}\mathbf{A}^*$ [9].

The 2-component complex vector qubit is a Weyl spinor corresponding to a massless particle with spin $\frac{1}{2}$ moving at the speed of light. Equation (5.20) shows correspondence between such a spinor and a 4D null vector (Fig. 5.3), which can be rewritten as Pauli matrices [9]:

$$\begin{aligned}\sigma_x &= \begin{pmatrix} 0 & 1 \\ 1 & 0 \end{pmatrix}, \quad \sigma_y = \begin{pmatrix} 0 & -i \\ i & 0 \end{pmatrix}, \quad \sigma_z = \begin{pmatrix} 1 & 0 \\ 0 & -1 \end{pmatrix} \\ V &= T\mathbf{1} + X\sigma_x + Y\sigma_y + Z\sigma_z, \\ V_i &= \frac{1}{2} \text{Tr}(\sigma_i V) = \text{Tr}(\sigma_i \psi \psi^*) = \psi^* \sigma_i \psi; \\ \sigma &= \{\sigma_x, \sigma_y, \sigma_z\}: (T\{X, Y, Z\}) = (\psi^* \psi, \psi^* \sigma \psi).\end{aligned}\quad (5.22)$$

5.3.2 Massive Particles

By introducing parity to the spinor representations, the generators \mathbf{K} change sign because they act as vectors but the generators \mathbf{J} do not because they act as axial vectors or pseudo-vectors. Thus, under parity, $(j, 0)$ and $(0, j)$ interchange accordingly giving $\xi \leftrightarrow \eta$ under parity operations, implying that extending the Lorentz group by parity can no longer be described by the 2-spinor representations; and we must introduce the 4-spinor representation. Following Vlasov and Yeh [13,14], massive spin $\frac{1}{2}$ particles such as an electron, e^- or neutrino, $\nu_e, \nu_\mu, \nu_\tau, \bar{\nu}_e, \bar{\nu}_\mu, \bar{\nu}_\tau$ for example, are described by two Weyl spinors with four complex components:

$$\psi \equiv \begin{pmatrix} \xi \\ \eta \end{pmatrix} = \begin{pmatrix} \varphi R \\ \varphi L \end{pmatrix} \varphi R, \varphi L \in \mathbb{C}^2; \quad \psi = \begin{pmatrix} \psi_0 \\ \psi_1 \\ \psi_2 \\ \psi_3 \end{pmatrix} \quad (5.23)$$

which can be considered as two qubits, $\psi = c_{00}|00\rangle + c_{01}|01\rangle + c_{10}|10\rangle + c_{11}|11\rangle$. For each $\varphi R, \varphi L$ the first index is like $|\uparrow\rangle$ and $|\downarrow\rangle$; and the second index corresponds to discretized coordinate transformations such as spatial reflection, $P: (t, \vec{x}) \rightarrow (t, -\vec{x})$ [14].

The 4×4 Dirac matrices, γ^μ can also be used as illustrated in

Fig. 5.5, $j^\mu = \psi^* \gamma^0 \gamma^\mu \psi$ which is always positive for $j^0 = \psi^* \psi = \sum_i |\psi_i|^2 = \|\varphi R\|^2 + \|\varphi L\|^2$, but j^0 is not Lorentz invariant. The Lorentz invariant scalar is, $\psi^* \gamma^0 \psi = \varphi^* R \varphi L + \varphi^* L \varphi R$ [9].

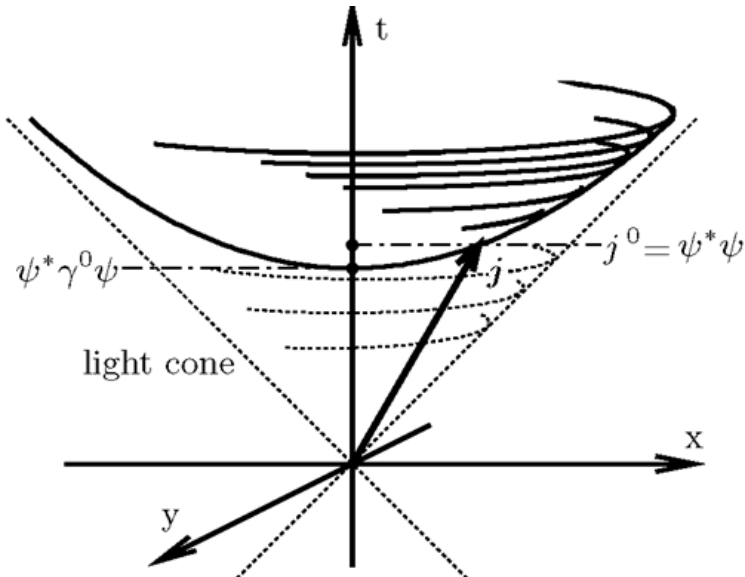


Fig. 5.3. Massive spin $\frac{1}{2}$ particle. Showing the Lorentz invariant scalar, $\psi^* \gamma^0 \psi = \varphi^* R \varphi L + \varphi^* L \varphi R$. Figure modified from [9].

Unitary transformations of a standard qubit correspond to 3D rotations of the Riemann Bloch sphere. Following Vlasov [9,14] for relativistic consideration of a qubit (r-qubit) an additional 4D parameter is added to equation (5.10):

$$\begin{aligned} \xi \bar{\eta} + \eta \bar{\xi} &\rightarrow X, & \xi \bar{\eta} - \eta \bar{\xi} &\rightarrow iY, \\ \xi \bar{\xi} - \eta \bar{\eta} &\rightarrow Z, & \xi \bar{\xi} + \eta \bar{\eta} &\rightarrow T \end{aligned} \quad (5.24)$$

5.3.3 Aspects of the Poincaré Transformation

Unitary representations preserve transition probabilities between two eigenstates measured in different reference frames; but the irreducible

spinor representation of the Lorentz group is not unitary because the Lorentz group is not compact since the Lorentz boost takes on values along an open line from 0 to 1, unlike the rotation group where the angle extends from $\theta = 0$ to 2π . Thus the true symmetry group for particles is not the homogeneous Lorentz group; but a symmetry group with translations in spacetime in addition to Lorentz boosts and rotations. This group is the inhomogeneous Lorentz group, or Poincaré group. The generator of spacetime translation, P_μ is given by the transformation:

$$x^\mu \rightarrow x'^\mu = x^\mu + a^\mu, \text{ and } P_\mu = i \frac{\partial}{\partial x^\mu}. \quad (5.25)$$

There are 4 translation generators in the Poincaré group, in addition to 3 generators for Lorentz boosts and 3 for rotations. Totaling 10 generators in the Poincaré group. The rank 2 Poincaré group has only two invariants that commute with all generators; these are the Casimir invariants or operators, C_1 associated with mass invariance and C_2 for spin invariance [13].

5.4 Additional Aspects of R-Qubits and Relativistic Computing

Let a and a^\dagger be two operators acting on an abstract Hilbert state space satisfying the commutation relation, $[a, a^\dagger] = 1$ with 1 is the Hilbert space identity operator. As well-known it is a fundamental axiom of Quantum Mechanics that the norm of all states in Hilbert space is positive. Therefore, the eigenvalues, α of the eigenstates of, a^\dagger must be non-negative real numbers. So that if the $|\alpha\rangle$ state is an eigenvector of the Hermitian operators, a, a^\dagger , the eigenvalue α is a real number. If identical particles are bosons, operators $\hat{a}(\phi)$ obey canonical commutation relations; and If the identical particles are Fermions, operators, $\hat{a}(\phi)$ obey canonical anti-commutation relations.

So called second quantization is used to describe quantum field theory, in which fields (wave functions) are field operators, similar to how the representation of position and momentum as operators in first quantization. The addition of creation and annihilation operators allow

particles to be added or removed from a many-body system, bridging the gap between the first and second-quantized states. Applying the creation or annihilation operator to a 1st-quantized many-body wave function will insert/delete a single-particle state from the wave function in a symmetrical way depending on particle statistics. For bosons, creation/annihilation operators are constructed as raising and lowering operators for a quantum harmonic oscillator, which are then generalized to field operators in the quantum field theory.

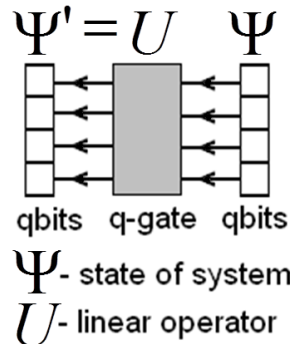


Fig. 5.4. Usual q-gate with constant number of states and particles.

The Fermi anti-commutator (1st quantization) relation

$$\{a^*, a\}_+ \equiv a^* a + a a^* = 1. \quad (5.26)$$

QFT utilizes wave functions as operators, which for bosons is,

$$\hat{\psi}_p = c_p e^{-ipx} + c_p^* e^{ipx} \quad (5.27)$$

With c_p and c_p^* the annihilation and creation operators. The Bose commutator for (2nd quantization) relation is

$$[c^*, c]_- \equiv c^* c - c c^* = 1 \quad (5.28)$$

The number of possible superposition states for such a register in a single molecule is potentially as high as 2^n states or (in the case where $n = 10$) 1,024 complex numbers. For our prototype solution (Chap. 14), the least-unit of this mesoionic crystalline structure is scalable suggesting

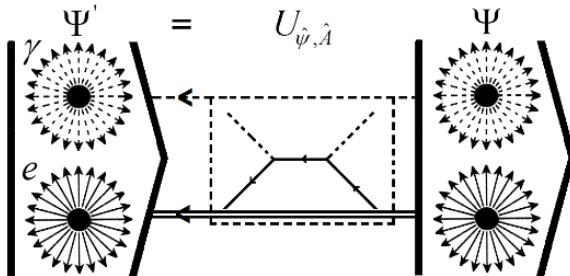


Fig. 5.5. Relativistic quantum gate, $\Psi' = U_{\hat{\psi}, \hat{A}} \Psi$ for r-qubits with constant particles but variable or infinite states with quantum field theoretic components, with wave vectors of fields, $\hat{\psi}', \hat{\psi}$ and wave operators, $\hat{\psi}, \hat{\phi}$. Redrawn from Vlasov [9].

putative utility for bulk NMR quantum computing. It will be shown that these 10-qubit registers are amenable to standard Deutsch-Jozsa, Shor and Grover algorithms. Additionally, we attempt to formalize I/O techniques for our Class II mesoionic xanthines based on a coherent control RF process of cumulative resonant interaction where by utilizing additional degrees of freedom pertinent to a relativistic basis for the qubit (r-qubit) new HD commutation rules putatively allow decoherence to be ontologically overcome.

5.5 Current Thinking on Relativistic Information Processing

Vlasov [9] in 1996 was first to suggest the concept of relativistic r-qubits; then in 2003 Peres and Terno's [10] detailed analysis of quantum information processing suggested that the whole basis of quantum information theory itself required reassessment. Now finally, in the last couple of years numerous papers on relativistic computing have appeared [15-18]. We will briefly review and contrast some of these ideas [14-23].

Jafarizadeh & Mahdian [15] show that projections of a relativistic spin operator (RSO), a massive spin-1/2 particle on a world-vector can be in a timelike or null tetrad direction, and are found to be proportional to the helicity or Bargman-Wigner (BW) qubit, respectively. The BW wave equations describe relativistic free particles of arbitrary spin, j . For integer bosons the spin is ($j=1, 2, 3, \dots$), and for half-integer spin fermions ($j = 1/2, 3/2, 5/2, \dots$). The solutions to the equations are wave functions, given the form of multi-component spinor fields [19,20].

Jafarizadeh & Mahdian also consider Lorentz transformations of 2-particle states, both constructed in the helicity basis using only the superposition of two momentum eigenstates (p_1 and p_2) for each particle. In a 2D momentum subspace, the structure of one particle in terms of the 4-qubit system leads to a new approach for the quantification of relativistic entanglement [15].

Xu and colleagues [18] are studying persistent currents (PCs) in relation to the Aharonov-Bohm (AB) Effect, known to vanish for Schrödinger particles in the presence of random scatterings like classical chaos. But would this still be the case for Dirac fermions? This is a significant issue because of the high interest in 2D quasiparticle anyon braiding modeling for quantum topological information processing. In that regard the team investigated relativistic quantum AB rings threaded by a magnetic flux and found PCs robust which they also found extended to highly asymmetric rings and Superpersistent Currents (SPCs).

In support of our UFM model, it is significant that SPCs can be attributed to “*a robust type of relativistic quantum states, i.e., Dirac whispering gallery modes (WGMs) that carry large angular momenta and travel along the boundaries*” [18]. With that finding Xu’s team proposed an experimental scheme using topological insulators to observe and characterize Dirac WGMs and SPCs, speculating that these features can potentially be the base for a new class of relativistic qubit systems. They consider their discovery of WGMs in relativistic quantum systems remarkable because, although WGMs are common in photonic systems, they are relatively rare in electronic systems [18]. In conclusion Xu states:

We formulate a relativistic version of AB chaotic billiards to study PCs in Dirac rings. We find that, in contrast to the nonrelativistic quantum counterpart where PCs vanish for chaotic rings, the currents continue to exist in the relativistic chaotic AB rings and, in this sense, they are superpersistent. We demonstrate that SPCs are a consequence of Dirac WGMs, and we develop an analytic understanding of their emergence in relativistic quantum systems. We also propose that, experimentally, chaotic rings patterned by magnetic domain heterostructures deposited on the surface of a 3D topological insulator can be a feasible scheme to observe and characterize chaotic Dirac WGMs and SPCs. The coexistence of inner and outer chaotic Dirac WGMs naturally forms a flux-tunable two-level system. To investigate the magnetic response of chaotic Dirac fermions is not only fundamental to the emerging field of relativistic quantum chaos, but also relevant to device applications based on Dirac materials [18].

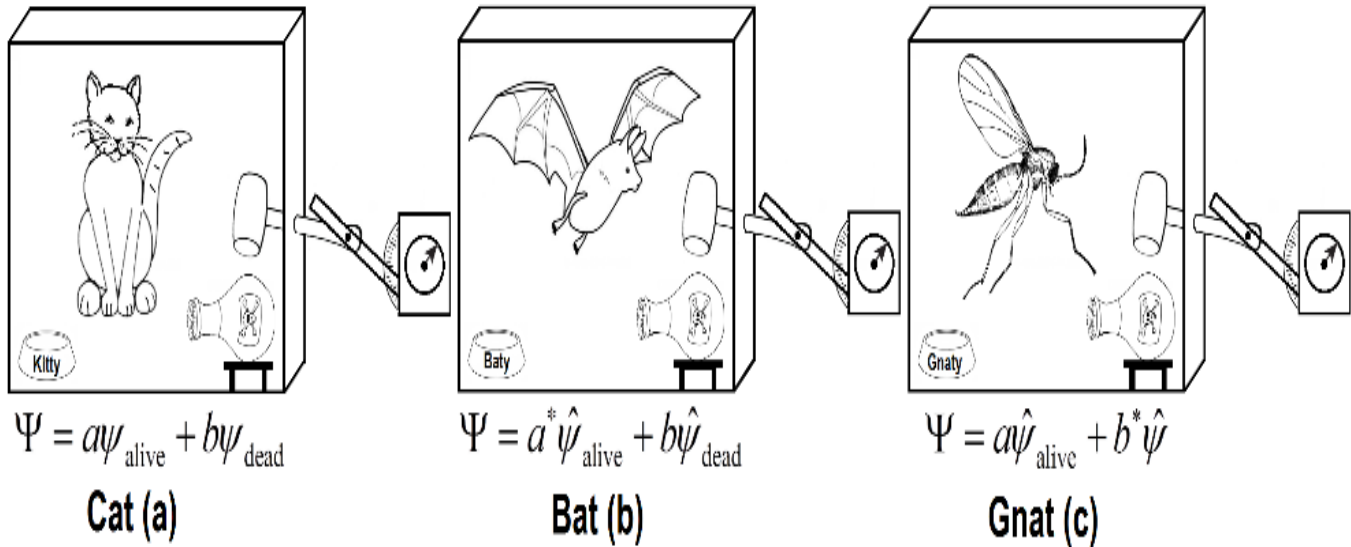


Fig. 5.6. Cat (a), Usual particulate quantum state with 50% probability at arbitrary time, t that the Cat is either dead or alive. Bat (b) and Gnat (c) are meant to represent quantum field (flying) theoretic annihilation-creation components of HD scale-invariant ‘copies’ of the Copenhagen level (Cat) quantum state potential. This is part of the newly discovered Calabi-Yau mirror symmetric brane elements comprising the hierarchy of the finite radius ‘manifold of uncertainty’.

5.6 Relativistic Quantum Information Theory and Computation

“The acquisition of information from a quantum system is at the interface of classical and quantum physics” [10]. This type of measurement occurs at the semi-classical limit, wherein quantum information processing has remained stuck at a few qubits hampered by decoherence. Increasing capacity requires another form of data acquisition occurring instead at a ‘semi-quantum limit’; thus it is postulated that usual theories of computation need to be merged not just with Relativistic Quantum Field Theory (RQFT) and Topological Quantum Field Theory (TQFT) but must also take an additional step. We know now that both RQFT and TQFT are required; we believe that a relativistic topological quantum field theory, if such is possible, is not the answer. We also know that to perform UQC, information theory needs to be extended not only to the 4D Poincaré group, but also into the HD realm of the 3rd regime of UFM [24-26]. In Chap.12 we outline a nascent ‘Ontological-Phase Topological Field Theory’ (OPTFT) to address the brane dynamics of the unified field.

A TQFT computes topological invariants (property of a topological space which remains unchanged when transformations are applied to the object under homeomorphisms). A topological isomorphism is a continuous function between topological spaces that has a continuous inverse function. Homeomorphisms are the isomorphisms in the category of topological spaces, that is, they are the mappings that preserve all the topological properties of a given space. Two spaces with a homeomorphism between them are called homeomorphic, and from a topological viewpoint they are the same space.

Assuming quantum field theory is a necessity for a consistent description of quantum interactions; suggests current concepts in quantum information theory likely require reassessment and will need to be brought in line with a relativistic quantum informational theory before quantum computation can be fully realized. New properties of this transformation also require a change in the usual model of a qubit. We agree with the assessment given by Perez ‘Most of the current concepts in quantum information theory may then require a reassessment’ [10]. Information needs a material carrier, and the latter must obey the laws of physics. Information is physical [12].

Relativistic kinematics is all about information transfer between observers in relative motion. Quantum mechanics texts tell us that observable quantities are represented by Hermitian operators,

$\int_{-\infty}^{\infty} \Psi^* \Psi d\tau \equiv \langle \Psi | \Psi \rangle$ in integral and Dirac notation respectively. Their possible values are the eigenvalues of these operators, and that the probability of detecting eigenvalue, λn corresponding to eigenvector, μv is $\langle \mu v | \Psi \rangle^2$, where Ψ is the pure state of the quantum system observed. If mixed states are included, the probability can be generally written, $\langle \mu v | \rho | \mu v \rangle$, where ρ is a mathematical expression that encodes information about measurements. “*This is nice and neat, but this does not describe what happens in real life. Quantum phenomena do not occur in a Hilbert space; they occur in a laboratory. If you visit a real laboratory, you will never find there Hermitian operators [10].*”

Drell pointedly asked “*When is a particle?*”[27]. A wave function is not defined in spacetime, but in a multidimensional mathematical representation called Hilbert space. It has become necessary to physicalize quantum information processing to an actual real multidimensional space. Dirac wrote “*a measurement always causes the system to jump into an eigenstate of the dynamical variable being measured [28].*” Collapse of the wavefunction ‘happens’ in our description of the system, not to the system itself. Von Neumann also ‘speculated’ that the final step involves the consciousness of the observer [29].

Another consequence is a change of the environment in which the quantum system evolves after completion of an intervention. For example, the measuring apparatus can generate a new Hamiltonian which depends on the recorded result. Classical signals may be emitted for controlling the execution of further interventions. These signals are of course limited to the velocity of light (until now). These interventions, as defined above, start by an interaction with a measuring apparatus [10]. Following Peres, the quantum system and the apparatus are initially in a state, $\sum_s c_s |s\rangle \otimes |A\rangle$, and become entangled into a single composite system C :

$$\sum_s c_s |s\rangle \otimes |A\rangle \rightarrow \sum_{s,\lambda} c_s U_{s\lambda} |\lambda\rangle, \quad (5.29)$$

where $\{|\lambda\rangle\}$ is a complete basis for the states of C . It is the choice of the unitary matrix, $U_{s\lambda}$ that determines which property of the system under study is correlated to the apparatus, and therefore is measured. An essential

property of the composite system C , which is necessary to produce a meaningful measurement, is that its states form a finite number of orthogonal subspaces which are distinguishable by the observer [10].

Up to now, the quantum evolution is well defined and is in principle reversible. It would remain so if the environment “*could be perfectly isolated from the macroscopic degrees of freedom of the apparatus ... This demand is of course self-contradictory, since we have to read the result of the measurement if we wish to make any use of it.*” (See Chaps. 7&8) States of the environment that are correlated to subspaces of C with different labels, μ can be treated as if they were orthogonal [10].

To become fully relativistic, the conception of intervention needs refinement. The precise location of an intervention is important in a relativistic information process. It is the point from which classical information is sent that can affect the input of other interventions. A simpler case of space-like separated interventions, amenable to complete analysis, is Bohm’s version of the EPR paradox with two coordinate systems in relative motion [10]. Such phenomena are often attributed to quantum nonlocality and the possibility of superluminal or rather instantaneous communication. Herbert’s proposal on this matter [30] led to the discovery of the no-cloning theorem [31,32]. (Note: We will address this issue later; surmounting uncertainty also obviates the no-cloning and quantum non-copying theorems.)

Bell’s theorem asserts that it is impossible to mimic quantum theory by introducing a set of objective ‘local hidden variables’ so that any classical imitation of quantum mechanics must be nonlocal. But, there is no inherent suggestion for the existence of nonlocality in Bell’s theorem.

Importantly, RQFT is manifestly local. Peres states ‘the obvious fact is that information must be carried by material objects, quantized or not’ [10]. Therefore, quantum measurements do not allow any information to be transmitted faster than the characteristic velocity that appears in the Green’s functions of the particles emitted in the experiment. In a Lorentz invariant theory, this limit is the velocity of light. Relativistic causality cannot be violated by quantum measurements. The only physical assumption needed to prove this is that Lorentz transformations of spacetime coordinates are implemented in quantum theory by unitary transformations of operators [10]. This is the same as saying that the Lorentz group is a valid symmetry of the physical system [33].

A profound conceptual revolution is about to occur. We have touted the imminent rise of RIP in this chapter; but this is only an intermediate step. OPTFT will allow an instantaneous algorithm Chap. 12.

5.7 Physical Reality of Quantum States

The fundamental objects of quantum theory are mathematical objects defined on an abstract configuration space, rather than the Euclidean 3-space of our reality. There has been considerable debate as to whether a pure quantum state corresponds to physical reality or merely some observed form of information about that state. Is the nonlocal nilpotent ‘invisible potentia’ before observation the actual physical reality we should be dealing with? An emphatic yes, is our answer in this volume. This will be the realization of Bohm’s superimpose order.

The quantum interference demonstrated by the 2-slit experiment strongly indicates that a ‘real’ wave causes the interference. Alternatively, numerous physicists have proposed that the quantum state is not real; only representing cursory information of some aspect of reality in relation to the observer [34-41]. Ah, the observer, there’s the rub. Most physicists believe, additional dimensions (if they exist) are curled up microscopically at the Planck scale because we don’t see them; but this is not the only interpretation for XD. Likewise, it is a challenge to change the current regime of observation from Euclidean space, to that of routinely doing physics from a base of operations with a vantage point in the HD potentia. Progress will be delayed until this is the case; in this scenario, Euclidean 3-space is a ‘shadow’ of the HD UFM space. Figure 5.7.

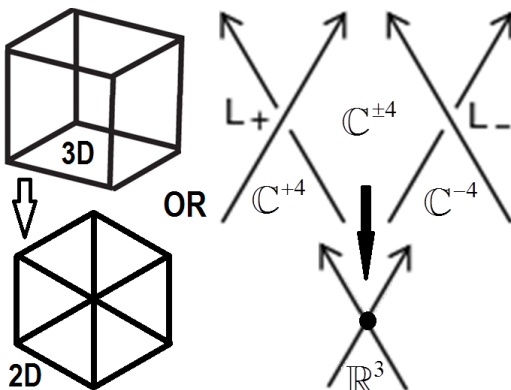
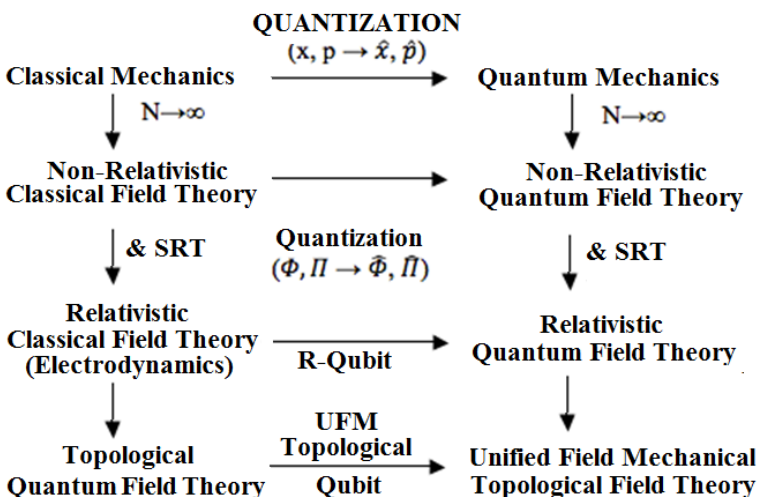


Fig. 5.7. Euclidean 3-space is a mere shadow of the more complete XD nonlocal potentia, hinted at to a certain degree by the Dirac 360-720° spherical rotation of the electron as it passes through space and anti-space to complete a rotation. By shadow we mean, (term from knot theory) that the bottom resultant figs. have lost degrees of freedom.

The Copenhagen Interpretation has become more and more challenged. The argument is whether or not the state vector (wavefunction) is a calculation tool or physically real and needs to be addressed as such for quantum computing to succeed. One argument is that a quantum system has a ‘real physical state’ that is not described completely by quantum theory, but is objective and independent of the observer. Such an assumption is denied by the instrumentalist approach to quantum theory, suggesting again that the quantum state is only a calculation tool for making predictions concerning macroscopic measurements and results [42,43]. Quantum Mechanics is not the ‘basement of reality’.

Table 5.1 EVOLUTION OF QUANTUM INFORMATION PROCESSING



In contrast to many other physical theories there is no canonical definition of what a QFT is. If one thinks of QM as a single particle theory, one can then think of QFT as an extension of QM to systems of many particles and a concomitant large number of degrees of freedom. Then the transition from QM to QFT allows treatment of both particles and fields within a uniform theoretical framework.

One might say that QFT results from the successful reconciliation of QM and SRT. But the locality postulate of SRT, in terms of EPR correlations of entangled quantum systems manifests a contradiction in the dynamics. The Schrödinger equation doesn't obey the relativistic requirement that all physical laws of nature be invariant under Lorentz transformations. The Klein-Gordon and Dirac equations, resulting from

the search for relativistic analogues of the Schrödinger equation meet the requirement of Lorentz invariance; but they are not complete descriptions because they do not allow fields in a fully quantum-mechanical way [44].

5.8 Unified Field Mechanical Ontological-Phase TFT

Just a brief mention here to give context; the discourse on OPTFT is given in Chap. 12. It seems likely that the imminent age of discovery will be described topologically. Field theory has evolved from classical field theory to the current 2nd regime modes of QFT, RQFT and TQFT. It is proposed *hypothesis non fingo*, that the 3rd regime of reality, Unified Field Mechanics (UFM) will be described by an Ontological-Phase Topological Field Theory (OPTFT). In terms of the nature of reality, QIP and the measurement problem, there has been a recent introduction of relativistic parameters including relativistic r-qubits bringing into question the historically fundamental basis of ‘locality and unitarity’. A dilemma in terms of Bell’s inequalities, the no-cloning theorem and correspondence to the epistemic view of the Copenhagen Interpretation versus the ontic consideration of objective realism and as merged by W. Zurek’s epi-ontic blend of quantum redundancy in quantum Darwinism [31,43]. The scenario for an ontological-phase topology of UFM requires a new set of topological transformations beyond the Galilean and Lorentz-Poincaré (Chap. 11).

References

- [1] Nielson, M.A., & Chuang, I.L. (2000) *Quantum Computation and Quantum Information*, Cambridge: Cambridge Univ. Press.
- [2] Feynman, R.P. (1982) Simulating physics with computers, *International Journal of Theoretical Physics* 21, 467-488.
- [3] Feynman, R.P. (1986) Quantum-mechanical computers, *Foundations of Physics* 16, 507-531.
- [4] Deutsch, D. (1985) Quantum theory, the Church-Turing principle and the universal quantum computer, *Proceedings of Royal Society of London, A* 400, 97-117.
- [5] Deutsch, D. (1989) Quantum computational networks, *Proceedings of Royal Society of London, A* 425, 73-90.
- [6] Schumacher, B. (1995) Quantum coding, *Physical Review A* 51, 2738-2747.
- [7] Bennett, C. (1995) Quantum information and computation, *Physics Today* 4810, 24-30.

- [8] 't Hooft, G. (2007) Lie Groups in Physics, <http://www.staff.science.uu.nl/~hooft101/lectures/lieg07.pdf>
- [9] Vlasov, A.Y. (1999) Quantum theory of computation and relativistic physics, PhysComp96 Workshop, Boston MA, 22-24 Nov 1996, arXiv: quant-ph/ 9701027v4.
- [10] Peres, A. & Terno, D.R. (2004) Quantum information and relativity theory, Rev. Mod. Phys. 76, 93; arXiv:quant-ph/0212023v2; Introduction to relativistic quantum information (2006) arXiv:quant-ph/0508049v2.
- [11] Shannon, C. E. (1948) Bell Syst. Tech. J. 27, 379, 623.
- [12] Landauer, R. (1991) Information is physical, Physics Today 44 (5), 23.
- [13] Yeh, N-C (2007) http://www.its.caltech.edu/~yehgroup/NTU_2007SummerLectures/NTU2007_Supplement_3.pdf.
- [14] Vlasov, A.Y. (1996) Quantum theory of computation and relativistic physics, in T. Toffoli, M. Biafore & J. Leao (eds.) Physcomp96, Cambridge: New England Complex Systems Institute; and additional material from private communication.
- [15] Jafarizadeh, M.A. & Mahdian, M. (2011) Quantifying entanglement of two relativistic particles using optimal entanglement witness, Quantum Information Processing, 10:4, pp. 501-518.
- [16] Amoroso, R.L. (2016) A unified field mechanical approach to the arrow of time utilizing large size extra dimensions, in preparation.
- [17] Felicetti, S., Sabin, C., Fuentes, I., Lamata, L., Romero, G. & Solano, E. (2015) Relativistic motion with superconducting qubits, arXiv:1503.06653v2 [quant-ph].
- [18] Xu, H., Huang L., Lai, Y.C. & Grebogi, C (2015) Superpersistent currents and whispering gallery modes in relativistic quantum chaotic systems, Sci Rep. 11:5:8965.
- [19] Bargmann, V. & Wigner, E.P. (1948). Group theoretical discussion of relativistic wave equations, Proceedings of the National Academy of Sciences of the United States of America 34 (5): 211-23.
- [20] Dvoeglazov, V.V. (2010) The Bargmann-Wigner formalism for higher spins (up to 2), arXiv:1011.1696v1 [math-ph].
- [21] Banerjee, S., Fransson, J., Black-Schaffer, A.M., Ågren, H. & Balatsky, A.V. (2015) Bosonic Dirac materials in two dimensions, arXiv:1511.05282v2 [cond-mat.mes-hall].
- [22] Wang, J., Deng, S., Liu, Z. & Liu, Z. (2015) The rare two-dimensional materials with Dirac cones, Natl. Sci. Rev. 2 (1), 22-39; <http://arxiv.org/ftp/arxiv/papers/1410/1410.5895.pdf>
- [23] Pletikosic, I., Kralj, M., Pervan, P., Brako, R., Coraux, J., N'Diaye, A.T., Busse, C. & Michely, T. (2009) Dirac cones and minibands for graphene on Ir(111), arXiv:0807.2770v2 [cond-mat.mtrl-sci].
- [24] Amoroso, R.L & Rauscher, E.A. (2009) The Holographic Anthropic Multiverse: Formalizing the Geometry of Ultimate Reality, Singapore: World Scientific.
- [25] Amoroso, R.L., Kauffman, L.H. & Rowlands, P. (2013) The Physics of Reality: Space, Time, Matter, Cosmos, Hackensack: World Scientific.
- [26] Amoroso, R.L., Kauffman, L.H. & Rowlands, P. (eds.) (2016) Unified Field Mechanics: Natural Science Beyond the Veil of Spacetime, Hackensack: World Scientific.
- [27] Drell, S. (1978) Am. J. Phys. 46, 597; Physics Today 31 (6) 23.
- [28] Dirac, P.A.M. (1947) The Principles of Quantum Mechanics, Oxford: University Press, p. 36.
- [29] von Neumann, J. (1955) Mathematical Foundations of Quantum Mechanics, R.T. Beyer (trans.) Princeton: Princeton Univ. Press, p. 418.
- [30] Herbert, N. (1981) Found. Phys. 12, 1171.

- [31] Wootters, W.K. & Zurek, W.H. (1982) A single quantum cannot be cloned, *Nature*, 299 (5886) 802-803.
- [32] Dieks, D.G.B.J. (1982) Communication by EPR devices *Physics Letters A*, 92(6) 271-272.
- [33] Weinberg, S. (1995) *The Quantum Theory of Fields Vol. 1*, Cambridge: Cambridge University Press.
- [34] Einstein, A., Podolsky, B. & Rosen, N. (1935) *Phys. Rev.*, 47, 777.
- [35] Popper, K.R. (1967) in M. Bunge (ed.) *Quantum Theory and Reality*, Springer.
- [36] Ballentine, L.E. (1970) *Rev. Mod. Phys.*, 42, 358.
- [37] Peierls, R.E. (1979) *Surprises in theoretical physics*, Princeton University Press.
- [38] Jaynes, E.T. (1980) in A. O. Barut (ed.) *Foundations of Radiation Theory and Quantum Electrodynamics*, Plenum.
- [39] Zeilinger, A. (1999) *Phys. Today*, 52, 13.
- [40] Caves, C.M., Fuchs, C.A. & Schack, R. (2002) *Phys. Rev. A*, 65, 022305; arXiv:quant-ph/0106133.
- [41] Spekkens, R.W. (2007) *Phys. Rev. A*, 75, 032110; arXiv:quant-ph/0401052.
- [42] Pusey, M.F., Barrett, J. & Rudolph, T. (2012) On the reality of the quantum state, arXiv:1111.3328v3 [quant-ph].
- [43] Jaynes, E.T. (1990) in W.H. Zurek (ed.) *Complexity, Entropy, and the Physics of Information*, Reading: Addison-Wesley.
- [44] Kuhlmann, M., (2015) Quantum Field Theory, in E.N. Zalta (ed.) *The Stanford Encyclopedia of Philosophy*, <http://plato.stanford.edu/archives/sum2015/entries/quantum-field-theory/>.

Chapter 6

Utility of Unified Field Mechanics

At one time, Classical Mechanics governed our whole understanding of the physical universe; then a 2nd regime of reality Quantum Mechanics was discovered, giving insight into the microscopic realm. Now we prepare to pragmatically enter a 3rd regime of natural science, Unified Field Mechanics (UFM). A 4th regime, beckoning just beyond our reach, is also postulated that will take us experimentally from Universe to Multiverse (infinite number of nested Hubble Spheres, each with their own fine-tuned laws of physics); but this 4th regime is beyond the scope of this monograph. In this chapter we introduce some of the, putative at this time, aspects of UFM deemed essential for Universal Quantum Computing (UQC).

If [all physicists] follow the same current fashion in expressing and thinking about electrodynamics or field theory, then the variety of hypotheses being generated ... is limited. Perhaps rightly so, for possibly the chance is high that the truth lies in the fashionable direction. But, on the off chance that it is in another direction - a direction obvious from an unfashionable view of field theory - who will find it? Only someone who sacrifices himself ... from a peculiar and unusual point of view, one may have to invent for and himself - *Richard Feynman*, Nobel Prize lecture.

6.1 Unified Field Mechanics: What is it, What are the Implications?

A brief introductory survey of Unified Field Mechanics (UFM) is given from the perspective of a Holographic Anthropic Multiverse cosmology in 12 ‘continuous-state’ dimensions (6 spatial, transformed by 3 temporal and guided by 3 UFM control factors). This paradigm with many new parameters is cast in a scale-invariant conformal covariant Dirac polarized vacuum utilizing extended HD forms of the de Broglie-Bohm and Cramer interpretations of quantum theory. The model utilizes a unique form of M-Theory based in part on the original hadronic form of string theory that had a variable string tension, T_S and included a tachyon. Fortunately, the

model is experimentally testable, thus putatively able to demonstrate the existence of large-scale additional dimensionality (LSXD), test for QED violating tight-bound state spectral lines in hydrogen ‘below’ the lowest Bohr orbit, and surmount the quantum uncertainty principle utilizing a hyperincursive Sagnac Effect resonance hierarchy [1,2].

Recently we hear more and more physicists saying, ‘spacetime is doomed’, ‘spacetime is a mirage’, the ‘end of spacetime’, ‘spacetime is not fundamental but emergent’ etc. “*Henceforth space by itself and time by itself are doomed to fade into the mere shadows, and only a union of the two will preserve an independent reality [3].*” We have come full circle from the time of Minkowski’s 1908 statement to the brink of an imminent new age of discovery. The basis of our understanding of the natural world has evolved in modern times from Newtonian Mechanics to the 2nd regime of Quantum Mechanics; and now to the threshold of a 3rd regime - Unified Field Mechanics (UFM). The Planck scale stochastic quantum realm can no longer be considered the ‘basement’ or fundamental level of reality. As hard as quantum reality was to imagine so is the fact that the quantum domain is a manifold of finite radius; and that the ‘sacrosanct - indelible’ Quantum Uncertainty Principle can now be surmounted. For decades, main stream physicists have been stymied by efforts to reconcile General Relativity with Quantum Mechanics. The stumbling block lies with the two theories conflicting views of space and time: For quantum theory, space and time offer a fixed backcloth against which particles move. In Einstein’s relativities, space and time are not only inextricably linked, but the resultant spacetime is warped by the matter within it. In our nascent UFM paradigm for arcane reasons the quantum manifold is not the regime of integration with gravity; it is instead integrated with the domain of the unified field where the forces of nature are deemed to unify. We give a simplistic survey of the fundamental premises of UFM and summarize experimental protocols to falsify the model at this stage of the paradigm’s development.

Our approach differs from that of the physics community at large searching for a TOE to complete the 4D Standard Model of particle physics. It also differs in significant ways from the current 11D iteration of M-Theory; but is essentially an M-Theoretic model, albeit cast in 12D, reverting to some aspects of the original hadronic form of string theory with variable string tension, T_S and the inclusion of virtual tachyon-tardon interactions. The other key difference is that instead of the search for one unique brane compactification making correspondence to the 4D standard model; in our view compactification occurs as ‘a *continuous-state*

spin-exchange dimensional reduction compactification process' through all the dimensionalities by mirror symmetric Calabi-Yau brane topology [4-8]. As Newton claimed to give '*hypothesis non fingo*' [9]; likewise, we have found that this UFM model leads to one unique background independent string vacuum, out of the Googolplex of possibilities confounding the usual parameters of M-Theory. The solution to this conundrum occurred in developing an alternative derivation of string tension, T_S [6]. Most importantly string theory is now testable; and a program is in place preparing to perform the experimental tests [10-12].

The Unified Field (UF) is not only 'unified'; it is a unifier, providing an inherent 'force of coherence' driving the evolution of reality from within the domain of its overt action. This yields the first indicia of why UFM is of critical importance to the design and implementation of UQC. Feynman, early on, suggested that the optimal manner for developing quantum computing would be the utility of what he called a 'synchronization backbone' [13]. Feynman was not too clear on what he meant by this concept; but we have discovered in our preliminary studies of UFM dynamics that the continuous-state process is essentially an inherent synchronization backbone driving the evolution of M-Theoretic brane dynamics [1,2,6-8]. More profoundly this synchronization backbone contains scale invariant copies of the matter and quantum states observed in Euclidean-Minkowski space. As one might surmise this erases the perceived problem of the quantum non-cloning and no-erasure theorems [14,15]; leading also to the ability to surmount the Uncertainty Principle and supervene decoherence (Chaps. 7 & 8) [10,11].

6.2 Précis

Einstein failed in his quest for a unified theory, partly because of conceptual discontinuities, but most likely simply because he was far enough ahead of his time that the higher dimensional mathematical framework (barely available now) needed to construct a unified field theory wasn't known before he passed away in 1955. However, the correspondence path to a unified theory did begin in 1919 [4,5] but it wasn't until the 1940's that Kaluza-Klein theory was considered complete,

$$\begin{aligned}\tilde{g}_{\mu\nu} &\equiv g_{\mu\nu} + \phi^2 A_\mu A_\nu, \\ \tilde{g}_{5\nu} &\equiv \tilde{g}_{5v} \equiv \phi^2 A_\nu, \quad \tilde{g}_{55} \equiv \phi^2\end{aligned}\tag{6.1}$$

where index 5 is the 5th coordinate. This metric implies an invariant 5D line element:

$$ds^2 \equiv \tilde{g}_{ab} dx^a dx^b = g_{\mu\nu} dx^\mu dx^\nu + \phi^2 (A_\nu dx^\nu + dx^5)^2. \quad (6.2)$$

Now with the evolution of String/M-Theory, more and more physicists have begun to take on Einstein's quest. One can say string theory began in 1968; but followed a rather bumpy road until the 1st (1984-1994) and 2nd (1994-2003) Superstring revolutions garnered huge interest. Currently 11D M-Theory (not without severe challenges and criticism) is considered the most promising approach to extend the standard model.

We suspect there will be a 3rd superstring revolution, which we hope the reader will find we have shone some light on in this volume. Because the world is currently seen as fundamentally quantum, the disparity between quantum field theory and general relativity has been sought under the auspices of 'quantum gravity'; but what if, as Feynman hinted, gravity is not quantized [16]? This is the track presented here; that the regime of integration is not quantum, but occurs with the arena of the unified field.

Preparation for the birth of a comprehensive UFT came just in time for the Einstein Centenary in November 2015 [1,2]. Our symposia program to found UFM follows the format of the *Conseils Solvay*, taking place over five symposia from 1911 to 1927 that founded quantum mechanics; the 2nd in this series of Vigier symposia geared toward founding UFM took place in 2016 [2].

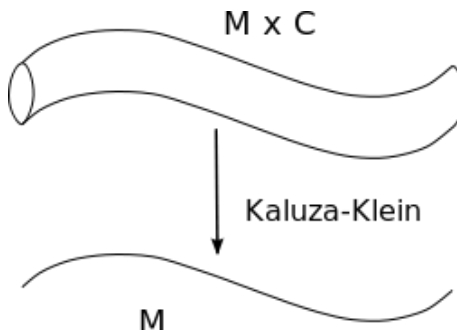


Fig. 6.1. The Kaluza-Klein space, $M \times C$ is compactified over the set C ; which after K-K decomposition produces a field theory over M .

In Table 6.1 we simplistically list various UFM parameters for a Holographic Multiverse [6-8]. UFM is not only a TOE; but brings us to the footstool of the multiverse, meaning it will lead to theoretical and empirical access beyond the ~ 14 bly radius Hubble sphere.

TABLE 6.1. Suggested UFM Multiverse Parameters

- 1) UFM suggests a 3rd physical regime in the progression: 3D Classical Newtonian Mechanics → 4D Quantum Mechanics → 12D Unified Field Mechanics (UFM).
- 2) Uncertainty is a manifold of finite radius that can now be experimentally surmounted [10,11].
- 3) Putative additional dimensions are not curled up microscopically at the Planck scale as originally thought [17].
- 4) Large-Scale additional dimensions (LSXD) of infinite size exist beyond the 'veil of uncertainty' [16].
- 5) Quantum - Gravity is not the regime of integration, rather the union occurs in the 3rd regime of UFM.
- 6) The unified field is not a 5th phenomenological field (i.e. mediated by exchange quanta) but a 'force of coherence' based on topological charge with instead an ontological 'energyless' phase exchange called 'topological switching' [6].
- 7) Reliance on scale-invariant covariant Dirac polarized vacuum, tiny photon mass, m_γ .
- 8) Reversion to original Hadronic form of String Theory with variable string tension, T_S , virtual Tachyons and a key unique 'Background Independent' string vacuum [6,12].
- 9) Additional Transform beyond the Galilean and Lorentz-Poincaré to handle LSXD UFM transformations.
- 10) Wave-Particle duality elevated to principle of cosmology.
- 11) Continuous-State 'spin exchange dimensional reduction compactification processes rather than fixed Planck-scale 'basement of a 4D reality' [6-8].
- 11) Not one unique compactification making correspondence to the Standard Model, rather continuous compactification mode from 12D to 0D with a '0 to infinity' rotation of the Riemann sphere Least Cosmological Unit (LCU) array.
- 12) Planck is a virtual asymptote never reached fundamentally that oscillates from asymptotic Planck to the Larmor radius of the Hydrogen atom, $\hbar + \Delta T_S$.
- 13) Spacetime not fundamental but emergent in a continuous-state process whereby annihilation-creation symmetry provides a 'beat frequency' to line element propagation.
- 14) Space is tessellated with an array of Least Cosmological Units (LCU) the nilpotent structure of which constitutes the new UFM designation of a 'singularity' or Fermion vertex.
- 15) The universe is a Holographic Anthropic Multiverse where the Hubble Sphere is finite and closed in time, but open and infinite in the atemporal LSXD realm with room for an infinite number of causally separated nested Hubble spheres each with their own fine-tuned laws of physics.
- 16) Relies on completed versions of the de Broglie-Bohm and Cramer interpretations of Quantum Theory extended to a LSXD Bohmian 'superimplicate order'.

6.3 The LCU Concept is Key to Developing Unified Field Mechanics

We claim unique insight into the required fundaments for implementing ‘Unified Field Mechanics’ (UFM). Firstly, the Universe is not fundamentally quantum, which for the last 100 Years was merely a convenient stopping place in the progress of Natural Philosophy. The LSXD appear ‘invisible’ not because they are curled up microscopically at the Planck scale as the accepted interpretation of Kaluza-Klein Theory proposed, but because of an inherent form of ‘subtractive interferometry’ related to the nature of the virtual reality limiting the Observer’s observation to Euclidean 3-space [18].

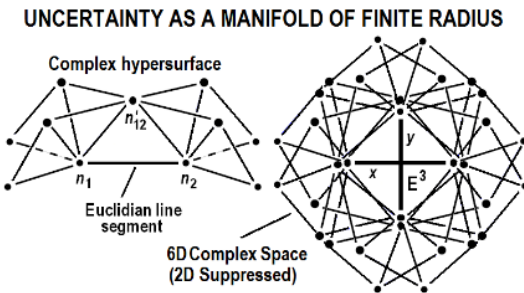


Fig. 6.2. Conceptual view of the space-antispace nilpotent ‘manifold of uncertainty’ with 64 quaternionic elements (some suppressed) with Euclidean space, E^3 as the resultant subspace of virtual ‘points’ forming observed reality.

According to Rowlands the units of the Dirac algebra can, like the gamma matrix products, be represented as a group of order 64, requiring only a *pentad* of 5 generators. Many sets of 5 generators can be derived, for example as in the asterisked units in the vector-quaternion set [19]:

$$\begin{aligned}
 & i \quad j^* \quad k \quad ii \quad ij \quad ik^* \quad i \quad 1 \\
 & i \quad j \quad k \quad ii \quad ij \quad ik \quad i \quad 1 \\
 & ii^* \quad ij \quad ik \quad iii \quad iij \quad iik \\
 & ji^* \quad jj \quad jk \quad iji \quad ijj \quad ijk \\
 & ki^* \quad kj \quad kk \quad iki \quad ikj \quad ikk
 \end{aligned}$$

The Standard Model seems to require one nilpotent set of space-antispace dual-quaternion nilpotent propagators ($ikE + i\bar{i}p_x + i\bar{j}p_y + i\bar{k}p_z + jm$)² = 0 [18]. Until it is known how to close-pack (see below) the array of LCU tessellating space (what spacetime emerges from) we cannot readily postulate whether the manifold of uncertainty is 2D or 5D. In either case

respectively the 3rd or 5th LSXD would be degenerate, i.e. the domain in atomic energy levels when the outermost electron acquires sufficient energy to escape to infinity. To clarify; if the manifold of uncertainty requires a single additional duality, degeneracy would occur at the 3rd LSXD and only two additional spectral lines would be found in hydrogen [7,8]. An additional anti-space duality could mean up to five additional spectral lines could be found. The reason for the complexity of the manifold of uncertainty is esoteric to discussion in this monograph.

A proposed radical paradigm shift will garner little attention/ respect from the physics community until it is empirically tested. For example, even Einstein himself after his *annum mirabilis* when he was for all practical purposes ‘Einstein’; was called an ‘idiot and a moron’ to his face when he proposed the photoelectric effect, an experiment that could easily today be performed in a kindergarten. Fortunately, the noetic model provides a clear pragmatic path for falsification [6-8]. If the protocol is successful it will not only help found UFM but also be a boon to M-Theory (demonstrate existence of additional dimensionality) and obviate the need for multi-billion dollar supercolliders [6-8].

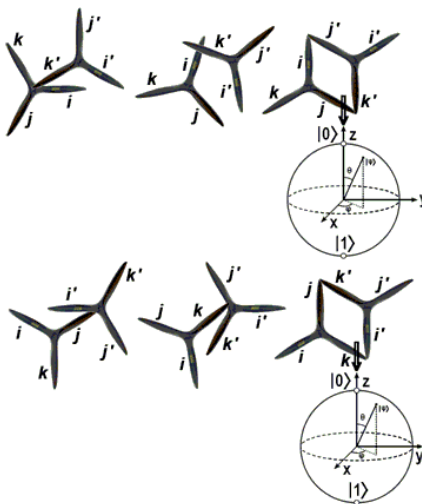


Fig. 6.3. An alternative (motive) rendition of Fig. 6.4 in nilpotent quaternionic form. A locus of HD mirror symmetric Calabi-Yau 3-tori here depicted as dual quaternion trefoil knots spinning relativistically and evolving quantum mechanically in time. The space-antispace nodes in the cycle are sometimes chaotic (degenerate) and sometimes periodically couple coherently into resultant quantum states in Euclidean 3-space depicted in the figure as faces of a 3-cube that reduce further to the Riemann Bloch 2-sphere at the bottom. The Bloch sphere is a knotted shadow of HD UFM and reason for uncertainty.

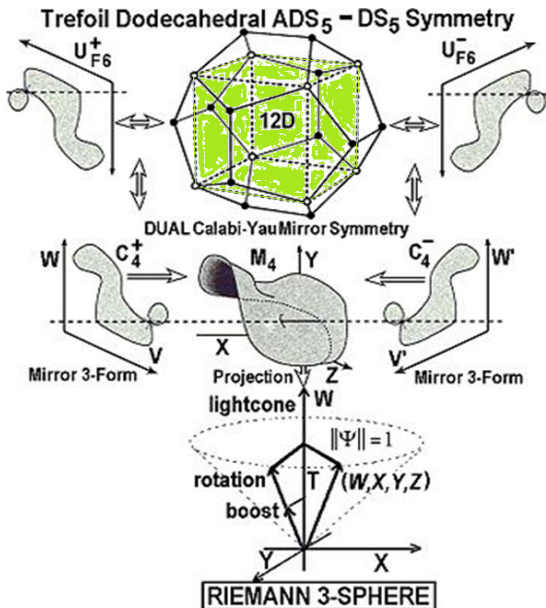


Fig. 6.4. Complete LSXD regime of 12D HAM cosmology illustrating the hierarchy of its geometric topology. Dodecahedral involute properties, as well as the continuous-state exciplex ‘hysteresis loop’ of noeon injection not shown. It represents a unique M-Theoretic model of ‘Continuous-State’ U_F dynamics as it relates to the LSXD topology of UFM and the putative exchange quanta of the U_F called the noeon.

Recent Planck satellite observations have not ruled out an AdS-dS wrap-around dodecahedral cosmology [20].

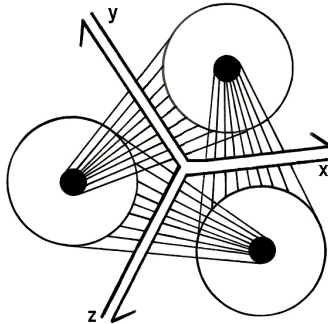


Fig. 6.5. Triune structure of a solitary LCU that like an isolated quark does not exist in nature. The central parallel lines, x, y, z are the Witten string vertex with properties of a complex Riemann sphere able to continuously rotate from zero to infinity. The field lines represent the HD ‘super quantum potential’ of the unified field, restricting 3-space.

Understanding the Least Cosmological Unit (LCU) is the essential key to the development and testing of Multiverse UFM. This will remain a major challenge to progress until we know how to understand what geometrical/topological form of close-packing its tessellation of space and spacetime takes. The problem arises because we don't know what form(s) of close packing occurs; it could be square or hexagonal for example.

We suspect even if LSXD are orthogonal and evenly spaced continuous compactification might change the dimensional radius. Continuous-state spin-exchange dimensional reduction compactification is a key UF process such that the force and dynamics of gravity are likely to be involved, suggesting that periodic deficit angles will occur in parallel transport during cyclical modes of the process. Extended de Broglie-Bohm Cramer contributions might restrict compactification pathways. Space charge may also contribute.

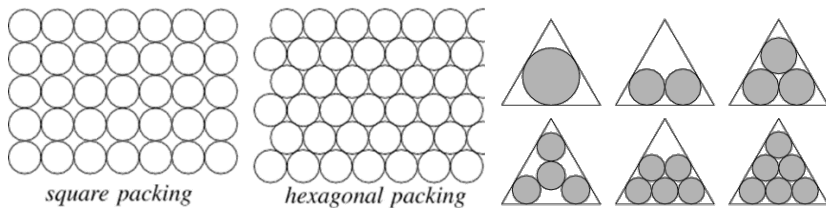


Fig. 6.6. a) Possibility of square and/or hexagonal LCU close-packing for tessellating space. It may be that the compactification process during parallel transport cyclically switches packing format to facilitate use of deficit angle creating crossover moves in the brane topology. b) Topological Calabi-Yau mirror symmetric brane boundary conditions and space ‘charge’ itself may restrict the form or size of the evolution of LCU close-packing.

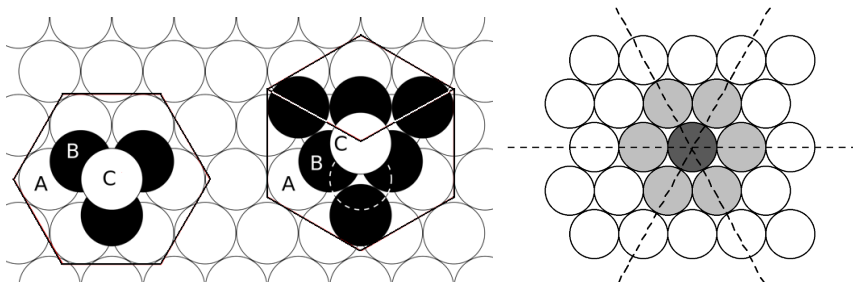


Fig. 6.7. a) The continuous-state compactification process may modulate the cyclical geometry of close-packing. b) What symmetrical form of HD hyperspherical LCU close-packing does Euclidean 3-space emerge from?

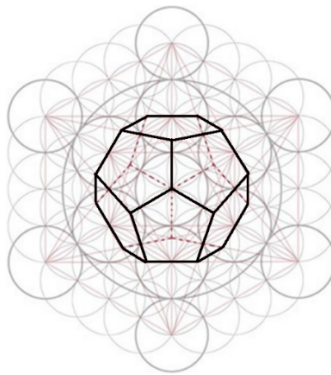


Fig. 6.8. The intellectual appeal of oscillating AdS₅-dS₅ Dodecahedral 12D to 15D LSXD space shown in Fig. 6.4 suggests LCU close-packing could take the form shown here.

Recent Planck satellite observation data has not ruled out the fact that the multiverse could take AdS₅-dS₅ dodecahedral wrap-around form [20]. Einstein himself stated that ‘if one could look far enough out into space one would see the back of one’s head’.

6.4 Pragmatic Testing of the UFM Paradigm

No idea in physics gets very far without empirical evidence. For example, Vigier’s seminal efforts begun in 1999-2000 on tight-bound states in hydrogen describing additional orbits below the lowest Bohr orbit [21,22] was considered to be nonsense at that time (including this author who was a close friend and colleague), and went virtually unnoticed. How could there be additional Bohr orbits below the lowest orbit by definition. And in addition Vigier was using this scenario to try to explain cold fusion, which even today it is considered to be on the foolish fringe of pseudoscience; but by 2012 the situation dramatically changed [23].

So our challenge is that this problem is not just atomic/nuclear physics but also a form of HD, LSXD M- theory. If one delves into string / M- Theory one can see it is quite a menagerie. Proponents don’t fully know what to do, they’re trying everything hoping to pick out of a 10^{Googolplex} or infinite number of possible string vacuums to try and find the one unique vacuum that makes correspondence to the standard model. We merely took all the pieces that were pertinent to the UFM model off the shelf and used them to develop the framework for this new model of tight-bound states (TBS). We started hundreds of years ago with Classical Newtonian

Mechanics in a 3D Euclidean space. Einstein and his contemporaries developed a 4D Minkowski-Riemann space for quantum mechanics and relativity; comprising the 2nd regime. The 3rd regime is suggested to be the realm where unified field mechanics (UFM) exists. The model used here is 12 dimensional; adding an additional UFM control factor to the 11D currently in vogue in M-Theory. Just as the tools of quantum mechanics were invisible to the tools of Classical Mechanics, so until now the tools of UFM are putatively invisible to the contemporary tools of experimental physics. As generally known spacetime is considered a stochastic foam with a zero-point field (ZPF) from which virtual particles restricted by the quantum uncertainty principle (to the Planck time) wink in and out of existence with *Zitterbewegung* explained as an interaction of a classical particle with the ZPF. Rowlands has extended this nicely with a space anti-space model [19].

The de Broglie Bohm theory didn't work very well formulated in 4D. Our program extends this model along with Cramer's Transactional Interpretation into HD space where it seems to work better. As you may know in the de Broglie Bohm model there is said to be no collapse of the wave function as in the Copenhagen interpretation but a continuous evolution where space-time and matter are continuously created annihilated and re-created with this evolution governed by a pilot wave or quantum potential.

This back cloth in our model is considered to be a covariant polarized vacuum of the Dirac type. A Dirac vacuum because it's proponents have applied extended electromagnetic theory with photon mass, m_γ , and such; but because of the great success of gauge theory the physics community has marginalized it perceiving a conflict. The best evidence for a Dirac vacuum is the Casimir effect. Lesser indicia of a Dirac vacuum include the Zeeman Effect and the Aharonov-Bohm Effect.

Regarding the putative Tight-Bound State (TBS) regimes in the hydrogen atom; what we are proposing in regards to these HD is to demonstrate their existence by observing new spectral lines in hydrogen. What this means as we will try to show is that the uncertainty principle is a manifold of finite radius (of 3 to probably 6 dimensions still to be determined). So we have a 3D asymptotically flat Euclidean space that we observe; then we have this manifold of uncertainty blocking another realm of dimensionality that is infinite in size. Lisa Randall is a major proponent of LSXD [16]. This model does not work in a 4D Big Bang cosmology. But because of certain inherent parameters within the new continuous-state multiverse cosmology it seems to work fine therein. This could be a

good thing, suggesting that we are on the correct track to new physics that might cause a reevaluation of Big Bang cosmology [6]. The main reason multiverse cosmology is perceived to have this success is that the continuous-state process allows the highest triplet of dimensions to be causally free of Euclidean space - crucial for surmounting uncertainty.

If one has familiarity with string theory one knows that the Planck constant is not considered fundamental. String tension, T_S is a factor added to the Planck constant. We were nonplussed for a while because the UFM model conflicts with the current incarnation of string theory in several ways. But this changed about a year or so ago when we uncovered the original hadronic form of string theory. String tension in the current model is fixed, one tension, T_S fixed for all strings. In the original hadronic model T_S fluctuated which is much more compatible with UFM multiverse cosmology. Another reason that the original hadronic form was rejected was that it contained a tachyon considered to be nonphysical. But the tachyon in terms of Cramer's model where the 'present is a standing-wave of the future-past' is a key element also deemed compatible with continuous-state cyclicity in conjunction with Calabi-Yau mirror symmetry. The tachyon appears to be virtual along with the tardyon as an interesting component allowed by the new set of UFM transformations beyond the Galilean-Lorentz-Poincaré; but that's an issue for later [12].

Following below is a brief outline of some of the ideas covered:

A) NEW HOLOGRAPHIC ANTHROPIC MULTIVERSE COSMOLOGY

- Derivation of Continuous-State Hypothesis
- Unique String Vacuum
- Derivation of Variable String Tension, $T_s = e/l = (2\pi\alpha')^{-1}$
- The Least Cosmological Unit (LCU) and relation to the Space-Antispace Quaternion Vertex
- Quantum Mechanical Uncertainty as a Manifold of Finite Radius
- Simplistic Calculation of New Spectral Lines Utilizing Common Hypervolume Formula

B) 12D M-THEORETIC CALABI-YAU MIRROR SYMMETRY

- The Conformal Covariant Dirac Polarized Vacuum With Continuous-State HD Copies of the Quaternionic or 4D Quantum 'Particle in a Box'.

C) TBS EXPERIMENTAL DESIGN

- Utility of Complex Quaternion Clifford Algebra for Protocol Design
- Sagnac Effect Incursive Oscillator Resonance Hierarchy
- Refined TBS Spectral line prediction utilizing Bessel Function parameters with corrections from string tension, T_s and the Fine Structure Constant.

6.5 Exploring Novel Cyclic Extensions of Hamilton's Dual-Quaternion Algebra

We make a preliminary exploratory study of higher dimensional (HD) orthogonal forms of the quaternion algebra in order to explore putative novel Nilpotent/Idempotent/Dirac symmetry properties. Stage-1 transforms the dual quaternion algebra in a manner that extends the standard anticommutative 3-form, i, j, k into a 5D/6D triplet. Each is a copy of the others and each is self-commutative and believed to represent spin or different orientations of a 3-cube. The triplet represents a copy of the original that contains no new information other than rotational perspective and maps back to the original quaternion vertex or to a second point in a line element. In Stage-2 we attempt to break the inherent quaternionic property of algebraic closure by stereographic projection of the Argand plane onto rotating Riemann 4-spheres. Finally, we explore the properties of various topological symmetries in order to study continuous anticommutative - commutative cycles in the periodic rotational motions of the quaternion algebra in additional HD dualities.

There is a world of strange beauty to be explored here... Baez [24].

6.6 Brief Quaternion Review

Since quaternions are not ubiquitously appreciated by physicists we review them briefly here. For many years prior to discovering the quaternions William Rowan Hamilton tried unsuccessfully to extend the common system of complex numbers, $a + bi$ where the real numbers, a are represented by the x -axis and the imaginary numbers, bi are represented orthogonally on the y -axis. Hamilton considered this a 2-dimensional (2D) space and desired to extend the system to 3D by utilizing an additional set of orthogonal complex numbers, cj . This attempt failed because he found that this system of ‘triplets’, $a + bi + cj$ did not exhibit the necessary algebraic property called ‘closure’ that would complete the algebra, i.e.

the product ij had no meaning within the algebra and therefore had to represent something else. In 1843 Hamilton finally realized he needed a 3rd system of imaginary numbers, dk to define an algebraic system properly exhibiting the needed property of closure [25-27] as in Fig. 6.9

$$i^2 = j^2 = k^2 = ijk = -1 \quad (6.3)$$

with additional anticommutative multiplication rules

$$ij = -ji = k, \quad jk = -kj = i, \quad ki = -ik = j. \quad (6.4)$$

which can be represented graphically as

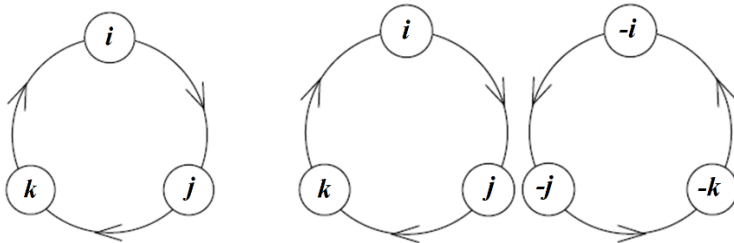


Fig. 6.9. a) Graphic summary of the quaternion cyclic permutation rules. b) The dual counterpropagating standing-wave mirror image. Adapted from. [24].

or represented in tabular form the dual quaternions, $\pm 1, \pm i, \pm j, \pm k$ form a non-Abelian group of order 8.

TABLE 6.2. Quaternion Cyclic Multiplication

	1	i	j	k
1	1	i	j	k
i	i	-1	k	$-j$
j	j	$-k$	-1	i
k	k	j	$-i$	-1

But by introducing the property of closure Hamilton sacrificed the principle of commutivity, $ij = -ji = k$. Frobenius proved in 1878 that no other system of complex algebra was possible with the same algebraic rules. This convinced him that he found a true explanation of the

3-dimensionality of space; with the 4th or real component in this case representing time as the real component (the 1 in quaternions, Tbl. 6.2). The Quaternion, Q_4 and Octonion, O_8 algebras arise naturally from restrictions inherent in the properties producing the discreteness of 3-dimensionality, i.e. the property of anticommutativity as realized by Hamilton as the key requirement for achieving the property of ‘closure’ when he discovered the i, j, k basis for the quaternion algebra or that in complex representation, $H = a \cdot 1 + bi + cj + dk$ is not commutative.

6.7 Background and Utility of New Quaternion Extensions

Our problem is similar to the one originally facing Hamilton. We also wish to add additional complex dimensionality but in a manner that also reintroduces commutivity, but only in a periodic manner. Our procedure in this exercise is to manipulate the inherent cyclicity of the normative quaternion algebra (anticommutative) in a manner that the property of closure is broken periodically during a transformation through a Large Scale Additional Dimensional (LSXD) ‘continuous-state’ mirror symmetric space evolving through periodic anticommutative and commutative modes [6,28]. This requires a new form of transformation of the line element. The usual representation of the line element, ds in an n -dimensional metric space is $ds^2 = dq \cdot dq = g(dq, dq)$ where g is the metric tensor, and dq an infinitesimal displacement. In n -dimensional coordinates $q = (q^1, q^2, q^3 \dots q^n)$ and the square of arc length is $ds^2 = \sum g_{ij} dq^i dq^j$. Indices i and j take values 1, 2, 3 ... n . The metric chosen determines the line element. We will continue this development in an ensuing section in terms of stereographically projected Riemann manifolds where a Riemann surface does not entail an inherent particular metric.

According to Rowlands [19,27,28-31] the usual quaternion cyclicity reduces the number of operators by a factor of 2 and prevents the possibility of defining further complex terms. To overcome this generalization of term limitations we explore utilizing shadow dualities employing additional copies of the quaternion algebra mapped into a 5D and 6D space to transform a new dualized ‘trivector’ quaternion algebra. As far as we know this can only occur under the auspices of a continuous-state cosmology within a dual metric where one coordinate system is fixed followed by the other being fixed in a sort of leap-frog baton passing fashion [6]. We will explain this in more detail later with as much rigor

currently at our disposal and conceptually in terms of a wonderfully illustrative metaphor in the ‘Walking of the Moai’ [32,33]. Correspondence is made to the usual 3D quaternion algebra as the resultant or re-closure that occurs at the end of the cycle repeats over and over continuously.

According to Rowlands’ the nilpotent duality or zero totality universe model requires an anti-commutative system that has this property of closure, whereas a commutative system remains open and degenerate to infinity [27]. However, this duality is fundamental to the continuous-state (like an internalized gravitational free-fall) postulate of Amoroso’s Holographic Anthropic Multiverse cosmology [6] which is compatible with Calabi-Yau mirror symmetry properties of M-Theory suggesting a putative relationship to physicality. We suspect also that in the future, correspondences will be found between the continuous-state hypothesis and the Rowlands’ nilpotent universal rewrite system [27].

6.8 A New Concept in Quaternion Algebra - The 1st Triplet

We start with a standard quaternion in italicized notation i,j,k which physically represents a fermionic vertex in space and therefore has a copy as a vacuum anti-space *Zitterberwegung* partner [19], **i,j,k** (bold italic notation) which together can form a nilpotent [27,29-31]. Multiplying the two (space-antispace) nilpotent components together we get 3 copies (3 sets of three) of the original quaternion (uppercase notation) at some new level of postulated higher space; but still with no new information such that each of the three copies commute with themselves internally. Our initial consideration is that these three copies are spin-like objects that conceptually represent 3 different views of a cube such as: **I**) planar face, **J**) edge and **K**) corner (as if collapsed to a hexagon).

We postulate the quaternion algebra extensions in Fig. 6.10 represent conceptually 3 different ways (orientations) of viewing a cube. The first, **Y_I** a usual planar face, second, **Y_J** perhaps like view onto an edge and the third, **Y_K** from a corner which would make the cube look like it was collapsed to a 2D hexagon. In summary: Fig. 6.10a) Usual i,j,k quaternion. 6.10b) Space-antispace dual quaternion, i,j,k and **i,j,k** . 6.10c) The new **IJK** nilpotent triplet. d) Reduced back to the original quaternion in 6.10a).

We pass through a stage of three commutative objects, each of which is constructed from ijk (original quaternion) and **ijk** (nilpotent vacuum copy) which are thus a set of dual quaternions. Knowing one of these gives us the other two automatically.

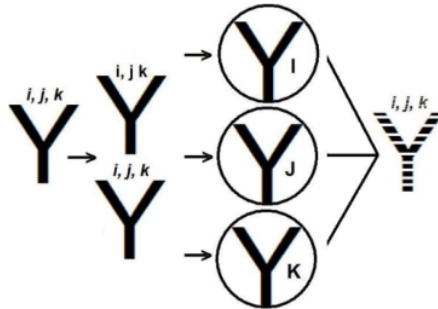


Fig. 6.10. This figure and next (Fig. 6.11) represent different aspects of the usual quaternion algebra containing no new information beyond the original fermionic vertex.

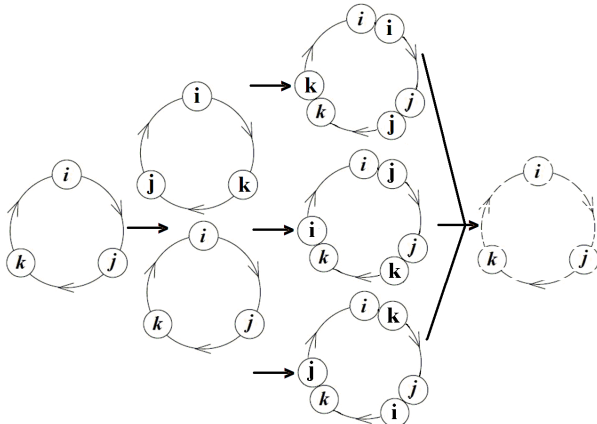


Fig. 6.11. Varied view of Fig. 6.10 but highlighting the cyclicity of the algebraic elements. Reduces to original i, j, k quaternion fermionic vertex. Also in summary (same as Fig. 6.9): Fig. 6.11a) Usual i, j, k quaternion. b) Space-antispace dual quaternion, i, j, k and $\mathbf{i}, \mathbf{j}, \mathbf{k}$. c) The new nilpotent triplet. d) Reduced back to the original quaternion in 6.11a).

Here is the algebraic derivation of the geometric objects shown in Figs. 6.10 & 6.11. In the quaternion algebra below, the usual italicized anticommutative quaternion, i, j, k acquires a dual vacuum (bold italicized) quaternion, $\mathbf{i}, \mathbf{j}, \mathbf{k}$. The product of these two quaternions becomes three commutative algebras (Figs. 6.10 & 6.11):

$$\begin{pmatrix} ii \\ jj \\ kk \end{pmatrix} \begin{pmatrix} ij \\ jk \\ ki \end{pmatrix} \begin{pmatrix} ik \\ ji \\ kj \end{pmatrix} \quad (6.5)$$

And their product becomes the new quaternion, **I J K** (Fig.6.11c). Each of these algebras is a copy of the others and each is commutative on itself. Selecting out the three versions makes an anticommutative set. In Eq. (6.5) our software would not allow bold font so we used regular and italic font to illustrate the quaternionic dualing.

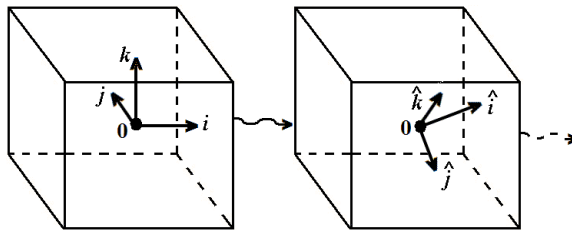


Fig. 6.12. Different complex orientations of the Euclidean 3-cube projected from a quaternion space-antispace fermionic vertex or singularity, i, j, k .

6.9 Vectors, Scalars, Quaternions and Commutativity

In this section notation is as follows. Vector are in regular and bold font. Quaternions are in regular italic and bold italic font. For the trivector we add the half quote mark ('').

i j k	<i>i i j i k</i>	<i>i'</i>	1
i j k	<i>i i j i k</i>	<i>i'</i>	1
<i>vector</i>	<i>bivector</i>	<i>trivector</i>	<i>scalar</i>
			<i>quaternions</i>

Vectors

i j k	anticommute
i j k	anticommute
ii jj kk	commute

Quaternions

<i>i j k</i>	<i>anticommute</i>
<i>i j k</i>	<i>anticommute</i>
<i>ii ij ik</i>	<i>j i'k</i>
<i>ii ij ik</i>	<i>j -</i>
	<i>nilpotent</i>
	<i>nilpotent</i>
	<i>(5th term automatic)</i>

$ii' jj' kk'$ commute

$ai\ bj\ ck$ 1d
 $Ai\ Bj\ Ck$ 1D

$ai\ bj\ ck$ 1d
 $ai\ bj\ ck$ 1D

$ii\ jj\ kk$
 $ij\ jk\ ki$
 $ik\ ji\ kj$

ijk anticommute SPACE

ijk anticommute VACUUM ANTISPACE

TOTAL 6 Degrees of freedom

This is Fig. 6.11 part b.

$ii\ jj\ kk$ commute SPINOR SPACE I

$ij\ jk\ ki$ commute SPINOR SPACE J

$ik\ ji\ kj$ commute SPINOR SPACE K

TOTAL 9 Degrees of freedom

The above (**I J K**) is Fig. 6.11 part c

IJ ($i i\ jj\ kk$) ($ij\ jk\ ki$) $\rightarrow (i\ j\ k\ -i\ -j\ -k\ -ik\ -ji\ -kj)$

JK ($ij\ jk\ ki$) ($ik\ ji\ kj$) $\rightarrow (i\ j\ k\ -i\ -j\ -k\ -ii\ -jj\ -kk)$

KI ($ik\ ji\ kj$) ($ii\ jj\ kk$) $\rightarrow (i\ j\ k\ -i\ -j\ -k\ -ij\ -jk\ -ki)$

Reverse **IJ** = $-JI$, **JK** = $-KJ$, **KI** = $-IK$. **I, J, K** anticommutative, becomes the new ijk at the next level in the cycle. Because of nilpotency, ijk and $ij\ jk$ are dual and contain the same information. Also, **I, J, K** is made up only of these terms and contains the same information again so we can map **I, J, K** directly onto ijk and then pull out its dual by nilpotency and go round the cycle again continuously. The **I, J, K** are a new set of quaternions with the same structure as ijk but with only the same information as contained in the usual ijk (real) and its dual $ij\ jk$ (vacuum).

We assume **I, J, K** are Dirac phase rotations of hypercube B. At phase K by stereographic projection (topological switching) a copy of A is boosted to a Riemann sphere ‘above’ K. We assume the Riemann sphere

by conformal scale-invariance inherent to the cosmology. This gives us $+ i,j,k$ and $- i,j,k$ on opposite sides of the boosted Riemann sphere. The **I**, **J**, **K**s all rotate so they take turns cyclically being in position to be boosted.

6.10 Toward Completing the Hypercube: The 2nd Triplet

In addition to boosting into the higher space we wish to turn the nilpotent into an idempotent that transforms into the vacuum in a similar manner. By multiplying we also get three copies that are three sets of three in the same manner as in the nilpotent boost into the higher space above that are also spin-like. And that will likewise by stereographic projection boost new copies into Riemann spheres above K.

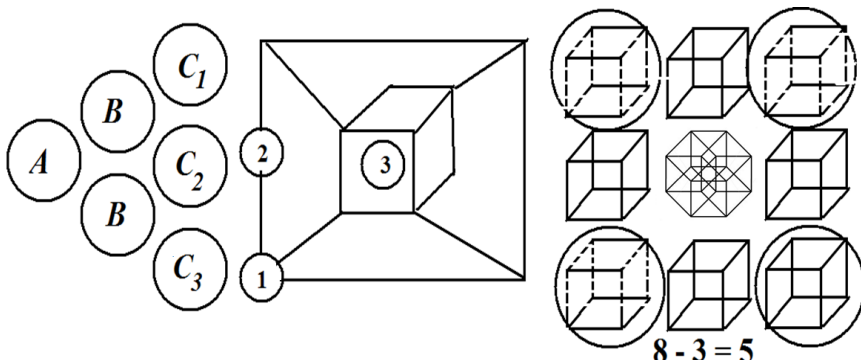


Fig. 6.13. The first part cycles A, B, C (as Figs. 6.9 & 6.11) is the algebra progression. The center hypercube represents the orientation provided by the three phases of the cube from C1, C2 & C3. The 3rd part (right) represents the 8 cubes exploded off a hypercube, suggesting that there are many orientations to explore with the new algebraic triplets.

It is suggested that the orientation of the Cs in Fig. 6.13 is periodic and that all three take turns boosting orientation information to the hypercube in the higher space. Through more layers of boosting into the higher space, in conjunction with additional symmetric idempotent copies in the vacuum space we wish to end up with a structure that is like a bag of close-packed ping pong balls or rotating Riemann spheres where the original quaternion sphere always remains at the center, but through a rewrite system (where the nilpotents are annihilation and creation ‘vectors’) that continuously boost copies of the original orientation information from the center to the surface spheres and back again. It is possible to describe these cubes as component hyperspheres or dodecahedral polyhedrons.

6.10.1 Higher Doublings - Planar to Riemann Sphere

Quaternions

$i j k$ anticommute SPACE (Real) \rightleftharpoons
Complex Argand Plane i

$i j k$ anticommute VACUUM (+C3) \rightleftharpoons
Complex Argand Plane i

$-i -j -k$ anticommute VACUUM (- C3) \rightleftharpoons
Stereographic Riemann Sphere I

$-i -j -k$ anticommute VACUUM (\pm Virtual) \rightleftharpoons
Stereographic Riemann Sphere I

These are not planar (as usual Q) but stereographic projections of a Riemann sphere. In the central portion closure (when it appears) subtracts the extra degrees of freedom in the extra duality. When not subtracted the Riemann sphere may “flip” the symmetry to achieve the basis for the commutative mode node. Doubled again, perhaps something like that shown in Fig. 6.11 to make it hyperspherical and causally separated.

In the London Underground tunnel near Imperial College there is an entrance to The Victoria and Albert Museum. In front of the entrance is a display sign encased in a 3 or 4-meter-long clear plastic tube about a meter in diameter. Inside the tube components of a large (V & A) rotate such that the A becomes the V and vice versa (with the help of the ampersand) [34,35]. These rotations are insufficient because they are planar and preserve the symmetry and closure of the original quaternion algebra [26,27]. With an additional copy on the Riemann sphere (mirror symmetries) 2 rotations occur simultaneously; but closure of the algebra is not yet broken. This requires a 3rd doubling in order to acquire properties of a dual Dirac spherical rotation. With sufficient degrees of freedom, one preserves the usual anti-commutative parameters of closure. The other by ‘boosting’ through an ambiguous Necker cube-like topological switching, reverses the symmetry and passes cyclically through a commutative mode. And then back down through a reverse Necker n-spinor switch to return to the origin or 2nd point in the line element reducing back to the usual quaternion form. The coordinate switching is also beautifully illustrated in the ‘Walking of the Moai on Rapa Nui’ [32,33].

6.10.2 Nilpotent Idempotent Vacuum Doublings

The nilpotent when multiplied by ζ becomes idempotent.

$$\begin{aligned}
 & (ikE + if + jm)(ikE + if + jm) \\
 & (ikE + if + jm)(ikE + if + jm) \\
 & (ikE + if + jm)(ikE + if + jm) \\
 & +()() = 0
 \end{aligned} \tag{6.6}$$

6.10.3 As Generalized Equation

The anticommutative

Anticommutative

$$(i_1 + j_1 + k_1)(i_2 + j_2 + k_2) =$$

Commutative Commutative Commutative

$$(i_1 i_2 + j_1 j_2 + k_1 k_2) + (i_1 j_2 + j_1 k_2 + k_1 i_2) + (i_1 k_2 + j_1 i_2 + k_1 j_2) =$$

$$I + J + K$$

a new iteration of the original i, j, k

6.10.4 As Tensor Transformation

Transform (X Y Z)

$$\begin{pmatrix} i_1 j_1 & i_2 j_2 & i_3 j_3 \\ j_1 k_1 & j_2 k_2 & j_3 k_3 \\ k_1 i_1 & k_2 i_2 & k_3 i_3 \end{pmatrix} = \begin{pmatrix} I \\ J \\ K \end{pmatrix} \tag{6.7}$$

6.11 Quaternion Mirrorhouses

Utilizing hypersets, to represent two parallel mirrors, a simple 2-mirror mirrorhouse may be represented as: $X = \{Y\}$, $Y = \{X\}$ (ignoring the

inversion effect of mirroring). In constructing a 3-mirror mirrorhouse interestingly the hyper-structure turns out to be precisely the structure of the quaternion imaginaries. Let i, j and k be hypersets representing three facing mirrors [36]. We then have

$$i = \{j, k\}, j = \{k, i\} \text{ and } k = \{i, j\} \quad (6.8)$$

where the notation $i = \{j, k\}$ means, e.g. that mirror i reflects mirrors j and k in that order.

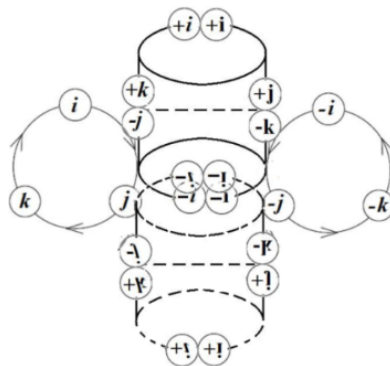


Fig. 6.14. Possible new duality doublings in higher space.

With three mirrors ordering is vital because mirroring inverts left/right-handedness. If we denote the mirror inversion operation by " $-$ " we have $i = \{j, k\} = -\{k, j\}$, $j = \{k, i\} = -\{i, k\}$ and $k = \{i, j\} = -\{j, i\}$ which is the structure of the quaternion triple of imaginaries: $i = j*k = -k*j$, $j = k*i = -i*k$, $k = i*j = -j*i$.

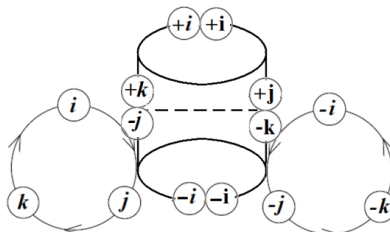


Fig. 6.15. With Rowland's intermediate skipped, center is straight to the spinor element (with additional duality to let the mechanism work cyclically), right is the symmetry reversing mechanism (when coupled at certain phase of the central spinor). To achieve causal separation, it is postulated this structure is doubled again?

The quaternion algebra therefore is the precise model of the holographic hyper-structure of three facing mirrors, where we see mirror inversion as the quaternionic anticommutation. The two versions of the quaternion multiplication table correspond to the two possible ways of arranging three mirrors into a triangular mirrorhouse.

Following Goertzel's [36] construction of a house of three mirrors; he demonstrates that the construction has the exact structure of the quaternion imaginaries. He lets i, j and k be hypersets representing the three facing mirrors such that $i = \{j,k\}$, $j = \{k,i\}$ and $k = \{i,j\}$. The notation $I = \{j,k\}$ means, e.g. that mirror i reflects mirrors j and k in that order. Goertzel points out that mirroring inverts left/right-handedness. Denoting mirror inversion by the minus sign " $-$ " yields $i = \{j,k\} = -\{k,j\}$, $j = \{k,i\} = -\{i,k\}$ and $k = \{i,j\} = -\{j,i\}$ which is the exact structure of the quaternion imaginary triplets: $i = j*k = -k*j$, $j = k*i = -i*k$, $k = i*j = -j*i$. Goertzel then claims the quaternion algebra is therefore the precise model of the holographic hyper-structure of three facing mirrors, where mirror inversion is the quaternionic anticommutation.

The two versions of the quaternion multiplication table correspond to the two possible ways of arranging three mirrors into a triangular mirrorhouse,

$$\begin{array}{ll} i*j = k & j*i = -k \\ j*k = i & k*j = -I \\ k*i = j & i*k = -j \end{array} \quad (6.9)$$

Which with dual counterpropagating mirror reflections is like a standing-wave.

6.11.1 Observation as Mirroring

To map the elements inside the mirrorhouse/algebraic framework noted previously, it suffices to interpret the $X = \{Y\}$, $Y = \{X\}$ as "X observes Y", "Y observes X" (e.g. we may have X = primary subset, Y = inner virtual other), and the above $i = \{j,k\}$, $j = \{k,i\}$, $k = \{i,j\}$ as "i observes {j observing k}" "j observes {k observing i}" and "k observes {i observing j}". Then we can define the - observation as an inverter of observer and observed, so that e.g. $\{j,k\} = -\{k,j\}$. We then obtain the quaternions

$$i = j*k = -k*j, j = k*i = -i*k, k = i*j = -j*i \quad (6.10)$$

where multiplication is observation and negation is reversal of the order of observation. Three inter-observers = quaternions.

This is where the standard mathematics of quataternion algebra has historically remained. In an actual mirrorhouse the reflections, like Bancos ghost extend into infinity. We wish to build an additional dual trivector mirrorhouse on top of the quaternion mirrorhouse that reduces back to the usual quaternion mirrorhouse. The idea is that in the additional mirrorhouses the cyclic reflections would reverse anticommutative effects to commutative effects.

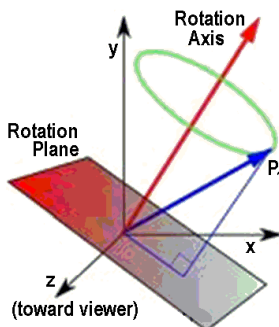


Fig. 6.16. A quaternion can be used to transform one 3D vector into another.

The quaternions can be physically modeled by three mirrors facing each other in a triangle; and the octonions modeled by four mirrors facing each other in a tetrahedron (a cube is a tetrahedron), or more complex packing structures related to tetrahedra. Using these facts, we wish to explore the structure of spacetime as structure that can be described by quaternions. Buckminster Fuller, for example, viewed the tetrahedron as an essential structure for internal and external reality. In addition, in nature the structure of HD space is an interacting tiling of topologically switching adjacent quaternionic or octonionic mirrorhouses that break Hamilton's closure cyclicity with an inherent natural periodicity that oscillates from Non-Abelian to Abelian continuously. A 3D quaternion transform is shown in Fig. 6.16.

This idea of quaternionic mirroring, beyond our current (temporary) ability to explain it mathematically, is conceptually the manner in which quantum data may be transferred ontologically by topological switching (like the ambiguous vertices of the Necker cube) to a detector without decoherence. The 'machine' to do this is the resonance hierarchy protocol described in Chap. 8 [10,11].

6.11.2 Mirror Symmetry Experiment

As a more visual person, I was curious to experience firsthand the symmetries of a quaternion mirrorhouse and obtained permission on 30 Jan 2012, 1:30 - 2 PM to use Sealing room 6, a four wall mirror house, in the Oakland, CA LDS Temple for an experiment.

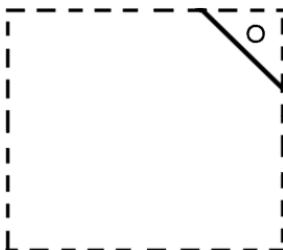


Fig. 6.17. Quaternion mirror house experiment. The dashed line-sided square represents the four mirrored walls of a large room. The solid line in the upper right corner a 6-foot mirror supported on a small table, and the circle a chair inside the mirror house corner.

Upon getting inside the mirror house, 4 images appeared. I initially thought it might be 3 images because I had made a triangle, but the 2 corners reflected off the mirror behind my head creating 4 proximal images. Not counting the observer it's like viewing an infinite series of quaternion vertices doubling *ad infinitum* with each mirror having the 4-fold quaternion vertex. Fig. 6.17.

If I closed my right eye, the face in the left vertex mirror closes its left eye (eye on the left). Then in the 2nd level image it is the right eye in right vertex image that closes. This is standard mirror symmetry imagery, but interesting to experience and verify 1st hand because it helps pondering how to reflect, rotate and invert more complex image components in order to create a new cyclical quaternion algebra that will both commute and anticommute periodically.

6.12 Calabi-Yau Manifolds - Brief Review

In superstring theory, the extra dimensions (XD) of spacetime are sometimes conjectured to take the form of a 6D Calabi-Yau manifold which led to the idea of mirror symmetry. The classical formulation of mirror symmetry relates 2 Calabi-Yau 3-folds M & W whose Hodge numbers three folds M $h^{1,1}$ and $h^{1,2}$ are swapped. Mirror symmetry is a special example of T-duality: The Calabi-Yau manifold may be written as

a fiber bundle whose fiber is a 3D torus. The simultaneous action of T-duality on all three dimensions of this torus is equivalent to mirror symmetry. Mirror symmetry allows physicists to calculate many quantities that seemed virtually incalculable before, by invoking the ‘mirror’ description of a given physical situation, which can be often much easier.

There are two different, but closely related, string theory statements of mirror symmetry.

1. Type IIA string theory on a Calabi-Yau M is mirror dual to Type IIB on W.

2. Type IIB string theory on a Calabi-Yau M is mirror dual to Type IIA on W.

This follows from the fact that Calabi-Yau Hodge numbers satisfy $h^{1,1} \geq 1$ but $h^{2,1} \geq 0$. If the Hodge numbers of M are such that $h^{2,1} = 0$ then by definition its mirror dual W is not Calabi-Yau. As a result, mirror symmetry allows for the definition of an extended space of compact spaces, which are defined by the W of the above two mirror symmetries.

Essentially, Calabi-Yau manifolds are shapes that satisfy the requirement of space for the six ‘unseen’ spatial dimensions of string theory, which are currently considered to be smaller than our currently observable lengths as they have not yet been detected. An unpopular alternative that we embrace and have designed experiments to test for [10,11] is known as large extra dimensions (LSXD). This often occurs in braneworld models - that the Calabi-Yau brane topology is large but we are confined to a small subset on which it intersects a D-brane.

6.13 Search for Commutative – Anticommutative Cyclical Algebra

We view the Hubble Universe, H_R as a nilpotent state of zero totality arising from a Higher Dimensional (HD) absolute space of infinite potentia. The world of apparent nonzero states that we observe, R must be associated with a zero creating conjugate, R^* such that $(R)(R) \Rightarrow (R)(R^*)$ in order to maintain the fundamental nilpotent condition of reality.

Since the quaternion set is isomorphic to the Pauli matrices we believe the Quaternion and Octonion sets are not merely a form of pure mathematics but indicative that the physical geometry of the universe is a

fundamental generator of these algebras. Baez [24] stated that the properties of these algebras have: “so far...just begun to be exploited”. Our purpose in this present work is to discover a new type of dualing in the cyclic dimensionality alternating between the principle of closure and openness, i.e. anticommutativity and commutativity. It appears that a Complex quaternion Clifford algebra can handle this effort.

For our purposes we wish to apply this to an extended version of Cramer’s Transactional Interpretation (TI) of quantum theory where according to Cramer the present instant of a quantum state is like a standing-wave of the future-past [37]. Cramer never elaborates on what he means by “standing-wave”. In our extension the standing-wave transactional present is a metaphorically more like a 6D hyperspherical standing wave with HD Calabi-Yau mirror house symmetry because the richer topology of brane transformations is equipped to handle the duality of closure and openness essential to our derivation of a new algebra to be used to design the protocol for testing for UFM [1,2].

We symbolize closure and openness as a form of wave-particle duality, which in our model we elevate to a principle of cosmology. So that rather than having the usual fixed closure built in to the quaternion algebra, we manipulate the standing-wave mirror house cycles so that closure is periodic instead. To do this we might keep a background doubling as a synchronization backbone rather than the ‘reduction by a factor of 2’ which as Rowlands states:

...describing a set of operators such as i, j, k as ‘cyclic’ means reducing the amount of independent information they contain by a factor of 2, because k for example arises purely from the product of jk . It could even be argued that the necessity of maintaining the equivalence of Q_4 and $C_2 \times C_2 \times C_2$ representations is the determining factor in making the quaternion operators cyclic [27].

Rowlands further discusses the dualing of Q_4 :

by complexifying it to the multivariate vector group, $1, -1, i, -i, \mathbf{i}, -\mathbf{i}, \mathbf{j}, -\mathbf{j}, \mathbf{k}, -\mathbf{k}, ii, -ii, ij, -ij, ik, -ik$ of order 16, which has a related $C_2 \times C_2 \times C_2 \times C_2$ formalism and which may also be written, $1, -1, i, -i, \mathbf{i}, -\mathbf{i}, \mathbf{j}, -\mathbf{j}, \mathbf{k}, -\mathbf{k}$, where a complex quaternion such as, ii becomes the equivalent of the multivariate vector \mathbf{I} [27].

There are two options

- 1) $(AB)(AB) \rightarrow (R^*)$ (Anticommutative)

$$2) \quad (AB)(AB) \rightarrow (R) \quad (\text{Commutative})$$

Option 1 was chosen by Hamilton when he discovered that the 3-dimensionality of the quaternion algebra required closure. The closed cycle of the anti-commuting option (zero creating) with distinguishable terms; but the commutative option has a series of terms that are completely indistinguishable (ontological) because the anticommuting partner must be unique. There are a number of forms of these open and closed dualities.

Planes through the origin of this 3D vector space give subalgebras of O isomorphic to the quaternions, lines through the origin give subalgebras isomorphic to the complex numbers, and the origin itself gives a subalgebra isomorphic to the real numbers.

What we really have here is reminiscent of a description of octonions as a ‘twisted group algebra’. Given any group G , the group algebra $\mathbb{R}[G]$ consists of all finite formal linear combinations of elements of G with real coefficients. This is an associative algebra with the product coming from that of G . We can use any function $\alpha: G^2 \rightarrow \{\pm 1\}$ to ‘twist’ this product, defining a new product $*\mathbb{R}[G] \times \mathbb{R}[G] \rightarrow \mathbb{R}[G]$ by: $g * h = \alpha(g, h)gh$ where $g, h \in G \subset \mathbb{R}[G]$. One can figure out an equation involving α that guarantees this new product will be associative. In this case we call α a ‘2-cocycle’. If α satisfies a certain extra equation, the product will also be commutative, and we call α a ‘stable 2-cocycle’. For example, the group algebra $\mathbb{R}[\mathbb{Z}_2]$ is isomorphic to a product of 2 copies of \mathbb{R} , but we can twist it by a stable 2-cocycle to obtain the complex numbers. The group algebra $\mathbb{R}[\mathbb{Z}_2^2]$ is isomorphic to a product of 4 copies of \mathbb{R} , but we can twist it by a 2-cocycle to obtain the quaternions. Similarly, the group algebra $\mathbb{R}[\mathbb{Z}_2^3]$ is a product of 8 copies of \mathbb{R} , and what we have really done in this section is describe a function α that allows us to twist this group algebra to obtain the octonions. Since the octonions are nonassociative, this function is not a 2-cocycle. However, its coboundary is a ‘stable 3-cocycle’, which allows one to define a new associator and braiding for the category of \mathbb{Z}_2^3 -graded vector spaces, making it into a symmetric monoidal category [38]. In this symmetric monoidal category, the octonions are a commutative monoid object. In less technical terms: this category provides a context in which the octonions are commutative and associative [24].

We do not believe at the moment a sole Octonion approach is correct for developing our new algebra and that octonions only provide a *gedanken* medium for exploring dualities and doublings; but additional clarity provided by the ‘Fano snowflake’ is changing that view. As in the Fano plane (Fig. 6.18) an ordinary 3-cube has 8 possible quaternionic vertices. A hypercube as in Fig. 6.13 explodes into eight 3-cubes for a total of 64 quaternionic vertices. Without yet having finished formalizing the new algebra we believe 64 symmetry components are required for its invention. See [27] for a discussion pertaining to 64 quaternionic elements.

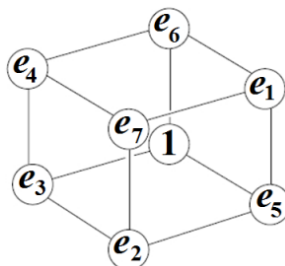


Fig. 6.18. The Fano plane is the projective plane over the 2-element field \mathbb{Z}_2 consisting of lines through the origin in the vector space \mathbb{Z}_2^3 . Since every such line contains a single nonzero element, we can also think of the Fano plane as consisting of the seven nonzero elements of \mathbb{Z}_2^3 . If we think of the origin in \mathbb{Z}_2^3 as corresponding to $1 \in O$, we get this picture of the octonions.

The quaternions are a 4D algebra with basis $1, i, j, k$. To describe the product, we could give a multiplication table, but it is easier to remember that:

- 1 is the multiplicative identity,
- i, j and k are square roots of -1 ,
- $ij = k, ji = -k$, and all identities obtained from these by cyclic permutations of (i, j, k) .

We can summarize the quaternion rule in a diagram, Fig. 6.9. When we multiply two elements going clockwise around the circle we get the next element: for example, $i, j = k$. But when we multiply two going around counterclockwise, we get *minus* of the next element: for example, $j, i = -k$ [24,27].

This cyclicity is key to our continuous-state commutative anti-commutative leap-frogging of the metric. Einstein believed ‘the photon provides its own medium and no ether is required’. This is true in general but the medium must be imbedded in a cosmology. Therefore, is the Rowland’s concept that the fermion vertex is fundamental similar, i.e. needing a cosmological embedding. Correspondence to Multiverse cosmology could provide the proper embedding. This is a primary postulate herein.

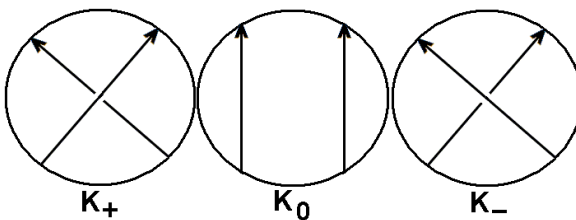


Fig. 6.19. Crossing change triple. Imagine embedded cyclically in Fig. 6.8.

In Fig. 6.19 the ordered set (K_+, K_-, K_0) is called a crossing-change-triple. Let (K_+, K_-, K_0) be a twist-move-triple See [39-41] for a variations and in depth discussion. This is only step one in developing the braided or knot topology required for the 6 spatial, 3 temporal and 3 control dimensions of the UFM ‘superimplicate order’. The crossing-triple reduces to the ‘shadow singularity in Euclidean 3-space.

Riemann sphere manifolds are key to algebraic topology. The Riemann sphere is usually represented as the unit sphere $x^2 + y^2 + z^2 = 1$ in real 3D space, $\mathbb{R}^3(x, y, z)$ where two stereographic projections from the unit sphere are made onto the complex plane by $\zeta = x + iy$ and $\xi = x - iy$, written as

$$\zeta = \frac{x + iy}{1 - z} = \cot\left(\frac{1}{2}\phi\right)e^{i\theta} \quad (6.11a)$$

and

$$\xi = \frac{x - iy}{1 + z} = \tan\left(\frac{1}{2}\phi\right)e^{-i\theta}. \quad (6.11b)$$

In order to cover the whole unit sphere two complex planes are required because each stereographic projection alone is missing one point, either the point at zero or infinity. The extended complex numbers consist of the complex numbers \mathbb{C} together with ∞ . The extended complex numbers

are written as $\hat{\mathbb{C}} = \mathbb{C} \cup \{\infty\}$. Geometrically, the set of extended complex numbers is referred to as the Riemann sphere (or extended complex plane) seen as glued back-to-back at $z = 0$. Note that the two complex planes are identified differently with the plane $z = 0$. An orientation-reversal is necessary to maintain consistent orientation on the sphere, and in particular complex conjugation causes the transition maps to be holomorphic.

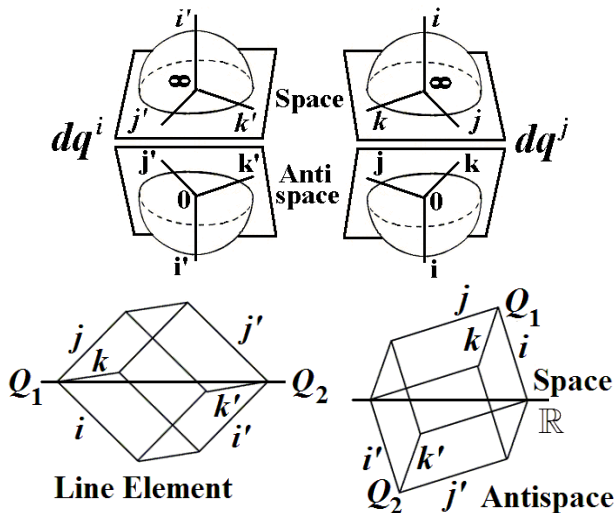


Fig. 6.20. Riemann sphere quaternionic line elements.

The transition maps between ζ -coordinates and ξ -coordinates are obtained by composing one projection with the inverse of the other. They turn out to be $\zeta = 1/\xi$ and $\xi = 1/\zeta$, as described above. Thus the unit sphere is diffeomorphic to the Riemann sphere. Under this diffeomorphism, the unit circle in the ζ -chart, the unit circle in the ξ -chart, and the equator of the unit sphere are all identified. The unit disk $|\zeta| < 1$ is identified with the southern hemisphere $z < 0$, while the unit disk $|\xi| < 1$ is identified with the northern hemisphere $z > 0$. A Riemann surface does not have a unique Riemannian metric which means we may develop a relevant metric for the noetic UFM transformation.

This implies a dual or mirror metricity where one is fixed in reality or 3-space and the ‘mirror’ confined to complex space where it then cyclically ‘topologically switches’ into real space and the real space metric takes its place in complex space. A component of the metric

fixing-unfixing when applied to the ‘Walking of the Moai on Rapa Nui’ relates symbolically to recent work of Kauffman on Laws of Form:

When the oscillation (Multiverse continuous-state) is seen without beginning or end, it can be regarded in two distinct ways: as an oscillation from marked to unmarked, or as an oscillation from unmarked to marked. In this way the re-entering marked becomes the recursive process generated by the equation and J is an algebraic or imaginary fixed point for the recursion.

$$R(x) = \boxed{x}$$

The analog with the complex numbers is sufficiently strong that we now shift to the complex numbers themselves as a specific instantiation of this recursive process. In the body of the paper we will return to the more rarified discussion leading from the distinction itself. We begin with recursive processes that work with the real numbers **+1** and **-1**. Think of the oscillatory process generated by $R(x) = -1/x$ [41].

The fixed point is **i** with $i^2 = -1$, and the processes generated over the real numbers must be directly related to the idealized **i**. There are two *iterant views*: **[+1,-1]** and **[-1,+1]**. Fig. 6.21.

These are seen as points of view of an alternating process that engender the square roots of negative unity.

$$\dots +1 -1 +1 -1 +1 -1 +1 -1 +1 -1 +1 -1 +1 -1 \dots$$

$$\dots +1, -1, +1, -1, +1, -1 \dots$$

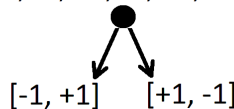


Fig. 6.21. Quantizing the Iterant views.

To see this, we introduce a *temporal shift operator*, \mathbf{h} such that $[\mathbf{a}, \mathbf{b}]\mathbf{h} = \mathbf{h}[\mathbf{b}, \mathbf{a}]$ and $\mathbf{h}\mathbf{h} = \mathbf{1}$ so that concatenated observations can include a time step of one-half period of the process ...abababab... [41], Fig. 6.21.

Figure 6.22 reminds us of the ‘walking of the Moai on Rapa Nui’ [32,33] because if for example the left foot is the *ababab* iterator, when it is lifted the *cdcdcd* iterator represents the ‘fixed metric’ and the *efefef* acts as the shift operator enabling a ‘complex crossing change’ from commutivity to anticommutivity or vice versa. However, as we already stated several more triune sets of additional mirror house doublings or dualings are required.

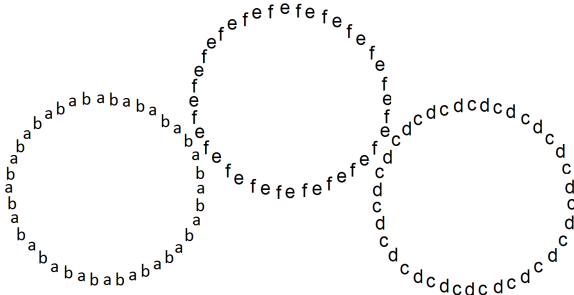


Fig. 6.22. Triune temporal shift operator for 1st triad duals. In reality involved as a trefoil knot or dual Calabi-Yau 3-torus. The contact points must include dynamic-static crossing change triples to cyclically break closure in the quaternion algebra.

The 3rd complex metric is involved in making an evolution from dual quaternions to a 3rd quaternion we choose to name a trivector that acts as a baton passing mechanism between the space-antispace or dual quaternion vector space. The trivector facilitates a ‘leap-frogging’ between anti-commutative and commutative modes of HD space. This inaugurates a Möbius transformation between the Riemann dual stereographic projection complex planes.

Dirac Spinor Rotation and Iterant Shift Operator [1,-1]& [-1,1]

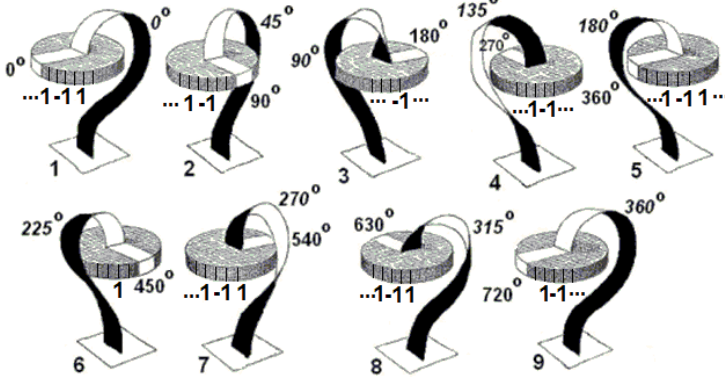


Fig. 6.23. Temporal i clock shift operator with addition of Dirac spherical rotation in preparation for Möbius transformation crossing changes. See Fig. 6.22.

In the midst of the UFM continuous-state dimensional reduction compactification process (U_F process) there is a central (focused around the singularity or LCU) coordinate ‘fixing-unfixing’. In prior work we [6]

have related this to the integration of G-em coordinates, in that initial case arbitrarily fixing one metric. That work proceeded discovery of the continuous-state process wherein now an inherent cyclicity occurs in first fixing one metric and then fixing the other. This is an essential aspect of the gating mechanism for the U_F dynamics to surmount quantum uncertainty. The ‘fixed’ knots can be ‘unfixed’ by topological moves.

Geometrically, a standard Möbius transformation can be obtained by first performing stereographic projection from the plane to the unit 2-sphere, rotating and moving the sphere to a new location and orientation in space, and then performing stereographic projection (from the new position of the sphere) to the plane. These transformations preserve angles, map every straight line to a line or circle, and map every circle to a line or circle. Möbius transformations are defined on the extended complex plane (i.e. the complex plane augmented by the point at infinity):

$$\hat{\mathbb{C}} = \mathbb{C} \cup \{\infty\}.$$

This extended complex plane can be thought of as a sphere, the Riemann sphere, or as the complex projective line. Every Möbius transformation is a bijective conformal map of the Riemann sphere to itself. Every such map is by necessity a Möbius transformation. Geometrically this map is the Riemann stereographic projection of a rotation by 90° around $\pm i$ with period 4, which takes the continuous cycle $0 \rightarrow 1 \rightarrow \infty \rightarrow -1 \rightarrow 0$.

An LSXD point particle representation of a fermionic singularity [1,6]. The $8 + 8$ or 16 ($\mathbb{C}^{\pm 4}$ complex space) 2-spheres with future-past retarded-advanced contours are representations of HD components of a Cramer ‘standing-wave’ transaction. This can be considered in terms of Calabi-Yau dual mirror symmetries. To produce the quaternion trivector representation (Figs. 6.10 and 6.11) a 3rd singularity-contour map is required which is then also dualized, i.e. resulting in 6 singularity/contour maps. This many are required to cycle from anticommutativity to commutativity to provide the cyclic opportunity to violate 4D quantum uncertainty [1,10,11]!

Figure 6.24 begins to illustrate the mirror symmetries involved in the more complex dualities. If the central points, P represent mirrored 3-cubes each of which already has 8 quaternionic vertices, then each sphere in Fig. 6.24 represents one of eight 3-cubes exploded off a hypercube which is each mirrored in the α and β singularities and contours. We believe one more mirror house doubling is required beyond that scenario to complete a commutative-anticommutative iterative shift operator!

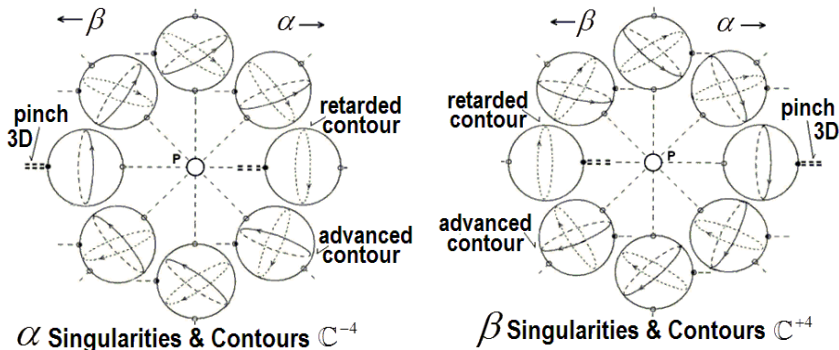


Fig. 6.24. Two of six required HD Nilpotent trivector complex quaternion symmetries.

6.14 Indicia for Unified Field Mechanics by Tight-Bound States (TBS)

A) SEARCH FOR LARGE-SCALE ADDITIONAL DIMENSIONS

A new program at CERN (proposed, not yet performed) seeks evidence of another host of particles that can only exist if there are more dimensions [42] than found in the Standard Model of particle physics.

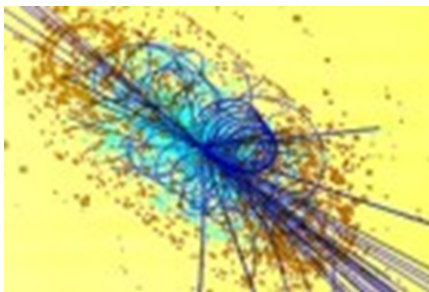


Fig. 6.25. CERN high energy collision cross section particle spray of the type that uncovered the Higgs mechanism.

Nothing in Physics bears much weight without experiment. We have proposed a low-energy tabletop model to ‘discover’ XD, that if successful puts an end to the need for large accelerators, provides the 1st test of M-Theory and opens the door to UFM, not to mention bulk UQC. The 1st step in describing the basis of HD UFM space begins with early work by Rauscher in describing a complex 8-space with a superluminal Lorentz transform boosting spatial dimensions to temporal dimensions [43].

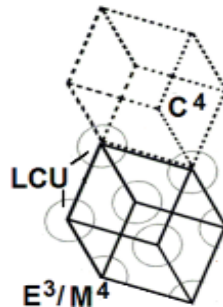


Fig. 6.26. Conceptual view of the Rauscher HD Complex C^4 space added to 4D Minkowski space, $\hat{M}^4 + \mathbb{C}^4$. Spatial dimensions are ‘boosted’ to temporal dimensions.

B) THE CONTINUOUS-STATE HYPOTHESIS

Derivation of continuous-state multiverse postulates led to a unique string vacuum based on a variable rather than fixed string tension and a virtual tachyon [6,12] that entered in by extending Cramer’s transactional interpretation. We will do our best to define this continuous-state process which is still very difficult to do in a manner others seem to comprehend.

The Planck scale is currently called the basement of reality starting from an essentially infinite size Hubble radius cosmology that reduces to a rigid microscopic Planck scale. In the holographic multiverse model, the 1st step is built as an extension of Rauscher’s complex 8-space, where she added a 4D complex space, C^4 to standard 4D Minkowski space, M^4 which isn’t deemed sufficient because her 4D complex space still reduced to a fixed rigid Planck barrier (Fig. 6.26).

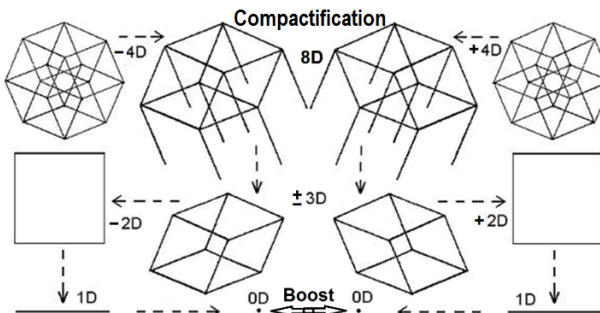


Fig. 6.27. Continuous mirror symmetric dimensional reduction from 8D to 0D where the Riemann sphere cyclically rotates from zero to infinity.

A second superluminal boost is required to transform the complex temporal dimensions to dimensions of energy, which become synonymous with a de Broglie-Bohm ‘super quantum potential’ or rather the coherent force of the unified field [2]. What is needed to develop the continuous-state model is a fundamental basis of reality that acts as if it is in a self-contained inherent freefall. So I added another set of complex dimensions to allow reality to cycle continuously at the fundamental level.

However, Elizabeth's complex 8-space also included superluminal Lorenz transformations that boosted a spatial dimension, s into a temporal dimension, t enhancing the process for conceptualizing the continuous-state scenario [1,6,43].

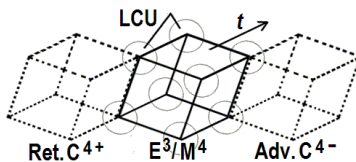


Fig. 6.28. 12D HAM cosmology with the addition of a 2nd complex 4-space resulting in $\hat{M}_4 \pm \mathbb{C}^4$. The $\pm \mathbb{C}^4$ spacetime packages must become described as involute (Fig. 6.30) before the continuous-state process can occur. We equate $\hat{M}_4 \pm \mathbb{C}^4$ with the dual Calabi-Yau 3-torus plus three additional dimensions undergoing the cyclic boosting process.

Then a second set of superluminal Lawrence transformations is applied boosting temporal dimensions, t to dimensions of energy, e . The energy dimension becomes compatible with a super-quantum potential eventually becoming synonymous with the ontological force of coherence of the unified field. This addition along with the second complex 4-space, $\pm \mathbb{C}^4$ dimensions completes geometrically at least the necessary components for continuous-state cyclicity providing a framework for one of the key elements of the model within which we propose experimental tests for new spectral lines in hydrogen in HD Cavity-QED volumes [7,8].

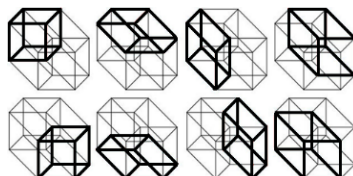


Fig. 6.29. View of 8 3D cubes comprising a 4D hypercube. See continuous-state involution metaphor in Fig. 6.30.

The other key element is that it is mandatory to surmount the sacrosanct uncertainty principle [6,10,11], as demonstrated by Copenhagen interpretation. The idea is simplistically to do something else!

Also in terms of the covariant Dirac vacuum, Calabi-Yau mirror symmetry which is a 6D dual 3-torus with a left-right symmetry. String theorists are searching for one unique compactification which will provide correspondence to the 4-space of the standard model. In physics generally a new theory must make satisfactory correspondence to existing theory.

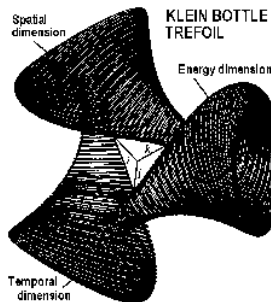


Fig. 6.30. A Klein bottle trefoil. A 6D Calabi-Yau 3-torus could also be used. A primitive metaphor to show rotation of continuous-state components. Not realized in 4D as shown; remember additional dimensionality is required to cyclically break the obvious closure shown in this figure illustrating the cycling of dimensional parameters if the 8-cubes of the 4D hypercube were doubled and put into cyclical motion not just exploded as in Fig. 6.29.

In the continuous-state paradigm compactification is different than in M-theory; rather than a search for one unique compactification making correspondence to the 4D standard model, UFM compactification is a ‘continuous-state spin-exchange dimensional reduction process occurring from 12D to ~0D (asymptotic Planck) where Riemann sphere (Kähler-Calabi-Yau) properties of the Least Cosmological Unit (LCU) rotate from zero to infinity in the same continuous-state standing-wave hyperspherical cycle such as left-right $11 \rightarrow 10 \rightarrow 9$ etc. down to ~ zero with alternating Calabi-Yau dual mirror symmetry.

Rauscher confided, she ‘*didn’t like the idea of a standing-wave as it seemed too simplistic*’; yes, when thought of as a 1D string on a musical instrument or even a 2D drum topology. But as a hyperspherical hyperdimensional Calabi-Yau 6D brane conglomerate one finds sufficient complexity to satisfy involute continuous-state process modeling.

The other important issue for the Dirac polarized vacuum is that it is conformal and scale-invariant. Because as we will see momentarily in

terms of our 3D or 4D quantum particle in a box, that the continuous-state cycle has inherent HD formatted Calabi-Yau mirror symmetric brane copies of the resultant 3D quantum state. This becomes important for surmounting the Uncertainty Principle as it is postulated that at 12D the mirror symmetric ‘copy’ is causally free of the 3D resultant, the whole hierarchy of which is nilpotent. The 12D ‘mirror image of the mirror image’ is the minimum dimensionality required for this to occur.

This is a boon for QIP because the quantum uncertainty principle in terms of supervening decoherence is the last main hurdle for the implementation of bulk UQC [6]. Whatever action is performed on the 12D copy has no effect on the 3D quantum particle in a box. There is in addition the other ontological properties associated with topological switching that may affect the dimensionality required for the process. Not only decoherence itself but the aspects of time or relativistic effects related to being able to maintain coherence. We won't get into this here because it is off the topic of formulating Unified Field Mechanics (UFM).

Concerning the importance of the original hadronic form of variable string tension; the main reason we were able to discover a unique string vacuum was by finding an alternative derivation of string tension; for which the traditional formula is, $T_s = e/l = (2\pi\alpha')^{-1}$. The UFM formula in unexpanded form simplistically became,

$$F_{(N)} = \frac{\aleph}{\rho} \quad (6.12)$$

where instead of energy, e over the length of the string, l topological charge or brane energy, \aleph is put over the brane topological radius, ρ of the relativistically rotating Riemann sphere LCU hyperstructure. $F_{(N)}$ is the noetic force of coherence of the unified field [1,2,6].

Of interest to note, which we will not get into here is that the fine structure constant is part of these parameters also. If the reader has delved into any of the fundamental constants, one knows that the fine structure constant and many other fundamental constants are derived in terms of themselves and therefore not yet fully understood fundamentally. It appears that further UFM development will show that the regime of unified field mechanics is where light is shed on the origin of the nature of the fine structure constant.

In a recent volume by Rowland's [44] we find a brief discussion of the abilities of complex quaternion Clifford algebra which we will need to

design the experimental protocol to search for new HD spectral lines in hydrogen. There are indicia for this model. One of the main indicia put forward by people like Nima Arkani-Hamad at the Princeton IAS and Lisa Randall [16] at CERN are to search for artifacts that will be indicative of additional dimensions in particle sprays. Such experiments have been suggested but not performed.

6.15 Building the UFM TBS Experimental Protocol

The best indicia for our model experimentally is suggested by work done by Chantler [45,46]. The data from his experiments over the last 10 years or so on hydrogen showed only a minute artifact proposed to violate QED; but more recently in 2012 for work on Titanium the QED violation effect was much larger. The beauty of this is that they stripped all the electrons off the Titanium atom except one creating a large hydrogen-like atom [46]. One wants to maintain the simplicity of the hydrogen atom to perform the experiment.

Vigier's seminal papers in 1999/2003 [21,22] are similar theoretically in some ways to Chantler's model. Vigier describes the first exploration made by Corben in an unpublished paper. Corben noticed that motion of a point charge in the field of magnetic dipole at rest, is highly relativistic and that the orbits are of nuclear dimensions. Further investigation was undertaken by Schild [47], but the most systematic treatment is given by Barut (see for example [48]). A 2-body system where magnetic interactions play the most significant role is in positronium. Both electron and positron have large magnetic moments which contribute to the second potential well in an effective potential, at distances much smaller than the Bohr radius. Barut and his coworkers predicted that this second potential well can support resonances. A 2-body model, suitable for non-perturbative treatment of magnetic interactions is presented by Barut [48] and Vigier [21,22].

Our approach doesn't fully correlate with Vigier's because at that time he had no consideration of additional dimensionality which is a dominant element in our multiverse model. For the first 10 years of Chantler's work the artifact said to violate QED was so small that it was essentially ignored by the physics community. But in the 2012 experiment [46] the QED violation was great enough ($\sigma 5$ level) that some elements in the news media suggested Nobel Prize; but as yet the majority of the physics community said the artifact is insufficient.

Now the reason we think the continuous-state model will work is for example, if you take the Bohr model of the hydrogen atom, spectroscopic measurements are taken as a 3D volume measurement from the space between the nucleus and the electrons orbit. For hydrogen, the first Bohr orbit has a radius of .5 Angstrom, and the second or orbit a radius of $\sim 2 \text{ \AA}$. This is the hundred-year history of spectroscopic measurements taken from within the fixed regime of the 4D standard model. A ‘hidden’ HD spectroscopic cavity is going to have different properties in a 12D holographic multiverse regime.

Firstly, we must make a postulate regarding the volume of additional dimensionality both within the finite radius manifold of uncertainty and beyond into the regime of LSXD. We attempt to make this assumption in a manner in which the conditions we are trying to apply can be sufficiently understood metaphorically. Remember that we have elevated wave particle duality to a principle of cosmology as it applies especially to the continuous-state postulate. We continue to mention the complex quaternion Clifford algebra under development to describe the continuous state process parameters for experimental design; the cyclicity has an inherent commutativity anticommutativity that Clifford algebra is equipped to handle symmetries with a 3D or 4D Euclidean/Minkowski manifold resultant covered with an 8D or 9D complex cycling of dimensions built on top of it. In the initial case of a single space anti-space dualing, the manifold of uncertainty represents a 4th, 5th and 6th additional hyperspherical dimensionality.

Recall our use of the Rauscher superluminal Lorentz transformation that boosts a spatial dimension into a temporal dimension wherein noetic UFM multiverse cosmology has added a second boost of dimensionality from temporal to that of energy (super quantum potential) as the exchange mechanism for topological charge in unified field theory. What we are trying to say is that behind or within the veil (manifold) of uncertainty these XD open and close volumetrically from zero, i.e. the usual 3D Euclidean QED cavity to the added volumetric structure of the 4th 5th and 6th dimensions yielding: $r_1 V_{3D}, r_2 V_{4D}, r_3 V_{5D}, r_4 V_{6D}$ enabling us to calculate the wavelength of three additional spectral lines in hydrogen based on the volume of these respective hyperspherical cavities!

We have not given sufficient thought to consider whether it's a viable assumption, to consider Von Neumann’s postulate of a ‘speed for collapse of the wave function’, hinting that Chantler’s switch from hydrogen to a hydrogen-like Titanium atom could provide a time delay factor sufficient to explain his QED artifact. In any case experimental success would provide the first indicia that something exists beyond the realm of QED.

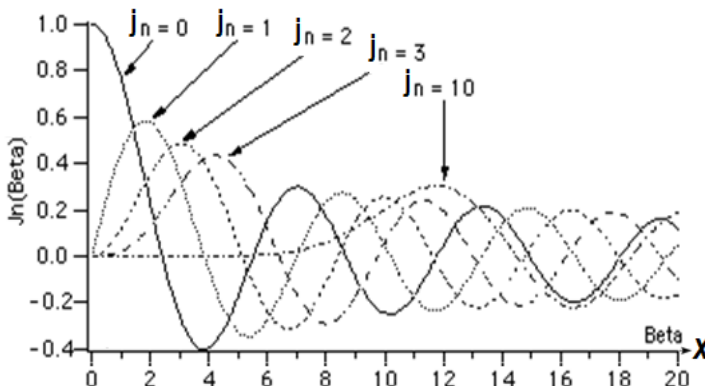


Fig. 6.31. Example of a Bessel Function necessary to couple the synchronization backbone with the Dubois incursive oscillator resonance hierarchy in order to access additional Tight Bound States (TBS) beyond the first. Even though we postulate how, surmounting uncertainty will not be a trivial experimental procedure.

We postulate applying the resonance hierarchy to open the first 4D TBS cavity will be relatively easy, but to open the 5th and 6D cavities probably requires the addition of a precision Bessel function [49] to the incursive resonance hierarchy that because of additional artifacts like those found in the refinements of the Born-Sommerfeld model; it will be a little tricky to master the protocol to measure these additional spectral lines because of the relativistic modes of mirror symmetric brane interactions. We do not mean this in calculating the TBS wavelength, but the tiniest propensity we do not sufficiently understand will probably keep the uncertainty principle cycle sufficiently active to keep the 5D cavity closed!

Common example of a Bessel function:

$$x^2 \frac{d^2 y}{dx^2} + x \frac{dy}{dx} + (x^2 - \alpha^2) y = 0 \quad (6.13)$$

This isn't the correct Bessel function, but we use a general form to illustrate that modes in the resonance hierarchy are believed to be required to get beyond the first TBS spectral line which will be relatively easy to find in comparison; and that the next will be more challenging as there will be some unexpected complexity that must be overcome that hasn't revealed itself to us as yet that will require a refined Bessel function

addition to adjust the spin-spin coupling parameters of the algebra precisely to the ‘beat frequency’ cycle in the spacetime backcloth.

For this reason, we haven’t performed a rigorous calculation, but preliminarily predict that these additional spectral lines will lie between the .5 Angstrom first Bohr orbit and the 2 Å second Bohr orbit.

We mentioned that this model only works within the continuous-state holographic multiverse scenario simply because without that utility, especially the inherent synchronization backbone, physics would not go beyond the Kaluza-Klein scenario and remain a ‘curled up at the Planck scale’ model of XD. It is only the continuous-state process of open-closed cyclicalities that allows access (by violating the uncertainty principle) to the additional LSXD. This restriction is not a negative aspect of this proposed multiverse cosmology, but we feel rather that it is suggestive of the correct path that must be taken as it is the actuality of 3rd regime reality.

The key element in this cosmology is the Least Cosmological Unit (LCU). We did not fully invent this concept; but extended the idea found within a chapter called, “The size of the least unit” in a collection edited by Kafatos [50]. But Stevens of course utilizing only the 4D of the standard model attempted to describe a Planck scale least unit. But hopefully you have realized by now that our LCU oscillates from virtual Planck, $(\hbar + T_s)$ to the Larmor radius of the hydrogen atom relative to the nature of its close-packed tiling the spacetime stochastic foam.

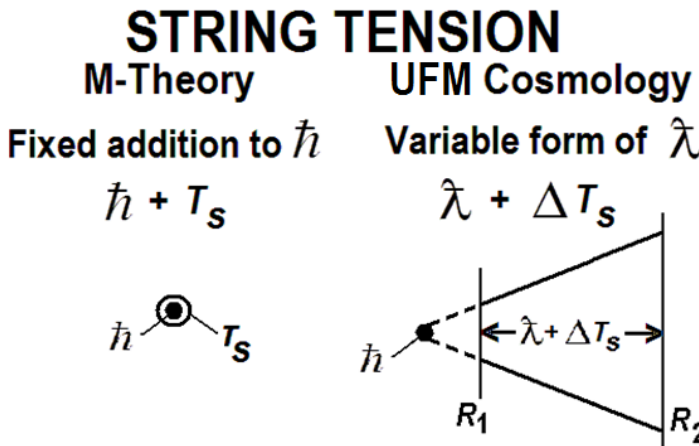


Fig. 6.32. Fixed string tension in M-Theory (left) and variable (right) as in the original hadronic form of string theory and UFM cosmology that also reverts to the original Stoney, $\hat{\lambda}$ rather than Planck’s constant, \hbar .

Since the Planck scale is no longer considered the basement of reality the 12D continuous-state process changes the size of the LCU in the process of Riemann sphere rotation from zero back to infinity continuously. Our choice of the upper limit of the Larmor radius is somewhat arbitrary, and has not been defined rigorously yet; but we assume it is in this ballpark. So just to make a note, we have this oscillating Planck unit, $\Delta\hbar$ at the microscopic level in conjunction with an oscillating $\Delta\Lambda$ lambda or cosmological constant at the macroscopic level.

As an aside this gives us the ability to describe dark matter/energy as an artifact of the rest of the multiverse outside our ~ 14.7 bly radius Hubble sphere. The multiverse has ‘room for an infinite number of nested Hubble spheres each with their own fine-tuned laws of physics’. That scenario provides a UFM model of dark energy. These nested Hubble spheres are closed and finite in time and causally separate in the dimensionality where gravity would take effect, so it’s not like there is an infinite mass acting on us but a much subtler interaction. As well-known the postulate of dark energy and dark matter comes from the knowledge that galactic rotation occurs like a phonograph record not a vortex.

If we think of these nested Hubble spheres like a bunch of grapes they are currently invisible to us because of the nature of the stalk holding the grapes. The parameters of the ‘stalk’ represent a 4th regime of reality. However, it will eventually be possible to design what we have called a Q-telescope to access them for SETI research utilizing UFM [6]. Also see the Drake equation therein.

One of the main conditions of the continuous-state hypothesis comes from an HD extension of Cramer’s Transactional Interpretation with future-past conditions resulting in a present moment [6,37]. This is considered by Cramer as a standing-wave of the future-past with all off diagonal elements considered physically real.

A demonstration of the TBS experiment can be made using a 3-blade ceiling fan symbolic of a quaternion fermion vertex. If one puts one of these fans in front of a mirror (real space) rotating clockwise the mirror image (anti-space) rotates counterclockwise with the blades coming occasionally into phase as in Fig. 6.33. Now we give a key insight into the conceptual simplicity of TBS experiment that Fig. 6.33 doesn’t have. If there is a light on by the fan in real space, i.e. the rf-pulse of our TBS experiment, periodically when the blades come into phase (Fig. 6.33 right side portions) meaning when a blade from real space comes into phase with a blade in the mirror antispace, the light is reflected off each blade (the mirror image of the mirror image) and a pulsating reflected flash of

light occurs in the direction back towards the source/detector. This is representative of how we expect to find the new spectral lines in hydrogen; that we would expect to see a flashing back like a rotating lighthouse beacon when the resonance hierarchy is aligned properly!

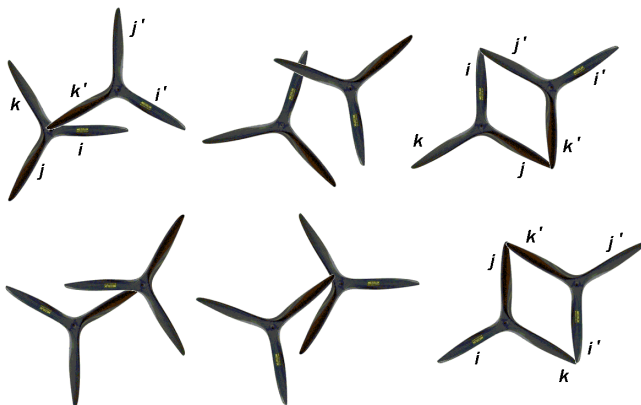


Fig. 6.33. Relativistically rotating quaternion fermionic vertices. In multiverse cosmology the line element, in this case a quaternion Fermionic vertex least cosmological unit (LCU), undergoes continuous-state evolution where as in the figure symmetry periodically arises from the stochastic quantum foam of spacetime possibly indicative of the emergence of observed 3D reality.

That ‘flash’ is would be of course, the 1st 4D TBS spectral line. The manifold of uncertainty (MOU) illustrated in Fig. 6.34 would still remain closed. To discover the 5D and 6D TBS spectral lines, a precision Bessel oscillation to experimentally ‘open’ the QED >4D cavity.

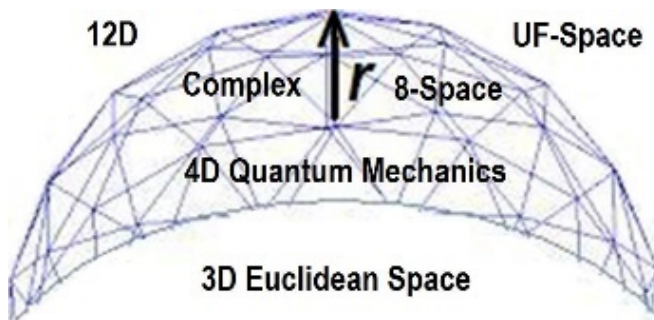


Fig. 6.34. Manifold of Uncertainty (MOU). Quantum Mechanical Uncertainty is predicted to be a Manifold of Finite Radius, r . Beyond the manifold LSXD are postulated.

Rowlands claims in his work using quaternions to describe the fermion as the fundamental condition of physics, that additional space anti-space dimensions are redundant (no new information); and that is acceptable, because that is what we actually want from an infinite nonlocal potentia that is nilpotent and redundant. Surmounting the quantum mechanical uncertainty principle occurs by the same process illustrated in Fig. 6.33 giving us a beat frequency inherent in the space-time backcloth.

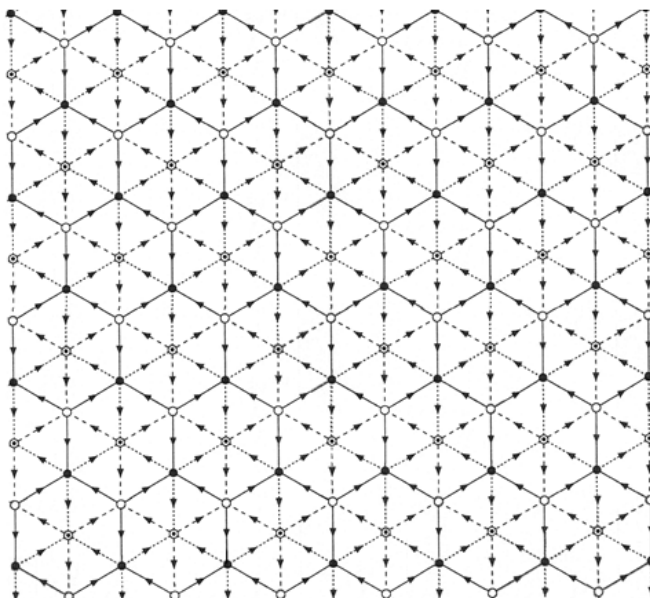
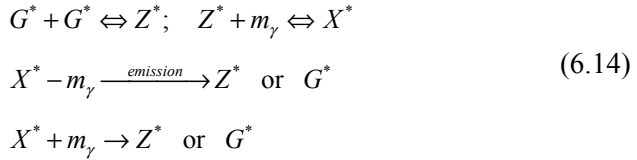


Fig. 6.35. LCU spacetime loses its stochasticity at the semi-quantum limit; and becomes more ordered by coherent control at the upper limit of the ‘manifold of uncertainty’.

The left-hand part of Fig. 6.32 shows the current thinking of string tension but. On the right we see a multiverse version with a variable string tension that oscillates from virtual plank to the Larmor radius of the hydrogen. Notice that the symbol for the Planck constant is different, we use the original Stony [6] that preceded Planck because it is electromagnetic and correlates better with the Dirac polarized vacuum which we want available for resonance hierarchy components of the experimental protocol. Virtual plank is the asymptotic zero point on the Riemann sphere that flips back to infinity in the continuous-state cycle.

The general equations for a putative experimental spacetime exciplex C-QED TBS emission cavity are (see Fig. 6.36):



If you know what an exciplex or excited complex is in chemistry you know that an exciplex never goes back to zero or the ground state. This is in contrast to the current quantum mechanical description of virtual ZPF particles winking in and out of existence at the Planck scale for the Planck time. The space-time exciplex model is one that correlates with the additional parameters of UFM. This again is inherent part of the continuous-state LCU process tessellating space. In terms of cosmology this exciplex provides a mechanism for kicking out a proton [51] where it is said only one proton is needed per 100 cubic kilometers according to Eddington. I mention this to lend support to the possible veracity of this multiverse cosmology. But in UFM cosmology an exciplex LCU structure provides a harmonic gating mechanism for ‘pumping’ coherent control.

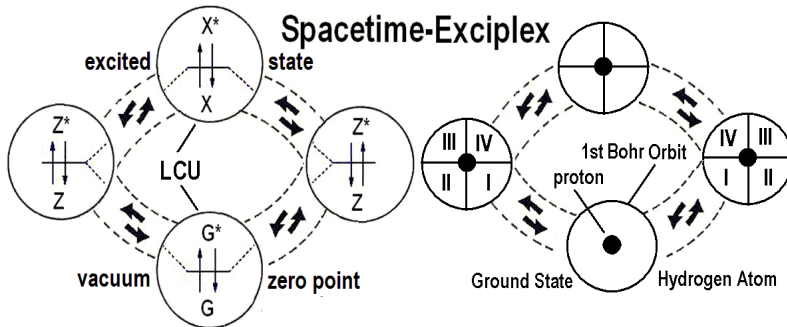


Fig. 6.36. Exciplex Properties of the hidden ‘beat frequency of Spacetime. Exciplex complex and conformal scale-invariant properties related to TBS in the hydrogen atom as it pertains to LSXD and an oscillating form of Planck’s constant fluctuating from asymptotic virtual Planck to the Larmor radius of the hydrogen atom.

In order to demonstrate existence of new spectral lines the TBS experiment itself requires surmounting the quantum uncertainty principle. We hope when applying the guidelines provided by a complex quaternion Clifford algebra it will tell us whether one or two additional doublings of the Rowlands’ space anti-space model are required and then let us know if there’s two or three or more consecutive doubling needed to find four or

five additional spectral lines revealing to us experimentally the complete size of the manifold of uncertainty. Issues of Experimental Design are taken up in Chap. 8. With phase differences the TBS method applies to operating the UFM model of UQC.

6.16 Some Concluding Remarks – Realm of Observation

The space of physical observation is generally considered as an infinite dimensional Euclidean 3-space with the addition of time forming a 4D spacetime continuum. For millennia this is the vantage from which we based our understanding of the universe. Now this is about to radically change. Space is a concept we know absolutely nothing about; likewise, physics has no idea of what a field is. We can label ‘it’ with a metric and measure some perceived properties. The philosopher Kant said, *‘neither space nor time can be empirically perceived; they are elements of a systematic framework that humans use to structure experience’*. Kant further stated that *‘space is subjective, a pure a priori form of intuition contributing to our faculties, a property of the theories we have about the world rather than as a property of the world itself. Physical space has no dimension. Space is defined entirely by the character of the phenomena being measured’* [52].

Kant rejected the view that space must be substantive or relational; he proposed that space and time are not objective features of the world, but are part of a framework for organizing experience [52]. Just as we eventually gave up the notion that the Earth is not the center of the Universe; now we must realize that the Euclidean space we observe and which until now, has been the basis of all physical experimentation, is not real but a virtual resultant or subspace of a deeper reality from which it reduces. This is the space of 12D UFM. There was a hint of this in the development of the quaternion algebra representation, where time was considered real and space complex instead of the obverse utilized instead by the more popular vector algebra which became the standard of physics because of a perceived simplicity for doing calculations.

It is not clear that redefining the basis of observation to HD UFM branes will solve the dilemma raised by Kant. Issues of the observer or the nature of awareness are however finally being brought to the forefront with prospects for empirical mediation [53,54]. Part of the problem that can only be resolved experimentally is the existence of XD [42]; and it won’t

be until then that real progress is made in comprehending why our sensory apparatus isn't built to perceive this HD segment of reality.

Alexander's horned sphere and cat tease our understanding of the uncertainty principle and how to solve the problem of surmounting it by breaking the chain links by implementing an ontological-phase topological field theory (Chap.12). Alexander's Horned Sphere is a fractal-like infinitely repeating pattern of perpendicular circles not quite touching, with an infinite never-ending regress of the same circles in the gap, as in Fig.6.37a [55].

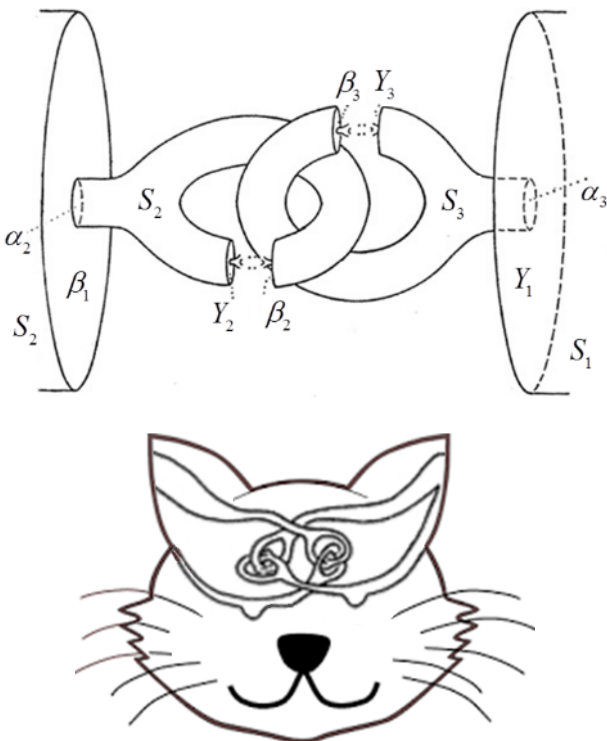


Fig. 6.37. a) Alexander's Horned Sphere. b) Alexander's horn eyed cat. Redrawn from [56]. A surprising ‘miracle’ of UFM is to untie the knot of uncertainty in the eyes of Schrodinger’s cat.

If ‘politically correct’ paths to investigate the fundaments of the observer are myopic to discovery, someone must push that limit. We take some risk here because the 3rd regime of reality, UFM, that we claim mandatory for UQC appears be the same regime that will clarify the role of the observer in observation or measurement [57]. It must be done.

References

- [1] Amoroso, R.L., Kauffman, L.H. & Rowlands, P. (eds.) (2013) The Physics of Reality: Space, Time, Matter, Cosmos, Hackensack: World Scientific.
- [2] Amoroso, R.L., Kauffman, L.H. & Rowlands, P. (eds.) Unified Field Mechanics: Natural Science Beyond the Veil of Spacetime, Hackensack: World Scientific.
- [3] Minkowski, H. (1908) *Raum und Zeit*, Space and Time, *Physikalische Zeitschrift* 10: 75-88.
- [4] Kaluza, T. (1921) *Zum Unitätsproblem in der Physik*. *Sitzungsber. Preuss. Akad. Wiss. Berlin, Math. Phys.* 966-972.
- [5] Klein, O. (1926) *Quantentheorie und funfdimensionale Relativitätstheorie*, *Zeits. Phys.* 37, 895.
- [6] Amoroso, R.L & Rauscher, E.A. (2009) The Holographic Anthropic Multiverse: Formalizing the Geometry of Ultimate Reality, Singapore: World Scientific.
- [7] Amoroso, R.L. & Vigier, J-P (2013) Evidencing ‘tight bound states’ in the hydrogen atom: empirical manipulation of large-scale XD in violation of QED, in Amoroso, Kauffman & Rowlands, The Physics of Reality, Hackensack: World Scientific; or <http://vixra.org/pdf/1305.0053v2.pdf>.
- [8] Amoroso, R.L. (2013) ‘Shut the front door!’: Obviating the challenge of large-scale extra dimensions and psychophysical bridging, in R.L. Amoroso, L.H. Kauffman, & P. Rolands, P. (eds.) The Physics of Reality: Space, Time, Matter, Cosmos, Hackensack: World Scientific.
- [9] Newton, I. (1689) *Philosophiae Naturalis Principia Mathematica*, Scholium to the Definitions, in Bk. 1; trans. A. Motte (1729), rev. F. Cajori, Berkeley: University of California Press (1934), pp. 6-12.
- [10] Amoroso, R.L. (2013) Simple resonance hierarchy for surmounting quantum uncertainty, in R.L. Amoroso, L.H. Kauffman & P. Rowlands (eds.) The Physics of Reality, Hackensack: World Scientific; or <http://vixra.org/pdf/1305.0098v1.pdf>.
- [11] Amoroso, R. L. (2010) Simple resonance hierarchy for surmounting quantum uncertainty, in AIP Conference Proceedings, Vol. 1316, No. 1, p. 185.
- [12] Amoroso, R.L. & Rauscher, E.A. (2010) Tachyon tardon interactions in a Dirac vacuum, in R.L. Amoroso et al (eds.) AIP Conf. Proceedings, Vol. 1316, No. 1, p. 199.
- [13] Biafore, M. (1994) Can quantum computers have simple Hamiltonians? in Physics and Computation, 1994, PhysComp'94, Proceedings, pp. 63-68, IEEE.
- [14] Lindblad, G. (1999) A general no-cloning theorem, Letters in Mathematical Physics, 47(2), 189-196.
- [15] Zhou, D.L., Zeng, B., & You, L. (2006) Quantum information cannot be split into complementary parts, Physics Letters A, 352(1), 41-44.
- [16] Feynman, R.P., Morinigo, F.B., & Wagner, W.G. (1971) Lectures on Gravitation, 1962-63, California Institute of Technology.
- [17] Randall, L. (2006) Warped Passages: Unravelling the Universe's Hidden Dimensions. London: Penguin.
- [18] Sen, R.N. (1999) Why is the Euclidean line the same as the real line? Foundations of Physics Letters 12(4): 325-345.
- [19] Rowlands, P. (2013) Space and antispace, in RL Amoroso, LH Kauffman, & P. Rolands, P. (eds.) The Physics of Reality: Space, Time, Matter, Cosmos, Hackensack: World Scientific.
- [20] Luminet, J.P. (1997) The wraparound universe, AMC, 10, 12.

- [21] Dragić, A., Marić, Z., & Vigier, J-P. (2000) New quantum mechanical tight bound states and ‘cold fusion’ experiments. Physics Letters A, 265(3), 163-167.
- [22] A. Dragic, Z. Maric, & J-P. Vigier (2003) On the possible existence of tight bound states in quantum Mechanics, in R.L. Amoroso et al (eds.) *Gravitation and Cosmology: From the Hubble Radius to the Planck Scale*, pp. 349-386, Dordrecht: Kluwer Academic.
- [23] Amoroso, R.L. (2013) Forward, Biographical reflections on an ‘emperor’s new clothes’ in R.L. Amoroso et al. *The Physics of Reality: Space, Time, Matter, Cosmos*, pp. vii-xii, Singapore: World Scientific.
- [24] Baez, J.C. (2005) On quaternions and octonions: their geometry, arithmetic, and symmetry by J.H. Conway and D.A. Smith, Bull. Amer. Math. Soc. 424, 229-243.
- [25] Hamilton, W.R. (1853) *Lectures on Quaternions: Containing a Systematic Statement of a New Mathematical Method*. Dublin: Hodges and Smith.
- [26] Hamilton, W.R. (1866) *Elements of Quaternions*. London: Longmans, Green.
- [27] Rowlands, P. (2007) *Zero to Infinity: The Foundations of Physics*, Singapore: World Scientific.
- [28] Kauffman, L.H. (2004) Non-commutative worlds. *New Journal of Physics*. 6, 2-46.
- [29] Rowlands, P. (1994) An algebra combining vectors and quaternions: A comment on James D. Edmonds’ paper, *Speculat. Sci. Tech.*, 17, 279-282.
- [30] Rowlands, P. (1996) Some interpretations of the Dirac algebra, *Speculat. Sci. Tech.*, 19, 243-51.
- [31] Rowlands, P. (1998) The physical consequences of a new version of the Dirac equation, in G. Hunter, S. Jeffers, and J-P. Vigier (eds.) *Causality and Locality in Modern Physics and Astronomy: Open Questions and Possible Solutions*, Fundamental Theories of Physics, vol. 97, 397-402, Dordrecht: Kluwer Academic Publishers.
- [32] Lipo, C.P., Hunt, T.L. & Haoa S.R. (2012) The ‘walking’ megalithic statues (moai) of Easter Island, *J Archaeological Science*, 1-8.
- [33] Amazing Video, Walking of the Moai on Rapa Nui (Easter Island) <http://www.youtube.com/watch?v=yvvES47OdmY>.
- [34] Amoroso, R.L. (2012) Rotation in Calabi-Yau Mirror Symmetry like the surface of a brane, London V & A Museum sign, side view, <http://www.youtube.com/watch?v=aat6Oic8biU>,
- [35] Amoroso, R.L. (2012) London V & A Museum sign, end view,<http://www.youtube.com/watch?v=i0QRRcc03wE>.
- [36] Goertzel, B., Aam, O., Smith, F.T. & Palmer, K. (2008) Mirror neurons, mirrorhouses, and the algebraic structure of the self, *Cybernetics & Human Knowing*, Vol. 15, No. 1, pp. 9-28(20)
- [37] Cramer, J.G. (1986) The transactional interpretation of quantum mechanics, *Reviews of Modern Physics*, 58(3), 647.
- [38] Conway J.H. & Smith D.A. (2003) *On Quaternions and Octonions: Their Geometry and Symmetry*, Natic: A.K. Peters Ltd.
- [39] Kauffman, L.H. (2013) Laws of form, Majorana fermions and discrete physics, in R.L. Amoroso et al. (eds.) pp. 1-18, *The Physics of Reality: Space, Time, Matter, Cosmos*, Singapore: World Scientific.
- [40] Kauffman, L.H. (2013) Iterants, Fermions and Majorana operators pp. 1-32, in R.L. Amoroso, L.H. Kauffman, & P. Rowlands (eds.) *The Physics of Reality: Space, Time, Matter, Cosmos*, London: World Scientific.
- [41] Kauffman, L.H. & Ogasa, E. (2012) Local moves on knots and products of knots, <http://arxiv.org/abs/1210.4667v1>.

- [42] Rowlands, P. (2015) How many dimensions are there? In R.L. Amoroso, L.H. Kauffman, & P. Rowlands (eds.) *Unified Field Mechanics: Natural Science Beyond the Veil of Spacetime*, Hackensack: World Scientific.
- [43] Rauscher, E.A., & Amoroso, R.L. (2011) *Orbiting the Moons of Pluto: Complex Solutions to the Einstein, Maxwell, Schrödinger, and Dirac Equations*, Singapore: World Scientific.
- [44] Rowlands, P. (2015) *The Foundations of Physical Law*, London: World Scientific.
- [45] Chantler C.T. (2004) Discrepancies in quantum electro-dynamics, *Radiation Physics & Chemistry* 71, 611–617.
- [46] Chantler, C.T., Kinnane, M.N., Gillaspy, J.D., Hudson, L.T., Payne, A.T., Smale, L.F., Henins, A., Pomeroy, J.M., Tan, J.N., Kimpton, J.A., Takacs, E. & Makonyi, K. (2012) Testing three-body quantum electrodynamics with trapped Ti^{20+} ions: Evidence for a Z-dependent divergence between experiment and calculation, *Physical Rev. Let.* 109, 153001.
- [47] Schild A. (1963) *Phys. Rev.* 131, 2762.
- [48] Barut A.O. (1980) *Surv. High Energy Phys.* 1, 113.
- [49] Feynman, R.P., Leighton, R.B., & Sands, M. (2013) *The Feynman Lectures on Physics*, Desktop Edition, Basic books.
- [50] Stevens, H.H. (1989) Size of a least unit, in M. Kafatos (ed.) *Bell's Theorem, Quantum Theory and Conceptions of the Universe*, Dordrecht: Kluwer Academic.
- [51] Amoroso, R.L. (2015) Multiverse space-antispace dual Calabi-Yau ‘exciplex-zitterbewegung’ particle creation, in R.L. Amoroso, L.H. Kauffman, & P. Rowlands (eds.) *Unified Field Mechanics: Natural Science Beyond the Veil of Spacetime*, Hackensack: World Scientific.
- [52] Kant, I. (1998) *Critique of Pure Reason*, P. Guyer (Trans.) Cambridge: Cambridge University Press.
- [53] Amoroso, R. L. (2013) Empirical protocols for mediating long-range coherence in biological systems, *J Consciousness Explor. & Res.*, Vol. 4:9, pp. 955-976.
- [54] Amoroso, R.L. & Di Biase, F. (2013) Crossing the psycho-physical bridge: elucidating the objective character of experience, *J Consciousness Explor. & Res.*, Vol 4:9, pp. 932-954.
- [55] Bing, R.H. (1983) *The Geometric Topology of 3-Manifolds*, Vol. 40, Am Math. Society.
- [56] Alexander, J.W. (1924) An example of a simply connected surface bounding a region which is not simply connected, *Proc. N. A. S.* 10, 8-10.
- [57] Amoroso, R.L. (2015) Toward a pragmatic science of mind, *Quantum Biosystems*, 6(1) 99-114; [http://www.quantumbiosystems.org/admin/files/QBS%206%20\(1\)%2099-114.pdf](http://www.quantumbiosystems.org/admin/files/QBS%206%20(1)%2099-114.pdf).

Chapter 7

Surmounting Uncertainty Supervening Decoherence

Eliminating ensemble decoherence time and uncertainty in the operation and measurement process of Quantum Information Processing (QIP) systems are remaining problems considered to be of paramount importance in the task of implementing viable bulk scalable Universal Quantum Computing (UQC). Most teams currently attempt to supervene decoherence by utilizing multimillion dollar room sized cryogenic apparatus. If our model is correct, it will allow tabletop room temperature UQC. We theoretically illustrate (in a manner empirically testable) that these conditions essentially become irrelevant in terms of the radical new Unified Field Mechanical (UFM) approach to QIP introduced here. It should be noted that the recent relativistic restrictions the QC research community has imposed on QIP point the way to our model. The additional degrees of freedom obtained by leaving the 3D realm of Euclidean space associated with Newtonian Classical Mechanics and entering the 4D domain of Minkowski 4-space had a profound effect on physics during the last century. Now as we enter a 12D M-Theoretic (String Theory) dual Calabi-Yau mirror symmetric 3-torus 3rd regime associated with UFM, more surprises like the ability to surmount the quantum uncertainty principle are proffered. In this chapter we review a UFM protocol for allowing uncertainty and decoherence to be routinely surmounted and supervened respectively, 100% of the time with probability, $P \equiv 1$. We begin with a discussion of Interaction-Free Measurement (IFM), an interesting 4D precursor providing another indicium of the 12D brane topology model introduced here. IFM is a novel quantum mechanical procedure for detecting the state of an object without an interaction occurring with the measuring device. What we propose is a radical extension of the various experimental protocols spawned by the recent Elitzur-Vaidman IFM thought experiment.

7.1 Phenomenology Versus Ontology

The highly speculative, at time of writing, UFM alternative to IFM protocols, is a single pass ontological method for surmounting uncertainty, without (phenomenological) quantal field interaction or collapse of the wave function. Surmounting the Quantum Uncertainty Principle with probability, $P \equiv 1$ is achieved through utility of the additional degrees of freedom inherent in a new cyclic interpretation of the Calabi-Yau mirror symmetric SUSY regime of string/brane theory. Just as the UV catastrophe provided a clue for the immanent transition from Classical to Quantum Mechanics, duality in the Turing Paradox (quantum Zeno Effect where an unstable particle observed continuously will never decay), suggests another imminent new horizon in our understanding of reality.

IFM as mentioned provides an intermediate indicator of this developing scenario. The quantum Zeno paradox experimentally implemented in IFM protocols hints at the duality between the regular phenomenological quantum theory and a completed unified or ontological model beyond the usual 4D Gauge formalism of the standard Copenhagen interpretation. Utilizing extended theoretical elements associated with a new formulation for the topological transformation of a ‘cosmological least unit’ (LCU), a putative empirical protocol for producing IFM with probability, $P \equiv 1$ is introduced in a manner representing a direct causal violation or absolute surmounting of the putatively inviolate quantum Uncertainty Principle imposed by 4D Copenhagen restrictions.

In the 1970’s the concept of quantum non-demolition (QND) [1] arose as a process for performing very sensitive measurements without disturbing an extremely weak signal which led to the Weber approach for gravitational interferometry. But there was a trade-off between the accuracy of a QND measurement and its inevitable back-action on the conjugate observable to that being measured. Recently myriad new terms have been introduced for programs exploring manipulation of the quantum uncertainty principle [2,3] for non-collapse of the wave function: Negative Result Measurement (NRM) [4], Quantum Non-Demolition (QND) [3,5,6], Interaction Free Measurement (IFM) [7-15], Quantum Zeno Effect (QZE) [16-19], Bang-Bang Decoupling (BBD) [20], Quantum Error Correction (QEC) [21], Quantum Interrogation Measurement (QIM) [22,23], Counter Factual Computing (CFC) [24,25], Absorption-Free Measurement (AFM) [26,27], Quantum Seeing in the Dark (QSD) [28], Quantum Erasure Experiment (QEE) [29,30], Interaction Free Imaging (IFI) [31] and the Bomb Testing Experiment (BTE) [7].

By definition an interaction (phenomenological) is any action, generally a force, mediated by an exchange particle for a field such as the photon in electromagnetic field interactions. This physical concept of a fundamental interaction regards phenomenological properties of matter (Fermions) mediated by the exchange of an energy/momentum field (Bosons) as described by the Galilean, or Lorentz-Poincaré groups of transformations. “*There has been some controversy and misunderstanding of the IFM system concerning what is meant by ‘interaction’ in the context of ‘interaction-free’ measurements. In particular, we stress that there must be a coupling (interaction) term in any Hamiltonian description.*” [32].

This is the distinction we are talking about. The Hamiltonian, H is generally used to express a systems energy in terms of momentum and position coordinates based on forces. While it might bring abject clarity to differentiate the differences between our model and the usual framework of Hamiltonian Mechanics; to do so is beyond the scope of this volume and will be addressed in detail elsewhere. Here we wish to introduce a new ontological type of homeomorphic transformation without the phenomenology of an exchange particle mediated by an ontological interactionless or ‘energyless’ topological switching process based on the concept of ‘topological charge’ in M-Theoretic brane configurations [33].

As indelibly ingrained in the current mindset; it is *impossible by definition* to violate the uncertainty principle, $\Delta x \Delta p_x \geq \hbar / 2$ or $\Delta E \Delta t_x \geq \hbar / 2$ within the framework of Copenhagen phenomenology arising from operation of a ‘Heisenberg Microscope’. This is a *fundamental empirical fact* demonstrated by the Stern-Gerlach experiment where space quantization is produced arbitrarily along the z axis by continuous application of a non-uniform magnetic field to an atomic spin structure [34], or as demonstrated by Young’s double-slit experiment [35] for example. Recent work stemming from the Elitzur-Vaidman bomb-test thought experiment [7] has begun to change the interpretation of this ‘immutable law’! The Elitzur-Vaidman bomb-test experiment was first demonstrated experimentally in 1994 [36] using a Mach-Zehnder interferometer (Fig. 7.1); and soon led to two main procedures for improving probability outcomes:

- 1) Multiple recycled Measurements and
- 2) Multiple array of Interferometers.

The Mach-Zehnder interferometer [37] works by using pairs of correlated photons produced by spontaneous parametric down-conversion from a molecular crystal such as LiIO_3 . Initially in the first experiments

for a 50-50 beam splitter with a 1-time measurement cycle, the IFM probability was 25% according to the formula in Eq. (7.1) [36]; but for repeated measurements and/or various forms of multiple interferometers it was found IFM probability could be arbitrarily increased toward unity as in Fig. 7.2.

$$\eta = \frac{P(Det2)}{P(Det2) + P(Bomb)} \quad (7.1)$$

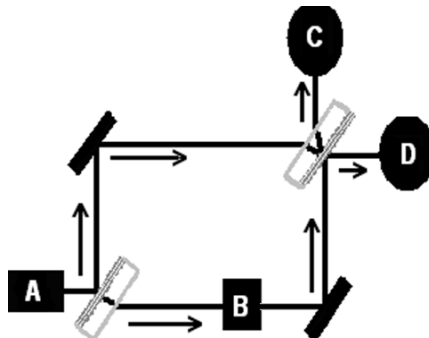


Fig. 7.1. General form of a Mach-Zehnder interferometer used to determine the phaseshift caused by placing a sample in the path of one of two collimated laser beams. **A** is the beam source, **B** the sample and **C & D** the detectors. Note the two types of mirrors utilized.

The probability for the IFM model was suggested to occur in powers of $\pi/2N$ by $P_{IFM} = [1 - 1/2(\pi/2N)^2 + \dots]^{2N}$ where N is the number of beam splitters in the Max-Zehnder interferometer. In his seminal paper (A thought experiment) Elitzur suggested a maximum IFM of 50%. Thereafter Kwiat's team developed a method to improve the model to 80% with $P_{QSD} = 1 - (\pi^2/4N) + O(1/N^2)$ where in this case N is the number of photon cycles through the apparatus [36]. In regards to the Elitzur and Vaidmann consideration that their model could be explained by the 'Many-Worlds' interpretation Cramer proposed, "they suggest that the information indicating the presence of the opaque object can be considered to come from an interaction that occurs in a separate Everett-Wheeler universe and to be transferred to our universe through the absence of interference" [38].

In terms of creative processes in the history of scientific progress, it is profoundly interesting to note that Cramer's suggestion, 'the idea of a Many-Worlds interpretation to explain how IFM works', is an LD shadow the new HD UFM model! In the UFM model of LSXD Calabi-Yau mirror symmetry the supposition is that the 4D Cavity-QED 'particle in a box' state has conformal scale-invariant Supersymmetric (SUSY) 'mirror copies' inherent in the HD Calabi-Yau brane topology [39,40]. Thus if the experimental protocol proposed here is successful it will demonstrate that the IFM model is not suggestive of a reality with 'many parallel worlds' but provides instead indicia of Calabi-Yau mirror symmetric topological 'copies' extending 'our' reality beyond the veil of stochastic spacetime [40] to a 3rd UFM regime with LSXD; and that these extra degrees of freedom, when properly accessed, allow the uncertainty principle to be surmounted in one pass with probability, $P \equiv 1$.

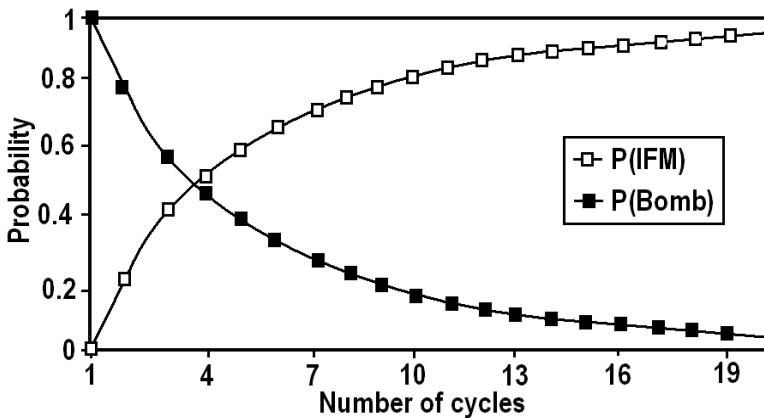


Fig. 7.2. IFM probability as shown to be arbitrarily increased toward unity by repeated measurements. Figure adapted from [36].

In this chapter a putative protocol is delineated, not for another sophisticated improvement of the varied stepwise degrees of violating the uncertainty relation by the several IFM protocols; but for completely surmounting the uncertainty relation directly, in a straight forward manner, for any and every singular resonant action, with probability, $P \equiv 1$. As stated in an unexpected way our model has similarities to IFM/QSD, but instead uses extended quantum theory and newly developing UFM theory [40] to fully complete the task of uncertainty violation. The HD regime of the unified protocol is like a complete IFM fun house 'hall of mirrors' where the whole battery of interferometers and

multiple cycling routines is inherent in the HD mirror symmetric brane regime, such that only one ‘ontological measurement’ is required to obtain probability, $P \equiv 1$. We emphasize that the methodology of this new empirical protocol is completely ontological (rather than usual phenomenological field couplings mediated by energy exchange quanta) with action in the HD SUSY regime in causal violation of the 4D Copenhagen phenomenology, not in an Everett ‘many-worlds’ sense [41], but in a manner that extends to completion the de Broglie-Bohm-Vigier causal interpretation of quantum theory [42] with a so-called ‘super-quantum potential’, the ontological ‘force of coherence’ of UFM (not a 5th force). The ontological basis is realized utilizing the additional degrees of freedom of a 12D version of M-Theory [43] along with the key supposition of conformal scale-invariance pertaining to the state of quantum informational SUSY brane mirror symmetric copies extended to Large-Scale Additional Dimensions (LSXD) [39].

While considerations of the vacuum bulk are of paramount concern for string theory, much of its putative essential parameters used here are ignored in the avid exploration of other parameters. The $P \equiv 1$ model also relies heavily on the existence of a Dirac covariant polarized vacuum [44-46]. Of primary concern at this point of our development is the Dirac vacuum inclusion of extended electromagnetic theory [47-49] which is a key element in manipulating the structural-phenomenology of LSXD SUSY brane topology with a spin-exchange resonant hierarchy.

The experimental design relies heavily on the utility of a new fundamental action principle inherent in the LSXD cyclical brane topology putatively driving the evolution of self-organization in spacetime as a complex system of cellular automata-like Least Cosmological Units (LCU) tessellating space [39]. Stated more directly, space, spacetime (no longer considered fundamental but emergent) and the HD mirror symmetric Calabi-Yau brane structure is an evolutionary form of self-organized complex system.

The new action principle is suggested not to be a 5th force of nature per se, but a combination of the four known forces as united in the unified field (not quantized). Initially this can appear confusing because the three known forces are phenomenological in action, i.e. mediated by the Hamiltonian for phenomenological energetic field exchange quanta, whereas the topological field is mediated by an ‘ontological charge’ of the unified field. Which is therefore energyless by definition, albeit it acts as a ‘force of coherence’ in conjunction with the driving of LSXD brane conformation dynamics. Continuous evolution of the ontology is a form

of ‘becoming’ or merging of one informational aspect with another without the exchange of energy, as in the until now usual sense of a physical field [39]. This key UFM aspect is difficult to comprehend at first, because it is also a challenge for us to explain.

Topologically, the HD Calabi-Yau mirror symmetric copies, $\pm\mathbb{C}^4$ in Fig. 7.3 are in constant motion [39,40]. Later we will see this inherent synchronization backbone (as called for by Feynman) is essential to providing a resonance hierarchy ‘beat frequency’ for surmounting uncertainty, and of paramount importance to QIP for bulk UQC.

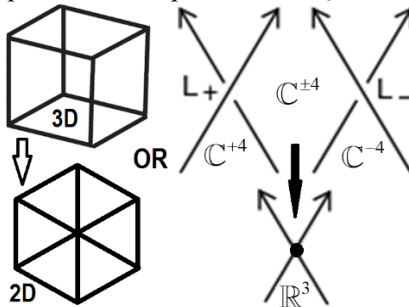


Fig. 7.3. Euclidean 3-space, \mathbb{R}^3 as a ‘fixed’ shadow of LSXD Calabi-Yau, L, R mirror symmetric topological brane (crossover) components in continuous-state cyclic evolution, with 4 complex HD dimensions suppressed for simplicity.

The field concept is a supporting paradigm of the entire edifice of modern physics; until now specifically for phenomenological field dynamics only. Be reminded that physically, physicists have no idea what a field is, we are only able to associate it with a metric and parametrize various phenomena. Our view of what constitutes an ontological field is radically different. We do not feel equipped to definitively define the distinction rigorously in this volume (as the whole nascent edifice of UFM has yet to even reach infancy); but realize we cannot get away with saying nothing either (Chap. 12). We want to let experiment drive theory at this moment in development [39,40]. Suffice it to say the ontological properties of the dynamics inherent in the HD unified field theoretic topological brane world do not transfer energy, and the ‘exchange’ of information also does not occur in time; further hinting at bringing into question the historically fundamental basis of ‘locality and unitarity’. The best metaphor we know for energyless ontological charge is the switching of central vertices of the ambiguous Necker cube when stared at (Fig. 7.4a).

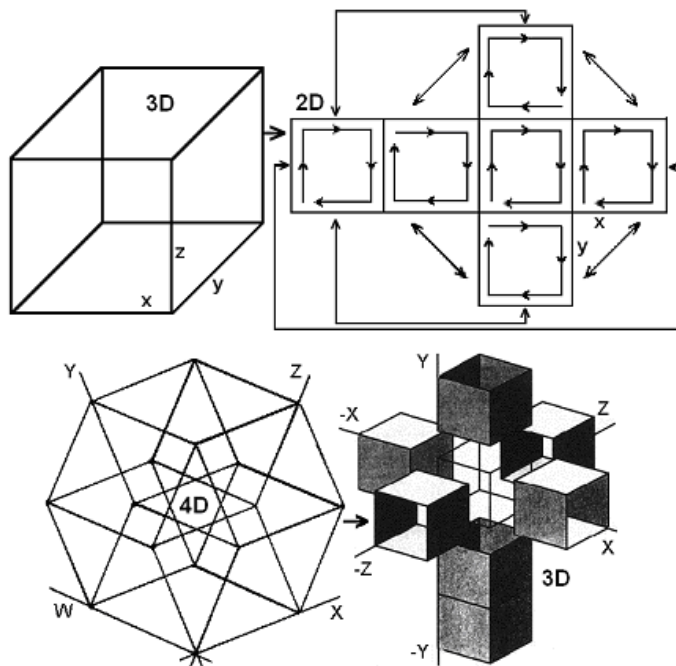


Fig. 7.4. Dimensional reduction. The suggestion is that the central translucent cube in the lower right represents a 4D CQED ‘particle in a box’ quantum state that through conformal scale-invariance remains physically real when the metaphor is carried to 12D where the nilpotent space-antispace state components become like the ‘mirror image of a mirror image’ and in that sense is causally free of the localized, E_3 quantum state, thereby open to ontological ‘energyless’ information transfer in violation of Copenhagen uncertainty.

Regarding Fig. 7.4, there is no ‘event’ relative to the perceived switching of the vertices of the metric of the cube in 3D (rather suggested to occur in 4D extensions like the spherical rotation of the Dirac electron requiring 720° to complete). For a cellular automata-like close-packed 12D dual space tessellation of an array of such hyperspherical objects, (the 3D nilpotent resultant designated as quantum particle/states in a box) we propose that quantum entanglement occurs in a conformal scale-invariant LSXD brane topology with inherent cyclic mirror symmetric copies of the usually considered stationary 3D Cavity-QED quantum ‘particle in a box’. This provides sufficient degrees of freedom for allowing quantum uncertainty to be surmounted, thus avoiding problems associated with decoherence times in QC. In this scenario quantum mechanical uncertainty is a manifold of finite radius separating two regimes of infinite size

dimensionality - the 3(4)D Euclidean/Minkowski and a complexified mirror symmetric 8D LSXD M-Theoretic brane world [40].

The de Broglie-Bohm-Vigier Causal [42] and Cramer Transactional Interpretations [38,50] have generally been ignored by the physics community for various reasons; most saliently considered to add nothing new or are incomplete interpretations. The Quantum Potential-Pilot Wave model is extended to a form of ‘Super Quantum Potential’ synonymous with a putative action of the Unified Field; the future-past parameters of Cramer’s model [50] enhance the hierarchy of Calabi-Yau mirror symmetry annihilation-creation parameters. The two theories together form key pillars for an ontological basis of the predicted ‘Force of Coherence’ of the Unified Field which is a mandatory requirement in the new model for developing UQC.

If the metaphor in Fig. 7.4 is carried to 5D, the ‘cross’ in the lower right corner would be comprised of 4D hypercubes instead of the 3-cubes shown in the dimensional reduction. Table 7.2 below shows the geometric content of spacetime carried to 12D. Our scale-invariant theory predicts that the 12D copy of the quantum state is causally free of the 3D shadow of this quantum state or ‘particle in a box’ (3D generator is a misnomer as used in terms of the usual sense of a Euclidean observer - The 3D quantum state or particle in a box is the resultant in terms of the 12D model of nilpotent potentia [39]). The task of this chapter is to elucidate the methodology for surmounting uncertainty in this LSXD context. The experimental apparatus, a multi-level rf-pulsed interferometer, is designed to focus/mediate/manipulate this unitary field. It is going to be a severe challenge for a while longer to encapsulate the observer physically. The 3-space we observe is virtual; the physically real space is the hidden HD space [39,40]. Fortunately, we can perform our proposed experiment without getting any acceptance of this temporary ‘heresy’; be advised von Neumann said something similar, only now we are nearly able to do something about it.

As we hope to show the protocol relies on the symmetry conditions of new self-organized cosmological parameters amenable to a resonant hierarchy of coherently controlled topological interactions able to undergo what Toffoli calls ‘topological switching’ as the energyless basis for the Micromagnetics [33] of information exchange. Finally, to complete the concatenation of concepts we utilize theoretical modeling in conjunction with the parameters associated with a covariant polarized Dirac vacuum [44-46] (another heresy) as described from the context of extended electromagnetic theory [47-49] (more heresy). In other Chaps. we show how this model relates to an M-Theoretic dual form of Calabi-Yau mirror

symmetry; the conceptual mantra of which is: Continuous-state, spin-exchange, dimensional reduction, compactification process. Not a unique 4D compactification to the standard model as sought by string theorists, but a continuous cyclic dimensional reduction $12D \rightleftharpoons \sim 0D$ symmetry exchange through pertinent aspects of all five M-Theories [39,40].

7.2 The Turing Paradox and Quantum Zeno Effect

By using the quantum Zeno effect, also known as the Turing paradox, the efficiency of an IFM can be made arbitrarily close to unity.

“It is easy to show using standard theory that if a system starts in an eigenstate of some observable, and measurements are made of that observable N times a second, then, even if the state is not a stationary one, the probability that the system will be in the same state after, say, one second, tends to one as N tends to infinity ... continual observations will prevent motion ...” – A. Turing [51].

The Turing Paradox, also called the Quantum Zeno Effect, is a scenario where a particle observed continuously will never decohere; in a sense the evolution of the system is frozen by frequent measurement in its initial state. More technically the Quantum Zeno Effect can suppress unitary time evolution not only by constant measurement, but applying a series of sufficiently strong fast pulses with appropriate symmetry can also decouple a system from its decohering environment or other stochastic fields [52-60].

Cramer has suggested that IFM can be interpreted by utilizing the Everett ‘Many Worlds Hypothesis’ to explain the subtleties of the quantum Zeno paradox [3,38]. While Cramer’s hypothesis is certainly logical we believe nature in higher dimensions (HD) is more surprising [39,40]. The Standard Model of Quantum Mechanics predicts that physical reality is influenced by events that can potentially happen (Heisenberg potentia) but factually do not occur. Peise [58] suggests that IFM exploits this counterintuitive influence to detect the presence of an object without requiring any interaction with it. *“Here we propose and realize an IFM concept based on an unstable many-particle system. In our experiments, we employ an ultracold gas in an unstable spin configuration, which can undergo a rapid decay. The object (realized by a laser beam) prevents this decay because of the indirect quantum Zeno effect and thus, its presence can be detected without interacting with a single atom. Contrary to existing proposals, our IFM does not require*

single-particle sources and is only weakly affected by losses and decoherence. We demonstrate confidence levels of 90%, well beyond previous optical experiments.” [58].

Our UFM model is radically different [39,40]. There is, in a sense, no interaction [32,39], but not in the sense Paise suggests. His claim is based on the usual ‘quantal or phenomenological’ form of interaction. But as we shall see in later chapters, there is another UFM type of ‘energyless’ ontological interaction or exchange of information based on ‘topological charge’ in HD brane topology [39,40] described by a new 3rd regime theory we call ‘Ontological-Phase Topological Field Theory’(OPTFT). This model arises in answer to recent forays into relativistic information processing [61-64] calling for an end to the historically fundamental utility of ‘locality and unitarity’ as the basis for describing the nature of reality [65-67]. The measurement problem is not yet solved.

The recent introduction of relativistic parameters, including relativistic r-qubits, into quantum information processing has compounded the dilemma bringing up new questions in terms of Bell’s inequalities, the no-cloning and quantum erasure theorems. Correspondence to the epistemic view of the Copenhagen Interpretation versus the ontic consideration of objective realism and as merged by W. Zurek’s epi-ontic blend of quantum redundancy in quantum Darwinism will be discussed [68,69]. Finally, after making further correspondence to current thinking in terms of the dual amplituhedron we delve into the ontological topology of UFM requiring a new set of topological transformations beyond the Galilean, Lorentz-Poincaré. We hope to have taken a bold step at least philosophically correct into the new UFM arena.

7.3 From the Perspective of Multiverse Cosmology

Comprehending the $P \equiv 1$ model from the perspective of cosmology is only necessary for more fully understanding the context from which developing the experimental protocol arises; otherwise the reader may skip to the next section, especially since no one seems to understand it very well yet anyway. When physicists last embraced a 3D Newtonian world view about a hundred years ago, the universe was believed to be a predictable mechanical clockwork. Since the advent of Quantum Theory (QT) reality has been considered to be stochastic and statistical or uncertain with a Planck scale basement. Following this line of reasoning when a Theory of Everything (TOE) is realistically discovered based on formalizing a unified field, should some form of fundamental monism be

embraced? Although the fermionic point-particle is considered the basic unit of physics, this concept is embedded in the global context of cosmology. We postulate that additional cosmology is required to understand the basis for bulk Universal Quantum Computing (UQC) because cosmology ultimately speaks to the nature of reality and the ultimate basis for the Fermionic singularity or point particle; and we are finding out that using a nonphysical mathematical calculation space is not sufficient for UQC implementation. The three regimes stated above (classical, quantum and unified field TOE) are currently thought to have a Planck-scale ‘basement of reality’. It remains impossible to surmount uncertainty in this context; it is perceived as an inadequate view requiring a reality with an open LSXD ‘continuous-state’ process instead of an impenetrable basement barrier [39]. Not seeing XD because they are curled up at the Planck scale is not the only interpretation. If the continuous-state process includes a form of ‘subtractive interferometry’, like discrete frames of film passing through a movie projector appearing continuous on the screen, additional dimensionality can be large scale. Experiments under development at CERN are trying to make this discovery, our proposal however, is tabletop and low energy [39,40].

Regarding ‘Continuous-State’: Imagine Einstein’s elevator metaphor with an observer inside in freefall. Next imagine an amusement park pin raster (pins as points in spacetime) with the little ball bouncing stochastically off the nails towards a slot at the bottom of the device. Now consider the observer inside the elevator to be the falling ball. But instead of the ball being drawn gravitationally toward a final slot at the bottom (pulled toward center of the Earth by G), imagine that the pin raster continuously rotates (hyperspherically) so that the ball perpetually remains at the center as if it were in continuous freefall. Also that the ball is not a OD vertex, but comprised of HD cyclic brane topology [39]; with a point in reality a dynamic transformation comprised of a Wheeler-Feynman-Cramer-like complementarity [50,70] of the three regimes in a background independent environment [71-74] as outlined in another chapter.

Einstein stated that ‘all of physics’ is based on measurements of *duration* and *extension*. This has occurred historically within the parameters of a 3D Euclidean, and in recent times, a 4D Minkowski-Riemann energy dependent spacetime metric, \hat{M}_4 under Gauge parameters utilizing various forms of the E_3 / \hat{M}_4 Galilean-Lorentz-Poincaré transformations describing classical, quantum and relativistic conditions. These criteria are perceived herein as insufficient for UQC operations, and

indeed our protocol for surmounting the uncertainty principle requires inclusion of another cosmological regime - Unified Field Mechanics (UFM) [39,40] described by a new set of 12D transformations we propose calling the ‘Noetic UFM Transformation’ because of its relevance to aspects of a Holographic Anthropic Multiverse correlated with the observer and meaning of the Greek term noetic as ‘hidden’. In this regard in spite of Bell’s theorem, following Einstein’s dice playing conundrum, we restate his complaint that quantum theory is incomplete and therefore inadequate in current form for supervening some quantum processes.

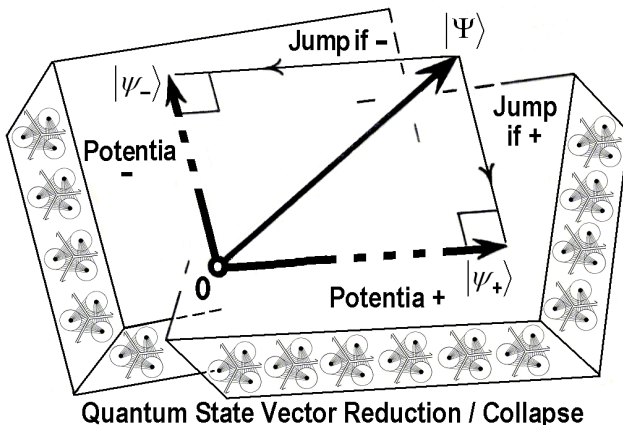


Fig. 7.5 A way to conceptualize a transaction as a collapse, $|\Psi\rangle$ to the 2D Euclidian plane from, in this case, an HD potentia of two possible orthogonal states, $|\psi_+\rangle, |\psi_-\rangle$ mediated by the underlying nilpotent annihilation-creation process inherent in the Least Cosmological Units (LCU) tessellating space behind the finite radius veil of uncertainty. The LCU array can be compared to Fig. 7.7 where a Euclidean cube emerges from spacetime ‘lattice gas’. (Illustrated here as a 3rd dimension with 9 others suppressed).

Cramer’s transactional model of QT [50] has been ignored by the physics community for a variety of reasons we will not address now. Its marginalization means that it’s utility as a key foundation of extended UFM cosmology is not well received. Cramer based his interpretation on the Wheeler-Feynman Absorber Theory [70]. Thus a *Cramer transaction* entails Wheeler-Feynman-like future-past, standing-wave symmetry conditions to describe a present instant which when extended to the HD SUSY regime readily lends itself as a foundation for Calabi-Yau mirror symmetry conditions inherent in a unique background independent 12D

brane iteration of M-Theory [43] (derived elsewhere). Note: Some have criticized Cramer's standing-wave concept as simplistic. This might of course be valid for a line element as a 1D string; but we feel the model when sufficiently developed for 9D hyperspherical brane topology as required by our model; it is sufficient as it becomes synonymous with a 6D Calabi-Yau Kahler manifold. In differential geometry, a Kahler manifold has three mutually compatible structures; a complex structure, a Riemannian structure, and a smooth symplectic differential 2-form.

Furthermore, we suggest that the UFM 12D noetic transform adds additional de Broglie-Bohm piloting-super-quantum potential [39,40] parameters, suggesting a duality to the regime of quantum mechanics – that of the observed 4D phenomenological interaction associated with the uncertainty principle; and another ontological HD nilpotent 'piloted' regime associated with the coherent force of the unified field. There seems to be a 'semi-quantum limit' associated with a manifold of uncertainty (MOU) of finite radius as the lower bound with an inherent gating mechanism (uncertainty) blocking entry to the LSXD beyond. Experiment will settle this issue [39,40].

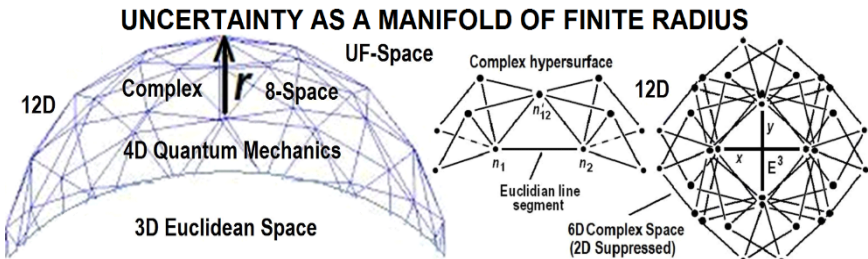


Fig. 7.6. Manifold of uncertainty of finite radius in the semi-quantum limit as a transition barrier between infinite dimensional Euclidean space and LSXD infinite dimensional UFM space. Because of Calabi-Yau dual 3-tori mirror symmetry we suspect it is a 5D manifold with the 6th dimension degenerate ending the domain wall. Experiment will test this limit.

As discussed in Chap. 3, reality completed by UFM, is a multi-tiered duality of a virtually static Euclidean subspace manifold with a dynamic HD de Broglie-Bohm piloted Cramer-like continuous-state standing-wave cyclical evolution. Because the external world we observe is this limited virtual submanifold of a more complete nilpotent (sums to zero) [39] contiguous superspace, some elements are removed from observation by subtractive interferometry [39]. This interpretation suggests that the reason additional XD brane dimensionality is not observed is not because

it is curled up microscopically at the Planck scale, but because subtractive interferometric annihilation-creation vectors of the nilpotent standing-wave process of the localized line element ‘erase’ the HD generators of the present moment keeping those parameters hidden from the observer’s view by a Heisenberg microscope because of the observational limit to our sensory apparatus provided by the veil of uncertainty.

In the standard Copenhagen Interpretation of QT an event emerges only as a result of measurement and objective reality is considered limited to probability. Cramer considers ‘all off diagonal elements of the line element physically real’ during the process of the offer-wave-confirmation-wave process preceding a local transaction (event) [50]. We may call the final event a resultant of the conditions of Heisenberg Potentia. Here we wish to consider (a more complete) reality that has remained illusory to the Minkowski observer hidden to the temporal observer behind the veil of the uncertainty principle.

Issues regarding the nature of the fundamental cosmological background continue to be debated with disparate views jockeying for philosophical supremacy; a scenario remaining tenable because experimental avenues for testing physics beyond the standard model have remained elusive. In our favor deeper and deeper cracks are occurring in QED violation [75]. QED is a relativistic quantum field theory of electrodynamics; the most stringently tested and most accurate theory in physics specifically for measurements of the fine structure constant, α , where $\alpha^{-1} = 137.035999074(44)$, from CODATA 2010. QED violation suggests we are on the brink of falsifying quantum mechanics in 4D [39,40,75]. Absolute truth occurs in science when a theory becomes falsified. In this respect with the advent of Quantum Mechanics the Newtonian Classical world view became an ‘absolute truth’ in the finite domain it describes. UFM is presenting a similar scenario for the falsification of Quantum Mechanics.

Here a putative empirical protocol is devised for manipulating a HD form of the so-called covariant Dirac polarized vacuum (DPV) [47-49] providing a methodology for both surmounting uncertainty and low energy protocols for testing the dimensionality of string theory. The DPV has a sixty-year history in the physics literature [44-49] which has for the most part been ignored by the main stream physics community for a number of philosophical conflicts most notably the DPV, and its associated Extended Electromagnetic Theory which includes photon mass, is erroneously perceived to conflict with the highly successful Gauge Theory. As well-known Gauge theory is an approximation, suggesting

additional physics. The problem of surmounting uncertainty is simplistically solved by the utility of additional degrees of freedom introduced by a UFM multiverse cosmology and the associated extended theoretical elements. We will develop salient features as we proceed.

7.4 Micromagnetics and LSXD Topological Charge Brane Conformation

An extensive body of literature exists for phenomena related to the zero-point field; but relative to unified theory this work is considered metaphorically descriptive only of the ‘fog over the ocean’ rather than the structural-phenomenology of the ocean itself. Instead a deep HD structure with a real covariant DPV at its foundation is utilized [44-46]. The Casimir, Zeeman, Aharonov-Bohm and Sagnac effects are considered evidence for a Dirac vacuum. New assumptions are made concerning the DPV relating to the topology of spacetime and the structure of matter cast in a 12D form of Relativistic Quantum Field Theory (RQFT) in the context of the Holographic Anthropic Multiverse (HAM) cosmological paradigm [39]. In this cosmology the observed Euclidian-Minkowski spacetime present, $E_3 - \hat{M}_4$ is a virtual standing wave of highly ordered Wheeler-Feynman-Cramer retarded-advanced future-past parameters respectively [50,70]. See Figs. 7.22 & 7.23 for a graphic illustration of this paradigm. An essential ingredient of HAM cosmology is that a new action principle synonymous with the force of coherence of the unified field arises naturally and is postulated to drive self-organization and evolution through all levels of scale [39,40].

In this context an experimental design [39,40] is introduced to isolate and utilize the new UFM action to test empirically its putative ability to effect conformational structure of the topology of spacetime to surmount the usual phenomenologically based uncertainty in an ontological matter with probability, $P \equiv 1$. Properties of the Least Cosmological Unit (LCU) is an essential key factor in the experimental design.

Unified Theory postulates that spacetime topology is ‘continuously transformed’ by the self-organizing properties of the long-range coherence of the unified field [39,40]. In addition to manipulating conformational change in HD brane topology, from the experimental results we attempt to calculate the energy Hamiltonian required to manipulate Casimir-like boundary conformation in terms of the unified field equation, $F_N = \mathbf{x} / \rho$

(simple unexpanded form - derived in Chap 3). This resonant coupling produced by the teleological action of the unified field driving its hierarchical self-organization has local, nonlocal and supralocal¹(complex LSXD) parameters. The Schrödinger equation, extended by the addition of the de Broglie-Bohm quantum potential-pilot wave mechanism has been used to describe an electron moving on a manifold; but this is not a sufficient extension to describe HD unified aspects of the continuous-state (Chap. 3) symmetry breaking of spacetime topology which requires further extension to include action of the unified field in additional dimensions.

The basic time dependent Schrödinger equation takes the form

$$i\hbar \frac{\partial}{\partial t} \Psi(r,t) = \left[-\frac{\hbar^2}{2m} \nabla^2 + V(r,t) \right] \Psi(r,t) \quad (7.2)$$

where i is the square root of -1, \hbar the reduced Planck constant, t time, r position, $\Psi(r,t)$ the wave function, ∇^2 the Laplacian operator and $V(x)$ is the potential energy as a function of position. The simplest de Broglie-Bohm pilot wave addition is

$$i\hbar \frac{\partial}{\partial t} \Psi(r,t) = \left[-\frac{\hbar^2}{2m} \nabla^2 + V(r,t) - Q \right] \Psi(r,t) \quad (7.3)$$

with the quantum force potential $Q = -\frac{\hbar^2}{2m} \frac{\nabla^2 \sqrt{\rho}}{\sqrt{\rho}}$.

I have not found any attempt in the literature to extend the de Broglie-Bohm pilot wave-quantum potential to String/M-Theory in the literature, which is one of several key criteria for developing our UFM model. But there is a small body of literature correlating de Broglie-Bohm with the Dirac equation [76].

¹ Nonlocal, complex regime of instantaneous action at a distance; by ‘supralocal’ we mean LSXD aspects with additional UFM complex topological properties. It may be that nonlocal should incorporate what we call here supralocal UFM parameters; but a distinction needs to be made and we are not there yet with clarity in that decision.

The nilpotent Dirac equation is an intermediate step for our UFM needs. Following Rowlands [77], who firmly believes in the utility of quaternionic algebra in simplifying particle physics [78-84].

Rowlands claims particle physics is more easily understood if the Dirac equation is expressed algebraically, replacing the gamma matrices by equivalent operators from vector and quaternion algebra [78-84]. Unit quaternion operators ($1, \mathbf{i}, \mathbf{j}, \mathbf{k}$) are defined according to the usual rules:

$$\begin{aligned} i^2 = j^2 = k^2 = ijk &= -1 \\ ij &= -ji = k; \quad jk = -kj = i; \quad ki = -ik = j, \end{aligned} \tag{7.4}$$

with multivariate 4-vector operators ($i, \mathbf{i}, \mathbf{j}, \mathbf{k}$), which are isomorphic to complex quaternions or Pauli matrices:

$$\begin{aligned} i^2 = j^2 = k^2 &= 1 \\ ij &= -ji = ik; \quad jk = -kj = ii; \quad ki = -ik = ij. \end{aligned} \tag{7.5}$$

Combination these two sets of units produces a 32-part algebra (group of order 64, with both + and - signs), which can be directly related to that of the five γ matrices, with mappings of the form:

$$\gamma^0 = -ii; \quad \gamma^1 = ik; \quad \gamma^2 = jk; \quad \gamma^3 = kk; \quad \gamma^5 = ij. \tag{7.6}$$

or, alternatively,

$$\gamma^0 = -ik; \quad \gamma^1 = ii; \quad \gamma^2 = ji; \quad \gamma^3 = ki; \quad \gamma^5 = ij. \tag{7.7}$$

Application directly to the conventional form of the Dirac equation,

$$\left(\gamma^0 \frac{\partial}{\partial t} + \gamma^1 \frac{\partial}{\partial x} + \gamma^2 \frac{\partial}{\partial y} + \gamma^3 \frac{\partial}{\partial z} + im \right) \psi = 0, \tag{7.8}$$

we obtain:

$$\left(-ii \frac{\partial}{\partial t} + ki \frac{\partial}{\partial y} + kj \frac{\partial}{\partial x} + kk \frac{\partial}{\partial z} + im \right) \psi = 0. \tag{7.10}$$

Multiplying the equation from the left by \mathbf{j} alters the algebraic representation to (7.10) and the Dirac equation becomes:

$$\left(i\mathbf{k} \frac{\partial}{\partial t} + i\mathbf{i} \frac{\partial}{\partial y} + i\mathbf{j} \frac{\partial}{\partial x} + i\mathbf{k} \frac{\partial}{\partial z} + ijm \right) \psi = 0. \quad (7.11)$$

The Dirac equation allows four solutions, corresponding to the four fermion – antifermion combinations, with spin up and spin down, which can be arranged in a column vector, or as a Dirac 4-spinor. Here, we identify the solutions as produced by the combinations of $\pm E, \pm \mathbf{p}$ (or $\boldsymbol{\sigma} \cdot \mathbf{p}$). Rowlands writes these terms in the form:

$$\begin{aligned} \psi_1 &= (\mathbf{k}E + i\mathbf{i}\mathbf{p} + ijm) e^{-i(Et - \mathbf{p} \cdot \mathbf{r})} \\ \psi_2 &= (\mathbf{k}E - i\mathbf{i}\mathbf{p} + ijm) e^{-i(Et + \mathbf{p} \cdot \mathbf{r})} \\ \psi_3 &= (-\mathbf{k}E + i\mathbf{i}\mathbf{p} + ijm) e^{i(Et - \mathbf{p} \cdot \mathbf{r})} \\ \psi_4 &= (-\mathbf{k}E - i\mathbf{i}\mathbf{p} + ijm) e^{i(Et + \mathbf{p} \cdot \mathbf{r})} \end{aligned} \quad (7.12)$$

and apply a single differential operator, but it is more useful to remove the variation in the signs of E and \mathbf{p} from the exponential term, by making the differential operator a 4-term row vector, which, in the equation, forms a scalar product with the Dirac 4- spinor. Incorporating all four terms into a single expression, we obtain

$$\left(\pm i\mathbf{k} \frac{\partial}{\partial t} \pm i\mathbf{\nabla} + ijm \right) (\pm \mathbf{k}E \pm i\mathbf{i}\mathbf{p} + ijm) e^{-i(Et - \mathbf{p} \cdot \mathbf{r})} = 0 \quad (7.13)$$

as the new version of the Dirac equation for a free particle [81]. Reducing this to the eigenvalue form, and multiplying out, produces the classical relativistic momentum-energy conservation equation:

$$(\pm \mathbf{k}E \pm i\mathbf{i}\mathbf{p} + ijm)(\pm \mathbf{k}E \pm i\mathbf{i}\mathbf{p} + ijm) = E^2 - p^2 - m^2 = 0. \quad (7.14)$$

It is significant that there are exactly four solutions to the Dirac equation. Both quaternion and complex operators require equal representation for + and – signs, suggesting eight possible sign

combinations for $\pm \mathbf{k}E \pm i\mathbf{p} + ij\mathbf{m}$; but only four of these will be independent, since the overall sign for the state vector is an arbitrary scalar factor. Thus the sign of one kE , $i\mathbf{p}$ or $ij\mathbf{m}$ must behave as if fixed. With only E and \mathbf{p} terms represented in the exponent, it is evident that the fixed term is m . Four solutions also result from the fact that quaternionic structure of the state vector can be related to the conventional 4×4 matrix formulation with quaternionic matrices. The conventional formulation is itself uniquely determined by the 4D spacetime signature of the equation, a 2nD spacetime requiring a $2^n \times 2^n$ matrix representation of the Clifford algebra [82].

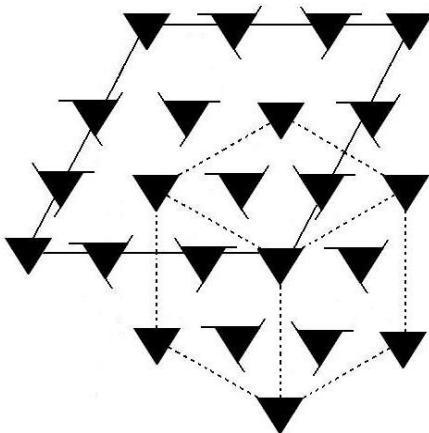


Fig. 7.7 HD emergence of structure from a LD lattice gas tessellation. If the central vertex of the projective cube represents a Euclidian point, the 12 satellite points represent HD control parameters. The triangles with obverse tails represent left-right raising and lowering nilpotent symmetry.

In the case of quaternionic matrices, it is significant that the hidden quaternion operators i, j, k applied, along with 1, to the rows and columns, and also to the rows of the Dirac 4-spinor, are identical in meaning to the same operators applied to the terms in the nilpotent state vector, as one can be derived from the other. There are good reasons for believing that the nilpotent form of the Dirac equation is the most fundamental. It is automatically second quantized, fulfilling all the requirements of a quantum field theory; it removes the infrared divergence in the fermion propagator, and the divergent loop calculation for the self-energy of the non-interacting fermion; and it introduces supersymmetry as a mathematical operation without the need for additional particles [84].

Physically, the fermion can be considered to see in the vacuum its ‘image’ or virtual antistate, producing a kind of virtual bosonic combination, and leading to an infinite alternating series of virtual fermions and bosons. Each real fermion state creates a virtual antifermion mirror image of itself in the vacuum, while each real antifermion state creates a virtual fermion mirror image of itself. The combined real and virtual particle creates a virtual boson state. Real fermions and real antifermions, of course, provide real mirror images of each other [84].

This is far as we will take the model in terms of development in this Chapter; what is needed for the next step is an additional space-antispace doubling, requiring a Complex Quaternion Clifford Algebra to describe. Compounded by development of the new UFM transformation cast in what we propose as an Ontological-Phase Topological Field Theory (OPTFT) going beyond the historic requirement for a fundamental basis of ‘locality and unitarity’ possibly utilizing an amplituhedron [65-67].

The Unified Field [40] produces periodic symmetry variations with long-range coherence that can lead to a topological phase effect like a coherently controlled Ising model lattice gas rotation of the Riemann sphere spacetime backcloth [85] (catastrophe theory Sect. 7.5). This can be described by a form of double-cusp catastrophe dynamics (Fig. 7.11).

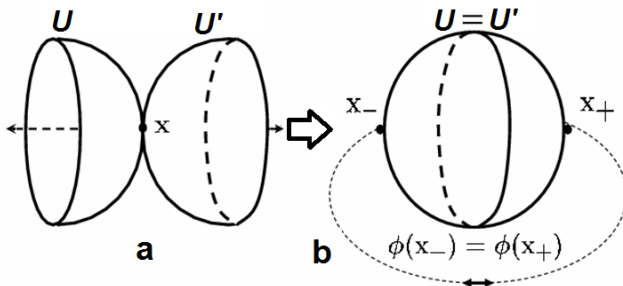


Fig. 7.8. Shadow point, x becomes unknotted (or knotted) in the continuous-state cyclic process that when various topological moves are performed dimensional raising and lowering may occur as part of cyclically opening and closing the algebraic description.

The coupled modes of this process rely on a special form of the harmonic oscillator called the Dubois incursive oscillator [86-90]. There is an inherent force of coherence [39,40,91]. For example, for an Earth observer’s temporal perception in Euclidean 3-space, railroad tracks recede into a point at the horizon. For an atemporal HD observer, the tracks remain parallel. This is the cyclic action of the coherence force forming an exciplex-like spacetime cellular automata logic gate driving equilibrium of the topologically charged Casimir boundaries to parallel or degenerate

modes thus giving rise to the possibility of effecting conformational state interactions ‘opened’ and ‘closed’ by resonant incursion [92]. These efforts will be clarified in Chaps. 9 & 11 on topological field theory.

Fig. 7.7 shows an attempt to illustrate an Ising model lattice gas mechanism for boosting and compactifying dimensionality as inherently driven by a de Broglie-Bohm super-quantum potential or ontological force of coherence of the unified field. We are still developing a format to clarify our explanation. Given that it is postulated that points in Euclidean space are knotted or braided ‘shadows’ of an HD topological brane structure that is continuously cycling stepwise through a L – R symmetry breaking compactification process; a structure of this sort applies. Relative to Figs. 7.3,7.8, there is no known sequence of Reidemeister moves that will untie a trefoil but moves based on Chern-Simons skein relations can [93].

GEOMETRIC REPRESENTATION OF THE NOETIC FIELD EQUATION

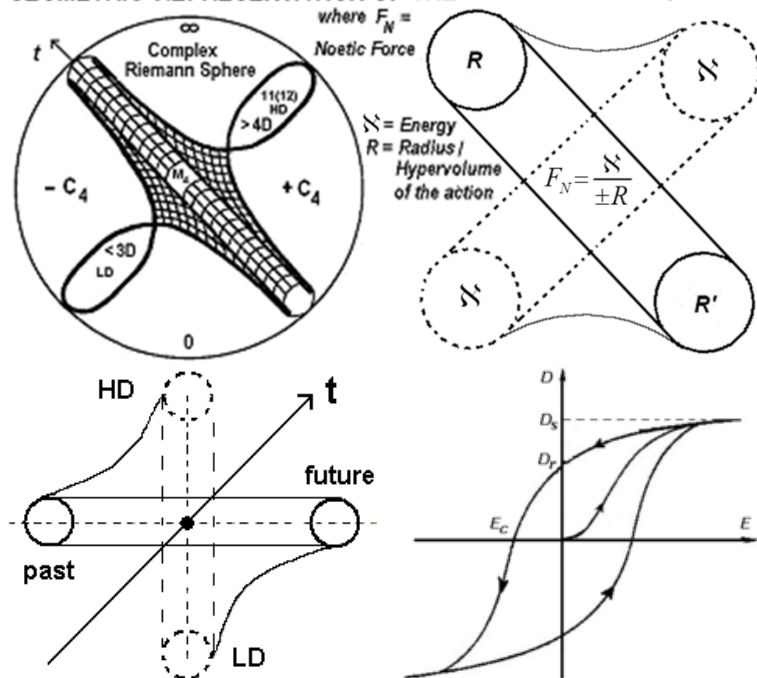


Fig. 7.9. Several topological and geometric idealizations of the putative unified field equation, $F_{(N)} = N / \rho$ describing an action of the unified field, a catastrophic ‘coherence effect’, on both biological and spacetime manifolds. Fig. 7.9d is a spacetime/brane hysteresis loop signifying the inherent energy of topological charge driving the ‘topological switching’ of catastrophe.

This is a boundary condition problem; here probably of the Born-von Karman type where the boundary conditions restrict the wave function to periodicity on a Bravais lattice of hexagonal symmetry, stated simply as $\psi(r + N_i a_i) = \psi_r$, where i runs over the dimensions of the Bravais lattice,

a_i are the lattice vectors and N_i are integers [85,91]. In this model presence of the periodic spherical rotation effects of the cyclical coherence-decoherence modes allow the cyclic action of the unified field. This Unified Processing is governed by the fundamental equation of unitarity, $F_{(N)} = \mathbf{x} / \rho$ (Fig. 7.9). Cyclotron resonance, logarithmic spiral, Kaluza-Klein or genus-1 helicoid ‘parking garage symmetry hierarchies (Chaps. 3,4) may be involved in maintaining piloting effects by the unified field or induce an electromotive ‘radiation pressure’ or topological switching coherence force that effects the topology of spacetime leading to conformational change in the static-dynamic [94-96] leapfrogging’ cycle of the topologically charged Casimir-like boundary conditions of HD Calabi-Yau mirror symmetric topological brane states.

We can’t be sure yet which of the hierarchical formalisms might be the physical one until some empirical work is performed. Intellectually we lean toward the concept of the action of a cyclotron resonance hierarchy acting on the genus-1 helicoid parking garage structure (Chaps. 3,4) modulated by a form of Bessel function embedded in the complex quaternionic Clifford algebra under study because this format also seems to meld well with catastrophe theory and the future-past symmetry breaking parameters we postulate in to be inherent in the structural-phenomenology of UFM continuous-state spacetime topology. We are utilizing a complex quaternionic Clifford algebra to develop this formalism in order to predict the resonance hierarchy bandwidth.

The structural-phenomenology of atoms and molecules is full of domain walls amenable to description by combinations of Gauss’ and Stokes’ theorems ordered in terms of Bessel Functions where boundary conditions create resonant cavities built up by alternating static and dynamic Casimir-like conditions [94-96]. As frequency increases central peaks occur with opposite or zero polarity at the domain edges. These properties are relevant to Ising Model [85] spin flips of the domains of the Riemann-Block Spheres effecting homeostatic planes of equilibrium (Fig. 7.11b). The UFM force of coherence can maintain equilibrium or produce catastrophes causing conformational change in the Casimir-like HD spacetime structures [92,97].

The UF ‘Coherence Effect’ is not a 5th phenomenological force (mediated by quantal field exchange); but an ontological charge or ‘Force of Coherence’ of energyless Calabi-Yau mirror symmetric (6D dual 3-tori) brane dynamics mediated by what is called topological switching [33] as described by a new set of transformations beyond the Galilean-Lorentz-Poincaré we chose to call the Noetic Transformation in terms of the meaning of the Greek term noetic as ‘hidden’ because it is deemed to operate in the regime of the as yet unobserved (LSXD) higher dimensions of spacetime [39,40] See Chap. 8 for complete delineation of the complex quaternionic Clifford algebra used for developing the preliminary formalism.

7.5 Catastrophe Theory and the M-Theoretic Formalism

Regarding *dynamical systems* that generally operate in a framework of stability and equilibrium – Technically these systems have a restrictive class called gradient systems which contain singularities or points of *extrema*. Some causal action can institute a bifurcation of an extrema that can initiate a qualitative change in the physical state of the system.

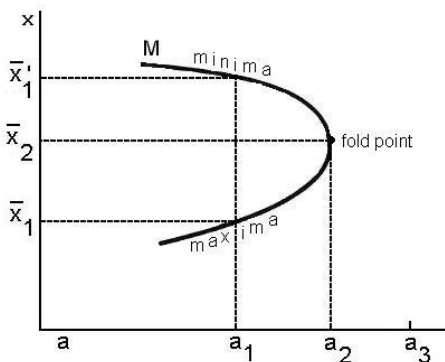


Fig. 7.10. Fundamental minima-maxima fold point basis of catastrophe theory.

Catastrophe theory² describes the breakdown of stability of any equilibrium system causing the system to jump to another state as the control parameters change. The changes in the singularities associated

² The groundwork for Catastrophe Theory began with Poincaré’s efforts in 1880 on the qualitative properties of solutions to differential equations; formalized in the 1950’s by R. Thom’s work mapping singularities in structural stability, he called catastrophes.

with the bifurcation of extrema are called elementary catastrophes [98-100] and can be described by real mathematical functions

$$f : R^N \rightarrow R . \quad (7.15)$$

The equation describing an elementary catastrophe utilizes variables representing *Control* and *State* parameters of the system and is a smooth real function of r and n where R represents the resultant singularity or catastrophe

$$f : R^r \times R^n \rightarrow R . \quad (7.16)$$

r (Control Factors)	Number of Catastrophes	Name		Dimensions
$r = 1$	1	A_2	Fold Catastrophe	2D
$r = 2$	1	$A_{\pm 3}$	Cusp Catastrophe	3D
$r = 3$	3	A_4	Swallowtail	4D
$r = 4$	2	$A_{\pm 5}$	Butterfly	5D
$r = 5$	4	A_6	Wigwam	6D
$r = 3$	-	D_{-4}	Elliptic Umbilic	5D
$r = 3$	-	D_{+4}	Hyperbolic Umbilic	5D
$r = 4$	-	D_5	Parabolic Umbilic	6D
$r = 5$	-	D_{-6}	2 nd Elliptic Umbilic	7D
$r = 5$	-	D_{+6}	2 nd Hyperbolic Umbil	7D
$r = 5$	-	$E_{\pm 6}$	Symbolic Umbilic	7D
$r = 6$	∞	X_9	Double Cusp	9-11D

Table 7.1 The general forms of catastrophes showing how dimensions increase as the number of control factors increase. The names bear some resemblance to the geometric pattern of the catastrophe. The double-cusp catastrophe is perceived as an aid to understanding the resonance hierarchy for surmounting uncertainty.

The r variables are the control parameters of the state variables, n . The function f is therefore an r -parameter family of functions of n variables.

If we let

$$f\left(a_1, \dots, a_r; x_1, \dots, x_n\right) \quad (7.17)$$

be a smooth real-valued function of $r + n$ real variables we get equation (7.17). The number of elementary catastrophes depends only on r and is finite for $r \geq 5$ totalling eleven (Table 7.1) and infinite for $r \geq 6$.

UNIFIED ACTION ON THE EQUILIBRIUM PLANE OF A DOUBLE-CUSP CATASTROPHE

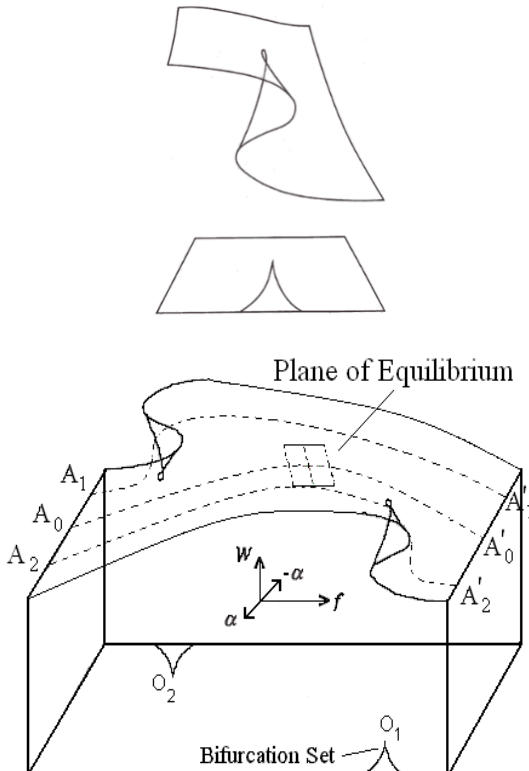


Fig. 7.11. The double-cusp catastrophe (DCC) illustration shows cusps at each end of the plane of equilibrium. The DCC occurs in ≥ 9 dimensions and thought to be the catastrophe form most compatible with UFM symmetry where the plane of equilibrium would be a topological manifold tiled of *least cosmological units* (LCU). This equilibrium manifold operates in conjunction with the inherent Feynman ‘synchronization backbone’ when undergoing a directed quantum computation best described as interactive computation.

This model can be utilized to call for a new field of vacuum engineering based on the structural-phenomenology of the unified field and whether resultant action of the ‘force of coherence’ of the unified field is positive or negative. Spacetime cellular automata exhibit complex selforganization. The unified field is the factor driving this self-organization [39,40]; therefore, we postulate hyperincursion and anticipatory properties are inherent in the fundamental hierarchical basis of this self-organization which could be formally described by Double-Cusp Catastrophe Theory.

Unit Circle and Associated Flag Manifold of Temporal Evolution for Noetic Catastrophe Cycle

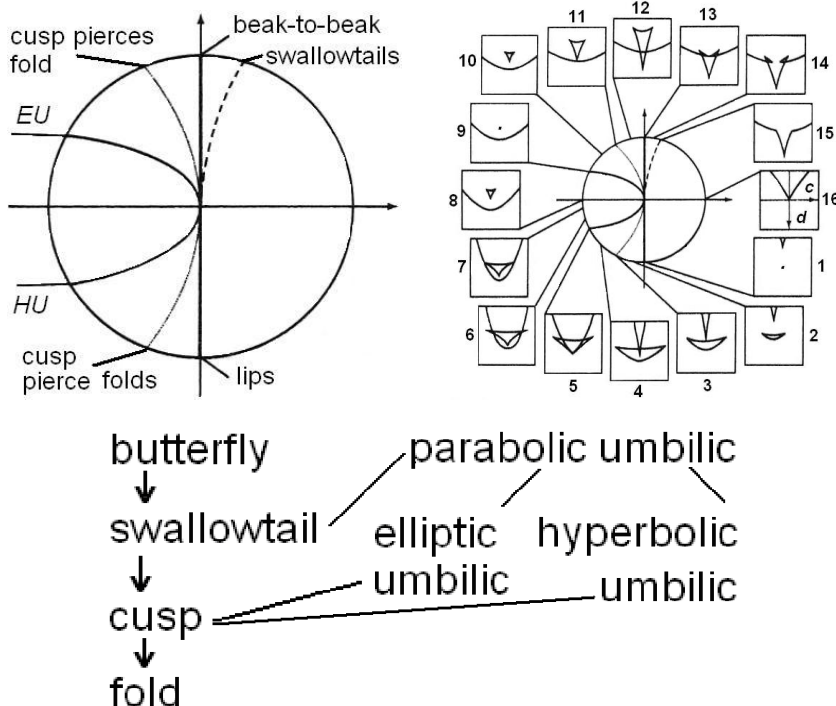


Fig. 7.12 a) represents a plane of the unit circle with corresponding cross sections in b: for example, shows a cusp. A single point in 1 grows to the ‘lips’ in 2. In 3 to 4 the original cusp 16 penetrates the mouth becoming a hyperbolic umbilic point at 5, turning into an elliptic umbilic at 6, shrinking to a point in 9. Growing again in 10 to pierce the fold line in 11 and through it in 12. A ‘beak-to-beak singularity in 13 breaks in 14, collapsing to a swallowtail 15. The seven fundamental catastrophes contain ‘subcatastrophes according to the diagram in c. Figures adapted from [98-100].

Fig. 7.11b (bottom) graphically illustrates the fundamental scale-invariant unified field equation $F_{(N)} = \aleph / \rho$ of the ‘force of coherence’ of unified field action. Any internal or external stress or change in \aleph is a nonlinear dynamic process producing stability or instability in the boundary conditions of ρ ; an instability in $\aleph \rightarrow$ stress \rightarrow displacement \rightarrow catastrophe \rightarrow jump...whereas stable flux is homeostatic. Further regarding Fig. 7.11b the plane of equilibrium entails a form of hysteresis loop of the Hamiltonian generalized in Fig. 7.9d as future-past parameters of HD spacetime. The area of the hysteresis loop represents the energy, \aleph of the unified force, F_N effecting the stability of the catastrophe as applied to manipulating the process for surmounting uncertainty.

TABLE 7.2 GEOMETRIC CONTENT OF 12D SPACETIME

N-Space	Points	Lines	Squares	Cubes	Tesseracts	5T	6T	7T	8T	9T	10T	11T	12T
0	1												
1	2	1											
2	4	4	1										
3	8	12	6	1									
4	16	32	24	8	1								
5	32	80	80	40	10	1							
6	64	192	240	160	60	12	1						
7	128	448	672	560	280	84	14	1					
8	256	1,024	1,792	1,792	1,120	448	112	16	1				
9	512	2,304	4,608	5,376	4,032	2,016	672	144	18	1			
10	1,024	5,120	11,520	15,360	13,440	8,064	3,360	960	180	20	1		
11	2,048	11,264	28,160	42,240	42,240	29,568	14,784	5,280	1,320	220	22	1	
12	4,096	24,576	67,584	112,640	126,720	101,376	59,136	25,344	7,920	1,760	264	24	1

The structural-phenomenology of Double-Cusp Catastrophe (DCC) Theory in $\geq 9D$ appears homeomorphic to the Riemannian manifold of both 10(11)D M-Theory and the 12D topological geometry of the mantra for the continuous-state spin-exchange dimensional reduction compactification process inherent in the action of the corresponding scale-invariant cosmological least-unit of UFM superspace as cast in UFM cosmology [39,40]. In this general framework the DCC equilibrium surface is analyzed in terms of a hierarchy of Ising-like lattice gas jumps in state providing a framework for considering the least-unit tiling [101] of the Planck backcloth as a complex HD catastrophe manifold mediated by the force of coherence of the unified field which because of the polarized properties of the Dirac vacuum lends itself to empirical mediation under certain restrictions.

The putative significance of Table 7.2 for the application of DCC theory to the UFM formalism is that the structure of possible boundary conditions and the number of control points is revealed. For example, in this simplistic view, a 3D point in real spacetime might have 16 control photon-gravitons (noeons - UF exchange unit) covering it. Carrying the analogy up to the 12D brane topology of the Multiverse, the same 3D point might be controlled or guided by a total of 8,176 noeon units. The number arrived at by summing the points of D4 to D12. No point in the universe is isolated; so this metaphor does not include the possible power factor by associated points in both the HD and LD UFM backcloth. Within the inherent continuous-state dimensional reduction compactification process, the LD domain (dimensions less than 3) might be coupled to orders of magnitude of more photon-gravitons. This detail of Unified Theory has not been completely worked out yet. $F_{(N)} = \aleph_{(N)} / \rho$

One can say that the cosmological least-unit [101] tiling the fabric of the continuous-state virtual Planck-scale backcloth is a complex HD catastrophe manifold with Dirac spherical rotation symmetry mediated by the unitary action of the unified field. Any internal or external stress or change in energy, \aleph is a nonlinear dynamical process producing stability or instability in the boundary conditions of ρ ; a causal instability in $\aleph \rightarrow$ stress \rightarrow displacement \rightarrow catastrophe \rightarrow Ising jump...whereas stable flux is homeostatic. The hysteresis loop of the unified field (Fig. 7.9d) is conformally scale invariant; the same processes occur in UFM cosmology and domains of the chemistry of living systems. The area represents the energy of the string tension, T_0 . This energy, $\aleph_{(N)}$ is measured in a unit similar to the *Einstein* in photometry, the fundamental physical quantity defined as a ‘mole’-Avogadro’s number (6.02×10^{23}) of bosons, defined here as noeons, the exchange unit of the unitary field.

Equation (7.18) describes the equilibrium surface of the DCC [98-100] as modeled in (Fig. 7.11); where $B \pm Q$ is the state variable and μ_d and v_d are the control parameters.

$$(B + Q)^3 + (B + Q)\mu_d + v_d = 0 \quad (7.18)$$

The position of the two cusps is found at $\mu_d = 0$ and $v_d = 0$. At any moment temporal permutations of the unified field catastrophe cycle evolve in time from future to past and higher to lower dimensions in the

same manner as the spacetime present of the cosmological least-unit of UFM cosmology for the spatial domains: $R^{12} \supseteq \dots R^4 \supseteq R^3 \supseteq R^2 \supseteq R^1 \supseteq R^0$; followed by a Riemann sphere Ising rotation where the cycle repeats.

7.6 Protocol for Empirically Testing Unified Theoretic Cosmology

Extrapolating Einstein's energy dependent or deformed spacetime metric, \hat{M}_4 [102-104] to a supersymmetric 12D standing-wave future-past advanced-retarded topology for a holographic multiverse we have designed a spacetime resonance hierarchy protocol for a covariant Dirac polarized vacuum which has properties akin to an 'ocean of light' or Wheeler Geon 'beyond the veil of spacetime [40]. If this is true emergent aspects of spacetime act like a 'surface wave' (Fig. 7.13) on the upper regime of the complex self-organized Dirac Sea and is therefore amenable to descriptive methods of nonlinear dispersive wave phenomena generally of the basic form

$$L(\mu) = \varepsilon N(\mu) \quad (7.19)$$

where L and N are Linear and Nonlinear operators respectively in the linear limit where $\varepsilon = 0$ with elementary dispersive wave solutions $\mu_i = A_i \cos \theta_i$, $\theta_i = k_i x - \omega(k_i)t$ for one dimension plus time where nonlinearity creates resonant interactions between the μ_i solutions and the Amplitude A_i depends on t , creating potentially substantial effects where initial absent modes can become cumulative interactions producing shock wave effects.

Motion of a one dimensional *classical* harmonic oscillator is given by $q = A \sin(\omega t + \varphi)$ and $p = m\omega A \cos(\omega t + \varphi)$ where A is the amplitude and φ is the phase constant for fixed energy $E = m\omega^2 A^2 / 2$. For state $|n\rangle$, with $n = 0, 1, 2, \dots, \infty$ and Hamiltonian $E_n = (n + 1/2)\hbar\omega$ the *quantum* harmonic oscillator becomes

$$\langle n | q^2 | n \rangle = \hbar / 2m\omega \langle n | (a^\dagger a + a a^\dagger) | n \rangle = E_n / m\omega^2 \quad (7.20)$$

and

$$\langle n | p^2 | n \rangle = 1/2(m\hbar\omega) \langle n | a^\dagger a + a a^\dagger = mE_n \quad (7.21)$$

where a & a^\dagger are the annihilation and creation operators,

$$q = \sqrt{\hbar/2m\omega}(a^\dagger + a) \text{ and } p = i\sqrt{m\hbar\omega/2}(a^\dagger a).$$

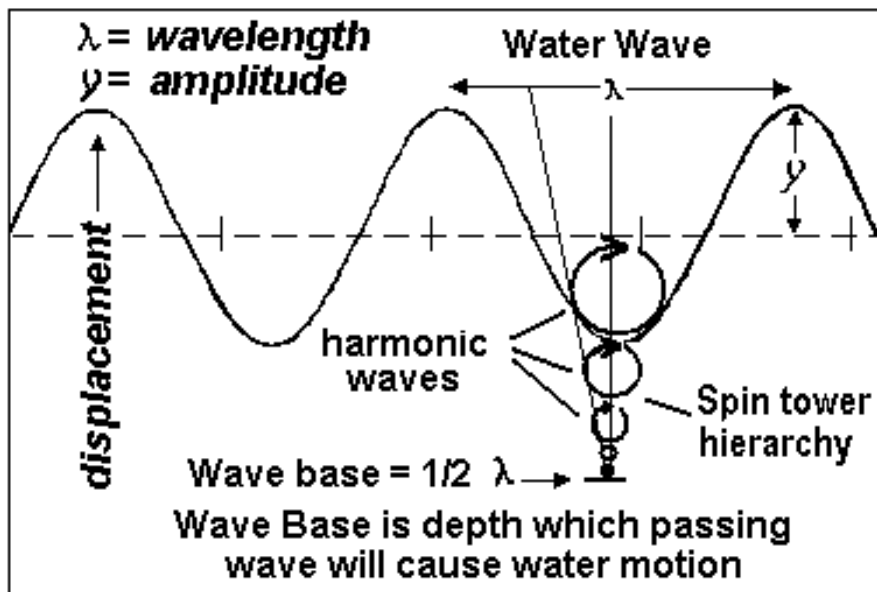


Fig. 7.13. The spacetime topological hierarchy may have properties like water waves where the wave (HD branes) moves but the water surface (local) remains stationary.

For the 3D harmonic oscillator each equation is the same with energies

$$E_x = (n_x + 1/2)\hbar\omega_x, E_y = (n_y + 1/2)\hbar\omega_y \quad (7.22a)$$

and

$$E_z = (n_z + 1/2)\hbar\omega_z [77,78]. \quad (7.22b)$$

In Dubois' notation the classical 1D harmonic oscillator for Newton's second law in coordinates t and $x(t)$ for a mass, m in a potential $U(x) = 1/2(kx^2)$ takes the differential form

$$\frac{d^2x}{dt^2} + \omega^2 x = 0 \quad \text{where} \quad \omega = \sqrt{k/m} \quad (7.23)$$

which can be separated into the coupled equations

$$\frac{dx(t)}{dt} - v(t) = 0 \quad \text{and} \quad \frac{dv(t)}{dt} + \omega^2 x = 0. \quad (7.24)$$

SPACETIME RESONANCE HAS SPHERICAL SYMMETRY

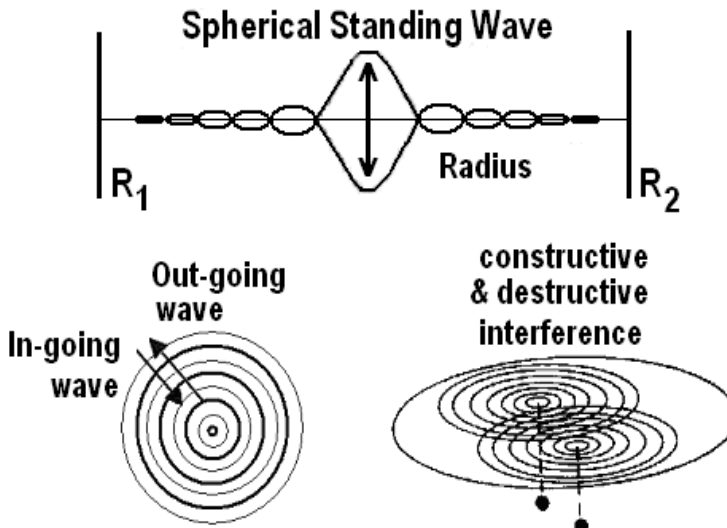


Fig. 7.14. The Dirac covariant polarized vacuum has hyperspherical symmetry. a) Metaphor for standing-wave present showing future-past elements, R_1, R_2 , 11D of 12D suppressed for simplicity. b) Top view of a) a 2D spherical standing-wave. c) Manipulating the relative phase of oscillations creates nodes of destructive and constructive interference as a substrate for incursion.

From incursive discretization, Dubois creates two solutions $x(t + \Delta t), v(t + \Delta t)$ providing a structural bifurcation of the system which together produce Hyperincursion. The effect of increasing the time interval discretizes the trajectory as in Fig. 7.15 below. This represents a background independent discretization of spacetime [86-90].

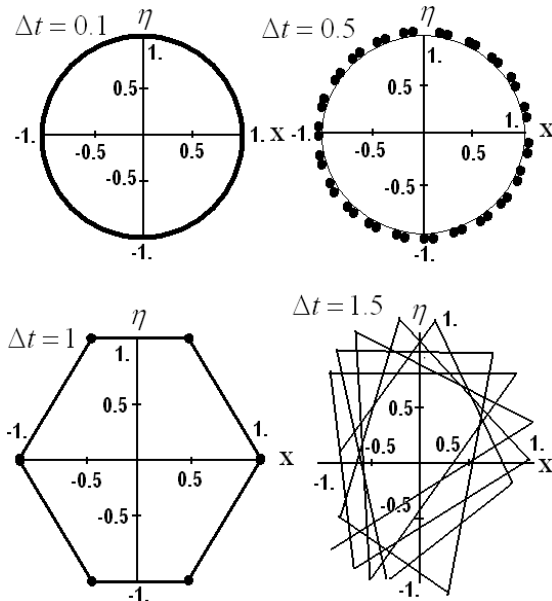


Fig. 7.15. Numerical simulation of the phase space trajectory of the Dubois *superposed incursive oscillator* based on coordinates and velocities $x_n = 1/2[x_n(1) + x_n(2)]$ and $v_n = 1/2[v_n(1) + v_n(2)]$ is shown in the figure for values of $\Delta\tau = \omega t$ equal to 0.1, 0.5, 1.0 and 1.5. Initial conditions are $\chi_0 = 1, \eta_0 = 0$ & $\tau_0 = 0$ with total simulation time $\tau = \omega t = 8\pi$. Figure adapted from [86-90].

7.7 Introduction to a $P \equiv 1$ Experimental Design

In a homogeneous magnetic field, the forces exerted on opposite ends of the dipole cancel each other out and the trajectory of the particle is unaffected. If the particles are classical ‘spinning’ particles then the distribution of their spin angular momentum vectors is taken to be truly random and each particle would be deflected up or down by a different amount producing an even distribution on the screen of a detector. Instead quantum mechanically, the particles passing through the device are deflected either up or down by a specific amount. This means that spin angular momentum is quantized (also called space quantization), i.e. it can only take on discrete values. There is not a continuous distribution of possible angular momenta. This is the usual fundamental basis of the

standard quantum theory and where we must introduce a new experimental protocol to surmount it. This is the crux of our new methodology: If application of a homogeneous magnetic field along a Z-axis produces quantum uncertainty upon measurement, then simplistically “*do something else*”.

In NMR spectroscopy often it is easier to make a first order calculation for a resonant state and then vary the frequency until resonance is achieved. Among the variety of possible approaches that might work best for a specific quantum system, if we choose NMR for the UFM Interferometer it is relatively straight forward to determine the spin-spin resonant couplings between the modulated electrons and the nucleons. But achieving a critical resonant coupling with the wave properties of matter with a putative beat frequency inherent in the HD spacetime backcloth is another matter. Firstly, for UFM cosmology \hbar is not a rigid barrier as in Standard Model Big Bang-Copenhagen cosmology; \hbar is a virtual limit of retarded-advanced elements of the continuous-state standing-wave present as it cyclically recedes into the past where the least unit [101] cavities tiling the spacetime backcloth can have cyclical radii \leq the Larmor radius of the hydrogen atom. This new Planck length ($\hbar + T_s$), where T_s is string tension, oscillates through a limit cycle from the Larmor radius of the hydrogen atom to standard \hbar , as asymptote never reached. As discussed in Chaps. 3,4, we utilize the original hadronic form of string tension which is variable, not the current M-Theoretic form which is fixed.

This cycle is like a wave-particle duality – Larmor radius at the future-retarded moment and \hbar at the past-advanced moment that opens and closes periodically into the HD regime. The dynamics are different for future-retarded elements which have been theorized to have the possibility of infinite radius for $D > 4$ [105]. This scenario is a postulate of string theory. Considering the domain walls of the least-unit structure, the $\pm\Delta\hbar$ -Larmor cyclical regime is considered internal-nonlocal and the Larmor-infinity regime rotation considered external-supralocal.

For simplicity we introduce our review of NMR concepts for the hydrogen atom, a single proton with magnetic moment, μ , angular momentum, J related by the vector $\mu = \gamma J$ where γ is the gyromagnetic ratio and $J = \hbar I$ where I is the nuclear spin. The magnetic energy $U = -\mu \cdot B$ of the nucleus in an external magnetic field in the z direction is $U = -\mu_z B_0 = -\gamma \hbar I_z B_0$ where the usual values of I_z , m_I are quantized

according to $m_I = I, I-1, I-2, I-3, \dots -1$ [106,107].

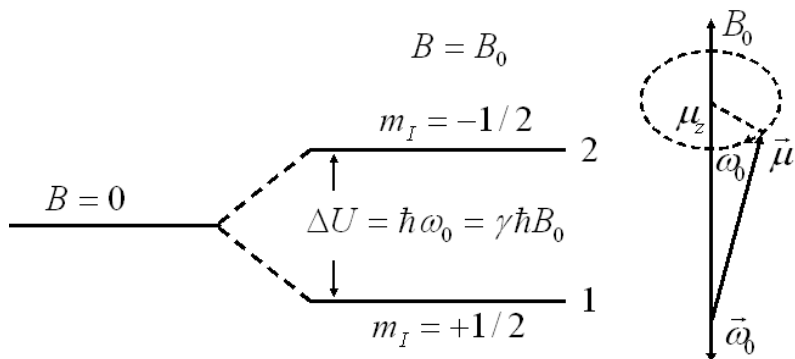


Fig. 7.16. a) The two magnetic energy states for the spin, $I = \frac{1}{2}$ single proton of a hydrogen atom in a magnetic field. b) Time variation of the magnetic moment of the proton in magnetic field B_0 with precession frequency, $\omega_0 = \gamma B_0$, the fundamental resonant frequency from a).

For most nuclear species the z -component of the magnetization, M grows exponentially until reaching equilibrium according to the formula $M_z(t) = M_0(1 - e^{-t/T_1})$ where T_1 is the spin-lattice relaxation time. Of interest for the noetic interferometer is the fact that (Fig. 7.16) as μ precesses cyclically from $m_I = -1/2$ to $m_I = +1/2$ the nucleons experience a torque, with τ changing J by $\tau = dJ/dt$ or $\mu \times B = dJ/dt$. Under thermal equilibrium the x-y components are zero; but M_z can be rotated into the x-y plane creating additional transverse M_x and M_y components $dM/dt = \gamma M \times B$ for the entire system by applying a rotating circularly polarized oscillating magnetic field $2B_1 \cos \omega \hat{i}$ of frequency ω in addition to the constant magnetic field, $B_0 \hat{k}$. Now the total time dependent field decomposes into the two counterpropagating fields

$$B_1(\cos \omega \hat{i} + \sin \omega \hat{j}) + B_1(\cos \omega \hat{i} - \sin \omega \hat{j}). \quad (7.25)$$

This more complicated form for use with multiple applied fields is necessary, as described below for use with the Sagnac Effect, quadrupole,

and dipole dynamics [108,109] required to operate the noetic interferometer.

Nuclear Quadrupole Resonance (NQR) is a form of NMR in which quantized energy level transitions are induced by an oscillating rf-magnetic field in the electric quadrupole moment of nuclear spin systems rather than the magnetic dipole moment. The nuclear quadrupole moment, Q is based on the nuclear charge distributions $\rho(r)$ departure from spherical symmetry defined as the average value of $1/2(3z^2 - r^2)\rho(r)$ over the nuclear volume. Q has the dimension of area where the nuclear angular momentum, for which $m_I = I$ where I is the nuclear spin quantum number and m_I is the quantum number for the z component of the spin, $m_I = -1, +1, \dots, I-1, I$. Nuclei with $I=0$ have no magnetic moment and are therefore magnetically inert. Similarly, in order for $Q=0$ the nucleus must be spherical with spin, $I \geq 0$. For spin $I=1/2$ nuclei have dipole moments, μ but no Q . Q is positive for prolate nuclei and negative for oblate nuclei [110,111].

For an isolated nucleus in a constant magnetic field, H_0 with nuclear spin number $I > 0$ the nucleus possesses a magnetic moment. From QT the length of the nuclear angular momentum vector is $[I(+)]^{1/2}\hbar$ where measurable components are given by $m\hbar$ with m the magnetic quantum number taking any $(2I+1)$ value from the series $I, I-1, I-2, \dots, -(I-1), -I$. For the $I=3/2$ case there are four values along the direction of the applied magnetic field, H_0 .

Of the three types of spin-spin coupling, this experiment relies on the hyperfine interaction for electron-nucleus coupling, specifically the interaction of the nuclear electric quadrupole moment induced by an applied oscillating rf-electric field acting on the nuclear magnetic dipole moment, μ . When electron and nuclear spins are strongly aligned along their z -components the Hamiltonian is $-m \cdot B$, and if B is in the z direction

$$H = -\gamma_N I \cdot B = -\gamma_N BI_x \quad (7.26)$$

with $m = \gamma_N I$, γ_N the magnetogyric ratio $\gamma_N = e\hbar / 2m_p$ and m_p the mass of the proton [112].

Radio frequency excitation of the nuclear magnetic moment, μ to resonance occurs for a nucleus collectively which rotates μ to some angle with respect to the applied field, B_0 . This produces a torque $\mu_i \times B_0$ causing the angular momentum, μ itself to precess around B_0 at the Larmor frequency $\omega_L = \gamma_N B_0$ [112-114]. This coherent precession of μ can also induce a ‘voltage’ in surrounding media, an energy component of the Hamiltonian to be utilized (Figs. 7.17,7.18) to create interference in the structure of spacetime.

Metaphorically this is like dropping stones in a pool of water: One stone creates concentric ripples; two stones create domains of constructive and destructive interference. Such an event is not considered possible in the standard models of particle physics, quantum theory and cosmology. However, UF science uses extended versions of these theories wherein a new teleological action principle is utilized to develop what might be called a ‘transistor of the vacuum’. Just as standard transistors and copper wires provide the basis for almost all modern electronic devices; This Laser Oscillated Vacuum Energy Resonator using the information content of spacetime geodesics (null lines) will become the basis of many forms of new UF technologies.

Simplistically in this context, utilizing an array of modulated tunable lasers, atomic electrons are rf-pulsed with a resonant frequency that couples them to the magnetic moment of the nucleons such that a cumulative interaction is created to dramatically enhance the Haisch-Rueda inertial back-reaction [115-118] in conjunction with the Dubois incursive oscillator [86-90]. The laser beams are counter-propagating producing a Sagnac Effect Interferometry to maximize the small-scale local violation of Special Relativity. This is the 1st stage of a multi-tier experimental platform designed (according to the tenets of UFT) to periodically ‘open a hole’ in the fabric of spacetime in order to isolate and utilize the force \hat{F}_U of the UFM Field.

The interferometer utilized as the basis for the vacuum engineering research platform is a multi-tiered device. The top tier is comprised of counter-propagating Sagnac effect ring lasers that can be built into an IC array of 1,000+ ring lasers. If each microlaser in the array is designed to be counterpropagating, an interference phenomena called the Sagnac Effect occurs that violates special relativity in the small scale [119]. This array of rf-modulated Sagnac-Effect ring lasers provides the top tier of the multi-tier Laser Oscillated Vacuum Energy Resonator. Inside the ring of

each laser is a cavity where quantum effects called Cavity-Quantum Electrodynamics (C-QED) may occur. A specific molecule is placed inside each cavity. If the ring laser array is modulated with resonant frequency modes chosen to achieve spin-spin coupling with the molecules electrons and neutrons, by a process of Coherent Control [120] of Cumulative Interaction an inertial incursive back-reaction is produced whereby the electrons also resonate with the spacetime backcloth in order to 'open an oscillating hole' in it. This requires a TFT compatible with the 12D version of M-theory [43] relying on the key 'continuous-state' symmetry conditions of UFM cosmology in which it is cast (Chap. 3).

LASER OSCILLATED VACUUM ENERGY RESONATOR (L.O.V.E.R.) Multi-Tiered Experimental Platform

TIER-I	Applied Tunable Laser RF Modulated Pulsed Quadrupole Resonant Counter-Propagating Sagnac Effect Interferometry of Electrons
TIER-II	For the Purpose of Spin-Spin Coupling of Tier-I Electrons to the Magnetic Moment of the Nucleons
TIER-III	By HD RQFT Tier-I & II Undergo Resonant Coupling with the Beat Frequency of the Fabric of Spacetime
TIER-IV	Producing a Multi-Tier Cumulative Interaction of Tier - I - II - III to Destructively Interfere with the Annihilation & Creation operators of Spacetime

Fig. 7.17. Design elements for the HD Cavity-QED trap of the UFM Noetic Interferometer postulated to constructively-destructively interfere with the topology of the 12D spacetime manifold to manipulate the unified field. Substantial putative effects are possible if cumulative interactions of the interference nodes of the cyclotron resonance hierarchy produce reactive incursive shock waves.

The first step in the interference hierarchy (Fig. 7.17) is to establish an inertial back-reaction between the modulated electrons and their coupled resonance modes with the nucleons. The complete nature of inertia remains a mystery [121]. It may later be shown that the continuous-state

energy in conjunction with the UF force of coherence will solve this mystery of Mach's Principle.

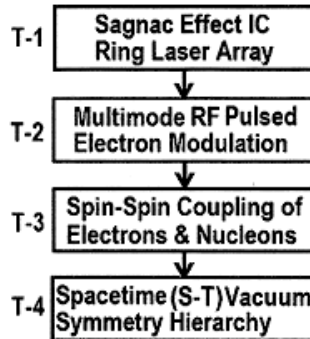


Fig. 7.18. Simplified description of the rf-pulsed resonance hierarchy for HD access.

It is critical to realize that the Standard Model contains no fundamental ‘beat frequency’ of a spacetime annihilation-creation cycle. Physicists have come to the realization recently that spacetime is not fundamental, but little has been said yet of the nature of its emergence. In our cosmological model, a key breakthrough is that this beat frequency arises as an inherent property of the continuous-state cycling.

But if one follows the Sakarov [122] and Puthoff [123] conjecture, regarding the force of gravity and inertia, the initial resistance to motion, are actions of the vacuum zero-point field. Therefore, the parameter m in Newton’s second law $f = ma$ is a function of the zero-point field [115-118,125-126]. Newton’s third law states that ‘every force has an equal and opposite reaction’. Haisch & Rueda [115-118] claim vacuum resistance arises from this reaction force, $f = -f$. We have also derived an electromagnetic interpretation of gravity and electromagnetism [127] that suggests this inertial back-reaction is like an electromotive force³ of the de Broglie matter-wave field in the spin exchange annihilation creation process inherent in a hysteresis of the relativistic spacetime fabric (Fig. 7.9b,d). In fact, we go further to suggest that the energy responsible for Newton’s third law is a result of the continuous-state flux of the ubiquitous UFM noetic field. For the Laser Oscillated Vacuum Energy Resonator we

³ Electromotive force, E : The internal resistance r generated when a load is put upon an electric current I between a potential difference, V , i.e. $r = (E - V)/I$.

assume the Haisch-Rueda postulate is sufficiently correct to be adapted for use in our rf-pulsed Sagnac Effect resonance hierarchy.

$$f = \frac{d\rho}{dt} - \lim_{\Delta t \rightarrow 0} \frac{\Delta\rho}{\Delta t} \equiv \frac{d\rho_*}{dt_*} - \lim_{\Delta t_* \rightarrow 0} \frac{\Delta\rho_*}{\Delta t_*} = f_* \quad (7.27)$$

where $\Delta\rho$ is the impulse given by the accelerating agent and thus $\Delta\rho_*^{zp} = -\Delta\rho_*$ [115-118].

The cyclotron resonance hierarchy must also utilize the proper spacetime beat frequency according to the mantra of the continuous-state dimensional reduction spin-exchange compactification process inherent in the symmetry of UF spacetime naturally ‘tuned’ to make the speed of light $c \equiv c$ and not infinite. With this apparatus in place, noetic theory suggests that destructive-constructive C-QED interference of the spacetime fabric occurs such that the UFM noeon wave, \mathbf{x} of the unified field, U_F is harmonically (like a light house beacon or holophote) released periodically into the cavity of the detector array. Parameters of the Dubois incursive oscillator are also required for aligning the interferometer hierarchy with the beat frequency of spacetime.

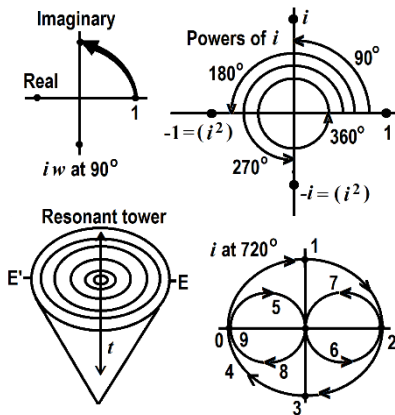


Fig. 7.19 Powers of i in the complex plane. For 90° to 360° the concept can be readily illustrated in 2D; but for 720° and above 4D is required which cannot easily be depicted in 3D so the representation in d) is used, which might also be represented by a Klein bottle which was not used because the torus in d) more easily shows the rotation topology, which for spin 1/2 is the Dirac rotation of the electron. c) is a simplistic representation of a powers of i resonance hierarchy.

If the water wave conception for the ‘Dirac sea’ is correct, the continuous state compactification process contains a tower of spin states from spin 0 to spin 4. Spin 4 represents the unified field making cyclic correspondence with spin 0 where Ising lattice Riemann sphere spin flips create dimensional jumps. Spin 0, 1/2, 1, & 2 remain in standard form. Spin 3 is suggested to relate to the orthogonal properties of atomic energy levels and space quantization. Therefore, the spin tower hierarchy precesses through 0, 720°, 360°, 180°, 90° & 0 (∞) as powers of i as illustrated in Fig. 7.19.

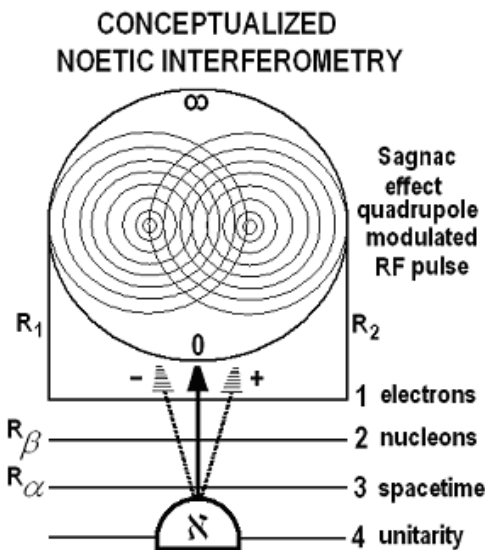


Fig. 7.20. Conceptualized Ising model Riemann sphere cavity-QED multi-level Sagnac effect interferometer designed to cyclically ‘penetrate’ space-time to emit the ‘noeon wave, \aleph ’. Experimental access to vacuum structure or for surmounting the uncertainty principle can be done by two similar methods. One is to utilize an atomic resonance hierarchy and the other a spacetime resonance hierarchy. The spheroid is a 2D representation of a HD Ising model Riemann sphere able to spin-flip from zero to infinity in conjunction with the putative ‘beat frequency’ of spacetime.

As illustrated in Figs. 7.17, 7.18 the coherent control of the multi-level tier of cumulative interactions relies on full utilization of the continuous-state cycling inherent in parameters of Multiverse cosmology. What putatively will allow noetic interferometry to operate is the harmonic coupling to periodic modes of Dirac spherical rotation in the symmetry of

the HD brane geometry. The universe is no more classical than quantum as currently believed; reality rather is a continuous state cycling of nodes of classical to quantum to unified, $C \rightarrow Q \rightarrow U$. We elevate the concept of wave-particle duality to a principle of cosmology especially in terms of the HD continuous-state cycle; this is what allows the UFM ‘mantra’ to operate. The salient point is that cosmology, the HD topology of spacetime itself, has a conformal rotation like the wave-particle duality Dirac postulated for electron spin. Recall that the electron requires a 4D topology and 720° for one complete rotation instead of the usual 360° to complete a rotation in 3D. The hierarchy of noetic cosmology is cast in 12D such that a pertinent form of ontological-phase topological field theory has significantly more degrees of freedom, whereby the modes of resonant coupling may act on the structural-phenomenology of the Dirac ‘sea’ itself rather than just the superficial zero-point field surface approaches to vacuum engineering common until now.

Hierarchical Harmonic Oscillator Parameters	
classical	$X = A \cos(\omega t)$
quantum	$\frac{\hbar^2}{2m} \frac{d^2\psi}{dx^2} + \left(E - \frac{kx^2}{2} \right) \psi = 0$
annihilation creation	$x(t) = x_0 [a \exp(-i\omega t) + a^\dagger \exp(i\omega t)]$
future-past retarded-advanced	$F_1 = F_0 e^{-ikx} e^{-2\pi i \frac{f}{\hbar}}, \quad F_2 = F_0 e^{ikx} e^{-2\pi i \frac{f}{\hbar}},$ $F_3 = F_0 e^{-ikx} e^{2\pi i \frac{f}{\hbar}}, \quad F_4 = F_0 e^{ikx} e^{2\pi i \frac{f}{\hbar}}$
incursive	$\frac{dx(t+\Delta t)}{dt} - v(t) = 0, \quad \frac{dv(t+\Delta t)}{dt} + \omega^2 = 0$

Fig. 7.21. Basic conceptual mathematical components of the applied harmonic oscillator: classical, quantum, relativistic, transactional and incursive are all required in order to achieve coherent control of the cumulative resonance coupling hierarchy in order to produce harmonic nodes of destructive and constructive interference in the spacetime backcloth by incursion.

The parameters of the noetic oscillator (Figs. 7.17, 7.18) seem best be implemented by an OPTFT using a form of de Broglie fusion. According to de Broglie a spin 1 photon can be considered a fusion of a pair of spin 1/2 corpuscles linked by an electrostatic force. Initially de Broglie thought this might be an electron-positron pair and later a neutrino and antineutrino. “*A more complete theory of quanta of light must introduce polarization in such a way that to each atom of light should be linked an internal state of right and left polarization represented by an axial vector with the same direction as the propagation velocity*” [128]. These prospects suggest a deeper relationship in the structure of spacetime of the Cramer Transaction type [50] (Fig. 7.22).

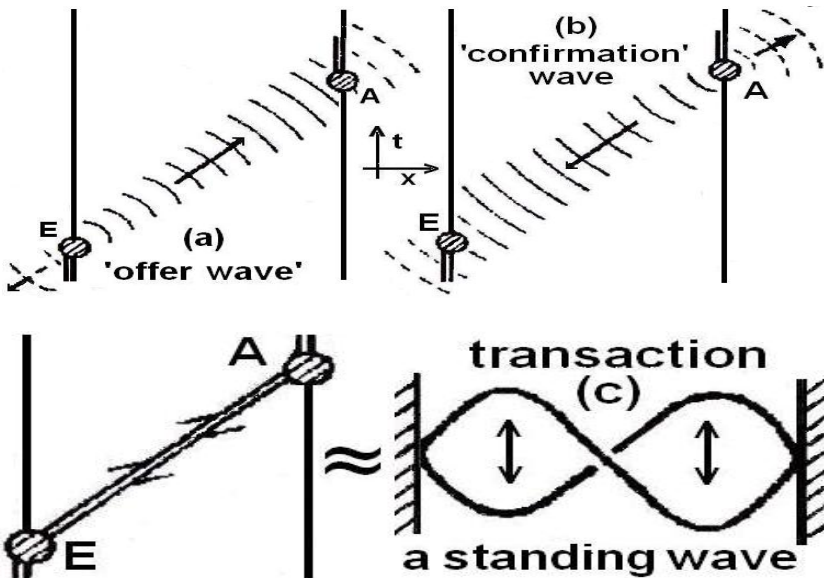


Fig. 7.22. Transactional model. a) Offer-wave, b) confirmation-wave combined into the resultant transaction c) which takes the form of an HD future-past advanced-retarded standing or stationary wave. Figs. Adapted from Cramer [50].

The epistemological implications of a 12D OPTFT must be delineated. The empirical domain of the standard model relates to the 4D phenomenology of elementary particles. It is the intricate notion of what constitutes a particle that concerns us here – the objects emerging from the quantized fields defined on Minkowski spacetime. This domain for evaluating physical events is insufficient for our purposes. The problem is

not only the additional degrees of freedom and the associated XD, or the fact that ‘particles’ can be annihilated and created but that in UFM cosmology they are continuously annihilated and recreated within the holograph as part of the annihilation and recreation of the fabric of spacetime itself. This property is inherent in the 12D Multiverse because temporality is a subspace of the atemporal 3rd regime of the UF. This is compatible with the concept of a particle as a quantized field. What we are suggesting parallels the wave-particle duality in the propagation of an electromagnetic wave. We postulate this as a property of all matter and spacetime albeit as continuous-state standing waves.

FUTURE-PAST PLANE-WAVE TRANSACTION

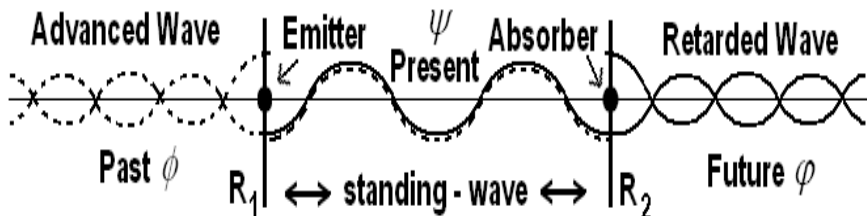


Fig. 7.23 Structure of a Cramer transaction (present state or event) where the present is a standing-wave of future-past elements. The separation of these parameters in terms of de Broglie’s fusion model is suggested to allow manipulation of the harmonic tier of the UF interferometer with respect to T-Duality or Calabi-Yau mirror symmetry.

For a basic description, following de Broglie’s fusion concept, assume two sets of coordinates x_1, y_1, z_1 and x_2, y_2, z_2 which become

$$X = \frac{x_1 + x_2}{2}, \quad Y = \frac{y_1 + y_2}{2}, \quad Z = \frac{z_1 + z_2}{2}. \quad (7.28)$$

Then for identical particles of mass m without distinguishing coordinates, the Schrödinger equation (for the center of mass) is

$$-i\hbar \frac{\partial \psi}{\partial t} = \frac{1}{2M} \Delta \psi, \quad M = 2m. \quad (7.29)$$

In terms of Fig. 7.23, Eq. 7.29 corresponds to the present and Eq. 7.30a corresponds to the advanced wave and (7.30b) to the retarded wave [98].

$$-i\hbar \frac{\partial \phi}{\partial t} = \frac{1}{2M} \Delta \phi, \quad -i\hbar \frac{\partial \varphi}{\partial t} = \frac{1}{2M} \Delta \varphi. \quad (7.30)$$

Extending Rauscher's concept for a complex 8-space differential line element $dS^2 = \eta_{\mu\nu} dZ^\mu dZ^{*\nu}$, where the indices run 1 to 4, $\eta_{\mu\nu}$ is the complex 8-space metric, Z^μ the complex 8-space variable where $Z^\mu = X_{\text{Re}}^\mu + iX_{\text{Im}}^\mu$ and $Z^{*\nu}$ is the complex conjugate [129,130]. This can be extended to 12D continuous-state UFM spacetime; we write just the dimensions for simplicity and space constraints:

$$x_{\text{Re}}, y_{\text{Re}}, z_{\text{Re}}, t_{\text{Re}}, \pm x_{\text{Im}}, \pm y_{\text{Im}}, \pm z_{\text{Im}}, \pm t_{\text{Im}} \quad (7.31)$$

where \pm signifies Wheeler-Feynman/Cramer type future-past/retarded-advanced dimensions. This dimensionality provides an elementary framework for applying the hierarchical harmonic oscillator parameters suggested in Figs. 7.17 and 7.21.

The concept conceptualized is that although commutativity was sacrificed by Hamilton in creating a closed quaternion algebra utilizing a 12D complex quaternion Clifford algebra approach to describe the Fermionic singularity; the additional degrees of freedom allow anticommutativity and commutativity to cycle periodically through the constraints of the algebra. This scenario when applied to the continuous-state cycle can be utilized to periodically via the suggested resonance hierarchy protocol to surmount the quantum uncertainty principle.

7.8 Conclusions

If the noeon interferometer resonance hierarchy is able to surmount the uncertainty principle as outlined and can isolate and manipulate the LSXD brane world, in addition to quantum computing it will lead to a new research platform for developing a whole new class of vacuum based technologies; whereas one could say virtually all electronic devices up to now are based on transistors and copper wires. The Laser Oscillated Vacuum Energy Resonator could lead to a transistor of vacuum cellular automata, where rather than copper wires, the geodesics or null lines of space would be utilized to transfer information topologically with no

quantal exchange particle mediating the ‘interaction’ in this scenario distinguishing phenomenology from unified field ontology.

This brief introduction is a primitive overview introducing the anticipated new field of vacuum engineering as Cramer stated in the 1st sentence of this chapter should revolutionize many fields of science [131].

When the great innovation appears, it will most certainly be in a muddled, incomplete form. To the discoverer himself it will be only half-understood; to everyone else it will be a mystery. For any speculation which does not at first glance look crazy, there is no hope [132].

Finally, we stress that vacuum energy is not ‘produced’ by the noeon interferometer. The interferometer manipulates the boundary conditions ‘insulating’ or ‘hiding’ the unitary geodesics of HD spacetime by constructive and destructive interference allowing vacuum energy to be ‘emitted’ as a form of cursory superradiance [133] of the dynamics of the hysteresis loop of inherent least-unit synchronization backbone energy (topological charge) in continuous-state parallel transport.

We have found already that a fair number of colleagues want to summarily dismiss this model because of its utilization of LSXD. This is the sort of myopic view that has consistently plagued the history of science whenever ‘big-leap’ innovation occurs. We hope readers here will not fall into this quagmire! The model is empirically testable hopefully making up for some of the lack of precision in our axiomatic approach or thin rigor in portions of our attempts at formalism. In addition to the protocol presented here we have described elsewhere an additional experiment to utilize the noeon \aleph -wave to study the putative manipulation of prion protein conformation responsible for degenerative neuropathies [92,97].

References

- [1] Thorne, K.S., Drever, R.W.P., Caves, C.M., Zimmermann, M. & Sandberg, V.D. (1978) Quantum nondemolition measurements of harmonic oscillators, *Phys. Rev. Lett.* 40; 667-671.
- [2] Teuscher, C. (ed.) (2004) Alan Turing: Life and Legacy of a Great Thinker, quoted by A. Hodges, p. 54, New York: Springer.
- [3] Cramer, J.G. (2000) The Alternate View: "Interaction-Free" Quantum Measurement and Imaging, Vol. CXX No. 6, pp. 78-81, Analog Science Fiction & Fact, Dell Magazines.
- [4] Gurvitz, S.A. (2003) Negative result measurements in mesoscopic systems, *Physics Letters A*, 311:4-5;292-296.
- [5] Braginsky, V.B., Vorontsov, Y.I. & Thorne, K.S. (1980) Quantum nondemolition measurements, *Science*, 209:4456, 547-557.

- [6] Ralph, T.C., Bartlett, S.D., O'Brien, J.L., Pryde, G.J & Wiseman, H.M. (2004) Quantum non-demolition measurements on qubits, arXiv:quant-ph/0412149v1.
- [7] Elitzur, A.C. & Vaidman, L. (1993) Quantum mechanical interaction-free measurements. Found. Phys. 23; 987-997.
- [8] Kwiat, P., Weinfurter, H., Herzog, T., Zeilinger, A. & Kasevich, M. (1995) Interaction-free quantum measurements. Phys. Rev. Lett. 74, 4763-4766.
- [9] du Marchie Van Voorthuysen, E.H. (1996) Realization of an interaction-free measurement of the presence of an object in a light beam, Am. J. Phys. 64:12; 1504-1507; or arXiv:quant-ph/9803060 v2 26.
- [10] Simon, S.H. & Platzman, P.M. (1999) Fundamental limit on “interaction free” measurements, arXiv:quant-ph/9905050v1.
- [11] Vaidman, L. (1996) Interaction-free measurements, arXiv:quant-ph/9610033v1.
- [12] Paraoanu, G.S. (2006) Interaction-free measurements with superconducting qubits, Physical Rev. Letters, 97.
- [13] Vaidman, L. (2001) The meaning of the interaction-free measurements, arXiv:quant-ph/0103081v1.
- [14] Vaidman, L. (2001) The paradoxes of the interaction-free measurements, arXiv:quant-ph/0102049v1.
- [15] Vaidman, L. (2000) Are interaction-free measurements interaction free?, arXiv:quant-ph/0006077v1.
- [16] Helmer, F., Mariantoni, M., Solano, E. & Marquardt, F. (2008) Quantum, Zeno effect in the quantum non-demolition detection of itinerant photons, arXiv:0712.1908v2.
- [17] Facchi, P., Lidar, D.A. & Pascazio, S. (2004) Unification of dynamical decoupling and the quantum Zeno effect, Phys Rev A 69, 032314; or arxiv:quant-ph/0303132.
- [18] Sudarshan, E.C.G. & Misra, B. (1977) The Zeno’s paradox in quantum theory, J Mathematical Physics 18:4; 756-763.
- [19] Facchi, P. & Pascazio, S. (2002) Quantum Zeno subspaces, arXiv:quant-ph/0201115v2.
- [20] Wocjan, P. (2004) Efficient decoupling schemes with bounded controls based on “Eulerian” orthogonal arrays, arXiv:quant-ph/0410107v1.
- [21] Knill, E., Laflamme, R., Ashikhmin, A., Barnum, H., Viola, L. & Zurek, W.H. (1999) Introduction to quantum error correction, arXiv:quant-ph/0207170v1.
- [22] Kwiat, P.G., White, A.G., Mitchell, J.R., Nairz, O., Weihs, G., Weinfurter, H. & Zeilinger, A. (1999) High-efficiency quantum interrogation measurements via the quantum Zeno effect, Phys. Rev. Lett. 83, 4725-4728; or arXiv:quant-ph/9909083v1.
- [23] Carroll, S.M. (2006) Quantum Interrogation, reprinted in The Open Laboratory: The Best Writing on Science Blogs, B. Zivkovic (ed.) (Lulu: Morrisville, NC), p. 123.
- [24] Jozsa, R. (1996) Counterfactual quantum computation, University of Plymouth preprint, unpublished.
- [25] Mitchison, G. & Jozsa, R. (2000) Counterfactual computation, Proc. Roy. Soc. (Lond) A; or arXiv:quant-ph/9907007v2.
- [26] Mitchison, G. & Massar, S. (2000) Absorption-free discrimination between semi-transparent objects, arXiv:quant-ph/0003140v2.
- [27] Nakanishi, T., Yamane, K. & Kitano, M. (2002) Absorption-free optical control of spin systems: The quantum Zeno effect in optical pumping, arXiv:quant-ph/0103034v2.
- [28] Kwiat, P.G., Weinfurter, H. & Zeilinger, A. (1996) Quantum seeing in the dark, Scientific American, Nov.
- [29] Elitzur, A.C. & Dolev, S. (2000) Nonlocal effects of partial measurements & quantum erasure, arXiv:quant-ph/0012091v12000.

- [30] Hiley, B.J. & Callaghan, R.E. (2006) What is erased in the quantum erasure? *Foundations of Physics*, 36:12.
- [31] White, A.G., Mitchell, J.R. Nairz, O. & Kwiat, P.G. (1998) Interaction-free imaging, *Physical Review A* 58; 605.
- [32] White, A.G., Mitchell, J.R., Nairz, O. & Kwiat, P.G. (1998) "Interaction-free" imaging, arXiv:quant-ph/9803060v2.
- [33] Kotigua, R.P. & Toffoli, T. (1998) Potential for computing in micromagnetics via topological conservation laws, *Physica D*, 120:1-2, pp. 139-161.
- [34] Gerlach, W & Stern, O. (1922) *Das magnetische moment des silberatoms*, *Zeitschrift für Physik* 9, 353-355.
- [35] Young, T. (1804) Experiments and calculations relative to physical optics, *Philosophical Trans. of the Royal Society of London* 94, 1-16.
- [36] Kwiat, P.G., Weinfurter, H., Herzog, T., Zeilinger, A. & Kasevich, M. (1995) Experimental realization of 'interaction-free' measurements, in D.M. Greenberger & A. Zeilinger (eds.) *Fundamental Problems in Quantum Theory*, A Conference held in Honor of Professor John A. Wheeler, *Annals of the New York Academy of Science*, Vol. 755, p. 383, New York: New York Academy of Science.
- [37] Jaekel, M.T. & S. Reynaud, S. (1990) Quantum limits in interferometric measurements, *Europhys. Lett.* 13, 301.
- [38] Cramer, J.G. (2006) A transactional analysis of interaction-free measurements, *Foundations of Physics Letters* 19: 1; 63-73; or arXiv:quant-ph/0508102v23, 2008.
- [39] Amoroso, R.L., Kauffman, L.H. & Rowlands, P. (eds.) (2013) *The Physics of Reality: Space, Time, Matter, Cosmos*, Singapore: World Scientific.
- [40] Amoroso, R.L., Kauffman, L.H. & Rowlands, P. (eds.) (2015) *Unified Field Mechanics; Natural Science Beyond the Veil of Spacetime*, Singapore: World Scientific.
- [41] Everett, H. (1957) Relative state formulation of quantum mechanics, *Reviews of Modern Physics*, Vol 29, pp 454-462.
- [42] Bohm, D. & Vigier, J-P (1954) Model of the causal interpretation of quantum theory in terms of a fluid with irregular fluctuations, *Phys. Rev.* 96:1; 208-217.
- [43] Kaku, M. (1999) *Introduction to Superstrings and M-Theory*, New York: Springer.
- [44] Dirac, P.A.M. (1952) Is there an ether? *Nature*, 169: 172.
- [45] Petroni, N.C. & Vigier, J-P (1983) Dirac's aether in relativistic quantum mechanics, *Foundations Physics*, 13:2, 253-285.
- [46] Vigier, J-P (1980) De Broglie waves on Dirac aether: A testable experimental assumption, *Lettere al Nuovo Cimento*, 29; 467-475.
- [47] Lehnert, B. (2002) New developments in electromagnetic field theory, in R.L. Amoroso, G. Hunter, M. Kafatos & J-P Vigier (eds.) *Gravitation & Cosmology: From the Hubble Radius to the Planck Scale*, Dordrecht: Kluwer Academic.
- [48] Lehnert, B. (1998) Electromagnetic theory with space-charges in vacuo, in G. Hunter, S. Jeffers & J-P Vigier (eds.) *Causality and Locality in Modern Physics*, Dordrecht: Kluwer Academic.
- [49] Proca, A, (1936) *Compt. Rend.*, 202, 1420.
- [50] Cramer, J.G. (1986) The transactional interpretation of quantum mechanics, *Rev. Mod. Phys* 58, 647-687.
- [51] Hofstadter, D. (2013) Alan Turing: Life and legacy of a great thinker, in C. Teuscher (ed.) p. 54, Springer Science & Business Media.
- [52] Sudarshan, E.C.G. & Misra, B. (1977) The Zeno's paradox in quantum theory, *Journal of Mathematical Physics* 18 (4): 756-763.
- [53] Nakanishi, T., Yamane, K., Kitano, M. (2001) Absorption-free optical control of spin

- systems: The quantum Zeno effect in optical pumping, Physical Review A 65 (1): 013404; arXiv:quant-ph/0103034.
- [54] Facchi, P., Lidar, D.A. & Pascazio, S. (2004) Unification of dynamical decoupling and the quantum Zeno effect, Physical Review A 69 (3).
- [55] Degasperis, A., Fonda, L. & Ghirardi, G.C. (1974) Does the lifetime of an unstable system depend on the measuring apparatus? *Il Nuovo Cimento A* 21 (3): 471-484.
- [56] von Neumann, J. (1932) *Mathematische Grundlagen der Quantenmechanik*, Springer; von Neumann, J. (1955) Mathematical Foundations of Quantum Mechanics, Princeton University Press. p. 366.
- [57] Mensky, M.B. (2000) Quantum Measurements And Decoherence, Springer.
- [58] Peise, J., Lücke, B., Pezzé, L., Deuretzbacher, F., Ertmer, W., Arlt, J., Smerzi, A., Santos, L. & Klempt, C. (2015) Interaction-free measurements by quantum Zeno stabilization of ultracold atoms, *Nature Communications*, 6,14.
- [59] Renninger, M. (1953) Zum Wellen-Korpuskel-Dualismus. *Zeitschrift für Physik* 136, 251–261.
- [60] Misra, B. & Sudarshan, E.C.G. (1977) The Zeno's paradox in quantum theory, *J. Math. Phys* 18, 756-763.
- [61] Vlasov, A.Y. (1999) Quantum theory of computation and relativistic physics, PhysComp96 Workshop, Boston MA, 22-24 Nov 1996, arXiv: quant-ph/ 9701027v4.
- [62] Peres, A. & Terno, D.R. (2004) Quantum information and relativity theory, *Rev. Mod. Phys.* 76, 93; arXiv:quant-ph/0212023v2; Introduction to relativistic quantum information (2006) arXiv:quant-ph/0508049v2.
- [63] Jafarizadeh, M.A. & Mahdian, M. (2011) Quantifying entanglement of two relativistic particles using optimal entanglement witness, *Quantum Information Processing*, 10:4, pp. 501-518.
- [64] Felicetti, S., Sabin, C., Fuentes, I., Lamata, L., Romero, G. & Solano, E. (2015) Relativistic motion with superconducting qubits, arXiv:1503.06653v2 [quant-ph].
- [65] Arkani-Hamed, N., & Trnka, J. (2013) The amplituhedron, arXiv:1312.2007.
- [66] Bai, Y., He, S., & Lam, T. (2015) The amplituhedron and the one-loop Grassmannian measure, arXiv:1510.03553.
- [67] Arkani-Hameda, N., Hodgesb, A. & Trnkac, J. (2014) Positive amplitudes in the amplituhedron, arXiv:1412.8478v1 [hep-th].
- [68] Wootters, W.K. & Zurek, W.H. (1982) A single quantum cannot be cloned, *Nature*, 299 (5886) 802-803.
- [69] Jaynes, E.T. (1990) in W.H. Zurek (ed.) Complexity, Entropy, and the Physics of Information, Reading: Addison-Wesley.
- [70] Wheeler, J.A., & Feynman, R. (1945) *Rev. Mod. Physics*, 17, 157;
- [71] Witten, E. (1993) Quantum background independence in string theory, arXiv:hep-th/9306122v1
- [72] Sen, A. & Zwiebach, B. (1994) Local background independence of classical closed string field theory, *Nucl. Phys.* B414, 649.
- [73] Sen, A. & Zwiebach, B. (1994) Quantum background independence of closed string field theory, *Nucl. Phys.* B423, 580.
- [74] Chu, S-Y (1993) *Physical Rev. Letters*, 71, 2847.
- [75] Chantler, C.T. et al. (2012) Testing three-body quantum electrodynamics with trapped Ti²⁰ ions: evidence for a Z-dependent divergence between experiment and calculation, *PRL* 109, 153001.
- [76] Ranganathan, D. (1988) The Dirac equation in the de Broglie-Bohm theory, *Physics Letters A*, Volume 128, Issues 3-4, pp. 105-108.

- [77] Rowlands, P. (2003) The nilpotent Dirac equation and its applications in particle physics; <http://arxiv.org/ftp/quant-ph/papers/0301/0301071.pdf>.
- [78] Rowlands, P. (1994) An algebra combining vectors and quaternions, *Speculat. Sci. Tech.*, 17, 279-282.
- [79] Rowlands, P. (1996) Some interpretations of the Dirac algebra, *Speculat. Sci. Tech.*, 19, 242-246.
- [80] Rowlands, P. (1998) The physical consequences of a new version of the Dirac equation, in G. Hunter, S. Jeffers, and J-P. Vigier (eds.), *Causality and Locality in Modern Physics and Astronomy: Open Questions and Possible Solutions*. Fundamental Theories of Physics, vol. 97, Kluwer Academic Publishers, Dordrecht, 397- 402.
- [81] Rowlands, P. & Cullerne, J.P. (2001) The connection between the Han-Nambu quark theory, the Dirac equation and fundamental symmetries, *Nuc Phys A* 684, 713-5.
- [82] Rowlands, P. & Cullerne, J.P. (2002) The Dirac algebra and its physical interpretation, arXiv:quant-ph/00010094.
- [83] Rowlands, P. & Cullerne, J.P. (2002) Applications of the nilpotent Dirac state vector, arXiv:quant-ph/0103036.
- [84] Rowlands, P. & Cullerne, J.P. (2004) The Dirac algebra and grand unification, arXiv:quant-ph/0106111.
- [85] Mackay, A.L. & Pawley, G.S. (1963) Bravais Lattices in Four-dimensional Space, *Acta. cryst.* 16: 11-19.
- [86] Antippa, A.F. & Dubois, D.M. (2004) Anticipation, orbital stability and energy conservation in discrete harmonic oscillators, in D.M. Dubois (ed.) Computing Anticipatory Systems, AIP Conf. Proceedings Vol. 718, pp.3-44, Melville: American Inst. of Physics.
- [87] Dubois, D.M. (2001) Theory of incursive synchronization and application to the anticipation of delayed linear and nonlinear systems, in D.M. Dubois (ed.) Computing Anticipatory Systems: CASYS 2001, 5th Intl Conf., Am Inst of Physics: AIP Conf. Proceedings 627, pp. 182-195.
- [88] Antippa, A.F. & Dubois, D.M. (2008) The synchronous hyperincursive discrete harmonic oscillator, in D. Dubois (ed.) AIP proceedings of CASYS07.
- [89] Dubois, D.M. (2008) The quantum potential and pulsating wave packet in the harmonic oscillator, in D. Dubois (ed.) AIP proceedings of CASYS07.
- [90] Dubois, D.M. (2016) Hyperincursive algorithms of classical harmonic oscillator applied to quantum harmonic oscillator separable into incursive oscillators, in R.L. Amoroso, L.H. Kauffman & P. Rowlands (eds.) *Unified Field Mechanics: Natural Science Beyond the veil of Spacetime*, Singapore: World Scientific.
- [91] Icke, V. (1995) *The Force of Symmetry*, Cambridge: Cambridge Univ. Press.
- [92] Amoroso, R.L. & Chu, M-Y.J. (2008) Empirical mediation of the primary mechanism initiating protein conformation in prion propagation, in D. Dubois (ed.) Partial Proceedings of CASYS07, IJCAS, Vol. 22, Univ. Liege Belgium.
- [93] Gambini, R. & Pullin, J. (1996) Variational derivation of exact skein relations from Chern-Simons theories, arXiv:hep-th/9602165v1.
- [94] Schwinger, J. (1992) Casimir energy for dielectrics, *Proc. Nat. Acad. Sci.* 89, 4091-3.
- [95] Schwinger, J. (1993) Casimir light: The source, *Proc. Nat. Acad. Sci* 90, 2105-6.
- [96] Schwinger, J. (1994) Casimir energy for dielectrics: spherical geometry, *Proc. Nat. Acad. Math. Psych.* 41:64-67, San Francisco: W.H. Freeman.
- [97] Amoroso, R.L. (2005) Application of double-cusp catastrophe theory to the physical evolution of qualia: Implications for paradigm shift in medicine & psychology, in G.E. Lasker & D.M. Dubois (eds.) *Anticipative & Predictive Models in Systems Science*,

- Vol. 1, pp. 19-26, Windsor: The International Institute for Advanced Studies in Systems Research & Cybernetics.
- [98] Gilmore, R. (1981) *Catastrophe Theory for Scientists & Engineers*, New York: Dover.
 - [99] Poston T. & Stewart, I (1978) *Catastrophe Theory & Its Applications*, New York: Dover; Gilmore, R. (1981) *Catastrophe Theory for Scientists & Engineers*, Dover.
 - [100] Qin, S. et al. (2001) *Int. J. of Solids & Structures*, 38, pp. 8093-8109.
 - [101] Stevens, H.H. (1989) Size of a least unit, in M. Kafatos (ed.) *Bell's Theorem, Quantum Theory and Conceptions of the Universe*, Dordrecht: Kluwer Academic.
 - [102] Cardone, F. & Mignani, R. (2004) *Energy and Geometry - An Introduction to Deformed Special Relativity*, Singapore: World Scientific.
 - [103] Cardone, F., Marrani, A. & Mignani, R. (2003) The electron mass from deformed special relativity, *Electromagnetic Phenomena* Vol.3, N.1; 9, special number dedicated to Dirac's centenary; (2008) hep-th/0505134.
 - [104] Cardone, F., Marrani, A. & Mignani, R. (2008) A new pseudo-Kaluza-Klein scheme for geometrical description of interactions, arXiv:hep-th/0505149v1.
 - [105] Randall, L. (2005) *Warped Passages. Unraveling the Mysteries of the Universe's Hidden Dimensions*, New York: Harper-Collins.
 - [106] Slichter, C.P. (1990) *Principles of Magnetic Resonance*, 3rd edition, Springer Series in Solid-State Sciences 1, New York: Springer.
 - [107] Schumacher, R.T. (1970) *Introduction to Magnetic Resonance*, Menlo Park: Benjamin-Cummings.
 - [108] Farrar, T.C. & Becker, E.D. (1971) *Pulsed and Fourier Transform NMR*, New York: Academic Press.
 - [109] Abragam, A. (1961) *Principles of Nuclear Magnetism*, Oxford: Clarendon Press.
 - [110] Dehmelt, H.G. (1954) Nuclear quadrupole resonance, *Am. J. Physics*, 22:110.
 - [111] Semin, G.K. Babushkina, T.A. & Yakobson, G.G. (1975) *Nuclear Quadrupole Resonance in Chemistry*, New York: Wiley.
 - [112] Atkinson, P.W. (1994) *Molecular Quantum Mechanics*, 2nd edition, Oxford: Oxford University Press.
 - [113] Haussler, O. (1974) Coulomb reorientation, in J. Cerny (ed.) *Nuclear Spectroscopy and Reactions*, Part C, New York: Academic Press.
 - [114] Humieres, D., Beasley, M.R., Huberman, B.A. & Libchaber, A. (1982) Chaotic states and routes to chaos in the forced pendulum, *Physical Rev A*, 26:6, 3483-34.
 - [115] Rueda, A. & Haisch, B. (1998) Contributions to inertial mass by reaction of the vacuum to accelerated motion, *Found. of Phys.*, 28:7, 1057-1108.
 - [116] Rueda, A. & Haisch, B. (1998) *Physics Lett. A*, 240, 115.
 - [117] Rueda, A., Haisch, B. & Puthoff, H.E. (1994) *Phys. Rev. A*, 49, 678.
 - [118] Rueda, A. & Haisch, B. (2002) The inertia reaction force and its vacuum origin, in R.L. Amoroso, G. Hunter, M. Kafatos & J-P Vigier (eds.), *Gravitation & Cosmology: From the Hubble Radius to the Planck Scale*, pp. 447-458, Dordrecht: Kluwer Academic.
 - [119] Vigier, J-P (1997) New non-zero photon mass interpretation of the Sagnac effect as direct experimental justification of the Langevin paradox, *Physics Let. A*, 234:2, 75-85.
 - [120] Garcia-Ripoli, J.J., Zoller, P. & Cirac, J.I. (2005) Coherent control of trapped ions using off-resonant lasers, *Phys. Rev. A* 71, 062309; 1-13.
 - [121] Vigier-J-P (1995) Derivation of inertial forces from the Einstein-de Broglie-Bohm causal stochastic interpretation of quantum mechanics, *Found. Phys.* 25:10, 1461-1494.
 - [122] Sakharov, A.D. (1968) Sov. Phys. Dokl. 12, 1040.

- [123] Puthoff, H.E. (2002) Polarizable vacuum approach to General Relativity, in R.L. Amoroso, G. Hunter, M. Kafatos & J-P Vigier (eds.), *Gravitation & Cosmology: From the Hubble Radius to the Planck Scale*, pp. 431-446, Dordrecht: Kluwer Academic.
- [124] Burns, J.E. (1998) Entropy and vacuum radiation, *Found. Phys.* 28 (7), 1191-1207.
- [125] Burns, J.E. (2002), Vacuum radiation, entropy and the arrow of time, in R.L. Amoroso, G. Hunter, S. Jeffers & M. Kafatos, (eds.) *Gravitation & Cosmology: From the Hubble Radius to the Planck Scale*, Dordrecht: Kluwer Academic.
- [126] Zeh, H.D. (1989) *The Physical Basis of the Direction of Time*, New York: Springer-Verlag.
- [127] Vigier, J-P & Amoroso, R.L. (2002) Can one unify gravity and electromagnetic fields? in R.L. Amoroso, G. Hunter, S. Jeffers & M. Kafatos, (eds.), *Gravitation & Cosmology: From the Hubble Radius to the Planck Scale*, Dordrecht: Kluwer Academic.
- [128] Borne, T., Lochak, G. & Stumpf, H. (2001) Nonperturbative Quantum Field Theory and the Structure of Matter, *The theory of light and wave mechanics*, pp. 4-38, Volume 114, *Fundamental Theories of Physics* Dordrecht: Kluwer.
- [129] Rauscher, E.A. (1983) *Electromagnetic Phenomena in Complex Geometries and Nonlinear Phenomena, Non-Hertzian Waves and Magnetic Monopoles*, Millbrae: Tesla Books; (2009) 2nd edition, Oakland: The Noetic Press, and references therein.
- [130] Rauscher, E. (2002) Non-Abelian gauge groups for real & complex Maxwell's equations, in R.L. Amoroso, G. Hunter, S. Jeffers & M. Kafatos, (eds.), *Gravitation & Cosmology: From the Hubble Radius to the Planck Scale*, Dordrecht: Kluwer.
- [131] Messiah, A. (1999) *Quantum Mechanics*, pp. 438-444, New York: Dover.
- [132] Dyson, F.J. (1958) Innovation in Physics, *Scientific American*, 199, No. 3.
- [133] Eberly, J.H. (1972) Superradiance revisited, *AJP*, 40; 1374-1383.

Chapter 8

Measurement with Certainty

Because of what Unified Field Mechanics (UFM) appears to tell us about the fundamental basis of matter (albeit a preliminary foray); it is postulated that a bulk UQC cannot be built without utilizing UFM parameters with an inherent ability to supervene the quantum uncertainty principle. Although no attempt has been made yet to make correspondence with M-Theoretic supersymmetry, since it remains sufficiently unfinished; the topological order envisioned for UFM additions to the structure of matter can probably readily be made to do so. Concepts required to supervene uncertainty, such as a Dirac polarized vacuum, the de Broglie-Bohm causal interpretation and Cramer's transactional interpretation are already well-known to physics, but generally ignored. Concepts like Large-Scale Additional Dimensions (LSXD), brane topology and the vision that spacetime is not fundamental, but emergent, are already known and under ongoing development. The three main additions we apply are the discovery of a manifold of uncertainty (MOU) with finite radius, to which the unified field provides an ontological force of coherence (not 5th force) and that the underlying bulk hidden behind the 'veil of uncertainty' is a tessellation of 'Least Cosmological Units' (LCU) annihilated and recreated with a cyclic beat frequency. May it become obvious, that this inherent LCU beat frequency is the key factor in supervening uncertainty for measurement with certainty.

The general principle of superposition of quantum mechanics applies to the states ... of any one dynamical system. It requires us to assume that between these states there exist peculiar relationships such that whenever the system is definitely in one state we can consider it as being partly in each of two or more other states ... indeed in an infinite number of ways. Conversely any two or more states may be superposed to give a new state ... The non-classical nature of the superposition process is brought out clearly if we consider the superposition of two states, *A* and *B*, such that there exists an observation which, when made on the system in state *A*, is certain to lead to one particular result, *a* say, and when made on the system in state *B* is certain to lead to some different result, *b*. What will be the result of the observation when made on the system in the superposed state? The answer is that the result will be sometimes *a* and

sometimes b , according to a probability law depending on the relative weights of A and B in the superposition process. It will never be different from both a and b . The intermediate character of the state formed by superposition thus expresses itself through the probability of a particular result for an observation being intermediate between the corresponding probabilities for the original states, not through the result itself being intermediate between the corresponding results for the original states – Dirac [1].

8.1 Introduction – Summary of Purpose

Generally, the 4-space of observation is restricted to a manifold inside a HD space, called the ‘bulk’ (hyperspace) by M-Theorists. If additional dimensions are compactified, then the observed universe would contain any possible extra dimensions; and no reference to a bulk is required. However, if a bulk with Large-Scale Additional Dimensionality (LSXD) does exist, a rich interacting brane-world influencing 4-space is postulated.

Kaluza-Klein XD compactification in string theory differs from the particle theory version in that a closed string can be wound several times around a rolled up dimension. A string with this property, has what is called winding mode oscillations that add additional symmetry not found in particle physics. A theory with a rolled up dimension of size R was found to be equivalent to a theory with a rolled up dimension of size L_s^2/R with winding modes and momentum modes exchanged in XD. (L_s is the string length scale.)

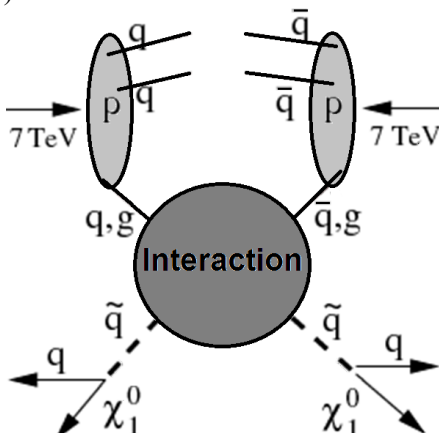


Fig. 8.1. An LHC p-p collision producing supersymmetric particles. Protons, p from the beams, are made of quarks, q and gluons, g . Their collisions produce supersymmetric particle pairs, \tilde{q} . The supersymmetric particles subsequently decay into ordinary particles and dark matter particles, χ_1^0 . Redrawn from [2].

This symmetry allows correspondence between theories with small XD to theories with LSXD, which is known as T-Duality. In superstring theory, Kaluza-Klein compactification must be applied to a 6D space. The well-known method of doing so is to use a heterotic dual Calabi-Yau 3-torus which determines the geometric topology of the symmetries and spectrum of the particle theory [3]. In our theory the manifold of uncertainty has a 6D topology [4,5] compatible with this type of supersymmetry. Braneworld models generally radically differ from superstring Kaluza-Klein compactification models because they require few steps between the Planck scale and electroweak scale. This huge difference between the Planck and the electroweak scale is called the gauge hierarchy problem [6-8].

Sufficient theoretical insight related to a new anthropic multiverse UFM cosmology [4,9-44] has occurred during the 17 intervening years since the prior work [45] to design rigorous empirical protocols for isolating and manipulating fundamental parameters related to long-range coherence in semi-quantum systems. A key premise is that the so-called Planck scale stochastic regime is not fundamental and need no longer be a barrier to the study coherent phenomena in quantum systems generally or biological systems. Since Heisenberg's 1927 discovery, the quantum uncertainty principle (4D) has been by empirical definition a barrier to accessing certain kinds of complementary biophysical information. As will be shown, the simple solution is - do something else! That is, use a different fundamental basis for quantum and biophysical 'measurement' criteria by utilizing additional degrees of freedom inherent in a noetic UFM cosmology. Nine experimental protocols are outlined for testing postulates of the model; which if successful will lead to bulk UQC, a standardized biophysical research platform and a new class of biosensors.

Noetic UFM cosmology makes correspondence to 11D M-Theoretic dual Calabi-Yau mirror symmetry, $M_{10} \rightarrow M_4 \times K_6$ [46-48] albeit with the addition of a twelfth dimension to incorporate Unified Field, U_F dynamics, $M_{12} \rightarrow M_4 \times K_8 \rightarrow \hat{M}_4 \times \hat{\mathbb{C}}_4^+ \times \hat{\mathbb{C}}_4^-$ [4,30]. String Theory has struggled to discover one unique vacuum compactification from the googolplex, 10^{googol} or infinite potentia provided by XD, with Standard Model Minkowski space, M_4 as the sought resultant [46-48]. Noetic UFM cosmology is different - All dimensionalities from 12D to 0D are cycled through continuously defined as a 'Continuous-state spin exchange dimensional reduction compactification process' that led to discovery of a unique string vacuum [4,44]. Note: The 'continuous-state' LCU is radically different than a Big Bang singularity [4,21,40,41].

Summary of salient theoretical postulates:

- The Unified Field, U_F provides an evolutionary ‘force of coherence’ guiding evolution in quantum systems.
- The HD U_F regime is accessible by surmounting the uncertainty principle (limitation imposed by space-quantization parameters of the Copenhagen Interpretation) by manipulating new cosmological parameters described by additional degrees of freedom related to a Large-Scale Additional Dimensionality (LSXD) version of M-Theory [41].
- Utilizing U_F parameters provides a new action principle with an inherent force of coherence acting like a ‘super-quantum potential’ or pilot wave [4,49-51] guiding the ‘continuous-state’ spin-exchange dimensional reduction compactification process of spacetime and evolution of complexity in quantum and the Self-Organized Living Systems (SOLS) it pervades [9].
- The putative unique 12D M-Theoretic regime of U_F action correlates parameters of Calabi-Yau mirror symmetry [49-51] with heretofore generally ignored properties of de Broglie-Bohm Causal and Cramer Transactional interpretations of quantum theory [49-52] and their higher dimensional (HD) extensions utilized in the new paradigm of noetic UFM cosmology [4,44].
- This unique string vacuum forms a conformal scale-invariant covariant polarized Dirac-Einstein energy dependent spacetime metric, $\hat{M}_4 \times \pm \mathbb{C}_4$ [4,53-55] which by nature of its inherent continuous-state dimensional reduction process [4] acts as a Feynman ‘synchronization backbone’ [56] facilitating/simplifying empirical accessibility.
- This empirical mediation of the LSXD polarized Dirac-Einstein metric, $\hat{M}_4 \times \pm \mathbb{C}_4$ (12D) [4,10,44,53-55] can be performed by a specialized incursive form of rf-modulated Sagnac Effect resonant interference hierarchy able to surmount the uncertainty principle [4,11].

Since 1993 the so-called Elitzur-Vaidman Interaction-Free Measurement (IFM) paradigm [57-65], a procedure for detecting the quantum state of an object without a phenomenological interaction occurring with the measuring device that ordinarily collapses the quantum

wave function, Ψ provides an indicia of our model suggesting it may be possible in general, as proposed here, to completely override the quantum uncertainty principle with probability, $p \equiv 1$ through utility of additional degrees of freedom inherent in the supersymmetric regime of string/brane theory. Note: in Newtonian mechanics the universe was 3D, Einstein introduced a 4D cosmology; now the next step seems to require 12D as the minimal dimensionality for producing causal separation from \hat{M}_4 .

The disadvantages of the IFM model is that in order to improve probability towards certainty more and more Mach-Zehnder interferometers and more and more cycles through the apparatus are required [58-61]; while our apparatus acts with a single cycle because it represents a true and complete overriding of the quantum uncertainty principle by utilization U_F dynamics [4,11]. We emphasize our position that it is impossible to violate the uncertainty principle in 4D (by empirical fact) which the IFM method is limited to. This duality in the Quantum Zeno Paradox as experimentally implemented in IFM protocols suggests a duality between the regular phenomenological quantum theory [66-70] and a completed unified or ontological model beyond the formalism of the standard Copenhagen Interpretation as proposed here [4,5,44,45,71]. Utilizing extended theoretical elements, a putative empirical protocol for producing IFM with probability $p \equiv 1$ is introduced in a direct causal violation or absolute surmount of the methodology of the current 4D Copenhagen quantum Uncertainty Principle.

8.2 The Principle of Superposition

Classical waves can interact with constructive or destructive interference or a combination of both. When two waves interfere, the resulting displacement of the medium at any location is the algebraic sum of the displacements of the individual waves at that same location. Quantum mechanically waves can exist in all possible states simultaneously; this known as a superposition of states. A state vector corresponding to a pure quantum state takes the form, $|\Psi\rangle$. For example, if electron spin is measured in a Stern-Gerlach apparatus, there are two possible results. By convention electron spin is described by a 2D Hilbert space represented as a pure state complex vector, (α, β) with a length one by $|\alpha|^2 + |\beta|^2 = 1$ where $|\alpha|$ and $|\beta|$ are the absolute values of α and β . The superposition

principle states that the net response at a given place and time caused by two or more stimuli is the sum of the responses which would have been caused by each stimulus individually. For example, a physically observable manifestation of superposition is interference peaks from an electron wave in a double-slit experiment or a qubit state as a linear superposition of the quantum basis states $|0\rangle$ and $|1\rangle$ in Dirac notation which convert to classical logic 0 or 1 by a measurement.

Accounting for interference effects in waves requires superposition such that an ensemble of quantum systems is described by wave functions with states, $\Psi_1, \Psi_2 \dots \Psi_n$. Thereby any linear combination

$$\Psi = c_1 \Psi_1 + c_2 \Psi_2 \dots c_n \Psi_n \quad (8.1)$$

with $c_1, c_2 \dots c_n$ being constants describes possible quantum states of the ensemble. The complex wave functions, $\Psi_1, \Psi_2 \dots \Psi_n$ are written as

$$\Psi_1 = |\Psi_1| e^{i\alpha_1}, \quad \Psi_2 = |\Psi_2| e^{i\alpha_2} \dots \Psi_n = |\Psi_n| e^{i\alpha_n}. \quad (8.2)$$

From (8.1) (simplified) the squared modulus of Ψ is

$$|\Psi|^2 = |c_1 \Psi_1|^2 + |c_2 \Psi_2|^2 + 2 \operatorname{Re} \{ c_1 c_2^* |\Psi_1| |\Psi_2| \exp[i(\alpha_1 - \alpha_2)] \} \quad (8.3)$$

Achieved by

$$\begin{aligned} |\Psi|^2 &= \Psi^* \Psi = (c_1^* \Psi_1^* + c_2^* \Psi_2^*) (c_1 \Psi_1 + c_2 \Psi_2) = \\ &c_1^* \Psi_1^* c_1 \Psi_1 + c_2^* \Psi_2^* c_2 \Psi_2 + c_1^* \Psi_1^* c_2 \Psi_2 + c_1 \Psi_1 c_2^* \Psi_2^* = \\ &|c_1 \Psi_1|^2 + |c_2 \Psi_2|^2 + c_1 \Psi_1 c_2^* \Psi_2^* + (c_1 \Psi_1 c_2^* \Psi_2^*)^* = \\ &|c_1 \Psi_1|^2 + |c_2 \Psi_2|^2 + 2 \operatorname{Re}(c_1 \Psi_1 c_2^* \Psi_2^*) \end{aligned} \quad (8.4)$$

and then substituting (8.1) one gets (8.2), such that in general

$$|\Psi|^2 \neq |c_1 \Psi_1|^2 + |c_2 \Psi_2|^2 \quad (8.5)$$

because of the Uncertainty Principle.

Note that $|\Psi|^2$ is unaffected if the wavefunction, Ψ is multiplied by a global phase factor, $\exp(i\alpha)$. However, if α is a real constant, it depends on the relative phase $(\alpha_1 - \alpha_2)$ of Ψ_1 and Ψ_2 which because of the third term on the right in (8.3) is an interference term [4,72].

8.3 Oscillatory Rabi NMR Resonance Cycles

A Rabi cycle is the cyclic behavior of a two-state quantum system in the presence of an oscillatory driving field. We are interested here in NMR-like Rabi cycles because our protocol for surmounting the uncertainty principle relies in part on a Rabi cycle resonance hierarchy. A two-state or two-level quantum system, such as the spin-1/2 electron ($\pm \hbar/2$) or atomic orbital transitions, has two possible states and can become ‘excited’ if energy is absorbed. For hydrogen in an electromagnetic field with the frequency tuned to the excitation energy, the electron would be in either the ground state or an excited state. If we initialize the hydrogen atom to one of these states, time evolution will cause each level to oscillate with a characteristic angular Rabi frequency represented by the basis vectors,

$$|1\rangle = \begin{pmatrix} 1 \\ 0 \end{pmatrix}, |2\rangle = \begin{pmatrix} 0 \\ 1 \end{pmatrix} [73].$$

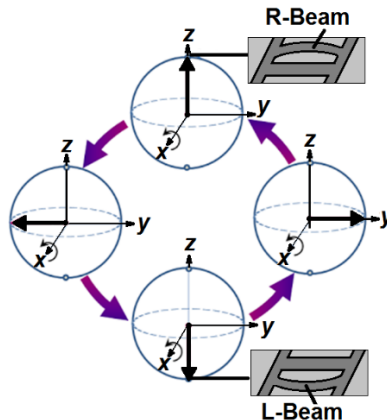


Fig. 8.2. Schematic evolution of coupled mechanical oscillators on the Bloch sphere when undergoing a Rabi cycle.

The NMR effect is produced by applying a strong static field, B_0 , called the holding field, to a nucleus. When an additional weak transverse field, B_1 oscillating at an rf-frequency, ω_r rotating in the xy -plane around B_0 is applied to the holding field, $B_0\hat{z}$, one has the time-dependent field:

$$\mathbf{B} = \begin{pmatrix} B_1 \cos \omega_r t \\ B_1 \sin \omega_r t \\ B_0 \end{pmatrix} [73]. \quad (8.6)$$

This is the right-handed rotating field; utilized in our protocol of counterpropagating Sagnac Effect rf-fields [4,5,44,71].

Whatever motions produce spectral lines, the application of a uniform magnetic field should produce changes because of Larmor precession. A general oscillation can be resolved into three harmonic components at right angles. If the magnetic field is in the $+z$ -direction, then the oscillation in the z -direction will be unaffected by the magnetic field, while the x and y motions will precess with the Larmor angular velocity $(e/2mc)B$ in a right-handed manner about the $+z$ -axis. An x -vibration $x = a \cos \omega t$ can be expressed as the sum of two circular motions $(a/2)e^{i\omega t}$ and $(a/2)e^{-i\omega t}$ rotating in opposite directions, and similarly for a y -oscillation. Clockwise motion will speed up by Larmor precession to $\omega + \omega_L$, and anticlockwise motion will slow down by the same amount [73-75].

8.4 The Problem of Decoherence

It could be that the universe has a very rich structure, with many different branes, on which there exist very different physics, living in an as yet unknown geometry.
 - L. Randall [7].

Except perhaps for quantum Hall quasiparticle protected anyons, in principle, quantum systems are open and not isolated from environmental noise or coupling. Decoherence, the destroyer of quantum superstition is essentially the only remaining barrier to bulk UCQ. It is curious that although anyonic TQC apparently has solved this dilemma by the braiding of topological phase; as yet there is no known method of accessing the protected qubits [76,77]. We suspect our proposed Ontological-phase Topological Field Theory (OPTFT) will provide a method of doing so; but

if such is the case, cryogenic temperatures would not be needed for UQC and an anyonic TQC might only be built as an interesting proof of concept.

One key to developing UQC is to have quantum states with lifetimes longer than it takes to perform a computing operation. Current records for maintaining coherence are curiously interesting. For isolated atoms in ultra-high vacuum chambers (no collisions with environment); the record for coherence is over 10 minutes. Solid-state silicon qubit systems cooled to absolute zero have long coherence times; but the new record is 39 minutes for room temperature silicon qubits [78].

In general, the problem of decoherence is strictly connected to the emergence of classicality in a world governed by the laws of quantum mechanics; and until now, any quantum information protocol must end up with a measurement converting quantum states into classical outcomes where decoherence plays a key role in this quantum measurement process [79-86]. The last statement is not true exactly in the manner stated. As we intend to show, the causally-free HD ontological-phase copy of the system may be read instead of the system itself, leaving the system itself untouched and free to continue its evolution. What this does to QC algorithms, or speedup remains to be determined [4,87,88] (Chap. 12).

The Heisenberg uncertainty principle, $\delta_x \delta_p \geq \hbar / 2$ says that there is an inherent uncertainty in the relation between position and momentum in the x direction. Matter was thought to consist of localized particles, but matter exhibits wave-like properties, which means that matter, like waves, isn't localized in space. The uncertainty principle is a direct consequence of the wave-like nature of matter, because you can't completely discretize a wave. As developed to a preliminary degree in Chap. 4, we move beyond these concepts of matter to one radically extended in HD UFM topology.

We concur with Randall that these dimensions can be of infinite size, which follows from the existence of branes with infinite spatial extent, a property of branes that occurs because they carry energy. If there is an energetic 4D flat brane in a 5D spacetime, the 5D space does not consist of flat, uniform, LSXD. To accommodate a flat brane requires that in addition to the tension of the brane itself, there is a bulk vacuum energy, closely aligned to the brane tension. The solution to Einstein's equations is then described locally as an anti-de Sitter (AdS) space, a space with a negative vacuum energy, although it is fundamentally 5D [7,89].

In this geometry, the length of a yardstick depends on position. Spacetime is ‘warped’ and HD do not have to be finite in size, because unlike the case of flat XD, the gravitational force spreads very little in the

direction perpendicular to the brane. To derive this form for the gravitational force, one solves Einstein's equations of general relativity in the presence of the brane. General relativity tells us that not only do gravitational forces affect matter, but matter determines the surrounding gravitational potential. In this case, the presence of a massive brane leads to a gravitational force highly concentrated near the brane. So although X_D can be very large (even infinite), the gravitational force is highly concentrated near the brane [6-8].

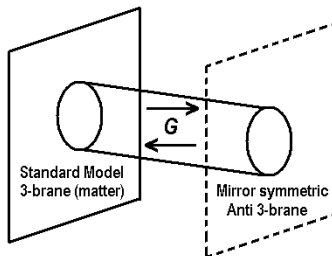


Fig. 8.3. Infinite size local 3-space and LSXD Braneworld and relate to gravity.

Randall says there is physics that ties X_D to observable low energy scales. Such theories, in which the X_D are tied to relatively low energy scales, have the enticing possibility that they can be observed in the next generation of LHC colliders. Our model, which may be a form of supersymmetric M-Theoretic T-Duality, is different, tabletop and low energy; if successful it will put an end to the need for supercolliders [90].

In a variant of the original proposal, in which the second brane does not end space but resides in an infinite extra dimension (essentially combining RS1 and RS2), one would have missing energy signatures identical to those one would obtain with six large ADD-type extra dimensions ... A five-dimensional AdS space is equivalent to a four dimensional scale-invariant field theory, in the sense that all properties of the four-dimensional theory can be computed from the five-dimensional gravitational theory, and in principle one can learn about the gravitational theory from the conformal field theory (this is known as a holographic correspondence) ... These include the existence of a four-dimensional domain in a higher dimensional space ... It is possible that one or several of these ideas will be relevant to the question of how string theory evolves from a higher dimensional theory to one that reproduces observed four-dimensional physics [7].

8.5 Insight into the Measurement Problem

In order to surmount quantum uncertainty and empirically access the hidden 3rd regime of reality (Classical → Quantum → Unified) new physics is required.

Here we introduce a new ontological type of homeomorphic transformation (a holomorphic-antiholomorphic duality) that Toffoli calls a ‘topological switching’ [75] by what Stern calls ‘topological charge’ [91,92] that we propose as an empirical basis for the Micromagnetics of spacetime/matter information exchange without usual phenomenological exchange quanta. Mediation occurs instead as an ‘ontological becoming’ or ‘being’ by operation of an energyless coherently controlled resonant hierarchy of the topology of LSXD brane interactions [4,87,88] which is not a local Hamiltonian phenomenon but perhaps a new form of ontological U_F Lagrangian topology. Topological switching can be represented metaphorically as the perceptual switching of the central vertices of a Necker Cube (Ambiguous cube) when stared at.

For example, imagine a usual 4D qubit or quantum particle in a box. In our noetic UFM interpretation the LSXD Calabi-Yau mirror symmetric regime contains a hierarchy of conformal scale-invariant ‘copies’ of the original 4D quantum state not independent Everett-Wheeler parallels [94,95]. Then in way of simplistic introduction in terms of our new operationally completed interpretation of quantum theory the ‘mirror image of the mirror image is causally free’ of the underlying uncertain 4D quantum state and is accessible by manipulating the resonance hierarchy of our empirical protocol! Many physicists have been reluctant to embrace HD or LSXD physics. We suspect success of our protocol would ease this philosophical conundrum.

In this volume a putative protocol is delineated not for another sophisticated improvement of the varied stepwise degrees of reducing the uncertainty relation by the several extant IFM protocols [93]; but for completely surmounting the uncertainty relation directly, in a straight forward manner, for any and every single action of the experiment with probability, $p \equiv 1$. In an unexpected way our model has similarities to IFM but by using extended theory fully completes the task of uncertainty violation. One could say the new noetic UFM protocol turns the IFM methodology upside down and inside out. The LSXD regime of the noetic UFM protocol accesses the complete ‘hall of mirrors’ simultaneously (ontologically) because the whole battery of IFM interferometers and multiple cycling routines is inherent in the conformal scale-invariant mirror symmetry of the LSXD regime, such that only one ‘measurement’ is required to achieve probability, $p \equiv 1$ when resonance is properly coupled and timed with the inherent continuous-state mirror symmetric synchronization backbone beat frequency.

The methodology of this new empirical protocol is fully ontological (rather than the usual phenomenology of field interactions) because action in the LSXD regime is in causal violation of Copenhagen phenomenology not in an Everett ‘many-worlds’ sense but in a manner that extends to completion the de Broglie-Bohm-Vigier causal interpretation of quantum theory [50]. In summary the ontological basis is realized utilizing the additional degrees of freedom of a unique 12D iteration of M-Theory along with the key supposition of conformal scale-invariance pertaining to the physicality of the dual mirror symmetric state of LSXD quantum information as geometric topology [4,5,44].

In Fig. 8.4a the suggestion is that the 3-cube (bottom left) represents the region of a Cavity-QED or 3D quantum ‘particle in a box’ that through conformal scale-invariance remains physically real when the metaphor is carried to 12D where the ‘mirror copy’ becomes like a ‘mirror image of a mirror image’ and in that sense is causally free of the E_3 quantum state thereby open to ontological information transfer in violation of Copenhagen uncertainty. A 5D hypercube would unfold into a cross of 4D hypercubes and so on to 12D.

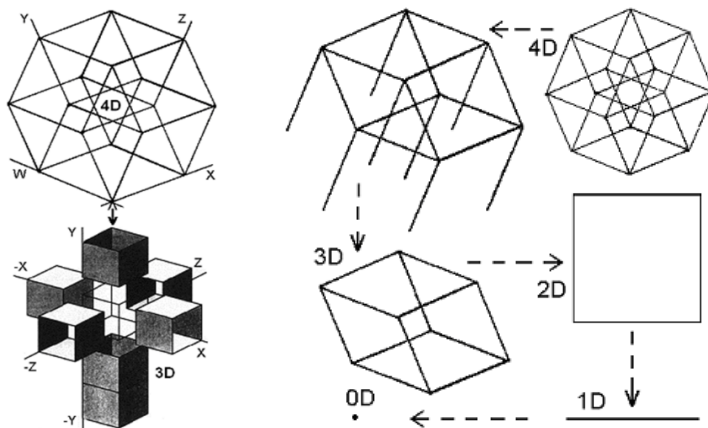


Fig. 8.4. a) Left, a 4D hypercube unfolds into a 3D cross of 8 cubes. b) Right. Dimensional reduction cycle from 4D to 1D.

Beyond 4D mirror symmetry adds a complexity in that the unfolding (Fig. 8.4b) has a knot or Dirac twist (not shown) that is part of the gating mechanism insulating quantum mechanics from the 3rd regime of UFM [5]. In Copenhagen the ‘handcuffs’ are on but during the LSXD cycle the handcuffs are periodically off and thus accessible resonantly.

8.6 New Physics from Anthropic Cosmology

Issues of the nature of the fundamental cosmological background continue to be debated with disparate views jockeying for philosophical supremacy; a scenario remaining tenable because experimental avenues for testing physics beyond the standard model have remained elusive until now. For the scientific perspective to evolve beyond the usual Copenhagen Interpretation of quantum theory requires a new cosmological paradigm. Full delineation of the new cosmology is beyond the scope of this volume, but introduced in [4,5,44,71,72]. In summary we axiomatically review pertinent concepts. The new noetic UFM cosmology is required to explain, utilize and design experimental access to the U_F regime where parameters required for UQC and for biophysical-bridging reside.

- The Planck scale can no longer be considered the most fundamental level of reality. Three regimes of reality must be addressed: Classical \Leftrightarrow Quantum \Leftrightarrow Unified Field; all of which cycle continuously [4].
- No ‘observer’ quantum state reduction exists in the usual sense of wave function collapse [71]; in the de Broglie-Bohm and extended Cramer interpretations of quantum theory [49-52] a continuous evolution operates instead [4,5,71]. Collapse of the wavefunction reduces a quantum state to a classical state, which does not generally happen in the nonlocal flux of qualia as the locus of awareness; especially since now more pertinently qualia are not quantum phenomena per se but unified field phenomena. Quale interface with the quantum regime as part of the sensory data transduction apparatus. The Planck scale is not an impenetrable barrier [5,44] even though considered so as an empirical fact demonstrated by the quantum uncertainty principle. This is a main problem with utilizing a Darwinian Naturalistic Big Bang cosmology originating from a putative singularity in time as the basis for cognitive theory. In an anthropic multiverse cosmology utilizing extended quantum theory and M-Theory the answer is simply: ‘do something else!’ which opens physical investigation into a new U_F realm of large scale additional dimensions (LSXD) [5,7,44,89]. The anthropic multiverse is closed and finite in time, i.e. the 14.7 billion light year Hubble radius, H_R , but open and infinite in atemporal eternity [4]. ‘Worlds without number, like grains of sand at the seashore’ [96] the multiverse has room for an infinite number of nested Hubble spheres each with their own fine-tuned laws of physics [4].

Fourteen empirical protocols are proposed [97,98] (9 reviewed here) for UQC, demonstrating, gaining access to and leading to a variety of experimental platforms for first hand investigation of awareness (qualia) breaking down the 1st person 3rd person barrier called for by Nagel [99].

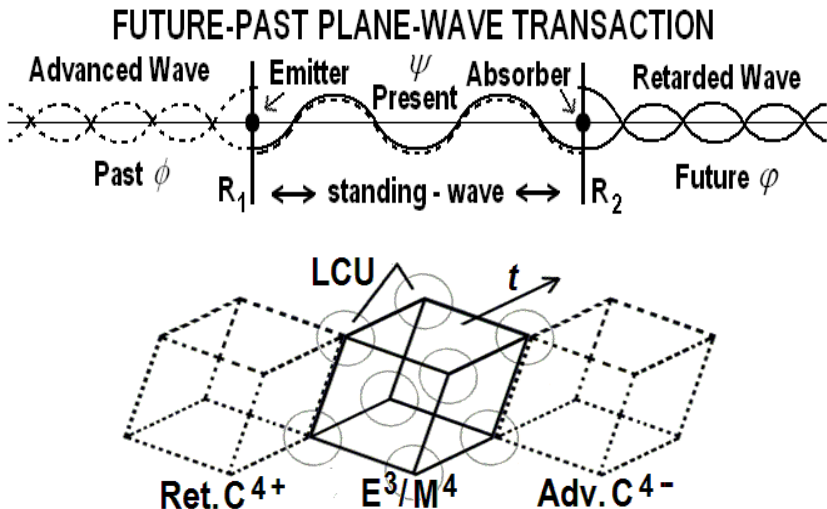


Figure 8.5. a) Conceptualized structure of a Cramer transaction (present state or event) where the present (simplistically) is a standing-wave of future-past potential elements. A point is not a rigid singularity (although still discrete) as in the classical sense, but has a complex structure like a mini-wormhole where R_1 & R_2 (like the frets holding the wire of a stringed instrument) represent opposite ends of its diameter. b) How observed (virtual) 3D reality arises from the infinite potentia of HD space (like a macroscopic transaction). The ‘standing-wave-like’ (retarded-advanced future-past) mirror symmetric elements C^{4+} / C^{4-} (where C^4 signifies 4D potentia of complex space distinguished from the realized 3D of visible space) of continuous-state spacetime show a central observed Euclidian, E_3 , Minkowski, M_4 space resultant. Least Cosmological Units (LCU) governing evolution of the ‘points’ of 3D reality are represented by circles. The Advanced-Retarded future-past 3-cubes in HD space guide the evolution of the central cube (our virtual reality) that emerges from elements of HD space.

String theory only has one parameter, string tension, T_S fraught with the dilemma of a Googolplex (10^{googol}) or infinite number of vacuum possibilities. Utilizing the Eddington, Dirac, and Wheeler large number hypothesis [5] we derived an alternative derivation of T_S leading to one unique string vacuum and what we call the ‘continuous-state hypothesis’ an alternative to the expansion/inflation parameters of Big Bang cosmology [4,5]. Simplistically the perceived inflation energy of Big Bang cosmology postulated as a Doppler expansion from a primordial *ex nihilo*

temporal singularity, instead according to the UFM noetic continuous-state hypothesis, is localized in an ‘eternal present’ as if in permanent ‘gravitational free-fall’ [4,5]. Since we are relativistically embedded in and made out of matter this condition means that all objects (in our 3D virtual reality) exist (in HD) as if they were in gravitational ‘free-fall’. This is better explained by two other interpretations of quantum theory generally ignored by the physics community because they are myopically considered to add nothing. That of the de Broglie-Bohm Causal Interpretation [49-51] and the Cramer Transactional Interpretation [52]; where spacetime and the matter within it (all matter is made of de Broglie waves) are created-annihilated and recreated cyclically over and over as part of the perceived arrow of time and creation of our 3D reality as a resultant from HD infinite potentia as a ‘standing-wave’ (Fig. 8.5) [4,5].

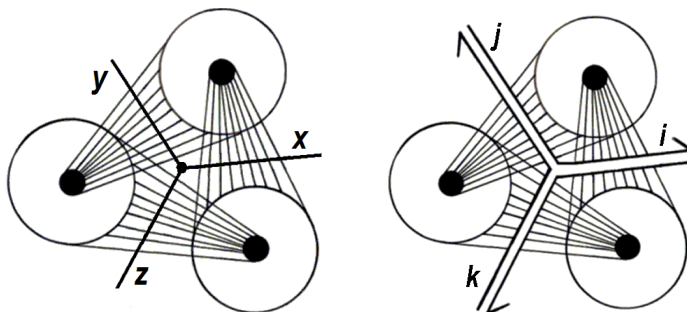


Fig. 8.6. Conceptualization of the cosmological Least-Unit (LCU) tessellating space which like quark confinement cannot exist alone. a) Current view of a so-called point particle or metric x,y,z vertex. The three large circles are an LCU array slice. It is a form of close-packed spheres forming a 3-torus; missing from the illustration are an upper and bottom layer covering the x,y,z vertex and completing one fundamental element of an LCU complex. The field lines emanating from one circle to another represent the de Broglie-Bohm concept of a quantum ‘pilot wave or potential’ governing evolution. b) Similar to a) but drawn with a central ‘Witten string vertex’ [100] and relativistic quantum field potentials (lines) guiding its evolution in spacetime. The Witten vertex is not a closed singularity and because of its open structure provides a key element to the continuous-state process and rotation of the Riemann sphere cyclically from zero to infinity which represents rotational elements of the HD exciplex brane topology.

The problem has to do with the nature of a point or 3D vertex in physical theory [4,100]. What extended versions of de Broglie-Bohm and Cramer bring to the table is a basis for defining a fundamental ‘point’ that instead of being rigidly fixed classically (Fig. 8.6a) is continuously transmutable (Fig. 8.6b) as in string theory. This represents in essence the elevation of the so-called wave-particle duality for quanta to a Principle of

continuous-state cosmology. What this does is cancel the troubling infinites in the standard model of particle physics in a natural way rather than by use of a mathematical gimmick called renormalization. We also build the continuous-state hypothesis around an object in string theory called the Witten Vertex [100] (Fig. 8.6b after noted M-Theorist David Witten). This means that when certain parameters (compactification, dimensional reduction etc.) associated with the Riemann sphere reach a zero-point; the Riemann sphere relativistically rotates back to infinity and so on continuously (Reminiscent of how water waves operate). The HD branes of so-called Calabi-Yau mirror symmetry are forms of Riemann 3-spheres or Kahler manifolds [15,46,47]. Instead of the insurmountable Plank foam, the gate keeper in this cosmology is an array of least cosmological units (LCU) [4,5,71,101] of which part (like the tip of an iceberg) resides in our virtual 4-space and the other part resides in the HD (12D) regime of a UFM version of M-Theory. These LCU exciplex gates govern the continuous-state process in the coherent ordering of matter embedded in a localized spacetime manifold (Chap. 4).

8.6.1 Spacetime Exciplex - U_F Noeon Mediator

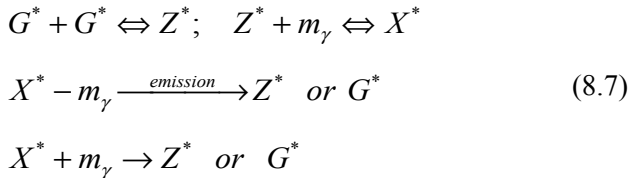
The spacetime exciplex or ‘excited complex’ of least cosmological units (LCU) is key to mediation of the U_F principles related to the observer. In the usual 4D interpretation of quantum theory limited by the uncertainty principle, virtual quanta in the zero point field wink in and out of existence limited to the Planck time, 10^{-43} s. For the noetic UFM spacetime exiplex the situation is radically different. The duality of its HD structure (i.e. living in both local 4-space and nonlocal 8-space) allows it to remain in an excited state in 4-space never fully coupling with the Planck-scale ground state. This holophote interaction is a noeon flux (exchange unit of the U_F) into every point (and thus atom) in spacetime (also animating living systems) by interaction with neural dendrons etc. for example as the flow of qualia as a form of superradiance into the brain.

Kowalski discovered that photon emission occurs only after electrons complete full Bohr orbits [102,103]. We apply this as a general principle for emission during rotation of the complex Calabi-Yau Riemann sphere which acts like a pinwheel-like scoop bringing in the next topologically switched hysteresis loop of semi-quantum interaction energy.

The exciplex concept as defined in engineering parlance is an ‘excited complex’ or form of excimer - short for excited dimer in chemistry nomenclature used to describe an excited, transient, combined state, of two

different atomic species (like XeCl) that dissociate back into the constituent atoms rather than reversion to some ground state after photon emission. An excimer is a short-lived dimeric or heterodimeric molecule formed from two species, at least one of which is in an electronic excited state. Excimers are often diatomic and are formed between two atoms or molecules that would not bond if both were in the ground state. The lifetime of an excimer is very short, on the order of nanoseconds. Binding a larger number of excited atoms form Rydberg clusters extending the lifetime which can exceed many seconds.

An Exciplex is also defined as an electronically excited complex, ‘non-bonding’ in the ground state. For example, a complex formed by the interaction of an excited molecular entity with a ground state counterpart of a different structure. When it hits ground a photon or quasiparticle soliton is emitted. In Noetic UFM Cosmology we have adapted the exciplex concept as a tool to describe the LCU gating mechanism between the quantum regime and the regime of the U_F . The exciplex LCU gate is key to understanding interaction of the physical mind of the observer and the basis for developing empirical tests. The general equations for a putative spacetime exciplex are:



where as seen in Fig. 8.7a, G is the ZPF ground state, Z intermediate cavity excited states and X the spacetime C-QED (Cavity-Quantum Electrodynamics) exciplex coupling. The numerous configurations plus the large variety of photon frequencies absorbed allow for a full absorption-emission equilibrium spectrum. We believe the spacetime exciplex model also has sufficient parameters to allow for the spontaneous emission of protons by a process similar to the photoelectric effect but from HD spacetime C-QED brane spallation rather than from a charged metallic surface. Not having a sufficient spacetime vacuum proton creation mechanism led to the downfall of Steady-State cosmology.

The new U_F basis centers on defining what is called a Least Cosmological Unit (LCU) [4,5,101] tessellating the spacetime backcloth. An LCU (Figs. 8.6,8.7) conceptually parallels the unit cell that builds up

crystal structure. The LCU entails the next evolutionary step for the basis of a point particle and has two main functions; it is the raster from which matter arises, and is a central mechanism that mediates the syntropic gating for physics of the observer parameters of the U_F . Syntropy is the negentropy process of expelling entropy by the teleological action of quantum biosystems.

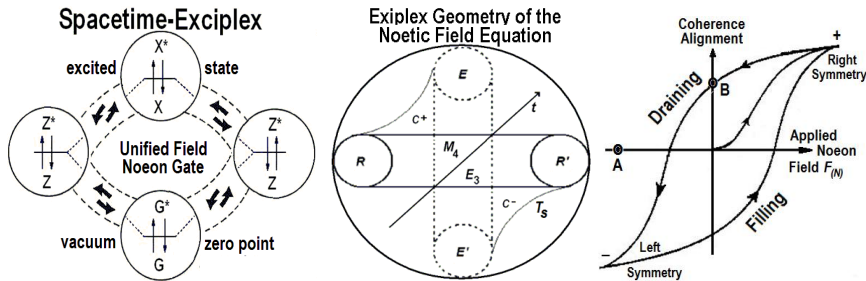


Fig. 8.7a) The geometry of the ‘spacetime exciplex’ (excited complex), a configuration of spacetime LCUs that act like a holophote laser pumping mechanism of U_F noeon energy and also how coherence of the U_F interacts with 3D compactified states. Locally the exciplex acts like an oscillating ‘cootie catcher’ [104]. b) Geometric representation of the Noetic Unified Field Equation, $F_{(N)} = \mathbf{x} / \rho$ for an array of cosmological LCUs. Solid lines represent extension, dotted lines field. Where $F_{(N)}$ is the anthropic or coherent force of the U_F driving self-organization, total energy, \mathbf{x} equals the c) hysteresis loop energy of the hypervolume, ρ is the scale-invariant rotational radius of the action and the domain wall (curves) string tension, T_0 .

The LCU change from the current concept of a fixed Planck scale point (Fig. 8.6a) to what is called a Witten string vertex [100] (Fig. 8.6b) is a form of Riemann sphere (model of the extended complex-plane with points at zero and infinity for stereographic projection to the Euclidean plane) cyclically opening into the LSXD regime of the U_F . Behind the current view of \hbar (Planck’s constant) as a barrier of stochastic foam is a coherent topology with the symmetry of a spin raster comprised of LCUs [4].

8.6.2 Quantum Phenomenology Versus Noetic UFM Field Ontology

There is a major conceptual change from Quantum Mechanics to Unified Field Mechanics (UFM). The ‘energy’ of the U_F is not quantized and thus is radically different from other known fields. Here is what troubled Nobelist Richard Feynman: "...maybe nature is trying to tell us something

new here, maybe we should not try to quantize gravity... Is it possible that gravity is not quantized and all the rest of the world is?" [105]. It turns out that not only is gravity not quantized but neither is the UFM coherent noeon energy of the U_F which is a step deeper than gravity.

Here is one way to explain it. In a usual field like electromagnetism, easiest for us to understand because we have the most experience with it, field lines connect to adjacent point charges. The quanta of the fields force is exchanged along those field lines (in this case photons). We perceive this as occurring in 4-space (4D). It is phenomenological. This is the phenomenon of fields. For topological charge as in the U_F with properties related to consciousness; the situation is vastly different. The fields are still coupled and there is tension between them but no phenomenological energy (i.e. field quanta) is exchanged. This is the situation in the ontological case. The adjacent branes 'become' each other as they overlap by a process called 'topological switching'. This is not possible for the 4-space field because they are quantized resultants of the HD topological field components. The HD 'units' (noeons) are free to 'mix' ontologically (ambiguous Necker cube vertices) as they are not resolved into points.

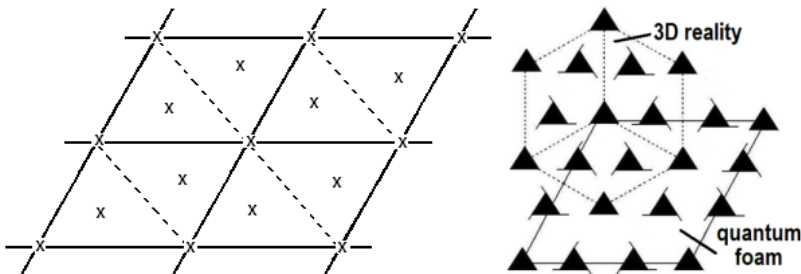


Fig. 8.8. a) 2D view of the LCU tiling of the spacetime backcloth (Fig. 8.6). b) Projective geometry topologically giving rise to HD (here the Fig. 8.8a 2D view extended to 3D). The triangles with tails represent trefoil knots and the naked triangles the resultant cyclic point or fermionic vertex quantum state in 3-space (Spheres in Fig. 8.7a,b).

The metric still has points, or it might be better to say coordinates; but in HD super space they are unrestricted and free to interact by topological switching which is not the case for an 'event' in 4-space. Whereas this singular quality (basis of our perceived reality) does not exist in the HD regime (U_F) of infinite potentia! So if the U_F is not quantized how can there be a force which is mediated by the exchange of energy? Firstly, the U_F does not provide a 5th force as one might initially assume; instead the ontological 'presence' of the U_F provides a 'force of coherence' which is

based on ‘topological charge’. It helps to consider this in terms of perception. If one looks along parallel railroad tracks they recede into a point in the distance, a property of time and space. For the unitary evolution of the mind of the observer [71] this would break the requirement of coherence. For the U_F which is outside of local time and space, a cyclical restoring force is applied to our *res extensa* putting it in a *res cogitans* mode. The exciplex mechanism [4] guides rotation of the Witten vertex Riemann spheres to maintain a consistent level of periodic coherence (parallelism). It is a relativistic U_F process. The railroad tracks do not recede into a point, but it is not observed because the Riemann sphere flips (our perception) by subtractive interference beforehand.

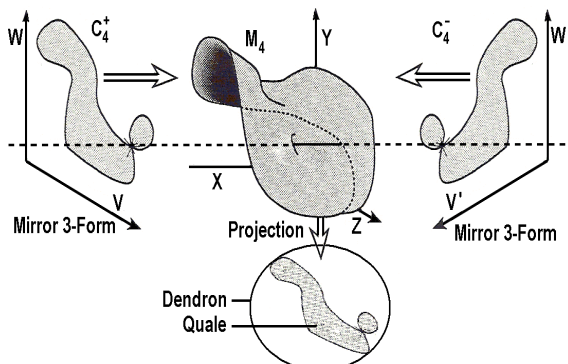


Fig. 8.9. Complex HD Calabi-Yau mirror symmetric 3-forms, C_4 become embedded in Minkowski space, M_4 and the U_F energy of this resultant is projected into localized matter as a continuous stream of evolving (evanescent) Bohmian explicate order. This represents the lower portion only that embeds in local spacetime; there is an additional duality above this projection embedded in the infinite potentia of the U_F from which it arises.

The U_F provides an inherent force of coherence just by its cyclical presence (perhaps a form of superradiance). This means that it is ontological in its propagation of information or ‘interaction’. The railroad tracks remain parallel and do not recede to a point as (perceived) in the 3D phenomenological realm where forces are mediated by a quantal energy exchange. Another way of looking at this is that the 3D observer can only look at one page of a book at a time while the HD observer (omniscient) can see all pages continuously. The LCU space-time exciplex is a mechanism allowing both worlds to interact locally-nonlocally.

Most are familiar with the ambiguous 3D Necker cube (center of Fig. 8.4a bottom is like a Necker cube) that when stared at central vertices topologically reverse. This is called topological switching [75]. There is

another paper child's toy called a 'cootie catcher' [104] that fits over the fingers and can switch positions. What the cootie catcher has over the Necker cube is that it has an easier to visualize a defined center or vertex switching point. So in the LCU Exciplex spacetime background we have this topological switching which represents the frame that houses the gate which is the lighthouse holophote with the rotating light on top.

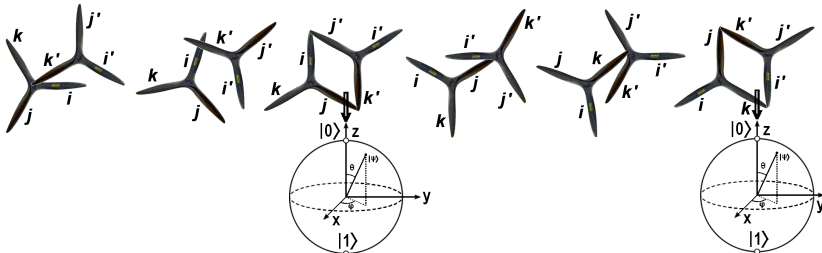


Fig. 8.10. Locus of nonlocal HD mirror symmetric Calabi-Yau 3-tori (here technically depicted as quaternionic trefoil knots) spinning relativistically and evolving in time. Nodes in the cycle are sometimes chaotic and sometimes periodically couple into resultant (faces of a cube) quantum states in 3-space depicted in the diagram as Riemann Bloch spheres, possibly indicative of the emergence of observed 3D reality. An animated version of Fig.8.9.

Now inside the structure there is also a 'baton passing'. The baton is like the lens that the light shines through but only at the moment of transfer (or coupling). In the HD U_F regime the 'light' is always on omnidirectionally but only 'shines' into 3-space when the gate is open during the moment of baton passing. In addition to baton passing there is also a form of 'leap-frogging'. The leap-frogging represents wave-particle duality (remember we elevated it to a principle of cosmology). The leaping moment represents the wave, and the crouched person being leapt over is the particulate moment. The particle moment acts like a domain wall and no neon light passes when its orientation is aligned towards the 3-D world resultant. This is also an important aspect of the gating mechanism. This is of course a relativistic process such that the 'beat frequency' giving rise to the arrow of time as a continuous LCU creation-annihilation cycle.

The trefoil knot, drawn as Planck-scale quaternion vertices in Fig. 8.10, is holomorphic to the circle. Since energy is conserved we may ignore the complexity of the HD symmetries and use the area of the circle for the neon hysteresis loop (Fig. 8.7c), in this case a 2D resultant as a 2-sphere quantum state as the coupling area of one LCU complex coupled to a HD neon brane array. This idea is further conceptualized in Fig. 8.8 illustrating how a 3D object emerges from close-packed spacetime LCUs.

8.7 The Basement of Reality - Through the Glass Ceiling

The anyon braid is topologically protected from decoherence but seemingly doubly inaccessible by the uncertainty principle. Few yet understand why UQC cannot be done from within the confines of the 4D standard model. The full power of quantum entanglement only comes to bear with access to the holographic properties of non-locality. Not as utilized now by parametric down conversion of a pair of EPR photons (points) embedded in spacetime. Many now realize space-time is emergent – not fundamental. So we want to gain access to a more fundamental arena, which is the HD regime of UFM. We need to Gödelize beyond quantum mechanics in the same way we Gödelized beyond classical mechanics; which we know everything about because of this transition. Gödelizing QM will give us full access to all that is quantum readily facilitating UQC. By Gödelizing, we mean going beyond the limits of the domain under study. Generalizing philosophically what Gödel said, ‘*a thing cannot be understood in terms of itself*’.

Let’s try to understand how to Gödelize beyond the Standard Model. Firstly, the world we observe is an asymptotically flat Euclidean 3-space of infinite size dimensionality. Current thinking suggests this reality has a ‘basement’; a fixed Zero-Point Field (ZPF) stochastic barrier or ‘quantum foam’ with *zitterbewegung* virtual particles winking in and out of existence for the Planck time, t_p . The Planck time, $t_p \equiv \sqrt{\hbar G/c^5} \approx 5.39106 \times 10^{-44}$ s represents the duration required for light to travel a distance of one Planck length ($l_p = \sqrt{\hbar G/c^3} \approx 1.61619 \times 10^{-33}$ cm), where, \hbar is the reduced Planck constant, G the gravitational constant, c the speed of light in vacuum and s the second. Quantum field theory covers aspects of both special relativity and quantum theory, \hbar sets the scale at which the uncertainty principle applies. In quantum theory \hbar appears in the commutation relation between momentum, p and position, q of a particle: $pq - qp = -i\hbar$, and similar commutation relations involving other complementary pairs of measurable quantities. Because our ability to measure two quantities simultaneously with complete precision is limited by their *inability to commute*, \hbar quantifies uncertainty for simultaneous measurement of all quantum properties!

If LSXD are shown to exist, the Planck length would have no fundamental physical significance. In string theory, the Planck length is claimed to be the mathematical order of magnitude of the oscillating strings that form elementary particles. The string scale l_s is related to the

Planck scale by $\ell_p = g_s^{1/4} l_s$, where g_s is the string coupling constant, which in actuality is not constant, but depends on the value of a volume factor when the size of XD is allowed to vary. Any physical calculation predicting length using only the constants c , G and \hbar must include the Planck length, possibly multiplied by a usually considered unimportant numerical factor like 2π . But these arguments are far from being settled; it may be, and this is our conjecture, that a numerical factor like 2π might be very important and take a value that is very large or very small [26]. If \hbar has physical significance (beyond its current use as a mathematical tool) it would apply to compactified black hole material.

How does this correlate the concept of a photon as a traveling wave along a 2D surface projecting at right angles to the direction of propagation with a photon with a particulate radius limiting the slit diameter it is able to pass through to $\sim 10^{-9}$ cm? These are unsettled issues in both the basis of quantum field theory itself and measurement theory. What we are getting at is that the uncertainty principle is hiding an inherent backcloth of cyclic bumps and holes in the Dirac polarized backcloth [4].

<i>n</i>	<i>V(n,1)</i>	
0	0	0
1	2	2
2	π	≈ 3.1416
3	$4/3\pi$	4.1888
4	$1/2\pi^2$	4.9348
5	$8/15\pi^2$	5.2638
6	Degenerate ?	∞

Table 8.1. Standard Hypervolume values for increasing n -dimensionality and radius, r of a unit sphere or n -ball equal to 1.

We have postulated a Manifold of Uncertainty (MOU) with a finite dimensional radius somewhat aligned with what string theory calls T-Duality [3-5]. For preliminarily predictions we could calculate hyperspherical volume or surface area of 2D-5D MOU (Fig. 8.11). The general n -volume equation is

$$V(n, r) = \pi^{\frac{n}{2}} r^n / \Gamma\left(\frac{n}{2} + 1\right) \quad (8.8)$$

where $V_{n,r}$ is volume per number of dimensions, n of radius r and Γ a factorial constant. These n -volume equations relate to volumetric

properties of the MOU for calculating an HD C-QED volume hierarchy for predicting new Tight-Bound State (TBS) spectral lines in hydrogen [31,35]. If LSXD exist, degeneracy would occur at the limit of r discovered in the same manner the outermost energy level of an atom is detected when an outer electron acquires sufficient energy to escape to infinity.

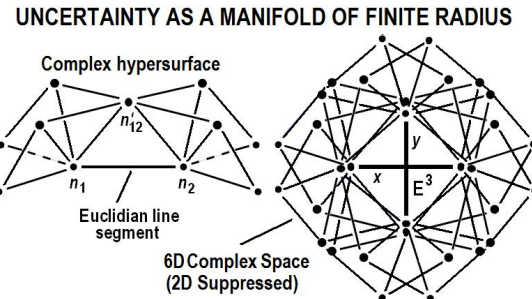


Fig. 8.11. Proposed 5/6D Manifold of Uncertainty (MOU) ‘guarding the door to LSXD. Dimensional suppressed planar views of quaternion vertices.

As shown in Fig. 8.11 we postulate existence of a ‘semi-quantum limit’ MOU 5D with the 6thD being degenerate (like the outermost atomic electron radius where the outer electron can escape to infinity when acquiring sufficient energy). We assume a 6D MOU based on an M-Theoretic Calabi-Yau dual 3-torus [3]. This is a 12D model with 6 spatial, 3 temporal and 3 super-quantum potential-like control parameters of the unified field. But because we don’t fully understand how to close-pack the LCU array tessellating spacetime we do not have much rigor yet [87,88].

8.8 Empirical Tests of UFM Cosmology Summarized

Viable experimentation will lead to new UFM research platforms for studying fundamental syntropic properties of quantum systems. We have proposed fourteen tests of UFM; in this chapter we summarize the main experimental protocol to test for the UFM noeon, Tight-Bound States (TBS) in hydrogen and the teleological ‘life-principle’ hypotheses. Note: Not all of the experiments relate directly to mediation of the U_F noeon, but all of the experiments manipulate the new physical regime of the U_F or importantly mediate the ‘gating mechanism’ by which access is gained to the 3rd regime of reality, thus facilitating mind-body research in addition to M-Theory, UQC and nuclear physics.

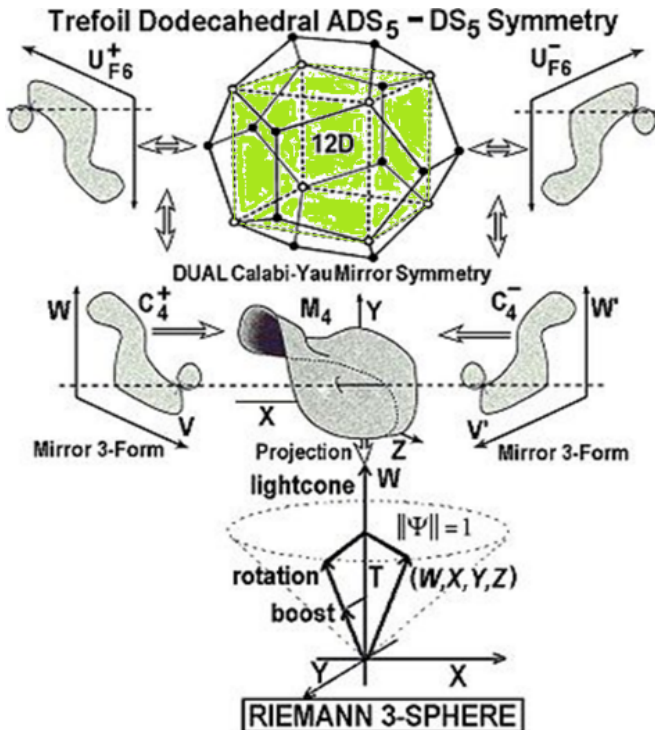


Fig. 8.12. Completion of Figs. 8.9 & 8.10 illustrating full extension to an HD ontological-phase topological field in continuous-state dual Calabi-Yau mirror symmetric UFM cosmology with Dodecahedral involute properties, as well as the continuous-state exciplex ‘hysteresis loop’ of noeon injection (not shown) as far as currently understood. The Bloch 2-sphere representation is also replaced with an extended Riemann 4-sphere resultant with sufficient parameters to surmount the uncertainty principle representing a unique M-Theoretic model of ‘Continuous-State’ U_F dynamics as it relates to UFM and its putative exchange quanta of the U_F , the noeon.

The 3-cube embedded in the dodecahedron (top of Fig. 8.12) represents what we term the ‘mirror image of the mirror image’ enfolding a scale-invariant ‘causally free’ copy of the Euclidean 3-space quantum ‘particle in a box’, accessible under a precise protocol surmounting uncertainty.

8.8.1 Summary of Experimental Protocols

If experimentation proves viable a new class of UQC biophysical research platform for studying fundamental properties of the spacetime vacuum as it relates to long-range coherence in living systems. We summarize eight

derivatives of the main experimental protocol to test the LSXD continuous-state Long-Range Coherence hypotheses:

1. Basic Experiment - Fundamental test that the concatenation of new OPTFT U_F principles is theoretically sound. A laser oscillated rf-pulsed vacuum resonance hierarchy is set up to interfere with the periodic (continuous-state) structure of the inherent ‘beat frequency’ of a covariant Dirac polarized spacetime vacuum exciplex to detect the new coherence principle associated with a cyclical holophote entry of the U_F into 4-space. This experiment ‘pokes a hole in spacetime’ in order to bring the energy of the U_F into a detector. The remaining protocols are variations of the parameters of this experiment.
2. Bulk Quantum Computing - Utilizing protocol (1) Bulk Scalable UQC can be achieved by superseding the quantum uncertainty principle. (see [31,35,87,88,97,98] for details) Programming and data I/O are performed without decoherence by utilizing the inherent mirror symmetry properties that act like a ‘synchronization backbone’ [4,] whereby ‘LSXD copies’ of the local 3-space quantum state are causally free (measureable without decoherence) at specific resonance nodes in the continuous-state conformal Calabi-Yau symmetry cycle hierarchy.
3. Protein Conformation - (similar to discussion in [13]). Utilizing more macroscopic aspects of protocols (1 & 2) dual Hadamard quantum logic gates are set as a Cavity-QED spacetime cellular automata [4,27] experiment to facilitate conformational propagation in the prion protein from normal cellular form, PrP^C to the pathological, PrP^{Sc} form by noeon bombardment with the ‘force of coherence’ of the U_F .
4. Manipulating a special case of the Lorentz Transformation [72] - Aspects of a spacetime exciplex model [4] in terms of restrictions imposed by Cramer’s Transactional Interpretation [52] on mirror symmetry can be used for the putative detection of virtual tachyon-tardyton interactions in *zitterbewegun* [37].
5. Extended Quantum Theory - Test of causal properties of de Broglie-Bohm-Vigier quantum theory by utility of the U_F holophote effect (protocol 1 parameters) as a ‘super quantum potential’ to summate by constructive interference the density of de Broglie matter waves [4].
6. Coherent Control of Quantum Phase - Additional test of the de Broglie-Bohm interpretation for existence of a nonlocal ‘pilot wave - quantum potential’ for manipulating the phase ‘space quantization’ in the double slit experiment by controlling which slit quanta passes through. Application to quantum measurement and transistor lithography refinement.

7. Manipulating Spacetime LCU Structure - (similar to protocol 6) Test of conformal scale-invariant properties of the putative Dirac conformal polarized vacuum, a possible ‘continuous-state’ property related to an arrow of time [4,21,34] (Also similar to basic experiment, but more advanced).
8. Testing for and Manipulating Tight Bound States (TBS) - (similar to protocol 4) Vigier [31,35] has proposed TBS below the 1st Bohr orbit in the Hydrogen atom. Utilizing tenets of the original hadronic form of string theory [4] such as a variable string tension, T_s where the Planck constant, \hbar is replaced with a version of the original Stoney, λ [4], where \hbar is an asymptote never reached, instead oscillating from virtual Planck to the Larmor radius of the hydrogen atom, i.e. the so-called Planck scale is a restriction imposed by the limitations of the Copenhagen Interpretation and is not a fundamental physical barrier. LSXD exist putatively behind the barrier of uncertainty and the oscillation of the Planck constant is part of the exciplex gating mechanism [4]. Utilizing ontological-phase topological field theory (OPTFT) at the moment of spin-spin coupling or spin-orbit coupling an rf-pulse is kicked at various nodes harmonically set to coincide with putative phases in the cycle between local and LSXD cavity TBS properties. [4,31,35]
9. Test for the noetic Unique String Vacuum - Until now the structure of matter has been explored by building ever bigger supercolliders like the CERN LHC. If the LSXD access model in terms of a Dirac covariant polarized energy dependent vacuum proves correct utilizing the inherent conformal scale-invariant mirror symmetry properties of de Broglie matter waves will allow examining various cross sections in the structure of matter in symmetry interactions during cyclic continuous-state future-past annihilation-creation modes of matter in the LCU tessellated spacetime metric without the need for supercolliders.

There are a number of very specific postulated cosmological properties required in order to perform these experiments [4,5,44].

8.8.2 Review of Key Experimental Details

To empirically gain access to the U_F , regime one must pass through the so-called Planck scale stochastic barrier. In order to do this, one must violate the heretofore sacrosanct quantum uncertainty principle. Since by

definition the standard methods of quantum theory produce the uncertainty principle; the simple solution is to do something else! Because of the great success of gauge theory, physicists have ignored the existence of a covariant Dirac polarized vacuum because they believe its existence would violate gauge principles. The methods of gauge theory however are only an approximation suggesting that there is additional new physics. Next we outline the general method for accessing the HD superspace of the U_F . Technical details can be found in references [4,87,88].

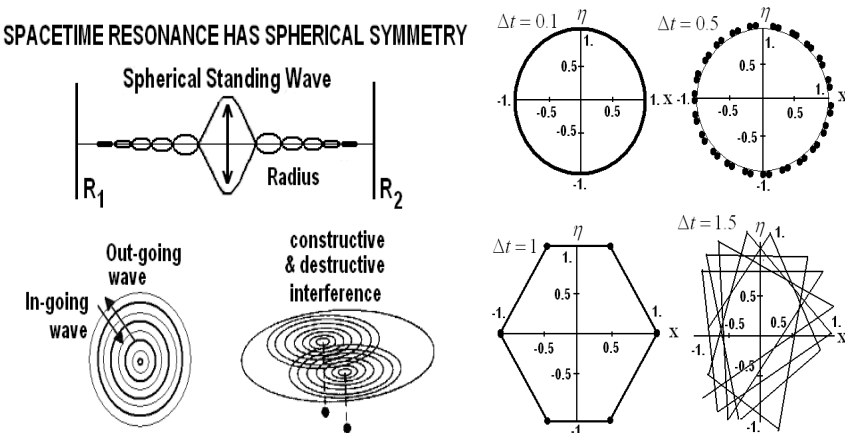


Fig. 8.13. The Dirac polarized vacuum has hyperspherical symmetry. a) Top left, metaphor for TI standing-wave present showing future-past elements, R_1, R_2 , eleven of twelve dimensions suppressed for simplicity. b) Bottom left, top view of a) 2D spherical standing-wave; c) Bottom left, right portion, manipulating the relative quantum/brane phase of oscillations creates nodes of destructive and constructive interference for incursive oscillation. d) Right, four numerical simulations of the phase space trajectory of the Dubois *superposed incursive oscillator*.

The Dubois superposed incursive oscillator based on coordinates and velocities takes the form:

$$x_n = 1/2[x_n(1) + x_n(2)], \quad v_n = 1/2[v_n(1) + v_n(2)]. \quad (8.9)$$

And it is shown in Fig. 8.13 (right) for values of $\Delta\tau = \omega t$ equal to 0.1, 0.5, 1.0 and 1.5. Initial conditions are $\chi_0 = 1, \eta_0 = 0$ & $\tau_0 = 0$ with total simulation time $\tau = \omega t = 8\pi$. Figure 8.13b adapted from [106-110].

Postulates introduced in this chapter are utilized; in general, the de Broglie-Bohm, ontological and Cramer, TI interpretations of quantum theory, the Dirac polarized vacuum, the Sagnac effect [4,49-55,111], the unique string vacuum derived from UFM cosmology and the special class of Calabi-Yau mirror symmetry conditions.

LASER OSCILLATED VACUUM ENERGY RESONATOR Multi-Tiered Experimental Platform

TIER-I	Applied Tunable Laser RF Modulated Pulsed Quadrupole Resonant Counter-Propagating Sagnac Effect Interferometry of Electrons
TIER-II	For the Purpose of Spin-Spin Coupling of Tier-I Electrons to the Magnetic Moment of the Nucleons
TIER-III	By HD RQFT Tier-I & II Undergo Resonant Coupling with the Beat Frequency of the Fabric of Spacetime
TIER-IV	Producing a Multi-Tier Cumulative Interaction of Tier -I - II - III to Destructively Interfere with the Annihilation & Creation operators of Spacetime

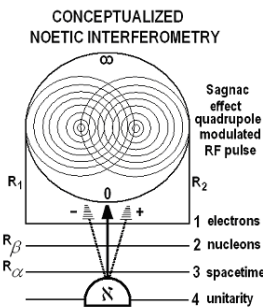


Fig. 8.14. a) Design elements of the Noetic Interferometer postulated to constructively-destructively interfere with the topology of the spacetime manifold to manipulate the unified field. The first three tiers set the stage for the critically important 4th tier which by way of an incursive oscillator ‘punches a hole’ in the fabric of spacetime creating a holophote or lighthouse effect of the U_F into the experimental apparatus momentarily missing its usual coupling node into an atom or biophysical system. b) Conceptualized Witten vertex Riemann sphere cavity-QED multi-level Sagnac effect interferometer designed to ‘penetrate’ space-time to emit the ‘noeon wave’, \mathbf{N} , of the unified field. Experimental access to vacuum structure or for surmounting the uncertainty principle can be done by two similar methods. One is to utilize an atomic resonance hierarchy and the other a spacetime resonance hierarchy. The spheroid is a 2D representation of a HD complex Riemann sphere complex able to spin-flip from zero to infinity continuously.

It is important to recall one of our main proposals concerning the wave structure of matter and that emergent spacetime is created, annihilated and recreated continuously. If one throws a stone in a pool of water concentric ripples occur. If one drops two stones into the water, regions of constructive and destructive interference occur. This is essentially how our resonant hierarchy operates as shown in Fig. 8.14b. The basic idea of the radio frequency or rf-modulated resonance hierarchy is as follows: in the first tier (Fig. 8.14a) a radio frequency is chosen to oscillate the electrons in the atom or molecule used in such a way that the nucleons will resonate. This is related to the principles of nuclear magnetic resonance (NMR). This couples electrons to the magnetic moment of the nucleons in tier 2. By the principles of relativistic quantum field theory (RQFT) tiers one and two undergo resonant coupling to the beat frequency of the fabric of

space-time. The multilayer cumulative interaction of tiers 1, 2 and 3 by application of the incursive oscillator can be set to destructively or constructively interfere with the annihilation or creation operators of space-time.

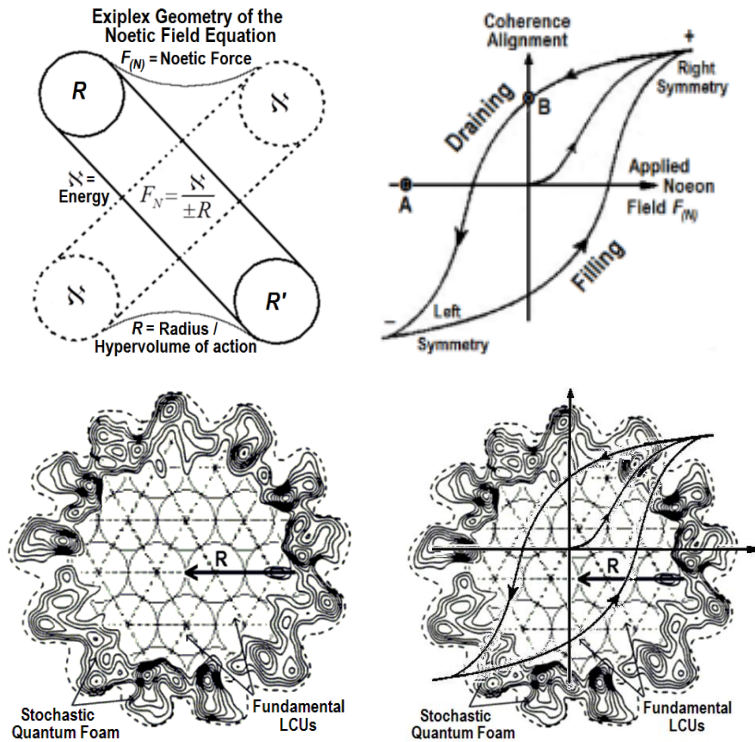


Fig. 8.15. a) Geometric topology of Noetic Field Equation $F_{(N)} = \mathbf{N} / \rho$ acting as a holophote (rotating lighthouse beacon) gating mechanism for entry of the nonlocal HD *UF* into local $M_4\text{-}E_3$ 3(4)-space. a) Wave-particle-duality is elevated to a principle of cosmology such that the solid bar, $R_1\text{-}R_2$ at one moment transforms to the dotted bar, \mathbf{N} at the next in a continuous relativistic wave-particle cycle with t the arrow of time. Fluctuating string tension, T_S (curves) helps drive the oscillation. b) *UF* Hysteresis Loop. Point A is a zero-point where the driving field reverses and increases. Point B is where the driving field drops but still retains considerable charge as a *UF* force of coherence related to the life-principle and quale. c) Noeon spacetime coupling to LCU tessellating space. d) Overlap of hysteresis loop with noeon coherent force spacetime interaction.

A final essential component of the vacuum interferometer is called an incursive oscillator [106-110] which acts as a feedback loop on the arrow of time [21,34]. Parameters of the Dubois incursive oscillator are also required for aligning the interferometer hierarchy with the beat frequency

of spacetime by $x(t + \Delta t) - v(t + \Delta t)$. Critically the size of Δt correlates with the bandwidth of the ‘hole’ to be punched in spacetime which also correlates with the wavelength, λ of the rf-resonance pulse.

Hysteresis is an important part of understanding how to quantify the topological charge with a unit of energy measure because it relates not to residual magnetization as in common usage but to the residual *UF* noeon charge. When the driving force drops to zero, the material retains considerable charge (coherence) for a period. The driving (noen) field must be continuously reversed and increased (holophote action) driving the charge to zero again. A Hysteresis Loop is a history dependence of a material (atom) at saturation (driven to). When the field is removed some retention occurs for a period of time. As noeon input alternately increases and decreases, hysteresis is the loop that the output forms (Fig. 8.15). A simple form of hysteresis is the lag-time between input (filling) and output (draining). An example of hysteresis is sinusoidal or harmonic input $X(t)$ and output $Y(t)$ separated by a phase lag, ϕ : $X(t) = X_0 \sin \omega t$ $Y(t) = Y_0(\omega t - \phi)$, this is the principle of hysteresis [11] - switching cycles that retain considerable charge (coherence in the case of the *UF* LCU noeon cycle).

In the current understanding of quantum cosmology where the Planck scale is the ‘basement of reality’ [4] there is a stochastic Zero Point Field (ZPF) where virtual quantum particles wink in and out of existence with a half-life of the Planck time. This is considered an impenetrable barrier imposed by the Uncertainty Principle. UFM has sufficient degrees of freedom to surmount uncertainty and allow a cyclic or harmonic emergence of the noeon into localized matter. This holophote mechanism can be metaphorically described as an Exciplex (Fig. 8.7a). In an exciplex (short for excited complex) heteronuclear molecules or molecules having more than two species are *exciplex* molecules that are often diatomic and composed of two atoms or molecules that would not bond if both were in the ground state - An Exciplex is a complex existing in an excited state that dissociates in the ground state.

8.9 Unified Field Mechanical (UFM) Précis - Required Parameters

Most physicists believe a *UF* theory (coined by Einstein) should be a quantum theory uniting the four fundamental interactions; but there is no *a priori* reason this should be the case and many physicists in recent

decades transferred the search to an 11D M-Theoretic (4D + 2D to 6D) brane world instead of the original 1D string) regime. The 11th dimension in M-Theory unites the five forms of string theory; and the 12th dimension of noetic UFM cosmology (OPTFT) introduces the coherent action of the *UF*. Classical Mechanics describes an event between two coordinate systems by what is called the Galilean transformation for uniform motion at velocities less than the speed of light in 3D Euclidean space.

Quantum mechanical events with relativistic velocities are described by the Lorentz-Poincaré group of transformations in 4D Einstein-Minkowski spacetime. To cross the manifold of uncertainty, noetic cosmology utilizes an extension of M-Theory requiring a new 12D set of transformations called the Noetic or UFM Transform [4] (provides actual bridge between the 2nd and 3rd regimes of reality) because it includes properties of inherent UFM principles in a ‘sea’ of infinite potentia simplistically like the entangled alive-dead quantum state of Schrödinger’s cat before realized local events occur and from which 4D reality of the observer cyclically emerges as nilpotent resultants (Figs. 8.9, 8.10). Norm zero nilpotency - technically meaning ‘sums to zero’ [111].

The key ingredients the HD regime of UFM provides for surmounting uncertainty and solving the observer or mind-body problem are:

- 1) Sufficient additional degrees of freedom to surmount the Uncertainty Principle,
- 2) An Exciplex gating mechanism to allow *UF* entry into 4-space [4],
- 3) Ontological UFM ‘Force of Coherence’ mediated by noeon topology and
- 4) Ability to define new physical unit of measure called the noeon to quantify mental energy [97,98].
- 5) Matter is not only a 3(4)D Euclidean/Minkowski substance; but an nD (12) nonlocal topological space, with a local manifold (shadow) homeomorphic to Euclidean space near each 3D point.

The force of coherence is described by the UFM Field Equation, $F_{(N)} = \mathbf{x} / \rho$ defining how to manipulate the topological charge of the Exciplex gate to perform UFM experiments. Since noeon flux is like a holophote, hysteresis loops can quantify the energy and duration of the coherence period applicable to a C-QED volume or surface area. This energy transfers information instantaneously as observed by the EPR experiment; presenting duality between our temporal 3-space and the atemporal unity of the UFM regime.

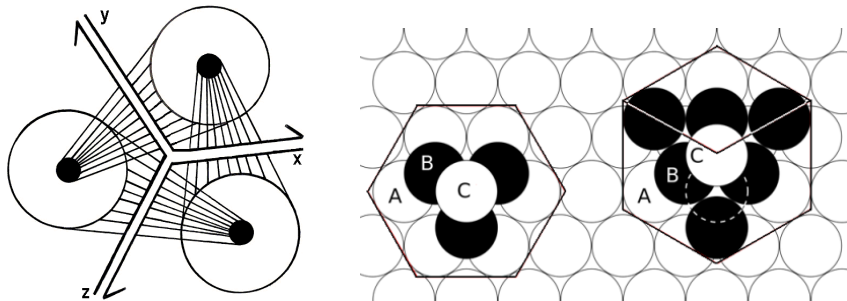


Fig. 8.16. a) Solitary triune LCU complex ‘component’ with a Whitten string vertex in 3-space represented by central x,x,z parallel lines; The 3 circles are super quantum potential field components coherently controlling the evolution of a local fermionic vertex with field lines of the UF . b) Possible ways to close-pack LCU arrays in spacetime tessellations.

8.10 Formalizing the Noeon, New Physical Unit Quantifying UFM Energy

Defining ‘noeon’ energy as a unit of physical measure helps formulate a comprehensive empirically testable UFM science. The Einstein, another physical unit of energy measure, named in honor of Albert Einstein for his explanation of the photoelectric effect in terms of light quanta (photons) bears conceptual similarity; thus our starting point.

The Einstein measures the power of em-radiation in photosynthesis where one Einstein represents one mole (Avogadro’s number) of photons (6.02×10^{23}). In general physics, the energy of n -photons is $E = n\hbar\nu = n\hbar(c/\lambda)$ where \hbar is Planck’s constant and ν frequency. The second part of the equation is energy in terms of wavelength, λ (in nanometers, nm) and speed of light, c . Adaptation of this photon energy equation to measure Einsteins is similar, $E = N_0\hbar\nu = N_0\hbar(c/\lambda)$ where energy of N_0 photons is instead in Einsteins, E . In photometrics the measure used is one microeinstein per second per m^2 , where one microeinstein, uE is one-millionth of an Einstein (6.02×10^{17}) photons imping leaf area.

We create a similar unit of measure to quantify noeon energy of the UF . The same unit can be applied to mental energy quantifying the mind of the observer (*quale* in terms of the Eccles’ Psychon) as one mole (Avogadro’s number) of ‘noeons’. Forces of the four known phenomenological fields

(electromagnetic, strong, weak and gravitational) have exchange quanta mediating field interactions by energy exchange. For em the exchange quanta is the photon. This quantal mediation has been experimentally verified for all fields except gravity because the graviton has not been discovered; and according to UFM is not expected to be, as the regime of unification is not quantum but instead correlates with ontological parameters of 3rd regime UFM [4,105].

Hypervolume charge in HD Calabi-Yau brane topology is complex and difficult to calculate at this stage of theoretical development. Since energy is conserved let's ignore this complexity and simply use area of the circle, or in this case resultant continuous rotations of two circles as a 2-sphere quantum state or perhaps better as a 3-torus as the noeon coupling area to one LCU complex. In considering noeon energy measure it seems easier to calculate nonlocal brane area of the spacetime exciplex (gating mechanism for passage of *UF* energy, Fig. 8.7a) rather than the volume or surface area of atoms which is unknown in this respect. Recall the surface area of small intestinal villi is about 4500 m²~area of a football field. We will not calculate here but leave for later publication since we still struggle with conceptual problems relating to the geometric-topology of noeon interaction coherence. The de Broglie-Bohm interpretation entails nonlocal pilot-waves or quantum-potentials guiding evolution of wavefunctions ontologically. This concept was not very successful in 4D, but when carried to Large-Scale Additional Dimensions (LSXD) [44] it works elegantly and the pilot-wave-quantum potential becomes a 'Super Quantum Potential' synonymous with coherent *UF* aspects in an arena seemingly corresponding to Bohm's super-implicate order.

More noeon-LCU theory: A torus is generated by rotating a circle about an extended line in its plane where the circles become a continuous ring. According to the torus equation, $\left[\left(\sqrt{x^2 + y^2} - R \right)^2 + z^2 = r^2 \right]$, where r is the radius of the rotating circle and R the distance between the center of the circle and axis of rotation. Torus volume is $2\pi^2 Rr^2$ and surface area is $4\pi^2 Rr$. In this Cartesian formula the z axis is the axis of rotation. We apply this to the holophote action of noeon exciplex flux with a hysteresis loop. In atomic theory electron charged particle spherical domains fill toroidal volumes of atomic orbits by their wave motion. If a photon of specific quanta is emitted while an electron is resident in an upper (U_F domain) more excited Bohr orbit, the orbit radius drops back down to the next lower energy level decreasing volume of the torus in the emission

process (noeon-psychon exciplex hysteresis loop maintaining a periodic syntropic force of coherence).

Summarizing pertinent aspects of noeon-LCU cosmology:

- Nature of point particles or singularities in physics has long been debated. In Noetic Cosmology it becomes a continuous Witten vertex [100] (Central x,y,z parallel lines, Fig. 8.16a).
- Energyless interaction of the U_F occurs by ‘topological switching’. Metaphorically like what happens by staring at an ambiguous Necker cube as the vertices ontologically oscillate back and forth. Like the exciplex gate in noetic cosmology [4].
- Like the Einstein, the noeon defines a measure of one mole of noeons, purported to be the topological exchange complex of the U_F providing the force of coherence that forms local material.

Using the noetic field equation, $F_{(N)} = \mathbf{x} / \rho$ (Fig. 8.15a) we could calculate the energy of the noeon field from its spacetime hysteresis loop (Fig. 8.15b,c). This is a practical and conceptual challenge currently hard to meet. Imagine a helicopter like those used to put out forest fires carrying a bucket of water retrieved from a nearby lake (UF). The volume of that bucket is known. So it is infinitely easier to work with the volume of the helicopter water bucket than to try to measure the surface area of trees and other objects on the ground. Until the experiment is performed; we could approximate the volume of the helicopter bucket with the energy of one LCU complex from parameters of Tbl. 8.1. As shown in Fig. 8.11 we are postulating that the Manifold of Uncertainty (MOU) has from 2D to 5D with either the 3rd or 6thD being degenerate (like atomic radius where an outer electron flies off to infinity). We don’t know yet if the MOU is 3D or 6D because we don’t fully understand how to close-pack the LCU array tessellating spacetime (Fig. 8.16). This model is compatible with M-Theoretic Calabi-Yau dual 3-tori [3,46,47]; but our theory cannot fully predict this until we know how many space-antispace doublings are required in LCU packing [112]. We discovered that a complex quaternion Clifford algebra can perform this task but our team hasn’t finished developing the equations at time of writing.

When first considering the noeon as a new unit of measure a correlation with an Avogadro’s number of noeons entering the picture wasn’t considered. Can we correlate helicopter buckets of UF brane topology with the volume or surface area of an array of LCUs modulating energy of coherence entering local spacetime? Yes, but we defer the calculation until

we have more maths or perform the experiment [31]. The exciplex LCU gate transforms continuously through HD M-Theoretic brane topology with cyclic compactification modes [4] until reaching a 4D ‘standing-wave’ [52,111] Minkowski spacetime of the standard model. Observed virtual reality, a gated domain-wall for entry of *UF* noeon energy pervading all spacetime and matter is mediated by a new set of transformations beyond the Galilean-Lorentz-Poincaré. Named the UFM Transform in deference to the anthropic multiverse it is cast in [4].

For preliminarily predictions we could calculate hyperspherical volume or surface area of 4D-5D MOU (Fig. 8.11). The general n -volume equation is $V(n, r) = \pi^{\frac{n}{2}} r^n / \Gamma\left(\frac{n}{2} + 1\right)$ where $V_{n,r}$ is volume per number of dimensions, n of radius r and Γ a factorial constant. These n -volume equations relate to volumetric properties of the MOU for calculating noeon brane volume of topological charge.

UF dynamics entails a ‘force of coherence’ not a 5th fundamental force. This ‘coherence’ is the resultant unitary unified action of the *UF* which is primary - originator of all other forces ‘pumping’ noeons, which are then immediately returned to the infinite sea of *UF* potentia. This cyclical process creates and annihilates matter. More work must be done on noeon dynamics. This is what the experimental protocols are designed for - rigorous investigation of ‘*some crazy theory*’, as Nobel Laureate D. Gross called it at the 2015 Singapore, NIAS 60 Years of Yang-Mills conference.

8.11 Quarkonium Flag Manifold Topology

In sections above we made a current best effort to describe in principle how an ‘Exciplex Topology’ acts as a gating mechanism for real *UF* noeons to pass from the 3rd regime of UFM to 4-space; a paradigm shift from current thinking of ZPF virtual particles of the 2nd regime of Quantum Mechanics. We know this gating mechanism pulses or oscillates cyclically like a lighthouse holophote beacon.

In this section we shed additional light on how the structure of the gating manifold hierarchy might operate:

- 1) 1st regime: A classical local Euclidean 3-space x, y, z fermion vertex with space-antispace *zitterbewegung*.
- 2) 2nd regime: In terms of an extended Cramer standing-wave transaction, is a mid-level future-past complex quantum space of which 3-space is the ‘resultant shadow’.

- 3) 3rd regime: UFM topology governing brane dynamics which is at the core of the gating mechanism.

In 1945 Wheeler and Feynman proposed an Absorber Theory as the mechanism for energy transfer by calculating em-radiation emitted from an accelerated electron. The electron generated outward and inward waves. Cramer's Transactional Interpretation of quantum theory is based on the Wheeler-Feynman Absorber Theory. M. Wolff further proposed a parallel model where spherical standing-waves created a 'particle effect' at their Wave-Center, suggesting a solution to the 70-year-old paradox of the Wave-Particle Duality of Matter [4].

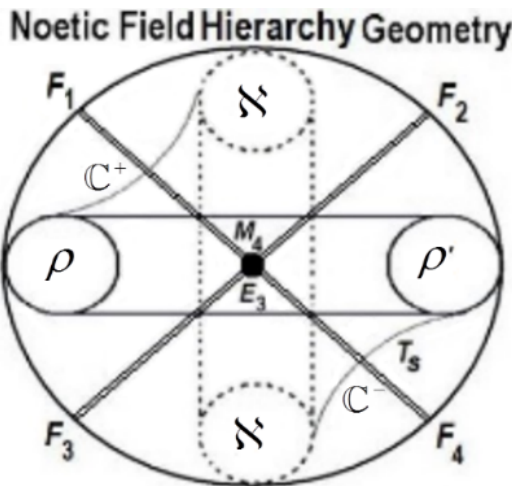


Fig. 8.17. Hierarchy of the three regimes of reality. a) Central black dot; a point in Euclidean space. b) Double lines, F_1 , F_2 , F_3 , F_4 (8.12) as future-past components of a Cramer transaction. c) Four LCU circles representing geometric topology of the UF and UF equation $F_{(N)} = \aleph / \rho$ for coherent control.

For a Cramer transaction emission locus at $x, t = 0, 0$; we are concerned with the boundary conditions in the region outside the event horizon. The scalar equation in spherical coordinates for wave motion in spacetime which has spherical symmetry

$$\nabla^2 \Phi - \frac{1}{c^2} \partial^2 \frac{\Phi}{\partial t^2} = 0 \quad (8.10)$$

where, Φ is the wave amplitude. The equation has two solutions

$$\begin{aligned}\Phi_{out} &= \frac{1}{r} \Phi_{\max} \exp(i\omega t - ikr), \\ \Phi_{in} &= \frac{1}{r} \Phi_{\max} \exp(i\omega t + ikr).\end{aligned}\quad (8.11)$$

which for the programming of spacetime can be applied to the propagation of Cramer's advanced retarded waves from an emission locus at $x, t = 0, 0$ by Eqs. (8.11 & 8.12) which form the advanced-retarded components of a transaction (Fig.8.5) [52].

$$\begin{aligned}F_{1-Ret} &= F_0 e^{-ikx} e^{-2\pi ift}, \quad F_{2-Ret} = F_0 e^{ikx} e^{-2\pi ift}, \\ F_{3-Adv} &= F_0 e^{-ikx} e^{2\pi ift}, \quad F_{4-Adv} = F_0 e^{ikx} e^{2\pi ift}.\end{aligned}\quad (8.12)$$

Another approach to formalizing noeon flux may be in terms of the 6D flag manifold that describes the geometry of quark confinement. A possible relationship to the noeon-LCU complex can make correspondence to work by Shipman correlating the flag manifold to a hexagonal structure of spacetime [113-115]. The structure of quarks in hadrons bears an uncanny geometric relation to the noetic UFM LCU.

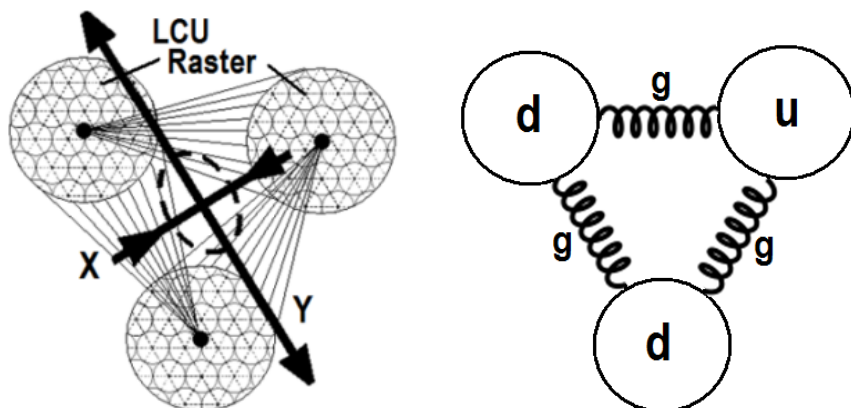


Fig. 8.18. Comparison of a) LCU array (with Euclidean x, y vertex) and b) Three quarks d, u, d with gluon, g force couplings.

8.12 Singularities, Unitary Operators and Domains of Action

Quantum systems decohere because they are open systems that couple to the environment. As we now begin to supersede Quantum Mechanics, leaving the challenges of decoherence and the Uncertainty Principle behind, by entering a 3rd regime of reality – that of Unified Field Mechanics (UFM); we have finally come full circle to Einstein's challenge of refuting indeterminism, that '*God does not play dice with the universe*'! Einstein felt that natural laws could not be like the throw of dice, incorporating an inherent structural randomness with access only probabilistically. But this is exactly what Quantum Mechanics tells us empirically – that at the fundamental level Nature is inherently stochastic or random, codified in Heisenberg's famous Uncertainty Principle. Physicists have now begun to suspect that spacetime is not fundamental but emergent. Spacetime is the domain of Quantum Mechanics; so now the challenge is that Quantum Mechanics along with its rigorous empirical tests of stochasticity can no longer be considered fundamental and will be superseded in a manner similar to Classical Mechanics. Here is where at the newly discovered 'semi-quantum limit' we begin to make correspondence to a regime of natural science where Einstein's wager finally becomes valid. Measurement with certainty is key to the Unified Field Mechanical or Noetic model of Universal Quantum Computing (UQC) being able to address quantum states without facilitating decoherence as it completely removes all aspects of that issue in QC operations.

If the Church-Turing Hypothesis (simplistically, any function that can be computed by a physical system can be computed by a Turing Machine) is correct, and that all quantum operators must be unitary (reversible), then UFM adds the ability to surmount uncertainty as a Gödelization beyond QM by the additional degrees of freedom.

8.12.1 Semi-Classical Limit

The Semi-classical limit refers to theoretical models or domains where one part of a physical system is described quantum mechanically and another corresponding part is treated classically [116]. This scenario is related to Bohr's Correspondence Principle, used generally to represent the idea that new theories should reproduce the results of established theories (as limiting cases) in domains where the earlier theories work. The Semi-classical limit is the arena in which quantum mechanics reduces to

classical mechanics. For example, Einstein's special relativity satisfies the correspondence principle because it reduces to classical mechanics in the limit where velocities are small compared to the speed of light. Another example is the Wentzel-Kramers-Brillouin (WKB) approximation [117].

8.12.2 Semi-Quantum Limit

The Semi-quantum limit refers to the domain where one part of a physical system is described by UFM and another corresponding part quantum mechanically [90]. This scenario is related to Bohr's Correspondence Principle, stating that new theories should reproduce the results of established theories in the limit where the earlier theory operates. The Semi-quantum limit is the arena in which UFM reduces to quantum mechanics; it is the one concerned with the duality of the interface with the finite dimensional radius of the manifold of uncertainty (MOU).

8.13 Measurement

A quantum system can be in a ground state $|0\rangle$ or excited state $|1\rangle$; but the superposition principle states that the system is in a linear superposition or combination of the two, $\alpha_0|0\rangle + \alpha_1|1\rangle$, simple if α represented probabilities, nonnegative real numbers adding to 1. However, the superposition principle allows them to be complex numbers if the square of their norms add to 1, $|\alpha_0|^2 + |\alpha_1|^2 = 1$. The coefficient α_0 represents the amplitude of the state $|0\rangle$, so it can thus refer to the probability, be negative or imaginary.

A linear superposition is the 'private world of the quantum state', $\alpha_0|0\rangle + \alpha_1|1\rangle$ with measurement outcome 0 having probability $|\alpha_0|^2$ and outcome 1 with probability $|\alpha_1|^2$, normalized to $|\alpha_0|^2 + |\alpha_1|^2 = 1$. This act of measurement causes the system to change state. This holds for k -level systems, such as $|0\rangle, |1\rangle, |2\rangle, \dots, |k-1\rangle$. Under these circumstances the superposition principle states, $\alpha_0|0\rangle + \alpha_1|1\rangle + \dots + \alpha_{k-1}|k-1\rangle$, with $\sum_{j=0}^{k-1} |\alpha_j|^2 = 1$. A measurement then has an outcome between 0 and

$k - 1$, with j 's probability $|\alpha_j|^2$ disturbing the system to $|j\rangle$ or the j th excited state.

To encode n qubits for two electrons for example, we have four possible states, 00, 01, 10, 11 (2 qubits) which in linear combination becomes

$$|\alpha\rangle = \alpha_{00}|00\rangle + \alpha_{01}|01\rangle + \alpha_{10}|10\rangle + \alpha_{11}|11\rangle, \quad (8.13)$$

Normalized to $\sum_{x \in \{0,1\}^2} |\alpha_x|^2 = 1$ where the probability of outcome is $x \in \{0,1\}^2$ is $|\alpha_x|^2$.

Now here's the rub; let's consider a general case of $n = 500$ qubits in a linear superposition of all 2^{500} possible classical states, much larger than the number of particles estimated in the classical universe (10^{80}):

$$\sum_{x \in \{0,1\}^n} \alpha_x |x\rangle. \quad (8.14)$$

This exponentially huge superposition is ‘the private world’ of the electrons involved and measurement only allows us to find the n bits (500) of information, $|\alpha_x|^2$. If our UFM model proves successful in surmounting uncertainty, then measurement does not change the system leaving all 2^{500} possible superposed states intact. This also leads to violation of the no-cloning theorem.

Input to quantum algorithms is by n classical bits - an n -bit string, x . After QC operations are performed, the n qubits have been transformed to the superposition, $\sum_y \alpha_y |y\rangle$ with output probability $|\alpha_y|^2$. This works by placing molecules in a magnetic field aligning spins of the nuclei and then flipping the spins with radio waves. Because each nucleus sits in a slightly different position in the molecule, each is addressed with slightly different frequencies, by a process known as nuclear magnetic resonance. The spins can also be made to interact with each other so that the molecule acts like a tiny logic gate when zapped by a carefully prepared sequence of radio pulses. In this way the molecule processes data. And because the spins of each nucleus can exist in a superposition of spin up and spin down states, the molecule acts like a tiny quantum computer [118-120].

A big question is, does an ontological measurement change the basis for quantum algorithms? Would such a scenario (other than putatively removing the need for error correction cycles) provide another category of speedup? We have considered that UFM based UQC is primarily a boon to measurement and possibly in that case classes of quantum algorithms might remain the same. Let's not call it 'parallel QC', but rather could we discover a class of 'holographic UQC' with asymptotically infinite speedup? As we devise in Chap. 13, it is not to be called infinite; but with EPR-like dual-Amplituhedron connectivity it is termed a new class of 'instantaneous' ontological algorithms!

The Larmor or cyclotron radius is the radius of the circular motion of a charged particle in the presence of a uniform magnetic field. Given in SI units by

$$r_L = \frac{mv_{\perp}}{|q|B} \quad (8.15)$$

where m is the mass of the particle, v_{\perp} the component of velocity perpendicular to the direction of the magnetic field, q the charge of the particle, and B the strength of the magnetic field. Proton, Electron, Photon? Gödelizing Fine Structure will reveal additional Unified Field Mechanical atomic structure beyond the current 4D model of the 3D Fermionic 0D singularity.

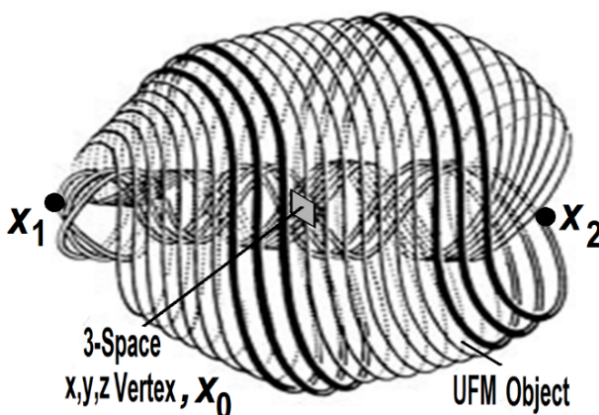


Fig. 8.19. Matter can no longer be considered as 3-space point particles, but needs to be studied with the inclusion of an HD topological brane manifold that it is embedded in and cyclically emerges from as a hyperspherical standing-wave.

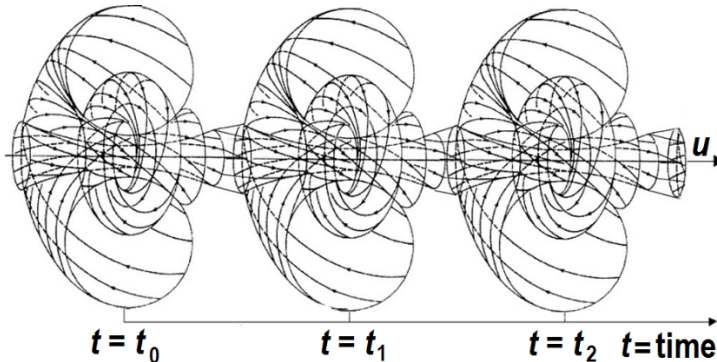


Fig 8.20. Symbolic diagram for LCU radius beat frequency of spacetime. Could be achieved by π rotations of the Riemann sphere LCU complex.

Coherent energy exchange can be achieved by dynamically coupling the mechanical oscillations of the two beams. This is realized by periodically modulating the spring constant of one beam at the frequency difference between the two beams. This periodic modulation, namely pumping, can be induced by applying gate voltage via the piezoelectric effect in this sample. This pumping enables strong vibrational coupling, leading to the cyclic (Rabi) oscillations between the two vibrational states (the beam-L state and the beam-R state) on the Bloch sphere. The Rabi cycle period, i.e., the coupling strength, is fully adjustable by changing the pump amplitude via the gate voltage. As a result, the vibration energy can be quickly transferred from one beam to the other enabling the vibration of the original beam to be switched off on a time-scale orders of magnitude shorter than its ring-down time. This quick energy transfer to the adjacent oscillator opens up the prospect of high-speed repetitive operations for sensors and logics using Nano-mechanical systems [121,122].

8.14 The No-Cloning Theorem (NCT)

The no-cloning theorem explicitly states that it is impossible to create an identical copy of an arbitrary unknown quantum state. We profess the NCT is only valid for the Copenhagen Interpretation, not for UFM. In theoretical physics, no-go theorems state that some situation is physically untenable. Specifically, the term describes results in quantum mechanics like Bell's theorem and the Kochen-Specker theorem that constrain the permissible types of hidden variable theories attempting to

explain the apparent randomness of quantum mechanics as a deterministic model featuring hidden states [123,124].

This no-go theorem of quantum mechanics was articulated by Wooters and Zurek [125] and Dieks [126], and has profound implications in quantum computing and related fields. The state of one system can be entangled with the state of another system. For instance, one can use the controlled NOT gate and the Walsh–Hadamard gate to entangle two qubits. This is not cloning. No well-defined state can be attributed to a subsystem of an entangled state. Cloning is a process whose result is a separable state with identical factors. The no-cloning theorem was prompted by a proposal of Herbert [127] for a superluminal communication device using quantum entanglement.

The no-cloning theorem is normally stated and proven for pure states; the no-broadcast theorem generalizes this result to mixed states [128-130].

§ The Quantum No-Cloning Theorem: *An unknown quantum state cannot be duplicated.*

8.14.1 Proof of the Quantum No-Cloning Theorem (NCT)

Let $|\phi\rangle$ be the state of quantum system A that we want copied. In order to clone state $|\phi\rangle$ we must take another quantum system B that has the same state space (general Hilbert abstract vector space) and its initial empty state $|e\rangle_B$ which must be independent of state $|\phi\rangle_A$ which must also be completely unknown. The composite A, B quantum system is designated by the tensor product $|\phi\rangle_A \otimes |e\rangle_B$. According to the tenets of quantum theory there are only two permissible quantum operations by which the composite system may be manipulated:

- An irreversible observation on the system could be made, collapsing the system into some observable eigenstate thereby corrupting the qubits information. This is not satisfactory.
- The Hamiltonian of the system can be controlled. Thus if the time-evolution operator, U up to some fixed time interval, yields a unitary operator U for a time-independent Hamiltonian, $U(t)=e^{-iHt/\hbar}$, with

$-H/\hbar$, the ‘translations in time’ generator, then U acts as a copier so long as $U|\phi\rangle A|e\rangle B = |\phi\rangle A|e\rangle B$ for all possible states $|\phi\rangle$ in the state space.

For the latter case we can select an arbitrary pair of states $|\phi\rangle A$ and $|\psi\rangle A$ drawn out of the Hilbert space. Since U is unitary, the inner product $\langle e|B\langle\phi|A\langle\psi|A|e\rangle B = \langle e|B\langle\phi|AU^\dagger U\langle\psi|A|e\rangle B = \langle\phi|B\langle\phi|A|\psi\rangle A|\psi\rangle B$, is preserved; and because all quantum mechanical states are assumed to be normalized, $\langle\phi a|\psi a\rangle\langle\phi b|\psi b\rangle = \langle\phi|\psi\rangle^2 = 1 = \langle\phi|\psi\rangle$.

Since this implies that either $\langle\phi|\psi\rangle = 1$ or $\langle\phi|\psi\rangle = 0$, two possibilities occur, either $\phi = \psi$ or that ϕ is orthogonal to ψ . Quantum theory however states that this cannot be true for two arbitrary states. Thus it is not possible for a single universal U to have the ability to clone a general quantum state which simply enough proves the Non-Cloning Theorem (NCT). However, one should be aware that that it is possible to find specific pairs that satisfy the algebraic requirement above. The following orthogonal states provide such an example $|\phi\rangle = 1/\sqrt{2}(|0\rangle + |1\rangle)$, $|\psi\rangle = 1/\sqrt{2}(|0\rangle - |1\rangle)$ and for this special case one can verify that $\langle\phi|\psi\rangle = 0 = \langle\phi|\psi\rangle^2$. And as one might surmise the relation doesn’t hold for more general quantum states [125].

And again, supposing the unknown quantum state, $|\psi\rangle = \alpha|0\rangle + \beta|1\rangle$, is it possible to take state $|\psi\rangle$ and produce copies of this state $|\psi\rangle \otimes |\psi\rangle$, essentially cloning it?

Proof: Show that for the evolution $|\psi\rangle \otimes |0\rangle \rightarrow |\psi\rangle \otimes |\psi\rangle$ for all possible states $|\psi\rangle$, there is no unitary cloning map operator, U allowing a $|0\rangle$ and $|1\rangle$ cloning operation: $U|0\rangle \otimes |0\rangle = |0\rangle \otimes |0\rangle$ and $U|1\rangle \otimes |0\rangle = |1\rangle \otimes |1\rangle$. If this operation holds, by the linearity of quantum theory, $U \frac{1}{\sqrt{2}}(|0\rangle + |1\rangle) \otimes |0\rangle = \frac{1}{\sqrt{2}}(|0\rangle \otimes |0\rangle + |1\rangle \otimes |1\rangle)$; but this is not equal to

the $\frac{1}{\sqrt{2}}(|0\rangle + |1\rangle) \otimes \frac{1}{\sqrt{2}}(|0\rangle + |1\rangle)$ required for a cloning unitary. The contradiction demonstrates that no such unitary exists for states that are elements of an unknown orthonormal basis [125,145].

8.14.2 Quantum No-Deleting Theorem

Similar in many ways to the no-cloning theorem, the quantum no-deleting theorem states that no quantum operation can erase an unknown quantum state. In order to manipulate, copy or delete quantum information a measurement must be performed by access to the state. While anyonic braiding TQC provides protected quantum states; they are currently too protected and inaccessible.

Ontological-phase topological field (OPTFT) theory will change this scenario. OPTFT has the ability to override the quantum no-cloning and non-erasure theorems; also allowing access to the topologically protected quantum Hall anyon braid states. (see Chap. 12).

8.15 The Tight-Bound State Protocol

Because Euclidean space is a ‘shadow’ of HD reality, gated by the Uncertainty Principle, and the current belief that the stochastic quantum foam is the ‘basement of reality’; it has not been evident that behind this veil (provided by a manifold of uncertainty of finite radius) there is a harmonic oscillation of the unified field, that opens and closes this gating mechanism with a ‘continuous-state’ periodicity. This is the key element of this scenario: in this regard there is a ‘beat frequency’ to the cyclic creation and annihilation of spacetime from the nilpotent potentia it is reduced (shadow) from. The symmetry occurs because of its inherent Cramer-like standing-wave structure with de Broglie-Bohm control parameters driving its evolution. The perceived extreme radical nature of these premises, they will be difficult to accept initially; but in our favor we have an experimental paradigm waiting in the wings to be performed.

We assume that all matter emerges from spacetime. In order to perform our experiment, we need to ‘destructively-constructively’ interfere with this process of continuous emergence. In the model being developed this requires finding a cyclical beat-frequency to the creation and annihilation process of space-time and matter. We believe this is best done by utilizing HD completed forms of the de Broglie-Bohm-Vigier causal and Cramer

transactional interpretations of quantum theory. Once we know the size of the close-packed LCU and apply this to our ‘zero to infinity’ rotation of the Riemann sphere (Kahler manifold) we will know the radius/time of this putative inherent beat-frequency. This is where the Sagnac Effect Dubois incursive oscillator is applied to the structure where the Δt hyperincursion [106-110] would correspond to a specific phase in the beat-frequency of spacetime and size of the hole utilized (punched by destructive interference) to send our signal through in order to detect several new TBS spectral lines in hydrogen [31].

We set the resonance hierarchy up in this case with hydrogen (simplest case with least amount of artifact from other electrons) where we jiggle the electron tuned to resonate with the nucleus tuned with the annihilation - creation vectors in the beat frequency of spacetime which putatively opens a hole into the HD ‘manifold of uncertainty’ cavities by a process which we have stated numerous times is a direct violation of the quantum uncertainty principle. Which as you recall, occurs when a field is arbitrarily set up along the z-axis to separate the states in the Stern-Gerlach apparatus, the historical beautiful empirical proof of the uncertainty principle.

So simplistically we’re going to do something else which you should by now have a glimmer of and the additional degrees of freedom required to perform this something else. This is why we have to have access to the physics inherent in this new cosmology. In the current model with the Planck basement there is no understanding of how to pass through; there is no XD cavities behind the Planck basement. It is finding the LCU beat frequency in the Dirac polarized vacuum that will give us success.

In summary, we have the 3-level tiered Sagnac Effect resonance hierarchy of electrons nucleons and spacetime. The counter-propagating properties of the Sagnac Effect that violates special relativity in the small-scale will most likely be relevant to this resonance process.

For the standing-wave oscillator, the gap between R_1 & R_2 in the beat frequency of spacetime we take our ‘little laser blaster’ starting at the R_1 bandwidth, when we reach the right point we will get a reflected blip, which will be our first new spectral line in hydrogen. So in a sense if you’ve been following along; you see in general how straightforward and really simple this experiment is. This is a paradigm shift and beneath this infinite as yet to the reader, concatenation of mumbo-jumbo lies the framework for performing the TBS experiment. Unfortunately, one can see that any part of these elements that I’ve been gerrymandering could each take several hours to describe properly. The continuous-state, deriving the alternative formula for string tension - any of these is in hour

lecture in itself. The importance of the LCU could require thousand page treatises. I've been trying to give an overview of the framework for UFM that we're in the process of discovering.

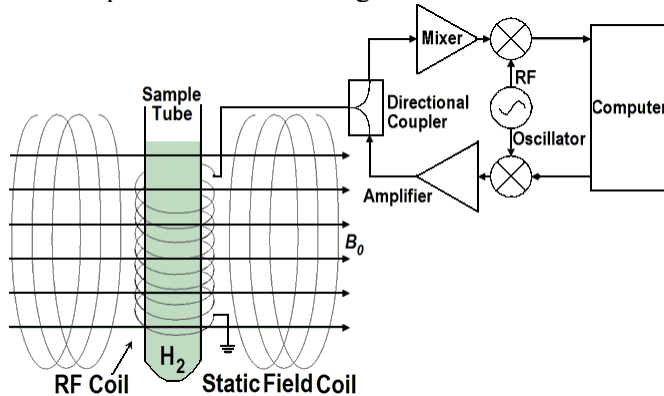


Fig. 8.21. NMR apparatus designed to manipulate TBS in Hydrogen. The figure only shows possible details for rf-modulating TBS QED resonance, not the spectrographic recording and analysis components. Conceptual model of a proposed TBS experiment where hydrogen is put in the sample tube to which resonances are applied in a manner opening the manifold of uncertainty for access to HD cavities correlated with new spectral lines in hydrogen.

Some experimental evidence has been found to support this view showing the possibility that this is the same property that the interaction of these extended structures in space involve real physical vacuum couplings by resonance with the subquantum Dirac ether. Because of photon mass the in CSI model, any causal description implies that for photons carrying energy and momentum, one must add to the restoring force of the harmonic oscillator an additional radiation (decelerating) resistance derived from the em (force) field of the emitted photon by the action-equal-reaction law. Kowalski has shown that emission and absorption between atomic states take place within a time interval equal to one period of the emitted or absorbed photon wave. The corresponding transition time correlates with the time required to travel one full orbit around the nucleus [102,103]. Individual photons with m_γ are extended spacetime structures containing two opposite point-like charges rotating at a velocity near c , at the opposite sides of a rotating diameter with a mass, $m = 10^{-65} g$ and with an internal oscillation $E = mc^2 = \hbar v$. Thus a new causal description implies the addition of a new component to the Coulomb force acting randomly and may be related to quantum

fluctuations. We believe this new relationship also has some significance for our model of vacuum C-QED blackbody absorption/ emission equilibrium [130].

8.16 Indicia of the UFM Tight Bound State CQED Model

A) SEARCH FOR LARGE-SCALE ADDITIONAL DIMENSIONS

CERN has begun a new program to find evidence of another host of particles that can only exist if there are more dimensions than found in the Standard Model of particle physics; experiments proposed, but not yet successfully performed.

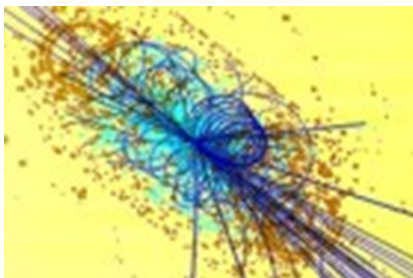


Fig. 8.22. CERN high energy collision cross section particle spray of the type that uncovered the Higgs mechanism.

CERN is trying to build larger and larger more powerful colliders like the LHC in the hopes of creating cross sections closer and closer to the Planck scale. Our UFM model is radically different; it is table-top and low energy. Why is that? If the matter right in front of our nose only appears solid and impenetrable because of a constructively interfered phase amplitude – of which we are made out of and imbedded in so that we have the same occlusion, then the uncertainty principle provides a simple gating mechanism to preclude us. Remember when ‘they’ first tried to fire a machine gun through the propeller of WWI airplanes – ‘They’ shot the propellers off until they timed the shots properly. Recall our mention of the inherent beat frequency hidden within the manifold of uncertainty.

B) THE CONTINUOUS-STATE HYPOTHESIS

Derivation of continuous-state multiverse postulates led to a unique string vacuum with as I've mentioned contains a variable string tension and a

virtual tachyon [6,7]. I will do my best to define this continuous-state process which is still very difficult for me to do. The Planck scale is currently called the basement of reality starting from an essentially infinite size Hubble radius cosmology that reduces to a rigid microscopic Planck scale. In the holographic multiverse model, built partly by the way on an extension of Rauscher's complex 8-space, where she added a 4D complex space, \mathbb{C}^4 to standard 4D Minkowski space, M^4 which didn't quite work for me because her 4D complex space still reduced to a fixed rigid Planck barrier.

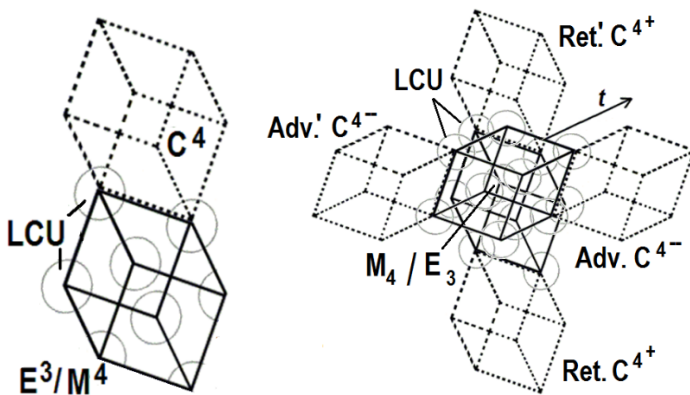


Fig. 8.23. a) Conceptual view of the Rauscher HD Complex C^4 space added to Minkowski space. b) 12D UFM Multiverse cosmology with the addition of a 2nd dual mirror symmetric complex 4-space resulting in $M_4 \pm C^4$. The $\pm C^4$ spacetime packages must become involute (like a trefoil or L-R dual Möbius Klein bottle (Fig. 8.26) before the continuous-state process flow can occur. Or better yet for Calabi-Yau manifolds, folded into a torus.

What was needed to develop the continuous-state model was to have a fundamental basis of reality that acted as if it was in a self-contained inherent freefall. So we added another set of complex dimensions to allow reality to cycle continuously at the fundamental level. However, Rauscher's complex 8-space also included superluminal Lorenz transformations that boosted a spatial dimension, s into a temporal dimension, t enhancing the process for conceptualizing the continuous-state scenario [10]. We then applied a second set of superluminal Lawrence transformations boosting a temporal dimension, t to dimension of energy, e . The energy dimension becomes compatible with a superquantum potential eventually becoming synonymous with the ontological force of coherence of the unified field. This addition along with the second

complex 4-space, $\pm\mathbb{C}^4$ dimensions completed geometrically at least the necessary components for continuous-state cyclicity providing a key framework for one of the most key elements of the model within which we propose new TBS spectral lines in hydrogen [31].

Concerning the importance of the original hadronic form of variable string tension; the main reason we were able to discover a unique string vacuum was by finding an alternative derivation of string tension; for which the traditional formula is, $T_s = e/l = (2\pi\alpha')^{-1}$. The multiverse UFM formula in unexpanded form became,

$$F_{(N)} = \frac{\aleph}{\rho} \quad (8.16)$$

where instead of energy, e over the length of the string, l topological charge or UF brane energy, \aleph was put over the brane topological radius, ρ of the relativistically rotating Riemann sphere LCU hyperstructure. $F_{(N)}$ is the noetic force of coherence of the unified field [31].

8.17 Building the UFM TBS Experimental Protocol

The best indicia for our model experimentally is suggested by work done by Chantler [132,133]. The data from his experiments over the last 10 years or so on hydrogen showed only a minute artifact proposed to violate QED; but more recently in 2012 for work on Titanium the QED violation effect was much larger. The beauty of this is that they stripped all the electrons off the Titanium atom except one creating a large hydrogen-like atom [133]. One wants to maintain the simplicity of the hydrogen atom to perform the experiment.

Vigier's seminal papers in 1999/2003 [134,135] are similar theoretically in some ways to Chantler's model. Vigier describes the first exploration made by Corben in an unpublished paper. Corben noticed that motion of a point charge in the field of magnetic dipole at rest, is highly relativistic and that the orbits are of nuclear dimensions. Further investigation has been undertaken by Schild [136], but the most systematic treatment of this problem is given by Barut (see for example [137]). A 2-body system where magnetic interactions play the most significant role is in positronium. Both electron and positron have large magnetic moments which contribute to the second potential well in an effective potential, at

distances much smaller than the Bohr radius. Barut and his coworkers predicted that this second potential well can support resonances. A 2-body model, suitable for non-perturbative treatment of magnetic interactions is presented by Barut [137] and Vigier [134,135].

Our approach doesn't fully correlate with Vigier's because at that time he had no consideration of additional dimensionality which is a dominant element in our multiverse model. For the first 10 years of Chantler's work the artifact said to violate QED was so small that it was essentially ignored by the physics community. But in the 2012 experiment [133] the QED violation was great enough ($>\sigma 5$) that media suggested Nobel Prize; but the majority of the physics community said the artifact is insufficient.

Now the reason we think the continuous-state model will work is for example if you take the Bohr model of the hydrogen atom, spectroscopic measurements are taken as a 3D volume measurement from the space between the nucleus and the electrons orbit. For hydrogen the first Bohr orbit has a radius of a .5 Angstrom, and the second or orbit a radius of ~ 2 Å. This is the 100-year history of spectroscopic measurements from within the fixed regime of the 4D standard model. A spectroscopic cavity is going to have different properties in a 12D holographic multiverse regime.

Firstly, we postulate the volumes of XD both within the finite radius MOU and beyond into the regime of LSXD. We continue to mention in terms of the complex quaternion Clifford algebra required to describe the continuous state process; that the cyclicity has an inherent commutativity anti-commutativity that the algebra can handle with a 3D or 4D Euclidean/Minkowski space resultant with 8D or 9D complex cycling dimensions built on top of it. Initially for a single space anti-space doubling, the MOU represents a 4th, 5th and 6th hyperspherical XD.

Recall our use of the Rauscher superluminal Lorentz transformation that boosts a spatial dimension into a temporal dimension, wherein multiverse UFM cosmology has added a second boost of dimensionality from temporal to that of energy as the exchange mechanism for topological charge in unified field theory. Behind or within the veil of uncertainty these XDs open and close volumetrically from zero i.e. the usual 3D Euclidean QED cavity to the added volumetric structure of the 4th 5th and 6th XD yielding: $r_1 V_{3D}, r_2 V_{4D}, r_3 V_{5D}, r_4 V_{6D}$ enabling us to calculate the wavelength of three additional spectral lines in hydrogen based on the volume of these respective hyperspherical cavities.

We haven't given enough thought to consider whether it's a viable addition to interpretation, but Von Neumann postulated a 'speed for collapse' of the wave function, suggesting that if we also used a hydrogen-

like Titanium atom there might be an additional helpful time delay factor. In any case the success of this experiment would provide the first indicia that something exists beyond the regime of Gauge theoretic SM QED.

Opening the 4D resonance hierarchy cavity will be relatively easy, but to open the 5th and 6D cavities probably requires the addition of some kind of precision Bessel function to the resonance hierarchy because additional artifacts like found in the refinements of the Born-Sommerfeld model; it will be a little tricky to master the protocol to measure these additional spectral lines. I do not mean this in calculating the wavelength, but the tiniest property we do not sufficiently understand will probably keep the uncertainty principle sufficiently active to keep the 5D cavity closed!

This TBS model only works within the continuous-state holographic multiverse scenario simply because without that utility physics would not go beyond 5D Kaluza-Klein and remain ‘curled up at the Planck scale’ model of XD. It is only the inherent continuous-state process of open-closed cyclicality that allows access (violating the uncertainty principle) to the additional infinite LSXD. This restriction is not a negative aspect of this proposed multiverse cosmology, but we feel rather that it is suggestive of the correct path to take as it is the actuality of physical reality.

The key element in this cosmology is the Least Cosmological Unit (LCU), not fully invented by us; but an extension of the idea found within a chapter called, “*The size of the least unit*” in a collection edited by Kafatos [101]. But Stevens of course utilizing only the 4D of the standard model attempted to describe a Planck scale least unit. But hopefully you have realized by now that our LCU oscillates from asymptotic virtual Planck, $(\hbar + T_s)$ to the Larmor radius of the hydrogen atom relative to the nature of its close-packing tiling the spacetime foam.

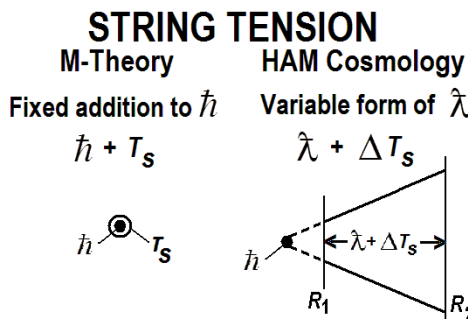


Fig. 8.24. Fixed string tension in M-Theory (left) and variable (right) as in the original hadronic form of string theory and HAM cosmology that also reverts to the original Stoney, λ rather than Planck's constant, \hbar .

The left-hand part of Fig. 8.24 shows the current thinking of string tension but, on the right we see a multiverse version with a variable string tension that oscillates from virtual plank to the Larmor radius of hydrogen. Notice that the symbol for the Planck constant is different, we use the original Stoney [4] that preceded Planck because it is electromagnetic and correlates better with the Dirac polarized vacuum which we want available for our resonance hierarchy component of the experimental protocol. Virtual plank is the asymptotic zero point on the Riemann sphere that flips back to infinity in the continuous-state cycle.

Since the Planck scale is no longer considered the basement of reality, the 12D continuous-state process changes the size of the LCU in the process of Riemann sphere rotation from zero back to infinity continuously. Choice of the upper limit as the Larmor radius is somewhat arbitrary. We cannot define this rigorously yet without experiment; but assume it is in this ballpark. So just to make a note we have this oscillating Planck unit, $\Delta\hbar$ at the microscopic level in conjunction with an oscillating $\Delta\lambda$ lambda or cosmological constant at the macroscopic level.

As an aside this gives us the ability to describe dark matter/energy as an artifact of the rest of the multiverse outside our ~ 14.7 bly radius Hubble sphere. The multiverse has ‘room for an infinite number of nested Hubble spheres each with their own fine-tuned laws of physics’. That scenario provides our model of dark energy. These nested Hubble spheres are closed and finite in time and causally separate in the XD where gravity would take effect, so it’s not like there is an infinite mass acting on us but something subtler. As generally known the postulate of dark energy and dark matter comes from the knowledge that galactic rotation occurs like a phonograph record not a vortex.

Think of these nested Hubble spheres as a stalk of grapes; they are invisible to current empirical means because the nature of the stalk holding the grapes, however, UFM allows design of a ‘Q-telescope’ to visualize them [4]. Also see the Drake equation therein.

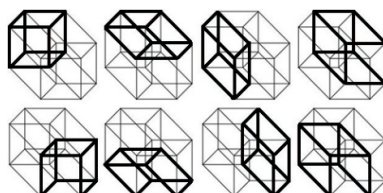


Fig. 8.25. View of 8 3D cubes comprising a 4D hypercube. See continuous-state involution metaphor in Fig. 8.5.

A main condition of the continuous-state hypothesis comes from an HD extension of Cramer's Transactional Interpretation of future-past elements resulting in a present moment [52]. Cramer considers this as a standing-wave of the future-past. In XD we build on superluminal Lorentz transformations, coupled to advanced-retarded future-past complex pairs.

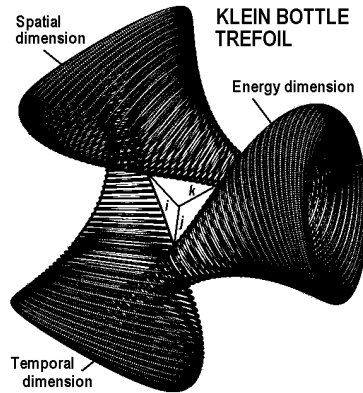


Fig. 8.26. A Klein bottle trefoil. A 6D Calabi-Yau 3-torus could also be used. A primitive metaphor to show rotation of continuous-state components. Does not really work in 4D. But I wanted to try to illustrate the cycling of dimensional parameters if the eight cubes of the hypercube put into motion not just exploded as in the figure.

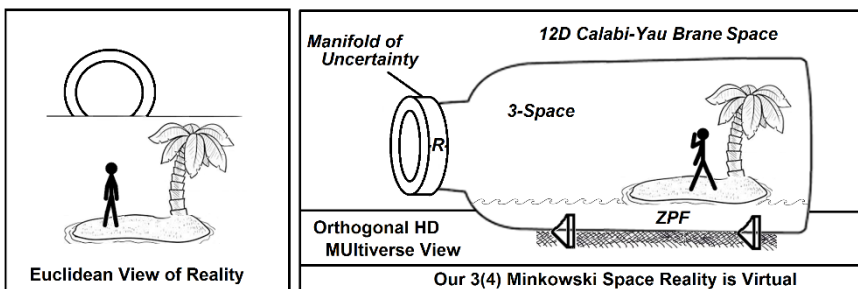


Fig. 8.27. Beyond the 4D Standard Model Lies Infinite Size Dimensionality (LSXD) 'Hidden' by Uncertainty.

What I have poorly tried to illustrate in Figs. 8.25 to 8.27 is some of the underlying topology of continuous-state topology. Figure 8.25 shows the dramatic increase in the number of cubes comprising HD space as we travel rectilinearly up the XD ladder. Figure 8.26 shows a key condition of involution allowing the continuous-state process to cycle continuously

when set in motion by the nature of HD reality. Figure 8.27 is also an attempt to speak to the rotational properties of cyclicity. Our 12D model must cycle through nodes of commutativity and anti-commutativity where one mode is degenerate and the other closed to observation. There are not sufficient degrees of freedom to cyclically break closure otherwise. Rowlands supports an inherent necessity of 3D for reality [138], so we have a doubling of the 1st 3D into another triplet of HD space. This might suggest indicia for the necessity of the 12D where UFM wants to lead us.

Imagine a 3-blade ceiling fan symbolic of a quaternion fermion vertex. If one puts one of these fans in front of a mirror (real space) rotating clockwise the mirror image (anti-space) rotates counterclockwise with the blades coming occasionally into phase as in Fig. (8.10). Now we give a key insight into the TBS experiment that Fig. 8.10 doesn't have. If there is a light on near the fan in real space, i.e. the rf-pulse of our TBS experiment. Periodically when the blades come into phase (Fig. 8.10 again) meaning when a blade from real space comes into phase with a blade in the mirror antispace the light is reflected off each blade (the mirror image of the mirror image) and a pulsating, reflected flash of light occurs in the direction back towards the source/detector! This is representative of how we intend to find the new TBS spectral lines in hydrogen; that we would expect to see a flashing back, like a rotating lighthouse beacon when the resonance hierarchy is aligned properly!

Rowlands suggests these additional space anti-space dimensions are redundant (no new information) [138] That's actually what we want from an infinite potentia that is nilpotent and redundant. Surmounting the quantum mechanical uncertainty principle occurs by this same process that gives us a beat frequency inherent in the spacetime backcloth.

In order to demonstrate existence of new spectral lines the experiment itself requires surmounting the quantum uncertainty principle. I hope when we apply the complex quaternion Clifford algebra it will tell us whether one or two additional doublings of Roland's original space anti-space model are required and then let us know if there's two or three or more consecutive doubling needed to find four or five additional spectral lines which of course tells us the complete size of the manifold of uncertainty.

From the common simple example of a Bessel function, with α an arbitrary complex number:

$$x^2 \frac{d^2 y}{dx^2} + x \frac{dy}{dx} + (x^2 - \alpha^2) y = 0 \quad (8.17)$$

we solve the Helmholtz equation in spherical coordinates by variable separation such that the radial equation takes the form

$$x^2 \frac{d^2 y}{dx^2} + 2x \frac{dy}{dx} + [x^2 - n(n+1)]y = 0. \quad (8.18)$$

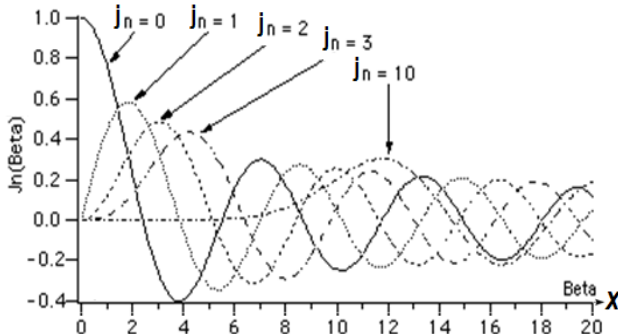


Fig. 8.28. Example of a Bessel Function that may be necessary to couple synchronization with the Dubois incursive oscillator in order access additional TBS beyond the first. Even though we think we know how, surmounting uncertainty will probably not be trivial.

The spherical Bessel functions, j_n , y_n are the two linearly independent solutions relate to the ordinary Bessel functions, J_n , Y_n as:

$$\begin{aligned} j_n(x) &= \sqrt{\frac{\pi}{2x}} J_{n+\frac{1}{2}}(x), \\ y_n(x) &= \sqrt{\frac{\pi}{2x}} Y_{n+\frac{1}{2}}(x) = (-1)^{n+1} \sqrt{\frac{\pi}{2x}} J_{-n-\frac{1}{2}}(x). \end{aligned} \quad (8.19)$$

When written as Rayleigh's formulas

$$\begin{aligned} j_n(x) &= (-x)^n \left(\frac{1}{x} \frac{d}{dx} \right)^n \frac{\sin(x)}{x}, \\ y_n(x) &= (-x)^n \left(\frac{1}{x} \frac{d}{dx} \right)^n \frac{\cos(x)}{x}, \end{aligned} \quad (8.20)$$

the first spherical Bessel functions are

$$\begin{aligned} j_0(x) &= \frac{\sin(x)}{x} \\ j_1(x) &= \frac{\sin(x)}{x^2} - \frac{\cos(x)}{x} \\ j_2(x) &= \left(\frac{3}{x^2} - 1 \right) \frac{\sin(x)}{x} - \frac{3\cos(x)}{x^2} \end{aligned} \quad [139] \quad (8.21)$$

and

$$\begin{aligned} y_0(x) &= -j_{-1}(x) = -\frac{\cos(x)}{x} \\ y_1(x) &= -j_{-2}(x) = -\frac{\cos(x)}{x^2} - \frac{\sin(x)}{x} \\ y_2(x) &= -j_{-3}(x) = \left(-\frac{3}{x^2} + 1 \right) \frac{\cos(x)}{x} - \frac{3\sin(x)}{x^2} \end{aligned} \quad [139]. \quad (8.22)$$

We show the 1st three Bessel function solutions of the 1st and 2nd kind to illustrate our process to locate the first TBS spectral line in hydrogen which will be relatively easy to find in comparison to finding the 2nd and 3rd. The additional lines will be more challenging as there will be some unexpected complexity in the Bessel harmonic oscillator that must be overcome. The restrictions related to this refinement have not revealed themselves to us as yet, that will require some additional adjustment to the spin-spin coupling parameters of the algebra describing the HD hyperspherical volume. Parallel transport of the gravitational curvature deficit angle kick in, in mirror symmetric brane topological form, with noeon topological charge corrections (not a quantized gravity).

The choice of linear combinations of Bessel solutions (8.5) depends on their asymptotic behavior at ∞ ,

$$J_n(x) \approx \sqrt{\frac{\pi}{2x}} \cos\left(x - \frac{\pi}{2}n - \frac{\pi}{4}\right); \quad Y_n(x) \approx \sqrt{\frac{\pi}{2x}} \sin\left(x - \frac{\pi}{2}n - \frac{\pi}{4}\right) \quad (8.23)$$

thus

$$H_n^\pm(x) \approx \sqrt{\frac{\pi}{2x}} \exp\left[\pm i\left(x - \frac{\pi}{2}n - \frac{\pi}{4}\right)\right] \quad [140]. \quad (8.24)$$

With the harmonic oscillator Bessel function solutions, the next step in the experimental design is to apply the Dubois incursive oscillator parameters as the final step in designing the Sagnac effect rf-pulses. The incursive algorithms are numerically stable and the numerical simulation of the pendulum will show the conservation of the energy. Let us consider the example of the harmonic oscillator, with m the oscillating mass and k the spring constant, represented by the ordinary differential equations:

$$\frac{dx(t)}{dt} = v(t) \quad (8.25a)$$

$$\frac{dv(t)}{dt} = -\omega^2 x(t) \quad (8.26b)$$

where $x(t)$ is the position and $v(t)$ the velocity as functions of the time t , and where the pulsation ω is related to k and m by $\omega^2 = k/m$ [141].

The solution is given by

$$x(t) = x(0) \cos(\omega t) + [v(0)/\omega] \sin(\omega t) \quad (8.27a)$$

$$v(t) = -\omega x(0) \sin(\omega t) + v(0) \cos(\omega t) \quad (8.27b)$$

with the initial conditions $x(0)$ and $v(0)$. In the phase space, given by $(x(t), v(t))$, the solutions are given by closed curves (orbital stability). The period of oscillations is given by $T = 2\pi/\omega$. The energy $e(t)$ of the harmonic oscillator is constant and is given by

$$e(t) = kx^2(t)/2 + mv^2(t)/2 = kx^2(0)/2 + mv^2(0)/2 = e(0) = e_0 \quad (8.28)$$

The simulation of differential equations is impossible. This is only the discrete transformation which is computable with recursive function.

In differential equations there is only the current time. In discrete systems, there are the current time t and the interval of time $\Delta t = h$. The discrete time is defined as: $t_k = t_0 + kh$ with $k = 0, 1, 2, \dots$ where t_0 is the initial value of the time and k is the counter of the number of interval of time h [141].

The discrete variables are defined as $x_k = x(t_k)$ and $y_k = y(t_k)$. The discrete equations used in the harmonic oscillator case for computing the position and the velocity at consecutive moments have the general form

$$x_{k+1} = Ax_k + Bv_k \quad (8.29a)$$

$$v_{k+1} = Cv_k - D\omega^2 x_k \quad (8.29b)$$

where A , B , C and D are coefficients with values specific to the numerical integration methods applied.

In eliminating v_k of Eq. (8.29a) in Eq. (8.29b), a second order discrete equation in x_k is given by

$$x_{k+2} - (A+C)x_{k+1} + (AC + BD\omega^2)x_k = 0. \quad (8.30)$$

The stability analysis for this discrete system can be performed by using the Z-transform

$$z^2 - (A+C)z + (AC + BD\omega^2) = 0 \quad (8.31)$$

which presents two poles:

$$z_{1,2} = ((A+C) \pm i\sqrt{-(A+C)^2 + 4(AC + BD\omega^2)}) / 2 \quad (8.32)$$

that are complex when

$$(A+C)^2 < 4(AC + BD\omega^2) \quad [141]. \quad (8.33a)$$

The position of the poles relative to the unit circle defines the system stability: a system is stable if the poles lie inside the unit circle, is unstable if the poles lie outside the unit circle and shows an orbital stability if the poles lie on the unit circle. It follows that the condition for stability is:

$$((A+C)^2 - (A+C)^2 + 4(AC + BD\omega^2)) / 4 \leq 1 \quad (8.33b)$$

or $AC + BD\omega^2 \leq 1$ and the orbital stability must satisfy the strict equality

$$AC + BD\omega^2 = 1 \quad (8.33c)$$

so, for the harmonic oscillator, the conditions for obtaining an orbital stability are given by relations (8.33a) and (8.33c), rewritten as

$$(A + C)^2 < 4 \text{ and } AC + BD\omega^2 = 1 \quad (8.34a,b)$$

in using the equality from the relation (8.33c), in the relation (8.34a) [141].

Let us first consider the well-known Euler and Runge-Kutta integration methods, e.g. Scheid [142]; and after that, the incursive methods will be analysed.

In terms of incursive discrete algorithms, Dubois defined a generalized forward-backward discrete derivative

$$D(w) = w Df + (1 - w) Db \quad (8.35)$$

where w is a weight taking the values between 0 and 1, and where the discrete forward and backward derivatives on a function f are defined by

$$D_f(f) = \Delta^+ f / \Delta t = [f_{k+1} - f_k] / h \quad (8.36)$$

and

$$D_b(f) = \Delta^- f / \Delta t = [f_k - f_{k-1}] / h \quad (8.37)$$

The generalized incursive discrete harmonic oscillator is given as:

$$(1-w)x_{k+1} + (2w-1)x_k - w x_{k-1} = hv_k \quad (8.38a)$$

$$w v_{k+1} + (1-2w)v_k + (w-1)v_{k-1} = -h \omega^2 x_k \quad (8.38b)$$

When $w = 0$, $D(0) = D_b$, this gives the first incursive equations:

$$x_{k+1} - x_k = h v_k \quad (8.39a)$$

$$v_k - v_{k-1} = -h \omega^2 x_k \quad (8.39b)$$

When $w = 1$, $D(1) = D_f$, this gives the second incursive equations:

$$x_k - x_{k-1} = h v_k \quad (8.40a)$$

$$v_{k+1} - v_k = -h \omega^2 x_k. \quad (8.40b)$$

When $w = 1/2$, $D(1/2) = [D_f + D_b]/2$, this gives the averaged (hyperincursive) equations:

$$x_{k+1} - x_{k-1} = 2 h v_k \quad (8.41a)$$

$$v_{k+1} - v_{k-1} = -2 h \omega^2 x_k \quad (8.41b)$$

These Eqs. (8.41a,b) integrate the two incursive equations.

This deals with a deduction of this forward-backwards discrete derivative, with the deduction of this time-symmetric discretization of the harmonic oscillator [141].

Next simulation of the incursive and hyperincursive algorithms of the classical harmonic oscillator. First, for the simulation of the classical harmonic oscillator, the dimensionless variables X , V and H , will be used [8], for the variables, x , v and $h : X(k) = \sqrt{[k/2]} x_k$, $V(k) = \sqrt{[m/2]} v_k$, $\tau = \omega t$ with $\omega = \sqrt{[k/m]}$, and $\Delta\tau = \omega\Delta t = \omega h = H$. So, the two incursive dimensionless harmonic oscillators are given by

$$X_1(k+1) = X_1(k) + H V_1(k) \quad (8.42a)$$

$$V_1(k+1) = V_1(k) - H X_1(k+1) \quad (8.42b)$$

$$V_2(k+1) = V_2(k) - H X_2(k) \quad (8.43a)$$

$$X_2(k+1) = X_2(k) + H V_2(k+1) \quad (8.43b)$$

and the hyperincursive dimensionless harmonic oscillator is given by

$$X(k+1) = X(k-1) + 2 H V(k) \quad (8.44a)$$

$$V(k+1) = V(k-1) - 2 H X(k) [141]. \quad (8.44b)$$

Table 8.2 shows the numerical simulations of algorithms (8.42-8.44).

Table 8.2. Simulation of Eq. (8.42, 8.43) of the two incursive harmonic oscillators with a cycle of $N = 6$ iterates and interval of time $H = 1.0$. The averaged energy $\langle E(k) \rangle = (E_1(k) + E_2(k))/2$ of the two oscillating energies is constant.

N	H	k	INCURSION 1			INCURSION 2			$\langle E(k) \rangle$
			$X_1(k)$	$V_1(k)$	$E_1(k)$	$X_2(k)$	$V_2(k)$	$E_2(k)$	
6	1	0	8.66	0.00	75	10.00	5.00	125	100
		1	8.66	-8.66	150	5.00	-5.00	50	100
		2	0.00	-8.66	75	-5.00	-10.00	125	100
		3	-8.66	0.00	75	-10.00	-5.00	125	100
		4	-8.66	8.66	150	-5.00	5.00	50	100
		5	0.00	8.66	75	5.00	10.00	125	100
		6	8.66	0.00	75	10.00	5.00	125	100

So, this confirms that the incursive and hyperincursive algorithms are totally numerically stable with the conservation of energy [141].

When the parameters for the experiment are coordinated and the rf-pulse sent into the MOU HD QED TBS hydrogen cavity, a positive result will retrieve a spectroscopic signal like the one represented in Fig. 8.29. A negative result would send back 0 amplitude [31].

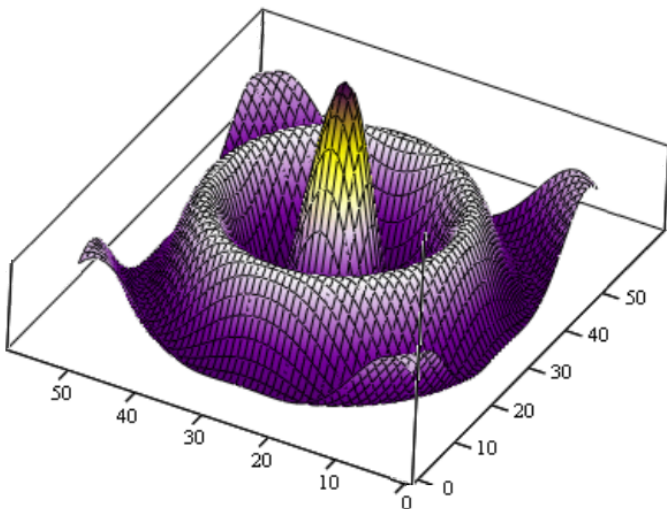


Fig. 8.29. First 4D TBS spectral line in hydrogen emerging from the 4D spherical potential well for $\alpha = \pm 1$. Fig. adapted from [143].

8.18 Issues of Experimental Design

In the simplistic model of doing the TBS experiment we put hydrogen in a sample tube (Fig. 8.21) and apply a series of resonant pulses in conjunction with the beat-frequency of space-time to open the HD QED-UFM cavity, send the signal in and allow the new TBS spectral line signal to be emitted back to the detector.

Remember we postulated that the HD continuous-state cycle must incorporate cycles of commutativity and anti-commutativity. This can be shown metaphorically in terms of logarithmic spirals applied to what is called perfect rolling motion (Figs. 8.30, 8.31).

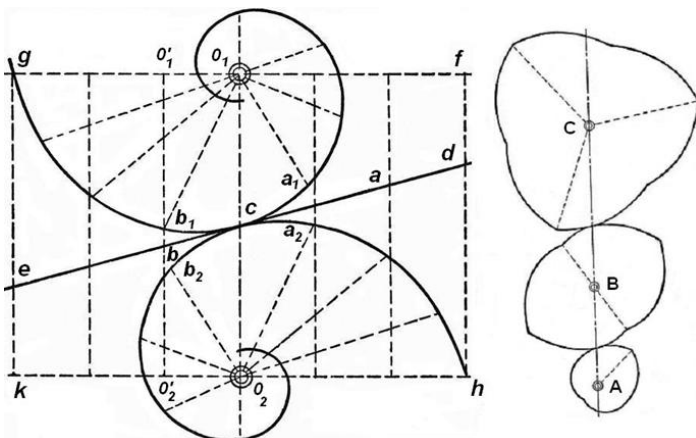


Fig. 8.30. Logarithmic spirals and ‘Perfect Rolling Motion. Segments of the logarithmic spiral are put together into the three spheroids on the right, A,B,C. Like the $320^\circ - 720^\circ$ spinor rotation of the Dirac electron; the spheroids will only return to the same configuration after a number of 360° rotations.

We've been arguing with colleagues for the last couple of years about aspects of quaternion algebra. I'm thankful especially to Peter Rowlands for helping me learn some of the properties of quaternions. As well-known Hamilton wanted to extend the complex number system algebraically by adding an additional j term to the i series; but the algebra didn't work. It was only when Hamilton added the 3rd k term that quaternion algebra became complete by closing the algebra and in the process, sacrificing commutativity. Is it any wonder that Rowlands resisted when I told him I wanted to open the algebra again so that it could cycle between modes of commutativity and anti-commutativity. Rowlands was very gracious and

allowed me to visit him for a week in Liverpool. We did find something interesting (see [143]) that is not yet a complete study, and not quite the cycle we've been looking for which with all profundity is going to be possible with a rather simple complex quaternion Clifford algebra [145].

How can we find this cycle in HD Calabi-Yau mirror symmetry? The logarithmic spirals in Fig. 8.30a are not free to rotate (Euclidean shadow). If we take pieces of the curve as in Fig. 8.30b and paste them together as shown; the three cycloids can cycle continuously. Perfect rolling motion in this case means a mechanical process where there is no slippage if this is applied to the mechanics of gears. As hopefully clear well before now to the reader, this represents a ‘closed’ non commuting algebra.

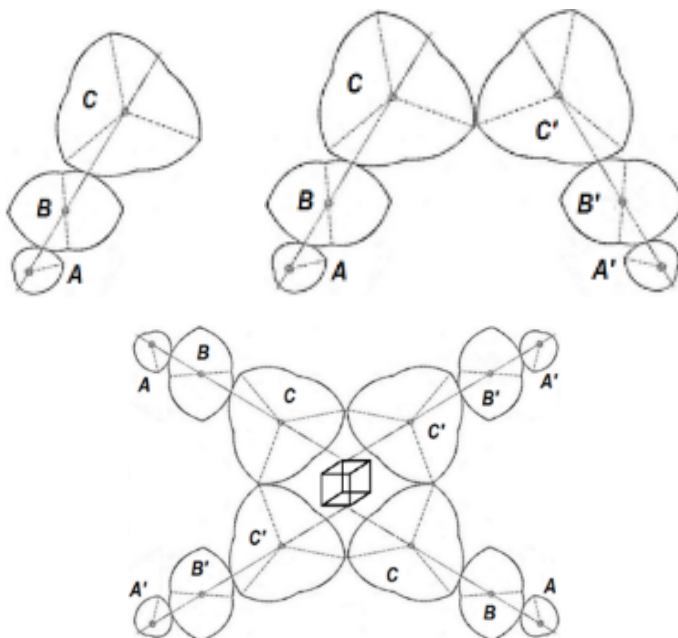


Fig. 8.31. a) Perfect rolling motion of logarithmic spiral components. b) Applied to left-right symmetry transformations of Calabi-Yau brane topology such that while the A,B,C tower is meant to represent the usual closed quaternionic space-antispace algebra; the A,B,C and A'B'C' towers together when doubled again as in c) will be able to cyclically commute and anti-commute (requires an additional mirror symmetric doubling with trefoil-like involution and parameters of parallel transport to finally cyclically break closure of the algebra. c) Hierarchical structure of HD space reducing to a 3-space resultant. The redundant A,B,C quaternionic copies shown for 2 cubic vertices, should be made to correlate with each of the 8 vertices of the Euclidean 3-space cube in order to fully represent complex 8-space, $\pm\mathbb{C}^4$, done beautifully with the Fano snowflake in Chap. 12.

If you're not a mechanical engineer, you may not have guessed already that after a certain number of cycles the set of three cycloids returns to the precise original position. Now in terms of the next figure (8.31) let's apply this to a second doubling or duality to Rowlands' space anti-space quaternion model which of course is going to have to include Calabi-Yau mirror symmetry. What we propose metaphorically here is that with the utility of the complex quaternion Clifford algebra we can mathematically describe how to break the closure inherent in one of the mirror symmetric partners and describe cycles relative to both mirror symmetric partners that additionally pass through cycles of commutativity and anti-commutativity with each other. We cannot surmount the uncertainty principle utilizing a closed algebra - the mathematical description of course.

This is similar to the property revealed in Fig. 8.10 with the rotating of the wind generator propellers cycling from Chaos to Order; and also similar to passing by a fruit orchard, rows of chairs in an auditorium or the tombstones in a graveyard where one's line of sight is alternatingly blocked and alternatingly open to infinity in similitude also to wave particle duality again in terms of the rotations inherent to the cyclicity of the LCU backcloth tessellating space antispace - talking about nodes in the hyperspherical structure inherent in the HD components 'behind' our 3-space virtual reality. We assume that all matter cyclically emerges from spacetime. In order to perform our experiment, we need to 'destructively-constructively' interfere with this process. In the model being developed this requires finding a cyclical beat-frequency to the creation and annihilation process of spacetime and matter.

In summary, we have the 3-level tiered Sagnac Effect resonance hierarchy of electrons nucleons and spacetime. The counter-propagating properties of the Sagnac Effect that violates special relativity in the small-scale will most likely be relevant to this process. For the standing-wave oscillator, the gap between R_1 & R_2 (Fig. 8.13) in the beat frequency of spacetime we take our 'little laser blaster' starting at the R_1 bandwidth, when we reach the right point we will get a reflected blip, which will be our first new spectral line in hydrogen.

Some experimental evidence has been found to support this view showing the possibility that this is the same property that the interaction of these extended structures in space involve real physical vacuum couplings by resonance with the subquantum Dirac ether. Because of photon mass the CSI model, any causal description implies that for photons carrying energy and momentum one must add to the restoring force of the harmonic oscillator an additional radiation (decelerating)

resistance derived from the em (force) field of the emitted photon by the action-equal-reaction law.

The corresponding transition time corresponds to the time required to travel one full orbit around the nucleus. Individual photons are extended spacetime structures containing two opposite point-like charges rotating at a velocity near c , at the opposite sides of a rotating diameter with a mass, $m = 10^{-65}$ g and with an internal oscillation $E = m^2 = h\nu$. Thus a new causal description implies the addition of a new component to the Coulomb force acting randomly and may be related to quantum fluctuations. We believe this new relationship has some significance for our model of vacuum C-QED blackbody absorption/emission equilibrium.

The purpose of this simple experiment is to empirically demonstrate the existence of LSXD utilizing a new model of TBS in the hydrogen atom until now hidden behind the veil of the uncertainty principle. If for the sake of illustration, we arbitrarily assume the s orbital of a hydrogen atom has a volume of 10 and the p orbital a volume of 20, to discover TBS we will investigate the possibility of heretofore unknown volume possibilities arising from cyclical fluctuations in large XD Calabi-Yau mirror symmetry dynamics. This is in addition to the Vigier TBS model. As in the perspective of rows of seats in an auditorium, rows of trees in an orchard or rows of headstones in a cemetery, from certain positions the line of sight is open to infinity or block. This is the assumption we make about the continuous-state cyclicity of HD space. Then if the theory has a basis in physical reality and we are able to measure it propose that at certain nodes in the cycle, we would discover cavity volumes of say 12, 14, and 16. We propose the possibility of three XD cavity modes like ‘phase locked loops’ depending the cycle position - maximal, intermediate and minimal.

Relation Between Power Loss & Hysteresis Loop Area

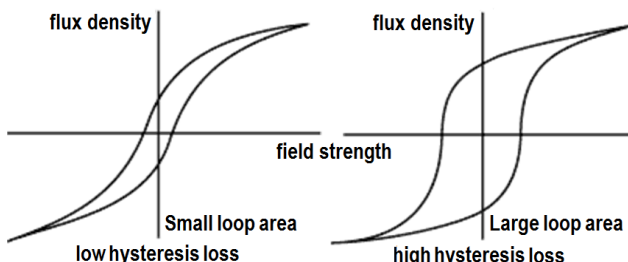


Fig. 8.32. We model our spacetime MOU QED cavity as a hysteresis loop of UFM charge. The cavity opens and closes; timing is crucial.

The lag of a magnetic material called Magnetic Hysteresis, relates to the magnetization properties of a material by which it first becomes magnetized and then de-magnetized. The magnetic flux generated by an electromagnetic coil is the amount of magnetic field force produced within a given area, called Flux Density. Using symbol B , the unit of flux density is the Tesla, T. Also the Magnetic Strength, H of an electromagnet depends on the number of turns of the coil around the core, and the current flowing through the core. The relative permeability, μ_r is defined as the ratio of the absolute permeability μ and the permeability of free space μ_0 (vacuum) which is a constant. The relationship of flux density, B and the magnetic field strength, H can be defined by the fact that the relative permeability, μ_r is not a constant but a function of the magnetic field intensity, so that the magnetic flux density is $B = \mu H$. Then the magnetic flux density in the material will be increased by a larger factor as a result of its relative permeability for the material compared to the magnetic flux density in vacuum, $\mu_0 H$ and for an air-cored coil this relationship is given as: $B = \Phi / A$ with $B / H = \mu_r$.

The magnetic flux does not completely disappear since the core material retains some of its magnetism even when the current has stopped flowing in the coil. The ability of a coil to retain some magnetism within the core after the magnetization process has stopped is called retentivity or remanence, while the amount of flux density still remaining in the core is called Residual Magnetism, B_R .

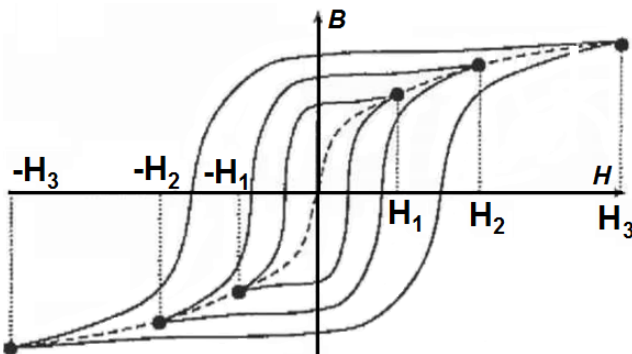


Fig. 8.33. The charge characteristics of nested Hysteresis loops can be used as a method for modeling the cyclic cavity dynamics of fermionic space-antispace parameters. Our postulate is that the Dirac polarized vacuum can demonstrate hysteresis properties.

References

- [1] Dirac P.A.M. (1930/1958) *The Principles of Quantum Mechanics*, p. 12. Oxford: Oxford Clarendon Press.
- [2] Allanach, B.C. (2014) Multiple solutions in supersymmetry and the Higgs, *Phil. Trans. Roy. Soc. Lond. A*373, 0035; arXiv:1401.8185 [hep-ph].
- [3] Becker, K., Becker, M. & Schwarz, J.H. (2007) *String Theory and M-Theory: A Modern Introduction*, Cambridge: Cambridge, Univ. Press.
- [4] Amoroso, R.L. & Rauscher, E.A. (2009) *The Holographic Anthropic Multiverse Formalizing the Complex Geometry of Reality*, London: World Scientific.
- [5] Amoroso, R.L., Kauffman, L.H. & Rowlands, P. (eds.) (2016) *Unified Field Mechanics: Natural Science Beyond the Veil of Spacetime*, Hackensack: World Scientific.
- [6] Arkani-Hamed, N., Dimopoulos, S., & Dvali, G. (1998) The hierarchy problem and new dimensions at a millimeter, *Physics Letters B*, 429(3), 263-272.
- [7] Randall, L., & Sundrum, R. (1999) Large mass hierarchy from a small extra dimension, *Physical Review Letters*, 83(17), 3370.
- [8] Cohen, A.G. & Kaplan, D.B. (1999) Solving the hierarchy problem with noncompact extra dimensions, *Physics Letters B*, 470(1), 52-58.
- [9] Amoroso, R.L. (2009) (ed.) *The Complementarity of Mind and Body: Realizing the Dream of Descartes*, Einstein and Eccles, New York: Nova Science Publishers.
- [10] Rauscher, E.A., & Amoroso, R.L. (2011) *Orbiting the Moons of Pluto: Complex Solutions to the Einstein, Maxwell, Schrödinger, and Dirac Equations* (Vol. 45) London: World Scientific.
- [11] Amoroso, R.L. (2010) Simple resonance hierarchy for surmounting quantum uncertainty, in R.L. Amoroso et al. (eds.) *AIP Conf. Proceedings*, Vol. 1316, p. 185.
- [12] Amoroso, R.L. (2009) Consciousness: The philosophical foundations of noetic field theory, in R.L. Amoroso (ed.) *The Complementarity of Mind and Body: Realizing the Dream of Descartes*, Einstein and Eccles, New York: Nova Science Publishers.
- [13] Chu, M-Y.J. & Amoroso, R.L. (2008) Empirical mediation of the primary mechanism initiating protein conformation in prion propagation, in D. Dubois (ed.) *Partial Proceedings of CASYS07, IJCAS*, Vol. 22, Univ. Liege Belgium.
- [14] Amoroso, R.L. (2005) Application of double-cusp catastrophe theory to the physical evolution of qualia: Implications for paradigm shift in medicine & psychology, in G.E. Lasker & D.M. Dubois (eds) *Anticipative & Predictive Models in Systems Science*, Vol. 1, pp. 19-26, Windsor: The Intl Inst Adv Studies in Systems Research & Cybernetics.
- [15] Amoroso, R.L., & Amoroso, P.J. (2004) The fundamental limit and origin of complexity in biological systems: A new model for the origin of life, in D. Dubois (ed.) *AIP Conference Proceedings* (Vol. 718, p. 144).
- [16] Amoroso R.L. (2003) Awareness: physical cosmology of the fundamental least unit, *Noetic J*, 4:1, 1-15
- [17] Amoroso, R.L. (2003) The Fundamental Limit and Origin of Biological Systems, *Noetic J*, 4:1; 24-32.
- [18] Amoroso, R.L. (2003) The physical basis of qualia: Overcoming the 1st person 3rd person barrier, *Noetic J*, 4:3, pp. 212-230.
- [19] Amoroso, R.L. & Martin, B.E. (2002) Consciousness: ‘A thousand points of light’, The emergence of self-organization from the noumenon of the conscious universe, *The Noetic Journal*, 3:4, 289-311.

- [20] Amoroso, R.L. (2002) The physical basis of consciousness: A fundamental formalism, Part 1 Noesis, XXVI, Bucharest: Romanian Acad.
- [21] Amoroso, R.L. (2000) The parameters of temporal correspondence in a continuous-state conscious universe, in R. Bucceri & M. Saniga (eds.) Studies in the Structure of Time: From Physics to Psycho(patho)logy, Dordrecht Kluwer Academic.
- [22] Amoroso, R.L. (2000) Consciousness, a radical definition: Substance dualism solves the hard problem, in R.L. Amoroso, R. Antunes, C. Coelho, M. Farias, A. Leite, & P. Soares (eds.) Science & the Primacy of Consciousness, Orinda: Noetic Press.
- [23] Amoroso, R.L (1999) An introduction to noetic field theory: The quantization of mind, Noetic J. 2:1, pp. 28-37.
- [24] Amoroso, R.L. (1997) Consciousness a radical definition: The hard problem made easy, The Noetic Journal 1:1, pp. 19-27.
- [25] Amoroso, R. L. (1997) A brief introduction to noetic field theory: The quantization of mind, in L. Rakic, G. Kostopoulos, D. Rakovic, & D. Koruga (eds.) Brain and Consciousness, Belgrade: ECPD.
- [26] Amoroso, R.L. & Martin, B. (1995) Modeling the Heisenberg matrix: Quantum coherence & thought at the holandscape matrix and deeper complementarity, in J. King & K.H. Pribram (eds.) Scale in Conscious Experience, Mahwah: Lawrence Earlbauum.
- [27] Osoroma, D.S. (2013) A programmable cellular automata polarized Dirac vacuum, 71-80, in R.L. Amoroso et al., The Physics of Reality: Space, Time, Matter, Cosmos, 504-509, New York: World Scientific.
- [28] Amoroso, R.L. Rowlands, P & Kauffman, L.H. (2013) Exploring novel cyclic extensions of Hamilton's dual-quaternion algebra, 81-91, in R.L. Amoroso et al., The Physics of Reality: Space, Time, Matter, Cosmos, 504-509, New York: World Scientific.
- [29] Amoroso, R.L (2013) Geometrodynamics: a complementarity of newton's and Einstein's gravity 152-163, in R.L. Amoroso et al., The Physics of Reality: Space, Time, Matter, Cosmos, 504-509, New York: World Scientific.
- [30] Amoroso, R.L & Dunning-Davies, J. (2013) A scintilla of unified field mechanics revealed by a conceptual integration of new fundamental elements associated with wavepacket dispersion, 239-248, in R.L. Amoroso et al., The Physics of Reality: Space, Time, Matter, Cosmos, 504-509, New York: World Scientific.
- [31] Amoroso, R.L & Vigier, J-P (2013) Evidencing 'tight bound states' in the hydrogen atom: empirical manipulation of large-scale XD in violation of QED, 254-272, in R.L. Amoroso et al., The Physics of Reality: Space, Time, Matter, Cosmos, 504-509, New York: World Scientific.
- [32] Amoroso, R.L Kauffman, L.H. & Giandinoto, S. (2013) Universal quantum computing: 3rd gen prototyping utilizing relativistic 'trivector' r-qubit modeling surmounting uncertainty, 316-325, in R.L. Amoroso et al., The Physics of Reality: Space, Time, Matter, Cosmos, 504-509, New York: World Scientific.
- [33] Dunning-Davies, J. & Amoroso, R.L (2013) Some thoughts on redshift and modern cosmology, 358-363, in R.L. Amoroso et al., The Physics of Reality: Space, Time, Matter, Cosmos, 504-509, New York: World Scientific.
- [34] Amoroso, R.L (2013) Time? in R.L. Amoroso et al., The Physics of Reality: Space, Time, Matter, Cosmos, 504-509, New York: World Scientific.
- [35] Amoroso, R.L (2013) "Shut The Front Door!": Obviating the challenge of large-scale extra dimensions and psychophysical bridging, 510-522, in R.L. Amoroso, L.H. Kauffman & P. Rowlands (eds.) The Physics of Reality: Space, Time, Matter, Cosmos, 504-509, New York: World Scientific.

- [36] Amoroso, R.L. (2012). Through the looking glass: Discovering the cosmology of mind with implications for medicine, psychology and spirituality, in I. Fredriksson (ed.) Aspects of Consciousness: Essays on Physics, Death and the Mind, 147, McFarland.
- [37] Amoroso, R.L., & Rauscher, E.A. (2010) Empirical Protocol for Measuring Virtual Tachyon/Tardon Interactions in a Dirac Vacuum, in R.L. Amoroso et al. (eds.) AIP Conference Proceedings (Vol. 1316, p. 199).
- [38] Kafatos, M. Roy, S. & Amoroso, R.L. (2000) Scaling in cosmology & the arrow of time, in R. Buccheri, V. Di Gesu & M. Saniga, (eds.) Studies on Time, Dordrecht: Kluwer Academic.
- [39] Amoroso, R.L. (2004) The fundamental limit and origin of complexity in biological systems: A new model for the origin of life, in D.M. Dubois (ed.) Computing Anticipatory Systems, AIP Conf. Proceedings Vol. 718, pp. 144-159, Melville: American Inst. of Physics.
- [40] Amoroso, R.L. (2002) Developing the cosmology of a continuous-state universe, in R.L. Amoroso, G. Hunter, M. Kafatos & J-P Vigier (eds.) Gravitation & Cosmology: From the Hubble Radius to the Planck Scale, Dordrecht: Kluwer Academic.
- [41] Amoroso, R.L. (2005) Paradigm for a continuous-state holographic conscious multiverse, in R.L. Amoroso & B. Lehnert (eds.) Extending the Standard Model: Searching for Unity in Physics, Oakland: Noetic Press.
- [42] Amoroso, R.L. (2009) Defining a context for the cosmology of awareness, in R.L. Amoroso (ed.) The Complementarity of Mind and Body: Realizing the Dream of Descartes, Einstein and Eccles,
- [43] Amoroso, R.L. (2009) The physical origin of the principle of self-organization driving living systems, in R.L. Amoroso (ed.) The Complementarity of Mind and Body: Realizing the Dream of Descartes, Einstein and Eccles, New York: Nova Science Publishers.
- [44] Amoroso, R.L., Kauffman, L.H. & Rowlands, P. (2013) The Physics of Reality: Space, Time, Matter, Cosmos, London: World Scientific Publishers.
- [45] Amoroso, R.L. (1996) The production of Fröhlich and Bose-Einstein coherent states in *in vitro* paracrystalline oligomers using phase control laser interferometry, Bioelectrochem. & Bioenergetics, 41:1, pp. 39-42; <http://vixra.org/pdf/1305.0106v1.pdf>.
- [46] Kaku, M. (1999) Introduction to Superstrings and M-Theory. Springer Verlag.
- [47] Polchinski, J. (1998) String Theory (Vols. 1&2) Cambridge university press.
- [48] Hübsch, T. (1992) Calabi-Yau Manifolds: A Bestiary for Physicists, Singapore: World Scientific.
- [49] Bohm, D. (1963) Quantum Theory, pg. 353, Englewood Cliffs: Prentice-Hall.
- [50] Bohm, D. & Vigier, J-P (1954) Model of the causal interpretation of quantum theory in terms of a fluid with irregular fluctuations, Phys. Rev. 96:1; 208-217.
- [51] Holland, P.R. (1995) The Quantum Theory of Motion: An Account of the de Broglie-Bohm Causal Interpretation of Quantum Mechanics, Cambridge: Cambridge Univ. Press.
- [52] Cramer, J.G. (1986). The transactional interpretation of quantum mechanics, Reviews of Modern Physics, 58(3), 647.
- [53] Dirac, P.A.M. (1952) Is there an ether? Nature, 169: 172.
- [54] Petroni, N.C. & Vigier, J-P (1983) Dirac's aether in relativistic quantum mechanics, Foundations Physics, 13:2, 253-285.
- [55] Vigier, J-P (1980) De Broglie Waves on Dirac Aether: A Testable Experimental Assumption, *Lettore. al Nuovo Cimento*, 29; 467-475.
- [56] Feynman, R.P. (1986) Quantum mechanical computers, Found. Phys. 6: 507-531.
- [57] Elitzur, A.C. & Vaidman, L. (1993) Quantum mechanical interaction-free measurements. Found. Phys. 23; 987-997.

- [58] Kwiat, P., Weinfurter, H., Herzog, T., Zeilinger, A. & Kasevich, M. (1995) Interaction-free quantum measurements. *Phys. Rev. Lett.* 74, 4763-4766; Kwiat, P.G., Weinfurter, H., Herzog, T., Zeilinger, A. & Kasevich, M. (1995) Experimental realization of ‘interaction-free’ measurements, in D.M. Greenberger & A. Zelinger (eds.) *Fundamental Problems in Quantum Theory, A Conference held in Honor of Professor John A. Wheeler*, Annals of the New York Academy of Science, Vol. 755, p. 383, New York: New York Academy of Science.
- [59] du Marchie Van Voorthuysen, E.H. (1996) Realization of an interaction-free measurement of the presence of an object in a light beam, *Am. J. Phys.* 64:12; 1504-1507; or arXiv:quant-ph/9803060 v2 26.
- [60] Simon, S.H. & Platzman, P.M. (1999) Fundamental limit on “interaction free” measurements, arXiv:quant-ph/9905050v1.
- [61] Vaidman, L. (1996) Interaction-free measurements, arXiv:quant-ph/9610033v1.
- [62] Paraoanu, G.S. (2006) Interaction-free measurements with superconducting qubits, *Physical Rev. Letters* 97, (2006) 180406.
- [63] Vaidman, L. (2001) The meaning of the interaction-free measurements arXiv:quant-ph/0103081v1.
- [64] Vaidman, L. (2001) The paradoxes of the interaction-free measurements, arXiv:quant-ph/0102049v1.
- [65] Vaidman, L. (2000) Are interaction-free measurements interaction free? arXiv:quant-ph/0006077v1.
- [66] Helmer, F., Mariantoni, M., Solano, E. & Marquardt, F. (2008) Quantum Zeno effect in the quantum non-demolition detection of itinerant photons, arXiv:0712.1908v2.
- [67] Facchi, P. Lidar, D.A. & Pascazio, S. (2004) Unification of dynamical decoupling and the quantum Zeno effect, *Phys Rev A* 69, 032314; or arxiv:quant-ph/0303132.
- [68] Sudarshan, E.C.G. & Misra, B. (1977) The Zeno’s paradox in quantum theory, *J Mathematical Physics* 18:4; 756–763.
- [69] Facchi, P. & Pascazio, S. (2002) Quantum Zeno subspaces, arXiv:quant-ph/0201115v2.
- [70] Kwiat, P.G. White, A.G., Mitchell, J.R., Nairz, O., Weihs, G. Weinfurter, H. & Zeilinger, A. (1999) High-efficiency quantum interrogation measurements via the quantum Zeno effect, *Phys. Rev. Lett.* 83, 4725-4728; or arXiv:quant-ph/9909083v1.
- [71] Amoroso, R.L. (2010) (ed.) Complementarity of mind and body: Realizing the dream of Descartes. Einstein and Eccles, New York: Nova Science.
- [72] Amoroso, R.L., & DiBiase, F. (2013) Crossing the psycho-physical bridge: Elucidating the objective character of experience, *J Cons. Explor & Res.*
- [73] Allen, L. & Eberly, J.H. (1987) Optical Resonance and Two-Level Atoms, New York: Dover.
- [74] Feynman, R.P. (1965) The Feynman Lectures on Physics: Vol. 3. Reading: Addison-Wesley.
- [75] Kotigua, R.P. & Toffoli, T. (1998) Potential for computing in micromagnetics via topological conservation laws, *Physica D*, 120:1-2, pp. 139-161.
- [76] Georgiev, L.S. (2006) Topologically protected gates for quantum computation with non-Abelian anyons in the Pfaffian quantum Hall state, *Physical Review B*, 74(23), 235112.
- [77] Jiang, L., Brennen, G.K., Gorshkov, A.V., Hammerer, K., Hafezi, M., Demler, E., & Zoller, P. (2008) Anyonic interferometry and protected memories in atomic spin lattices, *Nature Physics*, 4(6), 482-488.

- [78] Saeedi, K., Simmons, S., Salvail, J.Z., Dluhy, P., Riemann, H., Abrosimov, N.V., Becker, P., Pohl, H-V, Morton, J.J.L. & Thewalt, M.L.W. (2013) Room-temperature quantum bit storage exceeding 39 minutes using ionized donors in silicon-28, *Science*, Vol. 342, No. 6160, pp. 830-833.
- [79] Benenti, G. & Strini, G. (2007) A bird's eye view of quantum computers, arXiv:quant-ph/0703105v1.
- [80] Benenti, G., Casati, G., & Strini, G. (2004-2007), Principles of quantum computation and information, Vol. I: Basic concepts; Vol. II: Basic tools and special topics, Singapore: World Scientific.
- [81] Nielsen, M.A., & Chuang, I.L. (2000) Quantum Computation and Quantum Information, Cambridge: Cambridge University Press; Lloyd, S. (1996), Universal quantum simulators, *Science* 273, 1073.
- [82] Lidar, D.A. & Wang, H. (1999) Calculating the thermal rate constant with exponential speedup on a quantum computer, *Phys. Rev. E* 59, 2429.
- [83] Moore, G.E. (1965) Cramming more components onto integrated circuits, *Electronics*, 38, N. 8, April 19.
- [84] Aspect, A. (1976) Proposed experiment to test the nonseparability of quantum mechanics, *Phys. Rev. D* 14, 1944.
- [84] Ghirardi, G.C., Rimini, A., & Weber, T. (1986) Unified dynamics for microscopic and macroscopic systems, *Phys. Rev. D* 34, 470.
- [86] Kieu, T.D. (2003) Computing the noncomputable, *Contemporary Physics* 44, 51.
- [87] Amoroso, R.L., & Vigier, J-P (2013) Evidencing 'tight bound states' in the hydrogen atom: Empirical manipulation of large-scale XD in violation of QED, in R.L. Amoroso et al. (eds.) *The Physics of Reality: Space, Time, Matter, Cosmos*, pp. 254-272, Singapore: World Scientific.
- [88] Amoroso, R.L. (2010) Simple resonance hierarchy for surmounting quantum uncertainty, in R.L. Amoroso, P. Rowlands & S. Jeffers (eds.) *AIP Conference Proceedings-American Institute of Physics*, Vol. 1316, No. 1, p. 185.
- [89] Randall, L. (2005) *Warped Passages, Unraveling the Mysteries of the Universe's Hidden Dimensions*, New York: Harper-Collins.
- [90] Amoroso, R.L. (2015) Yang-Mills Kaluza-Klein equivalence: An empirical path extending the standard model of particle physics, Address given at the International Conference on 60 Years of Yang-Mills Gauge Field Theories, 25-28 May 2015, IAS, Singapore; <http://vixra.org/abs/1511.0257>; video: https://onedrive.live.com/?authkey=%21APfM4hcl_Mcv8dk&cid=F94F1346F17EA060&id=F94F1346F17EA060%21158&parId=F94F1346F17EA060%21117&o=OneUp.
- [91] Stern, A. (1992) Matrix logic and the Mind, a probe into a unified theory of mind and matter, Amsterdam: Northern-Holland.
- [92] Stern, A. (2000) *Quantum Theoretic Machines*, New York: Elsevier Science.
- [93] Gerlach, W & Stern, O. (1922) *Das magnetische moment des silberatoms*, *Zeitschrift Physik* 9, 353-355.
- [94] Cramer, J.G. (2006) A transactional analysis of interaction-free measurements, *Foundations of Physics Letters* 19: 1; 63-73; or arXiv:quant-ph/0508102v23, 2008.
- [95] Everett, H. (1957) Relative state formulation of quantum mechanics, *Reviews of Modern Physics*, Vol 29, pp 454-462.
- [96] Holy Bible, King James Version.
- [97] Amoroso, R.L. (2013) Empirical protocols for mediating long-range coherence in biological systems, *J Consciousness Exploration & Research*, Vol. 4, No. 9, pp. 955-976.

- [98] Amoroso, R. L. (2015) Toward a pragmatic science of mind, *Quantum Biosystems*, 6(1), 99-114.
- [99] Nagel, T. (1974) What's it like to be a bat? *Philosophical Rev.*, 83, pp. 435-450.
- [100] Witten, E. (1993) Quantum background independence In string theory, arXiv:hep-th/9306122v1.
- [101] Stevens, H.H. (1989) Size of a least unit, in M. Kafatos (ed.) *Bell's Theorem, Quantum Theory and Conceptions of the Universe*, Dordrecht: Kluwer Academic.
- [102] Kowalski, M. (1999) Photon Emission from Atomic Hydrogen, *Physics Essays*, Vol.12, 312-331.
- [103] M. Kowalski (2000) The process of photon emission from atomic hydrogen, in Amoroso, R.L. et al. (eds.) *From the Hubble Radius to the Planck Scale*, Dordrecht: Kluwer Academic, pp. 207-220.
- [104] Go to: www.Images.Google.com and type in “cootie Catcher” in the search box.
- [105] Feynman, R.P. (1971) *Lectures on Gravitation*, Pasadena: California Inst. Technology.
- [106] Dubois, D.M. (2001) Theory of incursive synchronization and application to the anticipation of delayed linear and nonlinear systems, in D.M. Dubois (ed.) *Computing Anticipatory Systems: CASYS 2001*, 5th Intl Conf., Am Inst of Physics: AIP Conf. Proceedings 627, pp. 182-195.
- [107] Antippa, A.F. & Dubois, D.M. (2008) The synchronous hyperincursive discrete harmonic oscillator, in D. Dubois (ed.) proceedings of CASYS07, preprint.
- [108] Dubois, D.M. (2008) The quantum potential and pulsating wave packet in the harmonic oscillator, in D. Dubois (ed.) proceedings of CASYS07, preprint.
- [109] Antippa, A.F. & Dubois, D.M. (2004) Anticipation, orbital stability and energy conservation in discrete harmonic oscillators, in D.M. Dubois (ed.) *Computing Anticipatory Systems*, AIP Conf. Proceedings Vol. 718, pp.3-44, Melville: American Inst. of Physics.
- [110] Dubois, D. (2016) Hyperincursive algorithms of classical harmonic oscillator applied to quantum harmonic oscillator separable into incursive oscillators, in R.L. amoroso, L.H. Kauffman, & p. Rowlands (eds.) *Unified Field Mechanics: Natural Science Beyond the Veil of Spacetime*, Hackensack: World Scientific.
- [111] Cramer, J.G. (2005) The quantum handshake: A review of the transactional interpretation of quantum mechanics, Time-Symmetry in Quantum Mechanics Conference, Sydney 23 July 2005.
- [112] Rowlands, P. (2007) *Zero to Infinity: The Foundations of Physics*. Singapore: World Scientific.
- [113] Shipman, B. A. (2002) On the fixed-point sets of torus actions on flag manifolds. *Journal of Algebra and Its Applications*, 1(03), 255-265.
- [114] Shipman, B. A. (1997). On the geometry of certain isospectral sets in the full Kostant-Toda lattice. *pacific journal of mathematics*, 181(1), 159-185.
- [115] Shipman, B. A. (2000) The geometry of the full Kostant-Toda lattice of sl (4, C). *Journal of Geometry and Physics*, 33(3), 295-325.
- [116] Child, M.S. (1991) *Semiclassical Mechanics with Molecular Applications* Oxford: Clarendon Press.
- [117] Spigler, R. & Vianello, M (1998) A Survey on the Liouville-Green (WKB) approximation for linear difference equations of the second order, in S. Elaydi, I. Györi, & G.E. Ladas (eds.) *Advances in Difference Equations: Proceedings of the 2nd Intl. Conf. on Difference Equations*: Veszprém, Hungary, August 7–11, 1995, p. 567, CRC Press.

- [118] Dasgupta, S., Papadimitriou, C.H. & Vazirani, U.V (2008) Algorithms, McGraw-Hill, New York.
- [119] Rosenbaum, D. & Perkowski, M. (2010) Superposed quantum state initialization using disjoint prime implicants (SQUID), <http://www.davidjrosenbaum.net/SQUID.pdf>.
- [120] Schulman, L.J. & Vazirani, M. (1999) Molecular scale heat engines and scalable quantum computation, STOC, ACM.
- [121] Petta, J.R., Johnson, A.C., Taylor, J.M., Laird, E.A., Yacoby, A., Lukin, M.D., Marcus, C.M., Hanson, M.P. & Gossard, A.C. (2005) Coherent manipulation of coupled electron spins in semiconductor quantum dots, *Science*, 309, 2180-2184.
- [122] Okamoto, H., Gourgout, A., Chang, C-Y, Onomitsu, K., Mahboob, I., Chang, Y. & Yamaguchi, H. (2013) Coherent phonon manipulation in coupled mechanical resonators, *Nature Physics*, 9, 480-484.
- [123] Bub, J. (1999) Interpreting the quantum world, revised ed., Cambridge: Cambridge University Press.
- [124] Holevo, A. (2011) Probabilistic and Statistical Aspects of Quantum Theory (2nd English ed.) *Pisa: Edizioni della Normale*.
- [125] Zurek, W.H. & Wootters, W.K. (1982) A single quantum cannot be cloned, *Nature* Vol. 299 , 802.
- [126] Dieks, D. (1982) Communication by EPR devices, *Phys. Letters A* 92 (6): 271-272.
- [127] Herbert, N. (1982) FLASH- A superluminal communicator based upon a new kind of quantum measurement, *Foundations of Physics*, Vol. 12. No. 12.
- [128] Lamas-Linares, A., Simon, C., Howell, J.C. & Bouwmeester, D. (2005) Experimental quantum cloning of single photons, arXiv:quant-ph/0205149.
- [129] Barnum, H., Caves, C.M., Fuchs, C.A., Jozsa, R. & Schumacher, B. (1996) Noncommuting mixed states cannot be broadcast, arXiv:quant-ph/9511010v1.
- [130] Chiribella, G., Yang, Y. & Yao, A.C-C (2013) Reliable quantum replication at the Heisenberg limit, arXiv:quant-ph/1304.2910v1.
- [131] Amoroso, R.L., & Vigier, J-P (2002) The origin of cosmological redshift and CMBR as absorption/emission equilibrium in cavity-QED blackbody dynamics of the Dirac vacuum, in R.L. Amoroso, Hunter, G., Kafatos, M. & Vigier, J-P (eds.) *Gravitation & Cosmology: From the Hubble Radius to the Planck Scale*.
- [132] Chantler, C.T. (2004) Discrepancies in quantum electro-dynamics, *Radiation Physics and Chemistry*, 71(3), 611-617.
- [133] Chantler, C.T. et al. (2012) Testing three-body quantum electrodynamics with trapped Ti²⁰ ions: evidence for a Z-dependent divergence between experiment and calculation, *PRL* 109, 153001.
- [134] Dragic', A. Maric', Z. Vigier, J-P (2000) New quantum mechanical tight bound states and 'cold fusion' experiments, *Physics Letters A*: 265;163-167.
- [135] Vigier, J-P (1993) New Hydrogen (Deuterium) Bohr Orbits, *Proceedings ICCF4*, Hawaii, Vol 4, p. 7.
- [136] Bhabha, H.J., & Corben, H.C. (1941) General classical theory of spinning particles in a Maxwell field, *Proceedings of the Royal Society of London Series A: Mathematical, Physical & Engineering Sciences*, 178:974, 273-314.
- [137] Barut, A.O. (1980) *Surv. High Energy Phys.* 1, 113.
- [138] Rowlands, P. (2015) How many dimensions are there? in R.L. Amoroso et al. (eds.) *Unified Field Mechanics: Natural Science Beyond the Veil of Spacetime*, *Proceedings of the IX Symposium Honoring Noted French Mathematical Physicist Jean-Pierre Vigier* (p. 46) Singapore: World Scientific.

- [139] Rowlands, P. (2013) Space and antispace, in R.L. Amoroso, P. Rowlands & L.H. Kauffman (eds.) Physics of Reality: Space, Time, Matter, Cosmos, London: World Sci.
- [140] Abramowitz, M. & Stegun, I.A. (eds.) (1983) Handbook of Mathematical Functions with Formulas, Graphs, and Mathematical Tables. Applied Mathematics Series 55, National Bureau of Standards; New York: Dover.
- [141] Gurarie, D. (2013) Bessel zoo and harmonic oscillator, <http://www.cwru.edu/artsci/math/gurarie/classes/445/lecture/bessel.pdf>.
- [142] Dubois, D.M. (2016) Hyperincursive algorithms of classical harmonic oscillator applied to quantum harmonic oscillator separable into incursive oscillators, in R.L. Amoroso, L.H. Kauffman & P.Rowlands (eds.) Unified Field Mechanics: Natural Science Beyond the Veil of Spacetime, London: World Scientific.
- [143] Scheid F. (1986) Theory and Problems of Numerical Analysis. McGraw-Hill.
- [144] Riffey, D.M. (2013) Lecture notes, http://www.physics.usu.edu/riffe/3750/lecture_notes.htm.
- [145] Bacon, D. (2006) CSE 599d - Quantum computing, the no-cloning theorem, classical teleportation and quantum teleportation, superdense coding, <http://courses.cs.washington.edu/courses/cse599d/06wi/lecturenotes4.pdf>

Chapter 9

Topological Quantum Field Theory

Among the dozens of theoretical elements and substrates proposed for Universal Quantum Computing (UQC), Topological Quantum Computing (TQC) is considered a leading contender. This is primarily because of the putative utility of fractional quantum Hall effect superconductors on 2D quasiparticles defined as non-Abelian anyons, whose world lines cross forming topological braids of quantum states which for all practical purposes are securely isolated from the environment and do not decohere. TQC is highlighted in this volume because many of its topological parameters are like a ‘shadow’ or lower dimensional (LD) ‘toy model’ of the higher dimensional (HD) Unified Field Mechanical QC model introduced in this monograph. However, the anyon TQC must operate at cryogenic temperatures, whereas our UFM model is designed to be tabletop and operate at room temperature. Topological Quantum Field Theory (TQFT) is quantum field theory based on topological invariants, which is a property of topological space invariant under homeomorphisms. Topological invariants are distinctly different from the unitary operators generally used in most other types of QC models under study. All known topological field theories are either the Schwarz-type TQFTs or the Witten-type TQFTs, which are sometimes referred to as cohomological field theories. A TQC précis is given as foundation for coming discussion.

9.1 Topological Quantum Field Theory (TQFT)

For a Topological Quantum Field Theory (TQFT), whenever a space, X contains topological invariants, every space homeomorphic to X also possesses that property. In a TFT, the correlation functions do not depend on the metric of spacetime. This means that the theory is not sensitive to changes in the shape of spacetime; if the spacetime warps or

contracts, the correlation functions do not change. Consequently, they are topological invariants. TFTs are trivial for the flat Minkowski spacetimes generally used in particle physics because they can be contracted to a point, and thus only able to compute trivial topological invariants. Usually then, TQFTs are applied to curved spacetimes like Riemann manifolds. The simplest concept allowing quantum field theory to be applied to topology is the functional:

$$S = \int_M A \wedge dA, \quad (9.1)$$

where A is a 1-form on a 3D compact manifold M , which is invariant with respect to gauge transformations, $A \rightarrow A + d\lambda$ [1].

TFTs have generally been defined on a spacetime of $D < 5$. Few higher-dimensional (HD) theories exist, and those that do are not well understood. This catches us on the ‘horns of a dilemma’ because we are sallying forth with a sortie of nomenclature we deem essential, not only for an HD TFT, but also one of a totally new kind incorporating ‘ontological-phase’ properties perceived to enable by careful definition, a new class of ontological moves inherent in the action of UFM brane topology (Chap. 12). Witten [2,3] and Atiyah [4] are said to be the creators of TQFT. Following Ivancevic, “*The ‘driving engine’ of quantum field theory is the Feynman path integral.*” Thus if one considers a set of fields, $\{\phi_i\}$ on a Riemannian n -manifold, M for metric, $g_{\mu\nu}$ with real functions of these fields, $S[\phi_i]$ which are the theories action. Including also a set of operators, $O_\alpha(\phi_i)$ with the same set of indices α , which are arbitrary functions of the fields, $\{\phi_i\}$ [5]; then the vacuum expectation value of the product of the operators is defined as the Feynman path integral [6]:

$$\langle O_{\alpha 1} O_{\alpha 2} \dots O_{\alpha p} \rangle = \int D[\phi_i] O_{\alpha 1}(\phi_i) O_{\alpha 2}(\phi_i) \dots O_{\alpha p}(\phi_i) \exp(-S)[\phi_i]. \quad (9.1)$$

A QFT is considered topological if it contains the property:

$$\frac{\delta}{\delta g_{\mu\nu}} \langle O_{\alpha 1} O_{\alpha 2} \dots O_{\alpha p} \rangle = 0, \quad (9.2)$$

such that if the vacuum expectation value of the chosen operators remains invariant under changes of the metric, $g_{\mu\nu}$ on M , the operators $O_\alpha(\phi_i)$ are observables [5]. There are two types of TQFTs satisfying condition (9.2), 1) The Schwarz-type and 2) The Witten-type theories.

9.2 Schwarz-Type Topological Field Theories

In Schwarz type theories, such as Chern-Simons or BF-theory (Background Field), the action is explicitly independent of the metric and correlation functions as computed by the path integral are considered independent of the metric. Background independence simply put, refers to a theory defined without a metric or coordinate system determining the shape of spacetime or values of fields within it [7]. Since string theory is currently all about quantum gravity, believed to be background-independent, thus the popularity of TQFT. For metric independence, parameters are calculated as the result of dynamical equations, from first principles rather than the structure of the metric determining what form they should take.

In Schwarz type theories, if both the action, S and operators, O_α are metric independent; this is the Schwarz and Chern-Simons type TQFTs where one must first construct an action independent of the metric, $g_{\mu\nu}$. Chern-Simons TQFTs are further differentiated in that invariants related to observables, $O_\alpha(\phi_i)$ are polynomial knot and link invariants like the Jones polynomial and its generalizations.

9.3 Witten-Type Topological Field Theories

In Witten-type TQFTs like the Donaldson or, Gromov-Witten theories, metric independence is subtler. In Witten theories, an initial metric must be chosen, but there are extra structures that allows one to compute some quantities that are metric independent. This is the second case where (9.2) is guaranteed by Witten-type TQFTs with a symmetry whose infinitesimal form, δ satisfies:

$$\delta O_\alpha(\phi_i) = 0, \quad T_{\mu\nu}(\phi_i) = \delta G_{\mu\nu}(\phi_i), \quad (9.3)$$

where, $T_{\mu\nu}(\phi_i)$ is the energy momentum tensor for the theory

$$T_{\mu\nu}(\phi_i) = \frac{\delta}{\delta g^{\mu\nu}} S[\phi_i], \quad (9.4)$$

with $G_{\mu\nu}(\phi_i)$ a tensor [4]. These second type TQFTs are called cohomological Witten type theories and are discussed in detail by Witten and a series of lectures by Cordes in [8,9].

9.4 Dodecahedral AdS⁵/CFT Duality

Another postulated approach to TQFT is the AdS⁵/CFT duality, which is believed to provide a full, non-perturbative definition of string theory in spacetimes with anti-de Sitter asymptotes. If developed, AdS⁵ / CFT duality could describe a superselection sector of the putative background-independent theories. The theory would remain restricted to anti-de Sitter space asymptotes, which some suggest disagrees with the current observations of our universe. But a careful examination of the satellite data reveals this interpretation is not yet completely valid; and when the Planck satellite is reset to different wavelengths in the future, observation is likely to support a ‘dodecahedral wrap-around’ cosmology in alignment with an AdS⁵/CFT duality TQFT [10,11]. It is interesting to note that, in our attempt to integrate Quantum Information Processing (QIP) with cosmology, we had already proposed that AdS⁵ dodecahedral wrap-around cosmology is compatible with parameters of our UFM multiverse cosmology [12-14].

The AdS/CFT correspondence is a duality relating quantum field theory (QFT) and gravity. More precisely, the correspondence relates the quantum physics of strongly correlated many-body systems to the classical dynamics of gravity in one XD. This duality is also referred to as the holographic duality or the gauge/gravity correspondence. In its original formulation [15-17], the correspondence related a 4D Conformal Field Theory (CFT) to the geometry of an anti-de Sitter (AdS) space in 5D.

9.5 Chern-Simons Theory with Knots and Links

TQFTs provide powerful tools for studying geometric topology in Low Dimensions (LD). 3D Chern-Simons theory is a Schwarz-type TFT that provides a natural framework for implementing knots and links. In this

section we review some of the operations used in doing computation with knot theory and links [18,19].

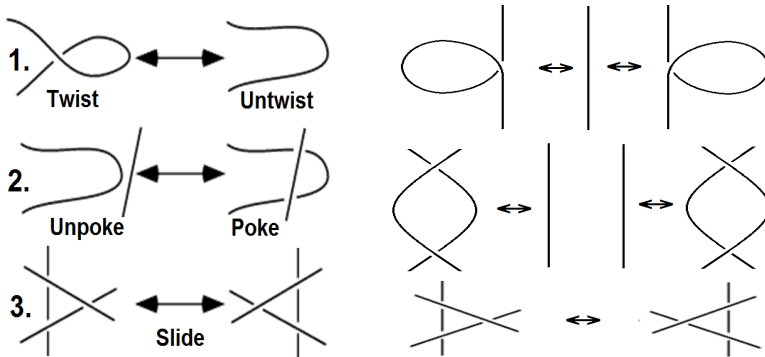


Fig. 9.1. Two renditions of the three types of Reidemeister moves.

Following Kauffman to develop notation, if one traverses a component R going under (U) x , over (O) y and then under z , one can then write, $R = UxOyUz$. Now let's see what the effect is on these codes when doing the Reidemeister moves, and thereby obtaining a language to study linking that is more sophisticated than the knot set theory. Firstly, for the Borromean Rings we have

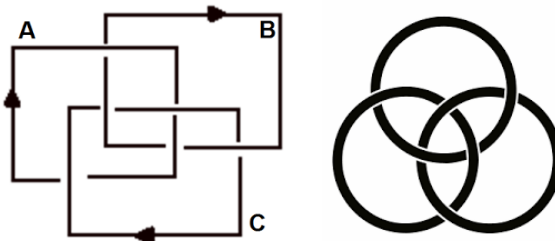


Fig. 9.2. Two graphic descriptions of Borromean ring crossings.

$$\begin{aligned} A &= OBUCOBUC \\ B &= OCUAOCUA \\ C &= OAUBOAUB. \end{aligned} \tag{9.5}$$

With the repetitions separated by symbol strings we can look at the effects on these symbol sequences by the Reidemeister moves [20].

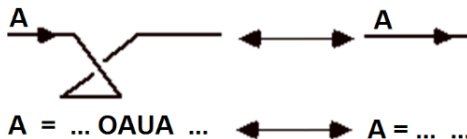


Fig. 9.3. Reidemeister move Type-I.

In the case of the first Reidemeister move, we see that we can, in the string corresponding to a label A, insert or remove an occurrence of OUAU or UAOA [20].

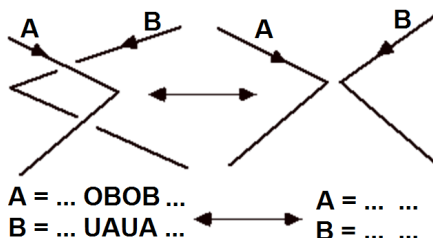


Fig. 9.4. Reidemeister move Type-II.

In the case of Reidemeister move II, notice we can still cancel consecutive occurrences of a symbol from a string, but that we need two overs in one string matched by two unders in the other as in Fig. 9.5.

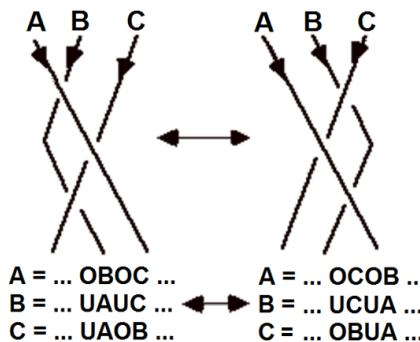


Fig. 9.5. Reidemeister move Type-III.

Finally, in Reidemeister move III we see that the pattern of triangle involvement is replaced by switching the order of encounters along each line [20].

The isotopy of links allows us to classify topological invariants such as the orientation of crossings, defined as right-hand and left-hand crossings:

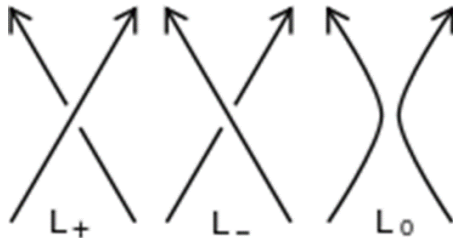


Fig. 9.6. An oriented link diagram where each component has a preferred direction indicated by the arrows.

For any crossing of the diagram (Fig. 9.6), let L_+, L_-, L_0 be the oriented link diagrams from changing the crossing orientation. The initial diagram could be either L_+ or L_- , depending on the chosen crossing configuration. Then the Alexander–Conway polynomial, $C(z)$, is recursively defined by the rule:

$$C(L_+) = C(L_-) + (L_0) \quad (9.6)$$

The following are the Conway's skein relations:

$$\nabla(O) = 1, \quad (9.7)$$

where O is any diagram of the unknot, and

$$\nabla(L_+) - \nabla(L_-) = z\nabla(L_0). \quad (9.8)$$

which relates to the standard Alexander polynomial by $\Delta_L(t^2) = \nabla_L(t - t^{-1})$. Where in this case ∇_L must be normalized by the multiplication of $\pm t^{n/2}$ in order to satisfy the skein relation $\Delta(L_+) - \Delta(L_-) = (t^{1/2} - t^{-1/2})\Delta(L_0)$ [21].

It is impossible to untie a trefoil knot by any sequence of Reidemeister moves, but a skein relation can untie a trefoil.

9.6 The Alexander Polynomial Skein Relation

The Alexander-Conway polynomial is defined in terms of links, consisting of one or more entangled knots. For a skein relation, the polynomial does not change under the three Reidemeister moves. Next we calculate the Alexander polynomial of the cinquefoil knot with crossing number 5.



Fig. 9.7. The cinquefoil knot with crossing number 5.

This alternating knot has five crossings in its minimal diagram. At each stage a relationship involving a more complex link and two simpler diagrams is exhibited. Note that the more complex link is on the right in each step below except the last. For convenience, let $A = x^{-1/2} - x^{1/2}$.

To begin, we create two new diagrams by patching one of the cinquefoil's crossings (dashed circle) so that

$$P\left(\text{cinquefoil}\right) = A \times P\left(\text{trefoil}\right) + P\left(\text{two unknots with four crossings}\right)$$

Fig. 9.8. Two new diagrams by patching one of the cinquefoil's crossings (dashed circle).

The first diagram is a trefoil; the second is two unknots with four crossings. Patching the latter

$$P\left(\text{cinquefoil}\right) = A \times P\left(\text{trefoil}\right) + P\left(\text{two unknots with four crossings}\right)$$

Fig. 9.9. A trefoil and two unknots with four crossings.

gives, again, a trefoil, and two unknots with two crossings (the Hopf link [22]). Patching the trefoil

$$P\left(\text{Trefoil}\right) = A \times P\left(\text{Trefoil}\right) + P\left(\text{Unknot}\right)$$

Fig. 9.10. Patching the trefoil gives the unknot.

gives the unknot and, again, the Hopf link. Patching the Hopf link

$$P\left(\text{Hopf Link}\right) = A \times P\left(\text{Hopf Link}\right) + P\left(\text{Unlink and Unknot}\right)$$

Fig. 9.11. Patching the Hopf link gives an unlink and unknot.

gives a link with 0 crossings (unlink) and an unknot. The unlink takes a bit of sneakiness:

$$P\left(\text{Unlink}\right) = A \times P\left(\text{Unlink}\right) + P\left(\text{Unknot}\right)$$

Fig. 9.12. Zero crossing unknots.

This is sufficient relations to compute the polynomials of all links we've shown [21].

9.7. The Jones Polynomial and Trefoil Knot Crossings

Since the Alexander-Conway polynomial is a knot invariant, the trefoil is not equivalent to the unknot, and is in actuality knotted. There are right and left-handed trefoil knots, which are mirror images of each other and are not equivalent (not amphichiral). An oriented knot that is equivalent to its mirror image is an amphichiral knot [23]. All prime alternating knots with an even crossing number are amphichiral knots. But for the

Alexander-Conway polynomial each type of trefoil will be the same, as seen by computing the mirror image.

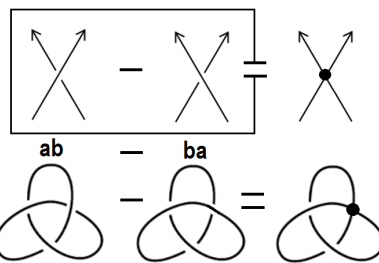


Fig. 9.13. Reducing a crossover link to a knot.

The Jones polynomial is able to distinguish between the left and right-handed trefoil knots [18] and is characterized by the fact that it takes the value 1 on any diagram of the unknot and satisfies the skein relation:

$$(t^{1/2} - t^{-1/2})V(L_0) = t^{-1}V(L_+) - tV(L_-) \quad (9.9)$$

where L_+ , L_- , L_0 are three identical oriented link diagrams except in one small region where they differ by the crossing changes or smoothing shown in the Fig. 9.14:

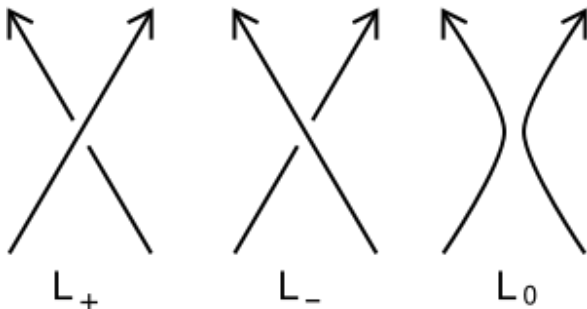


Fig. 9.14. Three oriented link diagrams.

For a knot K , the Jones polynomial of its mirror image is given by substitution of t^1 for t in $V(K)$. Therefore, an amphichiral knot, a knot equivalent to its mirror image, has palindromic entries in its Jones polynomial.

For an oriented link diagram (Fig. 9.15), each component has a preferred direction as shown by the arrow. For a given crossing indicated by, L_+ , L_- the resultants, L_0 and \mathbb{R}^3 change the diagram as indicated in the figure:

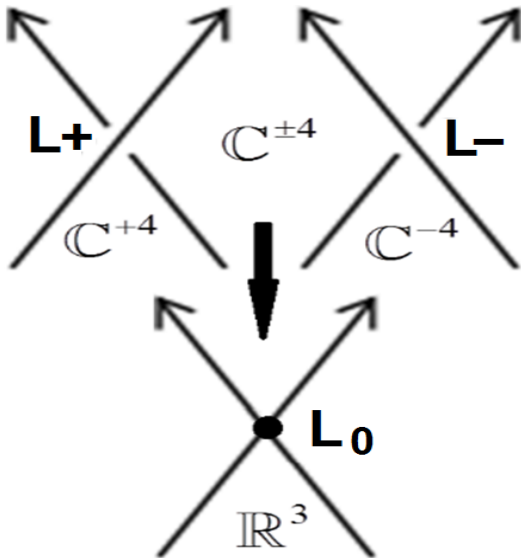


Fig. 9.15. How oriented left-right (over-strand, under-strand) crossover links, L^+ , L^- as proposed braid elements in the HD complex, $C^{\pm 4}$ brane world become a knotted shadow when projected onto Euclidean space, \mathbb{R}^3 .

A knot projected onto a plane casts a shadow. A small change in the angle of projection shows if it is one-to-one except at the crossings, where a ‘shadow’ of the knot crosses itself once transversely [23]. Analogously, knotted surfaces in 4-space can be related to immersed surfaces in 3-space.

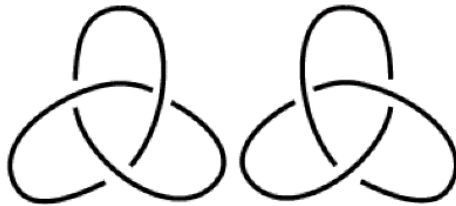


Fig. 9.16. Left and right handed trefoil knots are mirror images of each other.

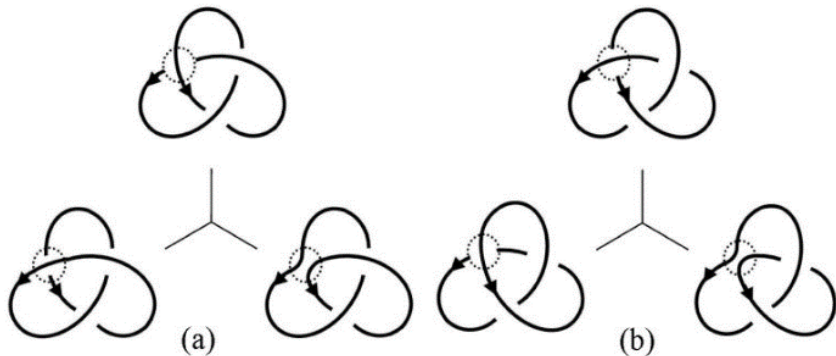


Fig. 9.17. Reduction scheme for computing the Jones polynomial from mirror trefoils.

Figure 9.17 is a reduction scheme for computing the Jones polynomial. Top diagrams: (a) left-handed and (b) right-handed trefoil knots. The bottom diagrams are obtained by switching an over-crossing (pictured in the dashed circle in top diagrams) into an under-crossing and a non-crossing of parallel strands. By using this reduction scheme recursively, any complex knot or link can be reduced to simpler configurations.

A knot in 3D can be untied when placed in a 4D space by changing crossings. If one strand is behind another, it is lifted into 4D with no barrier, then slid forward and dropped back to the front. Analogies for the plane would be lifting a string up off the surface, or removing a dot from inside a circle. In 4D, any non-intersecting closed loop of a 1D string is equivalent to an unknot. A loop is first pushed into a 3D subspace.

Since a knot can be considered topologically a 1D sphere, the next generalization is to consider a 2D sphere embedded in a 4-ball. Such an embedding is unknotted if there is a homeomorphism of the 4-sphere onto itself taking the 2-sphere to a standard round 2-sphere.

HD knots can also be added but there are some differences. While you cannot form the unknot in 3D by adding two non-trivial knots, you can form an unknot in HD, at least when one considers smooth knots in codimension of at least 3.

9.8 Cobordism in TQFT - Atiyah's Definitions

Typically, a cobordism is an n -manifold that connects together two $n-1$ D manifolds. Generally, we think of a cobordism as having a ‘direction’ so that some of its boundary components can be viewed as a ‘source’ and the others viewed as the ‘target’ of the cobordism.

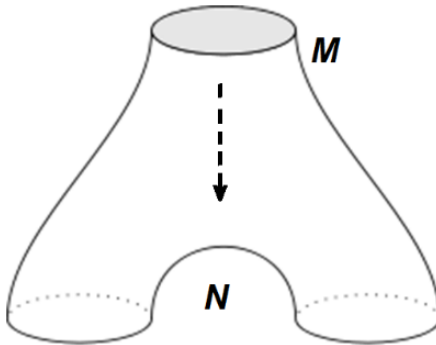


Fig. 9.18. A cobordism between a single circle (top) and a pair of disjoint circles (bottom), often called a ‘pants’ diagram.

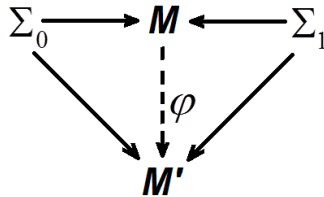
If M consists of a circle, and N two circles, M and N together make up the boundary of a pair of pants, W (Fig. 9.18). Thus, the pants is a cobordism between M and N . An advantage of TQFT is that fields are defined locally; meaning that invariants are computed by breaking manifolds into simpler pieces and computing on the pieces, often done by building up a closed n -manifold by gluing together simpler n -manifolds along their $n-1$ D boundaries. By definition, manifolds used to build up more complicated manifolds by gluing are called ‘cobordisms’ [24].

Here are three of Atiyah’s Definition of Cobordisms [25].

§1. Let $[\Sigma_0]$ and Σ_1 be closed $(n-1)$ -manifolds. A cobordism between Σ_0 and Σ_1 is an nD manifold with boundary $\partial M = \Sigma_0 \sqcup \Sigma_1$.

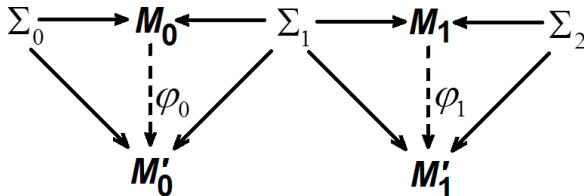
§2. Let Σ_0 and Σ_1 be closed oriented $(n-1)$ -manifolds. An oriented cobordism, M from Σ_0 to Σ_1 is a compact oriented manifold with a map $\Sigma_0 \rightarrow M$ taking Σ_0 diffeomorphically onto the ‘in-boundary’ of M and a map $\Sigma_1 \rightarrow M$ taking Σ_1 diffeomorphically onto the ‘out-boundary’ of M .

For example, the manifolds above can be regarded as an oriented cobordism once an orientation is chosen. When diagraming oriented cobordisms, the cobordism always goes from top to bottom so that the boundary components at the top form the in-boundary, and the ones near the bottom form the out-boundary [22].

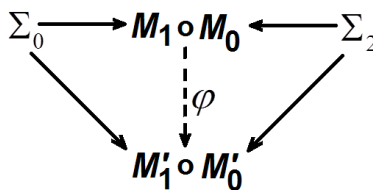


§3. Two cobordisms $\Sigma_0 \rightarrow M \leftarrow \Sigma_1$ and $\Sigma_0 \rightarrow M_0 \leftarrow \Sigma_1$ are equivalent if there exists an orientation-preserving diffeomorphism $\varphi: M \rightarrow M_0$ making the diagram above commute.

Suppose we are given composable cobordisms M_0 and M_1 which are equivalent (relative to the boundary) to cobordisms M'_0 and M'_1 :



Then we have the composition $M_1 \circ M_0$ and the composition $M'_1 \circ M'_0$, and the maps φ_0 and φ_1 glue to give a homeomorphism $\varphi: M_1 \circ M_0 \rightarrow M'_1 \circ M'_0$ which restricts to a diffeomorphism on each of the original cobordisms:



We can use this homeomorphism to define a smooth structure on $M'_1 \circ M'_0$. Although this smooth structure may not coincide with the original, it is implied that the two structures are diffeomorphic relative to the boundary. Thus there are well-defined ways to compose equivalence classes of oriented cobordisms [22,25].

Quantum Theory suggests that the laws of nature fundamentally describe time evolution using unitary operators. But this assumption needs to be dropped in models where the topology of space can change. In these cases, all morphisms in Hilb qualify as ‘processes’, just as all morphisms in $n\text{Cob}$ qualify as spacetimes. The resolution Baez makes for this puzzle he says is simple, but unsatisfactory to most category theorists: “*I admit that the inner product is inessential in defining the category of Hilbert spaces and bounded linear operators. However, I insist that it plays a crucial role in making this category into a $*$ -category*” [26].

A $*$ -category, is a category C with a map that sends each morphism $f : X \rightarrow Y$ to a morphism $f^* : Y \rightarrow X$, satisfying

$$1_X^* = 1_X, \quad (9.10)$$

$$(fg)^* = g^* f^*, \quad (9.11)$$

and

$$f^{**} = f. \quad (9.12)$$

To make Hilb into a $*$ -category we define T^* for any bounded linear operator $T : H \rightarrow H'$ to be the adjoint operator $T^* : H' \rightarrow H$, given by

$$\langle T^* \psi, \phi \rangle = \langle \psi, T \phi \rangle. \quad (9.13)$$

This formula shows that the inner product of both H and H' are required to define the adjoint of T [26].

This loose relation between $*$ operations and time reversal becomes precise in the case of $n\text{Cob}$, where the $*$ operation is time reversal. More precisely, given an n D cobordism $M : S \rightarrow S'$, we let the adjoint cobordism $M^* : S \rightarrow S'$ be the same manifold, but with the ‘past’ and ‘future’ parts of its boundary switched, as in Fig. 9.19. It is easy to check that this makes $n\text{Cob}$ into a $*$ -category [26].

In a so-called unitary topological quantum field theory (TQFT) terminology demands that the functor $Z : n\text{Cob} \rightarrow \text{Hilb}$ preserve the

$*$ -category structure in the following sense:

$$Z(M^*) = Z(M)^*. \quad (9.14)$$

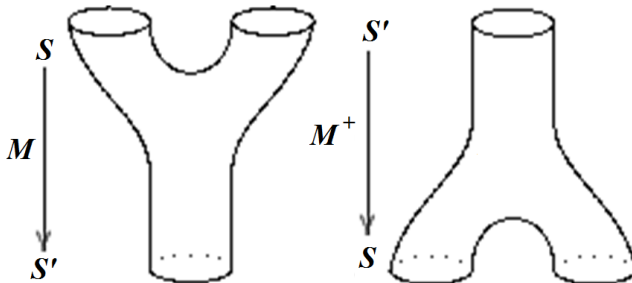


Fig. 9.19. A cobordism and its adjoint.

All the TQFTs of interest in physics have this property, and a similar property holds for conformal field theories and other quantum field theories on curved spacetime. This means that in the analogy between general relativity and quantum theory, “*the analogue of time reversal is taking the adjoint of an operator between Hilbert spaces*”. To ‘reverse’ a spacetime $M : S \rightarrow S'$ one formally switches the notions of future and past, while to ‘reverse’ a process $T : H \rightarrow H'$ we take its adjoint [26].

9.9 Ab Infinito Ad Infinitum

We have theorized that the Euclidean space of observation is not real, but merely an artifact of the observer (the best metaphor for which is the Analogy of Plato’s Cave [27]; and that in actuality the fundamental noumenon¹ is an as yet unobserved complex 12D space. It has taken a long time to formalize this philosophical posit in terms of physics; obviously

¹ Noumenon (in Kantian philosophy) a thing as it is in itself, as distinct from a thing as it is knowable by the senses through phenomenal attributes. The noumenon is a posited object or event that is known (if at all) without the use of the physical senses. The term noumenon is generally used in contrast with, or in relation to phenomenon, which refers to anything that can be apprehended by, or is an object of, the physical senses [28].

why the definition and ‘role of the observer’ has been such a conundrum to measurement theory. The most simplistic manner of looking at this conundrum of 3D matter as virtual arises from what is called the ‘shadow’ in knot theory. Not the knot itself as key element, but what this ‘chiasma’ does to the perceptual apparatus of the observer. It is the relation of the knot to the uncertainty principle; a locking mechanism shielding our view of the full reality like those chained in Plato’s analogy of the cave.

References

- [1] Schwarz, A. (2000) Topological quantum field theories, arXiv:hep-th/0011260v1.
- [2] Witten, E. (1988) Topological quantum field theory, *Com. Math. Phys.* 117(3), 353–386.
- [3] Witten, E. (1989) Quantum field theory and the Jones polynomial, *Comm. Math. Phys.* 121, 351.
- [4] Atiyah, M. (1988) Topological quantum field theories, *Pub. Math. l’IHÉS* 68, 175-186.
- [5] Ivancevic, V.G. & Ivancevic, T.T (2008) Undergraduate lecture notes in topological quantum field theory; arXiv:0810.0344v5 [math-ph].
- [6] Labastida, J.M.F. & Lozano, C. (1997) Lectures on Topological Quantum Field Theory, CERNTH/97-250; US-FT-30/97; hep-th/9709192, 1997.
- [7] Rickles, D. (2007) Who’s afraid of background independence? [http://philsci-archive.pitt.edu/4223/1/B1\(Rickles\).pdf](http://philsci-archive.pitt.edu/4223/1/B1(Rickles).pdf).
- [8] Witten, E (1991) Introduction to cohomological field theory, *Intl J Mod Phys A*, Vol. 6, No. 16, pp. 2775-2792; <https://ncatlab.org/nlab/files/WittenCQFT.pdf>.
- [9] Cordes, S., Moore, G. & Ramgoolam, S. (1996) Lectures on 2D Yang-Mills Theory, equivariant cohomology and topological field theories, arXiv:hep-th/9411210v2 26; hep-th/9411210 YCTP-P11-94.
- [10] Natsuume, M. (2015) AdS/CFT Duality user guide, arXiv:1409.3575v3 [hep-th].
- [11] Winkelnkemper, H.E (2014) A remark by Atiyah on Donaldson’s theory, AP theory and ADS/CFT duality, <http://www.math.umd.edu/~elmar/ymati3.pdf>.
- [12] Amoroso, R.L., Kauffman, L.H., & Rolands, P. (2013) *The Physics of Reality: Space, Time, Matter, Cosmos*, Hackensack: World Scientific.
- [13] Luminet, J-P, Weeks, J.R., Riazuelo, A., Lehoucq, R., & Uzan, J.P. (2003) Dodecahedral space topology as an explanation for weak wide-angle temperature correlations in the cosmic microwave background, *Nature*, 425(6958), 593-595.
- [14] Lachieze-Rey, M., & Luminet, J-P (1995) Cosmic topology, *Physics Reports*, 254(3), 135-214.
- [15] Hawking, S.W. & Page, D.N. (1983) Thermodynamics of black holes in anti-De Sitter space, *Commun. Math. Phys.* 87, 577.
- [16] Witten, E. (1998) Anti-de Sitter space, thermal phase transition, and confinement in gauge theories, *Adv. Theor. Math. Phys.* 2, 505; [arXiv:hep-th/9803131].
- [17] Balasubramanian, V. & Kraus, P. (1999) A stress tensor for Anti-de Sitter gravity, *Commun. Math. Phys.* 208, 413; [hep-th/9902121].
- [18] Lickorish, W.B. (1997) *An Introduction to Knot Theory*, Graduate Texts in Mathematics, Springer-Verlag.

- [19] Ramadevi, P. (1996) Chern-Simons theory as a theory of knots and links, www.imsc.res.in/xmlui/bitstream/handle/123456789/73/UNMTH49.pdf?sequence=1.
- [20] Kauffman, L.H. (2016) Pattern, sign and space, <http://homepages.math.uic.edu/~kauffman/MThoughts.htm>.
- [21] Morton, H.R. & Lukac, S.G. (2001) The Homfly polynomial of the decorated Hopf link, *J Knot Theory and Its Ramifications* 12:395-416; arXiv:math/0108011v1 [math.GT].
- [22] Taimanov, I.A. (2007) Topological library. Part 1: Cobordisms and their applications, Series on Knots and Everything, 39. S. Novikov (ed.) Hackensack: World Scientific.
- [23] Rolfsen, D. (1976) Knots and links (Vol. 346) American Mathematical Soc.
- [24] Dehn, M. (1914) *Die beiden Kleeblattschlingen*, *Mathematische Annalen*, 75(3), 402-413.
- [25] Allegretti, D.G.L. (2015) Notes on topological quantum field theory, <http://users.math.yale.edu/~dga4/TQFTNotes.pdf>.
- [26] Baez, J. (2004) Lessons from topological quantum field theory, <http://www.math.ucr.edu/home/baez/quantum/node2.html>.
- [27] Bloom, A.D. (1991) The republic of Plato, Basic Books.
- [28] Kant, I. (1998) Critique of Pure Reason (Trans./ Ed.) P. Guyer & A.W. Wood).

Chapter 10

Topological Quantum Computing

Topological Quantum Computation (TQC) is generally being studied with topologically protected non-Abelian anyons realized in 2D fractional quantum Hall quasiparticle states. Elementary qubits tested are being constructed by localizing Ising-model anionic excitations in films of super-cooled liquid helium on fractional quantum Hall antidots and various quantum gates where quantum information processing (QIP) in such multi-qubit register arrays are putatively implemented by the exchange or braiding of these non-Abelian anyons. While anyonic braiding promises unprecedented protection for QIP, the quantum states are currently so well ‘hidden’ that they are operationally inaccessible, raising concerns that the quantum non-cloning and quantum non-erasure theorems cannot be easily overcome if applicable in this case. The hope of TQC developers is that techniques like ‘experimentally’ detecting the signature of non-Abelian anyons in Coulomb blockaded quantum Hall islands could eventually be realized. We highlight TQC in this volume because we see it as a toy model precursor to our UFM model for UQC.

10.1 The Topological Quantum Computer (TQC)

Topological Quantum Computation (TQC) is considered a leading contender for bulk UQC because it has putatively solved the most persistent remaining problem slowing UQC implementation; that of decoherence. But the solution as profound as it is, essentially hides the anyons behind a moon on Pluto where they are inaccessible! TQCs, first proposed by Kitaev in 1997 [1], currently remain theoretical QCs employing 2D quasiparticles called anyons (intermediary fractional excitations between Fermi-Dirac spin $\frac{1}{2}$ and Einstein-Bose spin 1 statistics), have world lines that cross over one another forming topological braids in a 3D spacetime of one temporal and two spatial

dimensions. Most research has focused on gallium arsenide semiconductor lattices subjected to strong magnetic fields at temperatures < 5 mK. Quasiparticle pairs moving on the Ising lattice are annihilated to produce a unitary operation which depends only on the topology of the braid path. Virtual Abelian anyon vacuum bubbles with braiding phase, $\pm 2\pi\nu$ are a new model for detection by phase exchange statistic $\theta^* = \pi\nu$ [2].

Anyons have been physically classified as either Abelian or non-Abelian by the associative properties of their algebra. Under a particle exchange, the wavefunction of Abelian anyons acquires a phase that can be different π multiples. In contrast, for non-Abelian anyons exchanging two particles, the wavefunction operates as a non-diagonal unitary gate [3,4]. At the time of writing, experimental evidence only supports the existence of Abelian anyons in fractional quantum Hall fluids [5–7]; but in order to achieve universal TQC, non-Abelian anyons are required. To date only theoretical proposals to directly observe non-Abelian anyons in quantum Hall systems [2,8–10] and the honeycomb model exist [11–13].

10.2 Topological Quantum Computing

Topological braids form the logic gates comprising a TQC with the advantage over using other forms of trapped quantum particles in that the properties of anyonic braids are essentially free of environmental noise preventing decoherence.

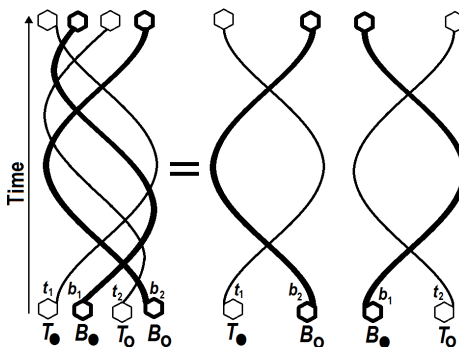


Fig. 10.1. Topological spin of the Abelian anyon. Figure redrawn from [14].

Following Teo, topological spin of the Abelian anyon TQC architecture (Fig. 10.1), $(T.)^{y1}(B.)^{b1}(T_0)^{l2}(B_0)^{b2}$ is evaluated for a 360° rotation, rendered

as $e^{2\pi i(t_2 b_1 - t_1 b_2)/k}$ for braid crossovers. Given a bipartite \bullet, \circ vertex assignment, each plaquette (hexagon), P has two stabilizing operators:

$$\hat{P}_\bullet = \prod_{v \in P} \sigma_v, \prod_{v \in P} \tau_v, \quad \hat{P}_\circ = \prod_{v \in P} \tau_v, \prod_{v \in P} \sigma_v, \quad (10.1)$$

where σ_v, τ_v are rotors at vertices, v around the plaquette and tensor products which have been suppressed. The bipartite structure ensures all plaquettes have the same number of \bullet and \circ vertices and two neighboring plaquettes share exactly one \bullet and one \circ vertex. Then (10.2) ensures mutual commutativity of the plaquette operators, which form a set of good quantum numbers referred to as \mathbb{Z}_k stabilizers or fluxes. The Hamiltonian is defined by the sum of stabilizers,

$$H = -J \sum_P (\hat{P}_\bullet + \hat{P}_\bullet^\dagger) - J \sum_P (\hat{P}_\circ + \hat{P}_\circ^\dagger) \quad (10.2)$$

Ground states are trivial flux configurations where $\hat{P}_\bullet = \hat{P}_\circ = 1$ for all stabilizers [14].

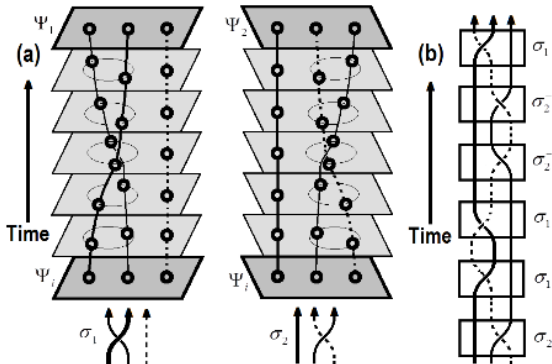


Fig. 10.2. Topological quantum computing schema of quasiparticle exchange. (a) Basic operations, σ_1 and σ_2 on three quasiparticle system. Top: Temporal evolution of the system from the initial state ψ_i to the final state $\psi_{1(2)} = \sigma_{1(2)}\psi_i$. Bottom: diagrammatic representations of the quasiparticle exchange operations. (b) Example of logic gate operations for the basic operations σ_1 and σ_2 shown in (a) and their inverses σ_1^{-1} and σ_2^{-1} . Redrawn from [15].

Notice that Hamiltonian (10.2) describes topological phase for two copies of the \mathbb{Z}_k Kitaev version of the toric code; the (10.2) model has a much richer S_3 symmetry extending the original \mathbb{Z}_2 charge-flux duality in the quantum double model generalizing Kitaev's toric code duality involving the geometric switching of vertices and plaquettes [1,8,14].

Following Muraki, the ground state of a system containing $2n$ non-Abelian quasiparticles has a $2^{n-1}D$ degenerate state space, serving as $n-1$ qubits. TQC exploits unitary transformations of a quantum state accompanying an exchange of two non-Abelian quasiparticles as a basis of quantum logic gates. The calculation depends solely on the order of the quasiparticle exchanges and not on the details of quasiparticle trajectories, lending TQC a certain imperviousness to error. By using a (2+1)D spacetime representation, one can express quasiparticle trajectories as world lines and quasiparticle exchanges as the braiding of two world lines around each other as shown in Fig. 10.2a. Two of three quasiparticles confined to a 2D plane are manipulated in a manner causing them to exchange positions by counterclockwise relative motion. Thick solid lines trace the position of quasiparticles in this spacetime representation forming quasiparticle world lines. Quantum information is encoded in braid topology. This means quantum information is not affected (topological protection) when quasiparticle trajectories undergo local perturbation. Figure 10.2b is an example of the basic logic gate operations shown in Fig. 10.2a and their inverses [15].

10.2.1 Quasiparticles in $v = 5/2$ FQH States

One of the prime candidates for physically hosting non-Abelian quasiparticles is an exotic 2D electron system (2DES), called the $v = 5/2$ FQH state [16] which emerges in a semiconductor heterostructure $< 5\text{mK}$ and high Tesla magnetic field. FQH effects are characterized by the quantization of Hall resistance occurring when the applied field B and the electron density, n take certain ratios [17]. Hall resistance R_{xy} is usually related to n and B as $R_{xy} = B/ne$, where e is the elementary charge. As a consequence of electron-electron interaction, an energy gap forms at the Fermi level for particular values of B/n , around which R_{xy} is pinned at a constant value over a finite range of n and B [18]. The energy gap also leads to the vanishing of longitudinal resistance R_{xx} [15].

Because of the energy gap that forms at particular values of B/n , the electron system tries to preserve the same B/n ratio to minimize the

interaction energy when B or n is slightly detuned. The resultant mismatch is accommodated by introducing point defects around which the local electron density is higher or lower than in the surrounding area. These point defects, which carry electric charge and behave like charged particles, are quasiparticles in FQH systems [18]. FQH quasiparticles have been shown to have a fraction of the electron charge [19,20] and are believed to be anyons [21]. Their properties, including their charge and statistics, are derived from the properties of the FQH state hosting them. The FQH states that emerge at $v = 5/2$, where $v = (h/e)n/B$, with h as Planck's constant, are believed to be non-Abelian quasiparticles [15,22].

10.2.2 Theoretical Models for the $v = 5/2$ State

The $v = 5/2$ FQH state [16,23] and its particle-hole counterpart $v = 7/2$ are the only FQH states with even-denominator v observed in a single-layer 2DES. Unlike other FQH states with odd-denominator v , the exact mechanism responsible for the energy gap formation at $v = 5/2$ has not yet been established. In the standard theory of FQH effects [18,24,25], the fermionic nature of electrons requires v to have an odd denominator. Breaking of the odd-denominator rule suggests a paired fermion state [26], [27]. Various theoretical models have been proposed and examined [22], [28-36], including those with non-Abelian and Abelian statistics.

Experiments reported thus far have neither demonstrated the non-Abelian nature of $v = 5/2$ quasiparticles nor pinned down precisely which theoretical model correctly describes the $v = 5/2$ ground state. The quasiparticle charge of $e/4$ observed in shot noise [37,38] and local compressibility [39] measurements indicates that the $v = 5/2$ state is indeed a paired state, but does not discriminate among different types of paired states which all have charge- $e/4$ quasiparticles. Notably, quasiparticle tunneling between FQH edges through a narrow constriction [40,41] has allowed the screening of different model wave functions through detailed comparison with theory. The likely candidates that emerged through these experiments so far include an undesirable Abelian wave function.

10.2.3 Spin Polarization of the $v = 5/2$ State

Most theories of topological quantum computation using the $v = 5/2$ state as a platform to manipulate non-Abelian quasiparticles [42,43] are based on the premise that the state is described by the wave function proposed by Moore and Read [22], which is considered to host non-Abelian

quasiparticles. An important feature of the Moore-Read theory is that it assumes that all the electrons have their spins, an internal degree of freedom of electrons making them behave like tiny magnets, aligned along the same direction. Numerical studies have shown that the ground state at $v = 5/2$ is spin polarized [44-46]. However, experiments reported thus far have indicated conflicting results for the spin polarization of the $v = 5/2$ state [47,48]. The addition of an in-plane magnetic field to increase the spin-splitting energy is known to weaken the $v = 5/2$ state [49,50], which hinted at an unpolarized or only partially polarized state. On the other hand, under a perpendicular magnetic field, the $v = 5/2$ state persists over a wide range of magnetic field, even up to 10T [51], suggesting full polarization. Recent optical measurements using photoluminescence [52] and inelastic light scattering [53] indicated an unpolarized state or an inhomogeneous state consisting of unpolarized or partially polarized domains, respectively. It is therefore of paramount importance to determine the spin polarization with a high level of confidence [15].

10.3 Quantum Hall Quasiparticle Anyon Braiding

Topology has been suggested as a unique method for stabilizing quantum information in anionic braids. A TQC would be capable of encoding information not in the usual $|0\rangle$ and $|1\rangle$ basis, but in configurations of different topological braids, which have some similarity to knots but with the addition of a number of threads intertwined around each other. The TQC would physically weave the braids in spacetime, allowing complex calculations to occur quickly. Utilizing braids instead of single particles represents a radical new approach to the problem of decoherence. Since decoherence is of penultimate importance in realizing bulk UQC, the possibility of error-correction is of extreme interest. Luckily, it is possible to represent quantum information redundantly; therefore, errors could be diagnosed and routinely corrected. [54-56].

Local geometry provides a redundant means of encoding topology:

Slightly denting or stretching a surface such as a torus does not change its genus, and small punctures can be easily repaired to keep the topology unchanged. Only large changes in the local geometry change the topology of the surface. Remarkably, there are states of matter for which this is more than just an analogy. A system with many microscopic degrees of freedom can have ground states whose degeneracy is determined by the topology of the system. The excitations of such a system have exotic braiding statistics, which is a topological selective interaction between them. Such a system is said to be in a topological phase [56].

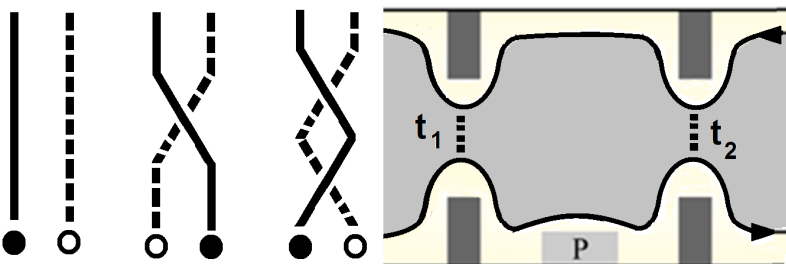


Fig. 10.3. Braiding of quantum Hall anyon quasiparticles. a) Evolution of a quantum Hall wave function by adiabatically moving one quasiparticle around another. b) experimental interferometer with a gate P that moves edge quasiparticles (arrows) around bulk quasiparticles (light gray); the total conductance through the point contacts (dark gray) is sensitive to quasiparticle statistics. Figure adapted from [54].

10.3.1 Topological Insulators

Topological insulators are recently discovered states of quantum matter which cannot be adiabatically connected to conventional insulators and semiconductors. They are characterized by a full insulating gap in the bulk and gapless edge or surface states which are protected by time-reversal symmetry. These topological materials have been theoretically predicted and experimentally observed in a variety of systems, including HgTe quantum wells, BiSb alloys, and Bi₂Te₃ and Bi₂Se₃ crystals [57].

Graphene inspired the discovery of the quantum spin-Hall effect [58], leading to the development of topological insulators. But the spin-orbit interaction is very weak in graphene so that spin-Hall effects have remained experimentally inaccessible. Study of the effect is made with very large magnetic field strengths reaching 60 Tesla which causes the formation of a zeroth Landau level, a hallmark of Dirac physics. Asymmetry in the sublattice of the zeroth Landau level causes a zero-bias peak when measuring the differential tunneling conductance on one sublattice and the occurrence of a Landau gap when measuring on the other [59,60].

An elegant approach to realize *artificial graphene* was recently taken by H.C. Manoharan and collaborators. Their experiment exploits that scanning tunneling microscopes allow for manipulating atoms or molecules adsorbed on metallic surfaces with atomic precision. This is used to arrange CO molecules into a hexagonal lattice on a Cu (111) surface which is known to have a band of surface states. The CO molecules impose a periodic potential on the surface electrons, resulting in a graphene-like bandstructure. When the lattice spacing is chosen on a nanometer scale, comparable to the Fermi wavelength of the surface electrons, this artificial-graphene

system has its Fermi energy close to the Dirac point. The lattices created in this experiment, consisting of hundreds of CO molecules, could then be probed by scanning tunneling spectroscopy [59].

The research is motivated to tune parameters in anyonic systems to find a mechanism for accessing topological braid phases currently inaccessible. One prospect for realizing topological phases could be by employing substrates with stronger spin-orbit coupling. The global nature of topological ordering makes topological phases robust and thus a promising research avenue for finding applications, but non-local properties of the topological order has left direct experimental access unresolved. Even for the simplest model of topological systems, interactions among the constituent particles add to this challenge. Our UFM experimental protocol is predicted to ameliorate this conundrum [61].

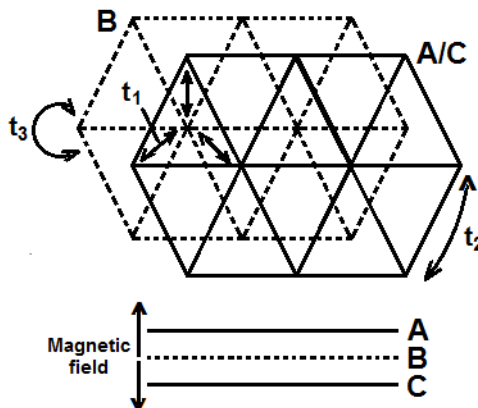


Fig. 10.4. Illustration of a 4-band non-interacting lattice model to which a 2-qubit model is mapped. The model consists of three stacked triangular lattices (A, B, and C), the middle of which (B) contains two spin/orbital states. In addition to nearest neighbor hopping (t_1) and on-site hybridization the B sublattice (t_2), electrons on the A and C sublattices experience a magnetic field that adds phase to the hopping ($t_2 e^{i\phi}$). Finally, an effective Zeeman field splits the spin/orbital states on all sublattices. Fig. redrawn from [61].

Experimental studies of topological phases have been primarily limited to indirect measurements. The nonlocal nature of topological ordering renders local probes ineffective, and when global probes, such as transport, are used, a fundamental problem in the interpretation of quantum theory itself occurs, requiring one to infer topological properties from the measurements [62] going all the way back to theoretical

generalizations by von Neuman suggesting that ‘unless special symmetry conditions occur in the Hamiltonian, three parameters must be tuned in order to reach degeneracy’ [62,63]. Nonlocal OPTFT probes are proposed.

The topological phases characterized by topological invariants, such as the first Chern number, Ch , whose discrete jumps indicate transitions between different topologically ordered phases [64,65]. For a quantum system, Ch is defined as the integral over a closed manifold S in the parameter space of the Hamiltonian as

$$Ch \equiv \frac{1}{2\pi} \oint_S \mathbf{B} \cdot d\mathbf{S}, \quad (10.3)$$

where \mathbf{B} is the Berry curvature which can be considered an effective magnetic field of points with ground state degeneracy acting as sources [61,66].

10.3.2 Quasiparticle Interferometry and Topological Protection

2D Topological phase supports anyonic quasiparticle excitations obeying neither bosonic nor fermionic statistics. These structures can carry global symmetries relating distinct anyons with similar fusion and statistical properties. Such anyonic symmetries associate topological defects or fluxes in topological phases. Since the symmetries are global and static, the defects are semiclassical objects behaving separately from conventional quantum anyons. Remarkably, even when the topological states supporting them are Abelian, they are generically non-Abelian and powerful enough for TQC [67].

Topological protection promises stable quantum gates that are able to be executed with extreme accuracy. Quasiparticle interferometry has arisen as a tool for constructing topologically protected gates [68]. 2D Topologically ordered states are exotic phases of matter that support fractional quasiparticle excitations with anyonic statistics [69-71]. Fundamental excitations in a fractional quantum Hall quasiparticle state carry fractions of an electric charge and do not obey either Bose-Einstein or Fermi-Dirac statistics. These unusual properties stem from long range entanglement of a ground state separated by an energy gap from all excitation states. Unlike ordinary phases of matter, like a superconductor, characterized by Landau order parameters and broken symmetries, topological phases can be featureless so that there are no apparent local order parameters. Their topological order (anyonic quasiparticle), does not

rely on a spontaneous symmetry breaking. However, topological phase can carry a symmetry or coexist with a symmetry breaking phase, which led to finer classes of Symmetry Protected/Enriched Topological phases (SPT/SET) [82-89]. For example, two phases with identical topological order can be separated by symmetries if there is no adiabatic path connecting the two phases without closing the bulk gap or breaking the symmetries. Fermionic topological insulators protected by time-reversal symmetry are examples [80-88]. Although these are short-range entangled states not supporting fractional excitations with anyonic statistics, the symmetry still enables a non-trivial bulk topology and anomalous boundary states [67].

In the fractional quantum Hall effect (FQHE) Hall conductance for 2D electrons determines precisely quantized plateaus at fractional values of e^2/h . This is a property of a collective state in which electrons bind magnetic flux lines making new quasiparticles, and excitations having fractional elementary charge and fractional statistics. Laughlin's explanation of the fractional quantum Hall effect introduced quasiparticles with fractional charges such as $e/3e/3$ possessing fractional statistics. If two identical quasiparticles are exchanged, the wavefunction picks up a factor $\exp(i\phi)$. In more complex quantum Hall states quasiparticle exchanges obey non-Abelian statistics (deemed essential for TQC), are represented by matrices for unitary transformations, describing quasiparticle 'braiding' which does not always commute [89].

Assuming corrections of the Moore-Read Model for $v = 5/2$'s FQHE [90] Freedman shows how to manipulate the collective state of two $e/4$ -charge anti-dots in order to switch the collective state from one carrying a trivial SU(2) charge, $|1\rangle$, to one carrying a fermionic SU(2) charge $|\epsilon\rangle$.

This is a NOT gate on the $\{|1\rangle, |\epsilon\rangle\}$, qubit which is effected by braiding an electrically charged quasiparticle carrying an additional SU(2)-charge. Read-out is accomplished by sigma-particle interferometry [66].

Understanding the $5/2$ state is relatively good; but for the experimentally observed $12/5$ state it is murkier. One possibility is that the $12/5$ state is the same as the observed Abelian $v = 2/5$ state. But, Read and Rezayi, in their initial work generalizing the non-Abelian 'Moore-Read state' [91] proposed that the $12/5$ state might be the particle-hole conjugate of their Z3 parafermion (SU(2) level 3) state. This is an interesting possibility because, unlike the $5/2$ non-Abelian Moore-Read state, the Z3 parafermion state would have braiding statistics for universal TQC [90].

A measurement of *statistics* requires a nonlocal process in which one quasiparticle moves either around another or around a suitable defect. Arbitrary phase factors, or even non-trivial unitary evolutions, can be obtained when two particles are exchanged [92–95]. Particles with such exotic statistics have been named anyons by Frank Wilczek [3,21,26]. The transformation of the anyonic wave function is consistent with the exchange symmetry. Indeed, similarly to the fermionic case the anyonic exchange transformations are not detectable by local measurements on the particles. This “indirect” nature of the statistical transformations of anyons is at the core of their intellectual appeal. It also provides the technological advantage of anyonic systems in performing quantum computation that is protected from a malicious environment. Geometric phases, also known as Berry phases [66]. These phases provide the natural mechanism that gives rise to the anyonic statistics in many-body quantum systems.

10.4 The Jones Polynomial

In the mathematics of knot theory, the Jones polynomial is a knot polynomial discovered by V. Jones in 1984 [96] that is an invariant of an oriented knot or link which assigns to each oriented knot or link a Laurent polynomial in the variable $t^{1/2}$ with integer coefficients [97,98].

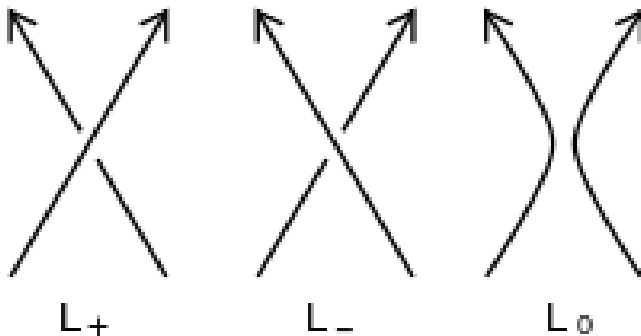


Fig. 10.5. The Jones Polynomial.

The Jones polynomial is characterized by the fact that it takes the value 1 on any diagram of the unknot and satisfies the following skein relation:

$$(t^{1/2} - t^{-1/2})V(L_0) = t^{-1}V(L_+) - tV(L_-) \quad (10.4)$$

where L_+ , L_- , and L_0 are three oriented link diagrams that are identical except in one small region where they differ by the crossing changes or smoothing shown in the figure above. The definition of the Jones polynomial by the bracket makes it simple to show that for a knot K , the Jones polynomial of its mirror image is given by substitution of t^{-1} for t in $V(K)$. Thus, an amphichiral knot, a knot equivalent to its mirror image, has palindromic entries in its Jones polynomial [98].



Fig.10.6 Amphichiral mirror image trefoil knot.

10.5 Anon ye Fabled Anyon

As a leading contender for UQC, anyons provide a radically different approach to the stability-decoherence problem in QC by using quasi-particles as threads and relying on braid theory to form stable logic gates [99-101]. Since late 1980s, we have noticed that Landau symmetry-breaking theory does not describe all possible orders. In trying to explain high temperature superconductivity a chiral spin state was introduced and physicists tried to use Landau symmetry-breaking theory to describe the new chiral spin state. The chiral spin state was taken to break time reversal and parity symmetries, but not spin rotation symmetry. But it was realized that many different chiral spin states have exactly the same symmetry. Symmetry alone was not enough to characterize different chiral spin states because chiral spin states contain a new kind of order outside usual descriptions of symmetry. The new kind of order was named ‘topological order’. New quantum numbers, such as ground state degeneracy and the non-Abelian geometric phase of degenerate ground states were introduced to characterize the various topological orders in chiral spin states.

Another important question about these phases is what kind of system and interactions are needed in principle to create them. Topological phases

could provide a way to operate a QC that would be much less sensitive to environmental noise than other approaches [102].

References

- [1] Kitaev, A.Y. (1997) Fault-tolerant quantum computation by anyons, arXiv:quant-ph/9707021v1; (2003) Annals of Physics, 303(1), 2-30.
- [2] Luo, X-W, Han, Y-J, Guo, G-C, Zhou, X. & Zhou, Z-W (2012) Simulation of non-Abelian anyons using ribbon operators connected to a common base site, arXiv: 1212.5001v1 [quant-ph]; Han, C., Park, J., Gefen, Y. & Sim, H-S (2016) Topological vacuum bubbles by anyon braiding Nature Comm, 7,1131, pp. 1-6.
- [3] Wilczek, F. (1982) Phys. Rev. Lett. 48, 1144.
- [4] Wen, X-G (2004) Quantum Field Theory of Many-Body Systems, Oxford: Oxford University Press.
- [5] Goldman, V.J. & Su, B. (1995) Science 267, 1010.
- [6] Camino, F.E., Zhou, W. & Goldman, V.J. (2005) Phys. Rev. Lett. 95, 246802.
- [7] Camino, F.E., Zhou, W. & Goldman, V.J. (2005) Phys. Rev. B 72, 075342.
- [8] Kitaev, A.Y. (2008) Anyons in an exactly solved model and beyond, arXiv:cond-mat/0506438v3 [cond-mat.mes-hall].
- [9] Sarma, S.D., Freedman, M. & Nayak, C. (2005) Phys. Rev. Lett. 94, 166802.
- [10] Bonderson, P., Kitaev, A. & Shtengel, K. (2006) Phys. Rev. Lett. 96, 016803.
- [11] Duan, L-M, Demler, E. & Lukin, M.D. (2003) Phys. Rev. Lett. 91, 090402.
- [12] Micheli, A., Brennen, G.K. & Zoller, P. (2006) Nature Phys. 2, 341.
- [13] Zhang, C-W et al. (2006) quant-ph/0609101; J. K. Pachos, quant-ph/0605068.
- [14] Jeffrey, C.Y., Teo, A.R. & Chen, X. (2014) Unconventional fusion and braiding of topological defects in a lattice model, Phys. Rev. B90,11, 115118; arXiv:1306.1538v2 [cond-mat.str-el].
- [15] Muraki, K. (2012) Unraveling an exotic electronic state for error-free quantum computation, NTT Technical Review, Vol. 10 No. 10.
- [16] Willet, R., Eisenstein, J.P., Stormer, H.L., Tsui, D.C., Gossard, A.C. & English, J.H. (1987) Observation of an even-denominator quantum number in the fractional quantum Hall effect, Phys. Rev. Lett., Vol. 59, No. 15, pp. 1776-1779.
- [17] Tsui, D.C., Stormer, H.L. & Gossard, A.C. (1982) Two-dimensional Magnetotransport in the extreme quantum limit, Phys. Rev. Lett., Vol. 48, No. 22, pp. 1559-1562.
- [18] Laughlin, R.B. (1983) Anomalous quantum Hall effect-an incompressible quantum fluid with fractionally charged excitations, Phys. Rev. Lett., Vol. 50, No. 18, pp. 1395-1398.
- [19] De Picciotto, R., Reznikov, M., Heiblum, M., Umansky, V., Buinin, G. & Mahalu, D. (1997) Direct observation of a fractional charge, Nature, Vol. 389, No. 6647, pp. 162-4.
- [20] Saminadayar, L., Glattli, D.C., Jin, Y. & Etienne, B. (1997) Observation of the e/3 fractionally charged Laughlin quasiparticle, Phys. Rev. Lett., Vol. 79, No. 13, pp. 2526-2529.
- [21] Arovas, D., Schrieffer, J.R. & Wilczek, F. (1984) Fractional statistics and the quantum Hall effect, Phys. Rev. Lett., Vol. 53, No. 7, pp. 722-723.
- [22] Moore, G. & Read, N. (1991) Nonabelions in the fractional quantum Hall effect, Nucl. Phys. B, Vol. 360, No. 2-3, pp. 362-396.

- [23] Pan, W., Xia, J-S, Shvarts, V., Adams, D.E., Stormer, H.L., Tsui, D.C., Pfeiffer, L.N., Baldwin, K.W. & West, K.W. (1999) Exact quantization of the even-denominator fractional quantum Hall state at $v = 5/2$ Landau level filling factor, Phys. Rev. Lett., Vol. 83, No. 17, pp. 3530-3533.
- [24] Haldane, F.D.M. (1983) Fractional quantization of the Hall effect - A hierarchy of incompressible quantum fluid states, Phys. Rev. Lett., Vol. 51, No. 7, pp. 605-608.
- [25] Jain, J.K. (1989) Composite-fermion approach for the fractional quantum Hall Effect, Phys. Rev. Lett., Vol. 63, No. 2, pp. 199-202.
- [26] Greiter, M., Wen, X.G. & Wilczek, F. (1992) Paired Hall states, Nucl. Phys. B, Vol. 374, No. 3, pp. 567-614.
- [27] Read, N. & Green, D. (2000) Paired states of fermions in two dimensions with breaking of parity and time-reversal symmetries and the fractional quantum Hall effect, Phys. Rev. B, Vol. 61, No. 15, pp. 10267-10297.
- [28] Burnell, F.J., Arovas, D.P. & Bernevig B.A. (2009) Scenario for fractional quantum Hall effect in bulk isotropic materials, Phys. Rev. B 79, 155310.
- [29] Burnell, F.J. & Simon, S.H. (2010) Space-time geometry of topological phases, Annals of Physics 325 2550.
- [30] Wen, X.G. (1991) Non-Abelian statistics in the fractional quantum Hall states, Phys. Rev. Lett., Vol. 66, No. 6, pp. 802-805.
- [31] Blok, B. & Wen, X.G. (1992) Many-body systems with non-Abelian statistics, Nucl. Phys. B, Vol. 374, No. 3, pp. 615-646.
- [32] Levin, M., Halperin, B.I. & Rosenow, B. (2007) Particle-hole symmetry and the pfaffian state, Phys. Rev. Lett., Vol. 99, No. 23, 236806.
- [33] Lee, S-S, Ryu, S., Nayak, C. & Fisher, M.P.A. (2007) Particle-hole symmetry and the $v = 5/2$ quantum Hall state, Phys. Rev. Lett., Vol. 99, No. 23, 236807.
- [34] Halperin, B. (1983) Theory of the quantized Hall conductance, Helv. Phys. Acta, Vol. 56, No. 1-3, pp. 75-102.
- [35] Overbosch, J. & Wen, X-G (2008) Phase transitions on the edge of the $v = 5/2$ pfaffian and anti-pfaffian quantum Hall state, [arXiv:0804.2087v1]
- [36] Ke, C.T. & Jain, J.K. (2006) Understanding the $5/2$ fractional quantum Hall effect without the pfaffian wave function, Phys. Rev. Lett., Vol. 96, No. 24, 246805.
- [37] Dolev, M., Heiblum, M., Umansky, V., Stern, A. & Mahalu, D. (2008) Observation of a quarter of an electron charge at the $v = 5/2$ quantum Hall state, Nature, Vol. 452, No. 7189, pp. 829-834.
- [38] Dolev, M., Gross, Y., Chung, Y.C., Heiblum, M., Umansky, V. & Mahalu, D. (2010) Dependence of the tunneling quasiparticle charge determined via shot noise measurements on the tunneling barrier and energetics, Phys. Rev. B, Vol. 81, No. 16, 161303(R).
- [39] Venkatachalam, V., Yacoby, A. Pfeiffer, L. & West, K. (2011) Local charge of the $v = 5/2$ fractional quantum Hall state, Nature, Vol. 469, No. 7329, pp. 185-188.
- [40] Radu, I.P., Miller, J.B., Marcus, C.M., Kastner, M.A., Pfeiffer, L.N. & West, K.W. (2008) Quasi-particle properties from tunneling in the $v = 5/2$ fractional quantum Hall state, Science, Vol. 320, No. 5878, pp. 899-902.
- [41] Lin, X., Dillard, C., Kastner, M.A., Pfeiffer, L.N. & West, K.W. (2012) Measurements of quasiparticle tunneling in the $v = 5/2$ fractional quantum Hall state, Phys. Rev. B, Vol. 85, No. 16, 165321.
- [42] Nayak, C., Simon, S.H., Stern, A., Freedman, M. & Das Sarma, S. (2008) Non-Abelian anyons and topological computation, Rev. Mod. Phys., Vol. 80, No. 3, pp. 1083-1159.

- [43] Das Sarma, S., Freedman, M. & Nayak, C. (2005) Topologically protected qubits from a possible non-abelian fractional quantum Hall state, Phys. Rev. Lett., Vol. 94, No. 16, 166802.
- [44] Morf, R. (1998) Transition from quantum Hall to compressible states in the 2nd Landau level: new light on the $v = 5/2$ enigma, Phys Rev Lett, Vol. 80, No. 7, pp.1505-8.
- [45] Dimov, I., Halperin, B.I. & Nayak, C. (2008) Spin order in paired quantum Hall states, Phys. Rev. Lett., Vol. 100, No. 12, 126804.
- [46] Feiguin, A.E., Rezayi, E., Yang, C. Nayak, C. & Das Sarma, S. (2009) Spin polarization of the $v = 5/2$ quantum Hall state, Phys. Rev. B, Vol. 79, No. 11, 115322.
- [47] Das Sarma, S., Gervais, G. & Zhou, X. (2010) Energy gap and spin polarization in the 5/2 fractional quantum Hall effect, Phys. Rev. B, Vol. 82, No. 11, 115330.
- [48] Jain, J.K. (2010) The 5/2 enigma in a spin, Physics, Vol. 3, p. 71.
- [49] Eisenstein, J.P., Willett, R., Stormer, H.L., Tsui, D.C., Gossard, A.C. & English, J.H. (1988) Collapse of the even-denominator fractional quantum Hall effect in tilted fields, Phys. Rev. Lett., Vol. 61, No. 8, pp. 997-1000.
- [50] Dean, C.R., Piot, B.A., Hayden, P., Das Sarma, S., Gervais, G., Pfeiffer, L.N. & West, K.W. (2008) Contrasting behavior of the 5/2 and 7/3 fractional quantum Hall effect in a tilted field, Phys. Rev. Lett., Vol. 101, No. 18, 186806.
- [51] Zhang, C., Knuuttila, T., Dai, Y., Du, R.R., Pfeiffer, L.N. & West, K.W. (2010) $v = 5/2$ fractional quantum Hall effect at 10 T: implications for the pfaffian state, Phys. Rev. Lett., Vol. 104, No. 16, 166801.
- [52] Stern, M., Plochocka, P., Umansky, V., Maude, D.K., Potemski, M. & Bar-Joseph, I. (2010) Optical probing of the spin polarization of the $v = 5/2$ quantum Hall state, Phys. Rev. Lett., Vol. 105, No. 9, 096801.
- [53] Rhone, T.D., Yan, J., Gallais, Y., Pinczuk, A., Pfeiffer, L. & West, K.W. (2011) Rapid collapse of spin waves in nonuniform phases of the second Landau level, Phys. Rev. Lett., Vol. 106, No. 19, 196805.
- [54] Sarma, S.D., Freedman, M., & Nayak, C. (2005) Topologically protected qubits from a possible non-abelian fractional quantum Hall state, Physical Review Letters (94): 166802; arXiv:cond-mat/0412343.
- [55] Nayak, C., Simon, S.H., Stern, A., Freedman, M. & Sarma, S.D. (2008) Non-Abelian anyons and topological quantum computation, Review of Modern Physics (80): 1083; arXiv:0707.1889.
- [56] Freedman, M.H. & Nayak, C.V. (2007) Quasiparticle interferometry for logical gates, US Patent, US007250624B1; Freedman, M.H., Nayak, C.V. & Sarma, S.D. (2008) Quasiparticle interferometry for logical gates, US Patent, US7394092 B2.
- [57] Qi, X-L & Zhang, S-C (2010) Topological insulators and superconductors, arXiv:1008.2026v1 [cond-mat.mes-hall].
- [58] Kane, C.L. & Mele, E.J. (2005) Phys. Rev. Lett. 95, 226801.
- [59] Polini, M., Guinea, F., Lewenstein, M., Manoharan, V. & Pellegrini, V. (2013) Artificial graphene as a tunable Dirac material, arXiv:1304.0750.
- [60] Kenjiro, K., Warren, G., Ko, M.W., Guinea, F., & Manoharan, H.C. (2012) Designer Dirac fermions and topological phases in molecular graphene, Nature 483, 306.
- [61] Roushan, P. et al. (2014) Observation of topological transitions in interacting quantum circuits, arXiv:1407.1585v1 [quant-ph].
- [62] Thouless, D.J., Kohmoto, M., Nightingale, M.P. & den Nijs, M. (1982) Quantized Hall conductance in a two-dimensional periodic potential, Phys. Rev. Lett. 49, 405-408.
- [63] Von Neumann, J. & Wigner, E.P. (1929) *Über merkwürdige diskrete eigenwerte*, Phys. Z. 30, 467.

- [64] Wen, X-G (2004) Quantum Field Theory of Many-body systems, Oxford.
- [65] Bernevig B.A. & Hughes, T.L. (2013) Topological Insulators and Topological Superconductors, Princeton: Princeton University Press.
- [66] Berry, M. (1984) Quantal phase factors accompanying adiabatic changes, Proc. R. Soc. Lond. A 392, 45–57.
- [67] Teo, C.Y. (2015) Globally symmetric topological phase: From anyonic symmetry to twist defect, arXiv:1511.00912v1 [cond-mat.str-el].
- [68] Ibanez, M., Links, J., Sierra, G. & Zhao, S-Y (2009) Exactly solvable pairing model for superconductors with a p+ip-wave symmetry, arXiv:0810.0340v3 [cond-mat.supr-con].
- [69] Wilczek, F. (1990) Fractional Statistics and Anyon Superconductivity, Singapore: World Scientific.
- [70] Fradkin, E. (2013) Field theories of condensed matter physics, 2nd ed., Cambridge: Cambridge University Press.
- [71] Wen, X-G (2004) Quantum Field Theory of Many Body Systems, Oxford: Oxford Univ. Press.
- [72] Levin, M. & Gu, Z-C (2012) Phys. Rev. B 86, 115109.
- [73] Chen, X., Gu, Z-C, Liu, Z-X & Wen, X-G (2012) Science 338, 1604.
- [74] Lu, Y-M & Vishwanath, A. (2012) Phys. Rev. B 86, 125119.
- [75] Mesaros, A. & Ran, Y. (2013) Phys. Rev. B 87, 155115.
- [76] Essin, A.M. & Hermele, M. (2013) Phys. Rev. B 87, 104406.
- [77] Wang, C., Potter, A.C. & Senthil, T. (2014) Science 343, 629.
- [78] Bi, Z., Rasmussen, A., Slagle, K. & Xu, C. (2015) Phys. Rev. B 91, 134404.
- [79] Kapustin, A. (2014) Symmetry protected topological phase, arXiv:1403.1467.
- [80] Hasan, M.Z. & Kane, C.L. (2010) Rev. Mod. Phys. 82, 3045.
- [81] Qi, X-L & Zhang, S-C (2011) Rev. Mod. Phys. 83, 1057.
- [82] Kane, C.L. & Mele, E.J. (2005) Phys. Rev. Lett. 95, 226801.
- [83] Konig, M., Wiedmann, S., Brüne, C., Roth, A., Buhmann, H., Molenkamp, L., Qi, X-L & Zhang, S. (2007) Science 318, 766.
- [84] Moore, J.E. & Balents, L. (2009) Phys. Rev. B 75, 121306(R).
- [85] Roy, R. (2009) Phys. Rev. B 79, 195322.
- [86] Fu, L., Kane, C.L. & Mele, E.J. (2007) Phys. Rev. Lett. 98, 106803.
- [87] Qi, X-L, Hughes, T.L. & Zhang, S-C (2008) Phys. Rev. B 78, 195424.
- [88] Hsieh, D., Qian, L., Wray, Y. Xia, Y., Hor, S., Cava, R.J. & Hasan, M.Z. (2008) Nature 452, 970.
- [89] Laughlin, R.B. & Girvin, S.M. (1987) Elementary theory: The incompressible quantum fluid, in R.E. Prange & S.M. Girvin (eds.) The Quantum Hall Effect, pp. 233-301, New York: Springer.
- [90] Moore, G. & Read, N. (1991) Nonabelions in the fractional quantum Hall effect, Nuclear Physics B360, 362-396.
- [91] Read, N. & Rezayi, E. (1999) Beyond paired quantum Hall states: Parafermions and incompressible states in the first excited Landau level, Phys. Rev. B 59, 8084; (1998). arXiv:cond-mat/9809384v2 [cond-mat.mes-hall].
- [92] Collins, G.P. (2006) Computing with quantum knots, Scientific American.
- [93] Sarma, S.D., Freedman, M. & Nayak, C. (2005) Topologically protected qubits from a possible non-abelian fractional quantum Hall state, Physical Review Letters (94): 166802. arXiv:cond-mat/0412343.

- [94] Nayak, C., Simon, S., Stern, H., Freedman, M. & Sarma, S.D. (2008) Non-Abelian anyons and topological quantum computation, *Review of Modern Physics* (80): 1083; arXiv:0707.1889.
- [95] Raussendorf, R., Harrington, J. & Koid, G. (2007) Topological fault-tolerance in cluster state quantum computation, arXiv:quant-ph/0703143.
- [96] Jones, V.F.R. (1985) A polynomial invariant for knots via von Neumann algebra, *Bull. Amer. Math. Soc. (N.S.)* 12: 103-111.
- [97] Futer, D., Kalfagianni, E. & Purcell, J.S. (2011) Jones polynomials, volume and essential knot surfaces: a survey, <https://math.byu.edu/~jpurcell/papers/fkp-survey7.pdf>
- [98] Lomonaco, S.J. Jr. & Kauffman L.H. (2006) Topological quantum computing and the Jones polynomial, arXiv:quant-ph/0605004v1.
- [99] Freedman, M., Kitaev, A., Larsen, M. & Wang, Z. (2002) Topological quantum computation, *Bulletin of the American Mathematical Society* 40 (1): 31-38.
- [100] Monroe, D. (2008) Anyons: The breakthrough quantum computing needs? *New Scientist* (2676).
- [101] Lechner, W., Hauke, P., Zoller, P. (2015) A quantum annealing architecture with all-to-all connectivity from local interactions, *Science Advances*, 1 (9).
- [102] Burnell, F.J. & Simon, S.H. (2010) Space-time geometry of topological phases, *Annals of Physics*, 325, 2550.

Chapter 11

A New Group of Transformations

Just as infinities in the Rayleigh-Jeans Law pointed the way to quantum mechanics; now infinities in the renormalization of quantum field theory provide indicia for the next age of discovery. Additionally, this imminent paradigm shift demands that the observational frame of reference be radically adjusted! Just as Copernicus (and Greek astronomer/mathematician Hipparchus 2,200 years prior), caused the switch to heliocentric cosmology (after a 150-year struggle to gain general acceptance); for natural science to observe the 3rd regime of reality (CM → QM → UFM) we must no longer consider Euclidean 3-space as the fundamental frame of reference. We hope the ‘update’ does not take 150 years this time. Physicists, so demanding of the utility of rigor in scientific method and principles, are often quite rigid in their belief system. Two contemporary examples are: 1) In the 2014 Hollywood biographical film, “The Theory of Everything”, Stephen Hawking says – “*Who is God to tell me how to write my equation?*”. 2) The field of Cognitive Science unscientifically tells its fundamental question, “*What processes in the brain give rise to awareness?*”, how to answer itself; the question should simply be posed, ‘What processes give rise to awareness?’’. The Observer continues to plague measurement theory. A frame of reference is typically a set of three orthogonal measuring rods with an associated clock to which a metric is attached for observing entities such as position, displacement, motion or energy. The frame of reference and observer or apparatus cannot be separated. We have come to the point of requiring another set of transformations beyond the Galilean, Lorentz-Poincaré to observe the UFM regime. This 3rd regime reveals an inherent new unified field ‘action principle’ driving self-organization, in a manner corresponding to a de Broglie-Bohm ‘super-quantum potential. Operationally this new set of transformations allows one to ontologically surmount the quantum condition, $\Delta x \Delta \rho \cong \hbar$) by an acausal, energyless topological interaction.

11.1 Introduction

Currently the Planck-scale stochastic foam of quantum mechanics is considered the basement of reality. If additional dimensionality exists, it is postulated to be curled up at 10^{-33} cm since it is not observed [1]. We propose, in a manner similar to Randall [2-4], that additional dimensionality is not compactified; and that the lack of observation of putative Large-Scale Additional Dimensionality (LSXD) is due instead to a process of ‘subtractive interferometry’ inherent in the evolution of the synchronized spacetime backcloth. This interferometric process creates an arrow of time related to the observer [5-7].

We further assume that the progression of our understanding of the universe (now an anthropic multiverse) proceeds from Classical Mechanics → Quantum Mechanics → to Unified Field Mechanics (UFM). The infinities in renormalizing quantum electrodynamics are indicative of a new age of discovery in the same manner the infinities in Rayleigh-Jeans Law for blackbody radiation provided indicia for the last age of discovery (quantum theory) requiring another new set of transformation beyond the Galilean-Lorentz-Poincaré related to UFM. This new set of UFM transformations allows violation of the quantum uncertainty principle and obviating the ‘No-Cloning’ and ‘Non-Erasure’ theorems, scenarios engendered by the limitations of the Copenhagen Interpretation.

Nobelst Paul Dirac is said to have told M-Theorist Ed Witten in the early 1980s that the most important challenge in physics was “*to get rid of infinity*”, which he helped overcome through renormalization in QED [8]. The equations for QED led to infinite results for the self-energy or mass of the electron, which was finally solved by a process called renormalization, which conveniently rolls up the infinities into the electron’s observed mass and charge, and then ignores them. Nobelst Richard Feynman pedagogically called this ‘sleight of hand’, “*brushing infinity under the rug.*” [9].

Interaction-Free Measurement (IFM) [10-21] provides additional indicia of the physicality of the putative new UFM group of transformations. Essentially the IFM procedure increases the number of Mach-Zehnder interferometers (determines relative phase shift variations between two collimated beams derived by splitting light from a single source) and the number of passes through the apparatus to increase outcome probability towards unity. The UFM transform is different, achieving probability, $P \equiv 1$ in a single pass by surmounting the

uncertainty principle. Surmounting the quantum uncertainty principle is required to observe the UFM regime [22,23].

11.2 Metric Space and the Line Element

In general, a line element is the spacetime interval separating two arbitrarily separate events; or the line segment for an infinitesimal displacement vector, ds in a metric space, most simply formulated in Cartesian coordinates as $ds^2 = dx^2 + dy^2 + dz^2$, where d is the metric and s the interval. For general relativity the line element is modeled on a spacetime with a curved Riemannian manifold by a metric tensor. For a space with metric, g_{ij} the infinitesimal line element is $ds^2 = g_{ij}du^i du^j$.

The length, d of a finite segment between points a and b is

$$d = \int_a^b \left(g_{ij} \frac{du^i}{dt} \frac{du^j}{dt} \right)^{1/2} dt, \quad (11.1)$$

where t parametrizes position along the line segment.

The choice of coordinate system basis is arbitrary, so we might for the sake of simplicity, say that all Galilean or Lorentz-Poincaré line-elements occur along the x -axis. Beginning with the non-relativistic Galilean group of transformations between the coordinates of two reference frames differing only by constant relative motion within the constructs of Newtonian physics we have

$$ds^2 = \begin{bmatrix} x' = x - vt \\ y' = y \\ z' = z \\ t' = t \end{bmatrix}. \quad (11.2)$$

Next recall that the usual Lorentz transformation is defined in a 4D real space. Consider two frames of reference, Σ , at rest and Σ' moving at relative uniform velocity v . We call v the velocity of the origin of Σ'

moving relative to Σ . A light signal along the x direction is transmitted by $x = ct$ or $x - ct = 0$ and also in Σ' as $x' = ct'$ or $x' - ct' = 0$, since the velocity of light in vacuo is constant in any frame of reference in 4-space. For the usual 4D Lorentz transformation, we have

$$\begin{aligned}x' &= \frac{x - vt}{\sqrt{1 - v^2/c^2}} = \gamma(x - vt) \\y' &= y \\z' &= z \\t' &= \frac{t - (v/c^2)x}{\sqrt{1 - v^2/c^2}} = \gamma\left(t - \left(\frac{v}{c^2}x\right)\right)\end{aligned}\quad (11.3)$$

for $\gamma = (1 - \beta^2)^{-1/2}$ and $\beta = v/c$.

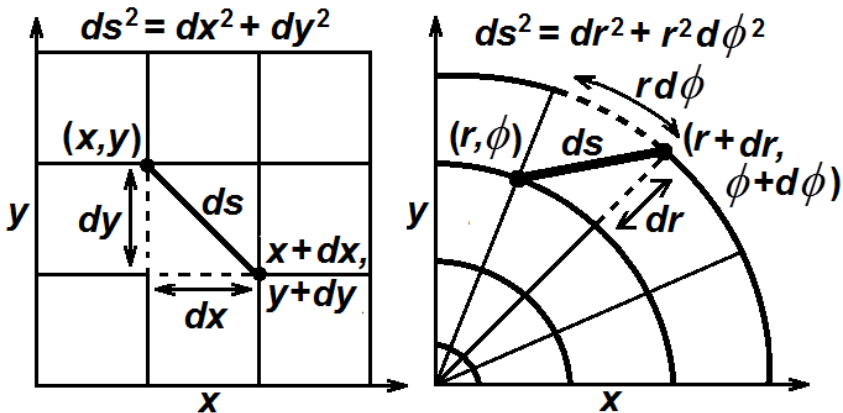


Fig. 11.1 Distance measure in Cartesian and plane polar coordinates in a Euclidean space is invariant for metric space transformations.

Figure 11.1a & b correspond to the same space, parametrized by different coordinates. Although the form of the line element is different, the distance between nearby points is still given by ds , which is independent of the coordinate system. Since the line element ds is invariant under coordinate transformations, we know generally that the distance between any two points is invariant under coordinate transformations for metric spaces.

11.3 Why a New Transformation Group?

The UFM Transformation is also called the Noetic Transform, T_N , as will become clear in the future. It is different from the Galilean and Lorentz-Poincaré group transformations in that in its simplest form it is stationary in ds_0 and has no temporal components (but still displacement). This is because its transformation process, which is cyclic, moves ‘upwards’ through HD brane topology. To further challenge the reader, it is also ‘ontological’ with no energy transferred; only topological information. The UFM transform is a topological-phase interaction, with an energyless ‘force of coherence’ mediated by ‘topological charge’ in conjunction with a nilpotent zero-totality, which will be defined in Chap. 12.

However, as all new theory must make correspondence to existing theory; when referring to a Standard Model particle in motion &c, the T_N would include all pertinent aspects of the Galilean and Lorentz-Poincaré transforms. This is no different than the additions made to CM with the discovery of QM.

11.4 Micromagnetics and LSXD Topological Charge Driving Brane Conformation

An extensive body of literature exists for phenomena related to the zero-point field; but relative to unified theory this work is considered metaphorically descriptive only of the ‘fog over the ocean’ rather than the structural-phenomenology of the ocean itself. Instead a deep HD structure with a real covariant Dirac polarized vacuum at its foundation is utilized [24-26]. The Casimir, Zeeman, Aharonov-Bohm and Sagnac effects are considered evidence for a Dirac vacuum. New assumptions are made concerning the Dirac polarized vacuum relating to the topology of spacetime and the structure of matter cast in a 12D form of Relativistic Quantum Field Theory (RQFT) in the context of the Holographic Anthropic Multiverse cosmological paradigm [5]. In this cosmology the observed Euclidian-Minkowski spacetime present, $E_3 - \hat{M}_4$ is a virtual standing wave of highly ordered Wheeler-Feynman-Cramer retarded-advanced future-past parameters respectively [27,28]. An essential ingredient of UFM cosmology is that a new action principle synonymous with the unified field arises naturally and is postulated to drive self-organization and evolution through all levels of scale [5,29].

In this context an experimental design [5-7] is introduced to isolate and utilize the new anthropic action to test empirically its putative ability to effect conformational structure of the topology of spacetime to surmount the usual phenomenologically based uncertainty in an ontological matter with probability $P \equiv 1$. The LCU (Least Cosmological Unit) is an essential key factor.

Unified Theory postulates that spacetime topology is ‘continuously transformed’ by the self-organizing properties of the long-range coherence of the unified field [5,29]. In addition to manipulating conformational change in HD brane topology, from the experimental results we attempt to calculate the energy Hamiltonian required to manipulate Casimir-like boundary conformation in terms of the unified field equation, $F_{(N)} = \kappa / \rho$ (simple unexpanded form). This resonant coupling produced by the teleological action of the unified field driving its hierarchical self-organization has local, nonlocal and global (complex LSXD) parameters. The Schrödinger equation, extended by the addition of the de Broglie-Bohm quantum potential-pilot wave mechanism has been used to describe an electron moving on a manifold; but this is not a sufficient extension to describe HD unified aspects of the continuous-state (Chap. 3) symmetry breaking of spacetime topology which requires further extension to include action of the unified field in additional dimensions.

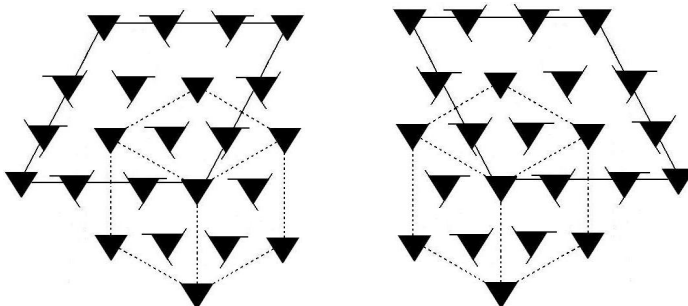


Fig. 11.2 HD emergence of Euclidean shadow vertices from local lattice gas array. If the central vertex of the cube represents a Euclidian point, the 12 satellite points represent HD control parameters. The triangles with obverse tails represent left-right nilpotent symmetry.

11.5 Lorentz Condition in Complex 8-Space and Tachyonic Signaling

In order to examine as the consequences of the relativity hypothesis that time is the 4th dimension of space, and that we have a particular form of

transformation called the Lorentz transformation, we must define velocity in the complex space. That is, the Lorentz transformation and its consequences, the Lorentz contraction and mass dilation, etc., are a consequence of time as the 4th dimension of space and are observed in three spaces [30]. These attributes of 4-space in 3-space are expressed in terms of velocity, as in the form $\gamma = (1 - \beta^2)^{-1/2}$ for $\beta \equiv v_{\text{Re}} / c$ where c is always taken as real.

If complex 8-space can be projected into 4-space, what are the consequences? We can also consider a 4D slice through the complex 8D space. Each approach has its advantages and disadvantages. In projective geometries information about the space is lost. What is the comparison of a subset geometry formed from a projected geometry or a subspace formed as a slice through an XD geometry? What does a generalized Lorentz transformation "look like"? We will define complex derivatives and therefore we can define velocity in a complex plane [30].

Consider the generalized Lorentz transformation in the system of x_{Re} and t_{Im} for the real time remote connectedness case in the $x_{\text{Re}}, t_{\text{Im}}$ plane. We define our substitutions from 4-to 8-space before us,

$$\begin{aligned} x &\rightarrow x' = x_{\text{Re}} + ix_{\text{im}} \\ t &\rightarrow t' = t_{\text{Re}} + it_{\text{im}} \end{aligned} \quad (11.4)$$

and we represented the case for no imaginary component of x_{Re} or $x_{\text{im}} = 0$ where the $x_{\text{Re}}, t_{\text{Re}}$ plane comprises the ordinary 4-space plane.

Let us recall that the usual Lorentz transformation conditions is defined in 4D real space. Consider two frames of reference, Σ , at rest and Σ' moving at relative uniform velocity v . We call v the velocity of the origin of Σ' moving relative to Σ . A light signal along the x direction is transmitted by $x = ct$ or $x - ct = 0$ and also in Σ' as $x' = ct'$ or $x' - ct' = 0$, since the velocity of light in vacuo is constant in any frame of reference in 4-space. For the usual 4D Lorentz transformation, we have as shown in Eq. (11.5), $x = x_{\text{Re}}, t = t_{\text{Re}}$ and $v_{\text{Re}} = x_{\text{Re}} / t_{\text{Re}}$.

$$\begin{aligned}
 x' &= \frac{x - vt}{\sqrt{1 - v^2/c^2}} = \gamma(x - vt) \\
 y' &= y \\
 z' &= z \\
 t' &= \frac{t - (v/c^2)x}{\sqrt{1 - v^2/c^2}} = \gamma \left(t - \left(\frac{v}{c^2} x \right) \right)
 \end{aligned} \tag{11.5}$$

for $\gamma = (1 - \beta^2)^{-1/2}$ and $\beta = v/c$. Here x and t stand for x_{Re} and t_{Re} and v is the real velocity.

We consider the $x_{\text{Re}}, t_{\text{Im}}$ plane and write the expression for the Lorentz conditions for this plane. Since again t_{Im} like t_{Re} is orthogonal to x_{Im} , and t'_{Im} is orthogonal to x'_{Im} ; we can write

$$\begin{aligned}
 x' &= \frac{x - ivt_{\text{Im}}}{\sqrt{1 - v^2/c^2}} = \gamma_v (x - vt_{\text{Im}}) \\
 y' &= y \\
 z' &= z \\
 t' &= \frac{t - (v/c^2)x}{\sqrt{1 - v^2/c^2}} = \gamma_v \left(t - \left(\frac{v}{c^2} x \right) \right)
 \end{aligned} \tag{11.6}$$

where γ_v represents the definition of γ in terms of the velocity v ; also $\beta_{v\text{Im}} \equiv v_{\text{Im}}/c$ where c is always taken as real [19] where v can be real or imaginary.

In Eq. (11.6) for simplicity we let x', x, t' and t denote $x'_{\text{Re}}, x_{\text{Re}}, t'_{\text{Re}}$ and t_{Re} and we denote script v as v_{Im} . For velocity, v is $v_{\text{Re}} = x_{\text{Re}}/t_{\text{Re}}$ and $v = v_{\text{Im}} = i_{\text{Im}}/it_{\text{Im}}$; where the i drops out so that $v = v_{\text{Im}} = x_{\text{Im}}/t_{\text{Im}}$ is a real value function. In all cases the velocity of light c is c . We use this alternative notation here for simplicity in the complex Lorentz transformation.

The symmetry properties of the topology of the complex 8-space gives us the properties that allow Lorentz conditions in 4D, 8D and ultimately

12D space. The example we consider here is a subspace of the 8-space of $x_{\text{Re}}, t_{\text{Re}}, x_{\text{Im}}$ and t_{Im} . In some cases we let $x_{\text{Im}} = 0$ and just consider temporal remote connectedness; but likewise we can follow the anticipatory calculation and formulate remote, nonlocal solutions for $x_{\text{Im}} \neq 0$ and $t_{\text{Im}} = 0$ or $t_{\text{Im}} \neq 0$. The anticipatory case for $x_{\text{Im}} = 0$ is a 5D space as the space for $x_{\text{Im}} \neq 0$ and $t_{\text{Im}} = 0$ is a 7D space and for $t_{\text{Im}} \neq 0$ as well as the other real and imaginary spacetime dimensions, we have our complex 8D space.

It is important to define the complex derivative in order to define velocity, v_{Im} . In the $x_{\text{Re}} t_{\text{Im}}$ plane then, we define a velocity of $v_{\text{Im}} = dx/dt_{\text{Im}}$. In the next section we detail the velocity expression for v_{Im} and define the derivative of a complex function in detail [5].

For $v_{\text{Im}} = dx / dt_{\text{Im}} = -idx / dt_{\text{Im}} = -iv_{\text{Re}}$ for v_{Re} as a real quantity, we substitute into our $x_{\text{Re}}, t_{\text{Im}}$ plane Lorentz transformation conditions as

$$\begin{aligned} x' &= \frac{x_{\text{Re}} - v_{\text{Re}} t_{\text{Im}}}{\sqrt{1 + v_{\text{Re}}^2 / c^2}} \\ y' &= y \\ z' &= z \\ t'_{\text{Im}} &= \frac{t_{\text{Re}} - v_{\text{Re}} x_{\text{Re}}}{\sqrt{1 + v_{\text{Re}}^2 / c^2}} \end{aligned} \quad (11.7)$$

These conditions are valid for any velocity, $v_{\text{Re}} = -v$.

Let us examine the way this form of the Lorentz transformation relates to the properties of mass dilation. We will compare this case to the ordinary mass dilation formula and the tachyonic mass formula of Feinberg [31] which nicely results from the complex 8-space.

In the ordinary $x_{\text{Re}} t_{\text{Re}}$ plane then, we have the usual Einstein mass relationship of

$$m = \frac{m_0}{\sqrt{1 - v_{\text{Re}}^2 / c^2}} \quad \text{for } v_{\text{Re}} \leq c \quad (11.8)$$

and we can compare this to the tachyonic mass relationship in the xt plane

$$m = \frac{m_0^*}{\sqrt{1-v_{\text{Re}}^2/c^2}} = \frac{im_0}{\sqrt{1-v_{\text{Re}}^2/c^2}} = \frac{m_0}{\sqrt{v_{\text{Re}}^2/c^2 - 1}} \quad (11.9)$$

for v_{Re} now $v_{\text{Re}} \geq c$ and where m^* or m_{Im} stands for $m^* = im$ and we define m as m_{Re} ,

$$m = \frac{m_0}{\sqrt{1+v^2/c^2}} \quad (11.10)$$

For m real (m_{Re}), we can examine two cases on v as $v < c$ or $v > c$, so we will let v be any value from $-\infty < v < \infty$, where the velocity, v , is taken as real, or v_{Re} .

Consider the case of v as imaginary (or v_{Im}) and examine the consequences of this assumption. Also we examine the consequences for both v and m imaginary and compare to the above cases. If we choose v imaginary or $v^* = iv$ (which we can term v_{Im}) the $v^{*2}/c^2 = -v^2/c^2$ and $\sqrt{1+v^{*2}/c^2}$ becomes $\sqrt{1-v^{*2}/c^2}$ or

$$m = \frac{m_0}{\sqrt{1-v_{\text{Re}}^2/c^2}} \quad (11.11)$$

We get the form of this normal Lorentz transformation if v is imaginary ($v^* = v_{\text{Im}}$)

If both v and m are imaginary, as $v^* = iv$ and $m^* = im$, then we have

$$m = \frac{m_0^*}{\sqrt{1+v^{*2}/c^2}} = \frac{im_0}{\sqrt{1-v^2/c^2}} = \frac{m_0}{\sqrt{v^2/c^2 - 1}} \quad (11.12)$$

or the tachyonic condition.

If we go "off" into x_{Re} t_{Re} t_{Im} planes, then we have to define a velocity "cutting across" these planes, and it is much more complicated to define the complex derivative for the velocities. For subliminal relative systems Σ and Σ' we can use vector addition such as $W = v_{\text{Re}} + iv_{\text{Im}}$ for $v_{\text{Re}} < x$, $v_{\text{Im}} < c$ and $W < c$. In general, there will be four complex velocities. The

relationship of these four velocities is given by the Cauchy-Riemann relations in the next section.

These two are equivalent. The actual magnitude of v may be expressed as $v = [vv^*]^{1/2} \hat{v}$ (where \hat{v} is the unit vector velocity) which can be formed using either of the Cauchy-Riemann equations. It is important that a detailed analysis not predict any extraneous consequences of the theory. Any new phenomenon that is hypothesized should be formulated in such a manner as to be easily experimentally testable.

Feinberg suggests several experiments to test for the existence of tachyons [31]. He describes the following experiment – consider in the laboratory, atom A , at time t_0 is in an excited state at rest at x_1 and atom B is in its ground state at x_2 . At time t_1 atom A descends to the ground state and emits a tachyon in the direction of B . Let E_1 be this event at t_1, x_1 . Subsequently, at $t_2 > t_1$ atom B absorbs the tachyon and ascends to an excited state; this is event E_2 , at t_2, x_2 . Then at $t_3 > t_2$ atom B is excited and A is in its ground state. For an observer traveling at an appropriate velocity, $v < c$ relative to the laboratory frame, events E_1 and E_2 appear to occur in the opposite order in time. Feinberg describes the experiment by stating that at t_2 , atom B spontaneously ascends from the ground state to an excited state, emitting a tachyon which travels toward A . Subsequently, at t_1 , atom A absorbs the tachyon and drops to the ground state.

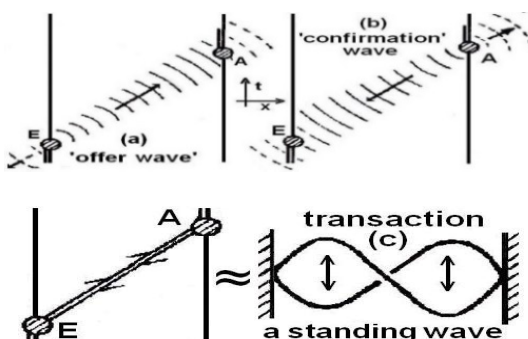


Fig. 11.3. Cramer's Transactional Interpretation model. a) Offer-wave, b) confirmation-wave combined into the resultant transaction c) which takes the form of an HD future-past advanced-retarded standing or stationary wave. Figs. Adapted from Cramer [28].

It is clear from this that what is absorption for one observer is spontaneous emission for another. But if quantum mechanics is to remain

intact so that we are able to detect such particles, then there must be an observable difference between them: The first depends on a controllable density of tachyons, the second does not. In order to elucidate this point, we should repeat the above experiment many times over. The possibility of reversing the temporal order of causality, sometimes termed ‘sending a signal backwards in time’ must be addressed [8]. Is this cause-effect statistical in nature? In the case of Bell’s Theorem, these correlations are extremely strong whether explained by $v > c$ or $v = c$ signaling.

Bilaniuk, et al formulated the interpretation of the association of negative energy states with tachyonic signaling [31,32]. From the different frames of reference, thus to one observer absorption is observed and to another emission is observed. These states do not violate special relativity. Acausal experiments in particle physics have been suggested by a number of researchers [33,34]. Another approach is through the detection of Cherenkov radiation, which is emitted by charged particles moving through a substance traveling at a velocity, $v > c$. For a tachyon traveling in free space with velocity, $v > c$, Cherenkov radiation may occur in a vacuum causing the tachyon to lose energy and become a tardon [23,31].

In prior volumes [5,31] in discussions on the arrow of time we have developed an extended model of a polarized Dirac vacuum in complex form that makes correspondence to both Calabi-Yau mirror symmetry conditions which extends Cramer’s Transactional Interpretation [5,28] of quantum theory to cosmology. Simplistically Cramer models a transaction as a standing wave of the future-past (offer wave-confirmation wave).

However, in the broader context of the new paradigm of Holographic Anthropic Multiverse (HAM) cosmology it appears theoretically straight forward to ‘program the vacuum’ The coherent control of a Cramer transaction can be resonantly programmed with alternating nodes of constructive and destructive interference of the standing-wave present. It should be noted that in UFM cosmology the de Broglie-Bohm quantum potential becomes an eternity-wave, \mathbf{x} or super pilot wave or force of coherence associated with the U_F ordering the reality of the observer or the locus of the spacetime arrow of time.

To perform a simple experiment to test for the existence of Tachyons and Tardyons an atom would be placed in a QED cavity or photonic crystal. Utilizing the resonant hierarchy through interference the reduced eternity wave, \mathbf{x} is focused constructively or destructively as the experimental mode may be and according to the parameters illustrated by Feinberg above temporal measurements of emission are taken.

11.6 Velocity of Propagation in Complex 8-Space

In this section we utilize the Cauchy-Riemann relations to formulate the hyperdimensional velocities of propagation in the complex plane in various slices through the hyperdimensional complex 8-space. In this model finite limit velocities, $v > c$ can be considered. In some Lorentz frames of reference, instantaneous signaling can be considered. It is the velocity connection between remote nonlocal events, and temporal separated events or anticipatory and real time event relations.

It is important to define the complex derivative so that we can define the velocity, $v_{y_{\text{Im}}}$. In the xit plane then, we define a velocity of $v = dx / d(i\tau)$. We now examine in some detail the velocity of this expression. In defining the derivative of a complex function we have two cases in terms of a choice in terms of the differential increment considered. Consider the orthogonal coordinates x and it_{Im} ; then we have the generalized function, $f(x, t_{\text{Im}}) = f(z)$ for $z = x + it_{\text{Im}}$ and $f(z) = u(x, t_{\text{Im}}) + iv(x, t_{\text{Im}})$ where $u(x, t_{\text{Im}})$ and $v(x_{\text{Im}}, t_{\text{Im}})$ are real functions of the rectangular coordinates x and t_{Im} of a point in space, $P(x, t_{\text{Im}})$. Choose a case such as the origin $z_0 = x_0 + it_{0\text{Im}}$ and consider two cases, one for real increments $h = \Delta x$ and imaginary increments $h = i\Delta t_{\text{Im}}$. For the real increments $h = \Delta t_{\text{Im}}$ we form the derivative $f'(z_0) \equiv df(z) / dz_{z_0}$ which is evaluated at z_0 a

$$f' = \lim_{\Delta x \rightarrow 0} \left\{ \frac{u(x_0 + \Delta x, t_{0\text{Im}}) - u(x_0, t_{0\text{Im}})}{\Delta x} + i \frac{v(x_0 + \Delta x, t_{0\text{Im}}) - v(x_0, t_{0\text{Im}})}{\Delta x} \right\} \quad (11.13a)$$

or

$$\begin{aligned} f'(z_0) &= u_x(x_0, t_{0\text{Im}}) + iv_x(x_0, t_{0\text{Im}}) \quad \text{for} \\ u_x &\equiv \frac{\partial u}{\partial x} \quad \text{and} \quad v_x \equiv \frac{\partial v}{\partial x}. \end{aligned} \quad (11.13b)$$

Again $x = x_{\text{Re}}$, $x_0 = x_{0\text{Re}}$ and $v_x = v_{x\text{Re}}$.

Now for the purely imaginary increment, $h = i\Delta t_{\text{Im}}$ we have

$$f'(z_0) = \lim \Delta t_{\text{Im}} \rightarrow 0 \left\{ \frac{1}{i} \frac{u(x_0, t_{0\text{Im}} + \Delta t_{\text{Im}}) - u(x_0, t_{0\text{Im}})}{\Delta t_{\text{Im}}} + \frac{v(x_0, t_{0\text{Im}} + \Delta t_{\text{Im}}) - v(x_0, t_{0\text{Im}})}{\Delta t_{\text{Im}}} \right\} \quad (11.14a)$$

and

$$f'(z_0) = -iu_{t\text{Im}}(x_0, t_{0\text{Im}}) + iv_{t\text{Im}}(x_0, t_{0\text{Im}}) \quad (11.14b)$$

for $u_{\text{Im}} = u_{t\text{Im}}$ and $v_{\text{Im}} = v_{t\text{Im}}$ then

$$u_{t\text{Im}} \equiv \frac{\partial u}{\partial t_{\text{Im}}} \text{ and } v_{t\text{Im}} \equiv \frac{\partial v}{\partial t_{\text{Im}}}. \quad (11.14c)$$

Using the Cauchy-Riemann equations

$$\frac{\partial u}{\partial x} = \frac{\partial v}{\partial t_{\text{Im}}} \text{ and } \frac{\partial u}{\partial t_{\text{Im}}} = -\frac{\partial v}{\partial x} \quad (11.15)$$

and assuming all principle derivations are definable on the manifold and letting $h = \Delta x + i\Delta t_{\text{Im}}$ we can use

$$f'(z_0) = \lim h \rightarrow 0 \frac{f(z_0 + h) - f(z_0)}{h} = \frac{df(z)}{dz} \Big|_{z_0} \quad (11.16a)$$

and

$$u_x(x_0, t_{0\text{Im}}) + iv_x(x_0, t_{0\text{Im}}) - \frac{\partial u(x_0, t_{0\text{Im}})}{\partial x} + i \frac{\partial v(x_0, t_{0\text{Im}})}{\partial x} \quad (11.16b)$$

with v_x for x and t_{Re} that is $u_{\text{Re}} = u_{x\text{Re}}$, with the derivative form of the charge of the real space increment with complex time, we can define a complex velocity as,

$$f'(z_0) = \frac{dx}{d(it_{\text{Im}})} = \frac{1}{i} \frac{dx}{dt_{\text{Im}}} \quad (11.17a)$$

we can have $x(t_{\text{Im}})$ where x_{Re} is a function of t_{Im} and $f(z)$ and using $h = i\Delta t_{\text{Im}}$, then

$$f'(z_0) = x'(t_{\text{Im}}) = \frac{dx}{dh} = \frac{dx}{idt_{\text{Im}}}. \quad (11.17b)$$

Then we can define a velocity where the differential increment is in terms of $h = i\Delta t_{\text{Im}}$. Using the first case as $u(x_0, t_{0\text{Im}})$ and obtaining $dt_{0\text{Im}} / \Delta x$ (with i 's) we take the inverse. If u_x which is v_x in the $h \rightarrow i\Delta t_{\text{Im}}$ case have both u_x and v_x , one can be zero.

Like the complex 8D space, 5D Kaluza-Klein geometries are subsets of the supersymmetry models. The complex 8-space deals in extended dimensions, but like the TOE models, Kaluza-Klein models also treat $n > 4$ D as compactified on the scale of the Planck length, 10^{-33} cm [5,31].

In 4D space event point, P_1 and P_2 are spatially separated on the real space axis as $x_{0\text{Re}}$ at point P_1 and $x_{1\text{Re}}$ at point P_2 with separation $\Delta x_{\text{Re}} = x_{1\text{Re}} - x_{0\text{Re}}$. From the event point P_3 on the t_{Im} axis we move in complex space from event P_1 to event P_3 . From the origin, $t_{0\text{Im}}$ we move to an imaginary temporal separation of t_{Im} to $t_{2\text{Im}}$ of $\Delta t_{\text{Im}} = t_{2\text{Im}} - t_{0\text{Im}}$. The distance in real space and imaginary time can be set so that measurement along the t_{Im} axis yields an imaginary temporal separation Δt_{Im} subtracts out, from the spacetime metric, the temporal separation Δx_{Re} . In this case occurrence of events P_1 and P_2 can occur simultaneous, that is, the apparent velocity of propagation is instantaneous.

For the example of Bell's Theorem, the two photons leave a source nearly simultaneously at time, $t_{0\text{Re}}$ and their spin states are correlated at two real spatially separated locations, $x_{1\text{Re}}$ and $x_{2\text{Re}}$ separated by $\Delta x_{\text{Re}} = x_{2\text{Re}} - x_{1\text{Re}}$. This separation is a space-like separation, which is forbidden by special relativity; however, in complex space, the points $x_{1\text{Re}}$ and $x_{2\text{Re}}$ appear to be contiguous for the proper path 'travelled' to the point.

11.7 Metaphor Series to Clarify the Transformation of HD Topology

The two stage triple coordinate boost of the UFM transformation rotates the Euclidian space through two sets of three mutually orthogonal complex planes (i.e. the future-past advanced-retarded coordinates). Each

coordinate is simultaneously ortho-rotated to HD in a process that violates the Copenhagen regime quantum uncertainty principle and the usual associated causal conditions. This is required to uncouple the observer from the Euclidian perspective in order to recouple ontologically to the HD perspective.

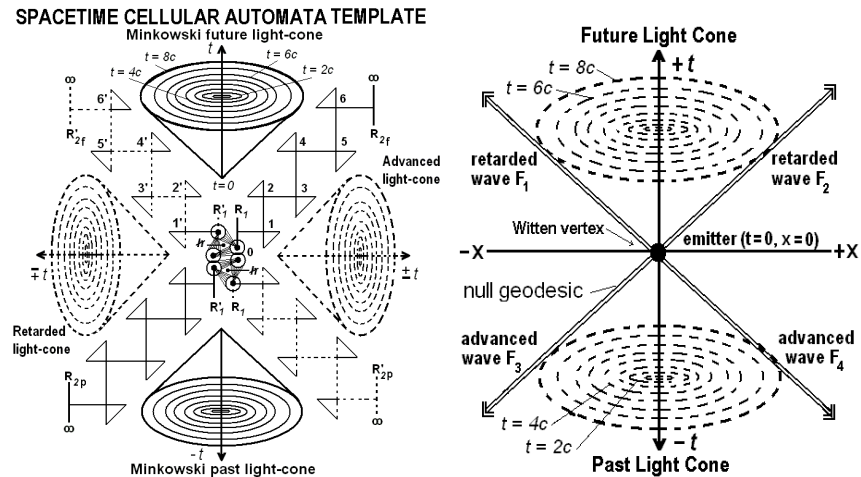


Fig. 11.4 Adaptation of a complex Minkowski light-cone showing advanced-retarded future-past Cramer wavefront transactions with a central Witten Ising lattice string vertex able to undergo symmetry transformations.

Four solutions emerge: two *retarded* (F_1 and F_2) connecting processes in the forward light cone and two *advanced*, (F_3 and F_4) connecting processes in the backward slight cone [28]. These four solutions are

$$\begin{aligned} F_1 &= F_0 e^{-i(-kx-\omega t)}, & F_2 &= F_0 e^{i(kx-\omega t)}; \\ F_3 &= F_0 e^{i(-kx+\omega t)}, & F_4 &= e^{i(kx+\omega t)}. \end{aligned} \quad (11.18)$$

with F_1 for a wave moving in the $(-x, +t)$ direction, F_2 is for a $(+x, +t)$ moving wave, F_3 is for a $(-x, -t)$ moving wave, and F_4 is a $(+x, -t)$ moving wave. F_1 and F_4 are complex conjugates of each other and F_2 and F_3 , are complex conjugates of each other, so that $F_1^+ = F_4$ and $F_2^+ = F_3$. Then the usual solutions to Maxwell's equations are retarded plane wave solutions.

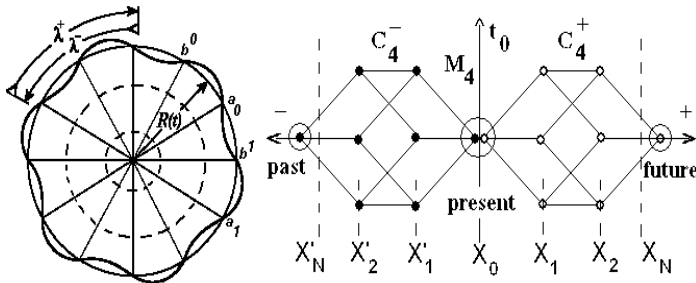


Fig. 11.5. Another conceptual view of the symmetry of a least-unit in UFM Superspace. a) 2D standing wave. b) 12D relationship depicted as points. The $12 \pm C_4$ points represent future-past potenia for a single M_4 point, X_0 the cyclic continuous iteration of which becomes the locus of points for the arrow of time t_0 . The larger center circle represents a Minkowski, M_4 present comprised of the smaller circles at each end representing future/past components that comprise it.

In Fig. 11.5 the twelve points labeled C_4 symbolize a conceptualization of the 12D comprising a fundamental least unit. The complex plane is suppressed for simplicity. Counterpropagating, complex, future-past, ‘hyper-Geon’ elements act in concert to ‘create’ instantaneous harmonic elements of localized Euclidian 3-sphere extension. They are ‘standing wave’ relational spacetime extensions $R(t)$ of the absolute 12D hyperspace that form the fundamental basis of observational reality representing a metric framework for events and interactions. Extension is mediated by the noumenal action principle of the unified field by $F_{(N)} = \aleph_n / R_{(t)}$, where \aleph_n is topological energy of the unified field (see Chaps. 3,4).

We begin discussion of the actual operation of the new transform by introducing the concept of planes or surfaces of constant phase which we hope to eventually correlate with the equilibrium regions on the genus-1 helicoid parking garage. But the starting configuration is shown in Fig. 11.6 below where k is the propagation vector for a plane wave along the z axis and the magnitude of k is the wavenumber

$$\psi \propto e^{i\phi}, \quad \phi = k \cdot r - \omega t \quad (11.19)$$

where $\omega = \omega(k)$ is the dispersion relation and $\lambda = 2\pi / k$ the wavelength. The positions of r at time, t where the phase, ϕ has a fixed value defines the planes of equal phase perpendicular to the propagation vector, k [5].

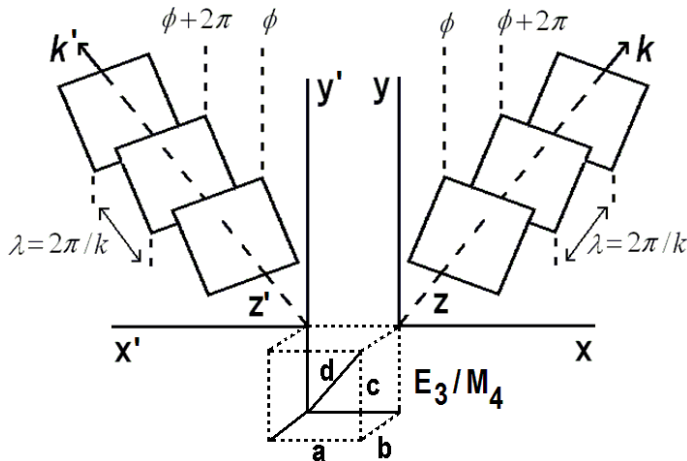


Fig. 11.6 Planes or surfaces of constant phase, ϕ along the z axis for the plane wave propagation vector k . For involute, see the ‘Fano snowflake’ (Chap. 12).

Next we want to associate these planes of equal phase with spherical sectors (Fig. 11.7 below) of the close-packed Riemann sphere least-units tiling the spacetime backcloth and then apply this to the harmonic oscillator properties of the future-past advanced-retarded standing-wave properties of a present instant. A spherical sector is generally formed by rotating a section of a circle about diameter where the volume of the spherical sector would be $V = (D^2 h)/2$ which can be considered to be a torus similar to the energy levels of a harmonic oscillator.

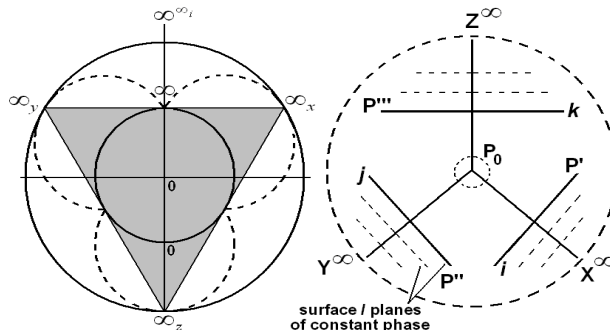


Fig. 11.7 a) Riemann sphere representation of subelements of toroidal phase. b) Combining symbolism of Figs. 11.8 & 11.9 to form hierarchical model of toroidal planes of equal phase.

Hyperspherical Dirac Rotation from LD to HD

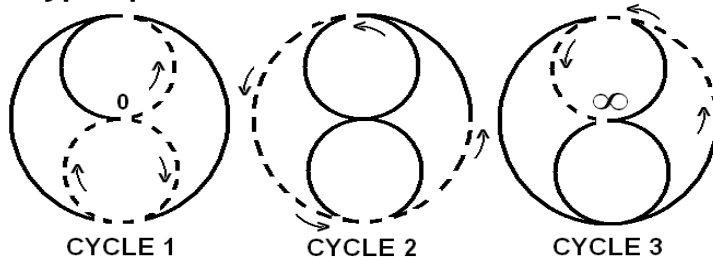


Fig. 11.8. Dirac hyperspherical rotation of the Riemann sphere from Euclidian 3-space to hyperspace during the 360-720° rotation process.

These additional figures above and below are meant to help illustrate some additional conceptual geometrical and topological components needed to develop the UFM transform.

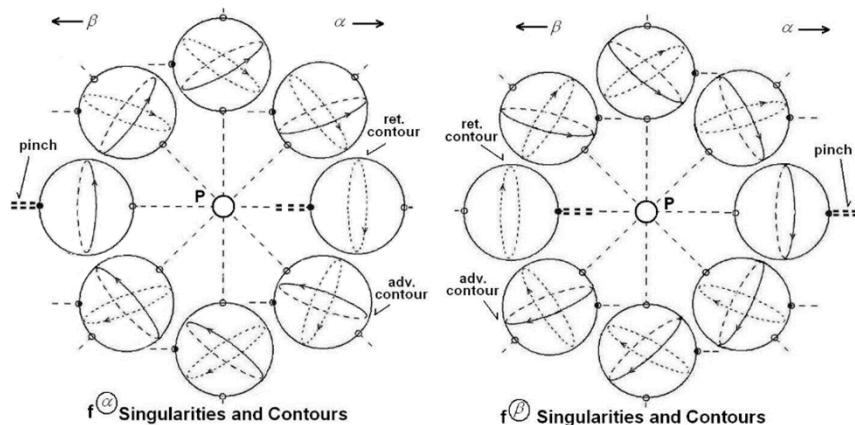


Fig. 11.9 Singularities and advanced-retarded phase contours for the Dirac rotation to reflect duality/Mirror symmetry. Figure adapted from [35].

Referring back earlier in the section to equations 11.32 & 11.33 these later figures are meant to graphically illustrate the action of the basic element of the UFM transform where unlike the Galilean and Lorentz/Poincaré transformations the action is both stationary and along all axes simultaneously. Figure 11.8 is simplistic rendition of the contours and pinches in Fig. 11.9. This is the Dirac spherical rotation originally for the spinor rotation of the electron through 720° which UFM cosmology

suggests is also a conformal scale-invariant parameter of the universe itself. It is easy to see the similarity of Figs. 11.7 to Fig. 11.10; the additional factor is that the topology of the inner core rotates to the outer skin in a continuous-state manner. Figure 11.10 is meant to illustrate (in the context of the other figures here) the additional requirements for boosting and transforming the coordinates, $s \rightarrow t \rightarrow E$.

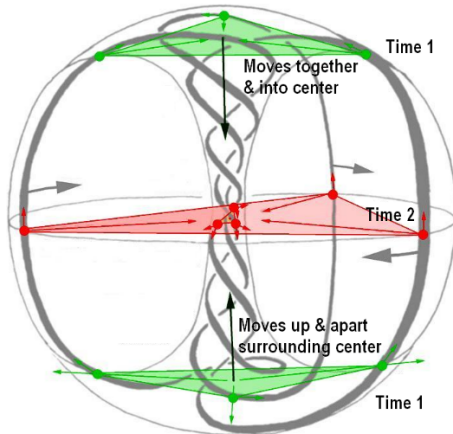


Fig. 11.10 Symbolic of how transformation of inner Euclidian coordinated rotate continuously to become external HD elements. Figure adapted from [36].

These last five figures above represent a final conceptualization as far as our thinking enables us to go at the time of this writing. Simply for the stationary Euclidian observer at point, 0 the first set of rotations and boosts complexify the space to an intermediate domain. Finally, a second set of boosts either recouples the observer to the HD unitary regime or if operated in reverse allows the HD UFM information to enter into the observers' awareness in the Euclidian ground state.

11.8 Spin Exchange Compactification Dynamics and Permutation of Dimensions in the UFM Transformation

Photon mass is not continuously maintained in UFM cosmology but occurs only during a period of internal motion (angular momentum) when the centrum of the wave - the particulate moment, couples to the vacuum; so the photon in propagation cycles harmonically from mass to zero mass as a property of the future-past symmetry of its wave-particle duality. This

is a new property of photon propagation introduced by the continuous-state parameters of UFM cosmology.

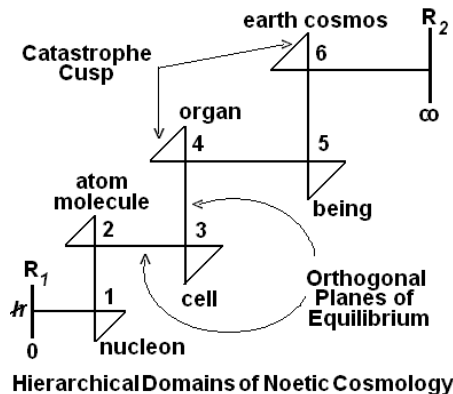


Fig. 11.11. Basic conceptualization of the covariant scale-invariant hierarchical structure and function of UFM cosmology from microscopic to cosmic.

Photon mass anisotropy is a major feature of the UFM model. It is indicative of the ubiquitous occurrence of the properties of spherical rotation discovered by Dirac initially attributed only to the spin of the electron where it 720° instead of 360° to return to the origin. The UFM spacetime Cavity-QED paradigm is based on the fundamental premise that the energetic interplay of the fundamental forces of nature, mass, inertia, gravitation and spacetime is based on a unified symmetry of internal spin-spin coupling and spin exchange compactification with a ‘super quantum potential’ [37] ultimately being the anthropic unitary action and control principle of the evolution of spacetime which within the Einstein Hubble 3-sphere is considered a complex self-organized system which gives it the known properties of such systems [38]. Spin exchange symmetry breaking through the interplay of a unique topological control package orders the compactification process providing a template from which superstring or twistor theory could be clarified if the tenets of Chap. 4 are applied (assuming they are correct). One purpose of compactification dynamics is to allow the Einstein 3-sphere of temporal reality to stochastically ‘surf’ as it were on the superstructure of an HD eternity creating our virtual reality and the perceived arrow of time allowing nonlocal interactions not possible in a Newtonian absolute space. Stated another way, the domain of quantum uncertainty stochastically separates the classical regime from

the unitary regime revealing why large XD can be relativistically unobservable.

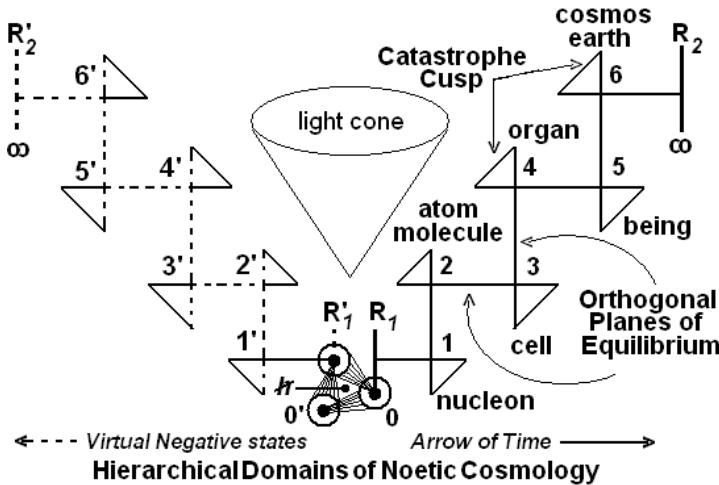


Fig. 11.12. Further conceptualization of the advanced-retarded future-past mirror symmetry/duality of the scale-invariance and function of the ‘standing-wave’ properties of UFM dimensionality from a 0D least-unit (LCU) to 12D limit of the Hubble 3-sphere setting the stage for application to a UFM model arrow of time.

By parallel transport of the topological boundary conditions of the continuous-state dimensional reduction compactification process the deficit-angle produced in the hysteresis loop of the standing-wave eternal present allows half of the parameters to drop out during the ‘leap-frogging’ of coordinate fixing and re-fixing as the awareness of the observer relativistically couples uncouples and re-couples as a baton passing in a relay race to observed reality. This seemingly complicated process creates the arrow of time and also reveals why the XD are not perceived even though they are large in scale during the retarded portion of the process. Only certain pathways for parallel transport by spin exchange dimensional reduction (D down scaling) and superluminal boosting (D up scaling) are allowed by the Wheeler-Feynman symmetry breaking relations in the continuous maintenance of the standing wave present.

It is useful to further clarify the utility of parallel transport begun in association with Fig. 11.13 below in terms of the Regge equations [39] relation to the Bianchi identity of a boundary of a boundary being equal to

zero ($\partial \circ \partial \equiv 0$) [39-41]. Figure 11.13 shows the counter-propagating circular permutations of the face plane of a tetrahedron representing parallel transport which creates a deficit angle [42] allowing uncoupling from Euclidian reality. Allowed pathways and orientations restricted by the symmetry breaking conditions allow boosting of the information or energy associated with one domain to transform by topologically switched parametric up-down conversion into another regime.

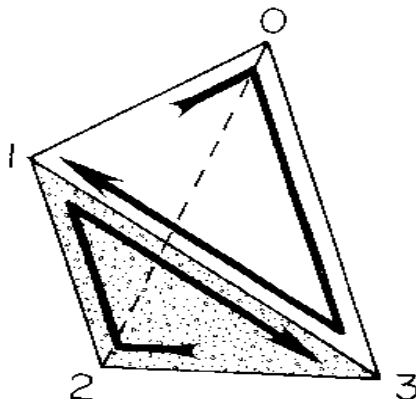


Fig. 11.13. Bianchi identities of absolute parallelism for a tetrahedron.

Ordering vertices as shown in Fig. 11.13 induces an orientation on the tetrahedron's two dimensional boundary, which consists of four oriented triangles by $\partial(0123) = (012) - (013) + (023) - (123)$. This in turn induces an orientation on the edges of the one dimensional boundaries $\partial(012) = (01) - (02) + (12)$. Summing the dimensional boundaries cancels them in pairs [$(01) - (01) = 0$]. This is the Bianchi identity $\partial \circ \partial = 0$ described by the Regge equations for parallel transport where the boundary of a boundary is zero. Or suggesting the tetrahedron is edgeless because the 1D boundary of the 2D boundary of the 2D region is zero [40-42].

11.9 Preparing the UFM Spacetime Transformation

There are several kinds of coordinate transformation, the Galilean transformation for small velocities, the Lorentz-Poincaré transformations for relativistic velocities and a newly proposed UFM transformation for ontological considerations.

Multiverse cosmology implies that so-called ‘real space’ is a relational standing wave subspace of an absolute HD space, where a continuous-state Dirac type spin-exchange dimensional reduction compactification process is central to the scale invariant periodic Ising model topological structure. It is useful to initiate the description by introducing a toy model of the lower D space and build it up toward the actual HD space.

Maintaining the extended Wheeler-Feynman-Cramer property of the present as a function of the advanced-retarded future-past (Figs. 11.12 & 11.4, 11.5). We begin by describing a discrete Einstein type point in the relational spacetime manifold. Since points are defined as singularities where dimensionality breaks down, a dimensionless 0D point cannot be topologically ‘covered’. This property will be shown to be a valuable criterion as a ‘hole’ for oriented orthogonal superluminal boosts in the UFM transformation. This also contrasts the nature of continuity (Absolute space) with discreteness (relational space); points are not absolute because the universe turns out not to be a Newtonian continuum. A transformation between inertial frames with the same orientation is called a boost. A Galilean boost is:

$$\begin{aligned} x' &= x'(xt) = y - vt \\ t' &= t'(x, t) = t \end{aligned} \tag{11.20}$$

11.10. Developing the Line Element for UFM Superspace

The real parameters for the line element in standard Einstein-Minkowski space, M_4 is

$$dS_0^2 = dx_1^2 + dx_2^2 + dx_3^2 - dt^2 \tag{11.21}$$

to which UFM superspace must make correspondence. We begin by developing the associated future-past and advanced-retarded 8D complex dual spaces following work initiated by Amoroso [29,38], Rauscher [43,44], Cole [45] and Hansen & Newman [46] on complex Minkowski space, $\hat{M}^4 \pm C^4$. For 12-space variable, Z^μ where $Z^\mu = \pm X_{\text{Re}}^\mu + iX_{\text{Im}}^\mu$ and $Z^{*\nu}$ is the complex conjugate of Z^μ so that $Z^\nu = \pm X_{\text{Re}}^\nu - iX_{\text{Im}}^\nu$ with the 12-space differential line element as

$$dS^2 = \pm \eta_{\mu\nu} dZ^\mu dZ^{*\nu} \quad (11.22)$$

with indices running 1 to 12 where $\pm X_{\text{Re}}$ is $\pm x_{\text{Re}}, \pm y_{\text{Re}}, \pm z_{\text{Re}}, \pm t_{\text{Re}}$, the usual 4D metric plus addition of Wheeler-Feynman-Cramer future-past conditions [27,28]. We then must finally introduce the additional complex UFM relations, $\pm N_8$ to include the advanced-retarded Dirac annihilation-creation ladder operators to complete the parameters required for the complex UFM transformation

$$W^{jk} = \pm [Z_{\text{Re}}^j + iZ_{\text{Im}}^k], \pm [\bar{Z}_{\text{ret}}^j + \bar{Z}_{\text{adv}}^k] \quad (11.23)$$

again with indices $j, k = 1$ to 12. Then for complex advanced space, $+N_4$ we have $Z_{\text{adv}}^{jk} = X_{\text{Re}(\text{adv})}^{jk} + iX_{\text{Im}(\text{adv})}^{jk}$, $\bar{X}_{\text{Re}(\text{adv})}^{jk} + \bar{X}_{\text{Im}(\text{adv})}^{jk}$ with $j, k = 1$ to 12. For complex retarded space, $-N_4$ the relation is $Z_{\text{ret}}^{jk} = X_{\text{Re}(\text{ret})}^{jk} + iX_{\text{Im}(\text{ret})}^{jk}$, $\bar{X}_{\text{Re}(\text{ret})}^{jk} + \bar{X}_{\text{Im}(\text{ret})}^{jk}$ with indices running $k = 1$ to 12. Then the UFM line element is

$$\Delta W^2 = \pm (\eta_{\mu\nu} dZ^\mu dZ^{*\nu} + \eta_{jk} dZ_{\text{adv}}^{jk} Z_{\text{ret}}^{jk}) \quad (11.24)$$

We have postulated an additional set of transformations beyond the Lorentz-Poincaré called the ‘noetic group’ with another causal relationship distinct from the strong causality of the standard model allowing spatially separated systems to exchange information without orthodox collapse of the wave function. This occurs through a nonlocal coupling of unitary field effects which produce a geodesic deviation mediated by intentionality or anthropic teleological control depending on the segment of the scale-invariant regime being acted upon. The dynamics of particle and fields are described by various groups of transformations; the Galilean group describes Newtonian mechanics, and the Lorentz transformations describe modern relativistic and quantum theories. This action is outside the current limits described by the Galilean, Lorentz and Poincaré groups of transformations. This additional UFM transformation of a normally null path is allowed in extended electromagnetic theory by nonzero restmass photon anisotropy [47] without violating gauge theory

[48]. The correspondences in physical theory, for example the reduction of quantum mechanics to classical mechanics or the recovery of thermodynamics from its successor statistical mechanics will also apply in relation to the mind and the nature of time. A correspondence between a complementary stable and unstable causality is shown to reduce to the null path of the standard model.

Current thinking for an ‘energy regime’ extends only to the indicia provided by the proposal of primal Kaluza-Klein theory of energy as a 5th dimension [49], Eastern philosophical dogma of ‘consciousness as the monistic ground of all being’ [50] or the Judeo-Christian doctrine ‘the spirit of God fills the immensity of space’ [34] which physicists like Einstein and Schrödinger equated with the unified field. Behind the facade of reality lies an atemporal hyper-geon [51] or ubiquitous unitary regime that is likened unto an ‘ocean of light’. Any usual EPR state is a parametric down-conversion [52] of simultaneity or bi-local entanglement of this holographic state [53,54] into the fabric of the spacetime view of the Euclidian observer. Our immediate question is if one is to parametric up-convert [52] such an entangled EPR state between two locally separated observers what should the description of the transformation to that state entail? The Lorentz transform [30,55] adds a relativistic warp factor to the Galilean transform for both x and t coordinates. In the UFM model do the rotating ends of the standing-wave strings have opposing ends with a velocity gradient or range from $v < c \rightarrow v \geq c$ which could be ignored for the purpose here if our interest remained only in delineating the final state; but the coupling/uncoupling process to this state’s intermediates would require elucidation of the dynamics of the complex topological gradient.

Another major issue is that resonance modes for each intermediate coordinate boost individually entail a description of orthogonal planes of equal phase; but the final result is the imbedding of the observer’s awareness in the surface of a hypersphere of information or charge equal to the area/volume of the topology where the mutually exclusive orthogonality of the intermediates is returned to parallelism allowing or producing independence from the initial Euclidian plane. We have two major problems at the moment keeping us from rigorously formalizing the UFM transformation;

- Where to draw the line in the sand. We have a 12D holographic model, but at this point following the Kaluza-Klein logic of ‘energy as a 5th dimension [49]; how many dimension does the transform requires to both contain and transform the topology in order to ontologically exchange the

information. So ‘today’ we make some best guesses and introduce a preliminary UFM transform based on postulates of M-theory and Anthropic philosophy [56]. If we start with the premise of string theory that ‘matter resides on the 3-brane and gravity is free to pass between branes’, then by including the premises of duality/mirror symmetry along with UFM cosmologies embrace of Wheeler-Feynman future-past symmetry conditions [27,28] we seem to end up with a local-nonlocal 6D QED spacetime cavity.

- Secondly, if the use of the transform happened to be the exchange of mental information between two separated subjects with the usual x' , x Lorentz coordinate separation which could be locally mapped; until the special class quantum computer is built there is no known manner of finding the correct holographic hyperplane resonance mode to couple the two systems to be entangled by the transform. Even if one logically assumes because of the holographic principle that the information to be transferred is ubiquitous there is still the same problem in initializing the receiver.

Physical understanding of coordinate transformation laws began with the Galilean transform for correlation between two Newtonian coordinate systems X' , X with velocity, $v < c$ with time absolute and independent of the motion of the different observers

$$x' = x - vt, \quad y' = y, \quad z' = z, \quad t' = t. \quad (11.25)$$

With the advent of quantum theory and special relativity the need for the Lorentz/Poincaré group of transformations arose for velocities, $v \leq c$ and time becoming a new concept of spacetime

$$x' = \gamma(x - vt), \quad y' = y, \quad z' = z, \quad \gamma(t - v_x/c^2) \quad (11.26)$$

with the ‘warp factor’ $\gamma = 1/\sqrt{1 - v^2/c^2}$. Now the need has arisen to fully integrate not only the role but also an inherent imbedding of the very existence of the observer as an essential element of the anthropic Multiverse; for which a new set of ‘UFM’ transformations is required. How to proceed has been fraught with challenging conceptual dilemmas like elucidating the proper cosmological framework and the restrictions imposed by extended em-theory, quantum and M-theories. Another challenge is reflected in what the nature or basis of the final state the

transform should be like, where it is and what happened to the information; because the observer has not necessarily traveled anywhere in Euclidian space as in the former transformation laws. We consider the Galilean-Lorentz-Poincaré transforms to reflect a virtual quantum reality of ‘parametric down-converted’ states; and what the new UFM transform requires is a description of a ‘parametric-upconverted’ state [52] that entangles the two observers in an HD regime with time again becoming independent of the final state. This is different than Newtonian temporal independence in that the Galilean conditions have no relevant quantum entanglement; and the Lorentz-Poincaré basis, although EPR entangled is lacking the overt simultaneity between the two observers that would be considered a violation of Copenhagen causality and the uncertainty principle. Also instead of the focus being for quanta in motion along a manifold the interest here lies with the information field itself and therefore must address conditions of relativistic quantum field theory with static de Broglie waves for all coordinates, x, y, z & x', y', z' simultaneously.

With this in mind we might begin outlining the UFM transform for a coordinate regions x', y', z' and x, y, z with each axis having their own warp factors, α, β, γ respectively as

$$\begin{aligned} x' &= \alpha(x - vt), \quad y' = \beta(y - vt), \quad z' = \gamma(z - vt), \\ t'_x &= \alpha(t_x - v_x / c^2), \quad t'_y = \beta(t_y - v_y / c^2), \quad t'_z = \gamma(t_z - v_z / c^2), \end{aligned} \quad (11.27)$$

with γ for example the usual Lorentz warp term

$$\gamma' \equiv \frac{1}{\sqrt{\left(\frac{v_x^2}{c^2} - 1\right)}} \quad (11.28)$$

But this is far too simplistic. In order to add Dirac spherical rotation as an element of the transformation for rotational parameters into HD one needs to apply additional superluminal Lorentz boost conditions and the XD supersymmetry conditions of UFM 12-space which is comprised of an energy dependent Minkowski spacetime present, \hat{M}_4 derived from an extended HD Cramer type [28] transaction; model where this ‘eternal’ present is a virtual standing-wave of Wheeler-Feynman advanced-retarded

future-past elements [27,57]. It is well known that superluminal Lorentz boosts may transform spatial dimensions into temporal dimensions [43,44]. The UFM transform requires a double boost; the former and a second boost which transforms the complex spatial dimensions into the original ‘Kaluza-Klein’ concept of energy dimensions [49] equated here with the unitary field. For simplicity we initially consider just the initial superluminal Lorentz transformation (boost), $v_x = \infty$ only along the positive x direction where the space and time vectors in a real Minkowski space, \tilde{M}_4 cyclically transform as [43]

$$x' = +t, \quad y' = -iy, \quad z' = iz, \quad t' = x \quad (11.29)$$

for real and imaginary parts separately, where x, y, z, t are real quantities for one frame, and x', y', z', t' are the real quantities in the second frame. For the initial 6D representation in complex Minkowski space, M_6 the above superluminal boost ($v_x = +\infty$) becomes [5,31,43,44]

$$\begin{aligned} x'_{\text{Re}} + ix'_{\text{Im}} &= t_{x,\text{Re}} + it_{x,\text{Im}}, \quad y'_{\text{Re}} + iy'_{\text{Im}} = y_{\text{Im}} - iy_{\text{Re}}, \\ z'_{\text{Re}} + iz'_{\text{Im}} &= z_{\text{Im}} - iz_{\text{Re}}; \quad t'_{x,\text{Re}} + it'_{x,\text{Im}} = x_{\text{Re}} + ix_{\text{Im}}, \\ t'_{y,\text{Re}} + it'_{y,\text{Im}} &= t_{y,\text{Im}} - it_{y,\text{Re}}, \quad t'_{z,\text{Re}} + it'_{z,\text{Im}} = t_{z,\text{Im}} - it_{z,\text{Re}}. \end{aligned} \quad (11.30)$$

The points of interest are that a superluminal Lorentz boost cyclically transmutes spatial dimensionality into temporal dimensionality while also preserving the magnitude of the line element but not the sign:

$$-x'^{\mu}x^{\nu} = x^{\mu}x^{\nu}, \quad (11.31)$$

where indices μ and ν run over 1,2,3,4 representing 1 as the time vector and 2,3,4 as spatial vectors with signature (+++-). Situation (11.29) must be carried out additionally for the y and z coordinates which we will discuss later on.

There are still a few things left to do; a second Lorentz boost to convert the first boosted $t_{x,\text{Re}} + it_{x,\text{Im}}$ dimensions to ‘energy’ dimensions is required to complete this component of the transformation such that $s \rightarrow t \rightarrow E$ which isn’t so terrible if we remember that the original

Kaluza-Klein model considered energy as the 5th dimension [49] or that in the usual signature +,+,+,- spatial dimensions could be considered as ‘realized’ or cut-offs of a topological field whereas the temporal dimension is a ‘field’ in flux. Of course here we consider this ‘energy’ regime as an indicator of a de Broglie-Bohm super-quantum potential [37] or in still higher dimensionality as the anthropic action principle. This additional HD domain is an essential part of the hysteresis loop of least-unit propagation as an inherent element of the 12D continuous-state.

§11.1 First boosted complex dimension $\dot{x}_{\text{Re}} + i\dot{x}_{\text{Im}} \rightarrow t_{x,\text{Re}} + it_{x,\text{Im}}$ is second boosted to an 8D hypersurface $E_{w,\text{Re}} + iE_{w,\text{Im}}$ where E_w is an HD Kaluza-Klein-like hypercube energy field coordinate. When the secondary boost is performed simultaneously along all 6 positive and negative axes including the temporal dimensions the temporal dimensions cancel and the ‘attachment’ of the observer couples to hypersphere coordinates.

Before elaborating on §11.1 we introduce another aspect of the transform. We have mentioned that in the UFM transformation it is necessary to double boost all three coordinates, x, y, z simultaneously such that $s \rightarrow t \rightarrow E$; this includes advanced-retarded future-past Cramer-like standing-wave parameters such that the double boost includes coordinates, $\pm x, y, z$ which could be considered action on a dual/mirror symmetry Calabi-Yau 3-form. For a boost singling initially an arbitrary direction with velocity, \vec{v} it is necessary to decompose the spatial vectors, \vec{r} into perpendicular, \vec{r}_\perp and parallel, \vec{r}_\parallel components to the velocity vector, \vec{v} ; then one may ‘warp’ only the \vec{r}_\parallel component of \vec{v} by the γ factor

$$\begin{aligned} t' &= \gamma \left(t - \frac{\vec{r} \cdot \vec{v}}{c^2} \right) \\ \vec{r}' &= \vec{r}_\perp + \gamma (\vec{r}_\parallel - \vec{v}t) \end{aligned} \quad (11.32)$$

where the γ factor then becomes

$$\gamma \equiv \frac{1}{\sqrt{1 - \vec{v} \cdot \vec{v} / c^2}} + \vec{r}' = \vec{r} + \left(\frac{\gamma - 1}{v^2} (\vec{r} \cdot \vec{v}) - \gamma t \right) \vec{v}. \quad (11.33)$$

This allows the perpendicular components, \vec{r}_\perp to remain stationery or coupled to the original local position of the observer. This separation of vectors allows an easier description for the implementation of § 11.1 for an Ising model rotation of \vec{r}_\parallel by a $0 \rightarrow \infty$ rotation of the Riemann sphere while the \vec{r}_\perp components remain coupled to the stationery Euclidean regime.

11.11 Dirac Spherical Rotation Inherent to Transformation of the Fundamental Least-Unit

Typically, the Dirac dual (2π) spinor rotation applies to the observation that an electron undergoes 720° of rotation (not the usual 360°) before returning to the initial orientation. Traditional thinking has assumed this to be some property of matter. But the discovery of the complex structure of spacetime has shown that this is not a property fundamental to the electron; but rather to the superspace the electron is imbedded in and part of. Dirac spherical rotation as it is also called, is more fundamentally a primary property of space than it is matter. This is revealed in the complex hierarchical structure of the least unit discussed in the paper.

Another version of the Dirac string trick is called the Philippine wine dance. A glass of water held in the hand can be rotated continuously through 720° without spilling any water. These types of geometrical demonstrations are related to the physical fact that an electron has spin $1/2$. A particle with spin $1/2$ is something like a ball attached to its surroundings with string. Its amplitude changes under a 360° (2π) rotation and is restored by rotation of 720° (4π). The formal description of such complex phenomena typically requires sophisticated mathematics (algebra, group theory, topology, quaternions...) since they are not part of everyday experience.

According to Kauffman, [58] features of certain spin networks can be viewed as particles with similarities to Bosons and Fermions of the standard model of particle physics by looking at topological elements of the Artin braid group [59-62] that could be used as the basis for introducing quantum numbers. The focus of Kauffman et. al. is the manipulation of braid forms, not specific correlations to actual physics, but the work establishes a useful basis for physical implications in future works especially for twist words for fermions that can be matched to quantum numbers such as weak isospin, hypercharge, baryon number or

lepton number, for example [58]. Kauffman says ‘The spinor rotation does not contain a twist of a knot (A knot is the closure of specific braids). What occurs in the Dirac ‘knot trick’ is that a certain kind of belt twist can model the fact that the first homotopy group of the rotation group $\text{SO}(3)$ is $\text{Z}/2\text{Z}$. This can be easily visualized giving an understanding of how the phase change in a fermion wave-function can occur as the result of a rotation in 3-space which can be represented via $\text{SU}(2)$ on the quantum wave function with $\text{SU}(2)$ appearing relative to $\text{SO}(3)$ as its double covering space’ [62].

The twist as demonstrated with a belt happens in 3-space. But this topology is not directly associated with a geometric linking of an electron with its surroundings. We only get there (using present theory) by noting that any quantum process must be modeled by a family of unitary transformations. And then a 360° rotation will be mapped up into $\text{SU}(2)$ and end up on the second sheet of the two sheeted covering space $\text{SU}(2)\text{-}\text{SO}(3)$. The topology of this covering space contains the essence of the Dirac belt trick. But the belt trick itself is part of something occurring in 4D, namely the quaternions. See [63] for a discussion of this relationship. A topological theory of the electron where the Dirac ‘belt trick’ rotation property is connected directly with the physical properties of a particle is currently stymied by the standard Copenhagen quantum theory because there is no ‘physical particle’ only the result of measurements of an electron wave function which gives only statistical parameters of the wave function.

But as well-known this is not true in the de Broglie-Bohm-Vigier (DBV) causal stochastic interpretation of quantum theory where wave and particle are physically real and may both exist simultaneously [64]. But DBV has not been completed. We believe when this explanatory gap has been filled it will show that there is no Quantum Gravity. The quantum regime ends with Copenhagen and the unification of quantum theory and gravity will be shown to occur at the level of unitarity. Our view here is initially more conceptual, we think that a certain rotation point of the belt where the twist occurs in 3D becomes like a Klein bottle that can only be untwisted by rotation through 4D where it is not intertwined. We encourage the reader to perform the little trick with belts or strings. When the electron is rotated 360° the 3D observer sees the twist that in that perspective cannot be untied except by another 360° rotation that occurs in 4D.

In string/brane theory there is a putative Kaluza-Klein spin tower compactification gradient of T-duality/Mirror symmetry for a pair of Calabi-Yau 3-forms or Kahler manifolds where the raising and lowering

of the dimensionality with the string/brane tension-coupling parameters passes through Fermi-odd and Bose-even spin symmetries relating the branes to each other. Our postulate is that the rotation of the electron is indicative of a topological process that might be conformally scale-invariant through this whole convoluted hierarchy of dimensionality...We assume, the Dirac 360-720° spherical spinor rotation of the electron contains a 'pinch or twist' in the midst of the transformation assumed to be indicative of a 4D topological background component of the rotation.

Is there a braid-form that might be scalable to even higher dimensions; a form that might require the mirror/dual symmetry conditions purported to occur in string-brane topologies to perform the pinch and unpinch? The Dirac spherical rotation concept appears to be indicative of a covariant scale invariant cosmological principle applying to the entire dimensional nature of reality itself not just the electron. This cosmological twist then would occur as the Copenhagen regime separating Newton classical mechanics from unitarity. We have done our best to introduce an empirical protocol to falsify this prediction (low energy methods without accelerator that can also test string theory).

11.12 Final Thought on the UFM Spacetime Transformation

UFM multiverse cosmology implies that so-called 'real space' is a relational standing wave subspace of an absolute HD space, where a continuous- state Dirac type spin-exchange dimensional reduction compactification process is central to the scale invariant periodic Ising model topological structure. It is useful to initiate the description by introducing a toy model of the lower D space and build it up toward the actual HD space.

Maintaining the extended Wheeler-Feynman-Cramer property of the present as a function of the advanced-retarded future-past (Figs. 11.3, 11.4 above). We begin by describing a discrete Einstein type point in the relational spacetime manifold. Since points are defined as singularities where dimensionality breaks down, a dimensionless 0D point cannot be topologically 'covered'. This property will be shown to be a valuable criterion as a 'hole' for oriented orthogonal superluminal boosts in the UFM transformation. This also contrasts the nature of continuity (Absolute space) with discreteness (relational space). Points are not absolute because the universe turns out not to be a Newtonian continuum, but holographic and therefore the information ubiquitous, that is the same

as being nowhere because one does not currently know how to address an infinite number of nonlocal nilpotent possibilities in a manner that automatically finds the one. In 3-space the unique signifier of an object is simply position; but in a holographic HD what does position mean in Einstein's relativistic sense of riding a photon and being everywhere at once. How does one plumb a point in that infinite ocean? But it is currently no trivial manner to mechanically create the simultaneity by parametric up-conversion that is so easily created by parametric down-conversion. But where in the wide holographic multiverse is this? How could it be accessed? MacKinnon [65] has given an idea that may prove helpful; he says a stationery de Broglie wave packet in some specific location is a result of a focus of the de Broglie waves of all observers in the whole universe.

Secondly, what conditions does string theory impose on the process. String theory states that 'matter resides on the 3-brane and gravity is free to pass between'. With duality/mirror symmetry this would take care of 6D. There are three time dimensions in UFM cosmology leaving three for the quantum or anthropic potential for a total of 12D. UFM cosmology equates gravitons with the unified field of anthropic information, but this doesn't yet help us either. Where do we draw the line? Einstein said 'if one could ride a photon, one could circumnavigate the universe without the passage of time'. Time is removed in the LSXD brane-world of the UFM transform. What is a field? In 3-space a field has a coordinate representation; but how can this be described in an ontological holographic arena of infinite potentia where 'something' is everywhere and nowhere? In this domain of ubiquity, the railroad tracks do not recede because of the atemporality; this is like viewing the inside and outside rotations of Fig. 11.10 simultaneously. So for the moment we can only go as far as intermediate stationery simultaneous coordinate boosts from E^3 to W^8 .

We are 'flatlanders' [66] to the complete nature of the multiverse. This is the great separator of the observers' awareness from the infinite potentia of noumenal reality of which the temporal reality of everyday existence is only a limited shadow, a virtual subspace. This entails a subtractive process that produces the arrow of time. One could say a stroboscopic beat frequency of the holophote action of the unitary field subtracts out the additional HD parameters because this mirror symmetric wave-particle duality of the topology of reality is a form of HD harmonic oscillator with nodes of constructive and destructive interference. Plato's cave again.

We are comprised of the 'matter', which is actually a resonant array of domain walls comprised mostly of empty space, projected from this

fundamental absolute space or potentia; and the observers' awareness is likewise coupled to that limited lower part of it, and imbedded in this same material. It is generally known that the standard models of quantum theory and cosmology do not include awareness or give an adequate description of the nature of time; suggesting that the elucidation of these ideas must come from extended theoretical insights; perhaps like those offered here. Human perception is indicative of a flow of time - from past, to present to future in accordance with the 2nd law of thermodynamics by appropriate changes in entropy of the system observed as it undergoes evolution. Thus the observed temporal order seems related to entropic order; and these dynamics constitute how we perceive 'action' or translation in this particular dimension, the dimension of time. It is a stretch; but probably the whole thermodynamic-entropic process is ultimately just a razzmatazz for the myopic virtual reality of the observer [67]. Believe it or not...

References

- [1] Kaloper, N., March-Russell, J., Starkman, G.D. & Trodden, M. (2000) Compact hyperbolic extra dimensions: branes, Kaluza-Klein modes, and cosmology, Physical Review Letters, 85(5), 928.
- [2] Randall, L. & Sundrum, R. (1999) An alternative to compactification, Physical Review Letters, 83(23) 4690.
- [3] Randall, L. (2006) Warped Passages: Unravelling the Universe's Hidden Dimensions, London: Penguin.
- [4] Randall, L. (2002) Extra dimensions and warped geometries, Science, 296 (5572) 1422-1427.
- [5] Amoroso, R.L. & Rauscher, E.A. (2009) The Holographic Anthropic Multiverse: Formalizing the Ultimate Geometry of Reality, Singapore: World Scientific.
- [6] R.L. Amoroso, L.H. Kauffman & P. Rowlands (eds.) (2013) The Physics of Reality: Space, Time, Matter, Cosmos, World Scientific, Singapore.
- [7] R.L. Amoroso, L.H. Kauffman & P. Rowlands (eds.) (2016) Unified Field Mechanics: Natural Science Beyond the Veil of Spacetime, Singapore: World Scientific.
- [8] Farmelo, G. (2009) The Strangest Man, The Hidden Life of Paul Dirac, Mystic of the Atom, Basic New York: Perseus.
- [9] Close, F. (2011) The Infinity Puzzle: Quantum Field Theory and the Hunt for an Orderly Universe, New York: Basic Books.
- [10] Elitzur, A.C. & Vaidman, L. (1993) Quantum mechanical interaction-free measurements, Found. Phys. 23; 987-997.
- [11] Kwiat, P., Weinfurter, H., Herzog, T., Zeilinger, A. & Kasevich, M. (1995) Interaction-free quantum measurements, Phys. Rev. Lett. 74, 4763-4766.
- [12] du Marchie Van Voorthuysen, E.H. (1996) Realization of an interaction-free measurement of the presence of an object in a light beam, Am. J. Phys. 64:12; 1504-1507; or arXiv:quant-ph/9803060 v2 26.
- [13] Simon, S.H. & Platzman, P.M. (1999) Fundamental limit on "interaction free" measurements, arXiv:quant-ph/9905050v1.

- [14] Vaidman, L. (1996) Interaction-free measurements, arXiv:quant-ph/9610033v1.
- [12] Paraoanu, G.S. (2006) Interaction-free measurements with superconducting qubits, Physical Rev. Letters 97, 180406.
- [15] Vaidman, L. (2001) The meaning of the interaction-free measurements, arXiv:quant-ph/0103081v1.
- [16] Vaidman, L. (2001) The paradoxes of the interaction-free measurements, arXiv:quant-ph/0102049v1.
- [17] Vaidman, L. (2000) Are interaction-free measurements interaction free?, arXiv:quant-ph/0006077v1.
- [18] Helmer, F., Mariantoni, M., Solano, E. & Marquardt, F. (2008) Quantum, Zeno effect in the quantum non-demolition detection of itinerant photons, arXiv:0712.1908v2.
- [19] Facchi, P. Lidar, D.A. & Pascazio, S. (2004) Unification of dynamical decoupling and the quantum Zeno effect, Phys Rev A 69, 032314; or arxiv:quant-ph/0303132.
- [20] Facchi, P. & Pascazio, S. (2002) Quantum Zeno subspaces, arXiv:quant-ph/0201115v2.
- [21] Kwiat, P.G. White, A.G., Mitchell, J.R., Nairz, O., Weihs, G. Weinfurter, H. & Zeilinger, A. (1999) High-efficiency quantum interrogation measurements via the quantum Zeno effect, Phys. Rev. Lett. 83, 4725-4728; or arXiv:quant-ph/9909083v1.
- [22] Amoroso, R.L. (2010) Simple resonance hierarchy for surmounting quantum uncertainty, in R.L. Amoroso,, P. Rowlands, & S. Jeffers (eds.) AIP Conference Proceedings, Vol. 1316, No. 1, pp. 185-193.
- [23] Amoroso, R.L. & E.A. Rauscher, E.A. (2010) Empirical protocol for measuring virtual tachyon/tardon interactions in a Dirac vacuum, in R.L Amoroso, P. Rowlands & S. Jeffers (eds.) Search for Fundamental Theory, AIP Conf. Proc. (Vol. 1316, No. 1, p. 199, 2010).
- [24] Dirac, P.A.M. (1952) Nature (London) 169, 702.
- [25] Cufaro, N., Petroni, C. & Vigier, J-P (1983) Dirac's ether in relativistic quantum mechanics, Found. Phys., 13, 253-286.
- [26] Burns, J.E. (1998) Entropy and vacuum radiation, Found. Phys. Let. 28:7; 1191-1207.
- [27] Wheeler, J.A. & Feynman, R. (1945) Rev. Mod. Physics, 17, 157.
- [28] Cramer, J.G. (1986) Transactional interpretation of quantum mechanics, Rev. of Modern Physics, 58:3; 647-687.
- [29] Amoroso, R.L. (2010) (ed.) Complementarity of Mind and Body: Realizing the Dream of Descartes, Einstein, and Eccles, New York: Nova Science Publishers.
- [30] Lorentz, H.A. (1904) Electromagnetic phenomena in a system moving with any velocity less than that of light, Proc. Acad. Science Amsterdam IV, 669-678.
- [31] Rauscher, E.A., & Amoroso, R.L. (2011) Orbiting the Moons of Pluto: Complex Solutions to the Einstein, Maxwell, Schrödinger, and Dirac Equations, Singapore: World Scientific.
- [32] Bilaniuk, O.M., & Sudarshan, E.G. (1969) Particles beyond the light barrier, Physics Today, 22(5), 43-51.
- [33] Zeh, H-D (1989) The Physical Basis of the Direction of the Arrow of Time, New York: Springer.
- [34] Kafatos, M., Roy, S. & Amoroso, R.L. (2000) Scaling in cosmology and the arrow of time, in R. Buccheri & M. Saniga, (eds.) Studies on the Structure of Time: From Physics to Psych(patho)logy, Dordrecht: Kluwer.
- [35] Penrose, R. (1982) Real-space topology for advanced-retarded twistor functions, Twistor Newsletter, No. 14, pp. 16-18.
- [36] Tenen, S. & Tenen, L. (2010) The Meru Foundation, www.meru.org/.

- [37] Holland, P.R. (1995) *The Quantum Theory of Motion: An Account of the de Broglie-Bohm Causal Interpretation of Quantum Mechanics*, Cambridge: Cambridge Univ. Press.
- [38] Amoroso, R.L & Amoroso, P.J. (2004) The fundamental limit and origin of complexity in biological systems: A new model for the origin of life, in D. Dubois, (ed.) *Computing Anticipatory Systems, Proceedings of CASYS04*, 6th Int, Conf., Liege, Belgium, 11-16 Aug, 2003, AIP Proceedings Vol. 718, pp. 144-159.
- [39] Misner, C.W., Thorne, K.S. & Wheeler, J.A. (1973) *Gravitation*, San Francisco: W.H. Freeman.
- [40] Cartan, E. (1966) *The Theory of Spinors*, New York: Dover.
- [41] Cartan, E. (1979) *Elie Cartan - Albert Einstein Letters on Absolute Parallelism 1929-1932*, R. Debever (ed.) Princeton: Princeton Univ. Press.
- [42] Schutz, B.F. (1980) *Geometrical Methods of Mathematical Physics*, Cambridge: Cambridge Univ. Press.
- [43] Rauscher, E.A. (1993) *Electromagnetic Phenomena in Complex Geometries and Nonlinear Phenomena, Non-Hertzian Waves and Magnetic Monopoles*, Millbrae: Tesla Books.
- [44] Rauscher, E.A. (2002) Non-Abelian gauge groups for real & complex Maxwell's equations, in R.L. Amoroso, G. Hunter, S. Jeffers & M. Kafatos, (eds.) *Gravitation & Cosmology: From the Hubble Radius to the Planck Scale*, Dordrecht: Kluwer.
- [45] Cole, E.A.B. (1977) *Il Nuovo Cimento*, 40:2, 171-180.
- [46] Hansen, R.O. & Newman, E.T. (1975) *Gen. Rel. and Grav.* 6, 216.
- [47] Amoroso, R.L., Kafatos, M. & Ecimovic, P. (1998) The origin of cosmological redshift in spin exchange vacuum compactification and nonzero rest mass photon anisotropy, in G. Hunter, S. Jeffers & J-P Vigier (eds.) *Causality and Locality in Modern Physics*, Dordrecht: Kluwer.
- [48] Atchison, I. & Hey, A. (1982). *Gauge Theories in Particle Physics*, Bristol: Adam Hilger.
- [49] Overduin, J.M. & Wesson, P.S. (1997) Kaluza-Klein gravity, *Physics Reports*, 283, pp. 303-378.
- [50] Goswami, A. (1995) *The Self-Aware Universe*, New York: Putnam.
- [51] Wheeler, J.A. (1955) Geons, *Physical Review*, 97:2, 511-536.
- [52] Marshall, T. (2002) Engineering the vacuum, in R.L. Amoroso, G. Hunter, S. Jeffers & M. Kafatos, (eds.), *Gravitation & Cosmology: From the Hubble Radius to the Planck Scale*, pp. 459-468, Dordrecht: Kluwer.
- [53] Susskind, L. (1994) The World as a Hologram, arXiv:hep-th/9409089 v2.
- [54] Bousso, R. (2002) The holographic principle, *Reviews Modern Physics* 74:825-874; arXiv:hep-th/0203101.
- [55] Lorentz, H.A. (1899) Simplified theory of electrical and optical phenomena in moving systems, *Proc. Acad. Sci. Amsterdam* I, 427-443.
- [56] Tipler, F. J., & Barrow, J. (1986). The anthropic cosmological principle. New York: Oxford University Press.
- [57] Franck, G. (2000) Time and presence, in *Science and The Primacy of Consciousness*, R.L. Amoroso et al, (eds.) Orinda: Noetic Press.
- [58] Bilson-Thompson, S., Hackett, J. & Kauffman, L.H. (2009) Particle topology, braids and braided belts, arXiv:0903.1376v1.
- [59] Bilson-Thompson, S.O. A topological model of composite preons, arXiv:hep-th/0503213.

- [60] Bilson-Thompson, S.O., Markopoulou, F. & Smolin, L. (2007) Quantum gravity and the standard model, *Class. Quant. Gravity* 24; 3975-3993; arXiv:hep-th/0603022.
- [61] Magnus, W (1974) Braid groups: A survey, In *Lecture Notes in Mathematics*, vol. 372, pp. 463-487; or (1974) *Proceedings of the 2nd Intl Conf. on the Theory of Groups*, Canberra, Australia, 1973, New York: Springer.
- [62] Personal communication, (2009) Lou H. Kaufman.
- [63] Kaufman, L.H. (2001) *Knots and Physics*, 3rd ed., Singapore, World Scientific.
- [64] Vigier, J-P (2000) selected papers, in S. Jeffers, B. Lehnert, N. Abramson, & L. Chebotarev (eds.) Jean-Pierre Vigier and the Stochastic Interpretation of Quantum Mechanics, Montreal: Aperion.
- [65] MacKinnon, L. (1979) The de Broglie wave packet for a simple stationery state, *Foundations of Physics*, 9:9-10; 787-791.
- [66] Abbot, E.A. (1983) Flatland, New York: Harper Perennial.
- [67] Drăgănescu, M.C. (1991) *The Philosophical tension and the cosmic feeling*, Bucharest: The Romanian Academy.

Chapter 12

Ontological-Phase Topological Field Theory

We thank Newton for inspiring strict adherence to *hypotheses non-fingo*¹, and claim reasonable *a posteriori* surely in positing the need for an Ontological-Phase Topological Field Theory (OPTFT) as the final step in describing the remaining requirements for bulk UQC. Let's surmise with little doubt that a radical new theory needs to be correlated with the looming 3rd regime of Unified Field Mechanics (UFM). If the author knows one thing for sure, it is that gravity is not quantized! The physics community is so invested in quantizing the gravitational force that it could still be years away from this inevitable conclusion. There is still a serious conundrum to be dealt with however; discovery of the complex Manifold of Uncertainty (MOU), the associated 'semi-quantum limit' and the fact of a duality between Newton's and Einstein's gravity, may allow some sort of wave-particle-like duality with a quanta-like virtual graviton in the semi-quantum limit. Why mention the gravitational field? Relativistic information processing (RIP) introduces gravitational effects in the 'parallel transport' aspects of topological switching in branes. There are A and B type topological string theories, and a related Topological M-Theory with mirror symmetry, that are somewhat interesting especially since they allow sufficient dimensionality with Calabi-Yau mirror symmetry perceived as essential elements for developing a UFM. But a distinction between these theories and the ontology of an energyless topological switching of information (Shannon related) through topological charge in brane dynamics, perhaps defined in a manner making correspondence to a higher dimensional (HD) de-Broglie-Bohm super-quantum potential synonymous with a 'force of coherence' of the

¹In B. Motte's 1729 English trans. of Newton's essay 'General Scholium', 2nd (1713) edition of *Principia*, phrase appeared as "*I do not frame hypotheses*". This translation was objected to by Koyre in 1965, who pointed out that 'fingo' means 'feign', not 'frame' [1].

unified field is of interest. Thus the term 'OPTFT' has been chosen to address this issue as best as the *Zeitgeist* is able to conceive at the time of writing....

It is possible to make 'intelligent guesses and conjectures – Atiyah [2].

12.1 Abductive *a Priori a Posteriori* Tautology

Not all who wander are lost. - J. R. R. Tolkien

Reality leaves a lot to the imagination. - John Lennon

And those who were seen dancing were thought to be insane by those who could not hear the music – Friedrich Nietzsche.

This is among the most challenging chapters of the volume for the author, the conception of which wasn't even in the list of topics when the book was first conceived in 2014; and not knowing sufficient Group Theory limits current enfolding. I didn't suspect there would be much to say about Anyon – quasi-particle – quantum Hall TQC [3] because it was perceived as an LD 'Toy Model' of the HD UFM UQC architecture proposed to take its place. My expertise at the time on TQFT and TQC was sparse, such that quite a can of worms was opened into my world view in bringing myself sufficiently up to speed with study and tad of tutoring given graciously by a world-renowned topologist.

The necessity of r-qubits (relativistic qubits) had already been embraced since first hearing of them at Physcomp96 [4]; and again in the course of getting up to speed, discovered that a corner of the QC R&D community finally began a discussion of their utility for modeling relativistic quantum computing (RIP) with a version of r-qubits [5-7].

I felt that attempting to develop a relativistic-TQFT was not a correct nomenclatural framework for both mathematical and physical reasons. Most acutely that the universe is not fundamentally quantum (anymore) and that gravitation, unlike the other three known phenomenological fields, is not quantized. The hearty belief in a quantum gravity persists only because of a herd mentality confounded by the current belief that fundamental reality is indeed quantum.

Most likely, the imminent age of discovery will be described topologically. Field theory has evolved from classical field theory to the current 2nd regime modes of QFT, RQFT and TQFT. It is proposed that the 3rd regime of reality, Unified Field Mechanics (UFM) will be described

by an Ontological-Phase Topological Field Theory (OPTFT). In terms of the nature of reality, quantum information processing and the measurement problem, there has been a recent introduction of relativistic parameters including relativistic r-qubits and not just an Amplituhedron but more saliently a dual-Amplituhedron replacing spacetime, all bringing into question the historically fundamental basis of and need to be restricted to ‘locality and unitarity’.

We briefly review this dilemma in terms of Bell’s inequalities, the no-cloning theorem and discuss correspondence to the epistemic view of the Copenhagen Interpretation versus the ontic consideration of objective realism and as merged by W. Zurek’s epi-ontic blend of quantum redundancy in quantum Darwinism [8-10]. Finally, we delve into the UFM ontological-phase topology requiring a new set of topological transformations beyond the Galilean, Lorentz-Poincaré.

A radical paradigm shift is needed to incorporate the new 3rd regime of Unified Field Mechanics (UFM), which appears to be inherently topological, suggesting extensions of current theory are required. If I was M. Atiya’s clone, I would write a seminal introduction to an extended topological field theory as he did in 1986 [11]. UFM does not imply a 5th force, is not quantized, but entails an ontological mediation of information by a ‘force of coherence’ transferring information (by a form of topological charge) in a Shannon sense in the geometric topology of branes. This process, as we continue to mention, is an energyless process called ‘topological switching’ utilizing ‘topological charge’ [12-14].

12.2 The Phasor (Phase Vector) Complex Probability Amplitude

As the first step in trying to figure out how to develop a new concept of Ontological-phase we wish to adapt the phasor or phase vector concept as a precursor for describing ontological topological phase. In general, a phasor is a complex number for a sinusoidal (π rotation) function with amplitude A, angular frequency ω and initial phase θ , which are all time invariant. The complex constant is the phasor [15].

Euler’s formula allows sinusoids to be represented as the sum of two complex-valued functions:

$$A \cdot \cos(\omega t + \theta) = A \cdot \frac{e^{i(\omega t + \theta)} + e^{-i(\omega t + \theta)}}{2}, \quad (12.1)$$

or as the real part of one of the functions:

$$A \cdot \cos(\omega t + \theta) = \operatorname{Re} \{ A \cdot e^{i(\omega t + \theta)} \} = \operatorname{Re} \{ A e^{i\theta} \cdot e^{i\omega t} \}. \quad (12.2)$$

The function $A \cdot e^{i(\omega t + \theta)}$ is the analytic representation of $A \cdot \cos(\omega t + \theta)$. Multiplication of the phasor $Ae^{i\theta}e^{i\omega t}$ by a complex constant, $B e^{i\phi}$, produces another phasor that changes the amplitude and phase of the underlying sinusoid:

$$\begin{aligned} \operatorname{Re} \{ (A e^{i\theta} \cdot B e^{i\phi}) \cdot e^{i\omega t} \} &= \operatorname{Re} \{ (AB e^{i(\theta+\phi)}) \cdot e^{i\omega t} \} \\ &= AB \cos(\omega t + (\theta + \phi)). \end{aligned} \quad (12.3)$$

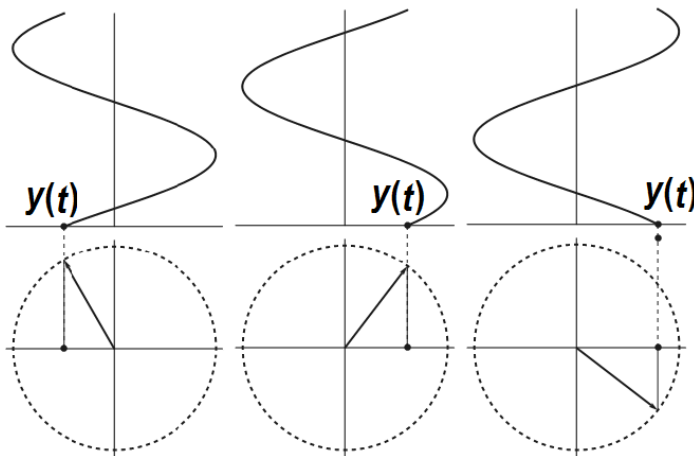


Fig. 12.1 Top sine waves - phase transform in the complex plane. Bottom, can also be thought of as 2D rotation of the reference circle, and 1D sliding point on the line segment, helping us ponder the 2D nature of anyon braid topology. Thus elements of the figure can be considered in 1D, 2D and 3D.

When function $A \cdot e^{i(\omega t + \theta)}$ is depicted in the complex plane (Fig. 12.1), the vector formed by the imaginary and real parts rotates around the origin. A is the magnitude, i is the imaginary unit $i^2 = -1$, one cycle is completed every $2\pi / \omega$ seconds, and θ is the angle formed with the real axis at $t = n \cdot 2\pi / \omega$, for integer values of n [16].

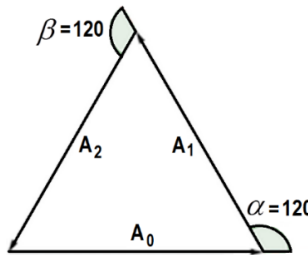


Fig. 12.2 Phasor diagram of three waves in perfect destructive interference.

This type of addition occurs when sinusoids interfere with each other constructively or destructively. Three identical sinusoids with a specific phase difference between them may perfectly cancel. To illustrate, we take three vectors of equal length placed head to tail so that the last head matches up with the first tail forming an equilateral triangle with the angle between each phasor being 120° ($2\pi/3$ radians), or one third of a wavelength $\lambda/3$. Thus the phase difference between each wave is 120° ,

$$\cos(\omega t) + \cos(\omega t + 2\pi/3) + \cos(\omega t - 2\pi/3) = 0. \quad (12.4)$$

In the example of three waves, the phase difference between the first and the last wave is 240° . In the limit of many waves, the phasors must form a circle for destructive interference, so that the first phasor is nearly parallel with the last. This means that for many sources, destructive interference happens when the first and last wave differ by 360° , a full wavelength, λ [16].

12.2.1 Complex Phase Factor

For any complex number written in polar form, such as $re^{i\theta}$, the phase factor is the complex exponential factor, $e^{i\theta}$. As such, the term ‘phase factor’ is related more generally to the term phasor, which may have any magnitude (i.e., not necessarily part of the circle group). The phase factor is a unit complex number of absolute value 1 as commonly used in quantum mechanics.

The variable θ is usually referred to as the phase. Multiplying the equation for a plane wave $A^{ei(k \cdot r - \omega t)}$ by a phase factor shifts the phase of the wave by θ :

$$e^{i\theta} A e^{i(k \cdot r - \omega t)} = A e^{i(k \cdot r - \omega t + \theta)}. \quad (12.5)$$

In quantum mechanics, a phase factor is a complex coefficient $e^{i\theta}$ that multiplies a ket $|\psi\rangle$ or bra $\langle\phi|$. It does not, in itself, have any physical meaning in the standard formulation of QM, since the introduction of a phase factor does not change the expectation values of a Hermitian operator. That is, the values of $\langle\phi|A|\phi\rangle$ and $\langle\phi|e^{-i\theta}Ae^{i\theta}|\phi\rangle$ are the same [17].

However, *differences* in phase factors between two interacting quantum states can be measurable under certain conditions such as in Berry phase, which has important consequences. The argument for a complex number $z = x + iy$, denoted $\arg z$, is defined as:

- Geometrically, in the complex plane, as the angle φ from the positive real axis to the vector representing z . The numeric value given by the angle in radians is positive if measured counterclockwise.
- Algebraically, the argument is defined as any real quantity φ such that $z = r(\cos \varphi + i \sin \varphi) = re^{i\varphi}$ for some positive real r (Euler's formula). The quantity r is the *modulus* of z , as $|z|: r = \sqrt{x^2 + y^2}$.

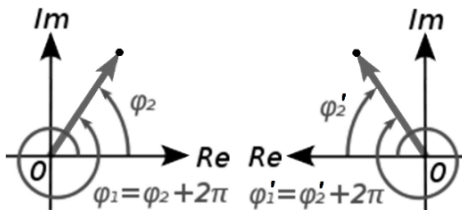


Fig. 12.3. Left-Right phase argument.

Use of the terms *amplitude* for the modulus and *phase* for the argument are sometimes used equivalently. Under both definitions, it can be seen that the argument of any (non-zero) complex number has many possible values: firstly, as a geometrical angle, whole circle rotations do not change the point, so angles differing by an integer multiple of 2π radians are the same. Similarly, from the periodicity of sin and cos, the second definition also has this property.

An N-particle system can be represented in non-relativistic quantum mechanics by a wavefunction, $\psi(x_1, x_2, \dots, x_n)$, where each x_i is a point in 3D space. A classical phase space contains a real-valued function in 6N dimensions (each particle contributes 3-spatial coordinates and 3-momenta). Quantum phase space involves a complex-valued function on a 3N dimensional space. Position and momenta are represented by operators that do not commute, and ψ lives in the mathematical structure of a Hilbert space. Aside from these differences, the analogy holds.

In physics, this sort of addition occurs when sinusoids interfere with each other, constructively or destructively. The static vector concept provides useful insight into questions like: What phase difference would be required between three identical sinusoids for perfect cancellation? In this case, simply imagine taking three vectors of equal length and placing them head to tail such that the last head matches up with the first tail. Clearly, the shape which satisfies these conditions is an equilateral triangle, so the angle between each phasor to the next is 120° ($2\pi/3$ radians), or one third of a wavelength $\lambda/3$. So the phase difference between each wave must also be 120° . In other words, what this shows is: $\cos(\omega t) + \cos(\omega t + 2\pi/3) + \cos(\omega t - 2\pi/3) = 0$.

12.2.2 Geometric Phase - Berry Phase

A Berry phase difference is acquired over the course of a cycle, when a system is subjected to cyclic adiabatic processes resulting from the geometrical properties of the parameter space of the Hamiltonian [18]. This phenomenon was first discovered in 1956, [19] and rediscovered in 1984 [20]. It can be seen in the Aharonov-Bohm effect and in the conical intersection.

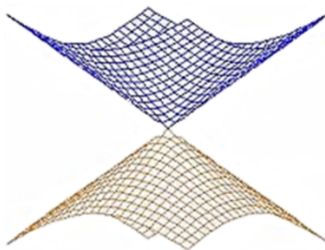


Fig. 12.4. Conical intersection of two potential energy surfaces.

A conical intersection of two potential energy surfaces is the set of geometrical points where the two potential energy surfaces are degenerate (intersect) and the non-adiabatic couplings between these two states are non-vanishing. For the Aharonov–Bohm effect, the adiabatic parameter is the magnetic field enclosed by two interference paths, and is cyclic because the two paths form a loop. For a conical intersection, the adiabatic parameters are molecular coordinates. In addition to quantum mechanics it can occur whenever there are at least two parameters describing a wave in the vicinity of a singularity or topological hole.

In a quantum system at the n^{th} eigenstate, if adiabatic (adapts to gradually changing external conditions; but for rapidly varying conditions there is insufficient time, so the spatial probability density remains unchanged) evolution of the Hamiltonian evolves the system such that it remains in the n^{th} eigenstate, while also obtaining a phase factor. The phase obtained has a contribution from the state's time evolution and another from the variation of the eigenstate with the changing Hamiltonian.

The second term corresponds to the Berry phase which for non-cyclical variations of the Hamiltonian can be made to vanish by a different choice of the phase associated with the eigenstates of the Hamiltonian at each point in the evolution. However, if the variation is cyclical, the Berry phase cannot be cancelled, it is invariant and becomes an observable property of the system. From the Schrödinger equation the Berry phase γ is:

$$\gamma[C] = i \oint_C \langle n, t | (\nabla_R | n, t \rangle) dR \quad (12.6)$$

where R parametrizes the cyclic adiabatic process. It follows a closed path C in the appropriate parameter space. Geometric phase along the closed path C can also be calculated by integrating the Berry curvature over surface enclosed by C [21].

One of the simplest examples of geometric phase is the Foucault pendulum [22]. The pendulum precess when it is taken around a general path C . For transport along the equator, the pendulum does not precess. But if C is made up of geodesic segments, precession arises from the angles where the segments of the geodesics meet; the total precession is equal to the net deficit angle, which equals the solid angle enclosed by C modulo 2π . We can approximate any loop by a sequence of geodesic segments, from which the most general result is that the net precession is equal to the enclosed solid angle. Since there are no inertial forces on the pendulum precess, precession, relative to the direction of motion along the

path, is entirely due to the turning of the path. Thus the orientation of the pendulum undergoes parallel transport [22].

12.2.3 The Toric Code

The toric code introduced by Alexei Kitaev, is named from its periodic boundary conditions having it the shape of a torus allowing the model to have translational invariance useful in TQC. Putative experimental realization requires open boundary conditions, allowing the system to be embedded on a 2D surface. Toric code and its generalized surface codes provides a basis for anyonic computation by braiding defects. The unique nature of topological codes, like Kitaev's toric code, is that stabilizer violations can be interpreted as quasiparticles [23].

Kitaev defines the Toric Code on a periodic 2D lattice, usually the square lattice, with a spin-1/2 degree of freedom located on each edge. Stabilizer operators are defined on the spins around each vertex v and plaquette p of the lattice:

$$A_v = \prod_{i \in v} \sigma_i^x, B_p = \prod_{i \in p} \sigma_i^z. \quad (12.7)$$

Where $i \in v$ denotes edges touching the vertex v , and $i \in p$ denotes the edges surrounding the plaquette p . The stabilizer space of the code is where all stabilizers act trivially,

$$A_v |\psi\rangle = |\psi\rangle, \forall v, B_p |\psi\rangle = |\psi\rangle, \forall p, \quad (12.8)$$

for any state $|\psi\rangle$. For the toric code, this is a 4D space, so it can store two qubits. The occurrence of errors moves the state out of the stabilizer space, resulting in vertices and plaquettes for which the above condition does not hold. The positions of these violations is the 'syndrome of the code', and is used for error correction. The unique nature of topological toric codes, is that stabilizer violations can be interpreted as quasiparticles. Specifically, if the code is in a state $|\phi\rangle$ such that, $A_v |\phi\rangle = -|\phi\rangle$, a quasiparticle called an e anyon exists on the vertex v [23,24].

Another method introduces a distance truncature at the antipode of each set of points. In Fig. 12.5, the square is a flat Euclidean torus with null curvature everywhere [25].

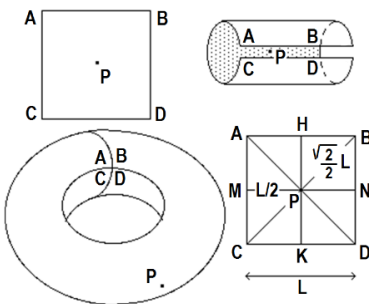


Fig. 12.5. a) Square Euclidean torus.

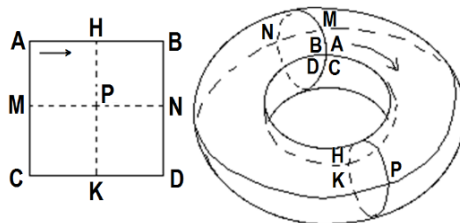


Fig. 12.6. The P torus point owns three antipodal points (A,B,C,D), (M,N) and (H,K).

From a geometrical point of view, the points A,B,C,D must be identified to an antipode of point P on the torus. For the Euclidean square torus, straight lines are geodesics of the torus. The gravitational action of a mass located at the antipodal point (A,B,C,D) on the point P is zero, which is the same for a mass located in (H,K) or (M,N) [25]. See fig. 12.6 (Right). The corresponding geodesic path lengths are basically different (Fig. 12.5) as shown in (12.9):

$$\begin{aligned} PA = PB = PC = PD &= \frac{\sqrt{2}}{2} L \\ PM = PN = PH = PK &= \frac{L}{2} \end{aligned} \quad (12.9)$$

Note that on a torus there are an infinite number of geodesics joining two given points, one being the shortest. When computing a corresponding gravitational interaction, both lengths must be considered, $d = \alpha R d' = R(2\alpha\pi - \alpha)$ [25].

12.3 Transitioning from TQFT to OPTFT

Topological quantum field theories (TQFT) were originally created to avoid the infinities plaguing quantum field theory [11,26]. Atiyah [11] initially to an axiomatic approach to TQFT, which has been realized in low dimensions and the primary method for modeling anyonic QC. The motivation for topological field theories stems from modern physical theories being defined by invariance under certain group actions like gauge groups in particle physics, diffeomorphism groups in general relativity, or unitary operator groups in quantum mechanics. In topological field theory, the concern is topological invariants, which are objects computed from a topological space (smooth manifold) without any metric [27]. Topological invariance is invariance under the diffeomorphism group of the manifold. Important milestones were Thom's theory of cobordism [28], de Rham cohomology, and knot theory. Through theories such as the Chern-Weil theory linking differential geometry and algebraic topology, abstract formalisms found powerful geometric applications which were applied to physics beginning in the 70's [29] and flourished through the work of Witten and Atiyah [30].

Fundamental strings map out 2D surfaces. The $N = (1,1)$ sigma model quantum field theory is defined on each surface. It consists of maps from the surface to a supermanifold interpreted physically as spacetime and each map is interpreted as the embedding of the string in spacetime. Only certain spacetimes admit topological strings. Classically one must choose a spacetime that allows an additional pair of supersymmetries, so in fact the theory is an $N = (2,2)$ sigma model. This is the case for a Kähler manifold where the H-flux is identically equal to zero [30].

Ordinary strings on special backgrounds are never topological. To make these strings topological, one needs to modify the sigma model by a procedure called a *topological twist* invented by Witten in 1988 [31]. The central observation is that these theories have two U(1) symmetries known as R-symmetries, where the Lorentz symmetry may be modified by mixing rotations and R-symmetries. One may use either of the two R-symmetries, leading to two different theories, called the A model and the B model. After this twist the action of the theory is BRST exact, and as a

result the theory has no dynamics, instead all observables depend on the topology of a configuration [26].

Twisting is not possible for anomalies. In the Kähler case where $H = 0$ the twist leading to the A-model is always possible, but that leading to the B-model is only possible when the first Chern class of the spacetime vanishes, implying that the spacetime is Calabi-Yau. More generally $N = (2,2)$ theories have two complex structures and the B model exists when the first Chern classes of associated bundles sum to zero, whereas the A model exists when the difference of the Chern classes is zero. In the Kähler case the two complex structures are the same and so the difference is always zero, which is why the A model always exists [31].

12.3.1 The A and B-Models of Topological Field Theory

The topological A-model comes with a target space which is a real-6D generalized Kähler spacetime describing two objects. There are fundamental strings, which wrap two real-dimensional holomorphic curves. Amplitudes for the scattering of these strings depend only on the Kähler form of the spacetime, and not on the complex structure [30].

The B-model also contains fundamental strings, but their scattering amplitudes depend entirely upon the complex structure and are independent of the Kähler structure. In particular, they are insensitive to worldsheet instanton effects and so can often be calculated exactly. Mirror symmetry then relates them to A-model amplitudes, allowing one to compute Gromov–Witten invariants. The B-model also comes with D(-1), D1, D3 and D5-branes, which wrap holomorphic 0, 2, 4 and 6-submanifolds respectively. The 6-submanifold is a connected component of the spacetime. The theory on a D5-brane is known as holomorphic Chern-Simons theory [29].

12.3.2 Dualities Between Topological String Theories (TSTs)

A number of dualities relate the above theories. The A-model and B-model on two mirror manifolds are related by mirror symmetry, which has been described as a T-duality on a 3-torus. The A-model and B-model on the same manifold are thought to be related by S-duality, implying the existence of several new branes, called NS branes by analogy with the NS5-brane, which wrap the same cycles as the original branes but in the opposite theory. Also a combination of the A-model and a sum of the B-model and its conjugate are related to topological M-theory by a kind of *dimensional reduction*. Here the degrees of freedom of the A-model and the B-models appear to not be simultaneously observable, but have a

relation similar to that between position and momentum in quantum mechanics [26,30].

12.3.3 The Holomorphic Anomaly

The sum of the B-model and its conjugate appears in the above duality because it is the theory whose low energy effective action is expected to be described by Hitchin's formalism. This is because the B-model suffers from a holomorphic anomaly, which states that the dependence on complex quantities, while classically holomorphic, receives non-holomorphic quantum corrections. In Quantum Background Independent String Theory, Witten argued that this structure is analogous to a structure that one finds geometrically quantizing the space of complex structures. Once this space has been quantized, only half of the dimensions simultaneously commute and so the number of degrees of freedom has been halved. This halving depends on an arbitrary choice, called a polarization. The conjugate model contains the missing degrees of freedom, and so by tensoring the B-model and its conjugate one reobtains all of the missing degrees of freedom and also eliminates the dependence on the arbitrary choice of polarization [23,24,26,30].

12.4 Topological Vacuum Bubbles by Anyon Braiding

According to a basic rule of fermionic and bosonic many-body physics, known as the linked cluster theorem, physical observables are not affected by vacuum bubbles, which represent virtual particles created from vacuum and self-annihilating without interacting with real particles. Here we show that this conventional knowledge must be revised for anyons, quasiparticles that obey fractional exchange statistics intermediate between fermions and bosons. We find that a certain class of vacuum bubbles of Abelian anyons does affect physical observables. They represent virtually excited anyons that wind around real anyonic excitations. These topological bubbles result in a temperature-dependent phase shift of Fabry-Perot interference patterns in the fractional quantum Hall regime accessible in current experiments, thus providing a tool for direct and unambiguous observation of elusive fractional statistics [32].

When two identical particles adiabatically exchange positions $r_i = 1,2$, their final state ψ , to dynamical phase, relates to the initial state through an exchange statistics phase θ^* ,

$$\psi(r_2, r_1) = e^{i\theta^*} \psi(r_1, r_2), \quad (12.10)$$

with $\theta^* = 0(\pi)$ [33].

In many-body quantum theory [33], Feynman diagrams are used to compute the expectation value of observables. This approach invokes vacuum bubble diagrams, which describe virtual particles excited from vacuum and self-annihilating without interacting with real particles. According to the linked cluster theorem [33], each diagram having vacuum bubbles comes with a partner diagram of the same magnitude but of opposite sign that it is exactly cancelled by. Consequently, vacuum bubbles do not contribute to physical observables.

This common wisdom must be revised for anyons because a certain class of vacuum bubbles of Abelian anyons does affect observables. These virtual particles, called topological vacuum bubbles, wind around a real anyonic excitation, gaining the braiding phase $\pm 2\pi\nu$ [32].

Han's team proposes an experimental procedure for detecting them and $\theta^* = \pi\nu$, where $\pi\nu$ is the anyon phase and θ the interference phase shift [32]. For an interference $a_1 a_2$ between processes a_1 and a_2 for propagation of a real particle, in a_1 , a virtual particle-hole pair is excited then self-annihilates after the virtual particle winds around the real particle, forming a vacuum bubble, which is not excited in a_2 . The winding results in a braiding phase $2\pi\nu$ and an Aharonov–Bohm phase $2\pi(\Phi/\Phi_0^*)$ from the magnetic flux Φ enclosed by the winding path, contributing to the interference signal as $e \exp i(2\pi(\Phi/\Phi_0^*) + 2\pi\nu)$; $\Phi_0^* = h/e^*$ as the anyon flux quantum [32].

The limiting cases of bosons ($\nu = 0$) and fermions ($\nu = 1$) imply that this bubble diagram appears together with, and is cancelled by, a partner diagram. The partner diagram has a bubble not encircling the real particle and involves only $2\pi(\Phi/\Phi_0^*)$. The two diagrams (and complex conjugates) yield

$$\begin{aligned} \text{Interference signal} &\propto \text{Re} \left[e^{i(2\pi(\Phi/\Phi_0^*) + 2\pi\nu)} - e^{2\pi i(\Phi/\Phi_0^*)} \right] \\ &= -\sin(\pi\nu) \sin(2\pi(\Phi/\Phi_0^*) + \pi\nu). \end{aligned} \quad (12.11)$$

For bosons and fermions, the two diagrams fully cancel each other with $\sin(\pi v) = 0$ in agreement with the linked cluster theorem; thus, the signal disappears. By contrast, for anyons they cancel only partially, producing non-vanishing interference in an observable, and are topological as the braiding phase is involved [32].

The astute reader will begin to notice, that the anyon braid topology begins to overlap with the UFM OPTFT. The question will be whether the cryogenic TQC will be built as a ‘proof of concept’ or a ‘leap-frog’ will occur to the table top room temperature UFM model. If the utility of the Aharonov-Bohm effect remains a key element of ‘Topological vacuum bubbles by anyon braiding’ interferometry; it is easy to add Aharonov-Bohm effect parameters to the OPTF dynamics.

12.5 Topological Switching – Key to Ontological-Phase

The 2-state formalism currently forms the basis of QC. Qubits, are 2-state systems. Any QC operation is a unitary operation that rotates the state vector on the Bloch sphere. To move from Hilbert space to ontological-phase space we must begin to define what we mean by topological switching [12-14]. We begin with a number of ways of looking at the ambiguous Necker cube [34].

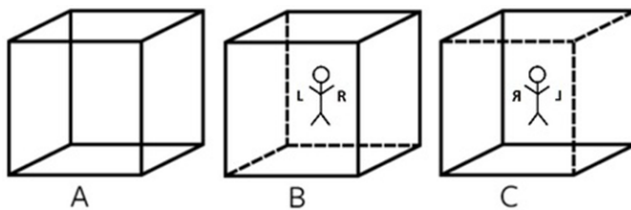


Fig. 12.7. Ambiguous Necker cube, left, mirror image, center and perceived shift between the two states in 4D.

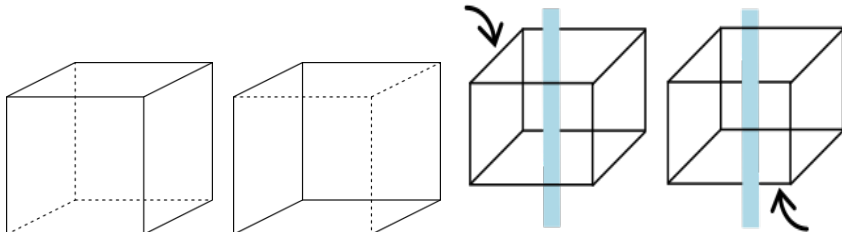


Fig. 12.8. Two states of the Necker cube. A physically real description is needed.

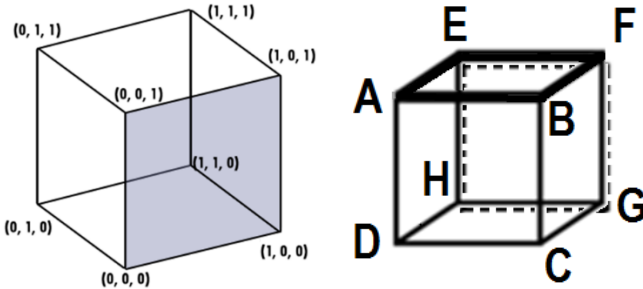


Fig. 12.9. A first step towards physicality might be distinguishing the vertices.

Quaternions have the ability to represent rotations of 3D space. If we represent 3-space, \mathbb{R}^3 as the set of pure quaternions of the form $\mathbb{Z} = ai + bj + ck$ with a, b, c real numbers, then g is a unit quaternion mapping $\rho : \mathbb{R}^3 \rightarrow \mathbb{R}^3$ defined by the equation $\rho(\mathbb{Z}) = g\mathbb{Z}g^{-1}$ describes a 3-space rotation by angle θ around axis μ when

$$g = \cos(\theta/2) + \sin(\theta/2)\mu. \quad (12.12)$$

In this manner, μ is a unit length quaternion giving a direction to a vector in 3-space, a rotation is specified by an angle θ about an axis U , which in the case below is in the positive direction [35].

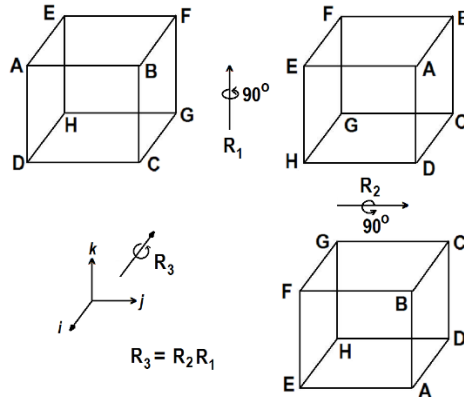


Fig. 12.10. Denoting two 90° rotations R_1 and R_2 , we write $R_3 = R_2R_1$ for the rotation obtained by 1st performing R_1 and then R_2 . R_3 fixes the corners B and H; thus R_3 is a 120° rotation about the diagonal axis.

Thus, following Kauffman [35],

$$\begin{aligned}
 e^{j(\pi/4)} e^{k(\pi/4)} &= \left(\frac{\sqrt{2}}{2} + j \frac{\sqrt{2}}{2} \right) \left(\frac{\sqrt{2}}{2} + k \frac{\sqrt{2}}{2} \right) \\
 &= \frac{1}{2}(1+j)(1+k) = \frac{1}{2}(1+j+k+jk). \\
 &= \frac{1}{2}(1+i+j+k) = \frac{1}{2} + \frac{\sqrt{3}}{2} \left(\frac{i+j+k}{\sqrt{3}} \right). \\
 \therefore e^{j(\pi/4)} e^{k(\pi/4)} &= e^{\left[(i+j+k)/\sqrt{3} \right] [2\pi/3]/2}
 \end{aligned}$$

↑ ↑
 diagonal axis 120° .

These quaternion rotations can be considered phase changes under certain conditions; but they do not correspond to the ontological phase we are looking for, because Euclidean geometry has no natural inherent perspective. It appears we need a duo-morphic projection perhaps involving Berry phase, because the ambiguous vertices of the Necker cube are not distinguished in Kauffman's quaternion rotation system [35].

To clarify how projective transformations lose orientable information, rotating a triangle in a plane is used as an illustration [36].

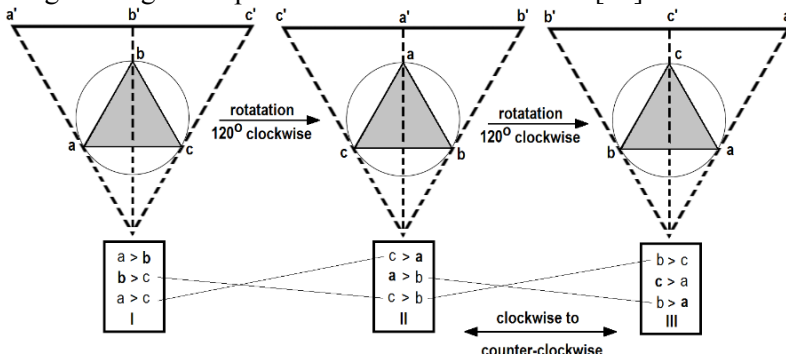


Fig. 12.11. Removing ambiguity from a projected rotation, with $>$ denoting order of sequence occurrence – to the left on the projective line. Bold letters are the front range of projective mapping. Fig. redrawn from [36].

The rotation sequences in Fig. 12.11 are I,II,III for clockwise and I,III,II for counter-clockwise. According to Shaw the direction of rotation reverses if the back and front ranges are interchanged. This is denoted by the connecting lines in the boxes below the rotation triangles. Bold letters mark the front range; this system is able to preserve orientation information under projected rotation.

The 3D wire-frame Necker cube can be projected onto a 2D surface, collapsing the cubes six faces into a complex of one to seven coplanar polygons depending on orientation of the cube.

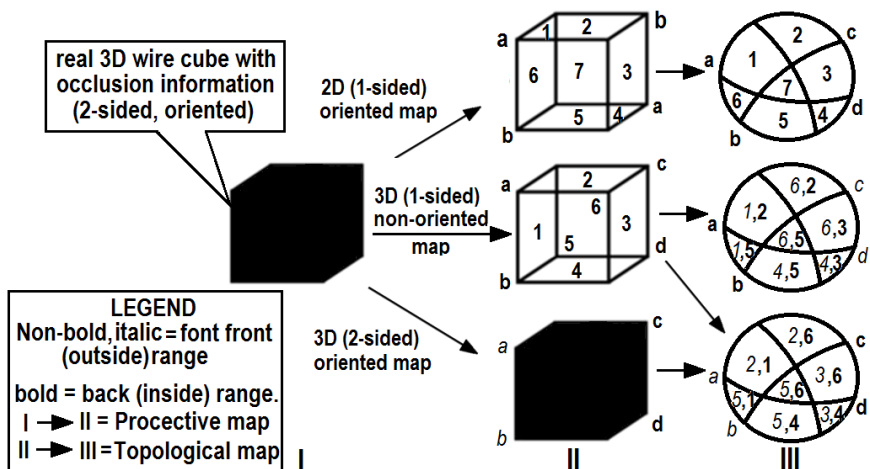


Fig. 12.12 Contrasting nonoriented - oriented projective geometries. Redrawn from [37].

Figure 12.12 illustrates three different forms of projection.

- I → II-Top → III-Top: no occlusion information
- I → II-Middle → III-Middle and III-Bottom: occlusion information is specified ambiguously
- I → II-Bottom → III-Bottom: occlusion information is specified unambiguously.

The Necker cube, like the Möbius strip is an ambiguous figure because of the problem of projective mapping. In ordinary projective space, the Möbius strip and Necker cube, are one-sided (Fig. 12.12). The spherical model of this geometry represents the fact that the projections of a point on the back of the sphere and of a point on its front both have the same

image in the Euclidean (projective) plane. All of the projected points, regardless of the hemisphere to which they belong, cover the projective plane in the usual way without any designation of where they originated. The loss of orientation is due to this failure of the projective mapping to preserve the distinction between the front and back range, collapsing both into positive values of the dimension of depth w . This loss of orientation is represented by the fact that relationships (e.g., the arrows) invert when the projective angle passes through the points at infinity [36].

To keep the front and back ranges distinguished, traditional computational geometries use the line at infinity as a reference; but this move is not a real solution to the orientation problem in projective geometry because it is tantamount to a return to Euclidean geometry which has no inherent natural perspective.

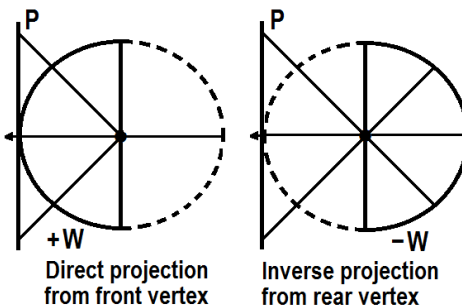


Fig. 12.13 Duo-morphic oriented projections (+W, -W) yield a double covering of the projective plane, P.

To distinguish front and back ambiguous vertices of the Necker cube is a problem of orientation. Oriented projective geometry introduces a methodology for distinguishing the ambiguous vertices of the Necker cube [36]. Shaw [37] assigns a dual range, +W and -W to represent front and rear ranges of a sphere.

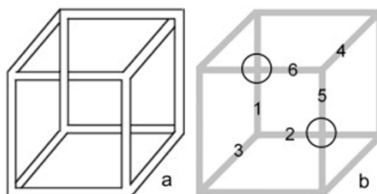


Fig. 12.14. Ambiguity needs a method of labeling for clarity.

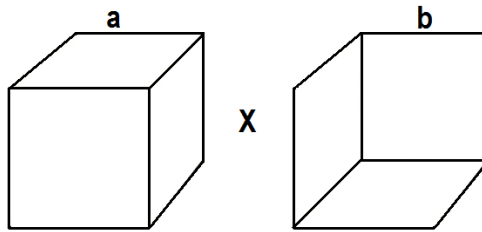


Fig. 12.15. Visual test of stereoscopic construction of a Necker cube.

Figure 12.15 separates the ambiguous Necker cube into its component perspectives. Although what we are about to illustrate is usually considered a mental construct, we use it here to illustrate what we mean by ontological phase and an ontological phase transformation. Focus on the 'X' halfway between the 2D L-R Necker perspectives; relax one's eyes and allow them to lose focus and cross. Soon, a 3rd image appears between the two printed L-R images fusing the original perspective into one apparent 3D image, confirmed by noticing the labels 'a' and 'b' are now superposed. This stereoscopic condition is the scenario we want to utilize to define ontological-phase.

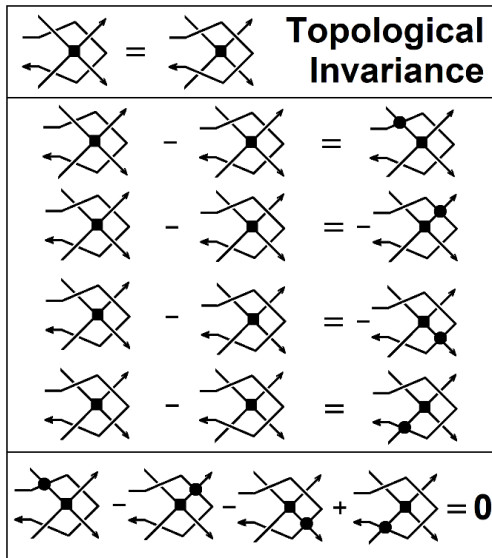


Fig.12.16. Topological Invariance must be included in any phase labeling. Figure redrawn from [25].

Masahide & Satoh generalize the class of roll-spun knots for 2-knot theory and show how to calculate the quandle cocycle invariant for any roll-spun knot [38]. For the case $X = S_4 = \mathbb{Z}[t, t^{-1}] / (2, t^2 + t + 1)$, the element $w = 1 \cdot t^{-1} \cdot 0 \cdot (t+1)^{-1}$ satisfies $\varphi_w = \text{id}_{S_4}$; such that we have

$$\begin{array}{ccccccc}
 0 & \xrightarrow{\varphi_1} & t+1 & \xrightarrow{\varphi_t^{-1}} & 1 & \xrightarrow{\varphi_0} & t & \xrightarrow{\varphi_{t+1}^{-1}} & 0 \\
 1 & \mapsto & 1 & \mapsto & 0 & \mapsto & 0 & \mapsto & 1 \\
 t & \mapsto & 0 & \mapsto & t+1 & \mapsto & 1 & \mapsto & t \\
 t+1 & \mapsto & t & \mapsto & t & \mapsto & t+1 & \mapsto & t+1
 \end{array} \tag{12.13}$$

Since $\text{ind}(w) = 0$, it holds that $w \in G_0(S_4)$. Figure 12.17 shows that $w^2 = 1$ in $\mathbf{G}_0(S_4)$, and that w is the generator of $G_0(S_4) \cong \mathbb{Z}_2$.

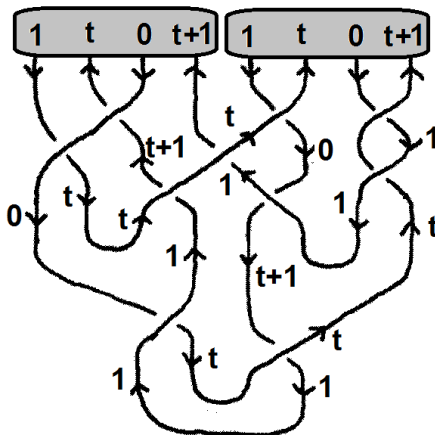


Fig. 12.17. Deform-spun knot tangle diagram. Redrawn from [38].

The spun knot is explored as a possible component topological move for ontological-phase transitions. When parallel transport creates a deficit angle in brane raising and lowering dynamics, in addition to Reidemeister moves, rotations, reflections and any other topological moves, spun knot components may add another type of phase transition with lattice charge.

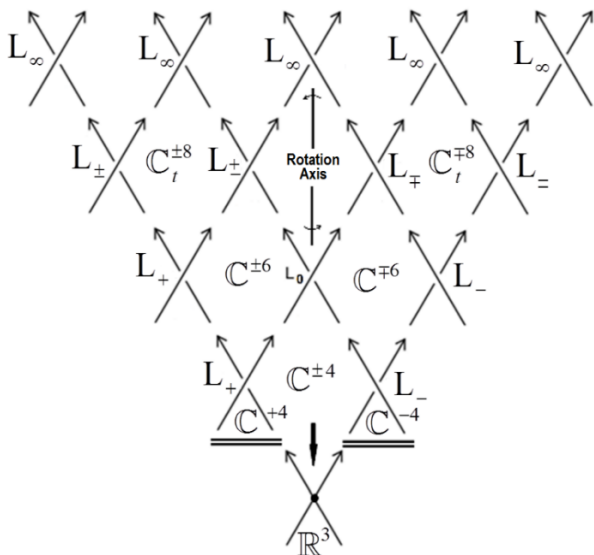


Fig. 12.18. Rolling spun knots. The infusion of topological charge as a UFM ‘force of coherence’ driving evolution throughout the multidimensional brane hierarchy can allow multiple types of moves to occur at multiple levels simultaneously.

An important feature of TQFTs is that they do not presume a fixed topology for space or spacetime. In other words, when dealing with an n -dimensional TQFT, one is free to choose any $(n-1)$ -dimensional manifold to represent space at a given time. Moreover, given two such manifolds, say S and S' , one is free to choose any nD manifold M to represent the portion of spacetime between S and S' . Mathematicians call M a ‘cobordism’ from S to S' . We write $M : S \rightarrow S'$, because we may think of M as the process of time passing from the moment S to the moment S' .

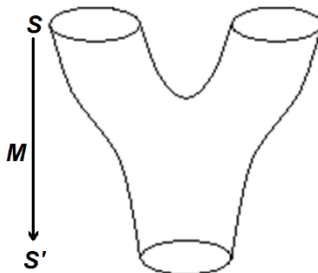


Fig. 12.19. A basic cobordism.

For example, in Fig. 12.19 we depict a 2D manifold M going from a 1D manifold S (a pair of circles) to a 1D manifold S' (single circle). Crudely speaking, M represents a process in which two separate spaces collide to form a single one! This may seem *outré*, but currently physicists are quite willing to speculate about processes in which the topology of space changes with the passage of time [39].

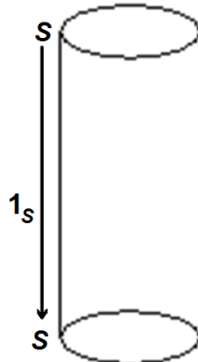


Fig. 12.20. Identity cobordism.

There are various important operations one can perform on cobordisms, but we only describe two. First, we may ‘compose’ two cobordisms $M : S \rightarrow S'$ and $M' : S' \rightarrow S''$, obtaining a cobordism $M'M : S \rightarrow S''$, as illustrated in Fig. 12.21. The idea here is that the passage of time corresponding to M followed by the passage of time corresponding to M' equals the passage of time corresponding to $M'M$. This is analogous to the familiar idea that waiting t seconds followed by waiting t' seconds is the same as waiting $t+t'$ seconds. The big difference is that in topological quantum field theory we cannot measure time in seconds, because there is no background metric available to let us count the passage of time! We can only keep track of topology change. Just as ordinary addition is associative, composition of cobordisms satisfies the associative law:

$$(M''M')M = M''(M'M). \quad (12.16)$$

However, composition of cobordisms is not commutative. As we shall see, this is related to the famous noncommutativity of observables in quantum theory [39].

Second, for any $(n-1)$ D manifold S representing space, there is a cobordism $1_S : S \rightarrow S$ called the 'identity' cobordism, which represents a passage of time without topological change. For example, when S is a circle, the identity cobordism 1_S is a cylinder, as shown in Fig. 12.20 In general, the identity cobordism 1_S has the property that for any cobordism $M : S' \rightarrow S$ we have $1_S M = M$, while for any cobordism $M : S \rightarrow S'$ we have $M 1_S = M$ [39].

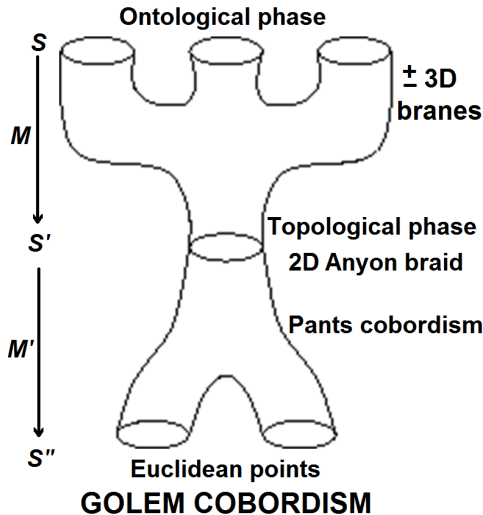


Fig. 12.21. The Golem, composition of cobordisms designed to handle ontological-phase.

These properties say that an identity cobordism is analogous to waiting 0 seconds: if you wait 0 seconds and then wait t more seconds, or wait t seconds and then wait 0 more seconds, this is the same as waiting t seconds.

These operations just formalize of the notion of 'the passage of time' in a context where the topology of spacetime is arbitrary and there is no background metric. Atiyah's axioms relate this notion to quantum theory as follows. First, a TQFT must assign a Hilbert space $Z(S)$ to each $(n-1)$ D manifold S . Vectors in this Hilbert space represent possible states of the universe given that space is the manifold S . Second, the TQFT must assign a linear operator $Z(M) : Z(S) \rightarrow Z(S')$ to each n D cobordism $M : S \rightarrow S'$. This operator describes how states change given that the portion of spacetime between S and S' is the manifold M . In other

words, if space is initially the manifold S and the state of the universe is ψ , after the passage of time corresponding to M the state of the universe will be $Z(M)\psi$ [39].

In addition, the TQFT must satisfy a list of properties. Let me just mention two. First, the TQFT must preserve composition. That is, given cobordisms $M : S \rightarrow S'$ and $M' : S' \rightarrow S''$, we must have $Z(M'M) = Z(M')Z(M)$, where the right-hand side denotes the composite of the operators $Z(M)$ and $Z(M')$. Second, it must preserve identities. That is, given any manifold S representing space, we must have $Z(1_S) = 1_{Z(S)}$, where the right-hand side denotes the identity operator on the Hilbert space $Z(S)$ [39].

Both these axioms are eminently reasonable if one ponders them a bit. The first says that the passage of time corresponding to the cobordism M followed by the passage of time corresponding to M' has the same effect on a state as the combined passage of time corresponding to $M'M$. The second says that a passage of time in which no topology change occurs has no effect at all on the state of the universe. This seems paradoxical at first, since it seems we regularly observe things happening even in the absence of topology change. However, this paradox is easily resolved: a TQFT describes a world quite unlike ours, one without local degrees of freedom. In such a world, nothing local happens, so the state of the universe can only change when the topology of space itself changes. The most interesting thing about the TQFT axioms is their common formal character. Loosely speaking, they all say that a TQFT maps structures in differential topology (the study of manifolds) to corresponding structures in quantum theory. In coming up with these axioms, Atiyah took advantage of a powerful analogy between differential topology and quantum theory, summarized in Table 12.1 [39].

This analogy between differential topology and quantum theory the sort of clue we should pursue for a deeper understanding of quantum gravity. At first glance, general relativity and quantum theory look very different mathematically: one deals with space and spacetime, the other with Hilbert spaces and operators. Combining them has always seemed a bit like mixing oil and water. But topological quantum field theory suggests that perhaps they are not so different after all! Even better, it suggests a concrete program of synthesizing the two, which many mathematical physicists are currently pursuing. Sometimes this goes by the name of 'quantum topology' [2,11].

DIFFERENTIAL TOPOLOGY	QUANTUM THEORY
(n - 1)-dimensional manifold (space)	Hilbert space (states)
cobordism between (n - 1)-dimensional manifolds (spacetime)	operator (process)
composition of cobordisms	composition of operators
identity cobordism	identity operator

Table 12.1: Analogy between differential topology and quantum theory.

Quantum topology is very technical, as anything involving mathematical physicists inevitably becomes. But if we stand back a moment, it should be perfectly obvious that differential topology and quantum theory must merge if we are to understand background-free quantum field theories. In physics that ignores general relativity, we treat space as a background on which states of the world are displayed. Similarly, we treat spacetime as a background on which the process of change occurs. But these are idealizations which we must overcome in a background-free theory. In fact, the concepts of 'space' and 'state' are two aspects of a unified whole, and likewise for the concepts of 'spacetime' and 'process'. It is a challenge, not just for mathematical physicists, but also for philosophers, to understand this more deeply [39].

We begin to explore various types of crossover inks and moves to start cataloguing the variety of moves that maybe applicable to ontological-phase transitions.



Fig. 12.22. Simple crossover links.

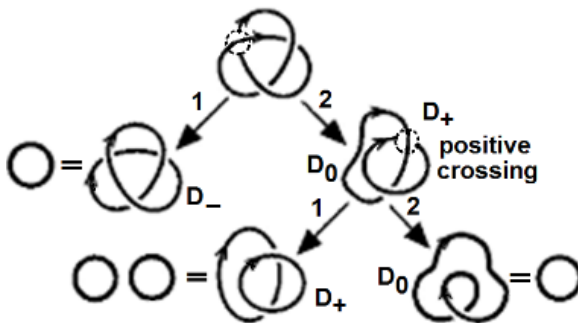


Fig. 12.23. Crossings for octonion trefoil knots.

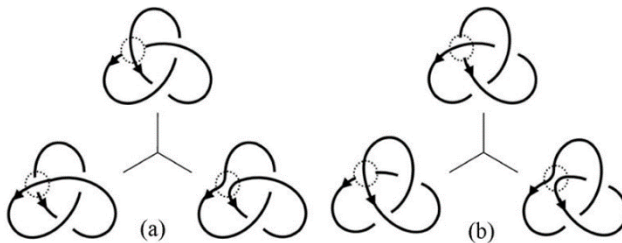


Fig. 12.24. Reduction schemes for the left- and right-handed trefoil knots. (a) Top: left-handed trefoil knot; bottom: writhe γ_- and a Hopf link H_- , with crossing -1 . (b) Top: right-handed trefoil knot; bottom: writhe γ_+ and a Hopf link H_+ , with crossing $+1$. The two knots are mirror images of one another. Figure adapted from [40].



Fig. 12.25. Reduction schemes for Whitehead links W_+ and W_- . (a) Top: Whitehead link W_+ with crossing $+1$; bottom: Hopf link H_- and the left-handed trefoil knot T^L . (b) Top: Whitehead link W_- with crossing -1 ; bottom: Hopf link H_+ , and a figure-of-eight knot F^8 . Figure adapted from [40].

Thus a true octonion contains three trefoil knots, whereas a split octonion may be specified by mixing a pair of quaternion trefoil lines. To define a tripled Fano plane requires three copies of Furey's particle zoo. It describes a set of $21 = 3 \times 7$ (left cyclic) modules over a noncommutative ring on eight elements. The ring is given by the upper triangular $[2 \times 2]$ matrices over the field with two elements. Similarly, for right cyclic modules [41,42].

The quaternions, H are a 4D algebra with basis $1, i, j, k$. To describe the product, it is easy to note that:

- 1 is the multiplicative identity,
- i, j, k are square roots of -1,
- we have $ij = k$, $ji = -k$ and all identities obtained from these by cyclic permutations of (i, j, k) .

We can summarize the last rule as a diagram

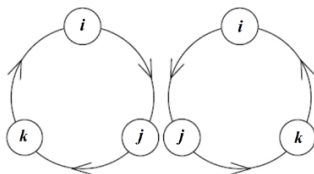


Fig. 12.26. Clockwise and counterclockwise rule for Quaternion cyclicity.

In multiplying two elements going clockwise around the circle we get the next one: for example, $ij = k$. But when we multiply two going around counterclockwise, we get *minus* the next one: for example, $ji = -k$. We can use the same sort of picture to remember how to multiply octonions:

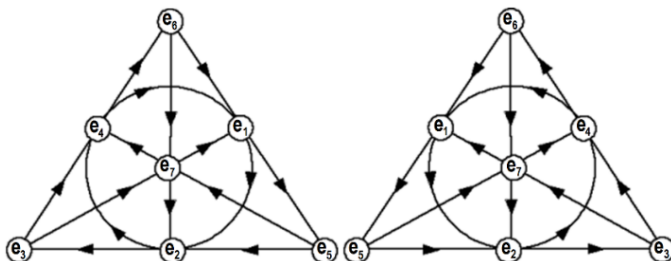


Fig. 12.27. The Fano plane and its mirror image.

The Fano plane is the finite projective plane of order 2, having the smallest possible number of points and lines, 7 each, with 3 points on every line and 3 lines through every point. The Fano plane has 7 points and 7 lines. The 'lines' are the sides of the triangle, its altitudes, and the circle containing all the midpoints of the sides. Each pair of distinct points lies on a unique line. Each line contains three points, and each of these triples has a cyclic ordering shown by the arrows. If e_i, e_j, e_k are cyclically ordered in this way then $e_i e_j = e_k$, $e_j e_i = -e_k$.

Together with these rules:

- 1 is the multiplicative identity,
- e_1, \dots, e_7 are square roots of -1,

the Fano plane completely describes the algebra structure of the octonions. Index-doubling corresponds to rotating the picture a third of a turn. Interestingly, The Fano plane is the projective plane over the 2-element field \mathbb{Z}_2 . In other words, it consists of lines through the origin in the vector space \mathbb{Z}_2^3 . Since every such line contains a single nonzero element, we can also think of the Fano plane as consisting of the seven nonzero elements of \mathbb{Z}_2^3 . If we think of the origin in \mathbb{Z}_2^3 as corresponding to $1 \in O$, we get the following picture of the octonions:

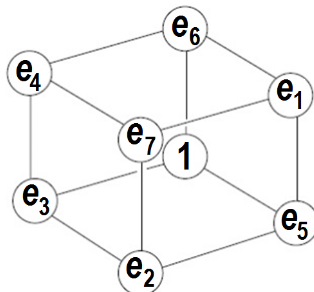


Fig. 12.28. The octonions for $1 \in O$.

Note that planes through the origin of this 3D vector space (Fig. 12.27) give subalgebras of O isomorphic to the quaternions, lines through the origin give subalgebras isomorphic to the complex numbers, and the origin itself gives a subalgebra isomorphic to the real numbers [39].

Now we finally arrive at the fundamental geometric topology for describing ontological-phase topological field theory. When the formalism is next written it will be created by utilizing both topology and complex quaternion/octonions Clifford algebra which is especially suited to handle the manifold embedding [43].

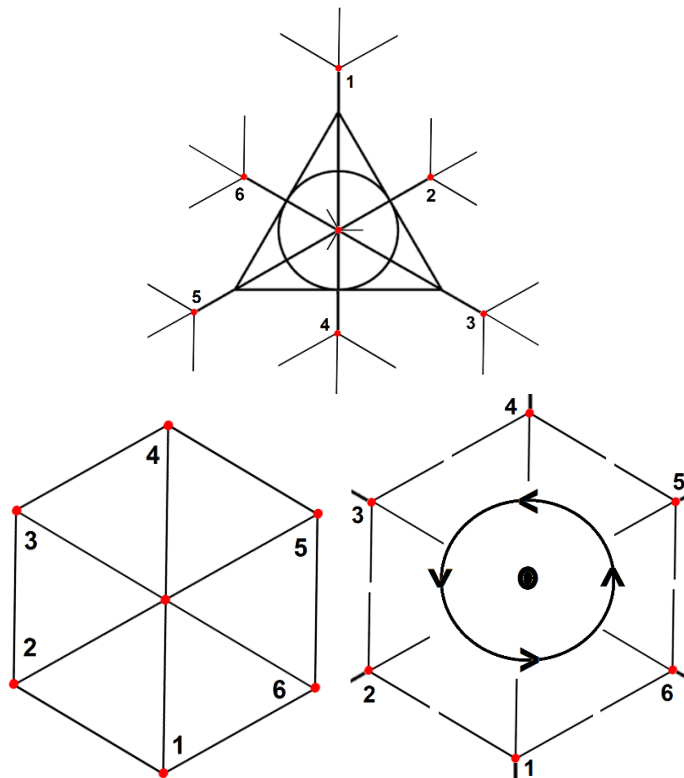


Fig. 12.29. The ‘antennas’ (snowflakes) on a Fano plane (top) represent vertices on the circumference of a hexagon or cube (bottom). The center rotates unconnected so position 1 or 2 can create the front/rear vertices of a Necker cube. b) Antennas 1-6 combine to form the outer vertices of a cube/hexagon depending on what dimensional phase the state is in.

The Fano snowflake configuration in Fig. 12.29 involutes to form a 2D hexagon or vertices of a Euclidean Necker 3-cube. We expect to require a dual set of twin Fano-snowflakes as would be derived from Fig. 12.27 to account for all the parameters necessary for ‘the mirror image of the mirror image to be causally free of the Euclidean 3-space QED quantum state.

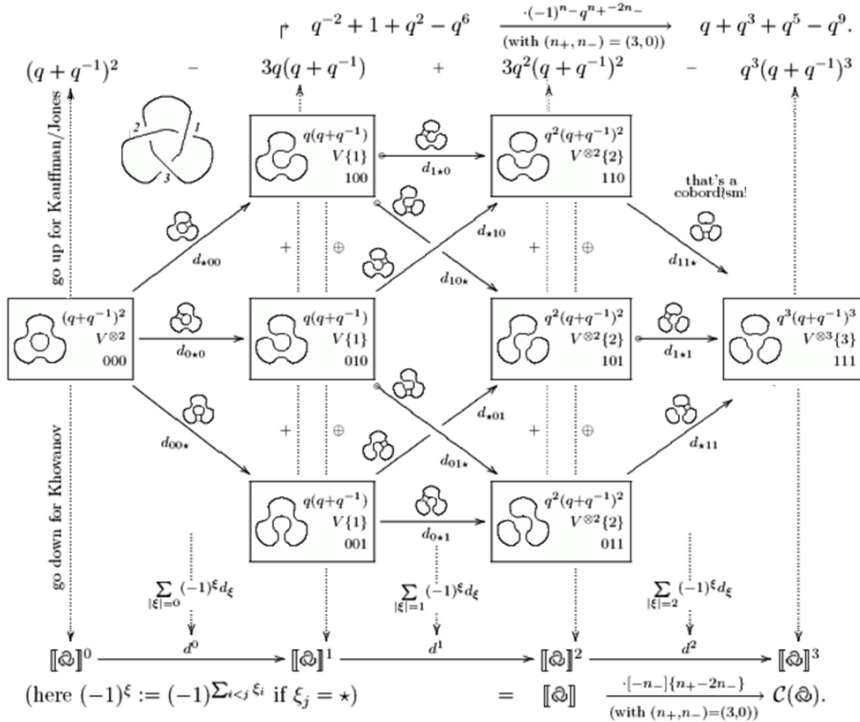


Fig. 12.30. Construction to improve Khovanov's seminal work on the categorification of the Jones polynomial. Figure adapted from [46].

Some of the complexity for categorizing the Jones polynomial is shown in Fig. 12.30 as it might apply to modeling ontological-phase.

12.6 Dual Amplituhedron Geometry and ‘Epionic’ Realism

The amplituhedron geometric jewel simplifies particle interaction calculations and challenges the notion that space and time are fundamental components of reality, advancing a long effort to reformulate quantum field theory, the body of laws describing elementary particles and their interactions by calculations with formulas thousands of terms long that can now be described by computing the volume of its amplituhedron, yielding an equivalent one-term expression. The new geometric version of quantum field theory could also facilitate the search for a theory of quantum gravity. Attempts thus far to incorporate gravity into the laws of physics at the

quantum scale have run up against nonsensical infinities and deep paradoxes. An amplituhedron type geometry could help by removing two deeply rooted principles of physics: locality and unitarity [47].

Locality is the notion that particles can interact only from adjoining positions in space and time. And unitarity holds that the probabilities of all possible outcomes of a quantum mechanical interaction must add up to one. The concepts are the central pillars of quantum field theory in its original form, but in certain situations involving gravity, both break down, suggesting neither is a fundamental aspect of nature. In keeping with this idea, the new geometric approach to particle interactions removes locality and unitarity from its starting assumptions. The amplituhedron is not built out of space-time and probabilities; these properties merely arise as consequences of the jewel's geometry. The usual picture of space and time, and particles moving around in them, is only a useful construct [47].

Because “we know that ultimately, we need to find a theory that doesn’t have” unitarity and locality, Bourjaily said, “*it’s a starting point to ultimately describing a quantum theory of gravity.*” The 1st part of Bourjaily’s statement is correct; however, the 2nd part is not. Most physicists still consider the quantum regime the basement of reality and thus automatically think to progress in unification gravity must be quantized. This is not the regime of integration and therefore obviously why there is no quantum gravity. But transition to the 3rd regime of UFM is confounded ‘epiontcs’. Reality acquires a semi-quantum (epi) limit on the way to the ontological (ontic) regime of UFM [47,48].

The amplituhedron in HD encodes in its volume “scattering amplitudes,” which represent the likelihood that a certain set of particles will turn into certain other particles upon colliding. The twistor theory at the root of it does this kind of simplification. It folds the speed of light into the geometry by mapping point particles to their light cones. The point becomes an intersection of the sphere of light rays that could radiate from it. Then you can do extra stuff like canceling out the asymmetry of universal expansion by mapping the larger future light cone on to the smaller past light cone [49].

Perhaps often, mathematics corresponds perfectly well to physical reality. But maybe now as we move away from a Hilbert space representation of qubit processing to a truly physical basis, we might surmise ‘No wonder it has been difficult to implement bulk QC’. For classical digital computing math itself was sufficient; but as we move to relativistic qubits and topological quantum field theory apparently this is not the case [50].

Jaynes had this to say:

“... our present formalism is not purely epistemological; it is a ... mixture describing in part realities of Nature, in part incomplete human information about Nature ... if we cannot separate the subjective and objective aspects of the formalism we cannot know what we are talking about ...” [50,51].

The term epistemic is used to represent – not real, mind of observer, in contrast to ontic – real; Zurek coined the term epiontic to merge the two philosophies into what he called Quantum Darwinism. Quantum Darwinism describes the proliferation, in the environment, of multiple records of selected states of a quantum system. It explains how the fragility of a state of a single quantum system can lead to the classical robustness of states of their correlated multitude; shows how effective ‘wavepacket collapse’ arises as a result of proliferation throughout the environment of imprints of the states of quantum system; and provides a framework for the derivation of Born’s rule, which relates probability of detecting states to their amplitude. Taken together, these three advances mark considerable progress towards settling the quantum measurement problem [48].

From copying to quantum jumps, Quantum Darwinism leads to appearance, in the environment, of multiple copies of the state of the system. However, the no-cloning theorem [52,53] prohibits copying of unknown quantum states. If cloning is outlawed, how can redundancy be possible? Quick answer is that cloning refers to (unknown) quantum states. So, copying of observables evades the theorem. Nevertheless, the tension between the prohibition on cloning and the need for copying is revealing: It leads to breaking of unitary symmetry implied by the superposition principle, accounts for quantum jumps, and suggests origin of the “wavepacket collapse”, setting stage for the study of quantum origins of probability [50].

Alexander's horned sphere is a convoluted, intertwined surface with a difficult to define inside and outside that is homeomorphic to a ball, meaning that it can be stretched into a ball without being punctured or broken or vice versa. Embedded in Euclidean 3-space, it can be constructed from a torus (Fig. 12.31) in the following manner:

1. Remove a radial slice of the torus.
2. Connect a standard punctured torus to each side of the cut, interlinked with the torus on the other side.
3. Repeat steps 1 & 2 on the two tori added in step two *ad infinitum*.

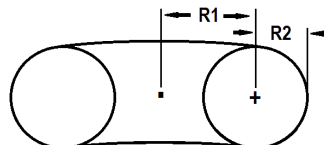


Fig. 12.31. Torus showing minor and major radii.

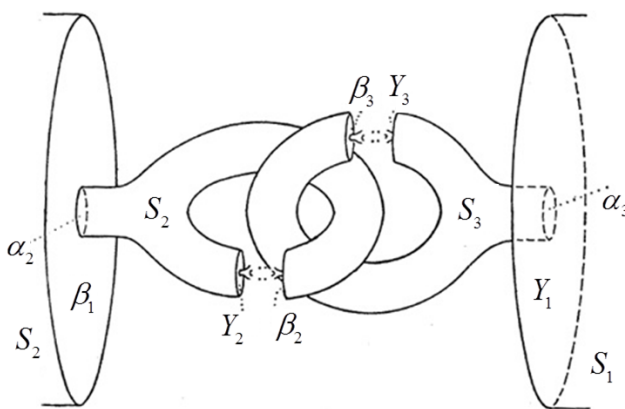


Fig. 12.32. Alexander's horned sphere with infinite fractal-like embeddings. With a finite number of links, we use it to illustrate the ‘chains’ of the manifold of uncertainty, that can be opened only by certain topological moves. Figure adapted form [54].

Time to peek out of the Schrödinger box with the eyes of Alexander’s horned cat...

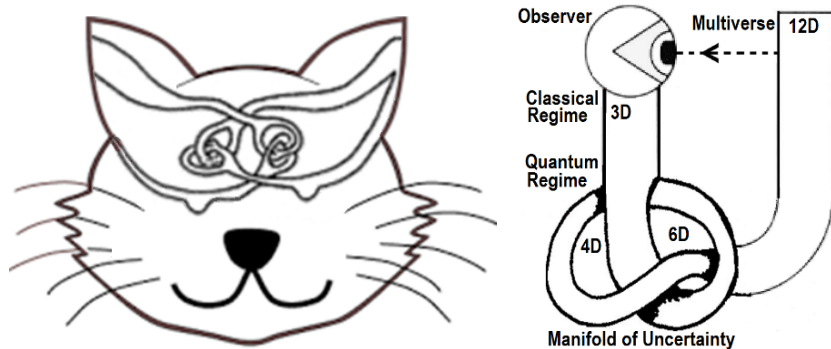


Fig. 12.33. a) Alexander’s horned sphere in the eyes of Schrödinger’s Cat. Is reality ‘created’ by the mind of the observer? Redrawn from [55]. b) Wheeler’s Self-Referential Universe, Does the act of observing the universe create it?

States with different topological orders or different patterns of long range entanglements cannot change into each other without a phase transition. In the case of Alexander's horned sphere, we believe this requires an ontological-phase topological transition.

The horned sphere, together with its inside, is a topological 3-ball, the Alexander horned ball, and so is simply connected; i.e., every loop can be shrunk to a point while staying inside. The exterior is *not* simply connected, unlike the exterior of the usual round sphere; a loop linking a torus in the above construction cannot be shrunk to a point without touching the horned sphere. This shows that the Jordan-Schönflies theorem does not hold in three dimensions as Alexander had originally thought. Alexander also proved that the theorem does hold in three dimensions for piecewise linear/smooth embeddings. This is one of the earliest examples where distinction between the topological category of manifolds, and the categories of differentiable manifolds, and piecewise linear manifolds was noticed.

Now consider Alexander's horned sphere as an embedding into the 3-sphere, considered as the one-point compactification of the 3D Euclidean space R^3 . The closure of the non-simply connected domain is called the solid Alexander horned sphere. Although the solid horned sphere is not a manifold, Bing showed that its double (which is the 3-manifold obtained by gluing two copies of the horned sphere together along the corresponding points of their boundaries) is in fact the 3-sphere. One can consider other gluings of the solid horned sphere to a copy of itself, arising from different homeomorphisms of the boundary sphere to itself. This has also been shown to be the 3-sphere. The solid Alexander horned sphere is an example of a crumpled cube; i.e., a closed complementary domain of the embedding of a 2-sphere into the 3-sphere [56].

References

- [1] Newton, I. (1726) *Philosophiae Naturalis Principia Mathematica*, General Scholium, 3rd edition, I.B. Cohen & A. Whitman's (trans.) (1999) pp. 943, Berkeley: University of California Press.
- [2] Atiyah, M. (1988) New invariants of three and four dimensional manifolds, Proc. Symp. Pure Math., American Math. Soc., 48: 285-299.
- [3] Nayak, C., Simon, S.H., Stern, A., Freedman, M. & Sarma, D.S. (2008) Non-Abelian anyons and topological quantum computation, arXiv:0707.1889v2 [cond-mat.str-el].
- [4] Vlasov, A.Y. (1999) Quantum theory of computation and relativistic physics, PhysComp96 Workshop, Boston MA, 22-24 Nov 1996, arXiv: quant-ph/ 9701027v4.

- [5] Peres, A. & Terno, D.R. (2004) Quantum information and relativity theory, *Rev. Mod. Phys.* 76, 93, arXiv:quant-ph/0212023v2.
- [6] Jafarizadeh, M.A. & Mahdian, M. (2011) Quantifying entanglement of two relativistic particles using optimal entanglement witness, *Quantum Information Processing*, 10:4, pp. 501-518.
- [7] Felicetti, S., Sabin, C., Fuentes, I., Lamata, L., Romero, G. & Solano, E. (2015) Relativistic motion with superconducting qubits, arXiv:1503.06653v2 [quant-ph].
- [8] Zurek, W.H. (2009) Quantum Darwinism, arXiv:0903.5082v1 [quant-ph].
- [9] Zurek, W.H. (2003) Quantum Darwinism and envariance, arXiv:quant-ph/0308163v1; in J.D. Barrow, P.C.W. Davies, & C.H. Harper (eds.) *Science and Ultimate Reality: From Quantum to Cosmos*, Cambridge University Press.
- [10] Zurek, W.H. (2003) Environment - assisted invariance, ignorance, and probabilities in quantum physics, *Phys. Rev. Lett.* 90, 120404.
- [11] Atiyah, M. (1989) Topological quantum field theories, *Inst. Hautes Etudes Sci. Publ. Math.* 68, 175-186.
- [12] Amoroso, R.L., Kauffman, L.H. and Rowlands, R. (eds.) (2016) *Unified Field Mechanics: Natural Science Beyond the Veil of Spacetime*, Singapore: World Scientific.
- [13] Kotigua, R.P. & Toffoli, T. (1998) Potential for computing in micromagnetics via topological conservation laws, *Physica D*, 120:1-2, pp. 139-161.
- [14] Stern, A. (1992) *Matrix logic and the Mind, a Probe Into a Unified Theory of Mind and Matter*, Amsterdam: Northern-Holland; Stern, A. (2000) *Quantum Theoretic Machines*, New York: Elsevier Science.
- [15] Zhang, K. & Li, D. (2007) *Electromagnetic Theory for Microwaves and Optoelectronics* (2nd ed.) Springer Science & Business Media.
- [16] Singh, R.R (2009) *Phasor Representation of Alternating Quantities, Electrical Networks*, McGraw Hill Higher Education.
- [17] Messiah, A. (1999) *Quantum Mechanics*, New York: Dover.
- [18] Solem, J.C.; Biedenharn, L.C. (1993) Understanding geometrical phases in quantum mechanics: An elementary example, *Foundations of Physics* 23 (2): 185-195.
- [19] Pancharatnam, I. (1956) Generalized theory of interference, and its applications, Part I. coherent pencils, *Proc. Indian Acad. Sci. A44*: 247-262.
- [20] Berry, M.V. (1984) Quantal phase factors accompanying Adiabatic changes, *Proceedings of the Royal Society A* 392 (1802): 45-57.
- [21] Xiao, D., Chang, M.C., & Niu, Q. (2010) Berry phase effects on electronic properties, *Reviews of modern physics*, 82(3), 1959.
- [22] von Bergmann, J. & von Bergmann, H.C. (2007) Foucault pendulum through basic geometry, *Am. J. Phys.* 75 (10): 888-892.
- [23] Kitaev, A.Y. (1997) Quantum communication, computing and measurement, in O. Hirota, A.S. Holevo & C.M. Caves (eds.) *Proceedings of the 3rd International Conference of Quantum Communication and Measurement*, New York: Plenum.
- [24] Kitaev, A.Y. (2006) Anyons in an exactly solved model and beyond, *Annals of Physics*, 321(1), 2-111.
- [25] Petit, J-P (2012) Twin universe astrophysics, <http://www.jp-petit.org/science/f300/f3800/f3802.htm>.
- [26] Witten, E. (1988) Topological quantum field theory, *Comm. Math. Phys.* 117, 353-386.
- [27] Witten, E. (1989) Quantum field theory and the Jones polynomial. *Communications in Mathematical Physics*, 121(3), 351-399.

- [28] Thom, R. (1954) *Quelques propriétés globales des variétés différentiables*, Comment. Math. Helv. 28, 17-86.
- [29] Chern, S-S & Simons, J. (1974) Characteristic forms and geometric invariants, The Annals of Mathematics, Second Series 99, 48–69.
- [30] Poelstra, A. (2013) A Brief overview of topological quantum field theory, <https://www.wpssoftware.net/andrew/school/tqfts.pdf>.
- [31] Baulieu, L., Losev, A., & Nekrasov, N. (1998) Chern-Simons and twisted supersymmetry in various dimensions, Nuclear Physics B, 522 (1) 82-104.
- [32] Han, C., Park, J., Gefen, Y. & Sim, H-S (2016) Topological vacuum bubbles by anyon braiding, Nature Communications, 7:11131, pp. 1-6.
- [33] Fetter, A.L. & Walecka, J.D. (1971) Quantum Theory of Many-Particle Systems, McGraw-Hill.
- [34] Necker, L.A. (1832) Observations on some remarkable optical phænomena seen in Switzerland; and on an optical phænomenon which occurs on viewing a figure of a crystal or geometrical solid, pp. 329-337, Vol. 1, No. 5, Philosoph. Magazine, Series 3.
- [35] Kauffman, L.H. (2016) From Hamilton’s quaternions to Graves and Cayley’s Octonions, <https://www.researchgate.net/publication/299575683>.
- [36] Stolfi, J. (1991) Oriented Projective Geometry, Boston: Academic Press.
- [37] Shaw, R.E. & Mace, W.M. (2005) The value of oriented geometry for ecological psychology and moving image art, in J.D. Anderson & B.F. Anderson (eds.) Moving Image Theory, Carbondale: S. Il. Univ. Press.
- [38] Iwakiri, M. & Satoh, S. (2011) Quandle cocycle invariants of roll-spun knots, <http://www.kurims.kyoto-u.ac.jp/~kyodo/kokyuroku/contents/pdf/1766-04.pdf>.
- [39] Baez, J.C. & Dolan, J. (1995) Higher dimensional algebra and topological quantum field theory, J. Math. Phys. 36, 6073, [arXiv:q-alg/9503002].
- [40] Liu, X. & Ricca, R.L. (2012) The Jones polynomial for fluid knots from helicity, J. Phys. A: Math. Theor. 45, 205501.
- [41] Furey, C. (2012) Unified theory of ideals, Physical Review D, 86(2), 025024.
- [42] <http://pseudomonad.blogspot.com/2011/02/theory-update-51.html>.
- [43] Schray, J. & Manogue, C.A. (1994) Octonionic representations of Clifford algebras and triality, arXiv:hep-th/9407179v1.
- [44] Saniga, M., Havlicek, H., Planat, M., & Pracna, P. (2008). Twin “Fano-Snowflakes” over the smallest ring of ternions. SIGMA, 4(050), 7.
- [45] Saniga, M., & Pracna, P. (2008) A Jacobson radical decomposition of the Fano-Snowflake configuration, SIGMA Symm. Integrability Geom. Methods Appl, 4(072), 7.
- [46] Bar-Natan, D. (2002) On Khovanov’s categorification of the Jones polynomial, Algebraic and Geometric Topology 2-16, 337-370, <http://www.math.toronto.edu/drorbn/papers/Categorification/>, arXiv:math.QA/9908171; arXiv:math.QA/0103190.
- [47] Wolchover, N. (2013) Scientists discover a jewel at the heart of quantum physics, Quanta Magazine, division of Simons foundation.org, <http://www.wired.com/2013/12/amplituhedron-jewel-quantum-physics/>.
- [48] Wootters, W.K., and Zurek, W.H. (1982) A single quantum cannot be cloned, Nature 299, 802-803.
- [49] Arkani-Hamed, N., & Trnka, J. (2013) The amplituhedron, arXiv preprint arXiv: 1312.2007.
- [50] Herbut, F. (2014) Fleeting critical review of the recent ontic breakthrough in quantum mechanics, arXiv:1409.6290v1 [quant-ph].

- [51] Jaynes, E.T. (1990) in Complexity, entropy, and the physics of information, p. 381, W.H. Zurek (ed.) Redwood City: Addison-Wesley.
- [52] Dieks, D. (1982) Communication by EPR devices, Phys. Lett. 92A, 271.
- [53] Zurek, W.H. (2009) Quantum Darwinism, arXiv:0903.5082v1 [quant-ph].
- [54] Alexander, J.W. (1924) An example of a simply connected surface bounding a region which is not simply connected, Proceedings of the National Academy of Sciences USA, 10 (1): 8-10.
- [55] Bing, R.H. (1983) The geometric topology of 3-manifolds, Vol. 40, American Mathematical Soc.
- [56] Bing, R.H. (1952) A homeomorphism between the 3-sphere and the sum of two solid horned spheres, Annals of Mathematics. Second Series 56: 354-362.

Chapter 13

New Classes of Quantum Algorithms

Quantum algorithm research and development remains in its infancy, because although a fair number of quantum gates and qubit technology platforms exist, it is safe to say that until an actual Universal Quantum Computer (UQC) implementation capable of bulk operation occurs, a complete conception of what sufficient quantum algorithms are seems unlikely; especially if much of the novel new parameters proposed in this monograph are required. Meaning for example, that the first bulk quantum computing system might in actuality be scalable, but there may be a dearth of quantum algorithms to implement sufficient quadratic speedup for practical utility beyond classical computing. We propose a new class of unified field mechanical (UFM) based holographic quantum algorithms with asymptotic speedup beyond the purely classical holographic reduction algorithmic process currently under development even to the point of a new class of instantaneous algorithms. There is recent talk of an end to locality and unitarity as a new basis for QC, along with the new field relativistic information processing (RIP); these scenarios may cause dramatic changes in QC research.

13.1 Introduction - From al-Khwarizmi to Unified Field-Gorhythms

The concept of ‘Algorithm’ reaches back to the creation of Arabic numerals in the 9th Century by Abu Jafar Muhammad ibn Musa al-Khwarizmi (Latin *Algoritmi*) and the methods of calculation utilizing them. He developed solutions to six varieties of linear and quadratic equations. His famous treatise on the subject, *Hisab al-jabr w'al-muqabala*, translated into Latin as *Liber algebrae et almucabala*, gave us the word ‘algebra’ [1,2]. The House of Wisdom at Baghdad during his lifetime was the Golden Age of Arabic science and mathematics.

In simplest terms, a classical algorithm is a finite sequence of instructions, step-by-step process or set of rules followed in calculations or other computed logical operations which always terminates. A quantum algorithm runs on a realistic model of quantum information processing, usually applied to algorithms that are inherently quantum using some essential feature of quantum computation such as quantum superposition or entanglement. The development of algorithms for simulating quantum mechanical systems was Feynman's original motivation for proposing a quantum computer [1]. Quantum algorithms require modules that are uniformly scalable and reversible (unitary) that can be efficiently implemented; the most commonly used model has been the quantum circuit model [3,4].

Generally, an algorithm is the procedure or set of instructions used to perform an information processing task. According to the strong Turing-Church thesis: Any algorithmic process can be simulated efficiently using a probabilistic Turing machine. Here, the word efficiently classifies algorithms into two main complexity classes - P and NP, where P is a polynomial type algorithm and NP the non-deterministic polynomial type algorithm. An algorithm is of the P-class if it has an 'efficient solution', meaning it runs in a polynomial time the size of the problem to be solved. An NP-class algorithm does not have an efficient solution or requires super-polynomial (usually exponential) time. For example, prime factorization of an integer is NP-type algorithm because no efficient solution is known for solving the problem. Deutsch first showed by a simple example the existence of an efficient QC solution for a classically classified NP problem [5]. In 1994, Shor demonstrated that prime factorization has an efficient solution in QC. But only a few NP-class problems can be solved efficiently with a QC [6]. Numerous NP-class problems exist for which no efficient algorithm is known even in QC. Although it is clear that P is a subset of NP, but whether $P = NP$ or $P \neq NP$ is still an unsolved puzzle to the QC research community [4].

In general, input to a quantum algorithm consists of n classical bits, and the output also consists of n classical bits. If the input is an n -bit string x , then the QC takes input as n qubits in state $|x\rangle$. Then a series of quantum operations are performed, at the end of which the state of the n qubits is transformed to some superposition $\sum_y \alpha_y |y\rangle$. Afterwards, a measurement is made, which has as output the n -bit string y with probability $|\alpha_y|^2$ [4].

13.2 The Church-Turing Hypothesis

The Church-Turing thesis states that any function that can be computed by a physical system can be computed by a Turing Machine. Many mathematical functions cannot be computed on a Turing Machine such as the halting function $h : \mathbb{N} \rightarrow \{0,1\}$ that decides whether the i^{th} Turing Machine halts or the function that decides whether a multivariate polynomial has integer solutions. Therefore, the physical Church-Turing thesis is a strong statement of belief about the limits of both physics and computation. Some functions can be computed faster on a quantum computer than on a classical one, but, as noticed by Deutsch [5,7], this does not challenge the physical Church-Turing thesis itself: a QC could even be simulated by pen and paper, through matrix multiplications. Therefore, what they compute can be computed classically.

Several researchers have pointed out that Quantum theory does not forbid, in principle, that some evolutions would break the physical Church-Turing thesis [8-10]. Technically, the only limitation upon quantum evolution is that it be by unitary operators. Then, as Nielsen argues, it suffices to consider the unitary operator, $U = \sum |i, h(i) \oplus b\rangle \langle i, b|$, with i over integers and b over $\{0,1\}$, to have a counterexample [9].

The paradox between Deutsch's and Nielsen's arguments is only an apparent one as both are valid; the former applies specifically to Quantum Turing Machines and the latter to full-blown quantum theory. This is not satisfactory; if Quantum Turing Machines are to capture Quantum theory's computational power, it falls short, and needs amending. Unless in contrast, quantum theory itself needs to be amended, and its computational power brought down to the level of the Quantum Turing Machine [11,12]. Most likely quantum theory will be amended.

It was known very early on that quantum algorithms cannot compute functions that are not computable by classical computers, however they might be able to efficiently compute functions that are not efficiently computable on a classical computer [5]. This scenario may evolve also.

13.3 Algorithms Based on the Quantum Fourier Transform

The first QC algorithms were called the ‘black-box or ‘oracle’ framework, where part of the input is a black-box implementing a function $f(x)$. The

only way to extract information about f was to evaluate it on the x inputs. These early algorithms used a special case of the quantum Fourier transform, the Hadamard gate. This allowed a problem to be solved with fewer black-box evaluations of f than a classical algorithm would need [12]. Deutsch [7] formulated the problem of deciding whether a function, $f : \{0,1\} \rightarrow \{0,1\}$ was constant. If one has access to a black-box implementing f reversibly by mapping $x, 0 \mapsto x, f(x)$; one further assumes that the black box does implement a unitary transformation U_f mapping $|x\rangle|0\rangle \mapsto |x\rangle|f(x)\rangle$. Deutsch's problem is to output "constant" if $f(0) = f(1)$ and to output "balanced" if $f(0) \neq f(1)$, given a black-box for evaluating f . Thus, to determine $f(0) \oplus f(1)$ (\oplus denotes addition modulo 2). Outcome '0' means f is constant and outcome '1' means f is not constant [12].

Classical algorithms would have to evaluate f twice to solve the problem. A quantum algorithm can only apply U_f once to produce

$$\frac{1}{\sqrt{2}}|0\rangle|f(0)\rangle + \frac{1}{\sqrt{2}}|1\rangle|f(1)\rangle. \quad (13.1)$$

With an end to the no-cloning theorem by UFM parameter based QC, another basis change will probably occur for QC development.

Under these conditions, if $f(0) = f(1)$, applying the Hadamard gate to the first register yields $|0\rangle$ with probability 1, and if $f(0) \neq f(1)$, then applying the Hadamard gate to the first register and ignoring the second register leaves the first register in the state $|1\rangle$ with probability 1/2; thus a result of $|1\rangle$ can only occur if $f(0) \neq f(1)$ [12].

Of special interest, given

$$\frac{1}{\sqrt{2}}|0\rangle|\psi_0\rangle + \frac{1}{\sqrt{2}}|1\rangle|\psi_1\rangle \quad (13.2)$$

a 'Hadamard test' can be performed if a Hadamard gate is applied to the first qubit. A measurement will give '0' with probability $\frac{1}{2} + \text{Re}(\langle \psi_0 | \psi_1 \rangle)$ [12].

13.4 Exponential Speedup by Quantum Information Processing

The salient utility of UQC is the offering of algorithms that will provide a fully exponential speed-up over classical algorithms, making them the most sought after research avenue for unleashing the power of QC's. Let's follow the work of Aaronson for finding a general theorem for developing exponential speedups from quantum algorithms; in recent efforts he makes two advances toward such a theorem in the black-box model where most quantum algorithms operate [13].

- First, Aaronson shows for any problem invariant under permuting inputs and outputs that has sufficiently many outputs (like collision and element distinctness problems), the quantum query complexity is at least the 7th-root of classical randomized query complexity. Earlier he found a 9th-root [14], resolving a conjecture of Watrous [15].
- Second, inspired by work of O'Donnell [16] and Dinur [17], he conjectured that every bounded low-degree polynomial has a 'highly influential' variable. (A multivariate polynomial p is *bounded* if $0 \leq p(x) \leq 1$ for all x in the Boolean cube.) Assuming this conjecture, he then showed that every T -query quantum algorithm can be simulated on most inputs by a $TO(1)$ -query classical algorithm. Essentially one cannot hope to prove $P \neq BQP$ relative to a random oracle.

Perhaps the central lesson gleaned from fifteen years of quantum algorithms research is this: Quantum computers can offer superpolynomial speedups over classical computers, but only for certain "structured" problems. The key question, of course, is what we mean by "structured." In the context of most existing quantum algorithms, "structured" basically means that we are trying to determine some global property of an extremely long sequence of numbers, assuming that the sequence satisfies some global regularity [13].

Aaronson offers period finding as a canonical example, the core of Shor's factoring algorithms and computing discrete logarithms [18] where black-box access to exponentially-long sequences of integers $X = (x_1, \dots, x_N)$ is given; that is, to compute x_i for a given i . We find the *period* of X , that is, the smallest $k > 0$ such that $x_i = x_{i-k}$ for all $i > k$ with the promise that X is indeed periodic, with period $k \ll N$ (and that the x_i values are approximately distinct within each period). The requirement of periodicity is crucial: it lets us use the Quantum Fourier Transform to extract the information we want from a superposition of the form

$$\frac{1}{\sqrt{N}} \sum_{i=1}^N |i\rangle|x_i\rangle. \quad (13.3)$$

For other known quantum algorithms, X needs to be a cyclic shift of quadratic residues [19], or constant on the cosets of a hidden subgroup.

By contrast, the canonical example of an ‘unstructured’ problem is the Grover search problem. Black-box access is given to an N -bit string $(x_1, \dots, x_N) \in \{0,1\}^N$, and we are asked whether there exists an i such that $x_i = 1$. Grover formulated a quantum algorithm to solve this problem using $O(\sqrt{N})$ queries [20], as compared to the $\Omega(N)$ needed classically. However, Bennett et al. showed this quadratic speedup is optimal [21]. For other “unstructured” problems see [22-26].

This ‘need for structure’ limits prospects for super-polynomial quantum speedups to areas of mathematics likely to produce similar periodic sequences or sequences of quadratic residues. This is the fundamental reason why the greatest successes of quantum algorithm research have been cryptographic, specifically in number-theoretic cryptography. This helps to explain why there are no fast quantum algorithm to solve NP-complete problems, or to break arbitrary one-way functions [13,27].

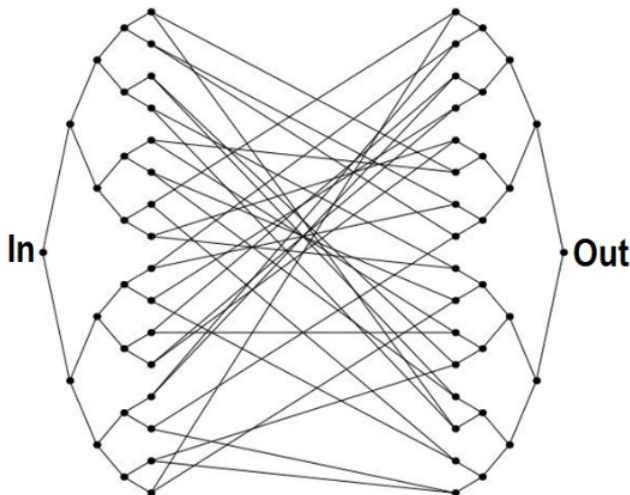


Fig. 13.1. Quantum walk algorithm graph. Figure adapted from [27].

Quantum walk algorithms can achieve provable exponential speedups over any classical algorithm (in query complexity), but according to Childs et al. only for extremely fine-tuned' graphs [27].

In the 20 years since the appearance of Shor's factoring algorithm only a few additional quantum algorithms like Grover's search and quantum walks have appeared. Aaronson claims that while there are a number of exponential and polynomial speedup algorithms, “*there just aren't that many compelling candidates left for exponential quantum speedups*” [28].

$$\begin{bmatrix} \mathbf{F1} \\ \mathbf{F2} \\ \mathbf{F3} \\ \mathbf{F4} \\ \mathbf{F5} \\ \mathbf{F6} \\ \mathbf{F7} \\ \mathbf{F8} \end{bmatrix} = \begin{bmatrix} \textcircled{-} \textcircled{-} \textcircled{-} \textcircled{-} \textcircled{-} \textcircled{-} \textcircled{-} \\ \textcircled{-} \textcircled{\frac{1}{2}} \textcircled{\frac{1}{2}} \textcircled{\frac{1}{2}} \textcircled{\frac{1}{2}} \textcircled{\frac{1}{2}} \textcircled{\frac{1}{2}} \\ \textcircled{\frac{1}{2}} \textcircled{-} \textcircled{-} \textcircled{-} \textcircled{-} \textcircled{-} \textcircled{-} \\ \textcircled{-} \textcircled{\frac{1}{2}} \textcircled{\frac{1}{2}} \textcircled{\frac{1}{2}} \textcircled{\frac{1}{2}} \textcircled{\frac{1}{2}} \textcircled{\frac{1}{2}} \\ \textcircled{-} \textcircled{-} \textcircled{-} \textcircled{-} \textcircled{\frac{1}{2}} \textcircled{\frac{1}{2}} \textcircled{\frac{1}{2}} \\ \textcircled{-} \textcircled{-} \textcircled{-} \textcircled{\frac{1}{2}} \textcircled{\frac{1}{2}} \textcircled{\frac{1}{2}} \textcircled{\frac{1}{2}} \\ \textcircled{\frac{1}{2}} \textcircled{-} \textcircled{\frac{1}{2}} \textcircled{\frac{1}{2}} \textcircled{\frac{1}{2}} \textcircled{\frac{1}{2}} \textcircled{\frac{1}{2}} \\ \textcircled{-} \textcircled{\frac{1}{2}} \textcircled{\frac{1}{2}} \textcircled{\frac{1}{2}} \textcircled{\frac{1}{2}} \textcircled{\frac{1}{2}} \textcircled{\frac{1}{2}} \end{bmatrix} \begin{bmatrix} f_1 \\ f_2 \\ f_3 \\ f_4 \\ f_5 \\ f_6 \\ f_7 \\ f_8 \end{bmatrix}$$

Fig. 13.2. Shor-like Fourier transform algorithms.

Factoring algorithms can break almost all public-key cryptosystems used today, but theoretical public-key systems exist that are unaffected, causing one to ask, ‘*Can Shor's algorithm be generalized to nonabelian groups?*’ [28].

Grover-like algorithms provide Quadratic speedup for any problem involving searching an unordered list, provided the list elements can be queried in superposition. This implies subquadratic speedups for many other basic problems [21]. For black-box searching, the square root speedup of Grover's algorithm is the best possible approach [29-31].

It was shown, if a fast, classical exact simulation of boson sampling is possible, then the polynomial hierarchy collapses to the third level. Experimental demonstrations with 3-4 photons were achieved [29-31].

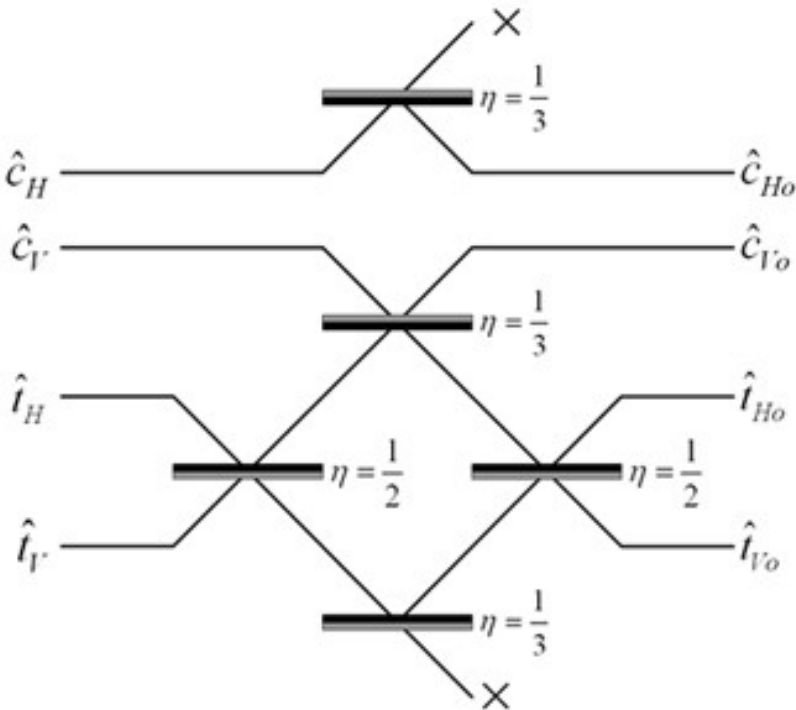


Fig. 13.3. Boson sampling algorithm. Identical single photons sent through network of interferometers, then measured at output modes. Figure adapted from [28].

13.5 Classical Holographic Reduction Algorithms

Yes, holographic algorithms (HA) already exist, a concept originated by Valiant in 2004 [32]. HA utilize a process called ‘holographic reduction’ mapping solution fragments ‘many-to-many’ so that the summation of solution fragments remains unchanged. Valiant coined the term HA because “*their effect can be viewed as that of producing interference patterns among the solution fragments*” [32]. The power of HA comes from the mutual cancellation of many contributions to a sum, analogous to the interference patterns in a hologram [33]. So far HA have discovered solutions to previously unsolved polynomial problems. Although HA have some similarities to quantum computation, they are currently completely classical in nature [34].

Holographic algorithms occur in the context of what is called Holant problems, which generalize counting Constraint Satisfaction Problems

(#CSP). A #CSP example is the hypergraph $G = (V, E)$ also called a constraint graph. Each hyperedge is a variable and each vertex, v is assigned a constraint, f_v . A vertex is connected to a hyperedge if the constraint on the vertex involves the variable on the hyperedge. The counting problem is to compute

$$\sum_{\sigma: E \rightarrow \{0,1\}} \prod_{v \in V} f_v(\sigma | E_{(v)}), \quad (13.4)$$

which is a sum over all variable assignments, the product of every constraint, where the inputs to the constraint f_v are the variables on the incident hyperedges of v .

A Holant problem is similar to a #CSP except the input must be a graph, not a hypergraph. For a #CSP instance, one replaces each hyperedge, e of size, s with a vertex, v of degree, s with edges incident to the vertices contained in e . The constraint on v is the equality function of s identifying all the variables on the edges incident to v . For Holant problems, Eq. 13.4 is called the Holant after a related exponential sum introduced by Valiant [35]. To further clarify, Holant is a framework of counting characterized by local constraints. It is closely related to other well-studied frameworks such as #CSP and Graph Homomorphism. An e dichotomy for such frameworks can immediately settle the complexity of all combinatorial problems expressible in that framework. Both #CSP and Graph Homomorphism can be viewed as sub-families of Holant with the additional assumption that the equality constraints are always available [35].

Considering holographic reduction, for a bipartite graph $G = (U, V, E)$ the constraint assigned to each vertex $u \in U$ is f_u , likewise for vertex $v \in V$ is f_v . This counting problem is $\text{Holant}(G, f_u, f_v)$. Thus for a complex 2×2 invertible matrix T , there is a holographic reduction between $\text{Holant}(G, f_u, f_v)$ and $\text{Holant}(G, f_u, T^{\otimes(\deg u)}, (T^{-1})^{\otimes(\deg v)} f_v)$. Thus, $\text{Holant}(G, f_u, f_v)$ and $\text{Holant}(G, f_u, T^{\otimes(\deg u)}, (T^{-1})^{\otimes(\deg v)} f_v)$ have precisely the same Holant value for all constraint graphs, essentially defining the same counting problem, which can also be proved using holographic reduction. Valiant's original application of holographic algorithms used holographic reduction which has since been used in polynomial time algorithms and proofs of #P-hardness [36].

13.6 Ontological-Phase UFM Holographic Algorithms

To try to stop all attempts to pass beyond the present viewpoint of quantum physics could be very dangerous for the progress of science and would furthermore be contrary to the lessons we may learn from the history of science. This teaches us, in effect, that the actual state of our knowledge is always provisional and that there must be, beyond what is actually known, immense new regions to discover – de Broglie [37].

A fundamental theory is needed which would tell us from first principles when quantum speedups are possible. There is a related longstanding open problem: Is there any Boolean function with a quantum quantum/classical gap better than quadratic? A Boolean function, f is simply

$$f : \{0,1\}^n \rightarrow \{0,1\} \quad (13.5)$$

with n input bits and a single output bit [4]. We will answer yes below.

There are new results from Ben-David: If $F : S_N \rightarrow \{0,1\}$ is any Boolean function of permutations, then $D(F) = O(Q(F)^{12})$. If F is any function with a symmetric *promise*, and at most M possible results of each query, then $R(F) = O(Q(F)^{12(M-1)})$ [38]. We need a ‘structured’ promise if we want an exponential quantum speedup. Exponential quantum speedups depend on structure. For example, abelian group structure, glued-trees structure, or relational structure...

The term Semiclassical in common usage means: intermediate between a classical Newtonian description and one based on quantum mechanics or relativity. Semiclassical physics, refers to a theory in which one part of a system is described quantum-mechanically whereas the other is treated classically. For example, external fields will be constant, or when changing will be classically described. In general, it incorporates a development in powers of Planck's constant, resulting in the classical physics of power 0, and the first nontrivial approximation to the power of (-1) . In this case, there is a clear link between the quantum mechanical system and the associated semi-classical and classical approximations.

Now for UFM, we create a new term, semi-quantum where one part will be quantum and the other part UFM. This is a small regime of finite radius called the Manifold of Uncertainty (MOU). This is the 1st step in the realization that the central pillars of quantum field theory, spacetime, locality and unitarity are to be superseded. In assuming the universe is a huge information processor, in terms of unitarity and locality

(phenomenal) each distinct point is like a central processing unit (CPU), but in the move to nonlocality and holographic (ontological) ballistic processing, there is no CPU; there is a simultaneity of information at each tessellated node. Clearly, I am trying to say this scenario is not classical or quantum, but a unified field mechanical ontology. It is hard to fathom what kind of algorithm, from a new class of holographic ontological algorithms able to operate without decohering the wavefunction, this leads to.

Creative thinking has already begun to skirt this empyrean realm:

All we experience is nothing but a holographic projection of processes taking place on some distant surface that surrounds us. - Brian Greene

Discovery of the amplituhedron could cause an even more profound shift ... That is, giving up space and time as fundamental constituents of nature and figuring out how the ... universe arose out of pure geometry ... In a sense, we would see that change arises from the structure of the object, but it's not from the object changing. The object is basically timeless. - Nima Arkani-Hamed

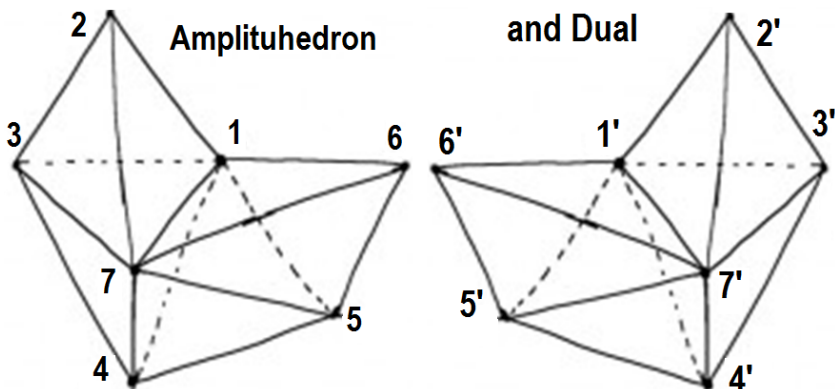


Fig. 13.4. 7-point Amplituhedron in P^3 with Amplitude for $[1^- 2^+ 3^+ 4^+ 5^+ 6^+ 7^- 8^-]$ and its dual. The Hubble sphere, H_R may be one huge geometric Amplituhedron.

Figure 13.4 is a sketch of the basic amplituhedron element, $A_{n,k,L;m}$ which lives in $G(k, k+m; L)$, the space of k -planes Y in $k+m$ dimensions, together with L 2-planes L_1, \dots, L_L in the m -dimensional compliment of Y [41], representing an 8-gluon particle interaction using Feynman diagrams. The amplituhedron is a newly discovered mathematical object resembling a multifaceted jewel in HD. Encoded in its volume are the most basic features of reality that can be calculated - the probabilities of outcomes of

particle interactions. This, or a similar geometric object, could help remove two deeply rooted physical principles: locality and unitarity from quantum field theories' basic assumptions [39-41].

The amplitude form is positive when evaluated inside the amplituhedron. The statement is sensibly formulated thanks to the natural 'bosonization' of the superamplitude associated with the amplituhedron geometry. However, this positivity is not manifest in any of the current approaches to scattering amplitudes, and in particular not in the cellulations of the amplituhedron related to on-shell diagrams and the positive Grassmannian. The surprising positivity of the form suggests the existence of a 'dual amplituhedron' formulation where this feature would be made obvious [41].

Locality is the idea that particles can interact only from adjoining positions in space and time, and unitarity states that the probabilities of all possible outcomes of a quantum mechanical interaction must add up to one. The amplituhedron is not built out of spacetime and probabilities; these properties merely arise as consequences of the jewel's geometry. The usual picture of space and time, with particles moving around in them, is a construct. "*Locality and unitarity emerge hand-in-hand from the positive geometry of the amplituhedron*" [39-41]. What is beyond the end to locality and unitarity as we know it?

In a confoundingly humorous parody Scott Aaronson has this to say about the amplituhedron:

My colleagues and I have been investigating a mathematical structure that contains the amplituhedron, yet is even richer and more remarkable. I call this structure the 'unitarihedron'...The unitarihedron encompasses, within a single abstract 'jewel,' all the computations that can ever be feasibly performed by means of unitary transformations, the central operation in quantum mechanics (hence the name). Mathematically, the unitarihedron is an infinite discrete space: more precisely, it's an infinite collection of infinite sets, which collection can be organized (as can every set that it contains!) in a recursive, fractal structure. Remarkably, each and every specific problem that quantum computers can solve - such as factoring large integers, discrete logarithms, and more - occurs as just a single element, or 'facet' if you will, of this vast infinite jewel. By studying these facets, my colleagues and I have slowly pieced together a tentative picture of the elusive unitarihedron itself [42]. – Scott Aaronson.

Aaronson's parody is of course justified, especially at this stage of development. The QC paradigm until now has been local and semiclassical. Aaronson himself said, '*UQC will require a new discovery in physics*'. Our *hypothesis non fingo* is that this putative discovery in physics is in fact a Gödelization beyond quantum mechanics (unitarity and locality) into the 3rd regime of reality dubbed UFM. We have seen that holographic computing algorithms are classical; we are not just looking

for a quantum holography (already exists in NMR spectroscopy), we are proposing a special new class of UFM algorithms. In the course of preparing this volume our opinion on this matter has evolved. We thought that the existing body of QC research would suffice; and what we had to add to the mix was ontological measurement without collapse and violation of the no-cloning theorem. We hope it is obvious that opinion has changed. If one has the stamina to read this whole volume, one sees we expend a lot of effort skirting around issues without doing much of the math. This is our excuse; NASA flew around the moon a couple times before actually landing on it.

Since the framework of quantum mechanics seems to rest on unitarity, most physicists will tend to look for possible ways to get around such a drastic modification. In quantum physics, unitarity is a restriction on the allowed evolution of quantum systems that ensures the sum of probabilities of all possible outcomes of any event is always 1.

Giving up space and time as fundamental constituents of nature and figuring out how the cosmological evolution of the universe arose out of pure geometry is a fascinating opportunity. In a sense, we would see that change arises from the structure of the object. But it's not from the object changing. The object is basically timeless. The revelation that particle interactions, the most basic events in nature, may be consequences of geometry significantly advances a decades-long effort to reformulate quantum field theory, describing elementary particles and their interactions. Interactions that were previously calculated with mathematical formulas thousands of terms long can now be described by computing the volume of the corresponding jewel-like 'amplituhedron,' which yields an equivalent one-term expression [39-41].

In the quantum world probabilities were expressed as complex numbers, with both a quantity and a phase, and these so-called amplitudes were squared to produce probability. This was the mathematical procedure necessary to capture the wavelike aspects of particle behavior. Probability amplitudes were normally associated with the likelihood of a particle's arriving at a certain place at a certain time [43]. Feynman said he would associate the probability amplitude '*with an entire motion of a particle - with a path*'. He stated the central principle of quantum mechanics: '*The probability of an event which can happen in several different ways is the absolute square of the sum of complex contributions, one from each alternative way*'. These complex numbers, amplitudes, were written in terms of classical action; Feynman showed how to calculate the action for each path as a certain integral [44-55].

13.7 The Superimplicate Order and Instantaneous UQC Algorithms

Who might have guessed there might be a class of QC algorithms better than polynomial and exponential speed QIP. Let's take a peek at the basis for possible instantaneous algorithms. It is generally known that information passes instantaneously in systems of EPR correlated photons. We know how to parametric down-convert entangled EPR pairs; what if we can learn parametric up-conversion utilizing the tenets of UFM?

Following Bohm, we assume a field, $\phi(x, t)$ will take the form of a wavepacket, $\alpha_c F_c(x, t) + \alpha_s F_s(x, t)$ with α_c, α_s real and positive proportionality factors; then functions, $\Gamma(x, t)$ orthogonal to $F_c(x, t)$ and $F_s(x, t)$ will have no effect on the factor in front of Ψ_0 , meaning their variation will be the same as in the ground state. Thus chaotic variation of the field will be modified by statistical tendencies to change around an average form of the wavepacket,

$$\Psi = \sum_k 'f_k q_k \Psi_0. \quad (13.6)$$

In (13.6) the sum is over all k and no restriction made that $f_{-k} = f_k^*$ because the wave function is complex even though $f(x)$ is real. Considering $q_{-k} = q_k^*$ we write

$$\Psi = \sum_k ' \left[f_k q_k + f_{-k} q_k^* \right] \Psi_0 \quad (13.7)$$

where \sum_k' indicates summation over a suitable half of the total set of k values. With the assumption in (13.7) that the space average of the field, $f_0 = 0$ we write

$$\Psi = \sum_k 'f_k q_k \exp[-ikt] \Psi_0. \quad (13.8)$$

Then write $g = \sum_k 'f_k q_k \exp[-ikt]$, giving $R = \sqrt{\Psi^* \Psi} = \sqrt{gg^*} \Psi_0$ [37].

According to Bohm, inside this wave packet the super-quantum potential introduces nonlocal connections between fields at different points separated by a finite distance (unlike ground state). Now we write the quantum potential as

$$Q = - \sum_k \frac{\partial^2 R}{\partial q_k^* \partial q_k} / R. \quad (13.9)$$

Now we evaluate the quantum potential change from the ground state,

$$\Delta Q = - \frac{1}{4} \sum_k \frac{f_k f_k^*}{g^* g} + \frac{1}{2} \sum_k \frac{k f_k q_k \exp[-ikt]}{g} + c.c. \quad (13.10)$$

For a wave packet with only a small range of wave vectors, the factor, k on the right reduces to the fixed number, k_0 , while the remaining factors reduce to unity. This term varies with time, but we are only interested in the wave packets for which the spread of k makes negligible contributions. But when the q_k are expressed in terms of $\phi(x)$ as in

$$q_k = 1/\sqrt{V} \int \exp[-ik \cdot x] \phi(x) dV \quad (13.11)$$

the quantum potential reduces to

$$\Delta Q = \frac{1}{4} \sum_k \frac{f_k f_k^*}{\sqrt{\int F(x, t) \phi(x) dV} \sqrt{\int F^*(x', t) \phi(x') dV'}}. \quad (13.12)$$

It should be obvious the term implies nonlocal interaction between $\phi(x)$ at one point and $\phi(x')$ at other points where the integrand is substantial. Writing $Q = \Delta Q + Q_0$, with Q_0 the quantum potential of the ground state as given in

$$\Psi_0 = \exp \left[- \iint \phi(x) \phi(x') f(x' - x) dV dV' \right] \quad (13.13)$$

as taken from (13.11) with the t coordinate suppressed and where $f(x' - x) = 1/V \sum_k 'k \exp[i k \cdot \leq(x' - x)]$, we can write the field equation

$$\frac{\partial^2 \phi}{\partial t^2} = \nabla^2 \phi - \frac{\delta Q}{\delta \phi} \quad (13.14)$$

as

$$\frac{\partial^2 \phi}{\partial t^2} = \nabla^2 \phi - \frac{\delta \Delta Q}{\delta \phi} - \frac{\delta Q_0}{\delta \phi}. \quad (13.15)$$

Using (13.13) and expressing Q in terms of $\phi(x)$ by Fourier analysis Bohm obtains, [37]

$$\begin{aligned} \frac{\partial^2 \phi}{\partial t^2} = & \frac{1}{8} \left(\sum_k 'f_k f_k^* \right) \times \\ & \frac{f_k f_k^*}{\left(\int F(x, t) \phi(x) dV \right)^{3/2} \left(\int F^*(x', t) \phi(x') dV' \right)^{1/2}} + c.c. \end{aligned} \quad (13.16)$$

Remember from the ground state, the field is static because the effect of the quantum potential cancels out the Laplacian, $\nabla^2 \phi$ in the field equation. ∇^2 is the Laplacian or divergence of the gradient of a function, $\Delta f(p)$ on a point, p in Euclidean space. Now with (13.16) in the excited state there is an additional term causing the wavepacket to move, and as happens with the quantum potential, the field equation is nonlocal and nonlinear [37].

The point we have been building up to in this section, is that the nonlocality represents an instantaneous connection of the field at different points in space. However, as Bohm reminds us, this is significant only over the extent of the wavepacket. In the usual interpretation, the spread of the wavepacket applies to a region within which, according to the uncertainty principle, nothing whatsoever can be said regarding what is happening. Therefore, the de Broglie-Bohm-Vigier causal interpretation [56] attributes nonlocality only to situations in which the usual interpretation cannot attribute well-defined properties [37].

It is of key importance to note that a wavefunction of the form $\Psi = q_k \exp[-ikt] \Psi_0$ does not correspond to the usual picture of an oscillation. This is shown by (13.16) because the term $\nabla^2 \phi$ is absent. This result follows because stationary wavefunctions usually correspond to static situations contradicting intuitive expectations of a dynamic state of motion [37].

But Bohm was only thinking from a 4D Standard Model perspective, in terms of an amplituhedronic-type (volume) for a Wheeler-DeWitt wavefunction of the universe, $H\Psi = 0$ instantaneous EPR-holographic algorithms should prove possible with sufficient UFM insight.

When considered in terms of our UFM brane topological additions to the structure of matter and Bohm's superimplicate order, full utility of nonlocal information as hinted by EPR correlations hints at the possibility of instantaneous algorithms.

13.8 Some Ontological-Phase Geometric Topology

The simplest example of ontological-phase eversion is in the transformation of the ambiguous vertices of the Necker cube. The form of a cube by itself is not oriented; any set diagonal pairs could apply to eversion. With 6 faces and 4 vertex positions each, this gives 24 possible directed orientations; the important point is that the phase eversion must be directed by the topological charge of the unified field.

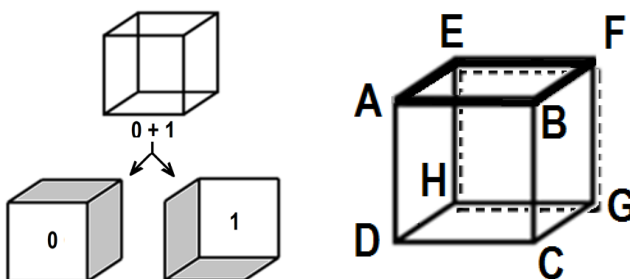


Fig. 13.5 a) The two ontological states of the ambiguous or Necker cube, 0 and 1. b) Vertices and ambiguous vertices labeled. Solid lines (B) front, dashed lines (H) rear.

With the 8 vertices labeled and 25 orientations, steps to create an algebra to describe rotations or dual-morphic projections can be taken. In

Fig. 13.5a there is no distinction between as to whether 0 or 1 represents the front or rear face. This is called the Topology of Ambiguity.

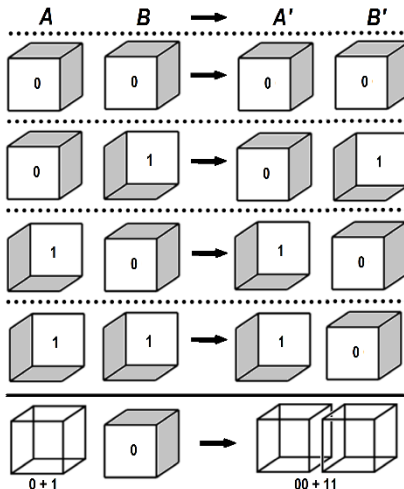


Fig. 13.6 Ambiguous truth table, showing how holographic r-qubits might be built up.

Ambiguous geometric/topology is the most rudimentary indicia of ontological information processing. For instantaneity to occur each point (no longer a point but structure beyond in nonlocality) must be a ballistic processor. In simplest form evolution is governed by a Bohmian superquantum potential or force of coherence of the unified field, $F_{(N)} = \kappa/\rho$, where κ is UFM topological charge, and ρ the radius of action.

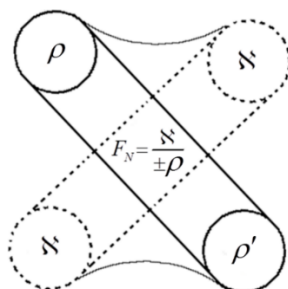


Fig. 13.7. Topological geometry of an isolated LCU described by the UFM equation. The center might be one oscillating L-R static-dynamic ‘Casimirirror’ half producing the knotted shadow fermion vertex in an x,y plane in 3-space.

The quaternions, H , are a 4D algebra with basis $1, i, j, k$. To describe the product, we could give a multiplication table, but it is easier to remember that:

- 1 is the multiplicative identity, $i, j,$
- and k are square roots of -1 ,
- we have $ij = k, ji = -k$, and all identities obtained from these by cyclic permutations of (i, j, k) [57].

The last rule is summarized in Fig. 13.8. below:

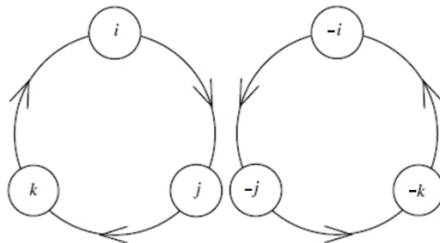


Fig. 13.8. Clockwise counterclockwise cyclicity of the quaternion algebra.

When we multiply two elements going clockwise around the circle we get the next one: for example, $ij = k$. But when we multiply two going around counterclockwise, we get *minus* the next one: for example, $ji = -k$. We can use the same sort of picture to remember how to multiply octonions:

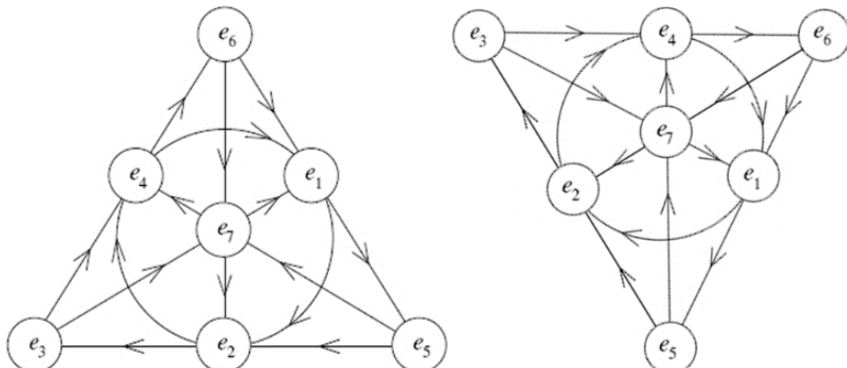


Fig. 13.9. The Fano plane, a) Graph showing the cyclic relationship of the Octonions. b) Index doubling by rotating the Fano plane $1/3$ of a turn.

The Fano plane (Fig. 13.9), a graphic with 7 lines and 7 points, completely describes the algebraic structure of the octonions, and the central circle describes the quaternions. The 'lines' are the sides and altitudes of the triangle, and the central circle contains all the midpoints of the sides. Each pair of distinct points lies on a unique line. Each line contains three points, and each of these triples has a cyclic ordering shown by the arrows. Index-doubling corresponds to rotating the plane 1/3 of a turn (right). If e_i, e_j , and e_k are cyclically ordered in this way then $e_i e_j = e_k$, $e_j e_i = -e_k$. Together with these rules:

- 1 is the multiplicative identity,
- e_1, \dots, e_7 are all square roots of -1 [57].

Can we go deeper? The Fano plane is the projective plane over the 2-element field \mathbb{Z}_2 . In other words, it consists of lines through the origin in the vector space \mathbb{Z}_2^3 . Since every such line contains a single nonzero element, we can also think of the Fano plane as consisting of the seven nonzero elements of \mathbb{Z}_2^3 . If we think of the origin in \mathbb{Z}_2^3 as corresponding to $1 \in O$, we get the following picture of the octonions:

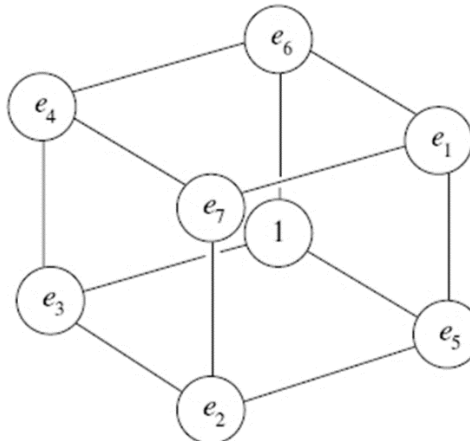


Fig. 13.10. Octonions subalgebras.

Planes through the origin of this 3D vector space give subalgebras of O isomorphic to the quaternions, lines through the origin give subalgebras

isomorphic to the complex numbers, and the origin itself gives a subalgebra isomorphic to the real numbers. This is a description of the octonions as a 'twisted group algebra'. Given any group G , the group algebra $\mathbb{R}[G]$ consists of all finite formal linear combinations of elements of G with real coefficients. This is an associative algebra with the product coming from that of G . We can use any function $\alpha: G^2 \rightarrow \{\pm 1\}$ to 'twist' this product, defining a new product $*: \mathbb{R}[G] \times \mathbb{R}[G] \rightarrow \mathbb{R}[G]$ by $g * h = \alpha(g, h)gh$, where $g, h \in G \subset \mathbb{R}[G]$. One can figure out an equation involving α that guarantees this new product will be associative. In this case we call α a '2-cocycle'. If α satisfies a certain extra equation, the product $*$ will also be commutative, and we call α a 'stable 2-cocycle' [57].

For example, the group algebra $\mathbb{R}[Z_2]$ is isomorphic to a product of 2 copies of \mathbb{R} , but we can twist it by a stable 2-cocycle to obtain the complex numbers. The group algebra $\mathbb{R}[Z_2^2]$ is isomorphic to a product of 4 copies of \mathbb{R} , but we can twist it by a 2-cocycle to obtain the quaternions. Similarly, the group algebra $\mathbb{R}[Z_2^3]$ is a product of 8 copies of \mathbb{R} , and what we have really done in this section is describe a function α that allows us to twist this group algebra to obtain the octonions. Since the octonions are nonassociative, this function is not a 2-cocycle. However, its coboundary is a 'stable 3-cocycle', which allows one to define a new associator and braiding for the category of $\mathbb{R}[Z_2^2]$ -graded vector spaces, making it into a symmetric monoidal category [58]. In this symmetric monoidal category, the octonions are a commutative monoid object. In less technical terms: this category provides a context in which the octonions are both commutative and associative [57].

Figure 13.11 is an adaptation of the Fano plane with many more degrees of freedom. Notice that the so-called Fano snowflakes involute into a 3-cube. The Fano snowflake graph also makes use of the 8th Necker ambiguous point. The central quaternionic cycle may also progress clockwise or counter-clockwise. Thus with rotations, mirror reflections, dimensional reduction and expansion of the Necker double covering point and other topological moves, there are sufficient degrees of freedom for

ballistically programming a nonlocal class of instantaneous UFM QIP algorithms. We would like to name the full set of moves - Ontological-phase eversion cycles.

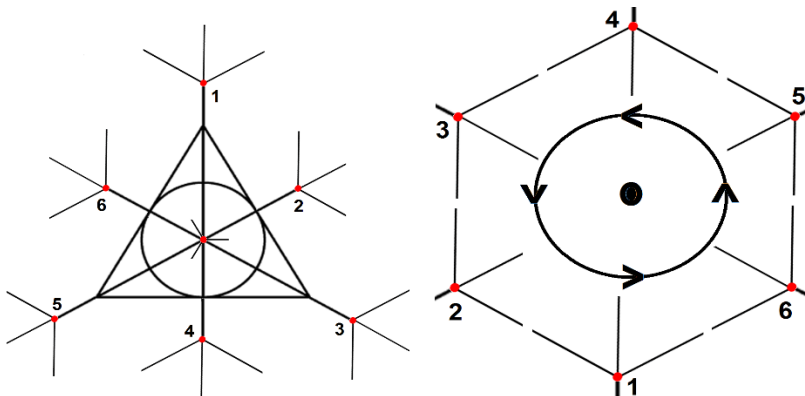


Fig. 13.11. a) Six snowflakes on the rim of Fano plane. b) Notice that that the 6 snowflakes involute to form a 3-cube which also contains the dual projection $(+\omega, -\omega)$ double covering point of the ambiguous Necker cube.

13.9 Summation

I recall a critic of Aaronson's Unitarihedron parody blog of the Amplituhedron calling Aaronson's Unitarihedron a diaperhedron! There is always risk when a 'bear' goes over the mountain '*to see what he could see*' as the old nursery song goes. I still remember vividly Tom Toffoli chastising Vlasov a young Russian postdoc at the time at Physcomp96 regarding his paper putting forth a relativistic qubit; now 20 years later, finally, there is more and more talk of r-qubits and a new field of relativistic information processing is well under way. In any case there is no need for us to 'shut up' because we have 'put up' viable protocols, much simpler and more revealing than those being processed by the CERN LHC.

Now here's the rub; let's consider a general case of $n = 500$ electron qubits in a linear superposition of all 2^{500} possible classical states, much larger than the number of particles estimated in the classical universe (10^{80}):

$$\sum_{x \in \{0,1\}^n} \alpha_x |x\rangle. \quad (13.17)$$

This exponentially huge superposition is ‘the private world’ of the electrons involved and measurement only allows us to find the n bits (500) of information, $|\alpha_x|^2$. If our UFM model proves successful in surmounting uncertainty, then measurement does not change the system leaving all 2^{500} possible superposed states intact. This also leads to violation of the no-cloning theorem.

I remember a quote by Feynman or Kip Thorne, (I forget which) ‘to be the 1st person on Earth to discover a new principle’. That’s the great fun of doing physics; enjoy a tiny moment before the hordes mass. I have to admit, ‘ontological-phase eversion cycles for instantaneous algorithms’, puts a spread of jam on my toast. I remember what noted Stanford neuroscientist (holographic brain) said to me once while we were watching a sunset by the ocean in Long Beach, CA USA arguing about how many images there were of the sun on the water surface, “*aren’t we all in this together?*”. Technological evolution continues to move asymptotically faster, 150 years for acceptance of Copernicus’ revolutions, 15 years to perform Einstein’s simple photoelectric effect experiment (after he was called an idiot and moron to his face). Any chance of getting one of the experiments proposed herein performed in 1.5 years? That would be about 2018... UQC could be that close if ‘angel investors’ appear in the midst.

References

- [1] Chabert, J.L. (1999) A History of Algorithms: From the Pebble to the Microchip, Berlin: Springer-Verlag.
- [2] Berlinski, D. (2001) The Advent of the Algorithm: The 300-Year Journey from an Idea to the Computer, Fort Washington: Harvest Books.
- [3] Alsuwaiyel, M.H. (2010) Algorithms: Design Techniques and Analysis, Singapore: World Scientific.
- [4] Nielsen, M.A. & Chuang, I.L. (2004) Quantum Computation and Quantum Information, Cambridge: Cambridge Univ. Press.
- [5] Deutsch, D. (1985) Quantum theory, the Church-Turing principle and the universal quantum computer, Proceedings of the Royal Society of London A, V. 400, pp. 97-117.
- [6] Shor, P.W. (1994) Algorithms for quantum computation: Discrete logarithms and factoring, Foundations of Computer Science, 1994 Proceedings., 35th Annual Symposium, pp. 124-134, IEEE.
- [7] Deutsch, D. (1989) Quantum computational networks, Proceedings of the Royal Society of London A: Mathematical, Physical and Engineering Sciences (Vol. 425, No. 1868, pp. 73-90).

- [8] Gu, M., Weedbrook, C., Perales, A. & Nielsen, M.A. (2009) More really is different, *Physica D: Nonlinear Phenomena*, 238 (9-10): 835-839.
- [9] Kieu, T.D. (2003) Computing the non-computable, *Contemp. Physics*, 44(1):51-71.
- [10] Nielsen, M.A. (1997) Computable functions, quantum measurements, and quantum dynamics, *Phys. Rev. Lett.*, 79 (15): 2915-2918.
- [11] Arrighi, P. & Dowek, G. (2011) The physical Church-Turing thesis and the principles of quantum theory, arXiv:1102.1612v1 [quant-ph].
- [12] Smith, J. & Mosca, M. (2010) Algorithms for quantum computers, arXiv:1001.0767v2 [quant-ph].
- [13] Aaronson, S. & Ambainis, A. (2014) The need for structure in quantum speedups, *Theory of Computing*, V. 10 (6), pp. 133-166; <http://theoryofcomputing.org/articles/v010a006/v010a006.pdf>.
- [14] Aaronson, S. & Ambainis, A. (2011) The need for structure in quantum speedups, Proc. 2nd Innovations in Computer Science Conference (ICS'11) pp. 338-352, Tsinghua, [arXiv:0911.0996] 138, 140.
- [15] Watrous, J. (2002) Limits on the power of quantum statistical zero-knowledge, Proceedings of the 43rd Annual IEEE Symposium on Foundations of Computer Science, pp. 459-468.
- [16] O'donnell, R., Saks, M.E., Schramm, O. & Servedio, R.A. (2005) Every decision tree has an influential variable, Proc. 46th FOCS, pp. 31-39. IEEE Comp. Soc. Press.
- [17] Dinur, I., Friedgut, E., Kindler, G. & O'donnell, R. (2007) On the Fourier tails of bounded functions over the discrete cube, *Israel J. Math.*, 160 (1):389-412; Preliminary version in STOC'06.
- [18] Shor, P.W. (1999) Polynomial-time algorithms for prime factorization and discrete logarithms on a quantum computer, *SIAM review*, 41(2), 303-332.
- [19] Van Dam, W., Hallgren, S. & Lawrence, I.P. (2006) Quantum algorithms for some hidden shift problems, *SIAM J. Comput.*, 36 (3): 763-778.
- [20] Grover, L.K. (1996) A fast quantum mechanical algorithm for database search, in Proc. 28th STOC, pp. 212-219, ACM Press.
- [21] Bennett, C.H., Bernstein, E., Brassard, G. & Vazirani, U.V. (1997) Strengths and weaknesses of quantum computing, *SIAM J. Comput.*, 26 (5): 1510-1523.
- [22] Beals, R., Buhrman, H., Cleve, R., Mosca, M. & De Wolf, R. (2001) Quantum lower bounds by polynomials, *J. ACM*, 48 (4): 778-797.
- [23] Ambainis, A. & De Wolf, R. (2001) Average-case quantum query complexity, *Journal of Physics A: Mathematical and General*, 34 (35): 6741.
- [24] Szegedy, M. (2004) Quantum speed-up of Markov chain based algorithms, in FOCS '04: Proceedings of the 45th Annual IEEE Symposium on Foundations of Computer Science, pp. 32-41, IEEE Computer Society, Washington, DC.
- [25] Bhaskar, M.K., Hadfield, S., Papageorgiou, A. & Petras, I. (2015) Quantum algorithms and circuits for scientific computing, arXiv:1511.08253v1 [quant-ph].
- [26] Cockshott, W.P. & Mackenzie, L.M. (2012) Computation and its Limits, <https://books.google.com/books?ISBN=0199640327>.
- [27] Childs, A.M., Cleve, R., Deotto, E., Farhi, E., Gutmann, S. & Spielman, D.A. (2002) Exponential algorithmic speedup by quantum walk, MIT-CTP #3309; arXiv:quant-ph/0209131v2.
- [28] Aaronson, S. (2015) When exactly do quantum computers provide a speedup?, www.scottaaronson.com/talks/speedup-austin.ppt.
- [29] Bremner, M.J., Jozsa, R., & Shepherd, D.J. (2011). Classical simulation of commuting quantum computations implies collapse of the polynomial hierarchy, in Proceedings of the

- Royal Society of London A: Mathematical, Physical and Engineering Sciences (Vol. 467, No. 2126, pp. 459-472) The Royal Society.
- [30] Ambainis, A. (2004) Quantum search algorithms, ACM SIGACT News, 35(2), 22-35.
- [31] Ambainis, A. (2007). Quantum walk algorithm for element distinctness, SIAM Journal on Computing, 37(1), 210-239.
- [32] Valiant, L. (2004) Holographic algorithms (Extended Abstract) FOCS 2004, Rome, Italy: IEEE Computer Society. pp. 306-315.
- [33] Hayes, B. (2008) Accidental algorithms, American Scientist.
- [34] Cai, J-Y (2008) Holographic algorithms: guest column. SIGACT News, New York: ACM 39 (2): 51-81.
- [35] Huang, S., & Lu, P. (2012) A dichotomy for real weighted Holant problems, in Computational Complexity (CCC), 2012 IEEE 27th Annual Conference on, pp. 96-106, IEEE.
- [36] Cai, J-Y, Pinyan, L. & Mingji, X. (2008) Holographic algorithms by Fibonacci gates and holographic reductions for hardness, FOCS, IEEE Computer Society, pp. 644-653.
- [37] de Broglie, L. (2004) Forward to, D. Bohm, Causality and Chance in Modern Physics, New York: Routledge.
- [38] Shalev-Shwartz, S., & Ben-David, S. (2014) Understanding Machine Learning: From Theory to Algorithms, Cambridge: Cambridge University Press.
- [39] Arkani-Hamed, N., & Trnka, J. (2013) The amplituhedron, arXiv:1312.2007.
- [40] Bai, Y., He, S., & Lam, T. (2015) The amplituhedron and the one-loop Grassmannian measure, arXiv:1510.03553.
- [41] Arkani-Hamed, N., Hodgesb, A. & Trnka, J. (2013) Positive amplitudes in the amplituhedron, arXiv:1412.8478v1 [hep-th].
- [42] Aaronson, S. (2013) The unitarifiedron: The jewel at the heart of quantum computing, <http://www.scottaaronson.com/blog/?p=1537>.
- [43] De Angelis, S.F. (2013) <http://www.enterrasolutions.com/2013/09/are-space-and-time-real.html>.
- [44] D'Ariano, G.M., Van Dam, W. & Mosca, M. (2007) General optimized schemes for phase estimation, Physical Review Letters 98(9), 090,501.
- [45] Papageorgiou, A. & Traub, J.F. (2014) Quantum algorithms for continuous problems and their applications, Vol. 154, Advances in Chemical Physics, pages 151-178, Hoboken: Wiley.
- [46] Harrow, A.W, Hassidim, A. & Lloyd, S. (2009) Quantum algorithm for linear systems of equations, Phys. Rev. Lett., 103:150502.
- [47] Portugal, R. & Figueiredo, C.M.H. (2006) Reversible Karatsubas algorithm, Journal of Universal Computer Science, 12(5):499-511.
- [48] Cao, Y., Papageorgiou, A., Petras, I., Traub, J.F. & Kais, S. (2013) Quantum algorithm and circuit design solving the Poisson equation, New Journal of Physics, 15: 013021.
- [49] Draper, T.G. (2000) Addition on a quantum computer, arXiv, quant-ph/0008033.
- [50] Wegner, P. (1997) Why interaction is more powerful than algorithms, Communications of the ACM, Vol. 40.
- [51] Wegner, P. (1998) Interactive foundations of computing, Theoretical Computer Science, Vol. 192, Issue 2, pp. 315-351.
- [52] Wegner, P. & Goldin, D. (2003) Computation Beyond Turing Machines, Communications of the ACM, Vol. 46, Issue 4.
- [53] Hopcroft, J.E. & Ullman, J.D. (1969) Formal Languages and Their Relation to Automata, Reading: Addison-Wesley.

- [54] Rice, J.K. & Rice J.N. (1969) Computer Science: Problems, Algorithms, Languages, Information and Computers, New York: Holt, Rinehart and Winston.
- [55] Goldin, D.Q., Smolka, S.A., Attie, P.C. & Sonderegger, E.L. (2004) Turing machines, transition systems, and interaction, *Information and Computation*, Vol. 194, Iss. 2, pp. 101-128.
- [56] Bohm, D. & Vigier, J. P. (1954) Model of the causal interpretation of quantum theory in terms of a fluid with irregular fluctuations, *Physical Review*, 96 (1), 208.
- [57] Baez, J. (2013) The Fano plane, <http://math.ucr.edu/home/baez/octonions/node4.html>.
- [58] Albuquerque, H. & Majid, S. (2012) Quasialgebra structure of the octonions, arXiv:math/9802116.

Chapter 14

Class II Mesoionic Xanthines as Potential Ten Qubit Substrate Registers

Class II mesoionic xanthines such as *anhydro*-(8-hydroxyalkyl-5-hydroxy-7-oxothia-zolo[3,2-a]pyrimidinium hydroxides) are unique, small atomic weight, stable crystalline organic compounds that can be represented as a combination of ten different resonance structures for each simple xanthine molecule. Each resonance structure contributes a certain percentage to the total resonance of the molecule. This unique resonance represents ten different quantum states of the entire molecule and can thus be exploited as a potential substrate for a ten-qubit register. The number of possible superposition states for such a register in a single molecule is potentially as high as 2^n states or (in this case where $n = 10$) 1,024 complex numbers. In solution the least-unit of this mesoionic crystalline structure is scalable suggesting putative utility for bulk NMR quantum computing. It will be shown that these ten-qubit registers are amenable to standard Deutsch-Jozsa, Shor and Grover algorithms. Additionally, we attempt to formalize I/O techniques for our Class II mesoionic xanthines based on a coherent control rf-process of cumulative resonant interaction where by utilizing additional degrees of freedom pertinent to a relativistic basis for the qbit (r-qbit) new HD commutation rules allow decoherence to be ontologically overcome.

14.1 Introduction

Mesoionic purinone analogs, a large and relatively new class of bicyclic heteroaromatic compounds, whose ring systems possess π -electron systems that are isoelectronic with those of the various known purinones, have been synthesized and characterized over the last few decades [1–7]. Class I mesoionic analogs have been classified and defined as being those

that are derived from known 5-membered mesoionic ring systems. Class II mesoionic analogs are those that are derived from known 6-membered mesoionic ring systems. In 1996, Giandinoto, *et.al* [8] had synthesized and characterized a number of novel Class II mesoionic xanthine acyclonucleosides as potential anti-neoplastic and antiviral agents. Class I and Class II mesoioic purinones have been formulated and examined from a quantum chemical standpoint [9-10]. The generalized structural representation of mesoionic xanthine acyclo-nucleosides is shown in Fig. 14.1 below.

In particular, the mesoionic xanthine acyclonucleosides where R' = H are especially useful since this moiety is ideal in giving the molecule a handle for attaching it to metallic, organic, polymeric or semiconductor surfaces substrates such as GaAs, GaN, CdSe/ZnS. The definition of a mesoionic compound is a compound that cannot be adequately represented by any single covalent or single dipolar resonance structure. These Class II mesoionic xanthines, such as *anhydro*-(8-hydroxyalkyl-5-hydroxy-7-oxothiazolo [3,2a] pyrimidinium hydroxides) cannot be adequately represented by fewer than ten different resonance contributors. Fig. 14.2 illustrates these ten resonance forms and all of their possible quantum inter-conversion states. Each resonance structure shown in Fig. 14.2 corresponds to an individual quantum state of the total molecule and all ten are required to adequately represent the molecule in its totality of superpositional quantum states. In quantum computing, there may be multiple quantum states in superposition. In this particular case where there are ten qubits, the quantum state of superposition would be the following orthonormal basis set

$$|\psi\rangle = \alpha_i |x_1 x_2 x_3 \dots x_n\rangle \quad (14.1)$$

for all i=1-1,024 and for all n=1-10 where x_n is either 0 or 1.

More succinctly the above may be written: $|\psi\rangle = \sum_{i=1}^N \alpha_i |i\rangle$ where $|i\rangle$ is a shorthand notation for an orthonormal basis set of indices $\{i_1, i_2, i_3 \dots i_j \dots i_n\}$ where $N = 2^n$.

The Greek letters α_i are referred to as the amplitudes of the register and are complex numbers. In a 10-qubit register, there are therefore 2^{10} or

1,024 complex numbers for the total register. Since the probability ($|\Psi|^2$) of a quantum state or set of quantum superpositional entangled states must always be equal to one, the following relationship for the coefficients of the quantum registers must also be true

$$\sum_{i=1}^{1,024} \alpha_i^2 \equiv |\Psi|^2 = 1. \quad (14.2)$$

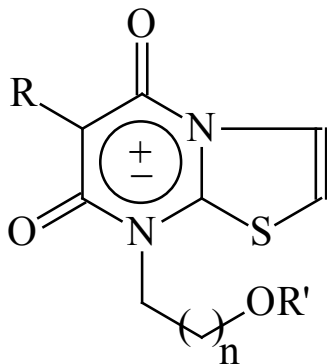


Fig. 14.1. Generalized structural representation of Class II mesoionic xanthine acyclonucleosides. $n = 1, 2$; $R = H, CH_3, CH_2CH_3, C_6H_5$; $R' = H, CH_3$.

For a 3-qubit register, there exists an 8-dimensional complex vector. For a 10-qubit register there exists a 1,024-dimensional complex vector. In order to initialize this vector space (register) for a quantum computer, an algorithm is necessary. In each step of the algorithm, the vector space is modified by multiplying it with a unitary matrix, which, by definition is a complex matrix.

14.2 Resonance stabilization in Class II Mesoionic Xanthines

Figure 14.2 illustrates at least ten different resonance contributors to the ground state of the Class II Mesoionic Xanthine molecule. Each resonance structure contributes a portion of its character to the overall nature of the molecule and to its ground state configuration.

Mesoionic xanthines are extremely unique and rare in this regard. Most molecules that exhibit resonance stabilization only have one or two resonance contributors to their ground state configuration.

Each resonance structure in Fig. 14.2 has a unique molecular wave function and a unique energy level characterized by its internal resonance structure. Looking carefully at Fig. 14.2 we can immediately see that the molecule in the middle (wave function Ψ_5) exhibits the most interconversions between other quantum states. It exhibits a total of eight interconversions. As a result, a large part of the molecule may be described using this one resonance structure. As a matter of fact, entering this particular resonance structure into a computer program (ACD Labs, Inc.), designed to predict ^{13}C NMR chemical shifts, was extremely accurate in predicting the actual chemical shifts of the molecule when compared to the experimental ^{13}C -NMR chemical shift values¹. This confirms the fact that the dominant resonance contributor of Class II Mesoionic Xanthines has the electronic configuration depicted in Ψ_5 of Fig. 14.2 with the positive charge on the nitrogen atom in the 4-position and the negative charge on the oxygen atom attached to the carbon atom at the 7-position of the fused ring structure.

The breakdown for the other resonance structures only in terms of total number of quantum interconversions between the different states is as follows:

$$\begin{aligned} \Psi_1 &= 4, \Psi_2 = 5, \Psi_3 = 5, \Psi_4 = 5, \Psi_5 = 8 \\ &\quad \quad \quad (14.3) \\ \Psi_6 &= 6, \Psi_7 = 4, \Psi_8 = 6, \Psi_9 = 4, \Psi_{10} = 5. \end{aligned}$$

There are thus a total of 52 quantum interconversions between all of the component resonant structures. It is generally known that in most cases, the more interconversions a particular resonant structure has, the more it contributes to the total ground state. Additionally, more interconversions usually indicate that a particular resonance contributor is more stable than one with less interconversions.

In this case, for example, the structure represented by Ψ_5 has the most interconversions and is thus the most stable and prominent contributor of all the quantum states. This is backed up by the ^{13}C -NMR data that was both experimentally and theoretically obtained using the ACD Labs software which accurately predicted the ^{13}C chemical shifts.

It is now a rather trivial procedure to calculate the actual probabilities in terms of coefficients of the individual quantum states. We simply take the above numbers for each state and divide them by the total number of

inter-conversion states. The following probabilities coefficients of the wavefunctions are thus obtained:

$$\begin{aligned}\alpha_1^2 &= \frac{1}{13}, \quad \alpha_2^2 = \frac{5}{52}, \quad \alpha_3^2 = \frac{5}{52}, \quad \alpha_4^2 = \frac{5}{52}, \quad \alpha_5^2 = \frac{2}{13} \\ \alpha_6^2 &= \frac{3}{26}, \quad \alpha_7^2 = \frac{1}{13}, \quad \alpha_8^2 = \frac{3}{26}, \quad \alpha_9^2 = \frac{1}{13}, \quad \alpha_{10}^2 = \frac{5}{52}\end{aligned}\quad (14.4)$$

We may now re-write the total wave-function Ψ in the following manner:

$$\begin{aligned}\Psi = & \frac{1}{13}\psi_1 + \frac{5}{52}\psi_2 + \frac{5}{52}\psi_3 + \frac{5}{52}\psi_4 + \frac{2}{13}\psi_5 + \\ & \frac{3}{26}\psi_6 + \frac{1}{13}\psi_7 + \frac{3}{26}\psi_8 + \frac{1}{13}\psi_9 + \frac{5}{52}\psi_{10}\end{aligned}, \quad (14.5)$$

where all of the coefficients of the individual wave-functions add up to equal one. We may also express the above wave-function in our more familiar quantum computer form as:

$$\begin{aligned}|\Psi\rangle = & \sum_{i=1}^N \sqrt{\frac{1}{13}}|i\rangle + \sqrt{\frac{5}{52}}|i\rangle + \sqrt{\frac{5}{52}}|i\rangle + \sqrt{\frac{5}{52}}|i\rangle + \sqrt{\frac{2}{13}}|i\rangle + \\ & \sqrt{\frac{3}{26}}|i\rangle + \sqrt{\frac{1}{13}}|i\rangle + \sqrt{\frac{3}{26}}|i\rangle + \sqrt{\frac{1}{13}}|i\rangle + \sqrt{\frac{5}{52}}|i\rangle\end{aligned}\quad (14.6)$$

or more succinctly as:

$$|\Psi\rangle = \sum_{i=1}^N 3\sqrt{\frac{1}{13}}|i\rangle + 4\sqrt{\frac{5}{52}}|i\rangle + 2\sqrt{\frac{3}{26}}|i\rangle + \sqrt{\frac{2}{13}}|i\rangle, \quad (14.7)$$

where $|i\rangle = \{i_1, i_2, i_3, \dots, i_n\}$ and $n = 10$; $N = 1,024$.

14.3 Projectors and Projection Operators

Let us examine the role of projectors and projection operators. A projection matrix P is an $n \times n$ square matrix that gives a vector space projection from R^n to a subspace W . The columns of P are the projections of the standard basis vectors and W is the image of P . Therefore, a square matrix P is a projection matrix if and only if $P^2 = P$. A projection matrix P is orthogonal if and only if $P = P^\dagger$.

Suppose W is a k -dimensional subspace of the d -dimensional vector space V . Using the Gram-Schmidt procedure, it is possible to construct an orthonormal basis $|1\rangle, \dots, |d\rangle$ for V such that $|1\rangle, \dots, |k\rangle$ is an orthonormal basis for W . We may represent this definition mathematically by stating that the projector P is the projector onto the subspace W using the

following equation: $P \equiv \sum_{i=1}^k |i\rangle\langle i|$. It can easily be shown that this

definition is independent of the orthonormal basis $|1\rangle, \dots, |k\rangle$ used for W .

It can further be shown that $|v\rangle\langle v|$ is Hermitian for any vector $|v\rangle$ and so

P is Hermitian, $P^\dagger = P$. We may now refer to P as the vector space onto which P is a projector. The *orthogonal complement* of P is the operator $Q \equiv I - P$. The operator Q is therefore a projector onto the vector space spanned by $|k+1\rangle, \dots, |d\rangle$ which we also refer to as the *orthogonal complement* of P , and may denote by Q .

Some of the most important of these unitary transformations or “quantum gates” are the following [11]:

Hadamard Gate:

$$\begin{array}{c} \boxed{\text{H}} \\ \xrightarrow{\hspace{1cm}} \end{array} \frac{1}{\sqrt{2}} \begin{pmatrix} 1 & 1 \\ 1 & -1 \end{pmatrix}$$

Identity matrix:

$$I \equiv \sigma_0 \equiv \begin{pmatrix} 1 & 0 \\ 0 & 1 \end{pmatrix}$$

Pauli X:

$$\begin{array}{c} \boxed{\text{X}} \\ \xrightarrow{\hspace{1cm}} \end{array} \begin{pmatrix} 0 & 1 \\ 1 & 0 \end{pmatrix} \equiv \sigma_x \equiv \sigma_1$$

Pauli Y:  $\begin{pmatrix} 0 & -i \\ i & 0 \end{pmatrix} \equiv \sigma_y \equiv \sigma_2$

Pauli-Z:  $\begin{pmatrix} 1 & 0 \\ 0 & -1 \end{pmatrix} \equiv \sigma_z \equiv \sigma_3$

$\pi/8$ Gate: $U_{\pi/8} = \begin{pmatrix} e^{-i\frac{\pi}{8}} & 0 \\ 0 & e^{i\frac{\pi}{8}} \end{pmatrix}$

CNOT Gate: $\begin{bmatrix} 1 & 0 & 0 & 0 \\ 0 & 1 & 0 & 0 \\ 0 & 0 & 0 & 1 \\ 0 & 0 & 1 & 0 \end{bmatrix}$ Controlled-Z: $\begin{bmatrix} 1 & 0 & 0 & 0 \\ 0 & 1 & 0 & 0 \\ 0 & 0 & 1 & 0 \\ 0 & 0 & 0 & -1 \end{bmatrix}$

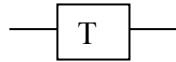
Controlled-Phase: $\begin{bmatrix} 1 & 0 & 0 & 0 \\ 0 & 1 & 0 & 0 \\ 0 & 0 & 1 & 0 \\ 0 & 0 & 0 & i \end{bmatrix}$

Phase Shift Gate: $R_\theta = \begin{bmatrix} 1 & 0 \\ 0 & e^{i\theta} \end{bmatrix}$ with symbol 

Since $e^{\pi i} = -1$ and $e^{\pi i/2} = i$, then $e^{\pi i/4} = \sqrt{i}$. Therefore, the $\pi/8$ gate is the square root of the phase gate and the phase gate is consequently the

square root of the Pauli-Z gate since $i = \sqrt{-1}$. An operator or matrix is defined as being unitary if the following operation is true: $UU^{-1} = I$.

Toffoli Gate:



$$\begin{bmatrix} 1 & 0 & 0 & 0 & 0 & 0 & 0 & 0 \\ 0 & 1 & 0 & 0 & 0 & 0 & 0 & 0 \\ 0 & 0 & 1 & 0 & 0 & 0 & 0 & 0 \\ 0 & 0 & 0 & 1 & 0 & 0 & 0 & 0 \\ 0 & 0 & 0 & 0 & 0 & 1 & 0 & 0 \\ 0 & 0 & 0 & 0 & 0 & 0 & 1 & 0 \\ 0 & 0 & 0 & 0 & 0 & 0 & 0 & 1 \\ 0 & 0 & 0 & 0 & 0 & 0 & 1 & 0 \end{bmatrix}$$

Also, if the complex conjugate transpose of a matrix U^\dagger equals its inverse, U^{-1} , it is considered to be unitary. For example, the Hermitian conjugate of a matrix A exhibits the following relationship: $A^\dagger = (A^T)^*$, where A^T is the transpose of the matrix A . Suppose we take the following [3×3] matrix A (where some or all of its elements are complex numbers) and perform the aforementioned operations.

$$A^T = \begin{pmatrix} a_{11} & a_{12} & a_{13} \\ a_{21} & a_{22} & a_{23} \\ a_{31} & a_{32} & a_{33} \end{pmatrix}^T = \begin{pmatrix} a_{11} & a_{21} & a_{31} \\ a_{12} & a_{22} & a_{32} \\ a_{13} & a_{23} & a_{33} \end{pmatrix}. \quad (14.8)$$

$$A^\dagger = (A^T)^* = \begin{pmatrix} a_{11}^* & a_{21}^* & a_{31}^* \\ a_{12}^* & a_{22}^* & a_{32}^* \\ a_{13}^* & a_{23}^* & a_{33}^* \end{pmatrix}. \quad (14.9)$$

The matrix A^\dagger is said to be self-adjoint or Hermitian conjugate. Each element of A^\dagger is the complex conjugate of the transpose of A . As another example, let's take the Pauli-Y gate and compute its Hermitian conjugate:

$$\sigma_y^\dagger \equiv \begin{pmatrix} 0 & -i \\ i & 0 \end{pmatrix}^\dagger = \begin{pmatrix} 0 & -i \\ i & 0 \end{pmatrix} \equiv \sigma_y. \quad (14.10)$$

Likewise, for the phase gate

$$S^\dagger \equiv \begin{pmatrix} 1 & 0 \\ 0 & i \end{pmatrix}^\dagger = \begin{pmatrix} 1 & 0 \\ 0 & -i \end{pmatrix}. \quad (14.11)$$

Notice that the Hermitian conjugate of the Pauli-Y gate is itself. However, the Hermitian conjugate of the Phase-gate S is not equal to itself. Both of these gates are unitary since the transpose of their complex conjugates are equal to their inverses.

14.4 Tensor Products and Associated Operators

A tensor product is an operation of putting vector spaces together to form larger vector spaces. This type of construction is absolutely essential to the understanding of the quantum mechanics of multiparticle systems. Let V and W be Hilbert vector spaces of dimension m and n respectively. Then $V \otimes W$ (read ‘ V tensor W ’) is a mn -dimensional vector Hilbert space [12]. The elements of $V \otimes W$ are linear combinations of tensor products $|v\rangle \otimes |w\rangle$ of elements $|v\rangle$ of V and $|w\rangle$ of W . Additionally, if $|i\rangle$ and $|j\rangle$ are orthonormal bases for the spaces V and W , then $|i\rangle \otimes |j\rangle$ is a basis for $V \otimes W$. The common abbreviated notations for this type of operation are $|v\rangle|w\rangle$, $|v, w\rangle$ or $|vw\rangle$ for the tensor product $|v\rangle \otimes |w\rangle$. Now suppose we introduce the operators A and B that are linear operators on V and W respectively. We can now mathematically show that the following is true: $(A \otimes B)(|v\rangle \otimes |w\rangle) \equiv A|v\rangle \otimes B|w\rangle$. Subsequently, it may also be shown that $(A \otimes B)\left(\sum_i a_i |v_i\rangle \otimes |w_i\rangle\right) \equiv \sum_i a_i A|v_i\rangle \otimes B|w_i\rangle$. The natural inner product of the spaces V and W on $V \otimes W$ may now be succinctly defined in the following equation:

$$\left(\sum_i a_i |v_i\rangle \otimes |w_i\rangle, \sum_j b_j |v'_j\rangle \otimes |w'_j\rangle \right) \equiv \sum_{ij} a_i^* b_j \langle v_i | v'_j \rangle \langle w_i | w'_j \rangle. \quad (14.12)$$

Resonance Stabilization in Class II Mesoionic Xanthines

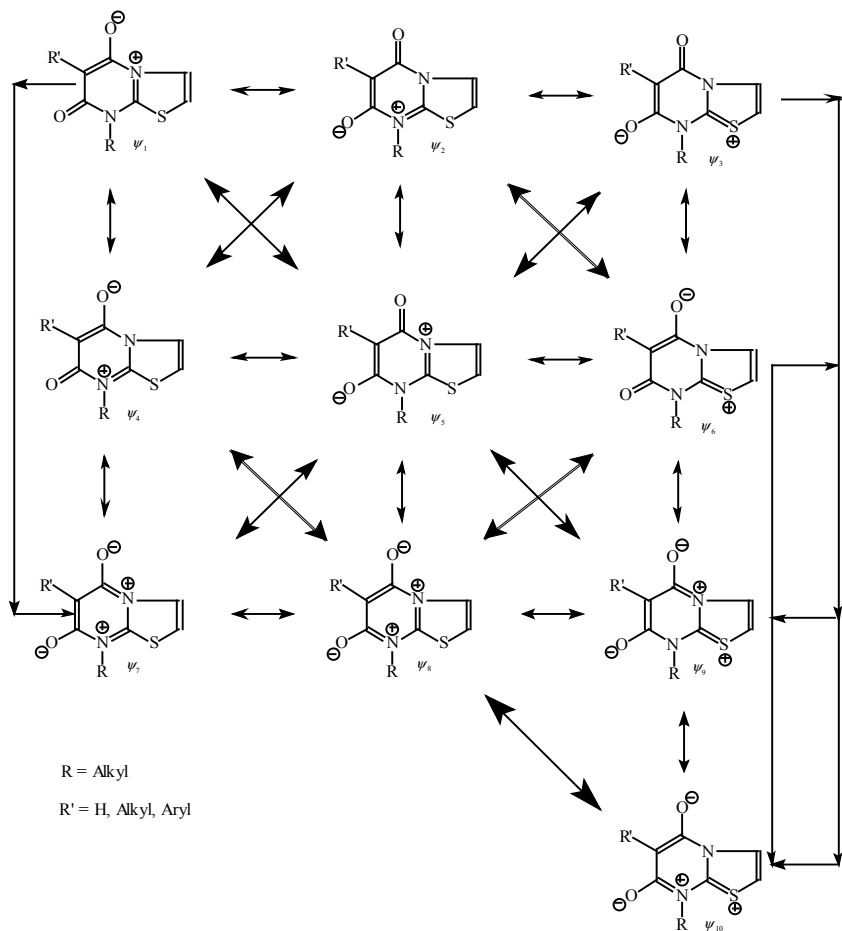


Fig. 14.2. Resonance stabilization in Class II Mesoionic Xanthines. Showing all 10 resonance contributors to the ground state of a Class II Mesoionic Xanthine. Each individual resonance contributor is of higher energy than the ground state. The arrows signify the conversion of one quantum state to another occurring naturally in the ground state of the molecule. As a QC substrate, each of these individual quantum states may be accessed or generated using an RF pulsed generator while under UV radiation at the λ_{\max} . Each resonance contributor represents a single wavefunction.

This well-defined inner product can be shown in a more concrete manner and a less abstract manner as a matrix or *Kronecker product* whereby A is an m by n matrix and B is a p by q matrix as shown below:

$$A \otimes B \equiv \begin{pmatrix} A_{11}B & \dots & A_{1n}B \\ \vdots & \ddots & \vdots \\ A_{m1}B & \dots & A_{mn}B \end{pmatrix}. \text{ In this form, terms like } A_{11}B \text{ refer to } p \text{ by } q$$

sub-matrices whose entries are proportional to B with the proportionality constant A_{mn} . As an example, the tensor product of the Pauli matrices X and Y is illustrated below:

$$X \otimes Y = \begin{pmatrix} 0Y & 1Y \\ 1Y & 0Y \end{pmatrix} = \begin{pmatrix} 0 & 0 & 0 & -i \\ 0 & 0 & i & 0 \\ 0 & -i & 0 & 0 \\ i & 0 & 0 & 0 \end{pmatrix}. \quad (14.13)$$

A close look at the 4×4 matrix shows that the product of the Pauli matrices X and Y is a compilation of two Pauli-Y matrices that are diagonalized from the upper right of the matrix to the lower left of the matrix with zeros everywhere else. A useful notation for a vector space that is tensored to itself is $|\psi\rangle^{\otimes k}$ where $|\psi\rangle$ is tensored with itself k times. For example, $|\psi\rangle^{\otimes 2} = |\psi\rangle \otimes |\psi\rangle$. Additionally, the Hadamard transform on n qubits,

$$H^{\otimes n}, \text{ may be expressed as: } H^{\otimes n} = \frac{1}{\sqrt{2^n}} \sum_{x,y} (-1)^{x.y} |x\rangle \langle y|.$$

14.5 Commutation Relations for the Pauli Matrices

Two operators are said to *commute* with each other *if and only if* the *commutator* between the two operators equals zero. For example, the commutator of Pauli-X and Pauli-Y matrices is shown as follows [13]:

$$[X, Y] \equiv XY - YX = \begin{pmatrix} 0 & 1 \\ 1 & 0 \end{pmatrix} \begin{pmatrix} 0 & -i \\ i & 0 \end{pmatrix} - \begin{pmatrix} 0 & -i \\ i & 0 \end{pmatrix} \begin{pmatrix} 0 & 1 \\ 1 & 0 \end{pmatrix} = 2i \begin{pmatrix} 1 & 0 \\ 0 & -1 \end{pmatrix} = 2iZ \quad (14.14)$$

Clearly, the Pauli-X and Y matrices are non-commutative as is demonstrated above. If the two operators A and B commute, $[A, B] = 0$ and are said to be *simultaneously diagonalizable*. This occurs if and only if there exists an orthonormal basis set (i.e., $|i\rangle$) that is some common orthonormal set of eigenvectors such that both A and B are diagonal with respect to that basis set. This would be the case if $A = \sum_i a_i |i\rangle\langle i|$, $B = \sum_i b_i |i\rangle\langle i|$.

On the other hand, two operators are said to *anti-commute* if the following operation is true: $\{A, B\} \equiv AB + BA = 0$. A is said to *anti-commute* with B if $\{A, B\} = 0$. The commutation relations for the Pauli matrices are: $[X, Y] = 2iZ$, $[Y, Z] = 2iX$ and $[Z, X] = 2iY$. An elegant way of writing this is by using the *Levi-Civita anti-symmetric permutation tensor* (actually a pseudo-tensor), ϵ_{jkl} on the three indices where $\epsilon_{jkl} = 0$ except where $\epsilon_{123} = \epsilon_{231} = \epsilon_{312} = 1$ and $\epsilon_{321} = \epsilon_{213} = \epsilon_{132} = -1$.

$$[\sigma_j, \sigma_k] = 2i \sum_{l=1}^3 \epsilon_{jkl} \sigma_l. \quad (14.15)$$

The quantum mechanical linear momentum operators are shown as [14]: $\hat{p}_x = -i\hbar \frac{\partial}{\partial x}$; $\hat{p}_y = -i\hbar \frac{\partial}{\partial y}$; $\hat{p}_z = -i\hbar \frac{\partial}{\partial z}$. The operator corresponding to \hat{p}_x^2 is $\hat{p}_x^2 = \left(-i\hbar \frac{\partial}{\partial x}\right)^2 = -\hbar^2 \frac{\partial^2}{\partial x^2}$ with similar expressions for \hat{p}_y^2 and \hat{p}_z^2 . The commutation relation for the positional vector \vec{x} and its component linear momentum operator in its direction is: $[\vec{x}, \hat{p}_x] = \left[x, -i\hbar \frac{\partial}{\partial x} \right] = \left[i\hbar \frac{\partial}{\partial x}, x \right] = i\hbar$. Likewise, the commutators for the positional vectors \vec{y} and \vec{z} and their corresponding component linear momentum operators (\hat{p} in the same direction) are also equal to $i\hbar$.

However, the commutators of the positional vectors in different directions from that of the momentum operators are, of course, equal to zero (*i.e.*, $[\vec{x}, \hat{p}_y] = 0$, $[\vec{x}, \hat{p}_z] = 0$, $[\vec{y}, \hat{p}_z] = 0$, etc.) and are thus commutative or said to commute with one another.

The classical mechanical *angular-momentum* \mathbf{L} of a particle is described in the following manner: $\mathbf{r} = \mathbf{i}x + \mathbf{j}y + \mathbf{k}z$ where \mathbf{r} is the vector from the origin to the instantaneous position of the particle and x , y , and z are the instantaneous coordinates of the particle. Therefore, the particle's *angular-momentum* \mathbf{L} with respect to the coordinate origin is $\mathbf{L} \equiv \mathbf{r} \times \mathbf{p}$, where \mathbf{L} is designated as the following determinant

$$\mathbf{L} = \begin{vmatrix} i & j & k \\ x & y & z \\ p_x & p_y & p_z \end{vmatrix}. \quad (14.16)$$

Therefore, we have the classical mechanical component *angular-momentum* vectors: $L_x = yp_z - zp_y$, $L_y = zp_x - xp_z$ and $L_z = xp_y - yp_x$.

The *angular-momentum* vector \mathbf{L} is perpendicular to the plane defined by the particle's position vector \mathbf{r} and its velocity vector \mathbf{v} (*i.e.*, $\mathbf{p} = m\mathbf{v}$). However, in the quantum mechanical realm there are two types of angular-momentum: *Orbital angular-momentum* which results from the motion of a particle through space, and is an analog of the classical-mechanical quantity \mathbf{L} and *spin angular-momentum* which is an intrinsic property of microscopic particles and which therefore has no classical-mechanical analog. The quantum-mechanical operators for the components of *Orbital angular-momentum* are designated below as follows:

$$\hat{L}_x = -i\hbar \left(y \frac{\partial}{\partial z} - z \frac{\partial}{\partial y} \right), \hat{L}_y = -i\hbar \left(z \frac{\partial}{\partial x} - x \frac{\partial}{\partial z} \right), \hat{L}_z = -i\hbar \left(x \frac{\partial}{\partial y} - y \frac{\partial}{\partial x} \right). \quad (14.17)$$

Also, $\hat{L}^2 = \left| \hat{L} \right|^2 = \hat{L} \cdot \hat{L} = \hat{L}_x^2 + \hat{L}_y^2 + \hat{L}_z^2$. It may now be shown that the

following commutation relations between the x , y and z components of the *orbital angular-momentum* operators are as follows:

$\left[\hat{L}_x, \hat{L}_y \right] = i\hbar \hat{L}_z$ and by performing two successive cyclic permutations on the coordinate indices we naturally obtain $\left[\hat{L}_y, \hat{L}_z \right] = i\hbar \hat{L}_x$ and $\left[\hat{L}_z, \hat{L}_x \right] = i\hbar \hat{L}_y$. The components of orbital angular-momentum therefore are non-commutative. Alternatively, however, it may be demonstrated that the total orbital angular-momentum \hat{L}^2 , commutes with each of its components as is shown:

$$\begin{aligned} \left[\hat{L}^2, \hat{L}_x \right] &= \left[\hat{L}_x^2 + \hat{L}_y^2 + \hat{L}_z^2, \hat{L}_x \right] = \left[\hat{L}_x^2, \hat{L}_x \right] + \left[\hat{L}_y^2, \hat{L}_x \right] + \left[\hat{L}_z^2, \hat{L}_x \right] = \\ &\quad \left[\hat{L}_y^2, \hat{L}_x \right] + \left[\hat{L}_z^2, \hat{L}_x \right] = \\ \left[\hat{L}_y, \hat{L}_x \right] \hat{L}_y + \hat{L}_y \left[\hat{L}_y, \hat{L}_x \right] + &\quad (14.18) \end{aligned}$$

$$\begin{aligned} \left[\hat{L}_z, \hat{L}_x \right] \hat{L}_z + \hat{L}_z \left[\hat{L}_z, \hat{L}_x \right] &= -i\hbar \hat{L}_z \hat{L}_y - i\hbar \hat{L}_y \hat{L}_z + i\hbar \hat{L}_y \hat{L}_z + i\hbar \hat{L}_z \hat{L}_y \\ \left[\hat{L}^2, \hat{L}_x \right] &= 0 \end{aligned}$$

Likewise, of course, the total angular-momentum operator also commutes with its y and z components \hat{L}_y and \hat{L}_z and therefore the commutation relations between \hat{L}^2 and these components are also zero. Analogous to the aforementioned orbital angular-momentum operators we also have the *spin angular momentum* operators $\hat{S}^2, \hat{S}_x, \hat{S}_y, \hat{S}_z$ which are both linear and Hermitian [15]. \hat{S}^2 is the operator for the square of the magnitude of the

particles total spin angular-momentum. As before with the orbital angular-momentum, we have $\hat{S}^2 = \hat{S}_x + \hat{S}_y + \hat{S}_z$. Also, as before, we have the following similar commutation relations for the spin angular-momentum operators: $[\hat{S}_x, \hat{S}_y] = i\hbar \hat{S}_z$, $[\hat{S}_y, \hat{S}_z] = i\hbar \hat{S}_x$ and $[\hat{S}_z, \hat{S}_x] = i\hbar \hat{S}_y$. Additionally, the *total spin angular-momentum* operators have the following commutation relations:

$$\left[\hat{S}^2, \hat{S}_x \right] = \left[\hat{S}^2, \hat{S}_y \right] = \left[\hat{S}^2, \hat{S}_z \right] = 0. \quad (14.19)$$

14.6 Quantum Superposition and Quantum Probabilities of 10-Qubit Mesoionic Registers

Quantum mechanically speaking, the ground and various excited state(s) of the mesoionic xanthines represented in Fig. 14.2 have the ability to exist in a total superposition of ten different quantum states simultaneously. It is this feature of these mesoionic xanthines that we attempt to exploit in terms of their utilization as potential substrates for 10-qubit quantum computer registers. Each resonance structure depicted in Fig. 14.2 is a distinct quantum state and can therefore be represented by a distinct wavefunction, ψ_i .

We therefore have ten different wavefunctions that can exist in a quantum superposition and quantum entangled states that may be represented by the following linear combination of wavefunctions: $\Psi = \psi_1 + \psi_2 + \psi_3 + \dots + \psi_{10}$. The state Ψ is the maximally entangled quantum state of the molecule and is therefore the lowest energy state or *ground state* of the molecule.

Each resonance structure depicted in Fig. 14.2 has a certain probability associated with that particular state. We determine these probabilities by utilizing a fundamental rule in quantum chemistry. This rule basically states the following: *The number of possible resonance inter-conversion states a particular resonance structure possesses is directly proportional to the probability of that quantum state*. As a few examples, using Fig. 14.2, let us first look at the most probable resonance structure designated as ψ_5 .

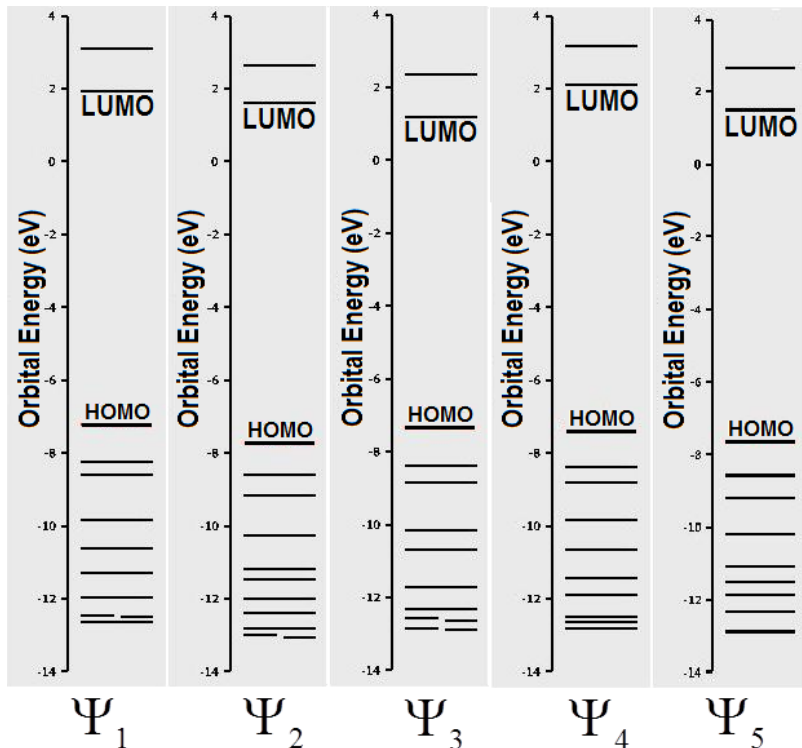


Fig. 14.3. Orbital energy LUMO and HOMO for Class II Mesoionic Xanthine quantum wavefunction states, 1 to 5. Notice that all 10 quantum states signified by Ψ_{1-10} are unique, and each state is represented by its unique energy levels.

Resonance structure or quantum state ψ_5 has a total of 8 possible resonance inter-conversions. These eight inter-conversions of quantum state ψ_5 are with the following quantum states: $\psi_1, \psi_2, \psi_3, \psi_4, \psi_6, \psi_7, \psi_8, \psi_9$. This is therefore the most probable quantum state of the molecule. As another example, let us count the number of possible inter-conversion states for ψ_1 . This state inter-converts with $\psi_2, \psi_4, \psi_5, \psi_7$, or a total of four quantum states. The list of possible inter-conversion states possible for each of the ten quantum states is listed below:

$$\psi_1 = 4, \quad \psi_2 = 4, \quad \psi_3 = 5, \quad \psi_4 = 4, \quad \psi_5 = 8 \quad (14.20)$$

$$\psi_6 = 4, \quad \psi_7 = 4, \quad \psi_8 = 4, \quad \psi_9 = 5, \quad \psi_{10} = 4$$

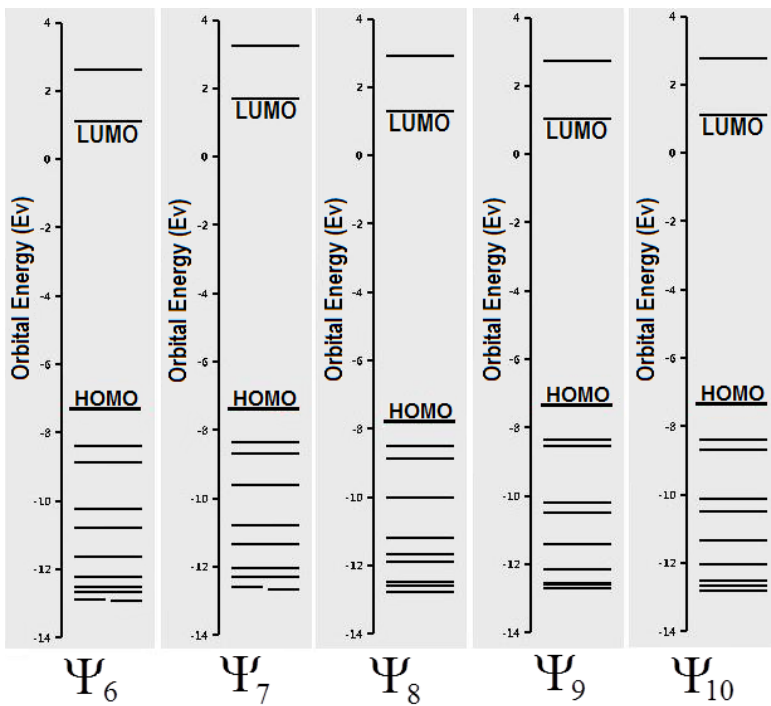


Fig. 14.4. Orbital energy, Lowest Unoccupied Molecular Orbital (LUMO) and Highest Unoccupied Molecular Orbital (HUMO) for Class II Mesoionic Xanthine quantum wavefunction states, 6 to 10.

The total number of quantum resonance inter-conversions is therefore equal to 52. It is now a rather trivial procedure to calculate the actual probabilities in terms of coefficients of the individual quantum states. We simply take the above numbers for each state and divide them by the total number of inter-conversion states. The following probabilities are thus obtained:

$$\alpha_1^2 = \frac{1}{13}, \quad \alpha_2^2 = \frac{5}{52}, \quad \alpha_3^2 = \frac{5}{52}, \quad \alpha_4^2 = \frac{5}{52}, \quad \alpha_5^2 = \frac{2}{13} \quad (14.21)$$

$$\alpha_6^2 = \frac{3}{26}, \quad \alpha_7^2 = \frac{1}{13}, \quad \alpha_8^2 = \frac{3}{26}, \quad \alpha_9^2 = \frac{1}{13}, \quad \alpha_{10}^2 = \frac{5}{52} \quad (14.22)$$

We may now re-write the total wavefunction Ψ in the following manner:

$$\begin{aligned}\Psi = & \frac{1}{13}\psi_1 + \frac{5}{52}\psi_2 + \frac{5}{52}\psi_3 + \frac{5}{52}\psi_4 + \frac{2}{13}\psi_5 + \\ & , \quad (14.23) \\ & \frac{3}{26}\psi_6 + \frac{1}{13}\psi_7 + \frac{3}{26}\psi_8 + \frac{1}{13}\psi_9 + \frac{5}{52}\psi_{10}\end{aligned}$$

where all of the coefficients of the individual wavefunctions add up to equal one. We may also express the above wavefunction in our more familiar quantum computer form as:

$$\begin{aligned}|\Psi\rangle = & \sum_{i=1}^N \sqrt{\frac{1}{13}}|i\rangle + \sqrt{\frac{5}{52}}|i\rangle + \sqrt{\frac{5}{52}}|i\rangle + \sqrt{\frac{5}{52}}|i\rangle + \sqrt{\frac{2}{13}}|i\rangle + \\ & (14.24) \\ & \sqrt{\frac{3}{26}}|i\rangle + \sqrt{\frac{1}{13}}|i\rangle + \sqrt{\frac{3}{26}}|i\rangle + \sqrt{\frac{1}{13}}|i\rangle + \sqrt{\frac{5}{52}}|i\rangle\end{aligned}$$

or more succinctly as:

$$|\Psi\rangle = \sum_{i=1}^N 3\sqrt{\frac{1}{13}}|i\rangle + 4\sqrt{\frac{5}{52}}|i\rangle + 2\sqrt{\frac{3}{26}}|i\rangle + \sqrt{\frac{2}{13}}|i\rangle, \quad (14.25)$$

where $|i\rangle = \{i_1, i_2, i_3, \dots, i_n\}$ and $n = 10$; $N = 1,024$.

14.7 Projectors and Projection Operators

Let us examine the role of projectors and projection operators. A projection matrix P is an $n \times n$ square matrix that gives a vector space projection from R^n to a subspace W . The columns of P are the projections of the standard basis vectors and W is the image of P . Therefore, a square matrix P is a projection matrix if and only if $P^2 = P$. A projection matrix P is orthogonal if and only if $P = P^\dagger$.

Suppose W is a k -dimensional subspace of the d -dimensional vector space V . Using the Gram-Schmidt procedure, it is possible to construct an orthonormal basis $|1\rangle, \dots, |d\rangle$ for V such that $|1\rangle, \dots, |k\rangle$ is an orthonormal basis for W . We may represent this definition mathematically by stating

that the projector P is the projector onto the subspace W using the following equation [16]: $P \equiv \sum_{i=1}^k |i\rangle\langle i|$. It can easily be shown that this definition is independent of the orthonormal basis $|1\rangle, \dots, |k\rangle$ used for W . It can further be shown that $|v\rangle\langle v|$ is Hermitian for any vector $|v\rangle$ and so P is Hermitian, $P^\dagger = P$. We may now refer to P as the vector space onto which P is a projector. The *orthogonal complement* of P is the operator $Q \equiv I - P$. The operator Q is therefore a projector onto the vector space spanned by $|k+1\rangle, \dots, |d\rangle$ which we also refer to as the *orthogonal complement* of P , and may be denoted by Q .

14.8 Density Measurement Operator and Quantum State Ensembles

Thus far, we have formulated our quantum mechanics using the concept or language of state vectors. An alternative formalism that is mathematically equivalent to the state vector approach is that of the density operator or density matrix. The density operator approach provides a much more convenient way for representing some commonly encountered scenarios within the framework of quantum mechanics. Suppose the quantum system is in one of a number of quantum states $|\psi_i\rangle$, where i is an index with respective probabilities p_i . We shall then call $\{p_i, |\psi_i\rangle\}$ an *ensemble of pure states*. The density operator for the system is defined by the following equation [17]: $\rho \equiv \sum_i p_i |\psi_i\rangle\langle\psi_i|$. As stated previously, the density operator is also known as the density matrix. The two terms may be used interchangeably. All of the postulates of quantum mechanics can be reformulated or expressed in terms of the density operator language. Both the density operator language and the state vector language give the exact same results, however the use of one over the other may make it easier to approach problems from one point of view rather than the other. Suppose that the evolution of a closed quantum system is described by the unitary operator U . If the system was initially in the state $|\psi_i\rangle$, with probability p_i then after the evolution has occurred

the system will be in the state $U|\psi_i\rangle$ with probability p_i . This is shown mathematically below:

$$\rho = \sum_i p_i |\psi_i\rangle\langle\psi_i| \xrightarrow{U} \sum_i p_i U |\psi_i\rangle\langle\psi_i| U^\dagger = U \rho U^\dagger. \quad (14.26)$$

The measurement operators M_m may also be described in terms of the density operator language. If the initial state of a quantum system is $|\psi_i\rangle$ then the probability of getting a result m is: $p(m|i) = \langle\psi_i|M_m^\dagger M_m|\psi_i\rangle = \text{tr}(M_m^\dagger M_m|\psi_i\rangle\langle\psi_i|)$, where we have used the known relationship, $\text{tr}(A|\psi\rangle\langle\psi|) = \sum_i \langle i|A|\psi\rangle\langle\psi|i\rangle = \langle\psi|A|\psi\rangle$ where the end result is that the operator is sandwiched between the two wavefunctions or quantum states. The notation whereby the operator, usually the Hamiltonian, is sandwiched between the two states is very common in quantum mechanics. Therefore, the probability of obtaining result m is:

$$p(m) = \sum_i p(m|i)p_i = \sum_i p_i \text{tr}(M_m^\dagger M_m|\psi_i\rangle\langle\psi_i|) = \text{tr}(M_m^\dagger M_m \rho). \quad (14.27)$$

Now suppose we wish to determine the density operator of the system after making the measurement m . If the initial state was $|\psi_i\rangle$ then the state after the measurement m is:

$|\psi_i^m\rangle = \frac{M_m|\psi_i\rangle}{\sqrt{\langle\psi_i|M_m^\dagger M_m|\psi_i\rangle}}$. After the measurement that yields the result m we have an ensemble of states $|\psi_i^m\rangle$ with respective probabilities $p(i|m)$ with the corresponding density operator

$$\rho_m = \sum_i p(i|m)|\psi_i^m\rangle\langle\psi_i^m| = \sum_i p(i|m) \frac{M_m|\psi_i\rangle\langle\psi_i|M_m^\dagger}{\langle\psi_i|M_m^\dagger M_m|\psi_i\rangle}. \quad (14.28)$$

Using the following definitions for probability theory, $p(i|m) = \frac{p(m,i)}{p(m)} = \frac{p(m,i)p_i}{p(m)}$ and with the appropriate substitutions,

we may further show that the following is true:

$$\rho_m = \sum_i p_i \frac{M_m |\psi_i\rangle\langle\psi_i| M_m^\dagger}{\text{tr}(M_m^\dagger M_m \rho)} = \frac{M_m \rho M_m^\dagger}{\text{tr}(M_m^\dagger M_m \rho)}. \quad (14.29)$$

We have thus proven that the basic postulates of quantum mechanics related to the unitary evolution and measurement can be viewed in terms of the density operator formalism. Furthermore, a quantum system whose state $|\psi\rangle$ is known exactly is said to be in a *pure state* (i.e., $\rho = |\psi\rangle\langle\psi|$). If the state function is not known exactly, then the density operator ρ is said to be in a *mixed state* which is simply a *mixture* of the different pure states in the ensemble for ρ . It may also be easily shown that for a pure state $\text{tr}(\rho^2) = 1$ and for a mixed state $\text{tr}(\rho^2) < 1$.

Now suppose we have a quantum system in the state ρ_i with a probability p_i . The system may therefore be described by the density matrix $\sum_i p_i \rho_i$. This can be proven by assuming that ρ_i arises from some ensemble of $\{p_{ij}, |\psi_{ij}\rangle\}$ pure states (where i is fixed) so that the probability for being in the state $|\psi_{ij}\rangle$ is thus $p_i p_{ij}$. The density matrix for this system is thus: $\rho = \sum_{ij} p_i p_{ij} |\psi_{ij}\rangle\langle\psi_{ij}| = \sum_i p_i \rho_i$, where we have used the definition $\rho_i = \sum_j p_{ij} |\psi_{ij}\rangle\langle\psi_{ij}|$. We conclude that ρ is therefore a *mixture* of the states ρ_i with probabilities p_i .

14.9 State-Function Time Evolution of a Closed Quantum System

The time evolution of a state function is given by the well-known Schrödinger equation, $i\hbar \frac{d|\psi\rangle}{dt} = H|\psi\rangle$ where H is the *Hamiltonian* of

the closed system [18]. Due to the fact the Hamiltonian is a Hermitian operator, it has a spectral decomposition: $H = \sum_E E |E\rangle\langle E|$ which

includes the eigenvalues E and their corresponding eigenvectors $|E\rangle$. The states $|E\rangle$ are referred to as the *energy eigenstates* or as *stationary states*, and E is the energy of the state $|E\rangle$. The lowest energy is known as the *ground state energy* and the corresponding energy eigenstate is known as the *ground state*. The energy eigenstates $|E\rangle$ are known as stationary states since their only change in time is to acquire an overall numerical factor, $|E\rangle \rightarrow e^{(-iEt/\hbar)}|E\rangle$. A simple example would be to consider a single qubit having the following Hamiltonian, $H = \hbar\omega X$, where $\omega = 2\pi f$ and f is the frequency of the particle or photon. The energy eigenstates of this Hamiltonian are $|0\rangle \pm |1\rangle / \sqrt{2}$ with corresponding energies $\hbar\omega$ and $-\hbar\omega$. The ground state is therefore $-hf$ and the ground state energy is $-\hbar\omega$ or $-hf$. The solution to the Schrödinger equation utilizing the unitary operator, U is shown below:

$$|\psi(t_2)\rangle = e^{(-iH(t_2-t_1)/\hbar)} |\psi(t_1)\rangle = U(t_1, t_2) |\psi(t_1)\rangle, \quad (14.30)$$

where

$$U(t_1, t_2) \equiv e^{(-iH(t_2-t_1)/\hbar)}. \quad (14.31)$$

Furthermore, it may be shown that any unitary operator U can be expressed in the compact form $U = e^{iK}$ for any Hermitian operator, K .

14.10 Quantum Simulations of Hamiltonians

Quantum simulations have largely concentrated on simulating Hamiltonians that are sums of local interactions. However, this is not a fundamental requirement! Efficient quantum simulations are possible

even for Hamiltonians which act non-trivially on all parts of a large quantum system. Suppose we have the Hamiltonian: $H = Z_1 \otimes Z_2 \otimes \dots \otimes Z_n$ which acts on an n -qubit system. We may apply a Hermitian phase shift $e^{-i\Delta t}$ to the system if the parity of the n -qubits in the computational basis set is even. If odd, the phase shift is $e^{i\Delta t}$. We may therefore efficiently simulate any Hamiltonian of the form: $H = \bigotimes_{k=1}^n \sigma_{c(k)}^k$, where $\sigma_{c(k)}^k$ is a Pauli matrix or the identity acting on the k^{th} -qubit, with $c(k) \in \{0, 1, 2, 3\}$ designating one of the matrices $\{I, X, Y, Z\}$. There are a couple of useful algebraic facts regarding the various quantum gates such as the Hadamard gate (H) and the various Pauli, phase and $\pi/8$ -gates. The Hadamard gate $H = (X + Z)/\sqrt{2}$ and the phase-gate $S = T^2$. The T-gate or $\pi/8$ -gate is called such since it contains $e^{\pm i\pi/8}$ appearing on its diagonals [19]:

$$T = e^{i\pi/8} \begin{pmatrix} e^{-i\pi/8} & 0 \\ 0 & e^{i\pi/8} \end{pmatrix}. \quad (14.32)$$

For a single qubit-vector state $|\psi\rangle = a|0\rangle + b|1\rangle$ parameterized by two complex numbers satisfying the relationship $|a|^2 + |b|^2 = 1$, the state may be visualized as a point (θ, φ) on the unit sphere where $a = \cos(\theta/2)$ and $b = e^{i\varphi} \sin(\theta/2)$. This is known as the Bloch sphere representation and the vector $(\cos \varphi \sin \theta, \sin \varphi \sin \theta, \cos \theta)$ is known as the Bloch vector. The value for a can be taken as a real number since the overall phase of the state is unobservable. Additionally, upon exponentiation, the Pauli matrices give rise to a very useful class of unitary matrices known as *rotation operators* about the x , y and z axes, defined by the equations below:

$$R_x(\theta) \equiv e^{-i\theta X/2} = \cos \frac{\theta}{2} I - i \sin \frac{\theta}{2} X = \begin{pmatrix} \cos \frac{\theta}{2} & -i \sin \frac{\theta}{2} \\ -i \sin \frac{\theta}{2} & \cos \frac{\theta}{2} \end{pmatrix} \quad (14.33a)$$

$$R_y(\theta) \equiv e^{-i\theta Y/2} = \cos \frac{\theta}{2} I - i \sin \frac{\theta}{2} Y = \begin{pmatrix} \cos \frac{\theta}{2} & -\sin \frac{\theta}{2} \\ \sin \frac{\theta}{2} & \cos \frac{\theta}{2} \end{pmatrix} \quad (14.33b)$$

$$R_z(\theta) \equiv e^{-i\theta Z/2} = \cos \frac{\theta}{2} I - i \sin \frac{\theta}{2} Z = \begin{pmatrix} e^{-i\theta/2} & 0 \\ 0 & e^{i\theta/2} \end{pmatrix} \quad (14.33c)$$

14.11 Initialization of Mesoionic Xanthine Registers

The mesoionic xanthine molecule, as depicted in Fig. 14.2, represents a molecule that is in a quantum superposition of at least ten distinct and unique quantum states. An efficient scheme for initializing quantum registers with an arbitrary superposed state, without the introduction of additional qubits (Ventura & Martinez 1999 [20]) has been developed by Long & Sun [21]. This scheme begins with the state $|0\dots0\rangle$ and is then transformed to a general superposed state of the following form:

$|\psi\rangle = \sum_{i=0}^{N-1} a_i |i\rangle$. In this particular case, $N = 1,024$ and $|i\rangle$ is the shorthand

notation for the basis set $\{i_1, i_2, i_3 \dots i_j \dots i_n\}$ where $n = \log_2 N$ and where i_j denotes the two possible states (0 or 1) of the j^{th} -qubit. The following diagram will illustrate this concept more easily:

$$i = \begin{cases} 0 \rightarrow \{000\dots000\} \\ 1 \rightarrow \{000\dots001\} \\ 2 \rightarrow \{000\dots010\} \\ 3 \rightarrow \{000\dots100\} \\ \vdots \\ N-1 \rightarrow \{111,\dots111\} \end{cases} . \quad (14.34)$$

The 14.34 diagram therefore illustrates that $|\psi\rangle$ is a general quantum superposition of N basis states and each basis state is a product state of n qubits. The initialization scheme involves only two types of unitary transformations or gate operations. The first gate operation is a single bit rotation

$$U_\theta, U_\theta \begin{bmatrix} 0 \\ 1 \end{bmatrix} = \begin{bmatrix} \cos \theta & \sin \theta \\ \sin \theta & -\cos \theta \end{bmatrix} \begin{bmatrix} 0 \\ 1 \end{bmatrix}. \quad (14.35)$$

This rotation differs from an ordinary rotation because it is an ordinary rotation only for the $|0\rangle$ bit but interjects a minus sign for the $|1\rangle$ bit. The operation thus converts a qubit in the state $|0\rangle$ to a superposition of the 2-state $(\cos \theta, \sin \theta)$ and a qubit in the $|1\rangle$ state to the superposition of the 2-state $(\sin \theta, -\cos \theta)$. When $\theta = 0$, the state $|0\rangle$ remains unchanged but converts the sign of state $|1\rangle$ (i.e., Pauli-Z gate). When $\theta = \pi/4$, U_θ is simply reduced to the Hadamard-Walsh transformation. When $\theta = \pi/2$ (90° rotation), it acts as the NOT operation (Pauli-X, σ_x) by changing $|0\rangle$ to $|1\rangle$ and $|1\rangle$ to $|0\rangle$.

The second type of gate operation is known as the controlled k -operation. This operation is constructed from a string of k -controlling

qubits as shown below:

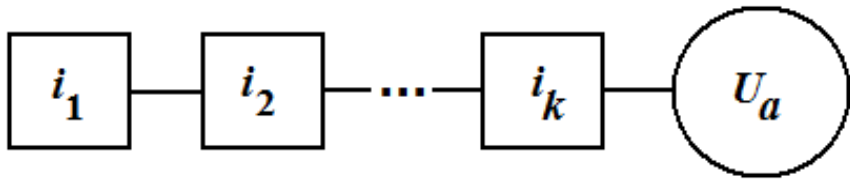


Fig. 14.5. k -controlling qubits.

The squares represent the controlling qubits $\{i_1, i_2, \dots, i_k\}$ and the circle is a unitary operation on the target qubit representing an angle of rotation. The uniqueness and power of this operation is that it is a conditional one that is activated only when the controlling qubits hold the respective values indicated in the squares. Controlled k -operations may be constructed using $O(k^2)$ standard 1- and 2-bit gate operations [22]. In order to more easily see how these operations are performed we may take a look at the simple example of a two qubit system.

$$|00\rangle \rightarrow \sqrt{|a_{00}|^2 + |a_{01}|^2} |00\rangle + \sqrt{|a_{10}|^2 + |a_{11}|^2} |10\rangle \quad (14.36)$$

Operation 1.) Single bit rotation α_1 ,

$$\rightarrow |0\rangle [a_{00}|0\rangle + a_{01}|1\rangle] + |1\rangle [a_{10}|0\rangle + a_{11}|1\rangle] \quad (14.37)$$

Operation 2.) Two controlled-operations $U_{\alpha_{2,i}}$ ($i = 0, 1$).

$$= a_{00}|00\rangle + a_{01}|01\rangle + a_{10}|10\rangle + a_{11}|11\rangle$$

The single bit rotation α_1 is equal to $\tan^{-1} \sqrt{\frac{|a_{10}|^2 + |a_{11}|^2}{|a_{00}|^2 + |a_{01}|^2}}$. We may now

represent the operations in matrix form as well:

$$U_{\alpha 2,0} = \begin{bmatrix} \frac{a_{00}}{\sqrt{|a_{00}|^2 + |a_{01}|^2}} & \frac{a_{01}}{\sqrt{|a_{00}|^2 + |a_{01}|^2}} \\ \frac{a_{01}^*}{\sqrt{|a_{00}|^2 + |a_{01}|^2}} & \frac{a_{00}^*}{\sqrt{|a_{00}|^2 + |a_{01}|^2}} \end{bmatrix} \quad (14.38a)$$

$$U_{\alpha 2,1} = \begin{bmatrix} \frac{a_{10}}{\sqrt{|a_{10}|^2 + |a_{11}|^2}} & \frac{a_{11}}{\sqrt{|a_{10}|^2 + |a_{11}|^2}} \\ \frac{a_{11}^*}{\sqrt{|a_{10}|^2 + |a_{11}|^2}} & \frac{a_{10}^*}{\sqrt{|a_{10}|^2 + |a_{11}|^2}} \end{bmatrix} \quad (14.38b)$$

The situation becomes even more interesting when using a larger register such as a 3-qubit register having 8 basis states:

- Starting from the state $|000\rangle$, a single bit rotation is operated on the 1st-qubit with the angle

$$\alpha_1 = \tan^{-1} \sqrt{\frac{|a_{100}|^2 + |a_{101}|^2 + |a_{110}|^2 + |a_{111}|^2}{|a_{000}|^2 + |a_{001}|^2 + |a_{010}|^2 + |a_{011}|^2}} \quad (14.39)$$

transforming the initialized state $|000\rangle$ to the state

$$\frac{\sqrt{|a_{000}|^2 + |a_{001}|^2 + |a_{010}|^2 + |a_{011}|^2}}{\sqrt{|a_{100}|^2 + |a_{101}|^2 + |a_{110}|^2 + |a_{111}|^2}} |000\rangle + \frac{\sqrt{|a_{100}|^2 + |a_{101}|^2 + |a_{110}|^2 + |a_{111}|^2}}{\sqrt{|a_{000}|^2 + |a_{001}|^2 + |a_{010}|^2 + |a_{011}|^2}} |100\rangle \quad (14.40)$$

2. Then, two controlled¹-rotations with angles

$$\tan^{-1} \sqrt{\frac{|a_{010}|^2 + |a_{011}|^2}{|a_{000}|^2 + |a_{001}|^2}} \text{ and } \tan^{-1} \sqrt{\frac{|a_{110}|^2 + |a_{111}|^2}{|a_{100}|^2 + |a_{101}|^2}} \text{ operate on the 2nd-qubit.}$$

The resulting superposed state vector therefore becomes:

$$\begin{aligned} & \sqrt{|a_{000}|^2 + |a_{001}|^2} |000\rangle + \sqrt{|a_{010}|^2 + |a_{011}|^2} |010\rangle + \\ & \sqrt{|a_{100}|^2 + |a_{101}|^2} |100\rangle + \sqrt{|a_{110}|^2 + |a_{111}|^2} |110\rangle \end{aligned} . \quad (14.41)$$

3. Finally, 4 controlled²-unitary transformations operate on the 3rd-qubit to generate the superposed state:

$$\begin{aligned} & a_{000} |000\rangle + a_{001} |001\rangle + a_{010} |010\rangle + a_{100} |100\rangle + a_{011} |011\rangle + \\ & a_{101} |101\rangle + a_{110} |110\rangle + a_{111} |111\rangle \end{aligned} . \quad (14.42)$$

These 4 controlled²-unitary transformations are:

$$U_{\alpha 3,00} = \begin{bmatrix} \frac{a_{000}}{\sqrt{|a_{000}|^2 + |a_{001}|^2}} & \frac{a_{001}}{\sqrt{|a_{000}|^2 + |a_{001}|^2}} \\ \frac{a_{001}^*}{\sqrt{|a_{000}|^2 + |a_{001}|^2}} & -\frac{a_{000}^*}{\sqrt{|a_{000}|^2 + |a_{001}|^2}} \end{bmatrix} \quad (14.43a)$$

$$U_{\alpha 3,01} = \begin{bmatrix} \frac{a_{010}}{\sqrt{|a_{010}|^2 + |a_{011}|^2}} & \frac{a_{011}}{\sqrt{|a_{010}|^2 + |a_{011}|^2}} \\ \frac{a_{011}^*}{\sqrt{|a_{010}|^2 + |a_{011}|^2}} & -\frac{a_{010}^*}{\sqrt{|a_{010}|^2 + |a_{011}|^2}} \end{bmatrix} \quad (14.43b)$$

$$U_{\alpha 3,10} = \begin{bmatrix} \frac{a_{100}}{\sqrt{|a_{100}|^2 + |a_{101}|^2}} & \frac{a_{101}}{\sqrt{|a_{100}|^2 + |a_{101}|^2}} \\ \frac{a_{101}^*}{\sqrt{|a_{100}|^2 + |a_{101}|^2}} & -\frac{a_{100}^*}{\sqrt{|a_{100}|^2 + |a_{101}|^2}} \end{bmatrix} \quad (14.43c)$$

$$U_{\alpha 3,11} = \begin{bmatrix} \frac{a_{110}}{\sqrt{|a_{110}|^2 + |a_{111}|^2}} & \frac{a_{111}}{\sqrt{|a_{110}|^2 + |a_{111}|^2}} \\ \frac{a_{111}^*}{\sqrt{|a_{110}|^2 + |a_{111}|^2}} & -\frac{a_{110}^*}{\sqrt{|a_{110}|^2 + |a_{111}|^2}} \end{bmatrix} \quad (14.43d)$$

For notation purposes we use an “angle” to label a controlled k -operation. If the coefficients are all real, it reduces to an ordinary rotation angle. The notations of angles of the controlled k -rotations, the first subscript designates the target qubit order number and the subscripts following the comma designate the quantum states of the controlling qubits. For example, 3 in $\alpha_{3,11}$ refers to the target qubit and the subscripts (11 in $\alpha_{3,11}$) refer to the controlling qubits. In the initialization, operations for the first $n-1$ qubits are controlled rotations where each rotation depends only on a single real parameter. The rotation angles take on the following general expressions. In the first qubit there is a 1-qubit rotation. The rotation angle is:

$$\alpha_1 = \tan^{-1} \sqrt{\frac{\sum_{i_2 i_3 \dots i_n} |a_{1 i_2 i_3 \dots i_n}|^2}{\sum_{i_2 i_3 \dots i_n} |a_{0 i_2 i_3 \dots i_n}|^2}}. \text{ In the } 2^{\text{nd}}\text{-qubit, there are two}$$

controlled¹-rotations:

$$\alpha_{2,0} = \tan^{-1} \sqrt{\frac{\sum_{i_3 i_4 \dots i_n} |a_{01 i_3 i_4 \dots i_n}|^2}{\sum_{i_3 i_4 \dots i_n} |a_{00 i_3 i_4 \dots i_n}|^2}} \text{ and } \alpha_{2,1} = \tan^{-1} \sqrt{\frac{\sum_{i_3 i_4 \dots i_n} |a_{11 i_3 i_4 \dots i_n}|^2}{\sum_{i_3 i_4 \dots i_n} |a_{10 i_3 i_4 \dots i_n}|^2}}.$$

In general, in the j^{th} -qubit, there are 2^{j-1} controlled $^{j-1}$ -rotations, with each of them having $j - 1$ controlling qubits labeled as $i_1 i_2 \dots i_{j-1}$. The rotation angle in the j^{th} -qubit ($j \neq n$) is given by:

$$\alpha_{j,i_1 i_2 \dots i_{j-1}} = \tan^{-1} \sqrt{\frac{\sum_{i_{j+1} \dots i_n} |a_{i_1 i_2 \dots i_{j-1} 1 i_{j+1} \dots i_n}|^2}{\sum_{i_{j+1} \dots i_n} |a_{i_1 i_2 \dots i_{j-1} 0 i_{j+1} \dots i_n}|^2}}. \quad (14.44)$$

For the last qubit, where $j = n$ we have 2^{n-1} controlled $^{n-1}$ unitary transformations where:

$$U_{\alpha_n, i_1 i_2 \dots i_{n-1}} = \begin{bmatrix} \frac{A_0}{\sqrt{|A_0|^2 + |A_1|^2}} & \frac{A_1}{\sqrt{|A_0|^2 + |A_1|^2}} \\ \frac{A_1^*}{\sqrt{|A_0|^2 + |A_1|^2}} & -\frac{A_0^*}{\sqrt{|A_0|^2 + |A_1|^2}} \end{bmatrix} \quad (14.45)$$

where $A_0 = a_{i_1 i_2 \dots i_{n-1} 0}$ and $A_1 = a_{i_1 i_2 \dots i_{n-1} 1}$.

If A_0 and A_1 are real, the operation is simply a rotation and the angle is given by:

$$\alpha_{n, i_1 i_2 \dots i_{n-1}} = \tan^{-1} \left(\frac{A_1}{A_0} \right). \quad (14.46)$$

We are now ready to initialize quantum superposition registers of three different types starting from the state $|0\dots0\rangle$:

1. The evenly distributed state $|\psi\rangle = \sum |i\rangle$ is the most common state in quantum computing. The Hadamard-Walsh gate operation on each qubit generates this form of superposition from the state $|0\dots0\rangle$. In this particular case, all of the rotation angles are $\pi/4$. In each qubit, the controlling qubits use up all possible combinations and therefore the 2^{j-1}

controlled Hadamard-Wash gate operations are reduced to a single Hadamard-Walsh transformation in the j^{th} -qubit.

2. The Greenberger-Horne-Zeilinger or GHZ state is the maximally entangled state with the superposition $\frac{1}{\sqrt{2}}(|0\dots0\rangle \pm |1\dots1\rangle)$. Suppose we would like to transform the state $|0000\rangle$ to the state $\frac{1}{\sqrt{2}}(|0000\rangle + |1111\rangle)$. The circuit below shows this diagrammatically:

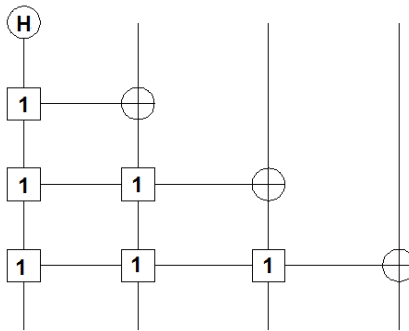


Fig. 14.6. Quantum Circuit for the GHZ state.

The rotation in the 1st-qubit is the Hadamard-Walsh transformation. There are two controlled operations $\alpha_{2,0} = 0$ in the 2nd-qubit that are equal to the identity operation and so does nothing to the qubit. However, $\alpha_{2,1} = \frac{\pi}{2}$ corresponds to the CNOT operation, so effectively, there is only one controlled-NOT gate in the 2nd-qubit. There are four gate operations in the 3rd-qubit. $\alpha_{3,11} = \frac{\pi}{2}$ is the $|11\rangle$ -CNOT gate and $\alpha_{3,00}$ is the identity operation. $\alpha_{3,01}$ and $\alpha_{3,10}$ are undetermined angles equal to $\frac{0}{0}$. Upon closer examination, however, these angles are equal to 0 and are therefore equal to the identity operation. Therefore, the only gate operation in the 3rd-qubit is the $|11\rangle$ -CNOT operation. Similarly, there is only the $|111\rangle$ -CNOT operation in the 4th-qubit. Should the circuit contain more than four

qubits, the same analysis applies until the last qubit. For the last qubit, the rotation is either $\frac{\pi}{2}$ for the state

$$\frac{1}{\sqrt{2}}(|0\dots0\rangle + |1\dots1\rangle) \text{ or } -\frac{\pi}{2} \text{ for the state } \frac{1}{\sqrt{2}}(|0\dots0\rangle - |1\dots1\rangle). \quad (14.47)$$

3. In the Grover search algorithm [23], the state vector is built up in a two-dimensional space spanned by the so-called “marked” state $|\tau\rangle$ and the “rest” state $|c\rangle = \sum_{i \neq \tau} |i\rangle$. At any step in the search, the state vector has the form $|\psi\rangle = \sin \theta |\tau\rangle + \cos \theta |c\rangle$. In order to initialize such a superposed state, we let $|\tau\rangle = |i_1 i_2 \dots i_n\rangle$ be the marked state. We may now construct the state $|\psi\rangle$ from $|0\dots0\rangle$. The amplitudes a_i of the basis states $|i\rangle$ are $a_\tau = \sin \theta$ and $a_i = \cos \theta / \sqrt{N-1}$ for $i \neq \tau$. According

to the equation, $\alpha_1 = \tan^{-1} \sqrt{\frac{\sum_{i_2 i_3 \dots i_n} |a_{1 i_2 i_3 \dots i_n}|^2}{\sum_{i_2 i_3 \dots i_n} |a_{0 i_2 i_3 \dots i_n}|^2}}$, the rotation

angle in the 1st-qubit is: $\alpha_1 = \begin{cases} \tan^{-1} \Omega_1, & \text{if } i_1 = 1 \\ \tan^{-1} \frac{1}{\Omega_1}, & \text{if } i_1 = 0 \end{cases}$, where

$$\Omega_1 = \sqrt{\frac{(N-2)\cos^2 \theta + 2(N-1)\sin^2 \theta}{N\cos^2 \theta}}. \quad (14.48)$$

In the k^{th} -qubit, the angle for the $|i_1 i_2 \dots i_{k-1}\rangle$ -controlled rotation is therefore:

$$\alpha_{k,i_1,i_2 \dots i_{k-1}} = \begin{cases} \tan^{-1} \Omega_k, & \text{if } i_k = 1 \\ \tan^{-1} \frac{1}{\Omega_k}, & \text{if } i_k = 0 \end{cases} \quad (14.49)$$

where $\Omega_1 = \sqrt{\frac{(N - 2^k) \cos^2 \theta + 2^k (N - 1) \sin^2 \theta}{N \cos^2 \theta}}$.

14.12 Xanthine Molecule Electrostatic Potentials

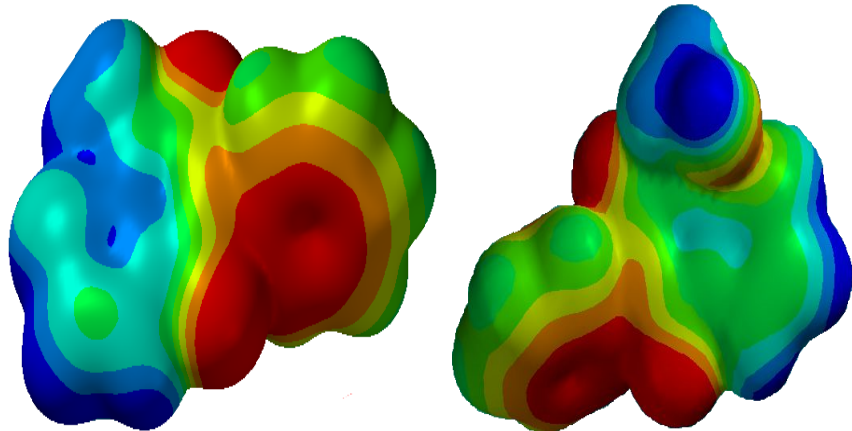


Fig. 14.7. Two of the 10 Electrostatic potentials of a Class II mesoionic xanthine molecule. These computer generated electrostatic potential plots illustrate the unique polarizability of Class II mesoionic xanthine showing one part of the molecule being electronegative in nature and the other part being electropositive. This characteristic plays an important role in the exploitation of these extraordinarily unique molecules making them excellent candidates for QIP substrates. Drawn with Spartan'14 software.

14.13 Conclusion

A viable organic molecule, a Class II mesoionic xanthine, has been introduced as a potential 10-qubit register substrate to prototype scalable quantum computing. This xanthine was chosen for prototyping bulk universal quantum computing because it remains stable at room temperature for a hundred ears, the 10-qubit states separate evenly under

ultraviolet light and will readily anneal to a variety of substrates. We have shown that the ground state of this xanthine molecule exists in a superposition of ten unique wavefunctions. These unique wavefunctions can form the basis of 10-qubit registers for the format of relativistic quantum computation. Additionally, a formalism was devised whereby these registers may be efficiently initialized, subsequently read into and transformed via standard unitary algorithms. We propose that polar solutions of the mesoionic xanthines, small crystalline quantum dots or a variety of doped quantum Hall effect substrates may be suitable for I/O techniques. At the time of writing the most suitable of these configurations is still under study. Furthermore, these solutions or quantum dots may be rf-laser pulsed at a certain hierarchical set of frequencies to produce a cumulative resonant interaction within the xanthines to exploit new unified field mechanical degrees of freedom resulting from new higher dimensional (HD) dual commutation anti-commutation rules developed utilizing a complex quaternionic Clifford algebra [24]. Relaxation of the numerous excited states via this new set of HD commutation rules are putatively a vehicle to ontologically overcome the decoherence problem associated with QC applications [25–27]; thus overcoming the penultimate obstacle for implementing bulk quantum computing.

The basis for the relativistic r-qubit in contrast to the current qubit represented on a Bloch sphere is 4-dimensional giving the r-qubit representation additional degrees of freedom required for surmounting the uncertainty principle in conjunction with Unified Field Mechanics. This extended basis is addressed in other chapters along with the key supposition that an additional M-Theoretic space-antispace [28] Calabi-Yau mirror symmetric duality cast in a complex 8-space [29] further dramatically extends the relativistic basis for an r-qubit. Although a major UQC obstacle is overcome by surmounting the uncertainty principle making true realization immanent; it has become apparent that there is more to the story. The extended r-qubit basis suggests that ‘Reality’ itself must be manipulated for implementing bulk UQC. Modeling makes it apparent that existing QC logic gates and algorithms will require profound extension and reconfiguration to higher dimensional unified field mechanical form.

Acknowledgement

Immeasurable thanks to Professor Salvatore Giandinoto for incalculable hours of work on this chapter and earlier derivations over the last decade.

References

- [1] Mbagwu, G.O., Bass, R.G. & Glennon, R.A. (1985) *J. Heterocyclic Chem.*, 22, 465.
- [2] Mbagwu, G.O., Bass, R.G. & Glennon, R.A. (1983) *Org. Magn. Reson.*, 21, 527.
- [3] Rogers, M.E., Glennon, R.A., Bass, R.G., Mbagwu, G.O., Smith, J.D., Boots, M.R., Nanavati, N., Maconaughey, J.E., Aub, D. & Thomas, S. (1981) *J. Med Chem.*, 24, 1284.
- [4] Mbagwu, G.O., Diss. Abs. (1982) Int., B42 4428.
- [5] Mbagwu, G.O., Bass, R. G. & Glennon, R.A. (1980) *Virginia J. Sci.* 31, 113.
- [6] Mbagwu, G.O., Bullock, B., and H.O., Greer (1988) *J. Heterocyclic Chem.*, 22, 475.
- [7] Mbagwu, G.O. & Garland, R. (1988) *J. Heterocyclic Chem.*, 22, 571.
- [8] Giandinoto, S., Mbagwu, G.O., Robinson, T.A., Ferguson, C. & Nunez, J. (1996) *J. Heterocyclic Chem.*, 33, 1839.
- [9] Coburn, R.A. (1971) *J. Heterocyclic Chem.*, 8, 881.
- [10] Coburn, R.A., Carapellotti, R.A. & Glennon, R.A. (1973) *J. Heterocyclic Chem.*, 10, 479.
- [11] Nielsen, M.A. & Chuang, I.L. (2005) *Quantum Computation and Quantum Information*, Cambridge University Press, p. xxiv, Eighth Printing.
- [12] Nielsen, M.A. & Chuang, I.L. (2005) *Quantum Computation and Quantum Information*, Cambridge University Press, pp. 71-5, Eighth Printing.
- [13] Nielsen, M.A. & Chuang, I.L. (2005) *Quantum Computation and Quantum Information*, Cambridge University Press, pp. 76-8, Eighth Printing.
- [14] Levine, I.N., *Quantum Chemistry* (1991) pp. 87-90, Prentice Hall, Englewood Cliffs, New Jersey, Fourth Edition.
- [15] Levine, I.N., *Quantum Chemistry* (1991) p. 259, Prentice Hall, Englewood Cliffs, New Jersey, Fourth Edition.
- [16] Nielsen, M.A. & Chuang, I.L. (2005) *Quantum Computation and Quantum Information*, Cambridge University Press, p. 70, Eighth Printing.
- [17] Nielsen, M.A. & Chuang, I.L. (2005) *Quantum Computation and Quantum Information*, Cambridge University Press, pp. 98-102, Eighth Printing.
- [18] Nielsen, M.A. & Chuang, I.L. (2005) *Quantum Computation and Quantum Information*, Cambridge University Press, pp. 82-4, Eighth Printing.
- [19] Nielsen, M.A. & Chuang, I.L. (2005) *Quantum Computation and Quantum Information*, Cambridge University Press, pp. 174-5, Eighth Printing.
- [20] Ventura, D. & Martinez, T. (1999) *Found. Phys. Lett.*, 12, 547.
- [21] Long, G.L. & Sun, Y. (2007) Efficient scheme for initializing a quantum register with an arbitrary superposed state, arXiv:quant-ph/0104030v1.
- [22] Barenco, A., et. al. (1995) *Phys. Rev. A* 52, 3457; Barenco, A. (1995) *Proc. R. Soc. London*, A449, 679.
- [23] Grover, L.K. (1997) *Phys. Rev. Lett.*, 79, 325.
- [24] Amoroso, R.L., Kauffman, L.H, Rauscher, E.A. & Rowlands, P. (2015) A new set of unified field transformations beyond the Galilean-Lorentz-Poincaré, in R.L. Amoroso et al., *Unified Field Mechanics: Natural Science Beyond the Veil of Spacetime*, Singapore: World Scientific.
- [25] Amoroso, R.L. (2008) Universal quantum computing: anticipatory parameters predicting bulk implementation, in D. Dubois, *Proceedings of CASYS07*, Liege, Belgium.
- [26] Amoroso, R.L. (2009) The bulk implementation of universal scalable quantum computing, in R.L. Amoroso & E.A. Rauscher, *The Holographic Anthropic Multiverse*, Singapore: World Scientific.

- [27] Amoroso, R.L., Kauffman, L.H. & Giandinoto, S. (2013) Universal quantum computing: 3rd gen prototyping utilizing relativistic ‘trivector’ r-qubit modeling surmounting uncertainty, in Amoroso et al. (eds.) *The Physics of Reality: Space, Time, Matter, Cosmos*, Singapore, World Scientific.
- [28] Rowlands, P., Space and antispace (2013) in Amoroso et al. (eds.) *The Physics of Reality: Space, Time, Matter, Cosmos*, Singapore, World Scientific.
- [29] Amoroso, R.L. & Vigier, J-P (2013) Evidencing ‘tight bound states’ in the hydrogen atom: empirical manipulation of large-scale XD in violation of QED, in R.L. Amoroso et al. (eds.) *The Physics of Reality: Space, Time, Matter, Cosmos*, Singapore, World Scientific.

Chapter 15

Universal Quantum Computing Prototype Modeling

Quantum Computing (QC) has remained elusive beyond a few qubits. Feynman's recommended use of a "synchronization backbone" for achieving bulk implementation has generally been abandoned as intractable; a conundrum we believe arises from limitations imposed by the standard models of Quantum Theory (QT) and Cosmology. It is proposed that Feynman's model can be utilized to implement Universal Quantum Computing (UQC) with valid extensions of QT and cosmology. Requisite additional degrees of freedom are introduced by defining a relativistic basis for the qubit (r-qubit) in a higher dimensional (HD) conformal scale-invariant context and defining a new anticipatory based cosmology (cosmology itself cast as a hierarchical form of complex self-organized system) making correspondence to 12D Calabi-Yau mirror symmetries in extended M-Theory. The causal structure of these conditions reveal an inherent new 'action principle' driving self-organization and providing a basis for utilizing Feynman's synchronization backbone principle. Operationally a new set of transformations (beyond the standard Galilean / Lorentz-Poincaré) ontologically surmount the quantum condition, $\Delta x \Delta \rho \cong \hbar$) by an acausal, energyless topological interaction. Utilizing ontological phenomenology of the HD regime requires new commutation rules and corresponding I/O techniques based on a coherent control process of cumulative interaction to manipulate applicable cyclic modes of HD brane manifolds as a spin-exchange continuous-state spacetime resonance hierarchy.

15.1 Introduction – Basics of Quantum Computing (QC)

Whereas a classical Turing machine using a register of binary bits, 1 or 0 can only be in one state at a time; a quantum computer (QC) with a sequence on n qubits that can be in a superposition of all the 2^n qubit states simultaneously. The simplest implementation would be a system of particles with two spin states as in Fig. 15.1.



Fig. 15.1. a) A qubit can be made from a particle with two spin states $|0\rangle$ and $|1\rangle$. b) A four-bit register with $2^4 = 16$ four-bit strings 0000, 0001, ..., 1111 with state $|1000\rangle$ representing the number 8 shown. While a classical bit is only in the single vector state, a qubit wavefunction is in superposition of all sixteen possibilities simultaneously.

It is easy to see the enormous power of quantum computing. A 1,000 qubit quantum register (possibly pin head in size) is described by 2^{1000} complex numbers which is many orders of magnitude more atoms than inside the Hubble radius (see Chap. 12). The main engineering problems for building a bulk quantum computer is decoherence during initialization and data readout, and quantum gates that operate faster than the decoherence time of the system which is often between nanoseconds and seconds. The ontological approach developed in this chapter makes decoherence on readout irrelevant because the methodology bypasses the quantum uncertainty principle (see also Chaps. 7,8 & 12).

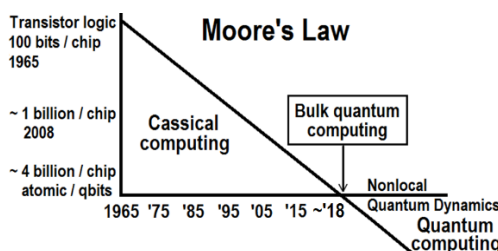


Fig. 15.2. Moore's law states that since the invention of the integrated circuit in 1958, the number of transistors on a chip doubles about every two years, as well as the processing speed, accompanied by a corresponding reciprocal shrinkage in the size of a transistor [1]. Right on schedule the Intel Itanium had 1 billion transistors in 2008. The graph predicts quantum computing should appear in about the year 2020.

The predictions of Moore's law have held true over the whole history of the transistor. Just for fun we use the reciprocal parameter to predict the appearance of bulk universal quantum computing (Fig. 15.2) with the utility of the principles delineated in this chapter; or will there be some sort of Snell Law phase transition from the classical to quantum regimes?

Eventually almost any quantum system could be used for various forms of bulk UQC. Some of the promising candidates currently being considered are: solid state and molecular solution nuclear magnetic resonance, superconducting, trapped ion, quantum dot, topological quasiparticle, optical lattice, cavity-QED, quantum optics, quantum spin, Bose-Einstein condensate, adiabatic, transistor based, molecular magnets, quantum Hall effect, Fullerene electron spin resonance, and diamond spin.

Some QC researchers claim quantum computers already exist; but this seems to be hype as the D-Wave QC is essentially a fancy logic gate. So since our Moore's law graph predicts ~ 2018 , does this mean Moore's Law will finally fail? *Aye mateys*, here's the rub; the transition from classical to quantum computing represents a 'phase change'. Ever stuck a stick in water? The stick bends by a transition phase angle. That angle, called the refraction angle is known for water, but what is it for a transition from local space to the nonlocal HD holographic brane space?

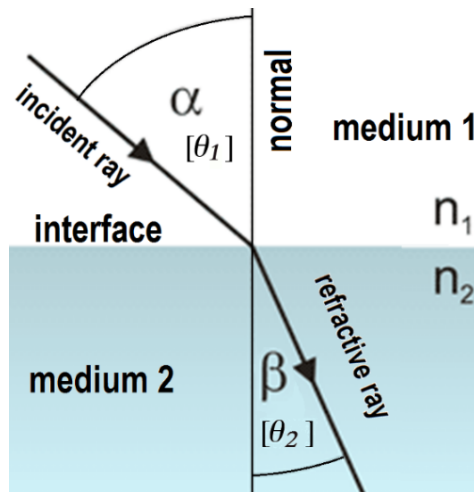


Fig. 15.3. The Snell-Descartes Law, showing refraction of light at the interface between two media of different refractive indices, with $n_2 > n_1$. Since the velocity is lower in the second medium ($v_2 < v_1$), the angle of refraction θ_2 is less than the angle of incidence θ_1 ; so the ray in the higher-index medium is closer to the normal. Note: Rotation of the reflected ray (not shown) is the same as the log spiral or dual quaternions.

We can quixotically use the Snell-Descartes refraction law to prove quantum computing will not be possible. Ah ha, since $V_2 > V_1$ because of nonlocality and the EPR paradox, θ_2 is ‘infinitely greater’ meaning there will never be quantum computers. OK not satisfied? This infinity in Moore’s Law is a similitude of the infinities in the Raleigh-Jeans Law and the infinities of Renormalization in Quantum Field Theory. Just sayin’. We could theorize instead because of the EPR paradox, the speed of ‘information’ is faster in nonlocal space increasing the angle of θ_2 so that instead of 2018 bulk UQC will appear by 2022. From our point of view; we are one experiment away, the UFM protocol surmounting uncertainty. UQC could occur immediately. It could realistically be done by 2018!

15.2 Overview of New Fundamental Parameters

The basis of our approach for the ontological realization of bulk or Universal Quantum Computing (UQC) is introduced conceptually utilizing an axiomatic approach to facilitate delineating the philosophy for the formalism. The theoretical model requires a new UFM cosmology based on an extension of Quantum Theory (QT) or vice versa depending on whether ones’ view is top-down or bottom-up. Both the new cosmology and extension of QT are anticipatory because they take the form of complex self-organized hierarchical systems [2-8]. The extended QT is derived from a combined relativistic extension of Cramer’s Transactional Interpretation [9], based on the Wheeler-Feynman Absorber Theory of Radiation [10], and an HD extension of the de Broglie, Bohm, Vigier Causal Interpretation of QT where $m_\gamma \neq 0$ [11,12]. The cosmology is that of a 12D Holographic Anthropic Multiverse making correspondence to the M-Theory [13] iteration of String Theory [2–5,7,8,14]. Why does UQC require an anticipatory approach cast in new QT and HAM cosmology? Salient reasons discussed are:

1. Causal conditions,
2. New Symmetry relations – Ontological phase commutativity
3. Utilization of Feynman’s suggestion, and
4. Coherent control methods of operation.

Interestingly, the self-organized parameters of the cosmology entail an inherent synchronization backbone, like getting half the UQC for free!

15.3 The Causal Separation of Phenomenology from Ontology

Because of the recent jump from Newtonian Mechanics to Quantum Mechanics most physicists believe we live in a quantum universe. The logical progression of this line of reasoning would suggest we live in a Unitary Universe once a unified field is empirically delineated. This is an erroneous conclusion. A better assumption based on anticipatory properties inherent in 12D UFM cosmology suggests that the universe is a continuous-state interplay of all three modes [2–5]. Because we only observe the Euclidean component of this world view, we assume reality is a complex virtual standing wave with the present a continuously created subspace of HD future-past parameters [2–10]. Our task is to demonstrate an ontological methodology for surmounting the inherent uncertainty conditions of Copenhagen regime phenomenology with a new set of transformations that utilize an ‘energyless topological switching’ to exchange information [15].

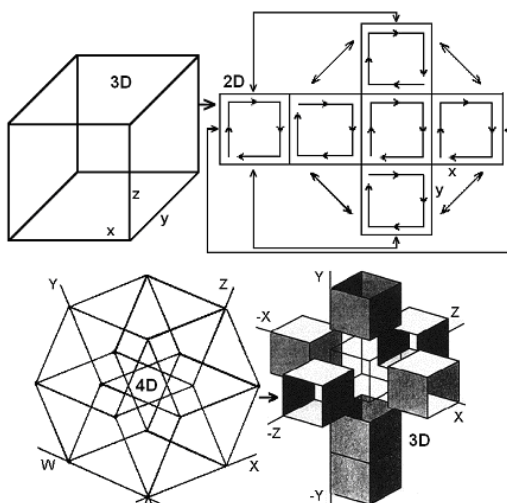


Fig. 15.4. Geometry of space in 3 & 4D. (top) A 3D cube unfolds into the 2D plane. This metaphor aids the visualization of HD space. (bottom) A 4D hypercube unfolds into 8 component 3D cubes as in (b). If a 5D hypercube were unfolded the 8 cubes forming the 3D cross (d) would be 4D hypercubes (tesseracts as in (c)). The translucent cube, called the central cube, represents observed reality, E_3 . This central cube is surrounded by six adjacent cubes. The 8th cube, the satellite cube, is placed arbitrarily on any adjacent cube. Carried to 12D the central cube and 12D satellite causally separate as a ‘mirror image of a mirror image’. This is why a commutative-anticommutative cycle is required.

Reality as locally observed, (Fig. 15.4 top) is Euclidean, E_3 or 3(4)D Minkowskian, \hat{M}_4 depending on whether time is introduced in the Newtonian or Einstein sense. In Fig. (15.4b) the 3D cube is shown unfolded into a cross in the 2D plane with arbitrary loss of the z direction. Fig. (15.4 bottom) shows a 4D tesseract that includes 4D designated as w . As in Fig. 15.4 top, the 4D tesseract is unfolded into a 3D cross as shown in Fig. 15.4d. Loss of the w direction makes it easier for the human mind to visualize a hypercube. For simplicity we use the 3(4)D cross to illustrate how ‘12’ is the minimum number of dimensions required to describe *eternity* (defined as causal separation from E_3) and conceptually reveal how to overcome the limitations of the quantum principle inherent in Copenhagen uncertainty; i.e. since the phenomenology of Copenhagen action produces uncertainty by definition - choose instead an ontological process that does not discretize the z field commutator as in Eq. (15.2).

Assume the translucent *central* cube (Fig. 15.4) represents local E_3 reality, a subspace surrounded by six *adjacent* HD cubes as components of the 4D tesseract in Fig. (15.4c). The 8th cube, the *satellite*, is arbitrarily attached to the y direction adjacent cube. Let the central cube hold a standard quantum state. A primary UFM assumption is that all eight 4D cubes (4096 in 12D) contain the information of the central cube’s state by superposition (an inherent property of the conformal invariance [16,17] of HD Relativistic Quantum Field Theory (RQFT)). This is a fundamental symmetry condition of the Superspace of UFM cosmology [2-5].

The satellite cube is *periodically causally free* of the E_3/M_4 central cube because of the nature of the relativistic transformation. This continuous-state topological transformation of the standing-wave modes is the inherent synchronization backbone in the backcloth of spacetime itself; as if half of the QC is obtained for free. In this context QC operations are ontological (if putatively performed in a specific manner described by the new UFM transform) without phenomenological collapse of the wave function with respect to quantum information contained in the central E_3 cube. This metaphor performed rigorously in a 12D context is able to surmount the uncertainty relation! Follow us in assuming \hbar is not the basement of reality. Recall passing along a cemetery, orchard or

auditorium where ones' gaze is sometimes blocked and sometimes open to infinity. It is this fundamental cycle hidden behind the 'veil of uncertainty that allows surmounting uncertainty opening the door to UFM.

15.4 Review of Angular Momentum and Pauli-Dirac Spin Matrices

The Schrödinger equation is invariant under Galilean, but not the Lorentz transformation and therefore incompatible with the principle of relativity and all phenomena relating to the interaction of light and matter leading to the concept of 2nd quantization [18]. Our 12D extension of QT goes beyond the usual Klein-Gordon and Dirac models of RQFT. This is an issue of the observer's cosmology with an inherent complementarity between 1st and 2nd quantization much like wave-particle duality. This is a continuous-state property [2–5] readily described by methods similar to that attributed to Dirac spherical rotation of the electron [2].

Separation of the Schrödinger equation into spherical coordinates reveals the Hamiltonian

$$H = \frac{1}{2m} \left(p_r^2 + \frac{L^2}{r^2} \right) + V(r), \quad (15.1)$$

where p_r is the radial momentum ($m\dot{r}$) and L the angular momentum vector. As well known, the three components of angular momentum, derived from each other by cyclic permutation, are $L_z = xp_y - yp_x$, $L_x = yp_z - zp_y$, $L_y = zp_x - xp_z$, $L = r \times \rho$ where the total angular momentum $L^2 = L_x^2 + L_y^2 + L_z^2$ has commutation rules $L \times L = i\hbar L$ [18–22]. SO(3) rotation generators l_1, l_2 and l_3 satisfy $l_1 l_2 - l_2 l_1 = l_3$, $l_2 l_3 - l_3 l_2 = l_1$, $l_3 l_1 - l_1 l_3 = l_2$; are related quantum mechanically to angular momentum components L_1, L_2, L_3 with $L_x = i\hbar l_1, L_y = i\hbar l_2, L_z = i\hbar l_3$ about Cartesian axes giving the usual commutation rules $L_x L_y - L_y L_x = i\hbar L_z$, $L_y L_z - L_z L_y = i\hbar L_x$, $L_z L_x - L_x L_z = i\hbar L_y$.

Angular momentum refers to intrinsic spin about a massive particles center of mass and its magnetic moment by SO(3) Lie algebra which is non-Abelian so the elements do not all commute. The Pauli matrices satisfy these commutation rules when acting on two component spinor wavefunctions $\{\psi_0(x), \psi_1(x)\} \equiv \Psi_A$; but by the uncertainty relation, $\Delta x \Delta p \cong \hbar$ only one set of these operators may commute at a time. Non-relativistic Fermi spin $1/2\hbar$ particles with spin angular momentum operator $S = 1/2\hbar\sigma$ can be expressed as the three anticommuting Pauli 2×2 spin matrices Eq. (15.2) satisfying $\sigma_x\sigma_y = -\sigma_y\sigma_x = i\sigma_z$ as derived empirically from the Stern-Gerlach experiments [18,20].

$$\begin{aligned} L_x &= \frac{\hbar}{2}\sigma_x = \begin{bmatrix} 0 & 1 \\ 1 & 0 \end{bmatrix}, & L_y &= \frac{\hbar}{2}\sigma_y = \begin{bmatrix} 0 & -i \\ i & 0 \end{bmatrix}, \\ L_z &= \frac{\hbar}{2}\sigma_z = \begin{bmatrix} 1 & 0 \\ 0 & -1 \end{bmatrix}. \end{aligned} \quad (15.2)$$

Here we demonstrate a complex HD geometric-micromagnetic [15] method where all commutator relations can periodically simultaneously commute like the Casimir-like ‘total spin’ operator, $\mathbf{J}^2 = L_x^2 + L_y^2 + L_z^2$ commutes with all three components of L in 3D [23-25]. This is possible in HD because E^3 (Fig. 15.4) in UFM cosmology has the same properties as the Dirac spherical rotation of the electron [2,5]. The topology of these boundary conditions is described by HD expansion of the UFM field equation, $F_n = \mathbf{N} / \rho$ [26]; F_N is the cyclic noetic force, \mathbf{N} the continuous-state Lagrangian and ρ the complex rotational coherence length [27].

Relativistic spin $1/2\hbar$ particles are described by Dirac’s formalism for the wave equation which has been expressed by several notations $E\psi + c(\alpha \cdot p)\psi + mc^2\beta\psi = 0$; or $i\hbar\frac{\partial\psi}{\partial t} - i\hbar c\alpha \cdot \text{grad}\psi + mc^2\beta\psi = 0$ [28] which when expressed by Dirac’s σ matrices can be expanded into the following 4×4 matrices:

$$\beta = \begin{bmatrix} 1 & 0 & 0 & 0 \\ 0 & 1 & 0 & 0 \\ 0 & 0 & -1 & 0 \\ 0 & 0 & 0 & -1 \end{bmatrix} \quad \alpha_x = \begin{bmatrix} 0 & \sigma_x \\ \sigma_x & 0 \end{bmatrix} = \begin{bmatrix} 0 & 0 & 0 & 1 \\ 0 & 0 & 1 & 0 \\ 0 & 1 & 0 & 0 \\ 1 & 0 & 0 & 0 \end{bmatrix} \quad (15.3a)$$

$$\alpha_y = \begin{bmatrix} 0 & 0 & 0 & -i \\ 0 & 0 & i & 0 \\ 0 & -i & 0 & 0 \\ i & 0 & 0 & 0 \end{bmatrix} \quad \alpha_z = \begin{bmatrix} 0 & 0 & 1 & 0 \\ 0 & 0 & 0 & -1 \\ 1 & 0 & 0 & 0 \\ 0 & -1 & 0 & 0 \end{bmatrix} \quad (15.3b)$$

which are Hermitian and readily seen to contain the 2×2 Pauli matrices (15.2) as in the center of matrix α_x for example [29]. An interesting point developed below is that in cases where $m = 0$ (or for high E where any massive particle behaves like $m = 0$) only three anticommuting matrices instead of four are required. This means the Pauli matrices will suffice and the spinor needs only 2 components which relates to the Wehl or chiral representation [30].

In another popular notation the Dirac equation is represented as

$$E + mc^2 + \frac{ke^2}{r} = \phi c + imc^2 = \vec{\phi} c + imc^2 \quad (15.4)$$

where $E \rightarrow -\frac{\hbar}{i} \frac{\partial}{\partial t}$; $\vec{\phi} \rightarrow \frac{\hbar}{i} \vec{\nabla}$ which has the general solution

$$\frac{\hbar c}{i} \left(\gamma_1 \frac{\partial}{\partial x} + \gamma_2 \frac{\partial}{\partial y} + \gamma_3 \frac{\partial}{\partial z} + \gamma_0 \frac{\partial}{\partialict} \right) \psi - mc^2 \psi = 0 \quad \text{which is easily}$$

shorthanded to $\left(\gamma^\mu \partial_\mu + i \frac{mc^2}{tc} \right) \psi = 0$. There are two non-relativistic limits; the

first $(E + mc^2 + ke^2 / r)^2 = (\phi c)^2 + (mc^2)^2$, is the well-known Klein-Gordon equation, and the second, $E + mc^2 + ke^2 / r = \sqrt{(\phi c)^2 + (mc^2)^2} \cong mc^2 \left[1 + \frac{1}{2} \left(\frac{\phi c}{mc^2} \right)^2 + \dots \right] \cong mc^2 + \frac{\phi^2}{2m} + \dots$ thus

becoming $E = \frac{\phi^2}{2m} - \frac{ke^2}{r}$, as a form of the Schrödinger equation. In this notation the matrices in (15.3) $\alpha_x, \alpha_y, \alpha_z, \beta_{ict}$ correspond to $\gamma_1, \gamma_2, \gamma_3, \gamma_0$,

respectively and ψ to the matrix $\psi = \begin{pmatrix} \psi_{e\uparrow} \\ \psi_{e\downarrow} \\ \psi_{\phi\uparrow} \\ \psi_{\phi\downarrow} \end{pmatrix}$.

15.5 Noumenal Reality Versus Phenomenology of Quantum Theory

Feynman has shown that reality can be considered incompatible with QT [31]. If we let A, B, C represent the three observables a, b, c , their values $P(a, b), P(b, c), P(c, a)$, their transition probabilities $a \rightarrow b, b \rightarrow c, c \rightarrow a$ and $\phi(a, b), \phi(b, c), \phi(c, a)$ the corresponding quantum mechanical amplitudes; the transition probabilities $P(x, y)$ ($x, y = a, b, c$) are measurable empirically by the classical rules of probability leading to

$$P(a, c) = \sum_b P(a, b) \cdot P(b, c) \quad (15.5)$$

with the summation taken over all values of observable B [31,32].

Measuring $P(x, y)$ in a case where the relative frequency of x is an ensemble prepared so that y is realized with certainty, the identity equation (15.6) can be shown to be wrong because the difference (called the interference term) between the right and left sides of (15.6) is found to be some orders of magnitude larger than the experimental error. If one calculates the interference terms according to the rules of QT from the empirically correct formula

$$\phi(a, c) = \sum_b \phi(a, b) \phi(b, c) \quad (15.6)$$

and utilizing the connection between probability and amplitude

$$|\phi(x, y)|^2 = P(x, y); \quad x, y = a, b, c \quad [31]. \quad (15.7)$$

This contradiction between the classical probability identity (15.5) and the Copenhagen interpretation (15.6) have been elucidated by Feynman:

...Looking at probabilities from a frequency point of view (15.5) simply results from the statement that in each experiment giving a and c , B had some value. The only way (15.6) could be wrong is the statement, “ B had some value”, must sometimes be meaningless. Noting that (15.7) replaces (15.6) only under the circumstance that we make no attempt to measure B , we are led to say that the statement, “ B has some value”, may be meaningless whenever we make no attempt to measure B ” [31].

Feynman’s statement delineates Schrödinger’s cat paradox. He states regarding the interference term that if we say “ B had some value” when we make no attempt to measure it is true we have a contradiction with experiment because there is a contradiction between objective reality and the validity of QT in the orthodox Copenhagen interpretation. For our purposes here we resolve this paradox by abandoning the notion of a local absolute objective reality by stating that the observer’s 3(4)D reality is virtual and that the 11(12)D Holographic Anthropic UFM Multiverse anticipatory reality is physically more complete. This is a key foundational element of our UQC model because we postulate firstly that the very existence of the observer discretizes this HD reality and secondly that the application of the arbitrary z -field discretizes L such that it does not universally commute. This is of course experimentally demonstrated as the standard interpretation of QT and is the basis for its formalism. This scenario avoided in the 12D anticipatory model of UQC is not possible by “law” if Copenhagen is applied. We demonstrate a model with zero commutator for all values of L where state evolution can be manipulated ontologically (from a position of causal separation) rather than the standard phenomenology of wave function collapse producing the uncertainty relation, $\delta x \delta p_x \geq 1/2\hbar$.

15.6 Justification for the Incursive UFM Model

If M-theory subsumes the standard model of particle physics and cosmology, strings will represent the primary physical element; and \hbar will no longer be considered a fundamental constant. First let’s consider the continuous-state compactification of UFM superspace. The 12th D (hyperplane of Fig. 15.17) is an absolute space signifying the geometric limit of our reality from which a 9 to 11D manifold drops out (site of

unified field) as the 1st continuous-state compactification of the harmonic superspace delineated as

$$x_N = x_N + 2\pi R \quad (15.8)$$

where $N \rightarrow$ from 1 to 8D and R the periodic radius of space N goes from $\hbar + \Delta T_s$ to ∞ . This condition exists because in this case, unit strings are not related to $\hbar = 1$, but to string tension, denoted simplistically as, $T_s = 1/\pi$ [33,34]. Fields on this periodic space therefore satisfy

$$\phi(x) = \phi(x + 2\pi r) \quad (15.9)$$

which means the field ϕ can be power expanded periodically with eigenfunctions

$$\phi(x) = \sum_k \phi_k e^{ipx} \quad (15.10)$$

where $p = k / R$ and k is an arbitrary integer so that the momentum conjugate, x is quantized in integers, a feature of all compactifications. Note for our purposes that compactification of a dimension quantizes the momentum corresponding to the compactified coordinate [13].

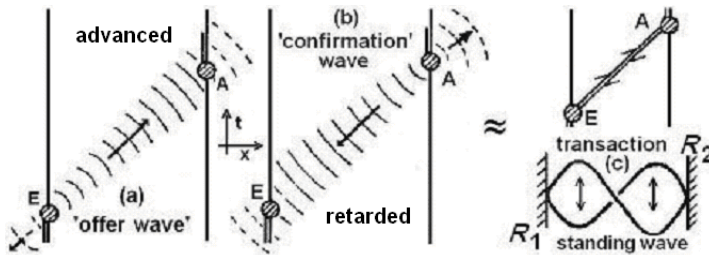


Fig. 15.5. Illustration of an event or transaction in Cramer's future-past standing-wave present interpretation of QT.

This has immediate repercussions for the anticipatory UQC model. For Copenhagen, only the z component of the angular momentum vector of a particle on a Riemann sphere is considered well defined.

The Dirac equation, usually formulated in 4D, must be recast in the 11(12)D superspace [35] to include additional causal action in the symmetry of advanced-retarded potentials and heterotic splitting of the 8D resonant tower (Figs. (15.5,15.6,15.7), where the wave function and all off diagonal elements are physically real and therefore accessible as in Cramer's hyperspherical standing-wave future-past Transactional Interpretation [9]. A transaction (Figs. 15.5,6) is represented as a form of standing wave both of which support the energy dependent nature [2] of the periodic 12D continuous-state Superspace. The separation of these parameters in terms of de Broglie's fusion model [36,37] is used for ontological manipulation of the harmonic tier (Figs. 15.5,6,7).

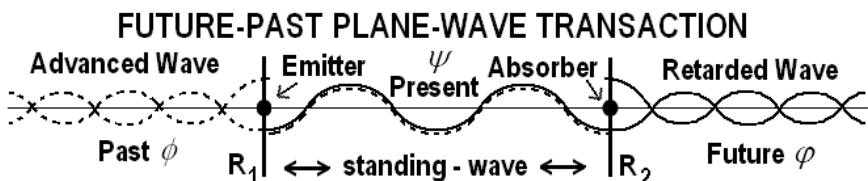


Fig. 15.6. Symbolic structure of a transaction (present state or event) where the present moment is a standing-wave of future-past retarded-advanced elements.

It is suggested that continuous compactification of UFM superspace in this framework produces a new singularity model (a cyclic wave-particle) which is the observed E_3 reality itself; and the 8-form factorizes into two 4-forms $N_8 \rightarrow X_4 \wedge X_4$, i.e. the advanced-retarded components of an HD extension of a Cramer transaction [9]. Because M_4 is Einstein's energy-dependent spacetime metric, \hat{M}_4 where strings are susceptible to *em*-charges, (p, q) ; the tension of these heterotic strings becomes

$$T_{p,q} = pe^{-\phi} + qe^{\phi} \quad (15.11)$$

which can be used to demonstrate that string tension, T vanishes at the singularity E_3 (Fig. 15.15) [13,38]. We define this new model of the singularity as a Least Cosmological Unit (LCU) tessellating spacetime in

a semi-quantum limit; with a superspace projection manifold in the HD Calabi-Yau brane world. The LCU is like a complex exciplex.

15.7 Essential Properties of Complex 12-Space

The UQC model relies on a new 12D Absolute Space (AS) (ultimate arena of reality) from which properties of a UFM Wheeler geon [39] or ‘ocean of light’ (unified field) emerge. The UFM AS is an atemporal, highly ordered and symmetric harmonic superspace from which all other space relative to an Earth observer is a composite subspace. The geon domain (9 to 16D) is the first compactification regime; and because of coherence of the unified field, railroad tracks would not recede but remain parallel.

A set of null lines (complex arrow of time), a loci of eternal points, remains hidden from local observed reality as an eternal present. This is part of the complex, $\pm C_4$ Wheeler-Feynman-Cramer duality of the future-past standing-wave comprising the continuous state present: ‘a relativistic spin-exchange dimensional reduction compactification process’ which represents a new set of transformations beyond Galilean and Lorentz/Poincaré to describe the inherent dynamics of this UFM domain and create the arrow of time [40]. This condition results in our $E^3\text{-}M^4$ domain being a subspace of eternity; and the essential process for producing the ‘synchronization backbone’ inherent in the backcloth of UFM cosmology [3–5]. ‘Eternity’ may not be a popular word choice; one could use null, atemporal or timeless instead. The instantaneity of nonlocality (EPR) suggests such.

As in special relativity where c remains constant and independent of the velocity of the source; the 12D AS remains static and absolute whether matter is stationery or in relativistic motion locally. In this context there is a duality in terms of conservation laws, annihilation/creation, advanced/retarded potentials or between space and energy including an asymmetry between the future-past. The new set of transformations makes correspondence with M-Theory and is conceptually considered an HD extension of Dirac Spherical Rotation of the electron [5,41–43].

Thus issues of the historical controversy between relational and AS are pushed to the new 12D domain. Within the Classical limit the former 3D Euclidean AS remains relative to the eternal present [44] of the subjective observer. Einstein demonstrated that the application of special

relativity to a 3(4)D Minkowski/Riemann manifold makes space relational. The new relational space extends Einstein's view from four to eleven dimensions. In the 12D UFM superspace, S_N the 11D unified field (and the local 3(4)D $B^{(3)}$ component of the *em*-field [45]) translates longitudinally, but the space (as in water waves) remains fixed because the wave bumps against the close-packed spheres or least units [8,46] (like the water molecules) allowing only transverse displacement while the wave is locally present. This wave cyclically undergoes $m_\gamma = 0$ and $m_\gamma \neq 0$ plus em- $B^{(3)}$ modes for certain polarizations.

Current thinking on the topology of space takes three general forms:

- 1) The most commonly accepted 3(4)D Minkowski/Riemann spacetime manifold; and two putative HD superspace additions,
- 2) Mirror symmetric Calabi-Yau space preferred by M-Theory and
- 3) Dodecahedral $\text{AdS}^5\text{-dS}^5$ wrap-around space.

Nature of the true vacuum remains an open question. The 3D absolute space of Newton became the 3(4)D relational spacetime of Einstein. The 12th D of UFM cosmology represents a new form of absolute space, a periodic superspace where the eternal twelfth dimension has a Wheeler Geon-like [39] ocean of UFM noeon 'light' (the unified field) as its $9 \rightleftharpoons 11$ D subspace. The relational 3(4)D Minkowski/Riemann spacetime manifold is a continuous-state standing wave subspace of the 12D UFM superspace; it acts as a topological cover of an eternal present [44] which is not observed and continuously decays into spacetime.

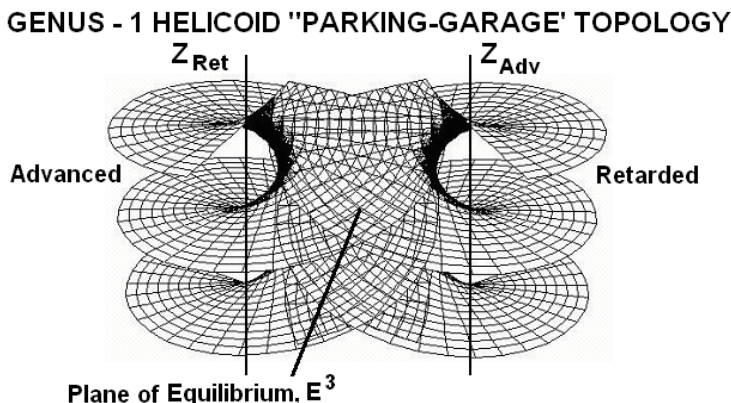


Fig. 15.7. The Helicoid, a minimal embedded surface [47], is swept out by a line rotating about and moving down the z axis. Here a double Genus-1 Helicoid is joined into a "parking garage" ramp structure representing the future-past hierarchical topology of UFM space. An ordinary 2D plane can be twisted into a helicoid. Also see [16].

'Space quantization' or the quantization of orientation of atomic systems observed empirically primarily by Stern-Gerlach [18] and secondarily in other phenomena like the Zeeman Effect in an inhomogeneous magnetic field led to the basis for representing spin $\frac{1}{2}$ fermions as a uniform Dirac spherical rotation through a 720° cycle [5,41-43] and the commutation relation for angular momentum in quantum theory. We explore extending these properties to 12D, 12D as required for UQC ontological operation.

If the UFM space water-wave conception is correct, the continuous-state compactification process contains a tower of spin state Lie groups from spin 0 to spin 4. Spin 4 represents the unified field and makes cyclic correspondence with spin 0 where spacetime lattice Riemann sphere Ising lattice spin flips [15,38] create dimensional jumps through the helicoids topology (Fig. 15.7). Spin 0, 1/2, 1, & 2 remain in standard form. Spin three is suggested to relate to the orthogonal properties of atomic energy levels and space quantization. Therefore, the spin tower hierarchy precesses through 0, 720° , 360° , 180° , 90° & 0 (∞) as powers of i , as conceptually illustrated in Fig. 15.8.

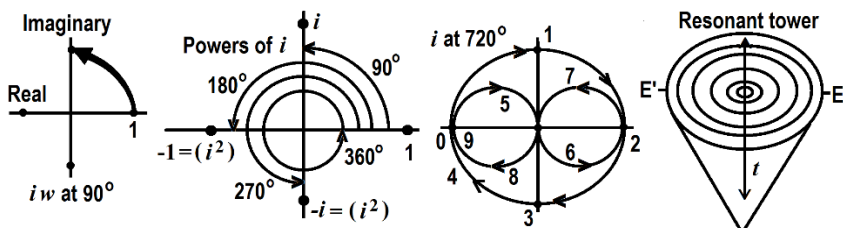


Fig. 15.8. a) Complex dimension at 90° from the real axis. b) Powers of i from 90° to 360° . c) Power of i at 720° . d) Resonant hierarchy comprised of powers of i in conjunction with the topology of the Genus-1 helicoid 'Parking-Garage' of the string vacuum with either Ising model, logarithmic spiral or cyclotron resonance hierarchy parameters for applying ladder operators of the resonant modes required to ontologically operate the UQC model.

An instant t , for position $r \equiv (x, y, z)$ or for the light cone (Fig. 15.9) $r = xdt$, defines a point or event $d = \sqrt{x^2 + y^2 + z^2}$ in ordinary spacetime coordinates, a pseudo-Euclidian metric tensor [48] representing the sixteen points of a 4-sphere (Fig. 15.4c)

$$G_{\mu\nu} = \begin{pmatrix} 1 & 0 & 0 & 0 \\ 0 & -1 & 0 & 0 \\ 0 & 0 & -1 & 0 \\ 0 & 0 & 0 & -1 \end{pmatrix}. \quad (15.12)$$

In summarizing the observer's relationship to the *Cosmological Principle* (that the universe is homogeneous and isotropic on average in the large-scale) [49,50] events are idealized instants in spacetime defined by arbitrary time and position coordinates t, x, y, z , written collectively as x^μ where μ runs from 0 to 3. For which the standard line element is

$$ds^2 = \sum_{\mu\nu} G_{\mu\nu} dx^\mu dx^\nu = G_{\mu\nu} dx^\mu dx^\nu, \quad (15.13)$$

where the metric tensor

$$G_{\mu\nu}(x) = G_{\mu\nu}(x) \quad (15.14)$$

is thus symmetric [48]. In local Minkowski form all the first derivatives of g_{ij} vanish at the event and equation (15.13) takes the form

$$ds^2 = c dt^2 - dx^2 - dy^2 - dz^2. \quad (15.15)$$

The Cosmological Principle generally suggests that the clocks of all observers are synchronized throughout all space because of the inherent homogeneity and isotropy of the universe. Because of this synchronization of clocks for the same world time t , for comoving observers the line element in (15.15) becomes

$$ds^2 = dt^2 + G_{\alpha\beta} dx^\alpha dx^\beta = dt^2 - dl^2, \quad (15.16)$$

where dl^2 represents special separation of events at the same world time, t . This spatial component of the event dl^2 can be represented as an Einstein 3-sphere

$$dl^2 = dx^2 + dy^2 + dz^2 + dw^2 \quad (15.17)$$

which is represented by the set of points (x, y, z, w) at a fixed distance R from the origin:

$$R^2 = x^2 + y^2 + z^2 + w^2 \quad (15.18)$$

where

$$w^2 = R^2 - r^2 \text{ and } r^2 = x^2 + y^2 + z^2 \quad (15.19)$$

so finally we may write the line element of the Einstein 3-sphere from equation (15.17) as

$$dl^2 = dx^2 + dy^2 + dz^2 + \frac{r^2 dr^2}{R^2 - r^2} [51]. \quad (15.20)$$

By imbedding Einstein's model of the 3-sphere in a flat HD space, specifically as a subspace of a new complex 12D superspace, [2-5,7] new theoretical interpretations of standard cosmological principles are feasible.

Although the Newton and Coulomb potentials have similar forms the two theories have developed separately. For our purposes, following the Sakharov-Puthoff conjecture [52], that gravity is a product of fluctuation of the zero-point field; we unify them with the Amoroso-Vigier methods [53,54] where both fields are represented by 4-vector field densities A_μ . Both phenomena are considered different types of motion within the same real physical field in flat spacetime as two different vacuum types of collective perturbations carried by a single vacuum field (unified). See (Fig. 15.12b).

Maxwell's equations traditionally describe only transverse elements that 'cut-off' at the vacuum. Here for Multiverse cosmology extended electromagnetic theory is utilized where the Einstein-de Broglie relation, $E = \hbar v = mc^2$ allows additional degrees of freedom such as longitudinal components $B^{(3)}$ and polarized vacuum conditions where $m_\gamma \neq 0$ suggests

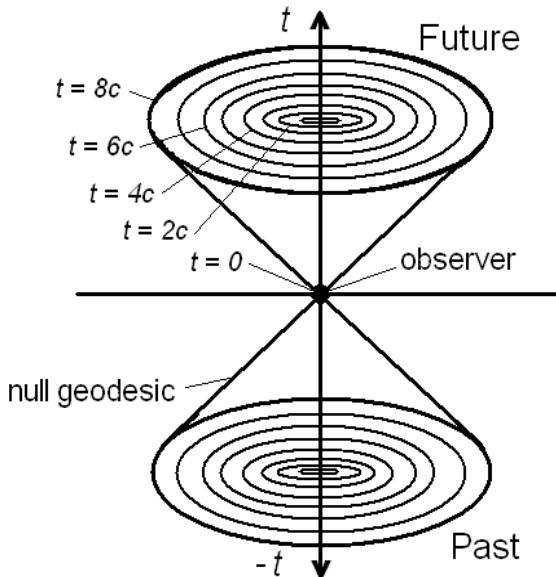


Fig. 15.9. Minkowski light cone with parameters for hierarchical conditions of Figs. 15.7, 15.8.

that the photon is piloted. These conditions suggest the need for both the standard em -field and extended $\mu\nu$ field coordinates; an understanding of which will be seen to be required for the ontological UQC operations.

In our original integration of G and em we chose to fix the $\mu\nu$ field coordinates [53,54]. Here we go a step further. Dirac himself suggested by the rule of coordinate law that the pilot wave and the photon decouples [55]. The two sets of coordinates em or $\mu\nu$ would normally be considered independent of each other. We integrate them in the topology of the Dirac polarized sea and alternate the fixing and decoupling of $\mu\nu$ and em coordinates as an inherent ‘leapfrogging’ (Fig. 15.10a) of the nonlocal-supralocal continuous-state standing-wave present [2-5,7]. Like wave-particle duality of matter, Multiverse cosmology $em - \mu\nu$ duality extends to spacetime itself in that the unified field harmonically discretizes into spatial boundary conditions of an Ising model Euclidian point (Fig. 15.10b). Two types of computer animation in terms of ‘figure’ and ‘ground’ illustrate this. First, the animated figure crosses (arrow of time) the stationery background from left to right, disappears off the screen and reappears cyclically with an inherent frame rate. Each L-R cycle can be considered as one discrete spacetime least-unit quantum to the

external observer. However as well known, our so-called quantum is actually comprised of a number of discrete frames that appear continuous to the external observer because of the refresh rate. This could be considered as the properties of quantum phase space and that material Fermi surfaces appear smooth because of the relativistic velocity of the surface electrons.

In the second case, the animated figure remains permanently fixed in the center of the screen and the background moves continuously from left to right (Arrow of time again) across the screen. For the sake of the metaphor one can say this latter case is introspective relative to the observer and the first case is objective (quantum) or external to an observer.

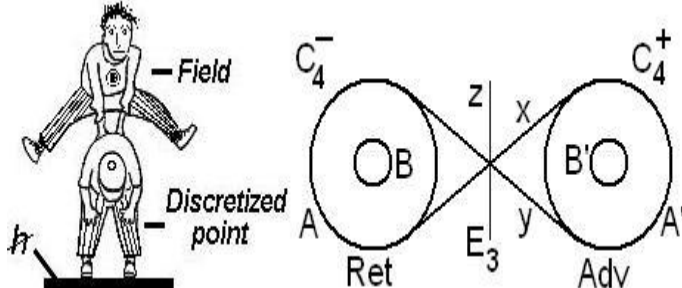
Neither of these two views offer a complete description of reality; as noted above, a third case of simultaneity is required. The apparent separateness of the two views; i.e. ‘we live in a quantum universe’ is the root of the problem because as proposed here we live in a continuous-state universe that is classical, quantum and unitary depending on perspective. The challenge here is to show that by adopting this view a model of Universal Quantum Computing with an inherent spacetime synchronization backbone can be delineated.

UFM Space “leapfrogs” from holographic unitarity to discretized reality. This simplifies the boundary conditions and variables needed for UQC operations. The 12D Multiverse surface is considered a new form of Absolute Space (AS) and our observed Euclidian E_3 is a pseudo-AS or subspace of this regime. Because of the leapfrogging which we suppose is a fancy form of Witten’s Ising flip [38] of the covariant string vertex (Fig. 15.11b). The E_3 pseudo-AS is a periodic discretization or ‘frozen moment’ of one 4D set of the 12D parameters (when time is included). This gives the least unit of the superspace the geometry of a torus; or in our Wheeler-Feynman future-past model considered as two 4D advanced-retarded tori. This suggests the boundary conditions A:B; A’:B’ (Fig. 15.8b) are HD boundary conditions of a harmonic oscillator allowing coherent control of the UQC to be operated with 4D parameters. As well known the usual form of Maxwell’s equations in vacuum with $m_\gamma \neq 0$ and $B^{(3)} = 0$ has infinite families of boundary free exact solutions with the Lorentz gauge vector potential $A_\mu = 0$; but in the UFM case with $m_\gamma \neq 0$ where Maxwell’s equations do not cut off at the vacuum, there is only one family and one set of boundary conditions, a model justified empirically by existence of the Casimir and Zeeman

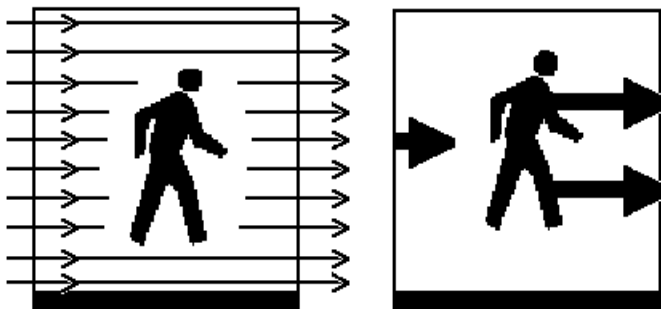
effects [18,23-25]. *Em*-theory implies the effects of the *em*-vector 4-potential A_μ on the phases, S of quantum mechanical waves

$$\Delta S = \frac{q}{h} \int \phi dt - \frac{q}{hc} \int \vec{A} \cdot d\vec{S}. \quad (15.21)$$

For the continuous-state integration the mass term, m_γ is introduced into Maxwell's equations. One may also describe gravity with a 4-vector density A_μ^g so that the Newton and Coulomb potentials take the same form but with different coupling constants suggesting both are different aspects of the same fundamental (unified) field with $A_\mu A_\mu \rightarrow 0$ where A_μ denotes the total 4-potential in a covariant polarized Dirac vacuum.



2 Types of Screen Animation



Background Moves, Figure
Walks Fixed in Place

Figure Moves,
Background Fixed

Fig. 15.10. a) Leapfrog metaphor of virtual reality. b) This metaphor adds Ising properties to the future-past transaction. The central Euclidian point, E_3 , is created and annihilated as a standing wave harmonic oscillator within the boundaries (denoted by $A:B$; $A':B'$) of two complex 4D tori. c) The leapfrog duality of the $em - \mu\nu$ metric also includes two types of spin exchange coupling-decoupling background-foreground interactions.

From the *em*-vector potential $A^\mu(x)$ where $F_{\nu\mu} = A_{\nu,\mu} - A_{\mu,\nu^*}$ the components of E and B form 2nd rank dual antisymmetric spacetime field strength tensors $F^{\mu\nu}$ (Adv), ${}^*F^{\mu\nu}$ (Ret) as $F^{\mu\nu} = \partial^\mu A^\nu - \partial^\nu A^\mu$ and ${}^*F^{\mu\nu} = \frac{1}{2}\epsilon \exp \mu\nu\rho\sigma F_{\rho\sigma}$ respectively as matrices [56, 57]

$$F^{\mu\nu} \equiv \begin{pmatrix} 0 & -E^x & -E^y & -E^z \\ E^x & 0 & -B^z & B^y \\ E^y & B^z & 0 & -B^x \\ E^z & -B^y & B^x & 0 \end{pmatrix}, \quad (15.22)$$

$${}^*F^{\mu\nu} \equiv \begin{pmatrix} 0 & -B^x & -B^y & -B^z \\ B^x & 0 & E^z & -E^y \\ B^y & -E^z & 0 & E^x \\ B^z & E^y & -E^x & 0 \end{pmatrix}$$

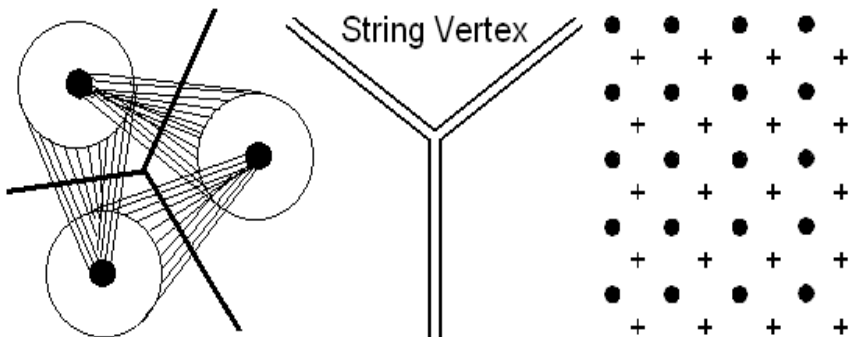


Fig. 15.11. a) Triune nature of least cosmological unit. b) Continuous Witten string vertex theory able to undergo Ising flips. c) Ising model background, descriptive elements of Riemann sphere rotation symmetry breaking.

If properties of the Dirac vacuum are expanded to conform with UFM cosmology Fig. 15.12b graphically represents the integration of Eqs. (15.12) and (15.13) on the top of the Dirac sea where the central point is a

space-like radial four-vector $A_\mu = r_\mu \exp(iS/\hbar)$ with frequency $\nu = m_\gamma c^2/\hbar$. The oppositely rotating dipoles $\pm e$ correspond to gravity and em with each individual sub-element four-momentum $\partial_\mu S$. For detailed discussion see [53,54]. Fig. 15.11a represents one close-packed UFM hypersphere least-unit just below this regime which is the vertex at 0 where further unification to the unified field occurs.

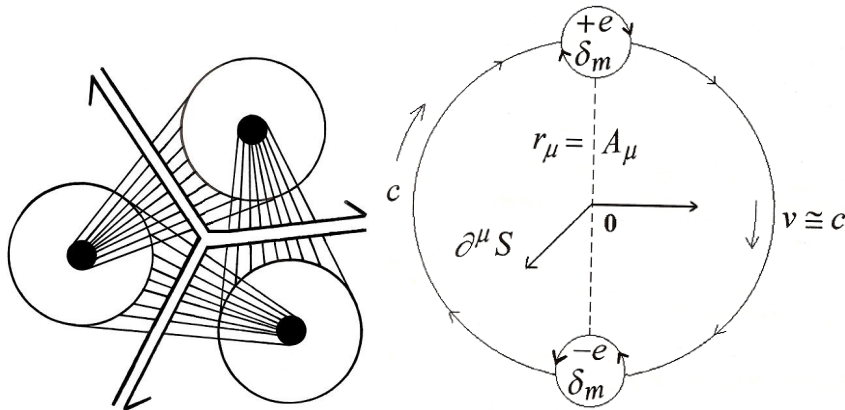


Fig. 15.12. Models of least-unit points tiling the Dirac backcloth in the UFM cosmology of 12D UFM superspace. a) Least cosmological unit (LCU) with a classical discrete \hbar vertex. b) Conceptualization of two oppositely charged vacuum subelements rotating at $v \approx c$ around a central point behaving like a dipole ($+e$) em ‘bump’ and ($-e$) G ‘hole’ on the topological surface of the covariant polarized Dirac vacuum.

This is only a superficial account of the highly essential relevance of the complementarity of the $G_{\mu\nu} - F_{\mu\nu}$ coordinate systems. More development is given in Chap. 6. Suffice it to simplistically summarize here that the dynamics of the continuous-state SUSY symmetry breaking are key to the ontological properties of this putative model of bulk QC. The G-em coordinates couple and uncouple fixing one and then the other in a dual seesaw-leapfrogging effect which is like a form of topological wave-particle duality. It is the utilization of this structural-phenomenology as a covariant resonant hierarchy that allows the ontological violation of the Copenhagen regime uncertainty principle. See Chap. 8 for a more complete description of the empirical protocol.

The triune geometry of Fig. 15.12a represents the point 0 in 15.12b shown as an Ising lattice array in 15.11c. This is similar to the vertex in string theory (Fig. 15.11b) able to topologically undergo spin flips of the Riemann sphere from zero to infinity (Fig. 15.20b). In these continuous-state points the Ising vertices as governed by the super quantum potential (unified field) as described by the UFM field equation [26]. There is a foreground and background duality as illustrated in Fig. 15.10 where the em and metrics continuously “leapfrog” in the spacetime backcloth. These factors are imposed on spacetime geometry by the symmetry conditions of UFM cosmology. Traditionally parallel transport of a vector or spinor around a closed path P,Q,R (Fig. 15.13a) or P,Q,R,S (Fig. 15.13b) generally results in a deficit angle, a mass deficit that signifies the amount of curvature at that vertex when the Riemann tensor is $\neq 0$ [30,58,59].

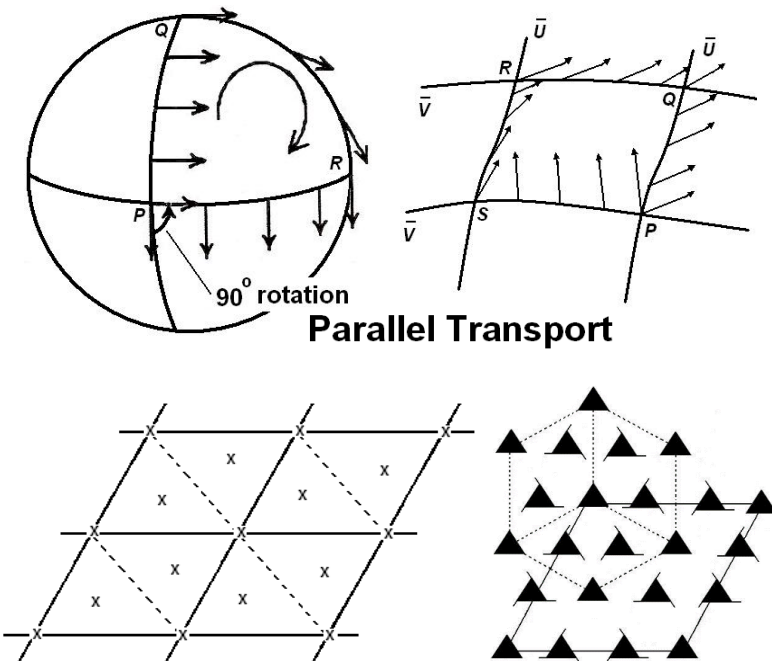


Fig. 15.13. a) Parallel transport of a vector or spinor around closed paths generally results in a deficit angle, a mass defect where the vector does not return to the original position P .
b) Tiling of the spacetime backcloth and projective geometry giving rise to higher dimensionality.

Tiny loops approximated by a parallelogram of two tangent vectors $\vec{\mu}$ and \vec{v} close (no deficit) if $[\vec{\mu}, \vec{v}] = 0$; then the curvature operator is the commutator of covariant derivatives along $\vec{\mu}$ and \vec{v} , $R(\vec{\mu}, \vec{v}) = [\nabla_{\vec{\mu}}, \nabla_{\vec{v}}]$ [30]. If $[\vec{\mu}, \vec{v}] \neq 0$, $[\nabla_{\vec{\mu}}, \nabla_{\vec{v}}]$ is subtracted from the commutator, the parallelogram doesn't close and the Riemann tensor is $\neq 0$.

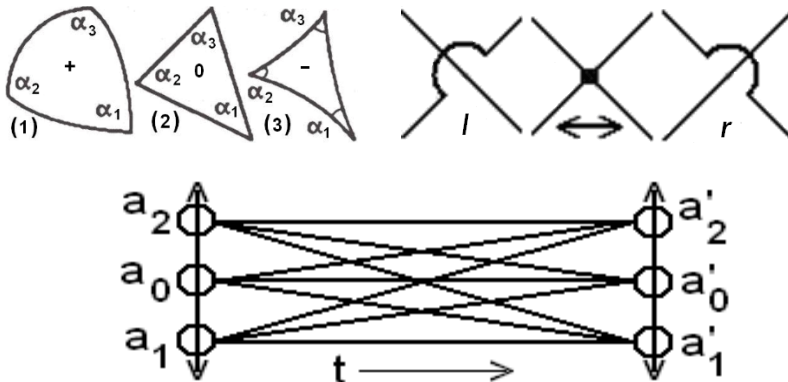


Fig. 15.14. a) Three types of geodesic triangles with Gaussian curvature. 1) Circumsphere with positive curvature, sum of internal angles $> \pi$. 2) Mesosphere, E^3 with zero curvature. 3) Insphere, internal angle sum $< \pi$ so curvature is negative. b) Chiral properties of a vertex where the coordinate basis topologically switches from fixed to l or r open. c) Triune elements of an HD transaction in UFM terms where the elements of a least-unit are tertiary.

In Fig. 15.14a, the sum of the three internal angles minus π is the Gaussian curvature integral $(\alpha_1 + \alpha_2 + \alpha_3) - \pi \int K dA$ where K is the Gaussian curvature. Taking Fig. 15.14 triangle (a) for example on a sphere of radius r with $\alpha_1 = \alpha_2 = \alpha_3 = \pi/2$ the area of the triangle is $(4\pi r^2)$ and the Gaussian curvature would be $K = 1/r^2$ which is positive [30].

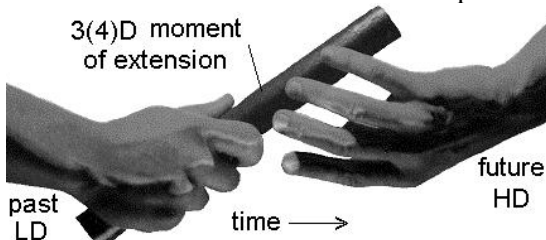


Fig. 15.15. Spin exchange. The spin exchange mechanism requires a coupling-decoupling moment between the $C \rightarrow q \rightarrow u$ components of the spacetime least-units (LCUs) like the passing of a baton in a relay race, a switch from anticommutativity to commutativity.

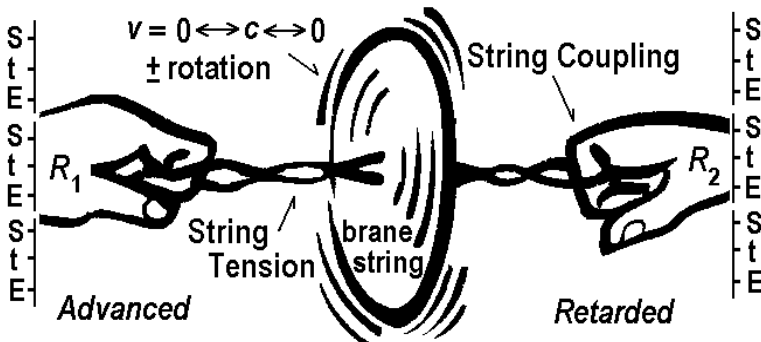


Fig. 15.16. Spin Exchange. The spinning disk toy further illustrates elements of the continuous-state. Imagine an array of disks as in Fig. 15.12b.

The spin-exchange hierarchy process has many components; more are shown in Fig. 15.17.

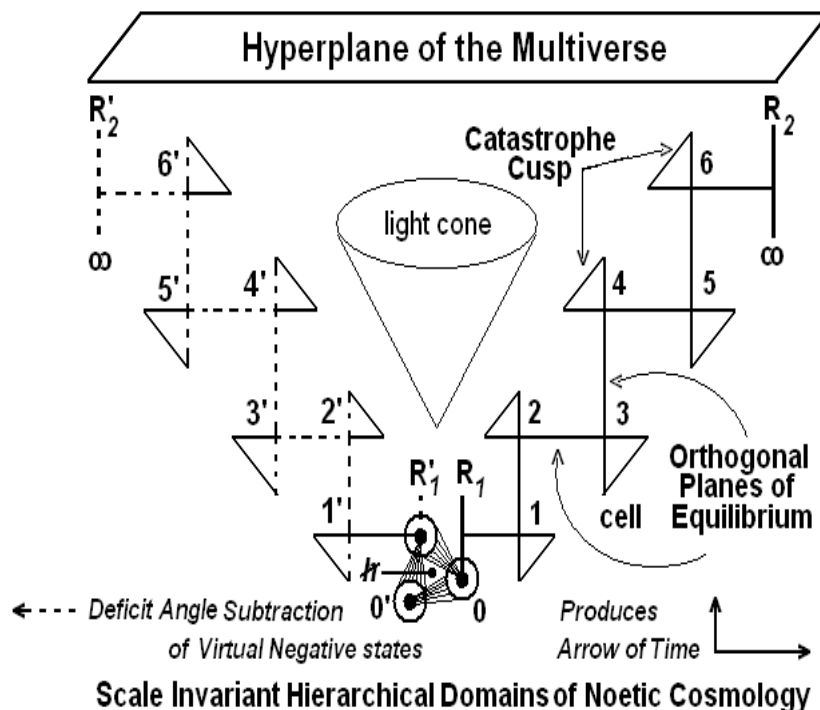


Fig. 15.17. Covariant scale invariant hyperplane domains in the hierarchy of UFM superspace.

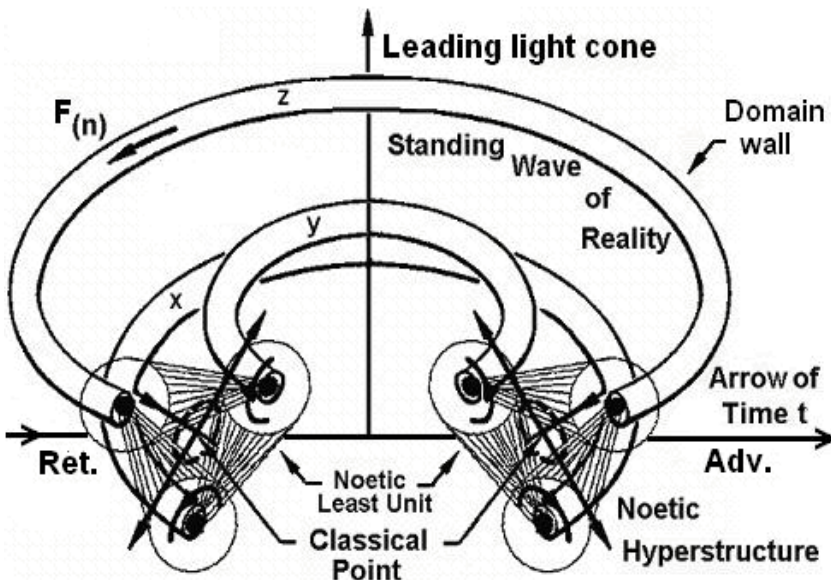


Fig. 15.18. A single future-past, retarded-advanced domain where the properties illustrated in Figs. 15.10, 15.11 & 15.12. interplay to produce the observed macroscopic arrow of time.

The dominant view among cosmologists regarding XD is that if they exist they must be microscopic because they are not observed. In UFM cosmology XDs are macroscopic and take part in the creation and recreation of spacetime, the arrow of time and observed macroscopic reality (Fig. 15.18). This scenario arises during the inherent ‘continuous-state spin-exchange dimensional reduction compactification process’ by parallel transport (Fig. 15.10) within the additional context of a dual Dirac spherical rotation of the least-unit topology (Fig. 15.8) of subspace elements producing deficit angles during decoupling-coupling allowing relativistic subtraction of supralocal-nonlocal domain components (Figs. 15.10, 15.11, 15.12 & 15.13) producing the arrow of time. The scaling process begins in the microscopic backcloth without a physical arrow of time and ramps up the helicoid hierarchy (Fig. 15.7) to the virtual standing-wave macroscopic present. Because of its relativistic nature the ‘baton’ passing (coupling-decoupling) between domains appears smooth to the observer. Fig. 15.13 is meant to be synonymous with the lightcone rings of Fig. 15.9 where the leapfrogging domain frequency provides the context for assigning coupling parameters required for utilizing the synchronization backbone for the UQC.

15.8 Geometric Introduction to the UFM QC Ontology

What are the topological conditions required to achieve a commutative ontology for UQC? Newton's 2nd Law of motion says position and velocity completely determine an observables 'state', (p, q) at an instant in time. Quantum mechanically an observable has a probabilistic distribution of values (P, Q) , with quantization making correspondence between the two [60]; conditions that delineate the uncertainty principle and provide no framework for a pragmatic absolute ontology. In UFM cosmology neither spacetime nor stochasticity is considered fundamental. This is not a different basis than the concept of Heisenberg's potential; so what is required is a new process. Spacetime is a continuous harmonic state comprised of the Amoroso-Vigier dual $em \rightleftharpoons \mu\nu$ metric [53,54] comprised of conventional transverse 'em' elements described by Maxwell's traditional equations plus longitudinal $\mu\nu$ elements with additional degrees of freedom derived from the Einstein-de Broglie relation $E = h\nu = mc^2$ (with $m = m_0(1 - v^2/c^2)^{-1/2}$) such that Maxwell's equations do not 'cut off' at the vacuum. Evidence for such a metric is implied by the Casimir, Zeeman & Aharonov-Bohm effects [61]. These two sets of coordinates EM + $\mu\nu$ would generally be exclusive and independent. The aim here is to reveal a framework for their 'continuous-state' integration, not in 4D as previously done [53,54] but in 12D where integration is completed to unitarity.

The close-packed least unit hypersphere tiling of this UFM superspace is a complex self-organized scale invariant anticipatory system. While beyond the scope of this paper, operational interplay of the parameters of the fundamental least unit is discretized macroscopically into perceived reality. Normally local application of an observational RF pulse in the z direction discretizes the uncertainty relations of microscopic quantum states for particles. To avoid production of these uncertainties inherent in the quantum principle, a new set of UFM transformations beyond the Galilean-Lorentz-Poincaré must be implemented by a cumulative interaction methodology to allow a 'coherent control' transformation of the phenomenology of discretization into an ontological superposition of the information.

To illustrate we apply general mechanical principles for 'pure rolling contact' [62] to the transmission of angular momentum translating through the topology of this HD spin tower (Figs. 15.7,9), the relative motion of consecutive elements propagate successively in proper order with the

elements of parallel axes in the corresponding topological surface. These motions may be \pm coupled combinations relative to the center of mass and components of angular momentum that are singular (degenerate), linear, circular, cylindrical, spherical and hyperspherical. This reveals the richness of the cosmological least unit (LCU) as it undergoes continuous-state spin-exchange (rolling contact) compactification (past orientation) and Ising dimensional flip (future orientation) in quantifiable stages of dimensional jumps from 12D to 0D by superluminal Lorentz boosts [2,63] in cyclic progression S \rightarrow t \rightarrow E and C \rightarrow Q \rightarrow U (space to time to energy; classical to quantum to unitary). The superluminal Lorentz boost to a temporal dimension sets the stage for the more critical 2nd boost to UF energy which allows coherent field action to cause raising or lowering moves of the topology cycling the commutative-anticommutative modes that open-close the topology.

12D, the minimum to describe eternity or escape from the temporal bounds of uncertainty is a result of the dimensional tower (Figs. 15.5, 15.6, & 15.7) where time and E_3/M_4 is a standing wave subspace of eternity. This structure whether Calabi-Yau, dodecahedral, or some M-Theory combination entails a reciprocal spiral topology. In this context we utilize logarithmic, helicoid or cyclotron resonance spirals (Fig. 15.19) to illustrate new angular momentum commutators. The future/past asymmetry has a Doppler relationship (Fig. 15.10) (relative only to the perception of the 4D observer). E & E' , (Fig. 15.6) therefore represent equal Wheeler-Feynman future/past symmetries. The Doppler effect arises because of inherent $E-E'$ boosts and compactifications. In this picture the Wheeler-Feynman-Cramer elements [9,6] may be understood conceptually by pairs of logarithmic spirals (Fig. 15.19a) of equal obliquity rolling on a common tangent, ed where each coupled point signifies a present spacetime moment; the locus of which (ed) is the arrow of time. A radiant of the spiral, r is

$$r = ae^{b\theta} \quad (15.23)$$

with a the value of r if $\theta = 0$, e base of the Naperian logarithms and $b = 1/\tan\phi$, with ϕ the constant angle between the tangent to the curve and radiant to the point of tangency [64]. If the value of θ takes uniform increase (quantized values) the radiants, r will be $ct = 0, 1, 2, 3, \dots, n$ in geometric progression relative to the hierachal topology of the space.

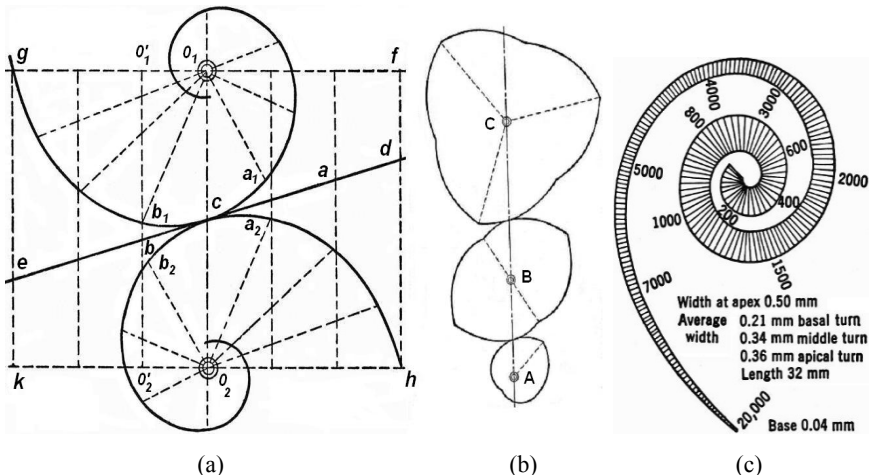


Fig. 15.19. a) Two logarithmic spirals illustrating perfect rolling contact (no slip) that cannot be continuous because of boundary limits. b) Continuous rolling contact by 1, 2 & 3 lobed spheres (segments of a)) illustrating how HD hierarchy nodes may be formed. c) The basilar membrane of the ear is tapered (like radians) roughly like a logarithmic spiral beginning at a Planck point and widening to the Larmor radius of an atom. Each width is frequency dependent causing sound input of specific frequencies to vibrate more in the location where the radius has the same characteristic resonant frequency.

These log curves are not closed; to adapt to continuous motion, pairs must be utilized. Joining corresponding sections of the spiral form symmetrical unilobed wheels. While sectors needn't be equal or symmetrical, the 'wheels' must be paired with sectors of equal obliquity in contact for pure rolling motion to occur. Wheels may also be bilobed or trilobed etc. up to ND to illustrate the Superspace. A tier of three symmetrical wheels is illustrated in Fig. 15.19b.

The mechanical concept of rolling contact is used to geometrically illustrate the ontological framework for the new UFM commutation rules of angular momentum. A logarithmic spiral coupled to another of the same obliquity undergoes perfect rolling motion (no slippage and constant touching) as long as arcs of the same obliquity coincide. This system of spirals reaches a limit that could be said to be points of Ising flip; but the rotation is not continuous. To make the rolling continuous one must take 2 sections of the logarithmic spiral (Fig 15.19) and join them into a spheroid. Then continuous motion may occur. As in Fig. 15.19b this single lobed gear may be made bilobed or trilobed, again for continuous or perfect rolling motion proper obliquity must be maintained.

So here as in the ear metaphor the points of contact correspond to frequencies. If the point of contact corresponds to the z axis we have moments of commutation of angular momentum. Leaving one gear set (the spin tower of frequencies) we have a system of close packed spheres of least cosmological units undergoing the UFM mantra (spin-exchange, dimensional reduction, compactification) which means that there are HD moments of commutation in the 12D structure.

Since angular momentum is the resultant of the atomic magnetic moment and (center of mass) harmonic frequencies (as in the cyclotron frequencies of synchrotron radiation) should make these other (x & y) components of angular momentum accessible. In any given discretized (composite) E_3 frame only the z axis will commute as per standard quantum theory; but in the complex HD space the E_3 non-commutative parameters commute periodically on rotation through mirror tangent nodes of proper obliquity in the continuous state topology; i.e. in considering all HD hyperplanes, there are periodic simultaneous moments where nodes of commutation may be accessible by synchronizing RF pulses of the proper harmonic cyclotron frequency.

Bessel functions could be used to manipulate the complex cavity (C-QED) resonance modes in the manifold of uncertainty (MOU). For example, in a generalized Cramer Transactional Interpretation event cavity (between future-past topological boundaries) the magnitude of a uniform applied electric field with E_0 constant can be taken as $E = E_0 e^{i\omega t}$. If the frequency increases, the electric field flux through any loop, Γ_1 produces an oscillating magnetic field $B = i\omega r / 2c^2 \cdot E_0 e^{i\omega t}$ proportional to r , the radius of the cavity. This varying magnetic field, proportional to the rate of change of E and thus ω , effects the electric field so it can no longer be uniform by Faraday's Law and also changes with r [65] which oscillates in the UFM C-QED model. This requires corrections to our original uniform field E_1 such that the corrected field must now be $E = E_1 + E_2 + E_3 \dots E_n$ which is best described by a Bessel function, J_0 , with $x = \omega r / c$:

$$J_0(x) = 1 - \frac{1}{(1!)^2} \left(\frac{x}{2}\right)^2 + \frac{1}{(2!)^2} \left(\frac{x}{2}\right)^4 - \frac{1}{(3!)^2} \left(\frac{x}{2}\right)^6 + \dots \quad (15.24)$$

such that E is now

$$E = E_0 e^{i\omega t} J_0 \left(\frac{\omega r}{c} \right). \quad (15.25)$$

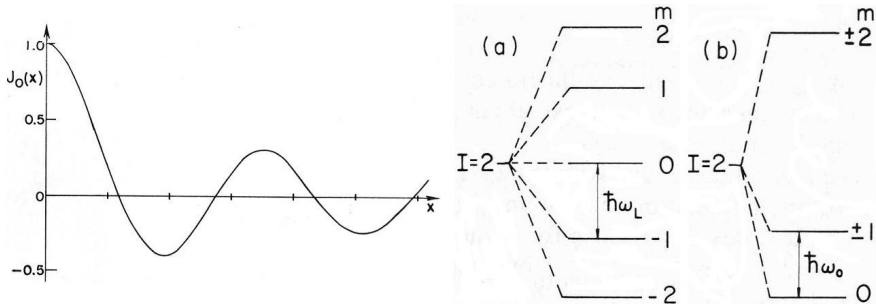


Fig. 15.20. (a) Graph of Bessel function $J_0(x)$ showing how J_0 oscillates as x increases. (b) Nuclear energy splitting of substates for total spin 2 in a magnetic field and (c) axially symmetric electric field with quadratic energy splitting, ω is the spin precession frequency.

15.9 Essential Parameters of the Incursive Oscillator

The evolution of physical theory from Classical to Quantum changed the fundamental understanding of a point or point particle from continuous – represented in 3D Euclidian space, to discrete fuzzy units with wave-particle duality–represented in 3(4)D Minkowski/Riemann spacetime. As physical cosmology has evolved towards M-Theory it is now realized that neither of these contexts is sufficient or complete. In Multiverse cosmology the nature of a vertex or point changes into a continuous-state 12D superspace. This means there are three regimes existing simultaneously/individually: Classical, Quantum and Unity depending on mode of observation.

Motion of a one dimensional *classical* harmonic oscillator is given by $q = A \sin(\omega t + \varphi)$ and $p = m\omega A \cos(\omega t + \varphi)$ where A is the amplitude and φ is the phase constant for fixed energy $E = m\omega^2 A^2 / 2$. For state

$|n\rangle$, with $n = 0, 1, 2 \dots \infty$ and with Hamiltonian $E_n = (n + 1/2)\hbar\omega$ the quantum harmonic oscillator becomes

$$\langle n | q^2 | n \rangle = \hbar / 2m\omega \langle n | (a^\dagger a + aa^\dagger) | n \rangle = E_n / m\omega^2 \quad (15.26)$$

and

$$\langle n | p^2 | n \rangle = 1/2(m\hbar\omega) \langle n | a^\dagger a + aa^\dagger = mE_n \quad (15.27)$$

where a & a^\dagger are the annihilation and creation operators, $q = \sqrt{\hbar/2m\omega}(a^\dagger + a)$ and $p = i\sqrt{m\hbar\omega/2}(a^\dagger - a)$. For the 3D harmonic oscillator each equation is the same with energies $E_x = (n_x + 1/2)\hbar\omega_x$, $E_y = (n_y + 1/2)\hbar\omega_y$ and $E_z = (n_z + 1/2)\hbar\omega_z$ [18,21].

In Dubois' notation the classical 1D harmonic oscillator for Newton's second law in coordinates t and $x(t)$ for a mass m in a potential $U(x) = 1/2(kx^2)$ takes the differential form

$$\frac{d^2x}{dt^2} + \omega^2 x = 0 \quad \text{where} \quad \omega = \sqrt{k/m} \quad (15.28)$$

which can be separated into the coupled equations (15.29)

$$\frac{dx(t)}{dt} - v(t) = 0 \quad \text{and} \quad \frac{dv(t)}{dt} + \omega^2 x = 0. \quad (15.29)$$

From incursive discretization, Dubois creates two solutions $x(t + \Delta t)$ $v(t + \Delta t)$ providing a structural bifurcation of the system which together produce Hyperincursion. The effect of increasing the time interval discretizes the trajectory as in Fig. 15.21 below [6,66-69]. This represents a background independent discretization of spacetime.

Each mode of a quantum harmonic oscillator is associated with cavity-QED dynamics, hexagon lattices (Fig. 15.21c) of spacetime topology undergoing continuous transitions. E is the state of energy for n photons. For $n = 0$ the oscillator is in the ground state, but a finite energy $1/2\hbar\omega$

of the ground state, called the zero-point energy, is still present in the region of the cavity. According to Eq. (15.30), the quantum harmonic oscillator field energy of the photons undergoes periodic annihilation and recreation in the periodic spacetime [70].

$$E_n = \left(n + \frac{1}{2}\right)\hbar\omega. \quad (15.30)$$

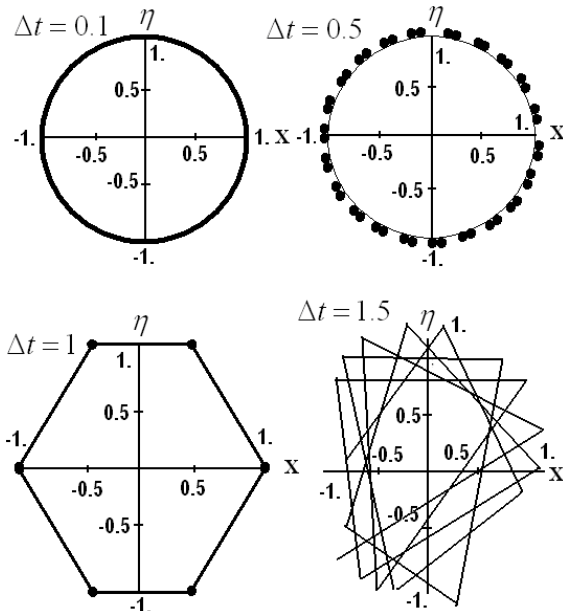


Fig. 15.21. Numerical simulation of phase space trajectory for Dubois' *superposed incursive oscillator* based on coordinates and velocities $x_n = 1/2[x_n(1) + x_n(2)]$, $v_n = 1/2[v_n(1) + v_n(2)]$ is shown for values of $\Delta\tau = \omega t$ equal to 0.1, 0.5, 1.0 and 1.5. Initial conditions are $\chi_0 = 1, \eta_0 = 0$ & $\tau_0 = 0$ with total simulation time $\tau = \omega t = 8\pi$. Figure adapted from [6,68].

15.10 Ontological I/O by Superseding Quantum Uncertainty

The critical problem in applying conventional QT to the bulk implementation of QC lies in the accompanying theory of measurement

[21]; variables observed change destructively in any interaction between particle and observing apparatus. This phenomenological *force of interaction* is mediated by particle exchange which modifies the Schrödinger equation. In conventional terms ‘physical reality’ is irreducibly quantum’ and a qubit resides at a Euclidian, E^3 or Minkowski, M^4 vertex.

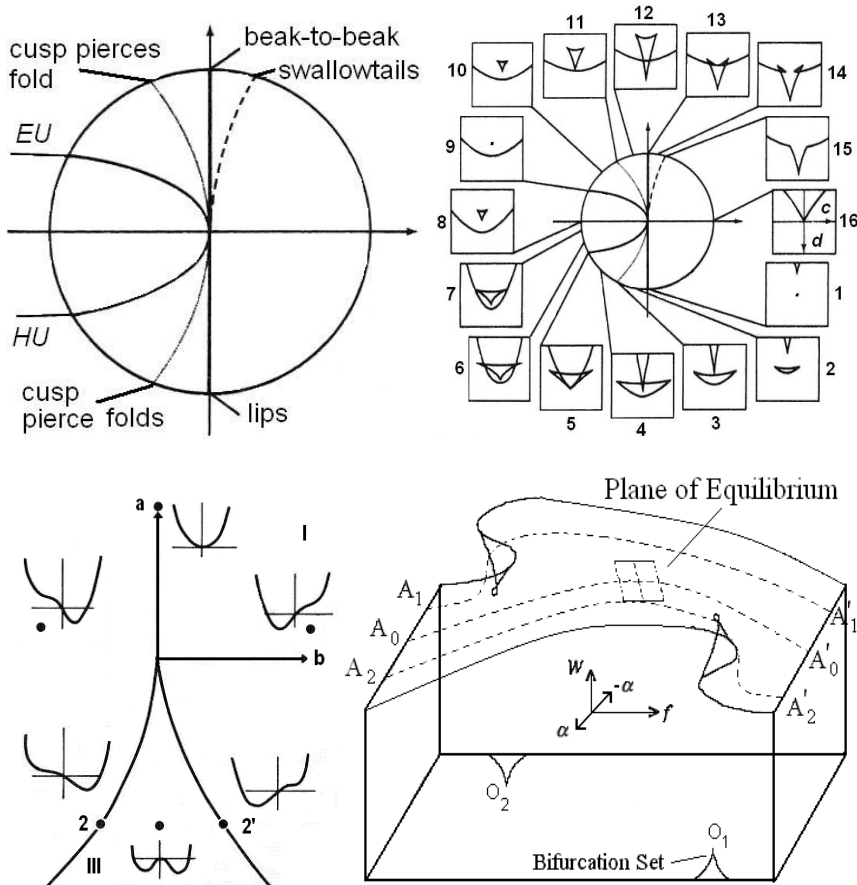


Fig. 15.22. A double-cusp catastrophe (DCC) provides a partial geometric and mathematical model of UFM superspace transitions. The inherent Dirac rotation is like a DCC.

All attempts for bulk QC have failed in the Copenhagen regime because measurement destroys the quantum system being measured. To

overcome this problem, the Dirac equation is hyperdimensionalized utilizing an extension of Cramer's Transactional Model of QT where all off diagonal elements are physically real and conformally invariant. Bulk implementation of UQC requires a new superspace N^{12} without a real vertex where not only is the arbitrarily chosen z -axis of angular momentum accessible; but the x and y components are also real and accessible by a new anticipatory transformation law for ontological evolution utilizing topological switching [15]. This is conceptually elucidated by unfolding a hypercube (Fig. 15.4). Relative to the subspace E_3 the extra square called a satellite is *causally free* of E_3 when carried to 12D unitarity.

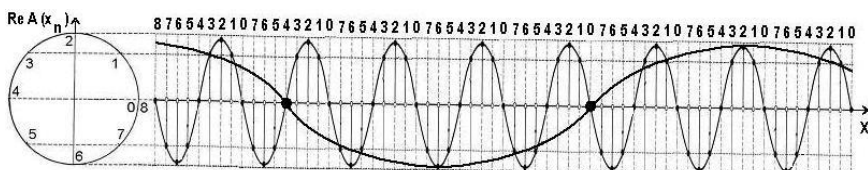


Fig. 15.23. Depiction of 2π and 14π harmonic waves coinciding at 2 points on the x -axis corresponding to points 4 and 0.8 on the reference circle. Reference circle geometry (2D for simplicity, an HD hypersphere) is utilized to set up RF harmonic oscillator π -pulse parameters for phase alignment with the inherent Adv-Ret elements of the spacetime synchronization backbone. Periodicity of the phase points ϕ are aligned to manipulate symmetries of corresponding regimes of commutative and noncommutative modes.

During the HD continuous-state topological transformation of the cosmological form of Dirac spherical rotation, a pinch or twist occurs in the middle of the transform followed by an Ising flip [38] of the close-packed complex Riemann spheres which can be driven by the micromagnetic spintronics [15] of fractional and integer quantum Hall effects because of the highly symmetric topological parameters [2] of driven Micromagnetics [15]. This UQC can be implemented in any sufficient multi-state quantum system, whether solid, liquid, bubble, crystal, dot, network, trap, well, vacuum backcloth, comprised of atoms, molecules, ions, photons, spins, NMR, threads, lines, block walls, domain walls, lattices or arrays able to utilize coherent control of the synchronization backbone [31]. In order to avoid the Copenhagen limitations of collapse and dissipation [71] UQC requires utilization of the hierarchical and recursive properties of complex self-organization inherent in the *whole universe*, not just a portion of its observed parameters. The critical condition is the introduction of a model for

evolution of the wave function making correspondence to a new non-collapse (ontological or energyless) version of RQFT.

By a coherent control of Ising spin flips [38] of the UFM spacetime least-units (a topological switching of metrics [15]) domains of discretization ($\Delta x \Delta \rho \cong \hbar$) may be avoided by utilizing periodic nodes in the resonant hierarchy that are commutative because the Riemann curvature tensor equals zero [72]. E_3 is a discretization, a composite of future-past potentials. In HD where the parameters are separated one can manipulate commutative and noncommutative regimes. Another way to illustrate the intended use of coordinated RF sine wave π -pulses (Fig. 15.20) with the geometry of spatial rotations of a pair of common dice to show that some rotations commute, $a \otimes b = b \otimes a$ and others are noncommutative $a \otimes b \neq b \otimes a$.

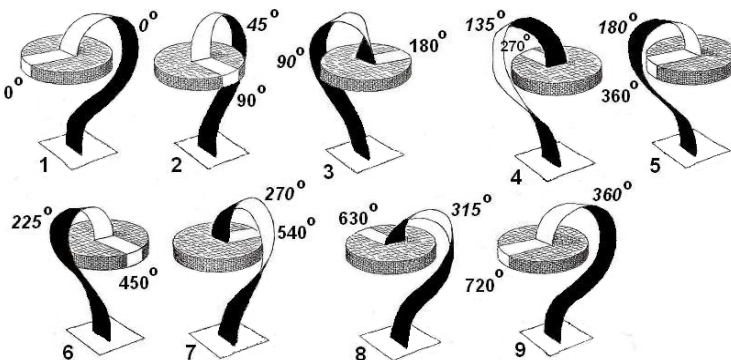


Fig. 15.24. Conceptualization of the spinor geometry of Dirac spherical rotation showing the 360° - 720° degree complementarity structure of spin $\frac{1}{2}$ particles without the topological pinch.

The topological pinch, shown more clearly in Fig. 15.27 is of critical importance to the continuous-state compactification process. Think of it as the centroid of the phase in an em-wave where for a moment the electric and magnetic moments are zero, like the cycle ends where the spin direction stops in Fig. 15.15 before reversing. This is a zero-mass moment in parallel transport where during deficit angle phase a compactification or boost may occur facilitating commutative anticommutative cycles breaking algebraic closure momentarily.

15.11 A Twistor Approach to the UQC I/O Ontology

Because of the essential requirement of utilizing an HD form of Dirac spherical rotation to access the inherent synchronization backbone in Multiverse cosmology; it is suggested that a Penrose twistor approach provides the most efficient methodology for coupling to the resonant hierarchy. We illustrate this only briefly here and leave it to a future paper or other QC researchers to develop more fully.

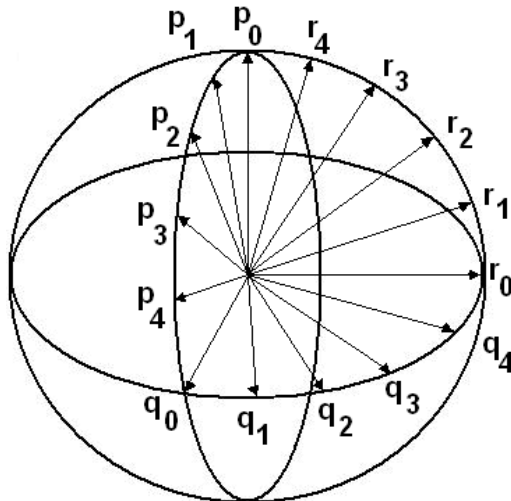


Fig. 15.25. Hyperspherical modeling as a visual aid for switching the coordination of phase angles for Dirac spherical rotation.

Given the worldline, $y^a(s)$ and then following Bailey and Penrose [73,74], from the fundamental twistor relation, $Z^\alpha = (\omega^A, \pi_A)$ the function $\xi^A(s) = \omega^A - iy^{AA'}(s)\pi_{A'}$ is then defined. Then for the scalar field contours (Fig. 15.23) we define a twistor function $f(Z^\alpha)$ by

$$f(Z^\alpha) = \oint \frac{ds \alpha \cdot \beta}{(\alpha \cdot \xi)(\beta \cdot \xi)} \quad (15.31)$$

where α_A and β_A are fixed spinors and $\alpha \cdot \beta = \alpha_A \beta^A$. In this regime the field produced by the unit charge has poles corresponding to advanced and retarded points on the worldline [73,74]. Taking an EM field potential

$\Phi A A'(x)$ with left and right handed components given by $\phi A' B' = \nabla_{A' \Phi B' A}^A$ and $\phi A B = \nabla_{A \Phi B A'}^{A'}$ respectively [73,74].

Twistor functions describe relative cohomology classes in \mathbb{PT} regions; but the same twistor functions may also be examined geometrically in M^4 [74]. The contour in Eq. (15.31) is a small loop around the $\alpha \cdot \xi = 0$ and $\beta \cdot \xi = 0$ poles (Fig. 15.27). There are two of these, one for advanced and one for retarded solutions. When a singularity is reached (Dirac pinch) one switches from $f(\alpha)$ to $f(\beta)$. In a small neighborhood U of L , U_α, U_β keeps away from the branching singularity of $f(\alpha), f(\beta)$. The process of doing contour integrals gives a well-defined field; choice of contour gives any linear combination of Adv. and Ret. solutions. The α and β spinors represent opposite directions in E^3 but not in the same regions. The contours move continuously from Ret to Adv [73,74].

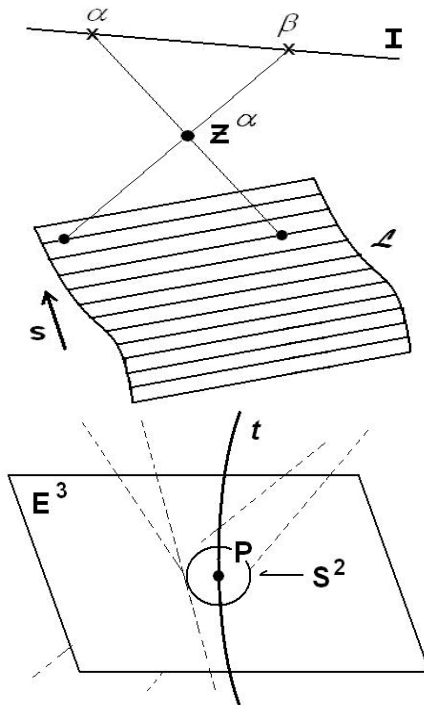


Fig. 15.26. (a) A piece of ruled surface L for worldline $y^a(s)$ where each line on the surface represents a point on the complex worldline I . (b) Small sphere, S^2 surrounds E^3 worldline P with null twistors Z^α representing null lines meeting S^2 .

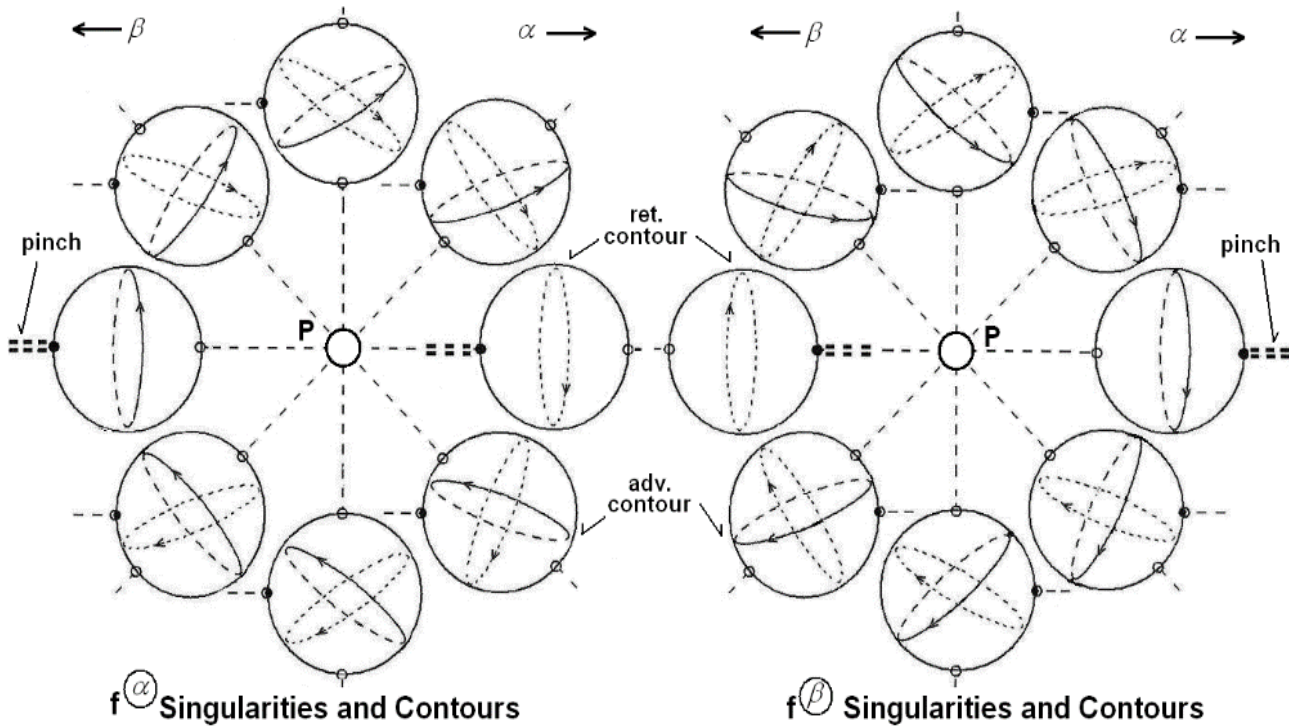


Fig. 15.27. Contours and singularities of two linearly independent advanced (solid lines) and retarded (dashed lines) fields that can be computed by contour integration.

Taking the spin structure hierarchy of 1-4 benzosemiquinone (Fig. 15.24) or class II mesoionic xanthines [75] for example and aligning it with the inherent synchronization-backbone of UFM cosmology using the Dirac spherical rotation contour integrals as defined by the Penrose twistor functions in Figs. 15.26 [73,74] as an intermediary we are able to achieve the rolling motion contacts suggested metaphorically in Fig. 15.24. but in the Dirac spherical rotation manner of Fig. 15.19. Why? This is to achieve ontological topological switching with the satellite regime of Fig. 15.4. UFM theory postulated that this path is only open in the continuous-state leapfrogging of the Vigier-Amoroso coordinates [53,54]. These coordinates fix and unfix; this is a cosmological utility of the Dirac rotation first discovered for the electron.

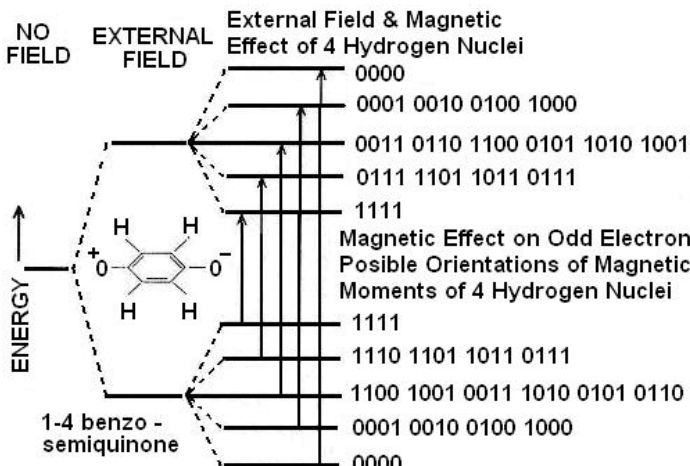


Fig. 15.28. The spin states of 1-4 benzosemiquinone, a molecule suitable for testing QC parameters by application of RF fields.

This complexity arises because the Dirac pinch (illustrated in Figs. 15.24, 15.27) is a fundamental process of reality (not just the electron) since the eternal origin of the unitary field is causally separated from E^3 . To comprehend one must hold the concept of Dirac spirical rotation in one's mind while wrapping it around the context where the interplay of the three regimes (classical, quantum, unitary) occurs. In order for the I/O pulses to achieve coupling to the proper leapfrogging contours the resonance modes of the RF pulses must align precisely with the inherent beat frequency of the spacetime backcloth, i.e. without the coherent

control [76-78] the inherent synchronization backbone provides there can be no cumulative interaction with the Dirac spherical rotation hierarchy and no ontological initialization or processing of the QC registers and the QC remains stuck at the ten qubit limit of the Copenhagen regime.

15.12 Class II Mesoionic Xanthines as Potential 10-Qubit Quantum Computer Substrate Registers

Perhaps better than the 1-4 benzosemiquinone, a molecule are Class II mesoionic xanthines such as *anhydro*-(8-hydroxyalkyl-5-hydroxy-7-oxothia-zolo[3,2-a] pyrimidinium hydroxides) are unique, small atomic weight, stable crystalline organic compounds that can be represented as a combination of ten different resonance structures for each simple xanthine molecule. Each resonance structure contributes a certain percentage to the total resonance of the molecule. This unique resonance represents ten different quantum states of the entire molecule and can thus be exploited as a potential substrate for a ten-qubit register. The number of possible superposition states for such a register in a single molecule is potentially as high as 2^n states or (in this case where $n = 10$) 1,024 complex numbers. In solution the least-unit of this mesoionic crystalline structure is scalable suggesting putative utility for bulk NMR quantum computing. It will be shown that these ten-qubit registers are amenable to standard Deutsch-Jozsa, Shor and Grover algorithms. Additionally, we attempt to formalize I/O techniques for our Class II mesoionic xanthines based on a coherent control RF process of cumulative resonant interaction where by utilizing additional degrees of freedom pertinent to a relativistic basis for the qbit (r-qbit) new HD commutation rules allow decoherence to be ontologically overcome.

Mesoionic purinone analogs, a large and relatively new class of bicyclic heteroaromatic compounds, whose ring systems possess π -electron systems that are isoelectronic with those of the various known purinones, have been synthesized and characterized over the last few decades [79-85]. Class I mesoionic analogs have been classified and defined as being those that are derived from known five-membered mesoionic ring systems. Class II mesoionic analogs are those that are derived from known six-membered mesoionic ring systems. In 1996, Giandinoto, *et.al* [86] had synthesized and characterized a number of novel Class II mesoionic xanthine acyclonucleosides as potential anti-neoplastic and antiviral agents. Class I and Class II mesoioic purinones

have been formulated and examined from a quantum chemical standpoint [87,88]. The generalized structural representation of mesoionic xanthine acyclonucleosides is shown in Figure 15.29 below.

In particular, the mesoionic xanthine acyclonucleosides where R' = H are especially useful since this moiety is ideal in giving the molecule a handle for attaching it to metallic, organic, polymeric or semiconductor surfaces/substrates such as GaAs, GaN, CdSe/ZnS. The definition of a mesoionic compound is a compound that cannot be adequately represented by any single covalent or single dipolar resonance structure. These Class II mesoionic xanthines, such as *anhydro-(8-hydroxyalkyl-5-hydroxy-7-oxothiazolo[3,2a]pyrimidinium hydroxides)* cannot be adequately represented by fewer than ten different resonance contributors. These ten class II mesoionic xanthine resonance forms and all of their possible quantum inter-conversion states are uniquely qualified for QC. Each resonance structure corresponds to an individual quantum state of the total molecule and all ten are required to adequately represent the molecule in its totality of superposed quantum states. In quantum computing, there may be multiple quantum states in superposition. In this particular case where there are ten qubits, the quantum state of superposition would be the following orthonormal basis set $|\psi\rangle = \alpha_i |x_1 x_2 x_3 \dots x_n\rangle$ for all $i=1-1,024$ and for all $n=1-10$ where x_n is either 0 or 1. (1)

More succinctly the above may be written: $|\psi\rangle = \sum_{i=1}^N \alpha_i |i\rangle$ where $|i\rangle$ is a shorthand notation for an orthonormal basis set of indices $\{i_1, i_2, i_3 \dots i_j \dots i_n\}$ where $N = 2^n$.

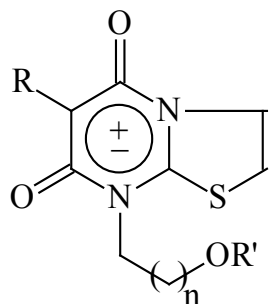


Fig. 15.29. Generalized structural representation of Class II mesoionic xanthine acyclonucleosides. $n = 1, 2$; $R = H, CH_3, CH_3CH_2, C_6H_5$; $R' = H, CH_3$.

The Greek letters α_i are referred to as the amplitudes of the register and are complex numbers. In a 10-qubit register, there are therefore 2^{10} or 1,024 complex numbers for the total register. Since the probability ($|\Psi|^2$) of a quantum state or set of quantum superposition entangled states must always be equal to one, the following relationship for the coefficients of the quantum registers must also be true

$$\sum_{i=1}^{1,024} \alpha_i^2 \equiv |\Psi|^2 = 1. \quad (15.32)$$

For an $n = 3$ -qubit register, there exists an 8-dimensional complex vector. For a 10-qubit register there exists a 1,024-dimensional complex vector. In order to initialize this vector space (register) for a quantum computer, an algorithm is necessary. In each step of the algorithm, the vector space is modified by multiplying it with a unitary matrix, which, by definition is a complex matrix.

15.13 Initialization of Mesoionic Xanthine Registers

The mesoionic xanthine molecule, as depicted in Fig. 15.29 was chosen because it remains stable at room temperature for over 100 years, and represents a molecule that can be in a quantum superposition of at least ten distinct and unique quantum states. An efficient scheme for initializing quantum registers with an arbitrary superposed state, without the introduction of additional qubits [89] has been developed by Long & Sun [90]. This scheme begins with the state $|0\dots0\rangle$ and is then transformed to

a general superposed state of the following form: $|\psi\rangle = \sum_{i=0}^{N-1} a_i |i\rangle$. In this particular case, $N = 1,024$ and $|i\rangle$ is the shorthand notation for the basis set $\{i_1, i_2, i_3 \dots i_j \dots i_n\}$ where $n = \log_2 N$ and where i_j denotes the two possible states (0 or 1) of the j^{th} -qubit. The following diagrams therefore illustrates that $|\psi\rangle$ is a general quantum superposition of N basis states

and each basis state is a product state of n qubits. The initialization scheme involves only two types of unitary transformations or gate operations. The first gate operation is a single bit rotation U_θ , $U_\theta \begin{bmatrix} 0 \\ 1 \end{bmatrix} = \begin{bmatrix} \cos \theta & \sin \theta \\ \sin \theta & -\cos \theta \end{bmatrix} \begin{bmatrix} 0 \\ 1 \end{bmatrix}$. This rotation differs from an ordinary rotation because it is an ordinary rotation only for the $|0\rangle$ bit but interjects a minus sign for the $|1\rangle$ bit. The operation thus converts a qubit in the state $|0\rangle$ to a superposition of the two states $(\cos \theta, \sin \theta)$ and a qubit in the $|1\rangle$ state to the superposition of the two states $(\sin \theta, -\cos \theta)$. When $\theta = 0$, the state $|0\rangle$ remains unchanged but converts the sign of state $|1\rangle$ (i.e., Pauli-Z gate). When $\theta = \frac{\pi}{4}$, U_θ is simply reduced to the Hadamard-

Walsh transformation. When $\theta = \frac{\pi}{2}$ (90° rotation), it acts as the NOT operation (Pauli-X, σ_x) by changing $|0\rangle$ to $|1\rangle$ and $|1\rangle$ to $|0\rangle$.

$$i = \begin{cases} 0 \rightarrow \{000\dots000\} \\ 1 \rightarrow \{000\dots001\} \\ 2 \rightarrow \{000\dots010\} \\ 3 \rightarrow \{000\dots100\} \\ \vdots \\ \vdots \\ N-1 \rightarrow \{111\dots111\} \end{cases} \quad (15.33)$$

The second type of gate operation is known as the controlled k -operation. This operation is constructed from a string of k controlling qubits. The squares represent the controlling qubits $\{i_1, i_2, \dots, i_k\}$ and the circle is a unitary operation on the target qubit representing an angle of

rotation. The uniqueness and power of this operation is that it is a conditional one that is activated only when the controlling qubits hold the respective values indicated in the squares. Controlled k -operations may be constructed using $O(k^2)$ standard 1- and 2-bit gate operations [91]. In order to more easily see how these operations are performed we may take a look at the simple example of a two qubit system.

$$|00\rangle \rightarrow \sqrt{|a_{00}|^2 + |a_{01}|^2} |00\rangle + \sqrt{|a_{10}|^2 + |a_{11}|^2} |10\rangle \quad \text{Operation}$$

1.) Single bit rotation α_1 , $\rightarrow |0\rangle [a_{00}|0\rangle + a_{01}|1\rangle] + |1\rangle [a_{10}|0\rangle + a_{11}|1\rangle]$
Operation

2.) Two controlled¹-operations $U_{\alpha_{2,i}}$ ($i = 0, 1$).

$$= a_{00}|00\rangle + a_{01}|01\rangle + a_{10}|10\rangle + a_{11}|11\rangle$$

The single bit rotation α_1 is equal to $\tan^{-1} \sqrt{\frac{|a_{10}|^2 + |a_{11}|^2}{|a_{00}|^2 + |a_{01}|^2}}$. We may now represent the operations in matrix form as well:

$$U_{\alpha_{2,0}} = \begin{bmatrix} \frac{a_{00}}{\sqrt{|a_{00}|^2 + |a_{01}|^2}} & \frac{a_{01}}{\sqrt{|a_{00}|^2 + |a_{01}|^2}} \\ \frac{a_{01}^*}{\sqrt{|a_{00}|^2 + |a_{01}|^2}} & \frac{a_{00}^*}{\sqrt{|a_{00}|^2 + |a_{01}|^2}} \end{bmatrix} \quad (15.34a)$$

$$U_{\alpha_{2,1}} = \begin{bmatrix} \frac{a_{10}}{\sqrt{|a_{10}|^2 + |a_{11}|^2}} & \frac{a_{11}}{\sqrt{|a_{10}|^2 + |a_{11}|^2}} \\ \frac{a_{11}^*}{\sqrt{|a_{10}|^2 + |a_{11}|^2}} & \frac{a_{10}^*}{\sqrt{|a_{10}|^2 + |a_{11}|^2}} \end{bmatrix} \quad (15.34b)$$

The situation becomes even more interesting when using a larger register such as a 3-qubit register having 8 basis states:

- Starting from state $|000\rangle$, a single bit rotation is operated on the 1st-qubit with the angle
$$\alpha_1 = \tan^{-1} \sqrt{\frac{|a_{100}|^2 + |a_{101}|^2 + |a_{110}|^2 + |a_{111}|^2}{|a_{000}|^2 + |a_{001}|^2 + |a_{010}|^2 + |a_{011}|^2}}$$
transforming the initialized state $|000\rangle$ to the state

$$\sqrt{|a_{000}|^2 + |a_{001}|^2 + |a_{010}|^2 + |a_{011}|^2} |000\rangle + \sqrt{|a_{100}|^2 + |a_{101}|^2 + |a_{110}|^2 + |a_{111}|^2} |100\rangle.$$

- Then, two controlled¹-rotations with angles

$$\tan^{-1} \sqrt{\frac{|a_{010}|^2 + |a_{011}|^2}{|a_{000}|^2 + |a_{001}|^2}} \text{ and } \tan^{-1} \sqrt{\frac{|a_{110}|^2 + |a_{111}|^2}{|a_{100}|^2 + |a_{101}|^2}}$$

operate on the 2nd qubit.

The resulting superposed state vector therefore becomes:

$$\begin{aligned} & \sqrt{|a_{000}|^2 + |a_{001}|^2} |000\rangle + \sqrt{|a_{010}|^2 + |a_{011}|^2} |010\rangle + \\ & \sqrt{|a_{100}|^2 + |a_{101}|^2} |100\rangle + \sqrt{|a_{110}|^2 + |a_{111}|^2} |110\rangle \end{aligned}$$

3. Finally, 4 controlled²-unitary transformations operate on the 3rd-qubit to generate the superposed state:

$$\begin{aligned} & a_{000} |000\rangle + a_{001} |001\rangle + a_{010} |010\rangle + a_{100} |100\rangle + \\ & a_{011} |011\rangle + a_{101} |101\rangle + a_{110} |110\rangle + a_{111} |111\rangle \end{aligned}$$

These 4 controlled²-unitary transformations are:

$$U_{\alpha^3,00} = \begin{bmatrix} \frac{a_{000}}{\sqrt{|a_{000}|^2 + |a_{001}|^2}} & \frac{a_{001}}{\sqrt{|a_{000}|^2 + |a_{001}|^2}} \\ \frac{a_{001}^*}{\sqrt{|a_{000}|^2 + |a_{001}|^2}} & -\frac{a_{000}^*}{\sqrt{|a_{000}|^2 + |a_{001}|^2}} \end{bmatrix}$$

$$U_{\alpha 3,01} = \begin{bmatrix} \frac{a_{010}}{\sqrt{|a_{010}|^2 + |a_{011}|^2}} & \frac{a_{011}}{\sqrt{|a_{010}|^2 + |a_{011}|^2}} \\ \frac{a_{011}^*}{\sqrt{|a_{010}|^2 + |a_{011}|^2}} & -\frac{a_{010}^*}{\sqrt{|a_{010}|^2 + |a_{011}|^2}} \end{bmatrix}$$

$$U_{\alpha 3,10} = \begin{bmatrix} \frac{a_{100}}{\sqrt{|a_{100}|^2 + |a_{101}|^2}} & \frac{a_{101}}{\sqrt{|a_{100}|^2 + |a_{101}|^2}} \\ \frac{a_{101}^*}{\sqrt{|a_{100}|^2 + |a_{101}|^2}} & -\frac{a_{100}^*}{\sqrt{|a_{100}|^2 + |a_{101}|^2}} \end{bmatrix}$$

$$U_{\alpha 3,11} = \begin{bmatrix} \frac{a_{110}}{\sqrt{|a_{110}|^2 + |a_{111}|^2}} & \frac{a_{111}}{\sqrt{|a_{110}|^2 + |a_{111}|^2}} \\ \frac{a_{111}^*}{\sqrt{|a_{110}|^2 + |a_{111}|^2}} & -\frac{a_{110}^*}{\sqrt{|a_{110}|^2 + |a_{111}|^2}} \end{bmatrix}$$

For notation purposes we use an “angle” to label a controlled k -operation. If the coefficients are all real, it reduces to an ordinary rotation angle. The notations of angles of the controlled k -rotations, the first subscript designates the target qubit order number and the subscripts following the comma designate the quantum states of the controlling qubits. For example, the 3 in $\alpha_{3,11}$ refers to the target qubit and the subscripts (11 in $\alpha_{3,11}$) refer to the controlling qubits. In the initialization, operations for the first $n-1$ qubits are controlled rotations where each rotation depends only on a single real parameter. The rotation angles take on the following general expressions. In the first qubit there is a 1-qubit

rotation. The rotation angle is: $\alpha_1 = \tan^{-1} \sqrt{\frac{\sum_{i_2 i_3 \dots i_n} |a_{1 i_2 i_3 \dots i_n}|^2}{\sum_{i_2 i_3 \dots i_n} |a_{0 i_2 i_3 \dots i_n}|^2}}$. In the 2nd

qubit, there are two controlled rotations:

$$\alpha_{2,0} = \tan^{-1} \sqrt{\frac{\sum_{i_3 i_4 \dots i_n} |a_{01 i_3 i_4 \dots i_n}|^2}{\sum_{i_3 i_4 \dots i_n} |a_{00 i_3 i_4 \dots i_n}|^2}} \text{ and } \alpha_{2,1} = \tan^{-1} \sqrt{\frac{\sum_{i_3 i_4 \dots i_n} |a_{11 i_3 i_4 \dots i_n}|^2}{\sum_{i_3 i_4 \dots i_n} |a_{10 i_3 i_4 \dots i_n}|^2}}.$$

In general, in the j^{th} -qubit, there are 2^{j-1} controlled $^{j-1}$ -rotations, with each of them having $j - 1$ controlling qubits labeled as $i_1 i_2 \dots i_{j-1}$. The rotation angle in the j^{th} -qubit ($j \neq n$) is given by:

$$\alpha_{j, i_1 i_2 \dots i_{j-1}} = \tan^{-1} \sqrt{\frac{\sum_{i_{j+1} \dots i_n} |a_{i_1 i_2 \dots i_{j-1} 1 i_{j+1} \dots i_n}|^2}{\sum_{i_{j+1} \dots i_n} |a_{i_1 i_2 \dots i_{j-1} 0 i_{j+1} \dots i_n}|^2}}. \quad (11.35)$$

For the last qubit, where $j = n$ we have 2^{n-1} controlled $^{n-1}$ unitary transformations where:

$$U_{\alpha_n, i_1 i_2 \dots i_{n-1}} = \begin{bmatrix} \frac{A_0}{\sqrt{|A_0|^2 + |A_1|^2}} & \frac{A_1}{\sqrt{|A_0|^2 + |A_1|^2}} \\ \frac{A_1^*}{\sqrt{|A_0|^2 + |A_1|^2}} & -\frac{A_0^*}{\sqrt{|A_0|^2 + |A_1|^2}} \end{bmatrix}$$

where $A_0 = a_{i_1 i_2 \dots i_{n-1} 0}$ and $A_1 = a_{i_1 i_2 \dots i_{n-1} 1}$.

If A_0 and A_1 are real, the operation is simply a rotation and the angle is given by:

$$\alpha_{n, i_1 i_2 \dots i_{n-1}} = \tan^{-1} \left(\frac{A_1}{A_0} \right). \quad (11.36)$$

We are now ready to initialize quantum superposition registers of three different types starting from the state $|0\dots0\rangle$:

- The evenly distributed state $|\psi\rangle = \sum_i |i\rangle$ is the most common state in quantum computing. The Hadamard-Walsh gate operation on each qubit generates this form of superposition from the state $|0\dots0\rangle$. In this particular case, all of the rotation angles are $\pi/4$. In each qubit, the controlling qubits use up all possible combinations and therefore the 2^{j-1} controlled Hadamard-Walsh gate operations are reduced to a single Hadamard-Walsh transformation in the j^{th} -qubit.
 - The Greenberger-Horne-Zeilinger or GHZ state is the maximally entangled state with the superposition $\frac{1}{\sqrt{2}}(|0\dots0\rangle \pm |1\dots1\rangle)$. Suppose we would like to transform the state $|0000\rangle$ to the state $\frac{1}{\sqrt{2}}(|0000\rangle + |1111\rangle)$.
- . The circuit below shows this diagrammatically:

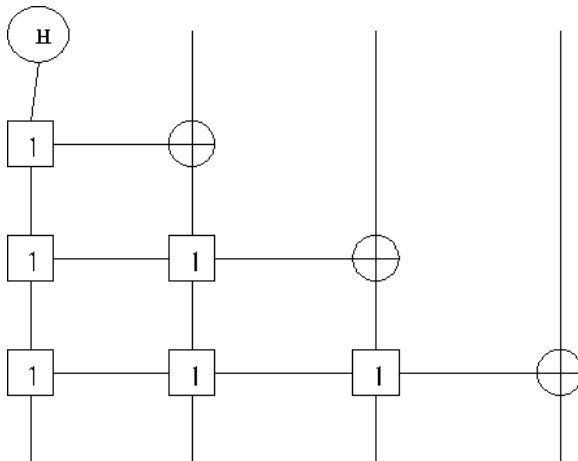


Fig. 15.30. Quantum Circuit for the GHZ state. Rotations can occur by utilizing the Hadamard-Walsh transformation.

The rotation in the 1st-qubit is the Hadamard-Walsh transformation. There are two controlled operations $\alpha_{2,0} = 0$ in the 2nd-qubit that are equal to the identity operation and so does nothing to the qubit. However,

$\alpha_{2,1} = \frac{\pi}{2}$ corresponds to the CNOT operation, so effectively, there is only one controlled-NOT gate in the 2nd-qubit. There are four gate operations in the 3rd-qubit. $\alpha_{3,11} = \frac{\pi}{2}$ is the $|11\rangle$ -CNOT gate and $\alpha_{3,00}$ is the identity operation. $\alpha_{3,01}$ and $\alpha_{3,10}$ are undetermined angles equal to $\frac{0}{0}$. Upon closer examination, however, these angles are equal to 0 and are therefore equal to the identity operation. Therefore, the only gate operation in the 3rd-qubit is the $|11\rangle$ -CNOT operation. Similarly, there is only the $|111\rangle$ -CNOT operation in the 4th-qubit. Should the circuit contain more than four qubits, the same analysis applies until the last qubit. For the last qubit, the rotation is either $\frac{\pi}{2}$ for the state $\frac{1}{\sqrt{2}}(|0\dots0\rangle + |1\dots1\rangle)$ or $-\frac{\pi}{2}$ for the state $\frac{1}{\sqrt{2}}(|0\dots0\rangle - |1\dots1\rangle)$.

3. In the Grover search algorithm [24], the state vector is built up in a two-dimensional space spanned by the so-called “marked” state $|\tau\rangle$ and the “rest” state $|c\rangle = \sum_{i \neq \tau} |i\rangle$. At any step in the search, the state vector has the form $|\psi\rangle = \sin \theta |\tau\rangle + \cos \theta |c\rangle$. In order to initialize such a superposed state, we let $|\tau\rangle = |i_1 i_2 \dots i_n\rangle$ be the marked state. We may now construct the state $|\psi\rangle$ from $|0\dots0\rangle$. The amplitudes a_i of the basis states $|\psi\rangle = \sum_{i=0}^{N-1} a_i |i\rangle$ are $a_\tau = \sin \theta$ and $a_i = \cos \theta / \sqrt{N-1}$ for $i \neq \tau$.

According to the following equation,

$$\alpha_1 = \tan^{-1} \sqrt{\frac{\sum_{i_2 i_3 \dots i_n} |a_{1 i_2 i_3 \dots i_n}|^2}{\sum_{i_2 i_3 \dots i_n} |a_{0 i_2 i_3 \dots i_n}|^2}}, \text{ the rotation angle in the 1st-qubit is:}$$

$$\alpha_1 = \begin{cases} \tan^{-1} \Omega_1, & \text{if } i_1 = 1 \\ \tan^{-1} \frac{1}{\Omega_1}, & \text{if } i_1 = 0 \end{cases} .$$

where $\Omega_1 =$

$$\sqrt{\frac{(N-2)\cos^2 \theta + 2(N-1)\sin^2 \theta}{N\cos^2 \theta}}$$

In the k^{th} -qubit, the angle for the $|i_1, i_2 \dots i_{k-1}\rangle$ -controlled rotation is therefore:

$$\alpha_{k,i_1,i_2 \dots i_{k-1}} = \begin{cases} \tan^{-1} \Omega_k, & \text{if } i_k = 1 \\ \tan^{-1} \frac{1}{\Omega_k}, & \text{if } i_k = 0 \end{cases} , \text{ where}$$

$$\Omega_k = \sqrt{\frac{(N-2^k)\cos^2 \theta + 2^k(N-1)\sin^2 \theta}{N\cos^2 \theta}} \quad (15.37)$$

A viable organic molecule, a Class II Mesoionic Xanthine, has been introduced as a potential 10-qubit register substrate for scalable quantum computing. We have shown that the ground state of this xanthine molecule exists in a superposition of ten unique wavefunctions. These unique wavefunctions can form the basis of 10-qubit registers for quantum computation. Additionally a formalism was devised whereby these registers may be efficiently initialized, subsequently read into and transformed via standard unitary algorithms. We propose that polar solutions of the mesoionic xanthines or small crystalline quantum dots may be suitable for I/O techniques. Furthermore, these solutions or quantum dots may be RF laser pulsed at a certain set of frequencies to produce a cumulative resonant interaction within the xanthines to exploit higher degrees of freedom resulting from new HD commutation rules. Relaxation of the numerous excited states via these HD commutation rules are putatively a vehicle to ontologically overcome the decoherence problem associated with QC applications [92,93]. This ability overcomes the major obstacle for bulk quantum computing.

15.14 Conclusions

The debate over the completeness of quantum theory has raged for nearly one hundred years. There is more to do; but in this volume we believe we will have brought it to its endgame experimentally. Completing QT to find a method for empirically surmounting the uncertainty principle has been no easy task. We have stated that bulk UQC cannot be achieved within the limits of Big Bang cosmology or the bounds described by the Copenhagen regime. Here we have produced a rudimentary path for the completion of QT through a model for the implementation of bulk UQC.

We doubt one can understand the ontology without sufficiently comprehending the new cosmology and have perhaps overdone the metaphors in hoping to facilitate this. We can only guess how difficult it will be to build a prototype utilizing our methodology. One could be like Edison trying 10,000 filaments (multiphase concatenation of resonant hierarchy coupling modes) and expect to achieve success with sufficient effort. Although this is not supposed to be necessary if our protocol is correct. Any style of sufficiently broad quantum system should be able to provide a vehicle for bulk implementation. DiVincenzo [78] has suggested five requirements the physical implementation of quantum computation:

- A physical system with scalable qubits
- Ability to initialize the qubit states
- Long decoherence times, longer than gate operation times
- Universal set of quantum gates
- Qubit measurement capability

We believe we have met these requirements and await the appearance of universal bulk quantum computing.

As a suggestion we have included what we believe to be a viable candidate organic molecule, that of the Class II Mesoionic Xanthine, because it has a potential scalable 10-qubit register substrate. Our general approach is based on a HD form of Dirac Spherical rotation in the context of a completed form of quantum theory able to ontologically surmount uncertainty. A formalism could be just as readily be designed around the nomenclature of the spacetime dynamics of M-Theory. Also our method could just as easily be translated into a form of Topological Quantum Field Theory (TQFT), which the brane-world closely resembles. This is also illustrated in the work of L.H. Kauffman, in papers such as [94] where he also integrates TQFT with knot theory for QC.

References

- [1] Moore, G.E. (1965) Cramming more components onto integrated circuits, *Electronics*, 38:8.
- [2] Amoroso, R.L. & Amoroso, P.J. (2004) The fundamental limit and origin of complexity in biological systems: A New model for the origin of life, in D.M. Dubois (ed.) CP718, Computing Anticipatory Systems: CASYS03-6th International Conference, Liege, Belgium, August 11-16, New York: American Inst. Physics 0-7354-0198-5/04.
- [3] Amoroso, R.L. (2002) Developing the cosmology of a continuous state universe, in R.L. Amoroso et al (eds.) *Gravitation & Cosmology: From The Hubble Radius to the Planck Scale*, Dordrecht: Kluwer.
- [4] Amoroso, R.L. (2006) Paradigm for the cosmology of a continuous state holographic conscious megaverse, in R.L Amoroso, B. Lehnert & J-P Vigier (eds.) *Extending the Standard Model: The Search for Unity in Physics*, Orinda: The Noetic Press.
- [5] Amoroso, R.L. (2008) Defining a context for the cosmology of awareness, in R.L. Amoroso (ed.) *The Complementarity of Mind and Body: Realizing the Dream of Descartes*, Einstein and Eccles, New York: Nova Science Publishers.
- [6] Antippa, A.F. & Dubois, D.M. (2004) Anticipation, orbital stability and energy conservation in discrete harmonic oscillators, in D.M. Dubois (ed.) Computing Anticipatory Systems, AIP Conf. Proceedings Vol. 718, pp.3-44, Melville: American Inst. of Physics.
- [7] Randall, L. (2005) *Warped Passages, Unraveling the Mysteries of the Universe's Hidden Dimensions*, New York: Harper-Collins.
- [8] Amoroso R.L. (2003) Awareness: physical cosmology of the fundamental least unit, *Noetic Journal* 4:1, 1-15.
- [9] Cramer, J.G. (1986) The Transactional Interpretation of Quantum Mechanics, *Rev. Mod. Phys* 58, 647-687.
- [10] Wheeler, J. & Feynman, R. (1945) Interaction with the Absorber as the Mechanism of Radiation, *Rev. Mod. Phys.* 17, 1578.
- [11] Holland, P.R. (2000) *The Quantum Theory of Motion: An Account of the de Broglie-Bohm Causal Interpretation of Quantum Mechanics*, Cambridge Univ. Press.
- [12] Vigier, J-P and Bohm, D., (1955) Model of the causal interpretation of quantum theory in terms of a fluid with irregular fluctuations, *Physical Rev.*, 96:1; 208-17.
- [13] Kaku, M. (1998) *Introduction to Superstrings & M-Theory*, 2nd ed., New York: Springer.
- [14] Amoroso, R.L., How to Build a Conscious Quantum Computer: The Immanent Era of Conscious Technologies, in process.
- [15] Kotigua, R.P. & Toffoli, T. (1998) Potential for computing in micromagnetics via topological conservation laws, *Physica D*, 120:1-2, pp. 139-161.
- [16] Penrose, R. (2005) *The Road to Reality*, New York: Knopf.
- [17] Peat, F.D. (1988) *Superstrings and the Search for the Theory of Everything*, Chicago: Contemporary Books.
- [18] Messiah, A. (1999) *Quantum Mechanics*, Mineola: Dover.
- [19] Atkins, P.W. (1994) *Molecular Quantum Mechanics*, Oxford: Oxford Univ. Press.
- [20] Brink, D.M. & Satchler, G.R. (1968) *Angular Momentum*, Oxford: Ox Univ. Press.
- [21] Bohm, D. (1989) *Quantum Theory*, New York: Dover.
- [22] Pauli, W. (1927) *Zeitschrift Physik*. 43: 601.
- [23] Schwinger, J. (1992) Casimir energy for dielectrics, *Proc. Nat. Acad. Sci. USA* 89, 4091-3.

- [24] Schwinger, J. (1993) Casimir light: The source, *Proc Nat Acad Sci USA* 90, 2105-6.
- [25] Schwinger, J. (1994) Casimir energy for dielectrics: spherical geometry, *Proc. Nat. Acad. Math. Psych.* 41:64-67, San Francisco: W.H. Freeman.
- [26] Amoroso, R.L. (2002) The physical basis of consciousness: a fundamental formalism, Part 1 *Noesis*, XXVI, Romanian Acad.
- [27] Jibu, M., & Yasue, K. (2005) *Quantum Brain Dynamics and Consciousness*, Amsterdam: John Benjamins.
- [28] Schiff, L.I. (1955) *Quantum Mechanics*, New York: McGraw-Hill.
- [29] Peebles, P.J.E. (1992) *Quantum Mechanics*, Princeton: Princeton Univ. Press.
- [30] Hatfield, B. (1992) *Quantum Field Theory of Point Particles and Strings*, Reading: Addison Wesley.
- [31] Feynman, R.P. (1948) Spacetime approach to non-relativistic quantum mechanics, *Rev. Mod. Phys.* 20:367-385.
- [32] Accardi, L. (1988) Foundations of quantum mechanics: A quantum probabilistic approach, in G. Tarozzi & A. van der Merwe (eds.) *The Nature of Quantum Paradoxes*, Dordrecht: Kluwer Academic.
- [33] Green, M.B., Schwarz, J.H. & Witten, E. (1987) *Superstring Theory V-1*, Cambridge: Cambridge Univ. Press.
- [34] Amoroso, R.L., Giandinoto, S. & Rauscher, E.A. (2008) Derivation of the string tension formalism, and super quantum potential as inherent parameters of a holographic conscious multiverse cosmology, in Cs. Varga, I. Dienes & R.L. Amoroso (eds.) *Unified Theories*, Oakland: The Noetic Press.
- [35] Rauscher, E.A. and Amoroso, R.L. (2008) The Schrödinger equation in complex Minkowski space, nonlocality and anticipatory systems, in D. Dubois (ed.) *Proceedings of CASYS07, IJCAS* Vo. 22, Liege, Belgium, August 2007.
- [36] Borne, T., Lochak, G. & Stumpf, H. (2001) *Nonperturbative Quantum Field Theory and the Structure of Matter*, Dordrecht: Kluwer Academic.
- [37] Chu, M-Y.J. & Amoroso, R.L. (2008) Empirical mediation of the primary mechanism initiating protein conformation in prion propagation, in D. Dubois (ed.) *Proceedings of CASYS07*, August, 2007, Vol. 22, Liege, Belgium.
- [38] Witten, E. (1996) Reflections on the fate of spacetime, *Physics Today*, pp. 24-30.
- [39] Wheeler, J.A. (1955) Geons, *Physical Review*, 97:2, 511-536.
- [40] Amoroso, R.L., Burns, J. & Rauscher, E.A. A relativistic approach to the arrow of time utilizing large size extra dimensions, in preparation.
- [41] Battey-Pratt, E.P. & Racey, T.J. (1980) Geometric model for fundamental particles, *Int. J. Theoretical Physics*, 19:6; 437-475.
- [42] Wolff, M. (1990) *Exploring the Physics of the Unknown Universe*, Manhattan Beach: Technotran Press.
- [43] Wolff, M. (2002) Cosmology, the quantum universe and electron spin, in R.L. Amoroso, G. Hunter, M. Kafatos & J-P Vigier (eds.) *Gravitation and Cosmology: From Hubble radius to the Planck scale*, *Proceedings of a symposium in Honour of the 80th Birthday of Jean-Pierre Vigier*, Dordrecht: Kluwer Academic Publishers.
- [44] Franck, G. (2000) Time and presence, in R.L. Amoroso, R. Antunes, C. Coehlo, M. Farias, A. Lieto & P. Soares (eds.) *Science and the Primacy of Consciousness: Intimation of a 21st Century Revolution*, pp. 187-189, Orinda: The Noetic Press.
- [45] Evans, M.W. & Vigier, J-P (1994) *The Enigmatic Photon; The Field B⁽³⁾*, Dordrecht: Kluwer Academic.
- [46] Stevens, H.H. (1989) Size of a least-unit, in M. Kafatos (ed.) *Bell's Theorem, Quantum Theory and Conceptions of the Universe*, Dordrecht: Kluwer Academic.

- [47] Meusnier, J. B. (1776) *Mémoire sur la courbure des surfaces*, *Mém. des savans étrangers* 10, 477-510, 1785.
- [48] Grotz, K. & Klapdor, H.V. (1990) The Weak Interaction in Nuclear, Particle and Astrophysics, New York: Adam Hilger.
- [49] Coles, P. & Lucchin, F. (2002) Cosmology, The Origin and Evolution of Cosmic Structure, Chichester: J. Wiley & Sons.
- [50] Narlikar, J.V. (2002) An Introduction to Cosmology (3rd Edition) Cambridge: Cambridge University Press.
- [51] Peebles, P.J.E. (1993) Principles of Cosmology, Princeton: Princeton Univ. Press.
- [52] Puthoff, H.E. (2002) Polarizable vacuum approach to General Relativity, in R.L. Amoroso, G. Hunter, M. Kafatos & J-P Vigier (eds.), Gravitation & Cosmology: From the Hubble Radius to the Planck Scale, pp. 431-446, Dordrecht: Kluwer Academic.
- [53] Vigier, J-P, & Amoroso, R.L. (2002) Can one unify gravity and electromagnetic fields? in R.L. Amoroso, G. Hunter, M. Kafatos & J-P Vigier (eds.) Gravitation and Cosmology: From the Hubble Radius to the Planck Scale, Dordrecht: Kluwer Academic.
- [54] Amoroso, R.L. & Vigier, J-P (2004) Toward the unification of gravity and electromagnetism, in V.V. Dvoeglazov & A.A. Espinoza Garrido (eds.) Relativity, Gravitation, Cosmology, New York: Nova Science.
- [55] Dirac, P.A.M. (1973) New ideas of space and time, *Naturwissen.* 32:6; 529-531.
- [56] Jackson, J.D. (1975) Classical Electrodynamics, 1st ed., New York: Wiley & Sons.
- [57] Baum, C.E. & Kriticos, H.N. (eds.) (1995) Electromagnetic Symmetry, Washington: Taylor & Francis.
- [58] Misner, C.W., Thorne, K.S., & Wheeler, J.A. (1972) Gravitation, San Francisco: Freeman & Company.
- [59] Schutz, B. (1980) Geometrical Methods of Mathematical Physics, Cambridge: Cambridge University Press.
- [60] Accardi, L., (1988) Foundations of quantum mechanics: A quantum probabilistic approach, in G. Tarozzi & A. van der Merwe (eds.) The Nature of Quantum Paradoxes, Dordrecht: Kluwer Academic.
- [61] Aharonov, Y. & Bohm, D. (1959) Physical Review 115, 485.
- [62] Shigley, J.E., and Uicker, J.J. Jr. (1980) Theory of Machines and Mechanisms, New York: McGraw-Hill.
- [63] Rauscher, E.A. (1983) Electromagnetic Phenomena in Complex Geometries and Nonlinear Phenomena, Non-Hertzian Waves and Magnetic Monopoles, Millbrae: Tesla Books; (2007) 2nd edition, Oakland: The Noetic Press.
- [64] Schwamb, P., Merrill, A.L. & James, W.H. (1930) Elements of Mechanism, New York: J. Wiley & Sons.
- [65] Feynman, R.P. (1966) The Feynman Lectures on Physics, Reading: Addison-Wesley.
- [66] Vlasov, A.Y. (1996) Quantum theory of computation and relativistic physics, in T. Toffoli, M. Biafore & J. Leao (eds.) Physcomp96, Cambridge: New England Complex Systems Institute; and additional material from private communication.
- [67] Dubois, D.M. (2001) Theory of incursive synchronization and application to the anticipation of delayed linear and nonlinear systems, in D.M. Dubois (ed.) Computing Anticipatory Systems: CASYS 2001-Fifth Intl Conference, Am Inst of Physics: AIP Conf. Proceedings 627, pp. 182-195.
- [68] Antippa, A.F. & Dubois, D.M. (2008) The synchronous hyperincursive discrete harmonic oscillator, AIP proceedings of CASYS07.
- [69] Dubois, D.M. (2008) The quantum potential and pulsating wave packet in the harmonic oscillator, proceedings of CASYS07, preprint.

- [70] Loudon, R. (1994) *The Quantum Theory of Light*, Oxford: Clarendon Press.
- [71] Kak, S. (1999) The initialization problem in quantum computing, *Foundations of Physics*, 29:2, 267-279.
- [72] Carruthers, P. & Nieto, M.M (1968) Phase and angle variables in quantum mechanics, *Rev. Mod. Physics*, 40:2; 411-440.
- [73] Bailey, T.N. (1982) Relative cohomology and sources on a line I & II, *Twistor Newsletter*, No. 14, pp. 9-15, 19-21.
- [74] Penrose, R, (1982) Real-space topology for advanced/retarded twistor functions, *Twistor Newsletter*, No. 14, pp. 16-18.
- [75] Giandinoto, S. & Amoroso, R.L. (2008) Class II Mesoionic Xanthines as Potential Ten-Qubit Quantum Computer Substrate Registers, in D. Dubois (ed.) *Proceedings of CASYS07*, IJCAS Vol. 22, Liege, Belgium.
- [76] Garcia-Ripoll, J.J., Zoller, P., & Cirac, J.I. (2005) Coherent control of trapped ions using off-resonant lasers, *Phys Rev A* 71, 062309.
- [77] Nielsen, M.A. & Chuang, I.L. (2000) *Quantum Computation and Quantum Information*, Cambridge: Cambridge University Press.
- [78] DiVincenzo, D.P. (2008) *The Physical Implementation of Quantum Computation*, arXiv:quant-ph/0002077v3.
- [79] Mbagwu, G.O., Bass, R.G. & Glennon, R.A. (1985) *J. Heterocyclic Chem.*, 22, 465.
- [80] Mbagwu, G. O., Bass, R. G. & Glennon, R. A., *Org. Magn. Reson.*, 21, 527, (1983).
- [81] Rogers, M.E., Glennon, R.A., Bass, R.G., Mbagwu, G.O., Smith, J.D., Boots, M.R., Nanavati, N., Maconaughey, J.E., Aub, D. & Thomas, S. (1981) *J. Med Chem.*, 24, 1284.
- [82] Mbagwu, G. O. (1982) *Diss. Abs. Int.*, B42 4428.
- [83] Mbagwu, G. O., Bass, R. G. & Glennon, R. A., Virginia (1980) *J. Sci.* 31, 113.
- [84] Mbagwu, G. O., Bullock, B., & H. O., Greer, (1988) *J. Hetero. Chem.*, 22, 475.
- [85] Mbagwu, G.O. & Garland, R. (1988) *J. Heterocyclic Chem.*, 22, 571.
- [86] Giandinoto, S., Mbagwu, G. O., Robinson, T. A., Ferguson, C., Nunez, J., (1986) *J. Heterocyclic Chem.*, 33, 1839.
- [87] Coburn, R. A., (1971) *J. Heterocyclic Chem.*, 8, 881.
- [88] Coburn, R.A., Carapellotti, R.A. & Glennon, R.A. (1973) *J. Hetero. Chem.*, 10, 479.
- [89] Ventura, D. & Martinez, T. (1999) *Found. Phys. Lett.*, 12, 547.
- [90] Gui-Lu Long & Yang Sun, (2007) Efficient scheme for initializing a quantum register with an arbitrary superposed state, arXiv:quant-ph/0104030v1.
- [91] Barenco, A., et. al. (1995) *Phys. Rev.* A52, 3457; *Proc. R. Soc. London*, A449, 679.
- [92] Grover, L.K. (1997) *Phys. Rev. Lett.*, 79, 325.
- [93] Amoroso, R.L. (2007) Universal quantum computing: anticipatory parameters predicting bulk implementation, in D. Dubois (ed.) *Proceedings of CASYS07*, IJCAS Vol. 22, Liege, Belgium.
- [94] Kauffman, L.H. & Lomonaco, S.J. (2007) q-Deformed spin networks, knot polynomials and anyonic topological quantum computation, arXiv:quant-ph/0606114v3.

Index

- 12D hyperspace, 65, 415
1st person – 3rd person barrier, 108
Aaronson, S., vi, 45, 479, 481, 486, 496, 498, 499
Abdollahi, A., 58, 61
Abelian anyons, 383, 449, 450
Absolute Space, 65, 70, 72-76, 95, 112, 118, 130, 209, 419, 422, 431, 433, 547, 550-1, 556
Absolute truth, 250
Absolute zero, 14, 23, 296
Additional dimensions, 65, 108, 131, 178, 187, 218, 220, 223, 241, 252, 288-9, 300, 321, 336, 404
Adiabatic/Adiabatic Quantum Computing, 6-7, 14-15, 42, 388, 391, 397, 443-4, 449, 472, 539
 AdS^5 , 128, 192, 367, 551
Age of discovery, vi, xiii, 40, 180, 184, 319, 400, 438
Aharonov-Bohm effect, 64, 193, 251, 403
Alexander polynomial, 370, 371
Alexander's horned sphere, 232, 235, 469-471, 474
Alexander-Conway polynomial, 370, 371
Algorithms, v, viii, xii, xiii, 1, 3, 15, 22-3, 31-2, 35, 37-8, 46, 56, 172, 177, 285, 296, 328-9, 346, 348-50, 475-500, 501, 503, 532, 534, 578, 580, 587-8
Allegory of the cave, 107
Amoroso, R.L., xii, 41, 44, 124-9, 198, 356-63, 422, 554, 564, 577
Amphichiral knots, 372-3, 393
Amplituhedron, viii, 246, 256, 284, 329, 439, 467-8, 473, 485-7, 491, 496, 499
Ancilla modes, 27, 28
Andrianov, 24, 43,
Anthropic Cosmology, 67, 82, 83, 96, 300
Anthropic Principle, 67, 83, 90, 93, 97, 98, 125
Anticommutative, 134, 135, 195-201, 204, 207, 209, 210, 217, 541, 565, 573
Anticommute, 93, 200, 208, 512
Antispace, 94, 132-136, 150-1, 157, 188-9, 193-4, 198-201, 216, 227, 243, 256, 322-3, 343, 352-3, 355, 534
Anyon braid topology, 440, 451,
Anyons, 33-5, 295, 359, 364, 382-3, 386, 390, 392-4, 449-51, 471,
Arrow of time, 66, 77-8, 95, 103-108, 115, 118-9, 126, 128, 181, 287, 302, 308, 314, 317, 400, 410, 415, 419-20, 432, 434, 550, 555-6, 563, 565, 591
Artin braid group, 122, 429
Atemporal realm, 139
Awareness, 74, 83, 103-6, 108, 112-4, 116, 119, 231, 300-1, 356, 399, 418, 420, 424, 432-3, 590

- Babbage, P., 46,
Baez, J., 195, 210, 378, 381, 473,
500,
Bancos ghost, 207
Beat frequency, 81, 108, 115, 117,
151, 156, 187, 226-30, 242, 269,
274-6, 288, 298, 308, 313, 316-7,
330, 333-4, 336, 343, 351, 353,
432, 577
Bell's inequalities, 3, 125, 177, 180,
235, 246, 248, 286, 330, 361, 410,
413, 419, 501,
Benioff, J., 38, 41,
Berry phase, 133, 392, 442-4, 453,
472
Bessel function, 195, 225, 258, 340,
343-6, 567, 568
Bessel oscillation, 228
Bianchi identities, 95, 111, 114, 119,
120, 420-1
Big Bang, 62-5, 67-8, 70, 74-7, 80-1,
91, 96, 98, 104, 128, 193-4, 269,
290, 300-1, 589
Black hole, 68-70, 125, 310, 380,
Blackbody radiation, vi, 63, 70, 81,
126, 336, 354, 362, 400
Bloch sphere, ix, x, 2, 3, 37, 44, 49,
52, 57, 62, 151, 161-2, 164-5, 169,
189, 294, 308, 312, 330, 451, 523,
534
Bohm, D., xii, 37, 64, 69, 79, 89, 96,
102-3, 114, 122, 127, 129, 144-5,
147-9, 158, 173, 177-8, 183, 191,
193, 220, 241, 249, 251-2, 257,
283, 284, 286, 288, 291, 299, 300,
302, 307, 313, 316, 321, 333, 358,
399, 403-4, 410, 428, 430, 437,
443-4, 450-1, 488-9, 490-2, 540,
564
Bohr magneton, 11
Bohr orbits, 184, 192, 224, 226, 303,
314, 321, 339,
Bohr radius, 19, 223, 339
Boltzman's constant, 31
Boolean function, 35, 46, 60, 479,
484
Born-Sommerfeld model, 144, 225,
258, 340, 469
Bose-Einstein Condensate, four, 23-
4, 43, 539
Braid crossover, 384
Braid group, 122, 130, 429, 436
Braid twists, 34,
Brane topology, v, vii, ix, xii, 37,
153, 160, 185, 191, 209, 236, 240-
1, 243, 246-7, 249, 251, 264, 288,
302, 321-3, 352, 365, 403, 404
Braneworld, 63, 209, 290, 297
Bravais lattice, 258, 285
Buckyball, 13, 14
Burell, S., 29, 44
Burns, J.E., 115, 116, 126, 128, 287,
434, 591
Calabi-Yau, x, xii, 37, 78, 84-5, 96-7,
99, 109, 123, 131, 152, 155, 157,
160, 174, 185, 189, 191, 194, 198,
208-10, 216, 220-1, 234-7, 240-2,
244, 248-9, 258-9, 279, 290-1,
298, 303, 307-8, 311-3, 316, 321,
337, 342, 352-4, 358, 410, 430,
437, 448, 534, 537, 550-1, 565
Carbon nanotube, 14
Casimir boundary conditions, 64, 95,
155-6, 170, 193, 251, 256, 258,
544, 556
Casimir mirror, 492
Catastrophe theory, 117, 256-64,
285-86, 356, 571
Cauchy-Riemann equations, 46, 409,
411-12
Causal separation, 65, 69, 76, 205,
292, 541-2, 547
Cavity-Quantum Electrodynamics,
273, 304,
CERN, v, vii, xii, 37, 92, 132, 218,
223, 247, 314, 336, 496
Chantler, J., 223-4, 235, 338-9,
362

- Charge, 7, 10, 15, 25, 30, 94, 108, 116, 131-5, 138, 142, 156, 187, 223
- Chern-Simons, 257, 285, 366-7, 380, 448, 473,
- Church-Turing principle, 38-9, 41, 45, 180, 326, 477, 497, 498
- Class II Mesoionic Xanthine, xi, 172, 501-533, 577-80, 588-9,
- Classical Mechanics, vi, ix, 39, 123, 183, 193, 236, 309, 319, 326, 400, 424, 431
- Clifford algebra, 133-5, 153, 155, 157, 195, 210, 222, 224, 230, 255-6, 258-9, 280, 322, 339, 343, 352-3, 466, 534
- Close pack, 77, 81, 109, 155, 157, 188, 191-2, 202, 226, 243, 308, 311, 320, 322, 334, 340, 416, 551, 559, 564-7
- Cluster-State, 5, 6, 41, 42, 398
- CNOT gate, 17, 21, 22, 26-8, 52-4, 58-60, 507, 531, 587
- Cobordism, 155, 375-9, 447, 458-61
- CODATA, 250
- Coherent control, xii, 172, 229, 230, 273, 276-7, 286, 313, 324, 410, 501, 537, 540, 556, 564, 572-73, 578, 593
- Commutation relation, 170, 309, 511-15, 552
- Commutative, 134-6, 138, 142, 195-201, 203-4, 207, 209-11, 213, 216-7, 459, 464, 495, 512-14, 541, 564-67, 572-73
- Compactification, 65, 70, 77, 79-82, 84-5, 91, 95, 97-99, 106, 108, 113, 115-19, 123-25, 184-85, 187, 191, 216, 221, 245, 257, 263-64, 275-76, 289-91, 303, 323, 418-20, 430-31, 433, 471, 547-50, 552, 563, 565, 567, 573
- Complementarity, 65, 73, 103, 106-9, 111-12, 125, 247, 356-59, 543, 559, 573, 590
- Complex 8-space, 218-20, 280, 337, 352, 404-7, 411, 413, 534
- Complex numbers, 3, 134, 162, 171, 195, 211, 213-16, 327, 465, 487, 495, 501-3, 508, 523, 538, 578, 580
- Complex plane, 165, 213-4, 216-7, 275, 305, 405, 411, 413, 415, 440, 442
- Complex space, 1, 214, 217, 219, 301, 337, 405, 413
- Complex vector space, 3, 36, 164
- Conformal Field Theory, 297, 367
- Continuous-State, 37, 63-4, 69, 70, 75, 77-80, 82, 91-99, 101-6, 109, 113-5, 117, 119, 128, 144, 149, 151, 155, 183-5, 187, 190, 191, 194, 197, 198, 213, 215-17, 219-222, 224, 226-30, 242, 245, 247, 249, 252, 256, 258, 263, 264, 269, 273-81, 290, 298, 301-3, 312-4, 333-42, 351, 354, 404, 418, 420, 428, 431, 537, 541-3, 547-77
- Conway's skein relations, 257, 370, 371, 373, 392
- Cooper pairs, 23, 42
- Copenhagen interpretation, 3, 49, 64, 74, 78, 80, 93, 96, 98, 113, 114, 122, 123, 143, 144, 146, 147, 160, 174, 179, 180, 193, 221, 237, 238, 241, 246, 250, 269, 291-2, 300, 314, 330, 400, 414, 426, 430, 439, 541, 547-8, 559, 571-2, 578, 589
- Copernicus, 67, 68, 399, 497
- Correspondence Principle, 326, 327
- Cosmological Least-Unit, 77, 95, 263-5, 302
- Cosmology, vii, ix, x, xi, 62-125, 160, 183, 187, 190, 193-4, 197-8, 202, 210, 213, 219, 220, 224, 226, 228, 230, 246-8, 251, 263-5, 269,

- 272-3, 276-9, 290-2, 300-4, 308, 316-9, 322, 334, 337, 339-40, 367, 399, 403, 410, 417-9, 574-589
Coulomb force., 19, 335, 354
Coulomb interaction, 33, 141
Cramer transaction, xii, 37, 77, 79, 82, 244, 248, 278-9, 291, 301-2, 324, 410, 549, 567
Creation operators, 140, 171, 266, 317, 569
Crossing change, 213, 215-6, 373, 393
Crossover links, 373-4, 462
Cryogenic, v, 33, 236, 296, 364, 451
Cyclically commute, 352
Dark energy, 69, 70, 81, 83, 89, 91, 95, 101, 132, 227, 341
Database search, xi, 498
de Broglie, L., xii, 30, 37, 64, 69, 79, 89, 96, 102-3, 114, 122, 124, 143-8, 183, 187, 191, 198, 220, 241, 244, 249, 252, 257, 274, 278-9, 288, 291, 299, 300, 302, 313, 314, 316, 321, 333, 399, 404, 410, 426, 428, 430, 432, 437, 484, 490, 540, 549, 554, 564
Decoherence, v, vi, xi, xii, 1, 3, 9, 10, 16, 20, 24, 33, 35, 36, 160, 164, 172, 175, 185, 207, 222, 236-7, 243, 258, 295-6, 309, 313, 326, 382-3, 387, 393, 501, 538, 578, 588-9
Decoherence time, 3, 9, 10, 20, 33, 236, 243, 538, 589
Deficit angle, 77, 79, 81, 91, 95, 96, 99, 106, 108, 113, 119, 191, 345, 420, 421, 444, 457, 560, 573
Degenerative neuropathies, 281
Destructive interference, 30, 272, 281, 292, 316, 334, 410, 432, 441
Deutsch, D., 5, 38, 39, 41, 172, 180, 476-8, 497, 501, 578
Differential topology, 461, 462
Dimensional reduction, 65, 77, 79, 81, 82, 84-6, 89, 91, 95-6, 98, 101, 106, 108, 113, 116, 119, 185, 187, 191, 216, 219, 221, 243-5, 263, 290-1, 299, 303, 420, 422, 431, 448, 495, 550, 563, 567
Dirac aether, 283, 335, 353, 358
Dirac equation, 133, 138, 139, 141, 157-8, 179, 234, 252-5, 284, 356, 434, 545, 549, 572
Dirac polarized vacuum, 80, 81, 108, when 83, 187, 194, 221, 229, 250, 265, 288, 315, 316, 334, 341, 355, 403
Dirac spherical rotation, 95, 120, 121, 123, 203, 216, 264, 278, 417, 426, 429, 431, 543, 550, 552, 563, 572, 573, 574, 577-8, 589
Dirac string trick, 121, 429
Dirac vacuum, 64, 75, 87, 99, 115, 193, 221, 233, 241, 244, 251, 263, 362, 357, 403, 410, 434, 557-9, Di Vincenzo, D.P, 3, 20-2, 41, 589
Dodecahedral wrap-around, 192, 367
Dodecahedral involute, 190, 312
Domain wall, 81, 102, 107, 109, 114, 145, 249, 258, 269, 305, 323, 432, 572
Donor electrons, 9, 10
Doppler effect, 75, 565
Doppler recession, 70
Doppler redshift, 69
Double-cusp catastrophe, 256, 260-3, 285, 356, 571
Double-slit experiment, 146, 238, 291, 313
Dubois, D., 125, 126, 225, 256, 266-8, 272, 285, 315, 317, 334, 344, 346-8, 356, 361, 363, 435, 535, 569, 570, 590-3
D-Wave, vi, 7, 8, 15, 539
Eddington, A., 230, 301
Eigenstates, 2, 9, 23, 165, 169, 170, 173, 176, 245, 331, 444, 522

- Einstein, A., ix, 4, 23, 24, 35, 43, 64-6, 70-6, 79, 81, 83, 85-9, 92-4, 97, 100, 102, 103, 107, 109, 111, 124, 131, 139, 143, 145, 147, 184-6, 190, 213, 247, 248, 265, 291, 296, 318-20, 327, 382, 390, 407, 419, 422, 431, 437, 497, 539, 542, 550, 553, 554, 564
- Electrode array, 11
- Electron bubbles, 12
- Electron spin, 10, 12, 13, 18, 21, 36, 42, 277, 292, 362, 539, 591
- Electron spin resonance, 13, 539
- Electrostatic potentials, 533
- Empirical protocol, 123, 155, 235, 237, 241, 250, 290, 292, 298, 299, 301, 431, 559
- Empirical tests, xi, 73, 91, 304, 311, 326
- Energy dependent spacetime, 81, 86, 88, 247, 291, 540
- Energy gap, 24, 32, 385, 390,
- Energyless process, 439
- Entelechies, 148
- Epi-ontic, 3, 180, 246, 439
- Epistemic, 3, 180, 246, 439, 469
- EPR Correlations, viii, 13, 14, 27, 60, 108, 177, 179, 182, 309, 319, 329, 362, 424, 491, 540, 550
- EPR pairs, 13, 488
- ESR spectroscopy, 4, 13, 22,
- Eternal now, 86, 108, 109
- Euclidean 3-space, x, 37, 41, 65, 149, 151, 156, 178, 188, 189, 191, 213, 231, 242, 256, 309, 312, 323, 352, 399, 466, 469
- Euler angles, 2
- Exciplex, 102, 152, 190, 229, 230, 256, 302-5, 307, 308, 312-4, 318, 319, 321-3, 550
- Exciplex complex, 230
- Exciton, 19, 30
- Fabry-Perot, 29, 449
- Fabry-Perot interference, 449
- Fano plane, 212, 464, 465-6, 493-5, 500
- Fano snowflake, xiii, 212, 352, 416, 466, 473, 495
- Fermi-Dirac statistics, 112, 390
- Fermionic point particle, x, xii, 131, 132, 217, 247, 302, 305, 322, 329, 468, 568, 591
- Fermionic singularity, x, xii, 133, 146, 280
- Feynman, R.P., ix, x, xii, 1, 37, 39, 41, 60, 64, 76, 81, 83-5, 91, 109, 116, 119, 160, 183, 185, 233, 242, 247, 261, 280, 291, 305, 324, 365, 400, 403, 420, 422-6, 431, 450, 476, 485, 487, 497, 537, 540, 547, 550, 565
- Fine Structure, 67, 195, 222, 250, 329
- Fine-tuned laws of physics, 63, 65, 66, 69, 76, 91, 183, 227, 341
- Flag manifold, 262, 323, 325, 361
- Floating-point operations, 2
- Flux qubits, 7, 8
- Force of coherence, 79, 117, 148, 153-6, 160, 185, 187, 220, 241, 244, 256-9, 262, 263, 274, 288, 291, 306, 313, 317, 319, 323, 338, 403, 410, 437, 439, 458, 492
- Fourier analysis, 490
- Fractional quantum Hall Effect, 33, 44, 364, 382, 383, 390, 394-7, 449
- Fredkin Gate, 54, 55, 57
- Fullerene, 4, 13, 14, 42, 539
- Fundamental noumenon, 112, 356, 379
- Furey's particle zoo, 464
- Fusion Power, xii, 119, 192, 234, 278, 362, 390, 458
- Future-past, 64, 65, 76, 77, 79, 82, 84, 85, 95, 109, 117, 118, 152-4, 194, 210, 217, 227, 244, 248, 251, 263, 265, 267, 278-80, 314, 323,

- 342, 403, 409, 410, 413-31, 541, 548-51, 556-7, 563, 573
Future-past parameters, 244, 251, 263, 403
Future-past transaction, 79, 95, 549, 557
Galileo, xv, 67
Gallium arsenide, 20, 383
Gamma matrix, 188
Gating mechanism, 132, 217, 230, 249, 299, 304, 308, 311, 314, 317, 319, 321, 323, 324, 333, 336
Gauge group, 71, 72, 126, 287, 447, Gauge symmetry, 72, 100, Gauge Theory, 77, 92, 94, 142, 193, 250, 315, 423
Gauge transformations, 365
Genus-1 helicoid, 97, 98, 153, 258, 415, 551, 552, 563, 565
Geometric phase, 392, 393, 443, 444
Geometrodynamics, 103, 129, 159, 357
Geon, 77, 78, 89, 90, 95, 99, 107-9, 126, 265, 415, 424, 435, 550, 591
Giandinoto, S., 357, 502, 534-6, 578, 591, 593
Gödelizing, 329
Gödel's incompleteness theorem, 96, 127
Golem, 155, 460
Golem cobordism, 460
Googolplex, v, 68, 91, 192, 290, 301
Graviton, 77, 90, 95, 110, 264, 321, 432, 437
Gromov-Witten invariants, 366, 448
Ground state, 3, 6-8, 23, 33, 71, 230, 294, 303, 304, 318, 327, 384-7, 390, 393, 409, 418, 488-90, 503, 510, 515, 522, 534, 569, 588
Group Theory, 35, 122, 163, 429, 438
Grover search algorithm, 532, 587
Hadamard gate, 5, 50, 56-8, 331, 478, 506, 523
Hadamard-Walsh gate, 586
Hadamard-Walsh transformation, 525, 531, 586
Hamed, N-A, viii, 128, 284, 356, 473, 485, 499
Hamiltonian, 7-11, 20, 31, 41, 49, 176, 238, 241, 251, 263, 265, 271, 272, 298, 331, 384, 390, 404, 443, 444, 520-3, 543, 569
Harmonic oscillator, 171, 256, 265, 277, 280, 285, 335, 345-53, 361, 416, 432, 556, 568-72, 590
Harmonic superspace, 83, 84, 548, 550
Hawking, S., 96, 125, 127, 380, 399
Helicoid, 97, 98, 153, 258, 415, 551, 552, 563
Heliocentricity, 68, 148
Hermitian conjugate, 508, 509
Hermitian operator, 170, 175, 176, 442, 522
Heterostructures, 12, 20, 173, 385
Heterotic strings, 100, 128, 549
Hidden variables, 41, 103, 158, 177, 330
Hierarchy problem, 93, 101, 290, 356
Higgs mechanism, 93-6, 143, 218, 336
Hilbert space, ix, 2-4, 36, 46, 62, 161-4, 166, 170, 176, 292, 332, 378, 443, 451, 460, 468, 509
Hipparchus, 68, 399
Holant problem, 482, 483, 499
Hologram, 68, 69, 108, 125, 435, 482
Holographic algorithm, 482-4, 491, 499
Holographic Multiverse, 69, 91, 95, 97, 187, 219, 224, 226, 265, 337, 339, 340, 432
Holographic reduction, 475, 482, 483, 499
Holomorphic Chern-Simons theory, 448

- Holophote, 109, 113, 115-7, 275, 303, 305, 308, 313, 316, 317-23, 432
- Homeomorphic manifold, 86
- Homeomorphisms, 175, 364, 375, 377, 471, 474
- Homomorphism, 483
- Hopf link, 372, 381, 463
- Hubble radius, 75, 78, 83, 89, 124, 126-8, 219, 284, 283, 286, 300, 337, 361, 362, 435, 538, 590-2
- Hubble sphere, 63, 65, 69, 76, 91, 97, 183, 187, 227, 300, 341, 485
- Huygens, 74, 109, 114, 117
- Hybrid quantum computer, 10
- Hypercube, 111, 155, 156, 201, 212, 217, 220, 244, 299, 341, 342, 428, 542, 572
- Hyperincursion, 262, 267, 334, 569
- Hyperspherical volume, 310, 323, 345
- Hypervolume, 156, 194, 305, 310, 321
- Hypotheses non Fingo, vi, 437
- Hysteresis loop, 94, 96, 119, 156, 190, 257, 263, 281, 303, 305, 308, 312, 317-9, 321, 322, 354, 355, 420, 428
- Idempotent, 195, 202, 204
- Incursive oscillator, 126, 195, 225, 256, 268, 272, 275, 285, 315-7, 334, 344, 346, 361, 568, 570
- Initial state, 5, 7-9, 22, 34, 245, 384, 449, 520
- Instantaneous algorithm, viii, xiii, 177, 475, 488, 491, 497
- Interaction-Free Measurement, xii, 34, 147, 159, 236-8, 282, 284, 291, 358, 359, 400
- Interference patterns, 69, 144, 146, 147, 449, 482,
- Ising model, 94, 95, 97, 98, 111, 155, 256-8, 276, 382, 422, 429, 431, 552, 558
- Jafarizadeh, M.A. & Mahdian, M., 172, 173, 181, 284, 472
- Jeong, H., 20, 43
- Jones polynomial, 366, 372, 373, 375, 380, 392
- Josephson junction, 7, 14
- Kafatos, M., 114, 124-8, 226, 235, 283, 286, 287, 340, 358, 434, 591
- Kahler manifold, 98, 123, 249, 303, 334, 430, 447
- Kaluza-Klein, 78, 85, 86, 98, 123, 142, 186, 258, 340, 360, 430
- Kaluza-Klein theory, 71, 72, 81, 125, 185, 188, 236, 286, 290, 413, 427
- Kantian antinomy, 63, 92
- Kauffman, L.H., 122, 215, 233-5, 357, 368, 429, 430, 453, 589
- k*-dimensional subspace, 506, 518
- Kitaev, A., 34, 44, 382, 385, 394, 398, 445
- Klein bottle, 94, 123, 221, 275, 337, 342, 430
- Knotted shadow, 149, 154, 189, 374, 492
- Kowalski, G., 303, 335, 361
- Lagrangian, 72, 298, 544
- Larmor precession, 295
- Larmor radius, 72, 78, 79, 86, 187, 226, 227, 230, 269, 340, 341, 566
- Laser Oscillated Vacuum Energy Resonator, 272, 274, 28
- Lattice gas array, 94, 248, 255-7, 263, 404
- LCU, 63, 65, 68, 81, 82, 95, 106, 109, 117, 120, 155-7, 179, 187, 188, 190-4, 216, 222-30, 248, 261, 301-8, 320, 323-35, 341, 404, 420, 492, 549, 559, 565
- Least Cosmological Unit, *See* LCU
- Leibniz, 46, 63, 74, 159,
- Leuenberger, A., 22, 43
- LHC, v, 96, 101, 132, 289, 314, 336, 496
- Lightcone, 75, 117, 154, 163, 563

- Line element, 71, 84, 88, 165, 186, 187, 195, 197, 203, 214, 228, 249, 250, 280, 401-3, 422, 427, 553, 554
- Linear algebra, 46
- Linear transformation, 48, 167
- Linked cluster theorem, 449-51
- Locality, v, ix, x, 3, 36, 105, 141, 161, 179, 180, 242, 246, 256, 309, 439, 468, 475, 486,
- Locality postulate, 179
- Logarithmic spiral, 258, 351, 352, 552, 565, 566
- Logic gates, v, x, xi, 1, 5, 7, 17, 21, 34, 46-61, 256, 313, 383-5, 534, 539
- Lorentz boost, 81, 166, 170, 426-7, 565
- Lorentz contraction, 405
- Lorentz invariance, 180
- Lorentz transformation, 87, 102, 164, 167, 173, 179, 214, 313, 339, 342, 401-8, 423, 427, 543
- Lorentz-Poincaré transform, 403, 417, 421, 426
- Loss, D., 20-4, 42, 43
- Lowest Bohr orbit, 184, 192
- LSXD, xi, 37, 65, 72, 78, 80, 95, 118, 144, 155, 184, 187-93, 197, 224,
- Mach's Principle, 77, 274
- Mach-Zehnder interferometer, 238, 239, 292, 400
- MacKinnon, K., 432, 436
- Magnetic anisotropies, 23, 25
- Magnons, 24, 43
- Majorana fermion, 33, 234
- Majorana zero modes, 33, 44
- Manifold of uncertainty, 78, 147, 152, 155, 156, 174, 188, 189, 193, 224, 228, 229, 231, 249, 288, 290, 310, 311, 319, 322, 327, 333-6, 343, 437, 484, 567
- Many Worlds Hypothesis, 245
- Many-Worlds' interpretation, 66, 239, 240
- Mass, 63, 64, 69, 70, 75, 77, 81, 83, 88, 92, 95, 99, 101, 115, 117, 118, 124, 131, 134, 135, 138, 139, 141, 143, 168-70, 187, 193, 250, 266, 277, 279, 297, 329, 341, 346, 354, 400, 407, 446, 497, 544, 557, 560
- Measurement, vii, xi, xii, 3-9, 16, 20, 25, 34, 38, 60, 70, 86, 105, 112, 113, 122, 144, 147, 159, 175-80, 232, 236-41, 250, 269, 281-4, 288-355, 380, 386-9, 399, 430, 476, 478, 497, 520, 570, 589
- Micromagnetic, 244, 251, 298, 359, 403, 544, 572
- Microphysics, 114
- Mind-body problem, 319
- Minkowski space, x, 65, 70, 76, 81, 84, 86-8, 165, 184, 193, 219, 224, 236, 247, 251, 278, 290, 301, 307, 319, 337, 339, 365, 403, 415, 422, 542, 551, 568, 571
- Mirror symmetry, x,xii, 37, 79, 84, 92, 95-7, 118, 156, 194, 208-9, 221, 240, 248, 279, 290, 299, 313-6, 353-4, 410, 420, 425, 428, 437, 448
- Mirrorhouse, 204-8
- Möbius strip, 454
- Möbius transformation, 216, 217
- Moore's Law, 36, 538-40
- Morello, J.D., 21
- MOU *See* Manifold of uncertainty
- M-Theory, viii, x, xii, xiii, 37-9, 66, 80, 83, 91, 93-100, 160, 186, 192, 221, 226, 241, 249, 253, 263, 273, 291, 299, 303, 319, 340, 425, 537, 540, 550, 565, 568
- Multiverse, x, 62-124, 148, 155, 183, 187, 191-4, 198, 213, 215, 224, 227-30, 246, 251, 265, 279, 290, 300, 336-41, 356, 367, 400, 410, 425, 431-3, 540, 554-6, 574

- Mysterium Cosmographicum, 40, 45
 Nanowire, 20, 33
 Narlikar, J., 101, 592
 n -bit register, 5
 Necker cube, 149, 203, 207, 298,
 306-8, 322, 451, 454-6, 466, 491
 Nested Hubble spheres, 63, 69,
 73, 76, 91, 183, 187, 227, 300,
 341
 Neutral Kaons, 105
 Neutrinos, 91, 92, 101, 127, 132,
 168, 278
 Newton, I., vi, vii, ix, 37, 63, 72,
 123, 147, 152, 185, 233, 274, 357,
 419, 431, 437, 471, 551, 554, 564,
 569
 Newtonian, 64, 70, 73-5, 88, 103-5,
 118, 131, 187, 192, 236, 246, 292,
 401, 419, 425, 484, 542
 Nilpotent, 133, 134, 139-43, 157,
 158, 178, 188, 189, 195, 198-200,
 202, 204, 209, 218, 222, 229, 243,
 249, 250, 319, 403, 404, 432
 Nitrogen-vacancy, 18
 NMR, 4, 9, 13, 25, 31, 172, 269, 294,
 316, 335, 487, 504, 572
 NMR quantum computing, 4, 30-3,
 44, 172, 501, 578
 No-cloning theorem, 3, 41, 60, 177,
 180, 233, 328, 330-3, 363, 469,
 478, 487, 497
 Noeon, 77, 89, 90, 95, 108-10, 116,
 155, 190, 264, 275, 281, 303,
 305-8, 311-3, 316-25, 345, 551
 Noetic equation, 77
 Noetic Interferometer, 270, 271, 273,
 316
 Noetic superspace, 84-86, 88
 Non-Abelian anyons, 359, 364, 382,
 383, 394, 471
 Nonconserved, 134
 Nondeterministic, 27
 Non-Erasure' theorems, 49, 333, 382,
 400
 Nonlocality, 141, 177, 485, 490, 492,
 540, 550, 591
 NOT gate, 21, 22, 26-8, 51-4, 58-60,
 331, 391, 507, 531, 587
 Noumenal Reality, 432, 546
 Noumenon, 112, 356, 379
 Nuclear Magnetic Resonance, 4, 9,
 13, 25, 31, 172, 269, 294, 316,
 335, 487, 504, 572
 Nuclear quadrupole, 25, 271, 286
 Nuclear Spin, 4, 9, 18, 31-3, 269, 271
 Observational limit, 65, 75, 77, 83,
 91, 250
 Observer, ix, xiii, 36, 37, 63, 68, 76,
 78, 83, 103-8, 112-9, 123, 156,
 175-9, 188, 206-8, 231, 244, 248,
 250, 256, 300-7, 319, 379, 400,
 414, 424-32, 470, 543, 553, 563
 Octonion, xiii, 134, 197, 207, 209,
 211, 212, 463-6, 493-5, 500
 Octonion trefoil knots, 463
 Ontological I/O, 570
 Ontological model, 237, 292
 Ontological-phase, viii, ix, 35, 37,
 150, 175, 180, 232, 246, 256, 277,
 295, 314, 333, 365, 437-471, 497,
 540
 OPTFT, viii, ix, 35, 37, 175, 180,
 232, 246, 256, 277, 295, 314, 437
 Optical beam splitter, 27
 Optical lattice, 4, 15, 28, 29, 44, 539
 Orbifold, 101
 Orbital angular-momentum, 513, 514
 Oriented knot, 372, 392
 Oriented link diagram, 370, 373, 374,
 393
 Orthogonal, 2, 27, 31, 50, 60, 87,
 108, 177, 191, 248, 276, 332, 399,
 406, 411, 413, 422, 431, 488, 518
 Orthonormal basis, 3, 48, 333, 502,
 506, 512, 519, 579
 Paradigm, v, viii, ix-xi, 37, 65, 101,
 118, 155, 183, 189, 192, 221, 242,
 291, 300, 333, 403, 410, 419, 486

- Paradigm shift, v, viii, x, 37, 155, 189, 323, 334, 399, 439
- Parallel transport, 77, 79, 81, 91, 95, 99, 111, 113, 119, 191, 281, 345, 352, 420, 437, 445, 457, 560, 563, 573
- Parallel Universe, 63, 66
- Pauli matrices, 8, 133, 135, 162, 168, 209, 253, 511, 523, 544-5
- Pauli-Y gate, 52, 508, 509
- Pauli-Z gate, 51, 52, 508, 525, 581
- Peebles, P.J.E., 62, 124, 592
- Penrose, R., 143, 158, 434, 574, 577, 590, 593
- Perfect rolling motion, 351, 352, 566
- Persistent currents, 173, 181
- Phase factor, 140, 161, 294, 392, 397, 441, 442, 444, 472
- Phase rotations, 201
- Phase Shift Gate, 51, 52, 507
- Phase space trajectory, 268, 315, 570
- Phase vector, 439
- Phasor, 439-443, 472
- Phonons, 11, 362
- Phosphorus donor, 9, 31
- Photoluminescence, 18, 187
- Photon mass, 69, 77, 81, 91, 92, 95, 99, 117, 118, 124, 130, 187, 193, 250, 286, 335, 353, 418, 419
- Photonic crystal, 19, 410
- Pilot wave, 89, 90, 144, 146-9, 193, 244, 252, 291, 302, 313, 321, 404, 410, 555
- Planck constant, 76, 79, 83, 86, 194, 229, 252, 309, 341
- Planck length, 72, 269, 309, 310, 413
- Planck scale, vi, vii, 71, 75-77, 85, 86, 89, 108, 116, 117, 124, 132, 156, 178, 184, 187, 188, 219, 226, 230, 246, 247, 264, 290, 300, 303, 305, 308, 310, 314, 318, 336, 340, 400, 590
- Planck time, 75, 132, 193, 230, 303, 309, 318
- Plaquette operators, 384, 385, 445
- Plato, 40, 45, 103, 107, 112, 156, 182, 379, 380, 432
- Point particle, x, xii, 131, 132, 217, 247, 302, 305, 322, 329, 468, 568
- Potentia, xi, 104, 112, 148, 178, 209, 229, 244, 245, 248, 250, 290, 301, 302, 306, 307, 319, 323, 333, 343, 433
- Potential energy surfaces, 443, 444
- Pribram, K.H., 37, 129, 357
- Proca equation, 64
- Protein-folding, 8
- Pseudovectors, 135, 136
- Psychon, 320, 322
- Psychosphere, 109, 113, 117
- Pure rolling contact, 566
- QC applications, xi, 588
- QED violation, 223, 250, 338, 339
- Quadratic speedup, 475, 480, 481
- Quadrupole photon, 77, 90, 95,
- Qualia, 109, 117, 285, 300, 301, 303, 356
- Quantized gravity, 345
- quantum algorithms, xi, 3, 31, 56, 328, 329, 475-490
- Quantum annealing, 7, 8, 14, 15, 42, 398
- Quantum braids, 34
- Quantum circuit, 4-6, 10, 26, 53, 58, 396, 476, 531, 586
- Quantum Darwinism, 3, 41, 180, 246, 439, 469, 472
- Quantum Dot, 4, 9, 11, 19-21, 30, 42, 43, 362, 534, 539, 588
- Quantum erasure theorem, 164, 237, 246, 282, 283
- Quantum gates, 3, 5, 7, 10, 12, 18, 22, 25, 43, 48, 50, 54, 172, 382, 390, 475, 506, 523, 538, 589
- Quantum gravity, 68, 83, 91, 92, 94, 96, 123, 127, 186, 366, 430, 436, 438, 461, 468

- Quantum Hall effect, 33, 364, 391, 394-7, 534, 539, 572
- Quantum parallelism, 39
- Quantum Phase, 313, 443, 556
- Quantum potential, 69, 79, 82, 89, 90, 95, 117, 118, 126, 144, 146, 153, 157, 190, 193, 220, 224, 241, 249, 252, 257, 291, 311, 313, 320, 337, 361, 399, 404, 410, 419, 428, 437, 489, 490, 492, 560, 591, 592
- Quantum register, 1, 31, 503, 524, 535, 538, 580, 593
- Quantum simulations, 522
- Quantum superposition, 476, 503, 515, 524, 530, 580, 585
- Quantum tunneling, 9, 15,
- Quantum uncertainty, vi, xiii, 1, 44, 118, 159, 184, 193, 217, 222, 230, 236, 237, 243, 269, 280, 288, 290, 292, 297, 300, 343, 400, 401, 419, 538, 570
- Quantum walk algorithm, 480, 481, 498, 499
- Quantum Zeno effect, 34, 237, 245, 282, 292, 359, 434
- Quark mass, 63
- Quasiparticles, 33-7, 173, 295, 304, 364, 382, 383-94, 445, 449, 539
- Quaternion rotations, 453
- Quaternionic Clifford algebra, 258, 259, 534
- Quaternions, 122, 133-5, 138, 141, 150, 153, 155, 157, 188, 189, 194-212, 214, 217, 222, 224, 228-31, 253-9, 280, 308, 311, 339, 343, 351-3, 429, 430, 452, 464-6, 473, 493-5, 534, 539
- Raleigh-Jeans Law, vi, 131, 540
- Randall, L., 193, 223, 233, 286, 295-7, 360, 400, 590
- Randall-Sundrum model, 100, 125, 356, 433
- Rare-Earth, 4, 25, 26, 43
- Rauscher, E.A., 87, 124, 218, 219, 221, 224, 280, 337, 339, 422
- Real numbers, 46, 47, 71, 134, 170, 195, 211, 215, 327, 452, 465, 495, 523
- Realiton, 62
- Regge equations, 119, 120, 420, 421
- Reidemeister moves, 150, 257, 368, 369-71, 457
- Relational spacetime, 65, 70, 73, 75, 77, 84, 89, 415, 422, 431, 551
- Relativistic information processing, viii, xii, 3, 62, 164, 172, 246, 437, 475, 496
- Relativistic kinematics, 175
- Relativistic Quantum Field Theory, 102, 175, 250, 251, 316, 403, 426
- Relativistic qubits, v, vii, x, xi, 1, 3, 160, 165, 169, 170-73, 180, 246, 357, 438-9, 468, 492, 496, 534, 537
- Renormalization, vi, 81, 93, 131, 132, 141, 303, 399, 400, 540
- res cogitans, 111, 307
- res extensa, 111, 307
- Resonance hierarchy, xiii, 44, 98, 152, 155, 184, 195, 207, 225, 228, 229, 242, 258, 260, 265, 273-6, 280, 294, 298, 313, 316, 334, 340-3, 353, 537, 552
- Riemann 3-sphere, 65, 303
- Riemann spheres, 82, 95, 98, 163, 165, 187, 190, 201-3, 213, 217, 209, 227, 229, 256, 265, 276, 302, 307, 316, 330, 334, 416, 429, 548, 552, 558, 560, 572
- Riemann surfaces, 197, 214
- Roll-spun knots, 457, 473
- Rotation gate, 55, 56, 59, 60
- Rotations and reflections, 48
- Rowlands, P., 133, 149, 153, 157-9, 193, 197, 198, 210, 229, 230, 233-5, 253, 254, 343, 351
- Rydberg states, 12

- Sagnac effect, 124, 130, 184, 195, 251, 270, 272, 275, 291, 295, 334, 346, 353, 403
Sakharov-Puthoff conjecture, 286, 554
Schöenflies theorem, 69, 71, 125
Schrödinger box, 470
Schrödinger equation, 49, 179, 180, 252, 279, 404, 444, 521, 522, 543, 546, 571, 591
Schrödinger's Cat, 157, 232, 319, 470, 547
Search algorithm, 22, 499, 532, 587
Self-organization, 63, 80, 82, 92, 96, 104, 156, 160, 241, 251, 252, 262, 305, 399, 572
Semi-classical limit, 36, 175, 326
Semi-quantum limit, ix, 1, 49, 149, 152, 155, 175, 229, 249, 311, 326, 327, 437, 550
SETI, 227
Shadow point, 151, 155, 256
Shor's factoring algorithm, 479, 481
Snell-Descartes Law, 539
Soliton, 146, 304
SOLS, 291
Spacetime backcloth, 63, 104, 109, 113, 151, 226, 256, 269, 273, 277, 304, 306, 343, 400, 416, 560, 577
Exciplex, 102, 155, 190, 229, 230, 256, 302-8, 312-4, 318-23, 550
Spherical harmonics, 89
Spherical symmetry, 153, 267, 271, 315, 324,
Spin angular-momentum, 268, 513-5, 544
Spin quantum number, 13, 271,
Spin-exchange dynamics, 105
Spun knot, 457, 458, 473
Square matrix, 50, 506, 518
SQUID, 7, 14, 362
Standard Model, viii, x, 49, 62-4, 72, 91, 92, 101, 104, 116, 132, 133, 164, 184, 186-8, 192, 218, 221, 224, 226, 245, 250, 269, 272, 274, 278, 290, 300, 303, 309, 323, 336, 339, 342, 403, 423, 429, 537, 547
Standing-wave, 15, 64, 65, 76, 78, 82, 84-6, 95, 108, 111, 113, 118, 194, 210, 217, 227, 248, 251, 265, 279, 301, 323, 333, 342, 353, 403, 410, 415, 420, 428, 541, 548-51, 557
Stark shift, 28
Steady-State Universe, 65, 82, 101, 304
Stereographic projection, 162, 163, 165, 195, 201-3, 213, 216, 217, 305
Stoney, 79-80, 95, 226, 314, 340-1
String coupling constant, 310
String tension, 78, 79, 83, 95, 102, 126, 156, 183-5, 187, 195, 219, 222, 226, 229, 264, 301, 305, 314, 317, 334, 336, 338, 340, 341, 548, 549, 591
String theory, 66, 68, 69, 77, 85, 91-3, 102, 123, 142, 183-7, 194, 209, 226, 241, 250, 269, 289, 297, 301-3, 310, 314, 340, 367, 425, 449, 540, 560
String vertex, 78, 79, 154, 155, 190, 302, 305, 320, 414, 556, 558
Structural-phenomenology, 73, 78, 94, 95, 109, 132, 144, 241, 251, 258, 263, 277, 403, 559
Subspace, 46, 65, 66, 73, 76, 78, 82, 85, 103, 108, 116, 173, 177, 188, 231, 249, 279, 375, 405, 422, 432, 506, 518, 519, 541, 550, 554, 556, 563, 565, 572
Substantivism, 70, 74
Subtractive interferometry, 65, 77, 80, 108, 118, 156, 188, 247, 249, 400
Sundrum, R., 100, 125, 127, 356, 433
Supercomputers, 2
Superconductor, 4, 14, 15, 364, 390

- Superfluid, 11, 144, 147
 Superimplyte order, 144, 148-53,
 156, 178, 187, 213, 488, 491
 Superluminal Lorentz boosts, 81,
 426, 427, 565
 Superpartners, 92-5
 Superposition, 1, 2, 16-18, 47, 48,
 56, 116, 141, 146, 165, 171, 288,
 292, 293, 327, 328, 469, 479, 481,
 496, 501-3, 515, 524, 525, 531,
 538, 542, 564, 579, 580, 585, 588
 Superposition principle, 327, 469
 Super-quantum potential, 69, 79, 82,
 95, 117, 118, 153, 154, 157, 190,
 220, 224, 244, 257, 291, 311, 320,
 399, 419, 428, 437, 489, 560
 Supersymmetry, 70, 71, 92, 98, 100,
 141, 157, 255, 288, 290, 356, 413,
 426, 473
 Supervening Decoherence, xi, xii, 1,
 35, 160, 164, 236-81
 Surfaces of constant phase, 415, 416
 Surmount uncertainty, 247, 318, 326,
 589
 Susskind, L., 68, 69, 83, 125, 435
 SUSY, 63, 65, 79, 92-6, 99, 237,
 240, 241, 248, 559
 Swap Gate, 51, 54
 Synchronization backbone, ix, x,
 160, 185, 210, 225, 242, 261, 281,
 291, 298, 313, 537, 540, 550, 556,
 563, 572, 577, 578
 't Hooft, G. 68, 69, 83, 125, 181
 Tachyon measurement, 98, 183, 358
 Tachyon-tardyion interactions, 184,
 187, 194, 219, 233, 313, 337, 404,
 407-10, 434
 TBS, 192, 193, 195, 218, 223, 225,
 228-31, 311, 314, 334, 335, 338,
 344-51, 354
 TBS experiment, 195, 223, 227, 230,
 334, 338, 343, 351
 T-duality, 95, 97, 99, 100, 153, 198,
 279, 290, 297, 367, 430, 448
 Teleological, 64, 67, 82, 90, 95, 99,
 108, 112, 116, 252, 272305, 311,
 404, 423
 Temporal shift operator, 215, 216
 Tensor product, 58, 133, 136, 331,
 384, 509, 511
 Theory of Everything, 83, 91, 96,
 246, 399, 59
 Thermodynamic equilibrium, 105
 Tight Bound States, *see* TBS
 Time, 3, 9, 11, 20, 48, 49, 56, 66, 75,
 79, 81, 86-91, 99, 104-8, 138, 223,
 245, 346, 427, 460, 521
 Time is an illusion, 106
 Tired-light, 69, 70, 81, 124
 TOE, *see* Theory of Everything
 Toffoli gate, 54-61, 508
 Topological braids, 33, 364, 32, 383,
 387, 389
 Topological charge, 77, 187, 222,
 224, 238, 246, 251, 257, 281, 306,
 307, 318, 338, 339, 345, 403, 437,
 439, 458, 491, 492
 Topological field, 147, 149, 241,
 306, 312, 314, 428
 Topological Field Theory, viii, ix,
 35, 37, 175, 180, 232, 246, 256,
 257, 277, 295, 333, 364, 366, 380,
 437-71
 Topological Invariance, 447, 456
 Topological invariants, 175, 364,
 365, 370, 390, 447
 Topological phase, 156, 256, 295,
 385, 387, 389-93, 403, 439
 Topolgical protection, 385, 390
 Topological Quantum Computing, 4,
 33-5, 364, 382-5
 Topological Quantum Field Theory,
 xi, 175, 364-380, 459, 461, 468,
 589
 Topological strings, 447
 Topological switching, 95, 116, 149,
 187, 201, 203, 207, 222, 238,, 244,

- 257-9, 298, 306-8, 322, 437, 439, 451, 541, 572, 577
- Topologically ordered phases, 390
- Topologically protected, viii, 44, 309, 333, 359, 382, 390, 396
- Toric code, 385, 445
- Toroidal phase, 416
- TQFT, *see* Topological Quantum Field Theory
- Transactional interpretation, 64, 78, 96, 193, 210, 219, 227, 234, 244, 283, 288, 291, 302, 313, 324, 334, 342, 361, 409, 410, 434, 540, 549
- Trapped ion, 14-17, 61, 286, 539
- Trivector, 135, 136, 197, 200, 207, 216-8, 357, 536
- Turing, A., 1, 4, 6, 18, 36, 38, 39, 74, 237, 245, 281, 326, 331, 476, 477, 538
- Twist Move, 150, 213
- Twistor theory, 118, 143, 419, 468
- UFM multiverse, 66, 73, 85, 118, 187, 194, 224, 251, 337, 367, 431, 547
- Uncertainty principle, v, vi, xii, 1, 98, 104, 107, 115, 131, 132, 144, 149, 151, 184, 185, 193, 221, 222, 225, 226, 229, 230, 232, 236-8, 240, 248-50, 276, 280, 288, 290-4, 296, 300, 303, 309-19, 326, 336, 340, 343, 353, 380, 400, 414, 426, 490, 534, 538, 559, 564, 589
- Unified field, 67, 69, 72, 77, 79, 89, 90, 103, 107-10, 115, 144, 148, 153-7, 175, 244, 246, 247, 249, 251, 256, 258, 262-4, 273, 281, 300, 305, 311, 333, 337-9, 399, 415, 424, 432, 491, 492, 541, 548
- Unified Field Mechanics, v, vi, xi, xii, 1, 4, 35, 41, 131, 160, 164, 180, 183-232, 236, 241, 288, 318, 326, 329, 364, 400, 437-9, 475, 485, 534
- Unified Field Theory, 103, 185, 224, 339
- Unitahedron, 486, 496, 499
- Unitarity, v, ix, 3, 36, 92, 123, 161, 180, 242, 246, 256, 258, 430, 431, 439, 468, 475, 484, 486, 487, 556, 564, 572
- Unitary matrix, 26, 27, 47, 50, 58, 163, 176, 503, 580
- Unitary transformations, 29, 48, 50, 122, 164, 169, 177, 385, 391, 430, 478, 486, 506, 525, 528, 530, 581, 583, 585
- Universal gate set, 3
- Vacuum engineering, 97, 262, 272, 277, 281
- Variable String Tension, 78, 156, 183, 184, 187, 194, 222, 229, 314, 336, 338, 341
- Vector potential, 556, 558
- Vector representation, 47, 217
- Veldhorst, H., 21, 43
- Vigier, J-P, xii, 37, 64, 96, 122-4, 144-8, 186, 192, 223, 233, 241, 244, 283-7, 299, 313, 314, 333, 338, 339, 354, 430, 490, 500, 536, 540, 554, 564, 577, 591, 592
- Virtual asymptote, 187
- Virtual reality, 73, 80, 107, 111, 112, 118, 188, 301, 302, 323, 353, 419, 433, 557
- Vlasov, A., xii, xiii, 61, 168, 169, 172, 181, 284, 471, 496, 592
- Von Neumann, J., ix, 176, 181, 224, 244, 284, 339, 396, 398
- Walking of the Moai, 198, 203, 215, 234
- Wavefunction, 14, 36, 140, 141, 144, 176, 179, 294, 300, 321, 383, 391, 443, 485, 491, 505, 510, 515-7, 520, 534, 538, 544, 588
- Weyl spinor, 168

- Wheeler Geon, 77, 78, 89, 90, 95, 99, 107-9, 126, 265, 415, 424, 435, 550, 591
Whitehead link, 463
Wineland, L., 16, 42
Witten, E., 72, 78, 79, 111, 125, 126, 154, 155, 190, 284, 302, 303, 305, 316,, 322, 361, 364-7, 380, 400, 414, 447-9, 472, 556, 558, 591
World as a hologram, 68, 125, 435
Wormhole concept, 94, 95, 127, 301
Yang-Mills, 323, 360, 380,
Zeh, Z., 115, 126, 287, 434
Zeitgeist, 148, 438
Zero totality, 134-6, 139, 141, 198, 209, 403
Zitterbewegung, 141, 143, 193, 235, 309, 323
Zurek, W., 3, 41, 60, 180, 182, 246, 331, 439, 469, 472-4